1987

Analytical studies on Australian oil shales

Jurgen Korth
University of Wollongong

ANALYTICAL STUDIES ON AUSTRALIAN OIL SHALES.

A thesis submitted in fulfilment
of the requirements for the award of the degree of

DOCTOR OF PHILOSOPHY

from

THE UNIVERSITY OF WOLLONGONG

by

JURGEN KORTH, B. Sc., M. Sc.

DEPARTMENT OF CHEMISTRY

1987

ABSTRACT.

Oil shale samples from the upper and lower units of the bipartite Duaringa oil shale deposit, Queensland Australia, have been analysed using a variety of fast characterisation procedures such as solvent extraction, pyrolysis-GC, isothermal pyrolysis and TGA. A CDS-150 pyroprobe was modified to simulate Fischer assay retort conditions on a micro scale basis and was used for the rapid assessment (pyrolysis-FID) of the hydrocarbon generating potential of these and other oil shale samples. Results obtained for Duaringa were extended to analytical studies on an extensive range of selected Australian and several overseas reference oil shales. An electronically-controlled tube-furnace retort was constructed to provide accurate control over heating rates and pyrolysis environments. The retort was used to produce shale oils for samples from both units of the Duaringa deposit, which were then compared with each other and with a Duaringa reference oil obtained using the conventional Fischer assay procedure. The retort was also used to study the composition of pyrolysate produced over narrow sequential temperature ranges to provide a better understanding of retort processes and pyrolysis mechanisms.

Solvent extracts of the Duaringa lamosites contain a homologous series of linear alkanals not previously reported in Australian oil shales. Following their characterisation in the Duaringa bitumen (based on mass-spectral data and retention-index values) these aldehydes were subsequently detected in extracts from other Australian oil shale deposits. The possible origins and significance of these and other components found in oil shale bitumen are discussed in relation to the source, environment of deposition, maturation and bio-degradation of the kerogen comprising these deposits.

Results obtained from the pyrolysis-FID procedures for Duaringa were used to characterise (type) the Australian and overseas oil shales on the basis of their relative abilities to generate (type-dependent) quantities of hydrocarbons (oil and gas) from the pyrolysis of their raw shale. For shales comprising type I and II organic matter, hydrocarbon oil and gas yields correlated positively with Fischer assay oil yields,

petrographic data, kerogen content and elemental composition. The procedure provides a rapid and inexpensive screening method for the accurate first assessment of the relative oil -generating potential of a given deposit.

Retort oils from the upper unit (resource seams) and lower unit (> 1000 m) were analysed by extraction and column chromatography, followed by detailed gas chromatography and mass spectrometry of each of the 19 fractions isolated. Hundreds of compounds were identified and their retention indices calculated where the components eluted as discrete peaks in respective gas chromatograms. Least-squares linear regression analysis of these data allowed retention-index equations to be calculated for a wide variety of different compound classes. Collectively this information provides reference data which should allow comprehensive chemical characterisation of shale oil to be achieved without the need for mass spectrometric analysis of each column fraction.

Despite the substantial difference in the depth of burial, the chemical composition of the upper- and lower-seam Duaringa shale oils was very similar and found to resemble those from non-carbonaceous seams of other Tertiary Australian deposits (Condor and Rundle). The distribution and relative abundances of some of the isomeric structures encountered in each of them indicate that retort-product concentrations are influenced by relative variations in the thermocatalytic activity of the mineral matrix. Accurate and class-specific quantitative data obtained for Duaringa phenols, nitriles and ketones suggest that these volatile components constitute only a minor portion of the otherwise non-volatile column fractions in which they are found. This implies that gravimetric data published for these compound classes for Condor and Rundle shale oils overestimate their abundance.

Data obtained from rapid characterisation techniques were interpreted in relation to the composition of the corresponding retort oils. Advantages and limitations of microscale screening techniques are discussed with reference to results obtained for Duaringa and other Australian oil shale deposits.

CONTENTS

ABBREVIATIONS USED IN TEXT.

NB. Unless otherwise stated, all aliphatic compounds are linear.

BP	-bonded phase.
C_n	-n carbon atoms.
C_{org}	-total organic carbon.
CI	-chemical ionisation.
CPI	-carbon preference index.
CP/MAS	-cross polarisation magic angle spinning ^{13}C NMR.
DSC	-differential scanning calorimetry.
DTA	-differential thermal analysis.
EA	-elemental analysis.
EI	-electron impact (ionisation).
FAB	-fast atom bombardment.
FA	-Fischer assay.
FID	-flame-ionisation detector.
FTIR	-fourier-transform infrared.
GC	-gas chromatography.
GC-MS	-gas chromatography-mass spectrometry.
HPLC	-high-performance liquid chromatography.
IR	-infrared.
IS	-internal standard.
LC	-liquid chromatography.
LTOM	-litres per tonne at zero % moisture.
MFA	-modified Fischer assay.
MI	-matrix isolation.
MID	-multiple-ion detection.
MS	-mass spectrometry.
NMR	-nuclear magnetic resonance.
PAH	-polycyclic aromatic hydrocarbon.
R	-correlation coefficient.
RI	-modified Kovats retention index.
SIM	-single-ion monitoring.
TGA	-thermogravimetric analysis.
TLC	-thin-layer chromatography.
TSQ	-triple-sector quadrupole.
UV	-ultraviolet.

CHAPTER ONE : INTRODUCTION .

1.1 OIL SHALES .

1.1.1 Definition.

Oil shales from different sources vary widely in composition and no precise definition for them exists. In practice they continue to be described primarily in terms of their behaviour according to economic criteria. Gavin (cited by Yen and Chilingarian, 1976) defines them as compact laminated rocks of sedimentary origin, yielding over 33 % of ash and containing organic matter that yields oil when distilled at 500-600° C, but not appreciably when extracted with commonly used hydrocarbon solvents. Materials yielding less than 33 % of ash should be considered as coal. Many oil shales as defined are not shales in the restricted sense of their lithology, but have mineral and textural features which allow them to be classified as siltstone, impure limestone, black shale or impure coal.

Simplistically oil shale may be regarded as a composite of tightly bound organic and inorganic material with the latter comprising quartz, feldspars, clays, carbonates, pyrites and other minerals. The organic material (usually) constitutes less than 20 % of the shale mass and may be subdivided into fractions either soluble (bitumen) or insoluble (kerogen) in common organic solvents. Both bitumen and kerogen dissociate when pyrolysed to form gaseous and liquid products. Commercially pyrolysis is carried out in a retort where some of the gases are reused as process fuels. The liquid crude (shale oil) is usually upgraded and refined to produce synthetic liquid fuels (synfuels). Because of its solubility bitumen is readily extracted from shale and is then available for analysis; however it rarely constitutes more than a few percent of the total organic shale content. The remaining insoluble kerogen is a tough geopolymer dispersed throughout the mineral matrix of the oil shale and requires specialized techniques for characterisation.

1.1.2 Environment of deposition.

In general terms oil shale formation may be regarded as the codeposition and lithification of finely divided mineral matter and the organic debris derived from the breakdown of biota. Conditions favourable for large accumulations necessarily include abundant organic productivity, early anaerobic conditions and a lack of destructive organisms. These conditions are met, at least in part, by bodies of still water and Duncan (1976) has suggested oil shales were probably deposited in small lakes, bogs, lagoons associated with coal-forming swamps, large continental lake basins and shelves in tranquil seas. Continued sedimentation, possibly coupled with subsidence, provided sufficient overburden pressure required for the compaction and diagenesis of organically rich strata to produce, over geological time, the fine-grained rocks of the definition.

Oil shales deposited in lacustrine basins include the thickest deposits known and are generally of the calcareous type, with associated sediments of volcanic tuffs, clastics and carbonate rocks. Inland waters are usually surrounded by thick margins of swamp vegetation which acted as an effective filter for all but the finest silt and clay brought in by rivers and the fine-grained detrital material consisted mostly of clays plus finely comminuted plant debris. Coarser material and large quantities of mud were introduced during flooding.

Marine oil shales deposited in shallow seas on continental platforms are characteristically thin and most have low oil yields; however reserves may cover hundreds of thousands of square kilometers. They are usually the siliceous type but some carbonate-rich shales do occur and most of the higher grade marine deposits are of this type. Oil shale deposits formed in small lakes, bogs and lagoons associated with coal producing swamps are relatively small although many are high grade resources.

1.1.3 Mineralogy.

It is the environment of deposition which determines the mineralogy of oil shales and information about the inorganic phase provides insight into the setting and process of their formation. The inorganic constituents of any deposit may be divided into detrital,

biogenic and authigenic minerals. To date only the Green River Formation of the U.S.A. has been studied extensively in this context. Shanks et al. (1976) have summarized some of the information available for this deposit but point out that the data obtained are not necessarily representative of other deposits; they allow only general conclusions about the mineral content of other oil shales to be made.

Detrital material is composed mainly of quartz, feldspars, clay minerals and volcanic debris, with the percentage of each determined by various factors such as source area, mode of transport and distance transported. Biogenic materials are primarily amorphous silica and calcium carbonate, but are not (generally) abundant. Authigenic minerals include metal sulphides, carbonates, phosphates and various saline minerals. Collectively the latter are important because they may provide information concerning the redox conditions during sedimentation. Authigenic sulphides, for example, are invariably present in oil shales and suggest formation in a reducing environment which, considering the oxidizing nature of the oceans and the atmosphere, indicates deposition regions of restricted water circulation. The fine grain size of detrital sediments included in oil shales is indicative of low energy environments and supports this interpretation. Authigenic carbonates and saline minerals are formed by evaporative concentration processes and, if present, indicate an arid climate.

Oil shale deposits containing substantial amounts of carbonate minerals include some of the higher-grade accumulations. The shales, particularly those of lacustrine origin, are generally hard rocks resistant to weathering and are commonly varved. The carbonate minerals, often calcite or dolomite, are fine-grained and may be the dominant constituents at the time of depositon. Most of the carbonates probably were precipitated at the time of deposition, whereas others may have formed as part of the process of oxidation of organic matter to carbon dioxide and its subsequent combination with calcium, magnesium and other elements. This process may have begun with the decay of organic matter during deposition and continued during the early stages of compaction of the shale. More than 20 such carbonate minerals have been described for the Green River Formation.

Oil shales devoid of significant amounts of carbonate minerals may have detrital

minerals as their main constituents. The siliceous shales are less resistant to weathering than carbonate-rich shales and the oil yield of older deposits is generally poor. This suggests that the combined effects of compaction, deformation and metamorphism have led to the progressive depletion of organic matter through the migration and release of mobile and volatile constituents.

1.1.4 Kerogen accumulation and abundance.

The general mineralogy of oil shales was briefly outlined in section 1.1.3; what follows is (almost) exclusively concerned with the study of their contained organic matter. This is not to understate the influence of mineral matter during all phases of deposition, burial and subsequent maturation of the oil shales, but reflects limitations imposed on the research by the range of analytical instruments available for our studies. Collectively any physical and chemical methods for oil shale analysis should converge to provide a coherent picture of the composite organic matter and its evolution. Before studying oil shales it is important to have some idea of organic source material likely to be involved in their formation and the chemical and geological processes which determined the evolutionary fate of the original sediment. Once incorporated in a sediment, the long-term prospects of organic matter are governed by both microscopic and macroscopic processes, the latter including tectonic events such as subsidence or phases of uplift and erosion which determine whether the organic content is preserved and transformed, or eroded and oxidised.

Sedimentary organic matter is derived from living organisms and the products of their metabolism. Mass production of organic matter on earth followed the emergence of photosynthesis as a global phenomenon more than 2 billion years ago. Primitive autotrophic organisms such as photosynthetic bacteria and blue-green algae utilized the procedure to produce vast quantities of organic matter through propagation and ultimate death as well as the metabolic processes of secretion and excretion. In doing so they sustained heterotrophic organisms, established the basis for the evolution of higher forms of life and enriched the earth's atmosphere in molecular oxygen. Globally less than 1 % of the organic matter synthesized by photosynthesis escapes the carbon cycle to be

accumulated through deposition in sediments. Kerogen represents the bulk of the preserved organic carbon in these sediments and is the most abundant "organic molecule" on earth. Hunt (1972) has estimated the total amount of organic carbon and graphite formerly representing sedimentary organic carbon to be 1.07×10^{16} t. Durand (1980) has taken this approximate figure, as well as data from various other sources, to draw up a comparison between the quantity of kerogen disseminated in various deposits and the ultimate fossil fuel resource that these represent (Figure 1.1). The estimate of kerogen in total oil shale resources (organic rich shales) remains very uncertain and Durand gives two values. One of 10^{14}t of kerogen, capable of producing 3×10^{13}t of oil by pyrolysis (equivalent to 75 times the petroleum resources) and one of 10^{12}t of kerogen, which represents an estimate of presently inventoried oil shale reserves exploitable using current technology. Using a conversion rate of 50% for transforming the kerogen content of these oil shale resources into fossil fuel this equates to 5×10^{11}t of shale oil. Yen and Chilingarian (1976) have put the total world potential of shale oil at 30×10^{12}bbls, with only about 2% available for present-day commercial exploitation. Using an average density of 0.9g cm^{-3} for shale oil this represents about 8.6×10^{11}t of shale oil, a figure close to that given by Durand.

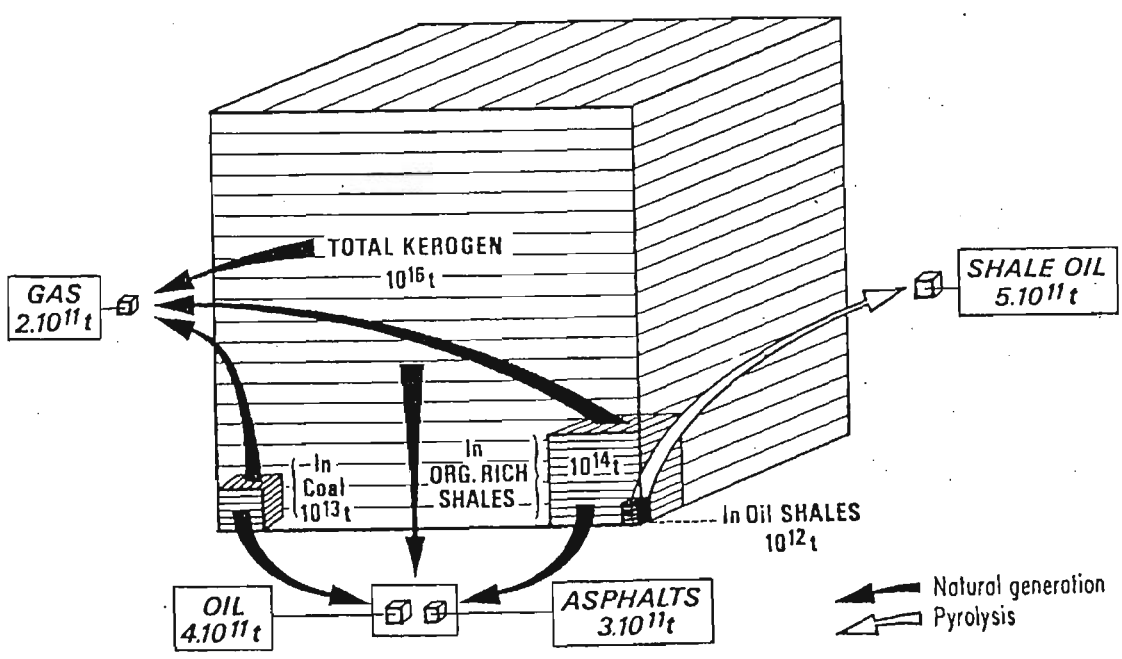

Figure 1-1. Comparison between kerogen abundance and ultimate resources of fossil fuel (from Durand, 1980).

Bacteria, phytoplankton, zooplankton and higher plants (the latter since Silurian-Devonian times) are the main contributors to organic matter in sediments. It is the natural associations of these groups of organisms in various facies provinces which determine both composition and type of organic matter to be deposited and incorporated in sediments. After the death of the organisms their component substances are subjected to varying degrees of decomposition dependent on the sedimentation medium, in particular its redox properties. The deposition of fine-grained sediments in subaquatic environments limits access of dissolved molecular oxygen and the activity of aerobic bacteria ceases once the limited amount of trapped oxygen has been exhausted. Sulphate-reducing bacteria (*Desulfovibrio)* produce H_2S and, where present, further limit bacterial attack by creating toxic gas-saturated conditions within and above the sediment-water interface, particularly in oxygen deprived bottom layers of stratified low energy bodies of water. By contrast, the presence of free air and moisture in subaerial environments allows profuse growth of bacteria with consequential breakdown of organic matter by chemical or microbial oxidation. As a result large quantities of kerogen are only formed and fossilized in subaquatic sediments, with contributions from allochthonous land-derived terrestrial plant material transported to respective sites of deposition by the (combined) actions of wind, rivers, ocean currents etc.. In both cases the most labile or assimilable compounds are depleted first and kerogen, a very inert fraction increases in relative proportion. Parts of the products of any decomposition are recycled by other organisms which use them as energy sources (heterotrophic organisms); simple molecules such as CO_2, H_2O, CH_4, NH_3, H_2S, etc. are formed as products of associated metabolic processes.

Organic matter available for accumulation comprises soluble (sugars, amino acids etc.) and particulate forms (water-insoluble lipid material as components of highly resistant parts of organisms such as spores, seeds, cell walls etc. or as part of the whole organism deposited directly in the sediment). Clay-sized minerals settling through the water column are readily coated with (polar) dissolved organic compounds to form suspended particulate matter which may be transported to, and laid down in, undisturbed

waters. This adsorption of hydrophilic compounds may be considered an extraction process, with attendant conversion of dissolved organic matter to particulate form. Further interactions between the various forms of organic matter and the mineral phase may cause phenomena such as coprecipitation, flocculation, protection, catalysis etc. to occur.

1.1.5 Kerogen source material.

All organisms are basically composed of the same groups of chemical constituents namely: proteins, carbohydrates, lignins (higher plants) and lipids.

Proteins are highly ordered polymers made from individual amino acids. In the presence of water, insoluble proteins may be broken down, by enzymatic hydrolysis of the peptide bond, to their water-soluble constituent amino acids with possible further breakdown to ammonia and amines. Cane (1976) suggested that some of the hetero-atoms originating from proteins were present in the intermediate breakdown products and were eventually "built into" the kerogen matrix. He supported this proposal by showing that the pyrolysis of polyene fatty acid polymers containing occluded aliphatic nitrogen compounds produces oil containing alkyl pyridines.

Carbohydrates are sources of energy and form the supporting tissues of plants and certain animals. The term is a collective name for individual sugars and their polymers, with cellulose and chitin among the most prominent polysaccharides occuring in nature. Degradation may proceed via bacterial or enzymatic attack to produce saccharides with possible subsequent hydrolysis to carbon dioxide and water. This mode of total degradation completely eliminates any potential input to kerogen and their contribution is small enough to be neglected (Cane, 1976).

Lignins occur as a three-dimensional network located between the cellulose micelles of supporting tissues of plants. They are high molecular weight aromatic derivatives of phenyl propane and may give rise to kerogenous material by demethylation, ring rupture and polymerization. Lignin is the major primary contributor of aromatic structures in Recent sediments. Pyrolysis of oil shales containing high terrestrial input should reflect this contribution and produce shale oil high in aromatic content, contrary

to what is (usually) found. Consequently it seems unlikely that lignins (or tannins-for similar reasons) played a significant role in oil shale kerogen formation, although some contribution by lignin and tannin material cannot be ignored, particularly in the coaly oil shales.

Lipids encompass fat substances, such as animal fats ,vegetable oils and waxes such as those occuring as surface coatings of leaves. Fats are involved in the energy budget of the organism whereas waxes are primarily designed for protective functions (eg. cuticle wax- to prevent excessive loss of water). Fatty acids of natural fats (mixtures of triglycerides) have an even number of carbon atoms because they are synthesized biochemically from C_2-units (acetate units). Unsaturated fats are common, especially in vegetable oils. Among algae, diatoms are known to contain great quantities of lipids, sometimes up to 70% on a dry mass basis especially if the algae grow under nitrogen-deficient conditions and in colder waters away from the euphotic zone. Alkanes of medium molecular weight are considered representative of both algal sources generally (Gelpi et al. 1970) and of cyanobacteria in specific cases (Blumer et al. 1971). These hydrocarbons result from the direct inheritance of individual components or may be derived from related fatty acids. The alkane distribution normally shows an odd over even-carbon-number preference with C_{15} and C_{17} usually most abundant.

Copepods constitute the largest single fraction of zooplankton in most waters. Composition of the lipids of calanoid copepods was investigated by Lee et al. (1970), who showed that the lipid content of certain wild types was unusually high, with wax esters of special interest because both the fatty acid and alcohol constituents are made up of long-chain carbon skeletons with 18 or more carbon atoms. Total carbon numbers for these esters were found to range from 30 to 44 and according to the authors the wax esters of marine copepods are very probably the main source of long-chain alcohols observed in marine sediments and in some ocean surface lipids. Blumer et al. (1963), found that the isoprenoid hydrocarbon pristane (2,6,10,14-tetramethylpentadecane) is a major component of the body fat of copepods, which use it for buoyancy purposes to maintain a suitable position in the water column. They concluded that pristane from the calanoid copepods

may be the major primary source of pristane in the marine environment.

The bulk material of terrestrial plants (especially shrubs and trees) is made up of cellulose and lignin (50-70%); however sections such as barks, leaves, spores, pollen, seeds and fruit may be highly enriched in lipids and lipid-like substances. Pollen usually contains 2-8% fats while leaves contain considerable amounts of lipids such as waxes, cutin, suberin etc. Waxes differ from fats in that glycerol is replaced by complex alcohols in the C_{16} to C_{36} range. Lipids derived from higher plants contain alkanes in the range C_{10} to C_{40} which show a strong predominance of odd over even-carbon-numbered alkanes with components C_{27}, C_{29} and C_{31} often most abundant in the order listed (Eglinton and Hamilton, 1963).

1.1.6 Kerogen evolution (maturation).

Once deposited, both lipid and non-lipid fractions are subjected to biological activity during the early stages of deposition, followed by deeper burial and the gradual combined effects of temperature and pressure. Given the comments about the biochemical fate of the four main classes of compounds representative of living matter, it may be deduced that the contribution of particulate lipid material (especially from exinite (liptinite) macerals) is of major importance for the formation of oil shales. Molecules which have been synthesized by living organisms and are deposited and preserved (relatively) unaltered are called geochemical fossils (biomarkers) (Eglinton and Calvin, 1967). They comprise mainly hydrocarbons or other lipids which have survived with carbon skeletons indicative of their biogenic origin. Biomarkers represent only a minor portion of oil shale bitumen with others possibly trapped in, or bound to, the kerogen polymer. They include alkanes, fatty acids, porphyrins, steroids and terpenoids. Terpenoids may occur as hydrocarbons, alcohols, aldehydes, ketones, acids and lactones and exhibit various degrees of unsaturation. They are produced by chain and ring polymerization of the isoprene unit, a prominent biochemical building block consisting of five C-atoms. Despite their low abundance biomarkers are extremely important since they provide chemical information about the original organic matter and possible kerogen precursors.

Freshly deposited subaquatic sediments comprise a chemically unstable mixture of water, minerals and living organisms as well as contemporaneous autochthonous or allochthonous, and reworked organic matter. During the formation and geological history of the sedimentary column the initial deposition may be succeeded by three main stages of evolution (Figure 1-2.).

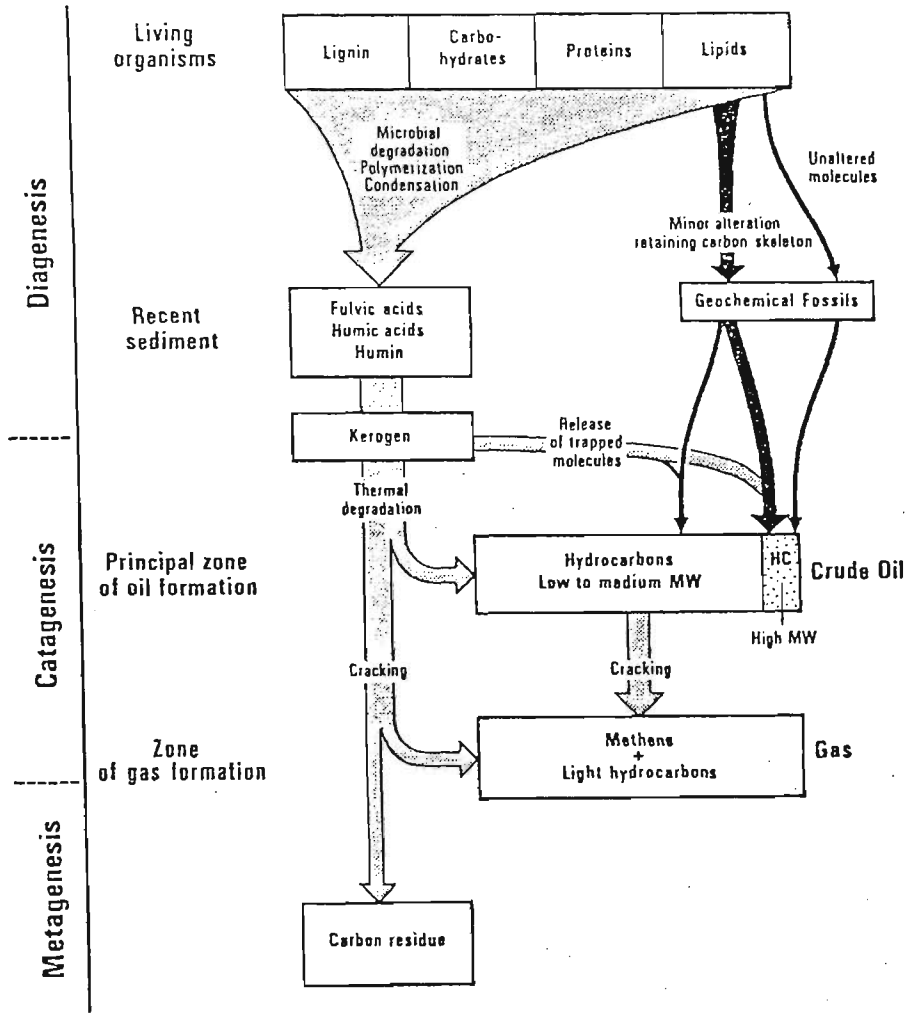

Figure 1-2.
Hydrocarbon sources from the evolution (maturation) of organic matter. Subsurface sources comprise geochemical fossils (black) and kerogen degradation products (grey). (from Tissot and Welte, 1984).

These are:

1. - **diagenesis**
2. - **catagenesis**
3. - **metagenesis/metamorphism**

The extent to which this sequence of evolutionary phases has progressed depends on the depth of burial of the deposit.

1. **Diagenesis** is a process through which the system tends to approach equilibrium under conditions of shallow burial and by which the sediment normally becomes consolidated. It begins with microbial activity as one of the main modes of transformation. Subsequent chemical rearrangements occur at shallow depths and result in polycondensation and insolubilization. Diagenesis results in the disappearance of oxygen containing functional groups which are eliminated in the form of CO_2, with accessory H_2O and CH_4 (the latter by *Methanobacteria* as the final stage in the anaerobic fermentation of oxidized forms of organic matter). At the end of these reactions, kerogen is impoverished in oxygen and almost completely defunctionalized. It ceases to be hydrolyzable and extractable humic acid content has decreased to minor levels. The latter is used as a chemical criterion to characterise the end of the diagenetic process which corresponds to a vitrinite reflectance level of ca. 0.5%.

Continued deposition of sediments, possibly coupled with tectonic events, results in deeper burial of previous beds and may reach thousands of metres. At these depths the kerogen is subjected to large increases in geostatic overburden pressure and depth-related increases in temperature. These increases again place the system out of balance and result in continuing chemical changes collectively designed to reestablish equilibrium conditions.

2. **Catagenesis** encompasses chemical changes which result largely from an increase in temperature, with pressure effects relegated to a subordinate role (rock compaction, expulsion of interstitial water, decrease in sediment porosity and permeability etc.). Temperature effects, which for this phase are restricted to the range 50-150^0 C, first produce hydrocarbons (oil and gas) from thermally degraded kerogen to be followed by the production of "wet gas" and condensate. Hydrocarbon production proceeds at the expense of hydrogen content and in the process increases kerogen aromaticity; free lipids present also undergo thermal evolution toward hydrocarbons. The end of catagenesis is chemically characterised by the disappearance of aliphatic chains in the kerogen structure, with basic units progressing structurally towards a hexagonal lattice. A vitrinite reflectance value of about 2.0% has been accepted to coincide with this stage of sediment maturity.

3. **Metagenesis** commences only under conditions of high temperature and pressure. Remaining hydrocarbons are converted to methane and residual kerogen, with kerogen as a whole expelling any last heteroatoms and evolving towards a carbon residue. **Metamorphism** occurs only in deep troughs or geosynclinal zones where the sediment has encountered very high temperatures and pressures. Here the constituents of residual kerogen are converted into graphitic carbon.

It is obvious from the above considerations that oil shales have not been subjected to any of the above processes other than those of diagenesis or possibly very early catagenesis. This is why their retort products contain relatively large quantities of oil and gas. The retorting process simulates the catagenetic phase of kerogen evolution and produces hydrocarbons characteristic of oil shale pyrolysis.

1.1.7 General classification of kerogens.

Practically all organic matter may be classified into two major groups, sapropelic and humic (Potonie, 1908 cited in Hunt, 1979). Sapropelic organic matter comprises the decomposition and polymerization products of high-lipid organic materials deposited under predominantly anaerobic conditions in the subaquatic muds of marine or lacustrine environments. It results from the reductive degradation of structured detritus of either algal or higher plant origin by anaerobic bacterial saprophytes. This sapropelization process produces an amorphous biomass high in bacterial bodies, relict and reworked algal and herbaceous lipids, microbial waxes, hydrocarbons and other lipids. An overall lipid-enrichment of the products is reflected by a higher H/C atomic ratio of the resultant protokerogen. Lijmbach (1975) found an increase in the organic matter to oil conversion (in conjunction with lower conversion temperatures) when heating bacterially reworked plankton, again indicative of overall lipid-enrichment. Humic organic matter is defined by the decomposition and polymerization products of the lignin, tannins, and cellulose of plant cell and wall material as well as carbonized organic matter deposited in swamps and soils under aerobic conditions with partial restriction of oxygen (Hunt, 1979). Within these broad groups (amorphous) kerogens may be differentiated into various (roughly

equivalent) categories using different optical criteria and into three distinct "types" based on results from the chemical analysis of three well-characterised reference deposits (Durand and Monin, 1980).

Optical examinations in transmitted light allow palynologists to classify mineral-free kerogen as algal, amorphous, herbaceous, woody and coaly. Coal petrographers study polished rock surfaces in reflected light (visible and ultraviolet) and base their classification on the presence of recognizable coal macerals and amorphous organic material. The latter is generally considered by petrographers as the organic matter richest in hydrogen and is consequently listed with the macerals of the liptinite (exinite) family. Elemental analysis of kerogen from amorphous organic matter has shown that this is not always the case and highlights the benefits of an interdisciplinary approach to classification in general (Durand and Monin, 1980). Another kerogen classification was established by Tissot et al. (1974) and characterises kerogen as types I, II, and III, depending on its elemental composition and its evolution path in a van Krevelen diagram.

The global atomic composition of shallow immature kerogens varies with the organic source material and the physicochemical conditions of deposition. Inherent differences evident in the major constituent elements C, H, and O may be substantial for different shallow sediments and, where this is the case, remain recognizable, albeit weaker, between deeper samples from the same formations. The H/C versus O/C ratio of each particular sample in the graph (van Krevelen diagram) provides a useful approach to the classifications of kerogens. Kerogens obtained at various depths from the same formation normally group along a curve called an evolution path which defines the kerogen type. Closely related environments of deposition result in the same path, with all paths ultimately converging to the carbon pole (graphitization) in concert with progressively deeper burial (Figure 1-3.). A plot of this kind was first used by van Krevelen (1961) to characterise coal macerals and their coalification paths (Figure1-4.). Oil shales may be characterised within the framework of these various systems of largely analogous classifications established primarily for the (amorphous) kerogens of petroleum source rocks.

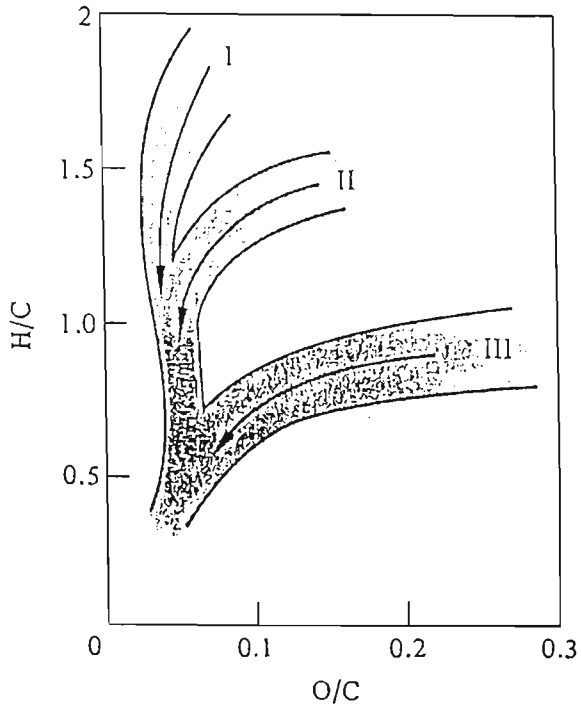

Figure 1-3.

Van Krevelen plot showing generalized evolution paths for type I, II, and III kerogen.

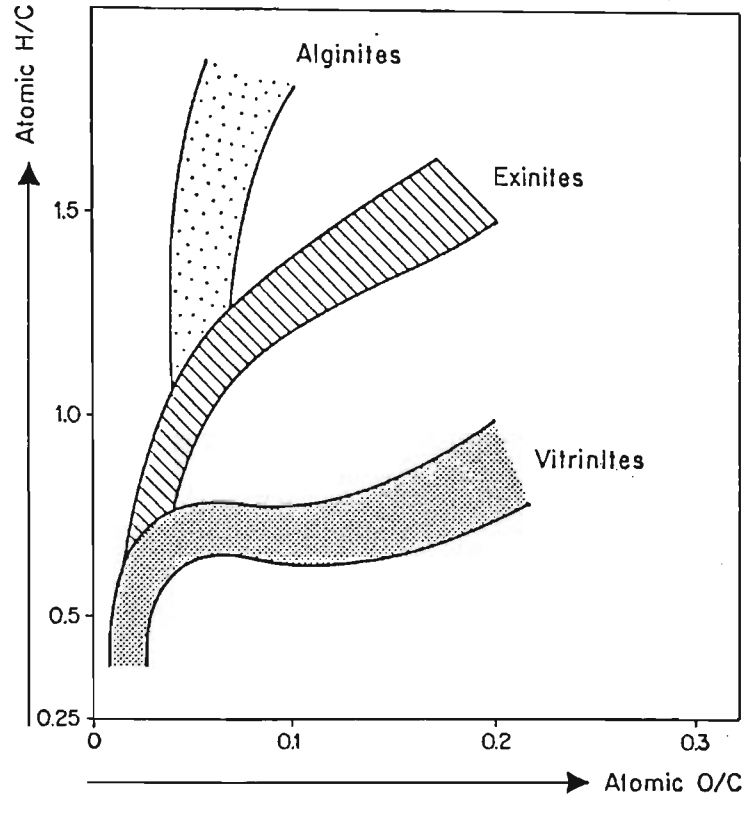

Figure 1-4.

Evolution paths of maceral groups in coals (from van Krevelen, 1961).

It should be noted that the three systems of classification based on optical and chemical criteria are not equivalent: boundaries between categories (types) within one system are not always sharply defined and do not necessarily coincide with those based on another system. An approximate relationship between the various classifications is given in Figure 1-5.

	SAPROPELIC			HUMIC	
KEROGEN (by transmitted light)	Algal	Amorphous	Herbaceous	Woody	Coaly (Inertinite)
COAL MACERALS	Liptinite (Exinite)			Vitrinite	Inertinite
(by reflected light)	Alginite	Amorphous	Sporinite Cutinite Resinite	Telinite Collinite	Fusinite Micrinite Sclerotinite
KEROGEN (by evolutionary pathway)	Types I, II		Type II	Type III	Type III
H/C	1.7–0.3		1.4–0.3	1.0–0.3	0.45–0.3
O/C	0.1–0.02		0.2–0.02	0.4–0.02	0.3–0.02
ORGANIC SOURCE	Marine and lacustrine		Terrestrial	Terrestrial	Terrestrial and recycled
FOSSIL FUELS	Predominately oil Oil shales, boghead and cannel coals		Oil and gas	Predominately gas Humic coals	No oil, trace of gas

Figure 1-5.

Classification systems for organic matter in sedimentary rocks (from Hunt, 1979).

In practice types I, II, and III are really mixtures, with type I generally comparable to the algal-amorphous categories typical of the kerogen of oil shales. Type II is comparable to amorphous-herbaceous-woody kerogen, and type III to woody-inertinite. A

comparison of the elemental composition of kerogen from oil shales shows that, according to the classification established above, the amorphous sapropelic organic matter of oil shales usually belongs to either type I or type II. There is no oil shale related to type III (Tissot and Welte, 1984). Concentrations of type III organic material, derived from higher plants, are usually classified as humic coals or carbonaceous shales accompanying coal.

Oil shales associated mainly with a single type of organism (e.g. algae) are anomalous from a geological point of view and cannot be readily compared with the classification given above. These classifications relate (primarily) to amorphous kerogens, as opposed to algal kerogens of oil shales such as torbanite and tasmanite. Algal-derived oil shales in general, and the unique Green River oil shales of the Uinta Basin (U.S.A.) in particular, are accomodated within a type I classification on the basis of the highly aliphatic character of their kerogen, as well as other criteria. The latter comprises only amorphous kerogen (microscopic examination shows practically no identifiable remains of organisms); it is the type I reference kerogen used by Tissot and co-workers (Tissot et al. 1974.). The former will be classified further in the section dealing with the organic petrography of oil shales.

Apart from sustained differences in elemental composition along respective evolution paths, the various kerogen types also exhibit other differences such as oil and gas generating potential (Figure 1-6.). Oil shale classifications within this type-system are largely predetermined by their oil yields. Sufficient kerogen of high atomic H/C ratios (1.25-1.75) combined with variable but normally low atomic O/C ratios (0.02-0.20) results in economically viable oil-generating potential. Estimates of oil yields to be expected can be made on the basis of H/C ratios and data obtained from other techniques such as thermogravimetric analysis (Durand-Souron, 1980). These data show, for the types which have been fully studied, that maximum quantities of hydrocarbons (oil + gas) formed per unit mass of initial kerogen are approximately 75% for type I, 50% for type II and 30% for type III. These values correlate well with the initial average H/C ratios for the kerogens which are respectively about 1.6, 1.3 and 0.9 (Durand and Monin, 1980).

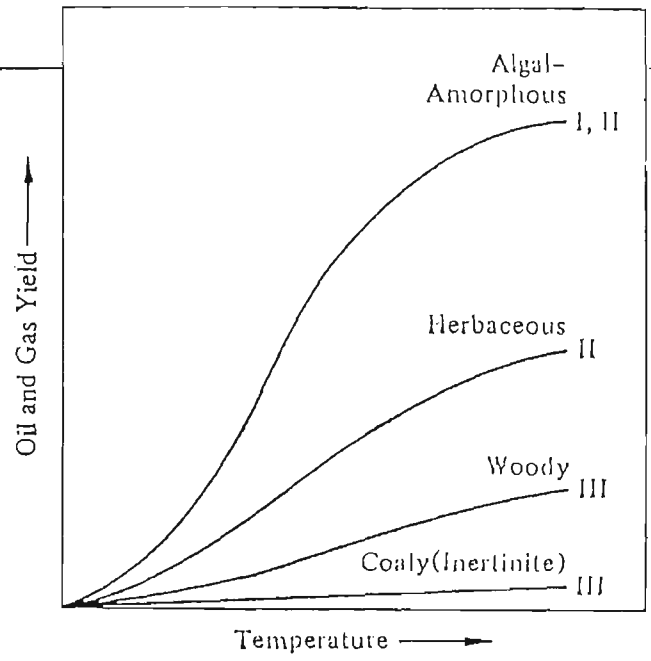

Figure 1-6.
Relative oil and gas yields for various kerogen types (from Hunt, 1979).

1.1.8 Organic Petrography .

Microscopic examination reveals that oil shales were laid down in the quiet ecosystems of the environments described in section 1.12. It appears that the major deposits were formed from the remains of algae which flourished in still waters, either marine or terrestrial, and that algal lipids were the main source of kerogen itself (Cane, 1976). Minor contributors were spores, pollen and remains of higher plants, with adventitious foreign matter such as insects, animal parts, fish, minute crustacea etc. also present. All deposits are microstratified and contain banded structures showing that environmental conditions varied on an annual, seasonal or irregular basis. Autochthonous organic material mixed in various proportions with allochthonous matter, clays and silt brought in by rivers and creeks, to produce stratification within the existing algal mass.

Any classification of oil shales should be based initially on easily recognisable features, primarily those of the organic matter. This relates directly to the use of oil shale as a fuel source and once sufficient relevant data have been established for a particular classification they may be related more generally to the chemistry of the shale and shale oil derived from it. Previous classifications have been based on criteria as diverse as industrial use, included mineral matter, density and ash relationships and the chemistry of kerogen, including its categorization into one of three types (Tissot and Welte, 1984). Organic matter type and abundance have rarely been the dominant criteria of those classifications which have gained wide acceptance.

The organic matter of oil shale may be differentiated microscopically into either amorphous or form preserving fractions. The amorphous fraction includes the maceral bituminite, but cannot be biologically defined because it lacks observable structure. Individual preserved forms, or macerals, may also be classified as belonging to one of the three maceral groups exinite, vitrinite, and inertinite. Petrographic examination of whole-rock is usually preferred over kerogen analysis because mineral-maceral inter-relationships are preserved and incident light examination allows a simultaneous determination of maturity parameters such as rank, to be made from vitrinite reflectance data.

Most forms of organic matter in oil shale are included within the exinite group of macerals as they are largely algal in origin (alginite) with a lesser contribution from spores, pollen and cuticle of higher plants (sporinite, cutinite). Significant differences occur in the nature of alginite from various oil shales, with the principal difference being the form of the macerals. Hutton et al. (1980), have divided alginite into two morphologically distinct submaceral groups to reflect these differences. They based a classification of oil shales on these subgroupings, using the dominant alginite submaceral as the foremost classification criterion. The groups comprise alginite A, consisting of discrete elliptical, spherical or disc-shaped algal bodies (both colonial and unicellular) which form the characteristic components of the oil shales known as torbanites, tasmanites and kukersites and alginite B, a finely banded lamellar alginite (green or blue-green algae) intimately interbedded with mineral matter in well laminated deposits. More recently this nomenclature has been changed and alginite A and alginite B are now respectively referred to as telalginite and lamalginite (Hutton 1982).

Botryococcus (green algae), *Tasmanites* (green algae) and *Gloeocapsomorpha* (primitive, blue-green) are representative of telalginite, while lamalginite is derived, at least in part, from the green planktonic alga *Pediastrum* and is generally referable to *Cyanophyceae* (blue-green algae) or *Chlorophyceae* (green algae). Using their established nomenclature, Hutton et al. (1980) proposed the term lamosite for laminated oil shale in which the dominant organic matter is lamalginite. Lamosite occurs as thick seams in some Tertiary sequences in eastern Queensland and in the Green River Formation which occurs

in four sedimentary basins in the western U.S.A.. The above terminology allows six major classes of oil shales to be described using a classification based solely on organic matter type.

These are:

Cannel coal - a dull black or brownish-black oil shale containing abundant liptinite derived from terrestrial plants, such as sporinite, cutinite, resinite and liptodetrinite with smaller amounts of vitrinite and inertinite.

Torbanite - black to greenish-black oil shale synonymous with boghead coal or kerosene shale. It is a form of sapropelic coal containing telalginite derived from algae related to the extant genus *Botryococcus*.

Tasmanite - a greyish-brown to black shale with its main organic constituent, telalginite , derived from the remains of the unicellular marine alga *Tasmanites* which closely resembles the extant genus *Pachysphaera*. Despite the widespread occurence of *Tasmanites* in marine sediments only two deposits are known (Tasmania and Alaska).

Kukersite - a shale of marine origin containing telalginite from algae referable to *Gloeocapsomorpha*.

Lamosite - a compact laminated organic-rich rock characterised by the presence of lamalginite as the dominant organic constituent. Hand-specimens are normally olive-grey or brown to brownish-black.

Marinite - (formerly **Mixed oil shale** , Hutton et al. 1980), - marine rocks containing a wide variety of organic matter which may include significant amounts of any or all of the macerals telalginite, lamalginite, sporinite, cutinite and vitrinite. Samples are generally greyish-brown to dark brown.

Classification by organic petrography allows Australian oil shales to be divided into five of the genetically different categories introduced above (Figure 1-7.).

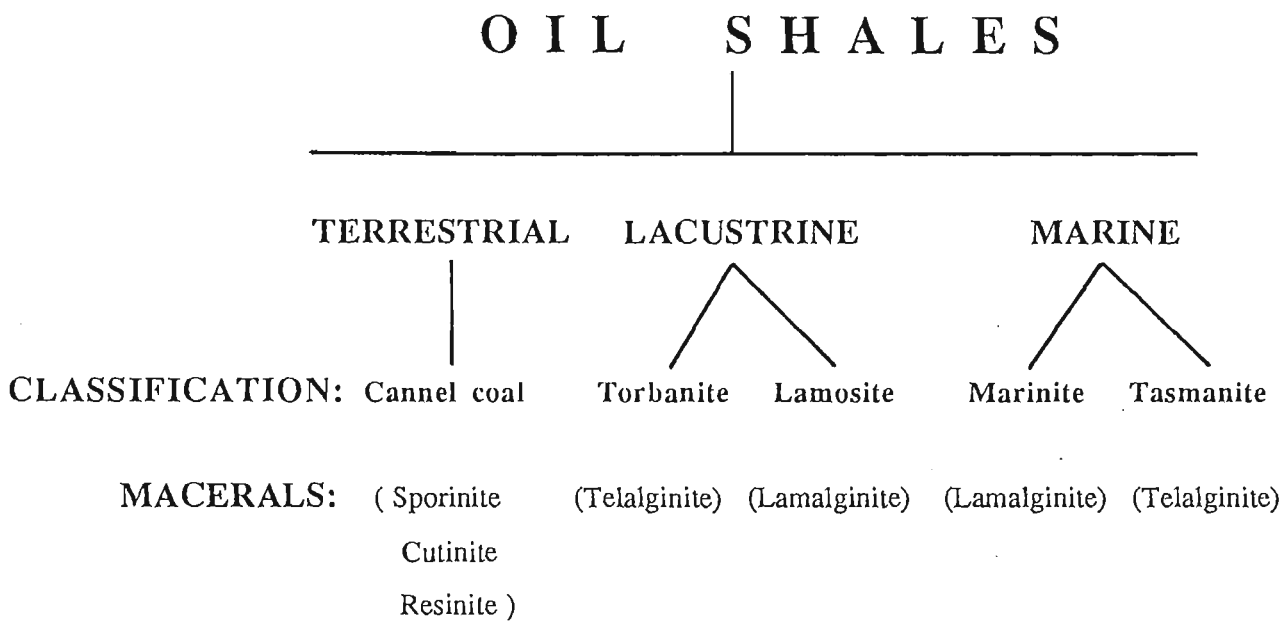

Figure 1-7.

Petrographic oil shale classifications representative of Australian deposits.

1.2 The shale oil industry.

The viability of a shale oil industry depends on the cost and quality of shale oil derived liquid fuels compared with conventional supplies or synfuels produced from coal or gas. The energy crisis of the 1970s created worldwide interest in synfuels which peaked about a decade later, but has declined since in line with sustained low crude oil prices. Research on oil shale today is particularly depressed as a direct consequence of the continuing supplier-controlled oil glut. World crude oil reserves are finite however and should a continuance of low oil prices lead to a return to earlier consumption patterns, then the next oil crisis could be much more severe than in 1974.

Lead times of more than 10 years just for the investigation, assessment and design phases preceding the construction of any large-scale shale oil facility highlight the need to continue research into all of the processes required to take oil shale out of the ground and into the marketplace. The current oil glut has made a potential industry even less competitive; but it has created an opportunity to continue fundamental research into retorting, product upgrading and waste management.

Any shale oil based synfuel industry will obviously be established first by those countries which are net importers of oil and/or have large reserves of exploitable oil shale. In meeting these criteria the U.S.A. appears to be a key player in the creation of such an industry, both for commercial as well as strategic resons. Other countries such as Australia and Japan may choose to develop the industry on a cooperative basis, applying technology and expertise from many sources to Australia's proven reserves.

1.3 Australian oil shale deposits.

Total world reserves (in-situ) of shale oil have been put conservatively at $30x10^{12}$ barrels (Yen and Chilingarian, 1976), with Australian resources making up an estimated 5% of this total. Oil shale deposits in Australia range in age from Cambrian to Tertiary and major resources are located mainly in the eastern part of the continent (Figure 1-8). Petrographic analyses have shown that liptinite is the dominant organic matter and (presumably) shale oil source (Crisp et al., 1987).

Shale oil was first produced in Australia about 100 years ago and was originally obtained from the relatively small torbanite deposits of New South Wales and the tasmanite deposits of Tasmania. Torbanite has the highest grade of all Australian oil shales because of the high percentages of liptinite normally present and probable higher specific oil yield of telalginite than other forms of liptinite. Utilization of established torbanite deposits has been sporadic and ultimately declined because of the small size of deposits, irregular seam thickness, unsuitability for mechanical mining and low production rates. The last remaining venture, the Permian deposit at Glen Davis ceased operation in 1952. Production of shale oil from tasmanite was centred on the Mersey River locality of Tasmania and ceased in 1934 after relatively small quantities had been won.

Figure 1-8.

Location of Australian oil shale deposits.

Despite a recent decline in interest in oil shales, research into their properties has continued generally and in Australia particularly for the Tertiary lamosites of coastal Queensland and the Cretaceous marinite of the Toolebuc Formation. Prospects for their development are discussed in section 1.4.

For Australian deposits much of the recent research information has been presented at one of the four workshops on oil shale held since 1983 and has been published in the proceedings covering these meetings. The workshops cover a diverse range of research interests in Australian oil shales and the proceedings include articles

dealing with the status of current Australian oil shale projects, the geology, petrology and mining of oil shales and their chemistry and characterisation. Other subjects covered include oil shale retorting , the analysis and upgrading of shale oil and environmental studies. In most published results little information is given about sample origin and the samples are often inferred to be representative of a particular deposit although, strictly speaking, no truly representative sample exists and in practice oil shale properties may vary significantly with depth and locality. While the workshops have proved an effective forum for the dissemination of progress in specific areas, particularly for major deposits with commercial potential, many of the other (minor) deposits have remained poorly characterised in terms of their geology and chemistry.

Crisp et al. (1987) have addressed some of the problems outlined above by producing a compendium of geological and chemical data for Australian oil shales. The study was carried out during 1984-1986 at the University of Wollongong (Department of Geology and Chemistry) and at the CSIRO Institute of Energy and Earth Resources (Division of Fossil Fuels). It presents petrographic, mineralogic and chemical data obtained under the same experimental conditions for specific samples from the range of Australian oil shale types presently known. General information provided includes a location map for each deposit, its geology and stratigraphy, the environment of deposition as well as a brief history and resource levels. Specific geological data includes an accurate description of the sample source and its petrographic and mineralogic properties. Chemical details of the shale include Fischer assay retort yields, elemental analysis of shale oil, kerogen content and kerogen elemental analysis. A chromatogram of the FA oil and pyrolysis-chromatogram of the raw shale are also given, with a brief description of prominent features of each profile accompanying the chromatograms. In conclusion the reader is directed to references considered important for the deposit under consideration. These references are listed in the compendium in a comprehensive bibliography covering research publications on Australian deposits over the last decade or so.

It is only by studying a large number of diverse samples under the same conditions that trends and correlations, if any, become evident. Interdisciplinary studies

such as those employed in the above project use different techniques to provide a variety of data for a particular sample. These need to be interpreted interdependently to establish a comprehensive picture of the oil shale. By doing this for a large number of sufficiently well-defined samples we can hope to establish a meaningful data base to which we can add more information as it becomes available and which allows us to compare new results with those already obtained.

1.4 Australian prospects for a shale oil industry.

To assess the need for Australia to establish a synfuel industry based on indigenous raw materials one must first look at any potential problems underlying the supply to its conventional petroleum industry. In 1985 Australia became virtually self-sufficient in oil for the first time; since then there has been a downward trend in oil prices through market manipulation by some O.P.E.C. producers, resulting in the current world-wide oil glut.

Locally this has resulted in a dramatic cut in exploration expenditure (Haselhurst,1986) which has serious long-term implications for Australian supplies. To maintain self-sufficiency Australia must find an additional 200 million barrels of reserves a year. That is double Australia's annual discovery rate over the last 15 years and coupled with the low level of exploration activity is a figure not likely to be achieved. With known oil reserves sufficient to meet consumption levels for only about 10 years we will see Bass Strait production declining to an estimated 75 % of current output by 1990 and to less than 40 % towards the end of the century.

Based on Australian oil and condensate demand and supply projections to the year 2000 (Figure 1-9), Mc Farlane (1984) concluded that Queensland's Condor oil shale deposit could provide 500,000 barrels of upgraded shale oil per day within about 18 years. Projected development costs were given at US $ 2.3 billion (mid-1983 base) with annual operating costs at full production put at US $ 265 million. Reddan et al. (1984) reported on the technical aspects of the major feasibility study of the Condor project,

carried out by Southern Pacific Petroleum (SPP)/Central Pacific Minerals (CPM) and the Japanese Australia Oil Shale Corporation (JAOSCO). Further studies are continuing under an agreement signed in July, 1984 between the venture partners and the Japan Oil Shale Engineering Corporation (JOSECO), a consortium of 36 interested Japanese companies.

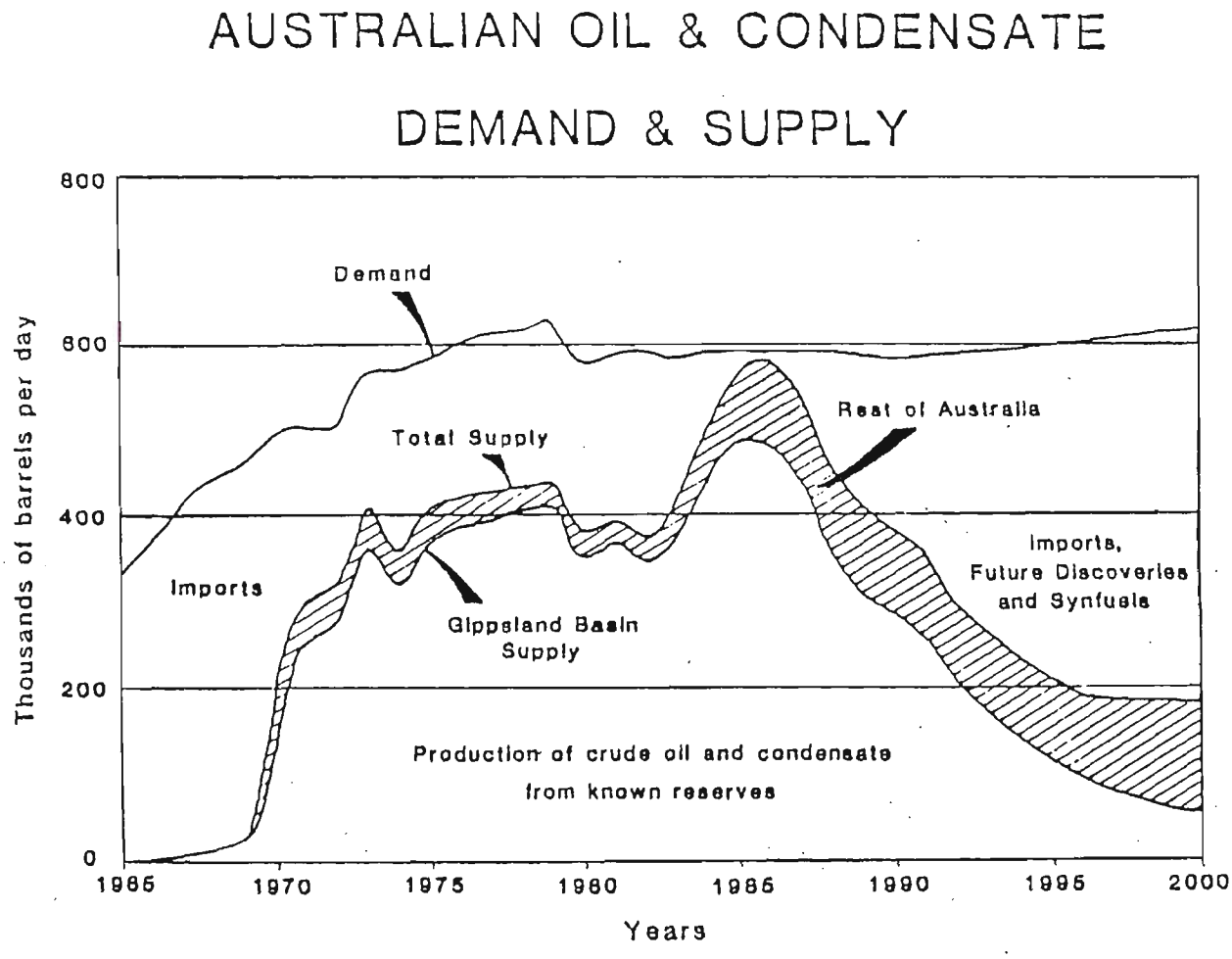

Figure 1-9.

Supply and demand graph for Australian oil and condensate requirements.

Progress in their development of new processing technology and efforts to construct a Japanese oil shale pilot plant with a 300 tonnes per day capacity is described in the paper by Uchida et al. (1986). Current Australian strategy favours a staged overall development based on smaller facilities and is focussed on the maximum utilization of known deposits

through the selective mining and upgrading of high-yield resources. The Kerosene Creek seam of the Stuart deposit meets the latter criterion and has proven reserves of 175 million tonnes of shale averaging 135 LTOM (litres per tonne at 0 % moisture) these could be high-graded by selective mining to around 70 million tonnes at 180 LTOM. Major operating cost reductions could be achieved by improved retort designs and/or higher throughputs and by reducing product-enhancement costs through selective upgrading of only part of the crude shale oil.

SPP/CPM envisage a first stage demonstration project producing 9,000 barrels per day, to be followed by a facility with a target design for 50,000 barrels per stream day. Such a facility at Stuart is estimated to cost just under US $1 billion and would produce over 300 million barrels of shale oil during its 20 year operational life-span, at a cost of approximately US $20 per barrel in terms of Middle East crude. Other deposits continue to be investigated with a view to commercial exploitation. Noon (1986), summarized oil shale exploration in Queensland during 1985-86, while Tolmie (1986), and Neale and Thompson (1986), reported on the technical status of the Julia Creek and Rundle oil shale projects respectively.

Synfuel production will not have to rely exclusively on shale oil for feedstock, since both gas and coal are abundantly available materials capable of supporting the industry. A study undertaken by BHP Petroleum concluded that the first large-scale production of synfuels will use gas as feedstock. This view is partly shared by Shell Australia who state that shale and gas have the best prospects for conversion to synfuels depending on the improvement of shale oil technologies and location of the gas fields (Curnow,1986). This assessment shows that research needs to continue into all aspects of oil shale utilization with the aim of making shale oil viable in a competitive marketplace. Areas where future savings should be realized include the mining, retorting, chemical characterisation, upgrading of raw materials and products and environmental management. Ultimately it will be commercial considerations in the Australian marketplace which determine the prospects of our shale oil; research alone will not produce a synfuel industry.

1.5 THE DUARINGA OIL SHALE DEPOSIT.

The Duaringa Tertiary oil shale deposit is one of at least 12 other Tertiary deposits located (mostly) along about 900 km of Queensland's east coast with a combined in-situ resource potential of 25 billion barrels of shale oil. Figure 1-10 shows the location of some of these deposits which collectively contain over 90% of the demonstrated resource.

1.5.1 Locality and setting.

The Duaringa deposit is part of the Tertiary sequence of the NW-SE trending Duaringa Basin, a half-graben approximately 180 km long and 20 km wide centred 110 km west of Rockhampton, Queensland (Figure 1-11 a). The sequence crops out in three topographic highs up to 100m above low-lying country. The basin sequence overlies the deformed eastern margin of the Permo-Triassic Bowen Basin and abuts the Connors Arch of pre-Permian intrusive rocks and the Gogango Overfolded Zone (an arcuate structure, composed of Permian sedimentary and volcanic rocks) along the eastern margin.

Permian sedimentary rocks of the Folded Zone are faulted against the Tertiary sedimentary rocks along the western edge of the basin (Figure 1-11 b).

1.5.2 History of the deposit.

Tertiary oil shale was discovered in the late nineteenth century during dredging of the Narrows Graben of coastal Central Queensland. In 1973, SPP/CPM commenced exploration in the area and by 1979 had delineated the Rundle deposit, a major oil shale resource with indicated in-situ reserves in excess of 2 billion barrels of shale oil. The success of this undertaking led to the search for similar deposits elsewhere, including an area of about 4000 sq. km in Central Queensland, effectively covering the Duaringa Basin. In that area, buff carbonaceous shale had been recovered from a bore in 1900 and an outcrop of oil shale was reported in 1928 in the banks of the Dawson River, near the confluence with the Don River. In 1938 oil shale was reported from a bore near Merion homestead, 115 km N- NE of Duaringa.

Deposit	Insitu Resources
CONDOR	8.14 billion barrels
DUARINGA	3.72 billion barrels
LOWMEAD	738 million barrels
NAGOORIN	2.65 billion barrels
NAGOORIN STH.	467 million barrels
RUNDLE	2.65 billion barrels
STUART	2.51 billion barrels
YAAMBA	2.82 billion barrels
Total	23.7 billion barrels

Figure 1-10.

Location and reserves of some of Queensland's major Tertiary oil shale deposits.

The first drilling was carried out by the Queensland Department of Mines who drilled three holes near Duaringa in 1942. SPP/CPM commenced drilling in 1978 and to date 66 holes, recovering 8856 m of core have been completed. The Geological Survey of Queensland (GSQ) drilled two stratigraphic holes to depths of 1224 m (GSQ Duaringa 3-5R) and 1303 m (GSQ Duaringa 1-2R) during 1979-80. During this drilling programme a lower oil shale unit separated from the known resource seams by a thick claystone interval, was discovered.

1.5.3 Geology of the deposit.

A drilling programme by SPP/CPM during 1978-79 delineated two thin but laterally extensive oil shale seams in the upper 100 m of the Tertiary sequence. These seams constitute the accessible resources and comprise an upper 8 m thick seam (unit D), separated from the lower 25 m thick seam (unit B) by 20-25 m of mudstone. Because the Duaringa tablelands have a deep soil and weathering profile ranging from 40-60 m, much of the upper seam as well as some of the lower seam has been affected where topographic relief is not very pronounced (Figure 1-11 c).

Two stratigraphic holes subsequently drilled by GSQ in the Central and Southern areas penetrated more than 1200 m of sedimentary rocks, most of it bioturbated silty and sandy oxidised claystone, and intersected a lower oil shale unit below about 600 m. The geology of the deposit has been briefly described by Ivanac (1983) and Lindner (1983), as well as in unpublished company reports (Green et al. cited in Hutton (1986).

Hutton (1986), in a comprehensive geological study of the deposit, described the Duaringa resource as a bipartite oil shale deposit comprising three distinct lithological units. The stratigraphically younger unit consists of dominantly grey to olive-green lamosites and claystone,with rare coaly intervals. The middle claystone interval contains negligible organic matter and overlays a lower unit of interbedded brown to dark greyish-brown lamosites, brown coal, carbonaceous shale and claystone (Figure 1-11 d.).

The oil shales from the two units have different physical and petrographic properties and are termed lamosites as defined by Hutton et al. (1980) because they contain abundant lamellar alginite derived from planktonic algae. The two lamosite dominated units

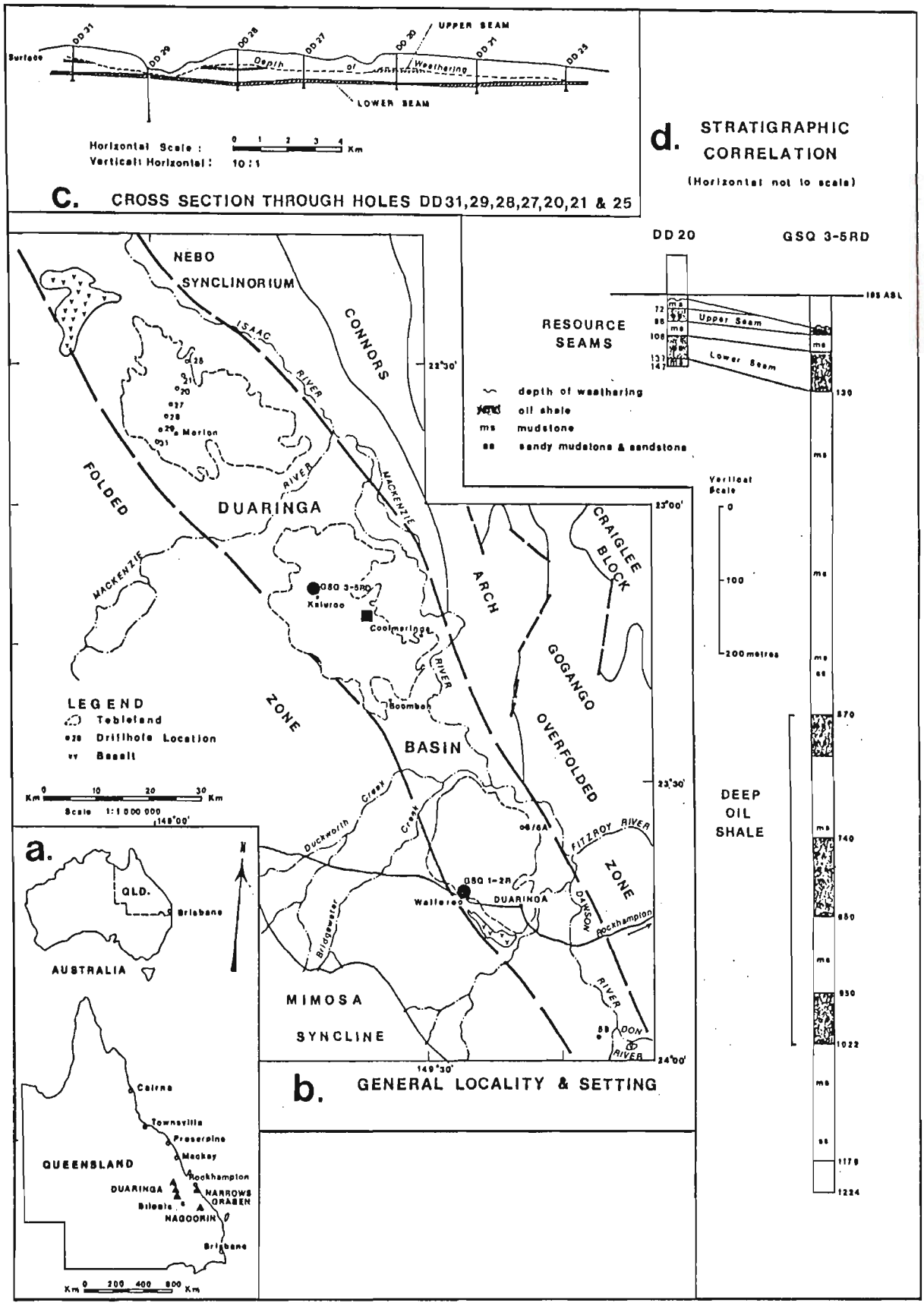

Figure 1-11a. - d.

Location map of the Duaringa oil shale deposit (**a.** and **b.**). Cross sectional profile of the northern plateau and stratigraphic sequence of GSQ 3-5RD are given in **c.**and **d.** respectively. (from Dixon and Pope, 1986).

may be categorised on the basis of data related to global properties such as hand-specimen colours, lamalginite fluorescence and abundance, humic matter content, precursor algae and reflectance of vitrinite macerals. Comparisons of these data distinquish the upper "Duaringa-type" lamosite from the lamosites of the lower oil shale unit which contain microflora similar to that of the Rundle-Stuart resource and (generally) possess many features in common with that deposit.

Based on these similarities Hutton concludes that the lower oil shale unit appears to be an equivalent of the Rundle-Stuart oil shale sequence, with minor differences between lamosites from the two localities probably related to local variations in conditions at the time of deposition.

1.5.4 Organic petrology.

Hutton (1981) has studied 60 core samples of oil shale, claystone and coaly material from GSQ Duaringa 1-2R for analysis of included matter and determination of reflectance. Samples were chosen so that data could be obtained for the entire Tertiary sequence of the Duaringa region. Results show that lamosites from the upper and lower oil shale units have markedly different hand-specimen and petrographic properties.

Lamosite from the upper unit is typically olive to olive-grey and contains abundant grey to greenish-yellow fluorescing lamalginite, much of which is derived from the algae *Pediastrum* and the dinoflagellate *Septodinium* as well as telalginite derived from *Botryococcus*. Samples contain up to 35% lamalginite and up to 25 % telalginite (although mostly less than 5 %). In many hand-specimen samples *Botryococcus* occurs as white, ovoid spots up to 1 mm diameter. An above-average abundance of *Botryococcus* accounts for the high shale oil yields obtained from stratigraphically equivalent intervals in several drill holes.

Lamosite from the lower unit is typically brown to dark greyish-brown and contains orange to yellowish-orange fluorescing lamalginite, most of which is derived from *Pediastrum,* with *Cleistosphaeridium* a precursor for a small proportion. Telalginite is derived from *Botryococcus* and samples contain up to 45 % lamalginite but less than 2 %

telalginite. Carbonaceous oil shale, termed carbonaceous lamosite, also occurs and is of two forms. The first comprises interlaminated (generally microlaminated) coal and lamosite whereas the second form is dominantly a lamosite with greater than 5 %, ubiquitous vitrodetrinite. Both forms are dark greyish-brown to black.

Brown coal contains vitrinite (composed of ulminite, corpohuminite, and minor resinite) and clarite (comprising ulminite, corpohuminite, attrinite, resinite, sporinite and cutinite). Thus the lamosite, carbonaceous lamosite and brown coal of the lower unit contain macerals with the same optical properties as corresponding macerals in lamosite from the Rundle-Stuart deposit.

Differences between the properties of macerals in the lamosites from the upper and lower units suggest that the environments of deposition in which the two were formed were not the same.

1.5.5 Environment of deposition.

Although any interpretation of the environment of deposition of an oil shale is dependent on a sound knowledge of the mineralogy, sedimentary structures and fossils (both macro- and micro-fossils) present in the oil shale, identification of the microfloral components permits some generalizations to be made. *Pediastrum* is the dominant alga in the Duaringa deposit. It is a blooming colonial green alga which swarms during the day under laboratory conditions. At least three well preserved types have been recognized in the lamosites and there are possibly further species. *Pediastrum* has been identified in other Australian Tertiary sediments as well as in those of other countries. In several of these occurrences the algae were associated with *Botryococcus* in sediments believed to be of freshwater lacustrine origin.

Pediastrum together with *Botryococcus* was found in Cainozoic sediment of Lake George, New South Wales and its occurrence, based on the alga's salinity tolerance, was believed to be an indicator of water depths of at least 7 m for long periods. *Botryococcus* was thought to indicate open water and a water depth of at least 7 m is therefore not unreasonable for the ancestral Lake Duaringa. The large area covered by the Tertiary lake provided water conditions ideal for growth and conducive to divergent

evolution of the *Pediastrum* genus. Large inputs of clastic sediment produced relatively low-grade lamosites. Stratigraphic variations in organic matter from GSQ Duaringa 1-2R allow five stages of sedimentation to be recognized in the deposit.

a). During the formation of the lower lamosite unit cyclic sedimentation of lamosite, carbonaceous lamosite and claystone predominated. The lake was shallow (possibly less than 10 m) and subject to periodic flooding. During flooding abundant sediment was deposited by streams which drained the undulating hills flanking the lake. Nutrient supply increased significantly and planktonic algae flourished. During sporadic dry periods marginal zones were characterised by low lying areas with algal-inhabited shallow pools. Carbonaceous layers of the lower oil shale unit probably represent both allochthonous plant matter carried into the lake by floods (represented by thin coaly layers interbedded with lamosite) with the thicker coaly layers representing limited encroachment of marginal swamps along waterways. Periods of flooding were probably infrequent. Partial degradation of plant matter would increase the nutrient supply and promote algal growth. Interbedded coal-carbonaceous shale and lamosite probably indicate fluctuating conditions. Anoxic conditions below or near the sediment-water interface, associated with the rapid accumulation of algal matter, probably promoted the accumulation and preservation of algal matter.

b). During the second stage, abundant clay-sized clastic detritus entered the lake. This stage is now represented by the thick sequence of claystone separating the upper and lower oil shale units. Conditions were evidently unsuitable for the vigorous growth of algae when this interval was deposited.

c). During the third stage the lower lamosite seam of the upper unit was deposited. Water depths and salinity parameters were probably similar to those prevailing when the lower oil shale unit was deposited. Algal bodies would have sunk to the bottom of the lake and mixed with incoming fine-grained mineral matter. Rapid burial inhibited bacterial degradation and much of the algal matter was preserved with little alteration.

Pyrite is much less abundant in the Duaringa deposit than elsewhere but reducing conditions probably still prevailed. Very little humic matter entered the basin at this time. Minor incursions of clastic sedimentation are indicated by claystone layers.

d). Algae were unable to survive during the fourth stage of deposition cycles which formed the claystone interval separating the upper resource seams. The rapid input of clastic sediment and consequently muddy waters, presumably inhibited algal growth.

e). The fifth stage is represented by the upper lamosite seam; conditions prevailing during formation would have been similar to those in force during stage three .

The discovery of the deeper oil shale unit is significant in that it illustrates that two alginite-bearing oil shales, with different petrographic properties, can form in the one basin given suitable conditions.

1.5.6 Resource potential and development status.

Implications from recent project studies on the Duaringa deposit were reported by Moore et al. (1986) and are summarized below.

Shale oil yields for the upper and lower resource seams are cited at 46-66 LTOM and 63-92 LTOM respectively. Using a cutoff grade of 50 LTOM and a minimum mining thickness of 4 m this equates to an average grade of 82 LTOM and combined in-ground reserves of 3.72 billion barrels of shale oil. Although the lower oil shale unit also contains significant reserves, its potential has not been assessed. During 1985 SPP/CPM conducted a prefeasibility study to examine the technical and economic viability of a project designed to produce 20,000 barrels of syncrude per day. To meet this target production requires the retorting of 66,000 tonnes of oil shale per stream day with total utilization of more than 500 million tonnes over a 30 year period; any of the three outcrops of the Duaringa deposit could satisfy this rate of shale production. Oil shale grade and depth of burial are important economic criteria in assessing the development prospects of any resource. There are obvious cost benefits in selecting the richest shale grades for retorting, while minimizing the amount of overburden to be removed will reduce overall mining costs. The Duaringa

Central plateau best meets both shale grade and strip ratio requirements and contains over 4 billion tonnes of oil shale with grades greater than 50 LTOM. A northern-edge section of this plateau could supply the tonnage required for the 30 year project life-span. It contains oil shale at a grade of 70 LTOM and has a volumetric overburden ratio of 2.7:1. In-situ moisture is very high at approximately 30 % of the shale mass as mined.

Compared to other resources Duaringa suffers the following disadvantages:

a. - shale is medium grade

b. - in-situ moisture is very high

c. - the deposit is remote from existing infrastructure.

The impact of the above factors on the overall energy balance results in the requirement of 2,000 tonnes of coal per stream day, mainly for pre-drying of retort feed. This represents a substantial cost penalty.

Based on the above considerations the prefeasibility study concludes that "development of the Duaringa deposit in the near term would not be commercially viable. However, on the basis that the real price of oil will return to 1985 levels by 1990 and then progressively increase through the end of the century, the project could show an adequate return on investment if constructed in the late 1990s". Prior to any resource development, the deposit needs to be fully characterised. This characterisation involves many areas of research and needs to include a detailed chemical analysis of retort products, in particular shale oil, since it represents the feed-stock for any marketable products. The chemical characterisation of Duaringa shale oil is one of the main objectives of the present study .

CHAPTER TWO : CHEMICAL CHARACTERISATION OF OIL SHALE AND SHALE OIL.

2.1 INTRODUCTION.

Information about oil shales can be obtained using various physical and chemical methods. These include extraction procedures, elemental analysis (EA), spectroscopy (e.g. IR, UV), thermogravimetric analysis (TGA) etc. Robinson (1969), has reviewed the main techniques of constitutional analysis for kerogen of the Green River Formation. More recently researchers at the Institut Francais du Petrole investigated various coherent stratigraphic sequences of organic matter and have published a complete review of the principal analytical techniques and their contribution to the understanding of kerogen structure (Durand and Monin, 1980; Durand-Souron, 1980; Rouxhet et al., 1980; Oberlin et al., 1980; Marchand et al., 1980; Vandenbroucke, 1980). Varied analytical procedures are collectively very important especially when, as in the above case, they are carried out on the same sample at one research facility. This allows data from one approach to be correlated with results obtained using complementary methods and ultimately provides a comprehensive picture for the composition and properties of the material under investigation.

The organic phases of interest in oil shales comprise shale extracts (bitumen), pyrolysis products (shale oil, gases) and kerogen, and exhibit an increase in structural complexity in the order listed. Bitumen usually makes up no more than a few percent of total organic content, but is readily extracted and may then be analysed (directly) using conventional methods. Shale oil, though substantially more complex than the corresponding bitumen is analysed using similar techniques and provides additional information about organic source material, while its detailed composition has obvious commercial implications (e.g. synfuel feedstock). Kerogen, a tough insoluble geopolymer is less accessible to direct analysis and requires specialized indirect techniques for

characterisation. Many chemical procedures, including those listed above, are global characterisation methods which provide only limited structural information about the heterogeneous materials under investigation. More specific data on constituents can only be obtained from these techniques in conjunction with prefractionation and isolation procedures or by using more sophisticated approaches such as gas chromatography (GC), liquid chromatography (LC), mass spectrometry (MS), nuclear magnetic resonance (NMR), etc. or a combination of some or all of these techniques (e.g. pyrolysis-GC, GC-MS). Although there are no direct chemical methods providing detailed structural information for solids at the molecular level, both IR spectroscopy and solid-state ^{13}C NMR (Cross Polarization, Magic Angle Spinning (CP/MAS) ^{13}C NMR) of the raw oil shale reveal certain structural features of its kerogen.

In general IR spectra of oil shales are similar to those for other carbonaceous solids such as humic substances and coals. They are characterised by several broad bands attributed variously to aliphatic, aromatic etc. structures, as well as to functional groups (e.g. hydroxyl, carboxyl, carbonyl). This information provides a semi-quantitative functional analysis of the complex solid and makes IR spectroscopy suitable for monitoring global changes coinciding with progressive evolution due to natural or artificially induced processes (Rouxhet et al., 1980). Fourier transform infrared spectroscopy (FTIR) has some advantages over dispersive IR including a high signal to noise ratio, high speed of operation and data handling capability. However, sample preparation for FTIR remains a difficult and time-consuming step in the overall analytical procedure. Krishnan et al. (1981) have avoided the sample preparation step by directly studying a variety of solid samples, including coal, using photoacoustic FTIR.

CP/MAS ^{13}C NMR allows an evaluation of the aliphatic/aromatic carbon in kerogen. Miknis et al. (1982) used the technique to evaluate the genetic potential of oil shales but noted limitations to the interpretation of NMR, due to the complexity of kerogen. Kalman and Saxby (1983) used it to study thermal alterations in Rundle oil shales caused by a small diabase sill intrusion in the deposit while Miknis et al. (1984) adopted the technique to study a range of oil shales from Queensland, Australia. Hagaman et al.

(1984) have reported that relative aliphatic resonance areas obtained for oil shales correlate linearly with oil yields thereby obviating the need to determine mass percent organic carbon for each specimen. Evans et al. (1986) have examined raw shale as KBr-shale discs (IR) and in the form of powders (CP/MAS ^{13}C NMR) to assess the aliphatic content of Australian oil shales. They used these data in conjunction with total organic carbon values to predict Fischer Assay oil yields.

Both oil shales and kerogens are best studied at the molecular level by analysis of their degradation products. When these products are generated naturally they are dependent on the burial history of the deposit and reveal information about the source, evolution and maturation of the kerogen. In the laboratory they are produced by chemical or thermal means. Natural degradation products are generated at lower temperatures and in conditions devoid of additional reactants. This ensures better preservation of structural information than is the case for laboratory simulation; however many natural products are less easily recovered under geological conditions than those generated by artificial degradation in a controlled environment. This applies particularly to the collection of gases, volatile hydrocarbons and water, all of which may disperse or migrate away from the region of their natural formation.

The various techniques used for the study on Australian oil shales are outlined below and often represent procedures available to us either directly, or after modifying existing equipment. The range of application is necessarily restricted by a desire to work with raw shale wherever possible, but this direct approach avoids the tedious and time-consuming step of kerogen isolation and the sample changes this procedure may produce. Most approaches are described in a cursory manner except in those cases where the technique is used extensively in subsequent sections. Even then the information is not in the form of a review, but is restricted to references most relevant to the specific context in which the method is used.

2.2 Solvent extracts.

Solvent extraction of the finely-crushed rock is a logical first step in the analysis

sequence for any oil shale. It liberates the bitumen fraction for subsequent study and prepares the oil shale for later demineralization and kerogen isolation. It is reasonable to expect different oil shales to yield different solvent extracts, however (quantitative) variability should also be anticipated for different samples from the same deposit, especially where these are taken from different levels of a highly-evolved stratigraphic sequence. Extractions should be carried out immediately after grinding of the shale, using solvents having little or no solvolysis effect. Most methods use ultrasonic agitation at room temperature, or Soxhlet extraction at the boiling point of the solvent (Robinson, 1969). Various solvents such as benzene (Anders et al., 1973), benzene/methanol (Burlingame et al., 1968), chloroform/methanol (Brown et al., 1980), dichloromethane (Wakeham et al., 1980) etc. have been used. Extraction yields generally increase with extraction temperature as well as solvent polarity and reactivity. Vitorovic and Pfendt (1967), have reported a hundred-fold increase in extractables from Aleksinac oil shale for aniline (~53%) over petroleum ether (~0.5%). The high extraction yield was associated with oxidation and chemical alteration, contrary to what is desired (the objective is to liberate only free components as opposed to fixed products, which are considered part of the kerogen polymer). Other reactions such as esterification of acid groups by methanol or ethanol may also occur, particularly when clay minerals are present to catalyze them (Arpino and Ourisson, 1971).

Treibs (1936) identified porphyrins in crude oils and proposed that they originated from the chlorophyll of plants. Since this pioneering work numerous types of hydrocarbons, or related structures, have been traced from living organisms through Recent sediments into ancient sediments and crude oils (Eglinton and Calvin, 1967; Maxwell et al., 1971; Blumer, 1973). These biomarkers (paraffins, terpanes, steranes etc.) resist chemical change and are preserved over geological times to be found in the extracts of almost all sediments, regardless of depth or age (Gallegos, 1976). They stem either directly from living organisms without chemical alteration, or indirectly with only minor changes. Most changes occur early during diagenesis of the young sediment and, depending on the molecules involved, may include loss of functional groups, stabilisation

by hydrogenation, aromatization etc.. The resultant molecules retain structures indicative of their biogenic origin and persist in a free state, or may be trapped in the kerogen network, or bound to it by chemical bonds. In the latter circumstances they are released from kerogen with an increase in depth and temperature. In this context certain biomarkers (e.g. alkanes) are less diagnostic for mature oil shales since highly evolved kerogens generate these hydrocarbons as part of any oil and gas production.

Once formed, biomarkers are not only stable over long periods of time in their geological environment but remain intact during extraction and analysis. Since they are also the easiest to isolate, they have been subjected to intensive investigation by an increasingly large number of researchers. They are important from the viewpoint of molecular origin since this provides information on kerogen source material and biological environment.

2.3 Elemental analysis (C, H, N, O, S).

Elemental analysis of kerogen is one of many approaches for characterising the origin and evolution of oil shales and establishes a broad framework within which other analytical methods can be used more effectively (Durand and Monin, 1980). However it is not very precise and lacks the ability to resolve globally similar materials disparate at the molecular level; consequently not too much should be expected from it alone and it needs to be used in conjunction with other relevant analytical techniques.

The elemental analysis of any kerogen is complicated by the need to isolate it from its mineral matrix. Ideally this is achieved by dissolution of the mineral phase while retaining chemically unaltered kerogen. In practice the methods most widely used are based on acid treatment of the finely-ground shale. Initially HCl is used to remove the bulk of the minerals (e.g. carbonates, oxides, sulphates etc.) and is followed by addition of HF to facilitate the removal of silicates. Several reviews have been published dealing with procedures for kerogen isolation and confirm that the isolated organic material (generally) represents chemically altered kerogen, particularly in the case of immature sediments (Robinson, 1969; Saxby, 1970, 1976).

Specific changes are sample-dependent but include:

1). -loss of organic matter

2). -decreases in the nitrogen content of residual kerogen

3). -increases in kerogen solubility

4). -interaction of the demineralizing agents with organic functional groups.

To minimize potential chemical alterations, acid treatment should be performed under mild conditions in a nitrogen atmosphere. A complete operating procedure, incoprporating these requirements in a patented apparatus, has been reported by Durand and Nicaise (1980). Acid treatment of oil shales invariably leaves residual minerals, most commonly pyrite, although heavy oxides, sulphates and silicates are also found. Complex fluorides may be formed during HF attack, while other indigenous minerals may survive, protected from the acids by a preservative coating of organic material which deactivates the encapsulated mineral grain. Pyrite removal constitutes a major problem, especially where it is associated with organic matter in framboidal form. Its abundance needs to be reduced before meaningful elemental sulphur values can be obtained for the kerogen. Various oxidative and reductive methods have been evaluated, with HNO_3 and $LiAlH_4$ reported as the most effective reagents (Saxby, 1970).

Elemental analyses are carried out on dried kerogen (1 hour at 105^0 C under nitrogen) and must be reported on a mineral-free basis, with corrections made for residual FeS_2, oxides, silicates and fluorides. To do this the true mineral content of the kerogen is determined from the ash yield and the corrected mineral-free elemental composition then calculated. H/C values give a first indication of the aromatic nature of the kerogen, while H/C and O/C atomic ratios may be plotted on a van Krevelen diagram to establish the kerogen type (cf. section 1.17). However, since elemental analysis does not differentiate between mixtures of different types of kerogen, any definitive typing should only be made in conjunction with supportive data obtained using other relevant techniques.

Elemental analysis of shale oil does not involve a prior isolation step, however the viscous oil is difficult to sample quantitatively, with at least some components lost during handling prior to analysis. Retort oil is wet when produced and contains dispersed or

dissolved water. The presence of water obviously modifies both H and O content and it needs to be removed prior to analysis. Drying agents such as magnesium sulphate are commonly used for this purpose and may involve further losses of components. To minimize oxidation of reactive components shale oil should be analysed as soon as possible after it is produced; where this is not possible it needs to be stored under nitrogen.

2.4 THERMAL DEGRADATION STUDIES ON OIL SHALES.

2.4.1 Fischer Assay.

The standard procedure for the laboratory evaluation of the oil generating capacity of oil shales is the modified Fischer Assay (MFA), described by Stanfield and Frost (1949).

A 100g charge of air-dried, crushed raw shale is loaded in 5 layers around a central vent tube in an aluminium retort. The layers are separated by perforated aluminium disks, which serve as vehicles for heat transfer. The retort is heated by a gas burner to 500° C at an approximate rate of 10°C min^{-1} and is held at that temperature until no further product formation is observed. Pyrolysis products (oil, gas, water) pass through a stainless steel transfer tube connected to a glass adaptor with a teflon plug. Condensable material is recovered in a 100 mL graduated centrifuge tube immersed in an ice bath (Fiure 2-1). The transfer tube is gently warmed to assist oil drainage and to ensure maximum product recovery. The collecting tube is then centrifuged to separate the water and oil phases; warming again facilitates this process. The entire procedure takes about an hour and the collected oil yield is generally reported as litres of oil $tonne^{-1}$ of shale at 0 % moisture (LTOM).

Although the assay is not a precise basic analysis and gives oil yields often lower than those obtained from modern commercial retorts, it continues to be used as the basis for the quantitative evaluation of their design and performance characteristics.

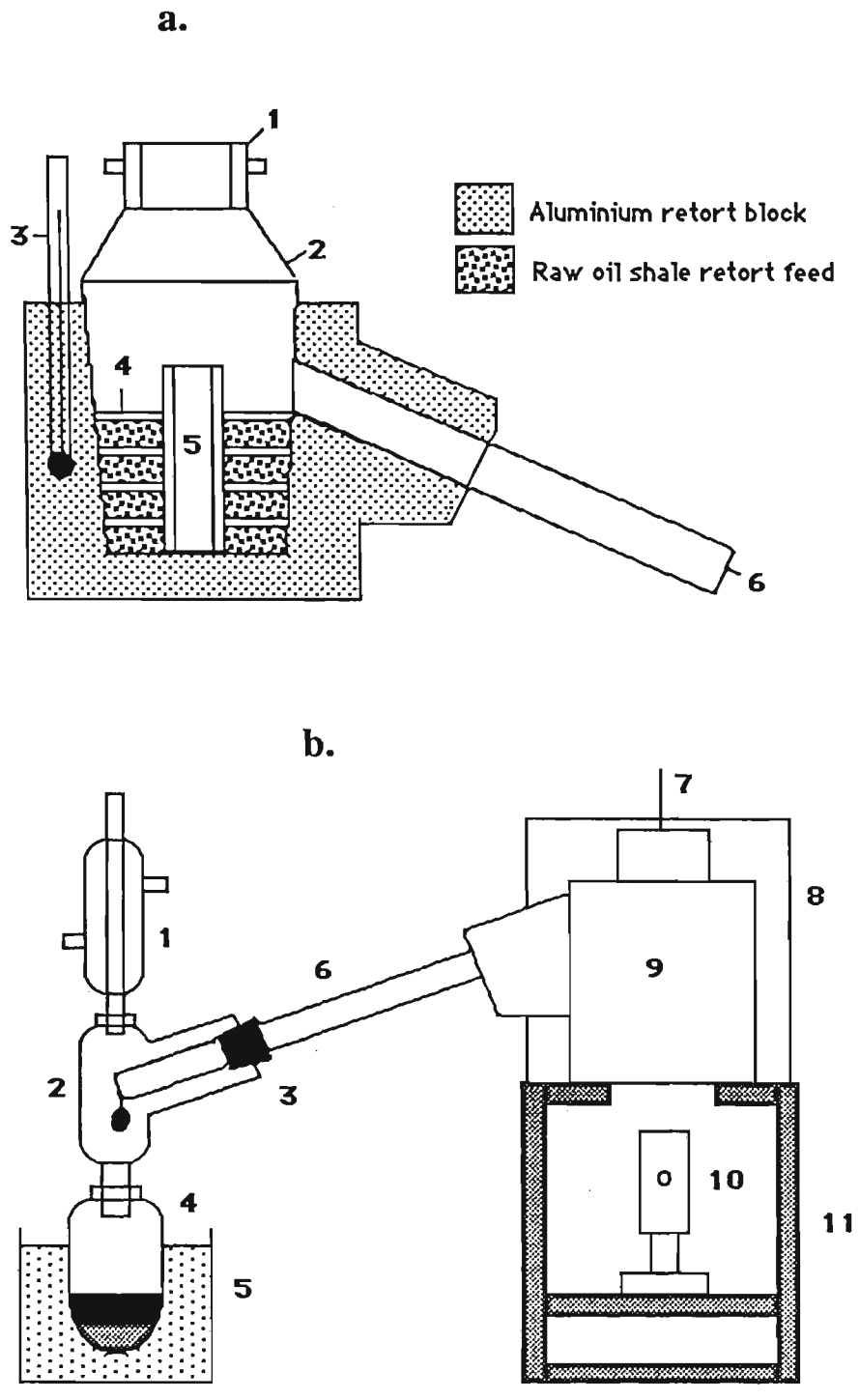

Figure 2-1.

Schematic diagram of Fischer Assay retort (a.) and retort assembly (b.). The retort is made up of: 1, lid; 2, retort housing; 3, thermometer; 4, perforated aluminium spacer discs; 5, perforated vent tube; 6, stainless steel transfer tube. The assembly comprises: 1, water cooled condenser; 2, glass adaptor; 3, teflon plug; 4, glass collecting tube; 5, ice bath; 6, s.s.transfer tube; 7, thermometer; 8, safety housing; 9, retort; 10, gas burner; 11, stand.

Fischer Assay oil may be used for the characterisation of the oil shale from which it is produced, but its composition is, at least partly, influenced by retort parameters such as:

1). -changes in raw shale particle size, packing density and retort atmosphere.

2). -variations in heating rates and final temperature.

3). -catalytic effects of the mineral matrix.

4). -homogeneity of the raw shale.

5). -residence time of pyrolysis products in the retort.

Some of these problems arise as a consequence of inherent design flaws in the Fischer retort, while others relate to the poor control exercised over the retorting process. The latter may be overcome by well-designed retorts monitored by, and operating under the control of, modern electronic devices.

2.4.2 Commercial retorts (shale oil production).

Shale oil is produced commercially using above-ground retorts, although subsurface in-situ retorting processes have also been investigated (Marcovich, 1983; Paine, 1983). The latter may offer an attractive alternative to conventional surface mining processes for shallow, thin oil shale deposits where high stripping ratios would otherwise preclude exploitation of the deposit.

Comprehensive literature on oil shale retorting technology is presented in the relevant sections of the proceedings of the three Australian workshops on oil shale held since 1983. The economic viability of oil shale production was discussed earlier (cf. sections 1.2 & 1.4); today the only commercial retorts continuing to operate are located in the U.S.S.R and China, with Brazil's embryonic industry ready to move into the semi -commercial phase (Prien, 1976).

Retorts may be grouped broadly into three categories according to the principle of heat transfer during the process of oil production. These categories include designs where the crushed shale is heated directly, by internal combustion gases produced in the retort, or indirectly by externally heated gases or solids. The latter design utilizes solids (e.g. hot

spent shale or heated ceramic balls) to achieve heat tansfer and oil recovery through contact mixing. Detailed descriptions of the various commercial retorts and their principles of operation are presented in the Oil Shale Data Book (1979). The most relevant current development is the proposed 300t day^{-1} pilot plant commissioned by JOSECO in 1981. This facility is based on a shaft-type retort which was chosen ahead of both fixed-bed and cross-flow designs following the evaluation of all three in bench-scale retorts of 3t day^{-1} capacity (Uchida and Yabushita, 1986). Directly heated retorts have high thermal efficiencies but produce low-BTU gas and achieve relatively poor oil recoveries (80-90 % of MFA yields). Indirectly heated designs produce better oil yields (up to 100 % of MFA) but exhibit lower thermal efficiencies.

All systems require large amounts of external energy and are capable of releasing at best only about 70 % of the total organic matter contained in oil shales. Mining, transport and crushing of the shale are major costs incurred in the overall shale oil production process. Retorted shale undergoes a volume increase of about 10 %, and the relocation of large amounts of spent shale presents a major disposal problem. In-situ retorting, although still in its infancy, offers potential answer to at least some of these problems since it does not involve the production and subsequent disposal of the oil shale. These benefits should realize major cost savings, however there are other problems associated with the process (e.g. the need for explosive fracturing of the rock to improve permeability; possible ground-water leaching of retort products etc.) and it needs to be fully evaluated before it is put into practice.

2.4.3 Thermogravimetric analysis.

Thermogravimetric analysis (TGA) and differential thermal analysis (DTA) are two fast techniques which respectively record weight-loss data (thermogram) and the speed, size, reversibility and temperature at which exothermic and/or endothermic reactions take place in the sample as it is subjected to increasing temperature. The two techniques are complementary and usually combined in the one instrument. This allows results obtained simultaneously on the one sample to be perfectly comparable.

Various factors, common to most thermal techniques, influence the degradation behaviour of samples analysed using TGA and DTA. These include equipment design, sample size and homogeneity, heating rates and pyrolysis atmosphere. Equipment variables are of concern primarily when relating data obtained by different laboratories. They are virtually eliminated when samples are analysed at only one facility using the same equipment under identical conditions. Sample size affects both the heat transfer into and out of the sample and the diffusion of products formed during heating. Diffusion of products from large samples may take long enough to allow secondary reactions to occur. These in turn may increase or decrease the loss of mass at a particular temperature. The overall influence of size variation is sample dependent and, if required, needs to be determined experimentally. Oil shale is a heterogeneous mixture of organic material disseminated through a mineral matrix. To ensure good sample representation and reproducibility, any specimen to be analysed must be ground to a fine powder and sieved to produce a uniform mixture of consistent particle size.

Samples may be heated in reactive (air, oxygen, hydrogen) or inert (nitrogen, helium) atmospheres to observe the effects of possible oxidation/reduction processes on the pyrograms and DTA curves. Although TGA may provide some global information about the kerogen structure (type) of oil shales, its main use has been to follow the evolution of kerogen within stratigraphic sequences and to simulate natural maturation of kerogen in the laboratory (Figure 2-2). In this regard shallow (immature) samples of the three types of kerogen have been artificially transformed using TGA and then compared to naturally transformed samples from greater depths of the same formation (Durand-Souron, 1980). When combined with anciliary procedures for characterising the products and residues from this pyrolysis, TGA provides valuable information on the kerogen structural type. The various techniques suitable in this context include many of those described in this chapter dealing, more generally, with the analysis of volatile products and solid residues.

Durand-Souron (1980) has reported the comprehensive analysis of volatile and residual matter obtained from the artificial maturation of kerogens by TGA and associated

techniques. Results obtained for several hundreds of kerogen samples from various origins were able to demonstrate TGA as a valid procedure for the simulation of kerogen maturation in the laboratory. This was established by comparing the simulation data with those obtained for naturally matured samples of the same kerogen. These detailed and comprehensive analyses delineated broad temperature regions within the TGA pyrolysis range that are associated with specific changes occuring in the kerogen structure.

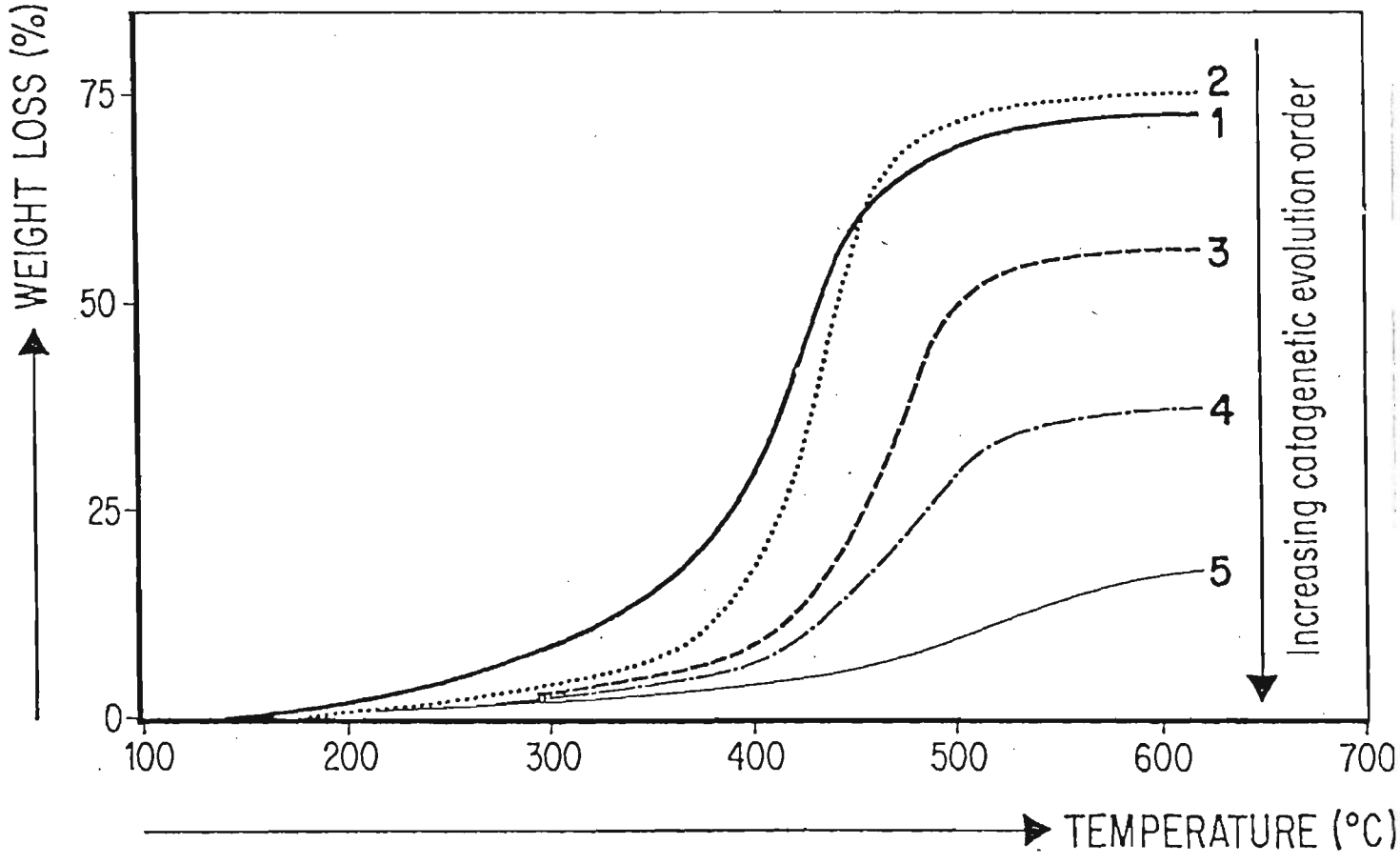

Figure 2-2.

TGA pyrograms for type II kerogens showing the effects of increasing maturation (from Durand-Souron, 1980).

For type II kerogen heated in non-oxidising atmospheres these are:

1). - a first stage up to ~350°C characterised by a (generally) small mass loss and associated with a decrease in oxygen content. This is indicated by a progressive disappearance of oxygen functionality in respective IR bands of the residue, most prominently C=O, and the release of water, carbon dioxide as well as small quantities of SO_2 and H_2S near the end of the temperature range. The observed data, including elemental analysis, correlate this artificial heating stage with subsurface late diagenesis equivalent to a burial depth of 1000-1500m.

2). - a second stage from ~350-500°C which involves a major mass loss and corresponds to the region of maximum oil formation. A decrease in hydrogen content (disappearance of IR band for C-H) for residual kerogen substantiates hydrocarbon production (mainly aliphatics) during this phase. Acids, esters and ketones are progressively eliminated and the overall effects of heating can be equated with natural catagenesis.

3). - a third stage from ~500-600°C which corresponds primarily to a structural reorganisation of the residual kerogen towards a thermodynamically more stable form (stacking of aromatic sheets to form aggregates or clusters) and does not involve any great mass loss. Observed transformations correlate with deeply buried, highly-evolved samples and this interval corresponds to natural metagenesis.

Absolute mass losses occuring within the first two of the above temperature regions characterise the kerogen as rich in oxygen or hydrogen, while relative mass losses serve to classify it according to its degree of evolution and its potential to generate hydrocarbons. Artificial evolution of type I and type III kerogens are comparable to those of type II, with quantitative variations reflecting compositional differences. Total amount of products generated, as measured by TGA mass loss, are highest for type I kerogen and least for type III. Consistent with the compositional criteria used for their typing, the proportion of hydrocarbons in these products is higher for types I and II and lower for type III kerogens.

Levy and Stuart (1983) have used TGA and derivative thermogravimetry (DTG) to

investigate several oil shale and kerogen samples from Australian deposits. They were able to correlate evolved gas analysis, and changes in infrared results observed during pyrolysis and oxidation of the kerogens, with their thermoanalytical data. Later the same authors extended their approach to include differential scanning calorimetry (DSC) in their investigations and used results from TGA in air and nitrogen for comparative studies of selected Australian oil shales (Levy and Stuart, 1984).

2.4.4 Isothermal pyrolysis.

Apart from the more common thermal techniques described above, there are many other pyrolysis procedures which provide fundamental information for oil shale studies. One technique, described by Wall and Dung (1984) is able to simulate various retort configurations and operating conditions and is suitable for studying pyrolysis kinetics of oil shales based on very accurate compositional data, which the method provides. Dried raw shale (~200mg) is heated rapidly (2000°C min^{-1}) to the selected temperature and is then held there (± 1°C) for the required period of time (usually 1000 s). Individual products (oil, gas, water) generated under these, essentially isothermal, conditions are quantitatively collected within the chilled quartz tube enclosing the sample holder. These products are subsequently analysed, with a mass balance better than 99 % routinely achieved for the entire procedure. Compositional data obtained at various discrete pyrolysis temperatures allows fractional conversions to be determined relative to product yields at 600°C. Finally, an oil yield equation is derived covering production over the entire range of temperatures investigated (~400-600°C). Apart from the kinetic data it produces, the technique is a very accurate and comprehensive approach for the comparative study of oil shales, particularly in terms of oil and gas generating potential. Further, analysis of the quantitative data produced for the entire range of products allows pyrolysis mechanisms to be investigated. The excellent mass balance gives an indication of the product partitioning for the constituent atoms of kerogen when these data are used in conjunction with relevant elemental data for the demineralized shale and shale oil.

2.4.5 Thermal distillation and pyrolysis-FID.

Pyrolysis-FID may be described as pyrolysis-GC without a chromatographic column. It is a rapid, quantitative technique suitable for very small quantities of untreated sample and may be used for crushed raw shale or kerogen concentrates. Data obtained for these samples characterise the oil shales and determine the extent of their evolution. Hunt (1979) has described some of the pyrolysis approaches employed to address these questions. There are many variations of the pyrolysis-FID procedure commonly in use. These include the commercially available Rock-Eval method for source rock characterisation and evaluation and others which may employ switching valves, sample traps and GC columns (Whelan et al., 1980). In most cases the technique consists of heating small samples of kerogen or finely-crushed rock (1-300 mg) in a stream of helium at a selected fixed rate (5-40°C min^{-1}), up to a temperature around 600-800°C. Hydrocarbons produced are selectively detected by a FID (the device does not respond to components such as H_2O, CO_2, H_2S, NH_3 etc.) with signal levels proportional to the total mass of those components reaching the detector. In this context the FID functions essentially as a hydrocarbon-selective mass detector.

Free hydrocarbons contained in pore water and adsorbed to mineral surfaces in the rock are released as a first peak (P_1) by thermal distillation in the temperature range of 100-200° C ; actual temperatures depend on programming rates and experimental conditions. Hydrocarbons, released by the thermal breakdown of kerogen in the sample, are observed at higher temperatures as a second peak (P_2). Its area (mass) may be considered as a measure of the potential of the sample to generate hydrocarbons with continued maturation. Pyrolysis-FID data need to be interpreted on a relative basis since procedural differences will give different absolute values for the same sample. Relative interpretations will be the same however provided the method is standardised and evaluated against known samples. The technique may be used for stratigraphic sequencing of prospective deposits since it reflects evolutionary changes occuring in the sample down the sedimentary column. In general, as burial depth increases so does the relative area of P_1 in

response to a progressive increase in generated free hydrocarbons produced at the expense of thermally altered kerogen; this causal relationship is reflected by a gradual shift in area from P_2 to P_1. At the same time the temperature corresponding to the P_2 maximum (T_{max}) moves to a relatively higher value, with both phenomena indicative of increasing maturation. Petroleum geochemists have quantified the peak area information by calculating a Production Index, or transformation ratio, to characterise the sample's evolutionary stage (Barker, 1974; Espitalie et al., 1977).

This is defined as : **PI = area P_1 / area (P_1 + P_2)** and is a measure of the quantity of previously generated but unmigrated hydrocarbons expressed as a percentage of the total generating potential (Figure 2-3). It is clear from the definition that low PI values are consistent with shallow, immature samples, which will yield large amounts of hydrocarbons with deeper burial. It should also be noted that PI data is able to identify migrated material within an otherwise continuous sequence. Upward migration of free hydrocarbons produced at greater depths, for example, is generally indicated by an index value greater than that expected for a sample corresponding to the respective depth within the stratigraphic column. Barker (1974) has looked more generally at the question of generated hydrocarbon migration. Using pyrolysis-FID he calculated a migration index from the relative abundances of benzene and octane contained in rock-pore micro -reservoirs and subsequently released by pyrolysis. He then used these values in an attempt to classify the rocks into source and nonsource categories.

The PI ratio for individual samples is obviously affected by the loss of volatile free hydrocarbons through evaporation and adverse sample handling; however relative values are again meaningful for samples with the same storage history. Barker (1974) studied only low molecular weight hydrocarbons up to ~C_{10} and avoided component losses by storing samples under water from the moment of production. Claypool and Reed (1976) adopted the opposite approach and oven-dried their samples to remove hydrocarbons up to about the C_{15+} range. They found that the first peak obtained up to 400°C correlates directly with the concentration of extractable C_{15+} hydrocarbons in the rock, while the

second peak is approximately proportional to the organic carbon content of the sample.

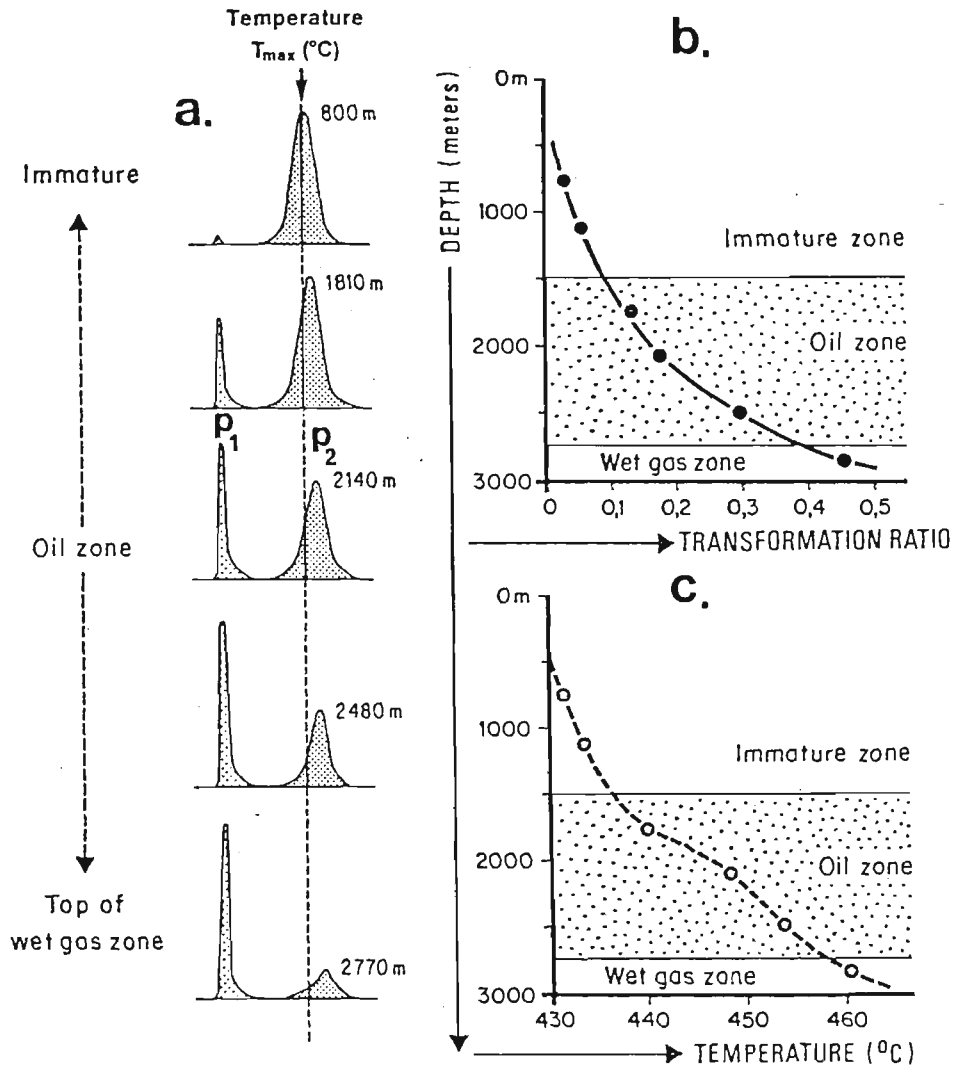

Figure 2-3.

Characterisation of source rock maturity by pyrolysis-FID, showing an increase in T_{max} (a) and (c), and transformation ratio (b), as a function of depth (Tissot and Welte, 1984).

2.4.6 Pyrolysis gas chromatography.

Pyrolysis gas chromatography is an indirect method in which the substance under investigation is characterised on the basis of the chromatographic profile (pyrogram) of the volatile products of its pyrolysis. The technique has found wide-spread acceptance for

studying polymers and has seen an exponential growth in practical applications since its inception, about 30 years ago. Various authors have presented detailed treatments of the terminology, apparatus, applications etc. since then. Berezkin (1981), has published a comprehensive review of the development of pyrolysis-GC .

By analysing pyrograms of the volatile pyrolysis products formed at different temperatures, one can arrive at conclusions about the structure and composition of oil shale kerogen, bitumen content and the likely composition of retort shale oil. Larter (1984) has reviewed the application of analytical pyrolysis techniques to kerogen characterisation and fossil fuel exploration/exploitation.

The pyrolysis unit is usually an independent device fitted (directly) to the gas chromatograph and can be classified as a static (enclosed) or dynamic (continuous flow) system. In static devices the primary products of thermal degradation can participate in various inter-and intramolecular reactions because of prolonged heating in a confined environment. Products from these secondary reactions make it very difficult to draw valid conclusions about the material under investigation and this approach will not be described further. Dynamic systems include pyrolyzers which are electrically heated conductors (filament or coil) or a rod of ferromagnetic material heated with a high-frequency current to the Curie-point temperature of the alloy. One advantage of the resistive device is the possibility of stepwise pyrolysis at several successively increasing temperatures (Leventhal, 1976). Curie-point pyrolyser temperatures can only be changed discretely to certain fixed temperatures within the range ~300-1000^0 C; actual Curie-point temperatures attained depend on the composition of the alloy used for the sample support. In dynamic systems the sample is rapidly heated in a continuous flow of carrier gas. Volatile pyrolysis products are diluted by carrier gas and swept away from the heated zone to the separation column. For oil shales the complex mixture (mainly hydrocarbons) is usually resolved on a capillary column under programmed-temperature conditions and using a (universal) flame ionization detector (FID), or others which are more selective. Specific requirements (e.g. gas analysis) may employ other combinations, such as packed molecular-sieve columns and thermal conductivity detectors.

To obtain reproducible results and characteristic pyrograms (fingerprint profiles), relevant experimental conditions must be established and once optimised need to be strictly standardised. This is essential since pyrograms reflect the influence of parameters such as:

1).-temperature and time of pyrolysis.

(Both factors interdependently control the extent of thermal degradation).

2).-sample size and homogeneity.

(Sample size influences heat transfer and diffusion processes within the sample and has a bearing on potential secondary reactions. Oil shales need to be finely ground for the sample to be representative)

3).-nature and flow rate of carrier gas.

(Chosing different gases allows pyrolysis to proceed in reactive (air, hydrogen etc.) or inert (nitrogen, helium) atmospheres. High carrier gas rates reduce product residence-time and minimize secondary processes).

4).-chromatographic separation and detection.

(Separation columns need to resolve (all) components of interest, while the detector must respond to each of them).

Pyrolysis-GC profiling of oil shales, using the dynamic technique, is a rapid procedure adequate for comparative purposes and provides information on kerogen source material, thermal history of the deposit and the kind of oil the shale can generate in commercial retorts. Reliable data on the relative abundances of the various components is normally obtained and quantitative values may be calculated by adding appropriate internal standard(s); however interpretations of the fingerprint profiles are rather subjective and cannot easily resolve differences between, for example, continuous series of mixed type II and type III kerogens. Pyrolysis-GC-MS is used, where required, to positively identify (all) individual peaks in the pyrogram; this is absolutely essential where the components of interest are present at low levels or obscured by major peaks.

Pyrolysis-GC and pyrolysis-GC-MS have been widely used in attempts to characterise petroleum source rocks, to elucidate the structure of kerogens and to type them according to their chemical properties and physical characteristics (Larter et al., 1978,1979;

Horsfield and Douglas, 1980; Solli et al., 1981; van Graas et al., 1981, 1983; Dembicki et al., 1983). Gallegos (1975) used pyrolysis-GC-MS to show that biomarkers (steranes and triterpanes) were produced by pyrolysis of Green River shale. Philp and Gilbert (1984) have used pyrolysis-GC-MS and multiple ion detection to characterise source rocks by determining the distribution of certain biomarkers, particularly triterpanes, produced during pyrolysis. They extended their investigation of source rock biomarker distributions to include asphaltenes and compared biomarkers produced by pyrolysis of the latter with those produced from the corresponding kerogens and soluble extracts (Philp and Gilbert, 1985). Larter and Senftle (1985) have reported an improved kerogen typing for petroleum source rock characterisation. The method provides an improved classification for kerogen at all maturity levels, particularly for those of mixed type from near-shore marine settings. It is based on a quantitative pyrolysis-GC approach using an internal standard, polymethylstyrene, to determine the absolute concentrations of specific kerogen pyrolysis products. Using cross-plots of normal hydrocarbons, aromatic hydrocarbons and total hydrocarbon yields from their kerogen pyrolysis-GC data, the authors were able to recognize eight separate nodes of kerogen composition. This represents an improvement over traditional kerogen typing based on microscopy and bulk chemical methods, which fail to provide adequate resolution of the complex mixture of kerogen components encountered in oil shales and petroleum source rocks. Crisp et al., (1986) have used flash thermal pyrolysis of oil shale powders, heated on nickel wires with a Curie-point temperature of 358°C, as an alternative to solvent extraction for the determination of C_8-C_{35} hydrocarbons in oil shales. They analysed samples from various deposits and proposed the technique as a qualitative exploration tool for oil shales and petroleum source rocks. Ellacott (1986) has used pyrolysis-GC-MS to establish a link between the chemistry and geology of a wide range of marine oil shales.

2.5 Chemical degradation of oil shales.

Chemical methods such as oxidative degradation, alkaline hydrolysis, functional group analysis etc. have been widely used to study kerogen structure. The main aim of

each approach is to make the degradation as specific as possible in an attempt to obtain smaller identifiable compounds which retain their structural relationship to the kerogen. In this respect chemical methods are more specific than the thermal procedures described in later sections. However any reconstruction of the products into a structure representative of the original kerogen is difficult since the nature of the linkages and bonds between the various fragments is not clearly defined. Chemical reagents attack primarily at, or next to, carbon atoms bearing a functional group and may consequently give misleading information about the functional groups from which they are derived. The oxidative production of carboxylic acids from various precursors is an example of this. Functional group analysis is therefore an important complementary method for any degradative approach.

Many oxidants have been employed for the study of kerogens, with alkaline potassium permanganate and chromic acid most frequently used, usually as part of a stepwise procedure to prevent further degradation of products formed at various stages of the oxidation sequence. Robinson et al. (1961) and Burlingame et al. (1968) have studied kerogen from the Green River Formation using oxidation procedures, in an attempt to characterise the structure of this type I geopolymer. The latter authors proposed a kerogen structure (Figure 2-4) based on their findings. Vitorovic (1980) has reviewed most of the procedures used for the structure elucidation of kerogen by chemical methods, with special emphasis on oxidative degradation. Vitorovic et al. (1984) have used multi-step alkaline permanganate oxidation to investigate the relationship between kerogen concentrates obtained from Green River (type I), Toarcian (type II) and Manville (Canada) shales (type III). GC-MS analysis of the methyl esters revealed typical saturated aliphatic mono- and dicarboxylic acids as the main components (>90 %) for type I kerogen and ranged to typical aromatic mono-, di- and tricarboxylic acids as the main products (>90 %) for type III kerogen. Type II kerogen yielded primarily aliphatic acids (ca. 80 %), with less, but significant amounts of, aromatic acids and subordinate quantities of alkane-polycarboxylic acids also produced. Costa Neto et al. (1984) have used a similar approach to study the stepwise oxidation of kerogen from Irati shales. GC-MS was again used to identify the

isolated carboxylic acids and revealed a product composition indicative of a type II kerogen. Chaffee and McLaren (1986) have used electrochemical oxidation to investigate the chemical structure of the kerogen concentrate from Julia Creek oil shale. The isolated acids were derivatised and analysed using capillary GC-MS. The authors showed that electro-oxidation leads to a complex mixture of both aliphatic and aromatic acids, with product distribution broadly similar to that obtained by permanganate oxidation of a type II kerogen.

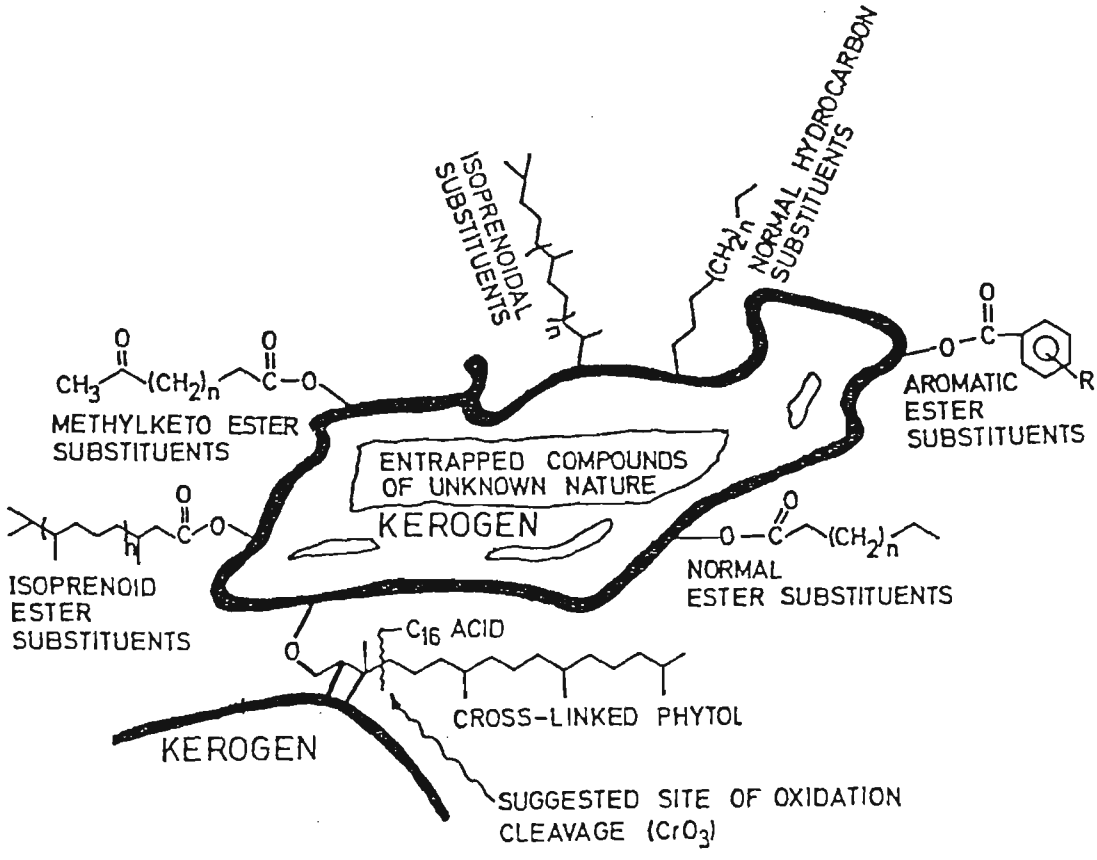

Figure 2-4.

Structure proposed for Green River Formation kerogen (type I). (From Burlingame et al., 1968).

2.6 CHROMATOGRAPHIC PROCEDURES.

2.6.1 Adsorption chromatography.

Shale oil and bitumen fractions may be analysed directly by GC without prior separation or fractionation. This direct approach has some of the disadvantages mentioned in the next section, while further problems associated with the procedure arise from the sample size restrictions imposed by the use of capillary columns. As a consequence low level components may be masked by coeluting peaks, obscured by very large peaks with similar retention times, or may not be detected at all if present at only very low concentrations. To overcome some of these limitations, samples are normally separated prior to analysis to obtain concentrates of fractions containing the components of interest.

Shale oil and bitumen samples are extremely complex mixtures of compounds including numerous homologous series of hydrocarbons and many classes of heterocyclic compounds of varying polarity. Many fractionation schemes have been reported in the literature to isolate these for further study. Most procedures achieve a class separation by using either open column or high performance liquid chromatography (HPLC) and adsorbents such as silica, alumina or a combination of both. Other adsorbents (Florisil, Sephadex etc.), reversed-phase and ion-exchange procedures as well as thin-layer chromatography (TLC) have also been used to isolate particular fractions. Jewell et al. (1972) adopted the widely-used SARA technique (saturates-aromatics-resins-asphaltenes) for the separation of petroleum distillates. This procedure combines ion-exchange, coordination-complex and adsorption chromatography (alumina or silica-alumina) to separate acidic, basic and neutral nitrogen compounds, saturated and aromatic hydrocarbons. Jones et al. (1977) have reported the separation of aliphatic and aromatic hydrocarbons as well as nitrogen heterocyclics and polar aromatic compounds in crude oil derived from coal and shale. They used acid-base extraction followed by solid-liquid chromatography on Sephadex LH-20, silicic acid and basic alumina to achieve this. Other researchers have used classical chromatography emloying both single- and dual-packed silica, alumina and alumina-silica columns to resolve heavy petroleum fractions, shale oil

and coal-derived liquids (Hirsch et al., 1972; Schwatzky et al., 1976; Shue et al., 1981; Later et al., 1981). Hertz et al. (1980) have used acid/base extraction followed by reversed -phase C-18 HPLC and GC, GC-MS to identify and quantify several phenols, N-heteroaromatic compounds and PAH in shale oil.

The use of HPLC, with activated silica as the stationary phase, has shown that petroleum feedstocks can be separated rapidly into saturates, aromatics and polar fractions with cleaner class separations compared to conventional chromatography. The inherent greater efficiency of HPLC has recently been augmented by improved selectivity through the development of bonded phases (Miller, 1982), the application of switching techniques and the introduction of high-resolution microcapillary columns. Despite the success of HPLC in resolving components within a chemical class and model compound mixtures, these separations have not translated directly to the analysis of complex oils, with the overlap of classes such as saturates/olefins and aromatics (mono-, di-, and polyaromatics) remaining a problem. Novotny et al. (1984) have used reversed-phase microcolumn-HPLC for the separation and characterisation of very large polycyclic molecules in the non-volatile neutral polyaromatic fraction of coal-derived fossil fuels. Using microcolumns with efficiencies over 200,000 theoretical plates they resolved over 170 components. Trapped components were analysed by MS, which showed the presence of numerous isomers of the parent and alkylated polycyclic compounds within five- to nine-ring structures. It is the presence of these isomers which normally prevents a clean separation of this fraction in shale oil using more conventional HPLC columns.

The class fractionation of fuel oils by TLC has not been widely reported. Column chromatography followed by TLC has been used by Hurtubise and Phillip (1979) to separate and identify the polyaromatic hydrocarbons in shale oil. Huc and Roucache (1981) have carried out a comparison between TLC and column chromatography as a technique for separating aliphatic, aromatic and polar compounds in the extracts from sedimentary material. Harvey et al. (1984) have used silica TLC to separate the organic components in shale oil into 14 classes. Individual compounds within these classes were identified using GC-MS and IR procedures.

Regtop (1983) has reviewed some of the more commonly used separation procedures including open column chromatography, HPLC and liquid-liquid extraction. Using a combination of alumina and silica adsorbents he isolated various fractions from Rundle shale oil and bitumen by eluting them from a gravity-fed chromatographic column using solvent mixtures of increasing polarity. The isolated fractions were then concentrated and analysed further by GC, GC-MS and gravimetry (Regtop et al., 1982; Regtop et al., 1983). Ingram et al. (1983) used the same procedure for the comparative study of oil shales and shale oil from the Mahogany Zone, Green River Formation and Kerosene Creek Seam, Rundle Formation. Rovere et al. (1983) modified the solvent elution program of the method to obtain 20 fractions for shale oil from the Condor deposit, Australia. Aliphatic fractions obtained from adsorption chromatography may be further fractionated by urea adduction or molecular sieving, to separate linear compounds from branched and cyclic components. It should be appreciated that the resolution achieved by any column (or other) -fractionation step is not as critical when the isolated fractions are subsequently analysed by GC, GC-MS or GC-FTIR. Under those circumstances the main requirement from these procedures are separation efficiencies adequate to obtain (clean) class separations and (complete) recovery of the sample. Other important considerations relate to cost, sample capacity, reproducibility and speed of the procedure. Apart from the latter, the use of the gravity-fed mixed-bed open column used by Regtop et al., (1983) has been shown to satisfy most of these criteria .

2.6.2 Gas chromatography.

Even narrow fractions obtained from adsorption chromatography often contain hundreds of components at varying concentrations. These components need to be resolved and subsequently identified, or simply monitored for the presence of a particular compound. Capillary-GC, interfaced to complementary equipment, goes a long way towards achieving most of these requirements.

Gas chromatography (GC) separates complex mixtures of chemicals into those constituent components amenable to the technique. A stream of inert gas carries a

vaporised sample of volatile components through a column containing a non-volatile stationary phase. The components that have little or no affinity for the stationary phase remain partitioned in the gas phase and are swept through the column quickly. Other components may interact with the stationary phase and be temporarily removed from the gas stream, with individual passage through the column dependent on the respective affinity. Where the affinity is too great, components may be totally retained, never to emerge from the column (e.g. some high molecular-weight polar or non-volatile compounds). The time from sample injection to component appearance (retention time) is characteristic of the component identity, assuming that the column, gas velocity, temperature and other appropriate parameters are held constant.

Mc Nair and Bonelli (1969) have covered the basic concepts of GC and Douglas (1969) has reviewed some of the earlier applications of gas chromatography to the field of organic geochemistry.

In the context of oil shale research, the most important recent advance in GC has been the development of fused-silica capillary columns coated with a cross-linked (bonded) stationary phase. Compared to the previously available packed or capillary columns made of either stainless steel or glass, fused-silica bonded-phase (BP) columns now routinely provide vastly improved column to column reproducibility, resolution and retention characteristics. Other advantages include the virtual elimination of breakage, a highly inert inner-column surface, a wide dynamic temperature range and rinsability. Collectively these attributes have made the large number of stationary phases previously required for packed and glass capillary columns virtually redundant. Jennings (1980) has reviewed the development and use of glass capillary columns leading up to this latest innovation.

It is the inertness, reproducibility and great resolving power which makes the use of BP capillary columns almost mandatory for the compositional analysis of such complex mixtures as bitumen and shale oil. Low-cost commercially available columns (25m) routinely exceed 100,000 effective plates and are available in a narrow range of non-polar (silicone rubber) to polar (carbowax) stationary phases. Used with high-speed modern integrators, they are capable of analysing almost the entire range of volatile components

normally found in the complex mixtures of organic compounds isolated from sediments, rocks and oil. In conjunction with specific detectors which are selective for, or enhance the signal of, nitrogen, sulphur, phosphorous and halogen containing molecules, they provide direct information about the presence of these compounds in complex mixtures without the need for prior fractionation or isolation. Earlier comments about retained components should caution the researcher against any direct analysis of complex mixtures. Indiscriminate injections of unknown samples may lead to the build-up of contaminants which may prove difficult, if not impossible, to remove from the column. When used with fractionation procedures, such as column chromatography, and followed by post-separation identification (GC-MS, GC-FTIR), BP columns form an indispensible part of the most powerful analytical approach available to the geochemist today.

The advent of BP capillary columns has rendered obsolete much of the early data obtained from packed or glass capillary columns using different phases; there is now a need to provide retention times obtained using BP columns under standard conditions. This will result in the establishment of a large data base of important and easily reproducible information (e.g. retention indices for GC-MS identified components in bitumen and shale oil).

2.7 Mass spectrometry.

Mass spectrometry has been used in the petroleum industry and related areas for many years. In the early stages it was used mainly to monitor refinery products and to determine crude oil compositions. Burlingame and Schnoes (1969) have reviewed the instrumentation, techniques and applications of this early work. Their comprehensive review covers the analysis of organic matter from geological sources but emphasises those applications in which mass spectrometry has played a major role in the structural characterisation of individual components within the main compound classes comprising crude oil.

The applications of MS to organic geochemistry, particularly in the case of GC-MS, have increased dramatically in the last few years. This has been in conjunction

with the development of high-resolution capillary columns, quadrupole and laminated -sector mass spectrometers, cheap and powerful computers and sophisticated software to control the instruments and process the data. Consequently GC-MS is now used routinely in fossil fuel studies for the identification of individual components in the complex oils and extracts obtained from a variety of sources. GC-MS is also used extensively to monitor and quantify biomarker compounds present in these mixtures, particularly where these components are present at relatively low concentrations and consequently obscured in the baseline of the respective chromatograms. Philp (1985) has compiled and published a comprehensive collection of mass spectra for these compounds. Their presence and distribution can provide valuable information about the evolution and source of a particular deposit and their study is proving to be an important tool in the area of petroleum exploration (Ourisson et al., 1984).

Many biomarkers and other molecules (e.g. members of homologous series) fragment in a systematic way to produce fragment ions characteristic of their structural identity. These characteristic ions can be used to detect and monitor individual components of that type within unresolved complex mixtures even in the presence of coeluting GC peaks, provided the coeluting component does not itself produce an ion of the same mass. This technique of multiple ion detection (MID) enhances the sensitivity of the MS dramatically. Since it obviates the need for complete scans, greater dwell-times are attained for the restricted number of discrete, preselected ions chosen to monitor the components of interest. Philp and Gilbert (1984) have used pyrolysis-GC-MS-MID to characterise selected Australian and Alaskan petroleum source rocks and oil shales. Later the same authors extended this approach to include the characterisation of asphaltene biomarkers produced by microscale pyrolysis of extracted source rocks, kerogens and asphaltenes (Philp and Gilbert, 1985). The GC-MS-MID mode of operation is particularly effective when used with high-resolution mass spectrometry. Choosing fractional-mass ions, totally specific for the monitored compounds, eliminates possible contributions at these masses from unrelated components and increases selectivity to the extent where complex mixtures may now be analysed without the need for time-consuming fractionation steps (Mackenzie et al., 1983).

An alternative approach to mixture analysis is to utilise a tandem MS-MS configuration either directly, using a batch inlet or direct-insertion procedure, or more appropriately, as part of a GC-MS-MS facility. Even further selectivity has been achieved in commercial systems in the form of a triple-sector quadrupole (TSQ) mass spectrometer. This configuration comprises three sequential quadrupole mass-filters and is able to utilise most of the available inlet systems and ionisation methods. The recent development of extremely compact ion-trap mass spectrometers offers the future possibility of stacked-array multiple-trap arrangements with virtually unlimited MS flexibility and selectivity. With continued innovations in instrument design and major advances in computer technology, it may eventually be only financial constraints that limit the complexity and availability of these extremely powerful systems.

Interfacing a high-resolution capillary GC to a modern fast-scanning mass spectrometer (quadrupole or sector) creates a combined GC-MS system capable of resolving and identifying most of the hundreds of components normally encountered in oil shale analysis. Most capillary columns are interfaced to the MS via an open-split coupling, or coupled directly, with the column terminating close to the MS ionising region. The former arrangement allows part of the column eluent to be diverted and recorded by a FID and retains the column's normal retention characteristics. The latter achieves maximum sensitivity with all components entering the MS source and avoids losses associated with problems in the interface (e.g. activity of the transfer line). In this case profiles almost identical to conventional FID traces are obtained from the total ion chromatogram produced by the MS data system.

High performance liquid chromatography-MS (LC-MS) is another combined technique which may play a greater part in future geochemical studies. Some of the early work was concerned with the analysis of PAH in coal-derived liquids (Dark et al., 1977). Ironically this is an area where fused-silica columns are now competing with HPLC, since relatively large polyaromatic compounds are now easily chromatographed using these columns (Hirata et al., 1981). However, with improvements in interfacing (e.g. thermospray) and the development of high-resolution microbore columns (Novotny et al.,

1984) it is now possible to take the total HPLC eluate directly into the ion source of the mass spectrometer system. The latter should provide an improvement for the analysis of high molecular-weight, polar compounds which may be retained by capillary columns or prove too labile to survive alternate MS introduction systems.

Mass spectra are normally produced by electron-impact (EI) ionisation, since this mode of operation achieves the highest sensitivity and provides maximum structural information for individual molecules; consequently all mass-spectral libraries are based on information obtained from this ionisation method. Chemical ionisation (CI) using various reagent gases may also be employed, although it is only suitable for restricted classes of compounds (Mackenzie et al., 1981). It is a soft ionisation technique involving ion-molecule reactions and has only limited applications to hydrocarbon-type analysis, however it may be more useful for heteroatomic molecules. This restricted application can be used to advantage in the analysis of suitable mixtures, since it may allow selective ionisation of certain classes of compounds in the presence of others. CI produces fewer fragments ions than the EI procedure and provides primarily molecular weight information for those molecules accessible by the technique. A common approach with older instruments is to analyse suitable GC-MS fractions sequentially in both the EI and CI mode, while some modern installations are capable of alternate scan EI/CI operation during a single analysis (Taylor et al.). The latter is invariably associated with the loss of some EI spectral resolution due to the higher MS source pressure required to produce CI conditions. Alternating positive-ion / negative-ion scans may also be performed with modern instruments. As with CI, the negative ion phase of this pulsed-mode of operation does not find universal application but gives selective information for specific compounds that produce a high proportion of negative ions under (predominantly) EI conditions.

Other ionisation techniques such as field ionisation, field desorption and fast atom bombardment (FAB) are also available but have not found wide-spread application in geochemical research. Ekstrom et al. (1983) have used FAB to study porphyrins isolated from shale extracts, but the technique is generally more popular in the biomedical field, where molecular weight information on complex molecules, of up to 5000 daltons, has

been obtained using this ionisation procedure. The need to analyse high molecular-weight molecules and polymers, from polar fractions such as the asphaltenes, will undoubtedly see an increase in the use of this approach in an effort to unravel fundamental kerogen/oil relationships.

2.8 Modern infrared techniques.

Most of the characterisation work on crude oils and rock extracts has been carried out using GC-MS techniques. Although this situation is likely to continue, relevant advances in other techniques will progressively contribute more and more complementary data obtained from alternate identification methods. Infrared spectrometry, for example, can now be combined with GC to obtain IR spectra for peaks eluting from capillary columns. GC-FTIR uses a light pipe approach to obtain real-time spectra as the compounds leave the column. An alternate, matrix-isolation infrared approach (MI-IR) was first demonstrated by Reedy et al. (1979). Their GC-MI-IR procedure immobilises the eluting molecules in a matrix of solid argon deposited on a gold-plated disk held at ~10K. The cryogenically trapped components are then analysed at the end of the chromatographic run, with a computer serving to synchronise the column peaks with respective disk positions.

Laude et al. (1984) have linked GC-FTIR-FTMS with integrated EI and CI ionisation to analyse a mixture of model compounds comprising a variety of functionalities including aliphatic and aromatic halogen, carbonyl and hydrocarbon compounds. The IR part of the linked technique is inherently less sensitive than the MS analysis and overall the procedure requires greater sample levels and a capillary column with consequently higher sample capacity to avoid column overloading. Smith (1986) has overcome the deleterious effects of high sample concentrations by using a two-dimensional capillary GC-FTIR. This involves two capillary columns of different polarities located in two discrete, independently controlled ovens in the same gas chromatograph. He used a heart-cutting technique to obtain FTIR spectra for components of a terpene mixture. Reedy et al. (1985) have used high-resolution GC-MI-IR to study a mixture of PAH, PCB, dioxin and aliphatic

hydrocarbon compounds. They obtained excellent IR spectra for 50 ng of fluorene, about 40 times better than the detection limit for the compound using a light pipe approach.

Infrared spectrometry is unique for every chemical compound and is consequently well suited to distinguish between closely related structures such as isomers. In mass spectrometry, identifications of chemical compounds are based on fragmentation patterns which may be similar for a variety of molecules. Infrared spectra are measured for intact molecules and any change in the identity or position of a substituent on a molecule alters the vibration modes of the molecule, resulting in distinctive infrared spectral features. Even in those cases for which neither MS nor IR nor a combination of the two is able to identify a particular compound, IR is a good source of information about the functional groups present in the molecule. This data often indicates whether the molecule may respond to CI-MS analysis. If so, the molecular weight, mass-spectral fragmentation pattern, and all of the IR information, may collectively allow complete structural assignments.

CHAPTER THREE : EXPERIMENTAL

3.1 General procedures.

Raw oil shale samples were crushed, as received, to < 2.8 mm diameter and divided into sub-fractions using a riffle sample splitter. The top size (1.4-2.8 mm) was used for retorting purposes, while the finely-powdered fraction was used for solvent extraction and pyrolysis-GC, pyrolysis-FID etc. All sieved fractions were stored in glass containers fitted with alfoil-lined lids.

All solvents were distilled prior to use and checked for chromatographic purity using GC. Water was triple-distilled (the last two distillations from a quartz still) to ensure the absence of plasticiser contaminants.

All glass containers were initially cleaned using a cycle of detergent, hot tap-water, Decon 90 (or chromic acid) washing, followed by rinsing with hot tap-water, distilled water, acetone and chromatographically-pure dichloromethane. All screw-cap vial lids were fitted with teflon-lined silicon-rubber septum-seals to maintain sample integrity and to prevent evaporation of the contents during prolonged storage.

3.2 Solvent extraction.

Finely-crushed raw shale (10 g) was placed into a 100 mL round-bottom flask and 50 mL dichloromethane added. The flask was placed in an ultrasonic bath filled with water (35°C) to a level ~1cm above the flask contents, which were then stirred for 4x15 min (Figure 3-1). At the end of each extraction period evaporated dichloromethane was replaced with fresh solvent and the bath adjusted to the initial temperature. After 60 min the solvent extract was decanted, filtered, concentrated to ca. 4 mL (rotary evaporator, 30°C, 4.7 kPa.), dried (anhydrous $MgSO_4$) and centrifuged. The supernatant was transferred to a 5 mL amber screw-cap vial and the solvent evaporated under a gentle stream of dry nitrogen until component concentrations suitable for GC analysis were obtained, or completely for gravimetric quantitation. When a large number of samples needed to be processed, smaller quantities (0.5 g) of powdered raw shale were extracted with 10 mL of solvent in 20 mL screw-cap vials bundled together with rubber bands. These vials were shaken gently for 12 h and the extracts then treated as described above.

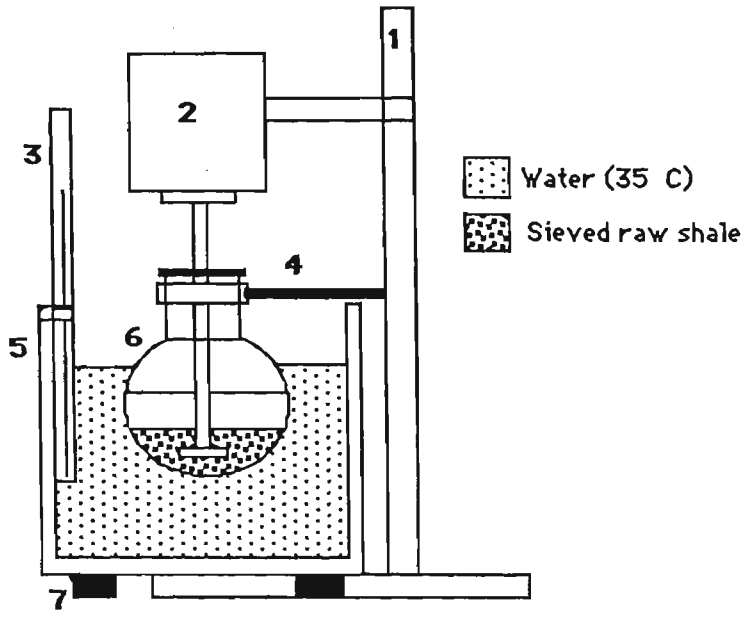

Figure 3-1.
Schematic diagram of ultrasonic extraction of raw shale : 1, retort stand; 2, stirrer motor; 3, thermometer; 4, flask clamp; 5, ultrasonic bath; 6, round-bottom flask.

3.3 THE RETORTING OF OIL SHALE.

Air-dried, crushed raw shale (60 g) from the Duaringa deposit (5391-C) was retorted using the modified Fischer Assay procedure of Stanfield and Frost (1949). The shale oil produced (**FA-retort oil**) was fully characterised and served as a reference sample for further studies.

3.3.1 Retort construction and shale oil production.

A copper tube-furnace and a stainless steel retort of ca.60 g capacity were constructed to overcome at least some of the inherent design problems evident in the F.A. retort (cf. section 2.4.1). The furnace was positioned centrally inside an aluminium can and thermally insulated from it with quartz wool. All other oil shales were retorted using this facility (Figure 3-2) and oil produced will be referred to as **retort oil,** to differentiate it from the oil obtained as above. The tube-furnace was controlled by a Varian column-oven linear temperature programmer, supplying two 115 V, 300 W cartridge heaters connected in series. Retort temperatures were monitored by a sensing probe located in a hole drilled close to the internal wall of the copper tube. Dry nitrogen sweep-gas was controlled by a fine needle valve and introduced to the furnace via a drilled-through 1/8" swagelok fitting silver-soldered to the retort lid. Retort products were collected in a

centrifuge tube(s) immersed in an ethanol bath held at -20°C by a cold finger (Neslab Cryocool).

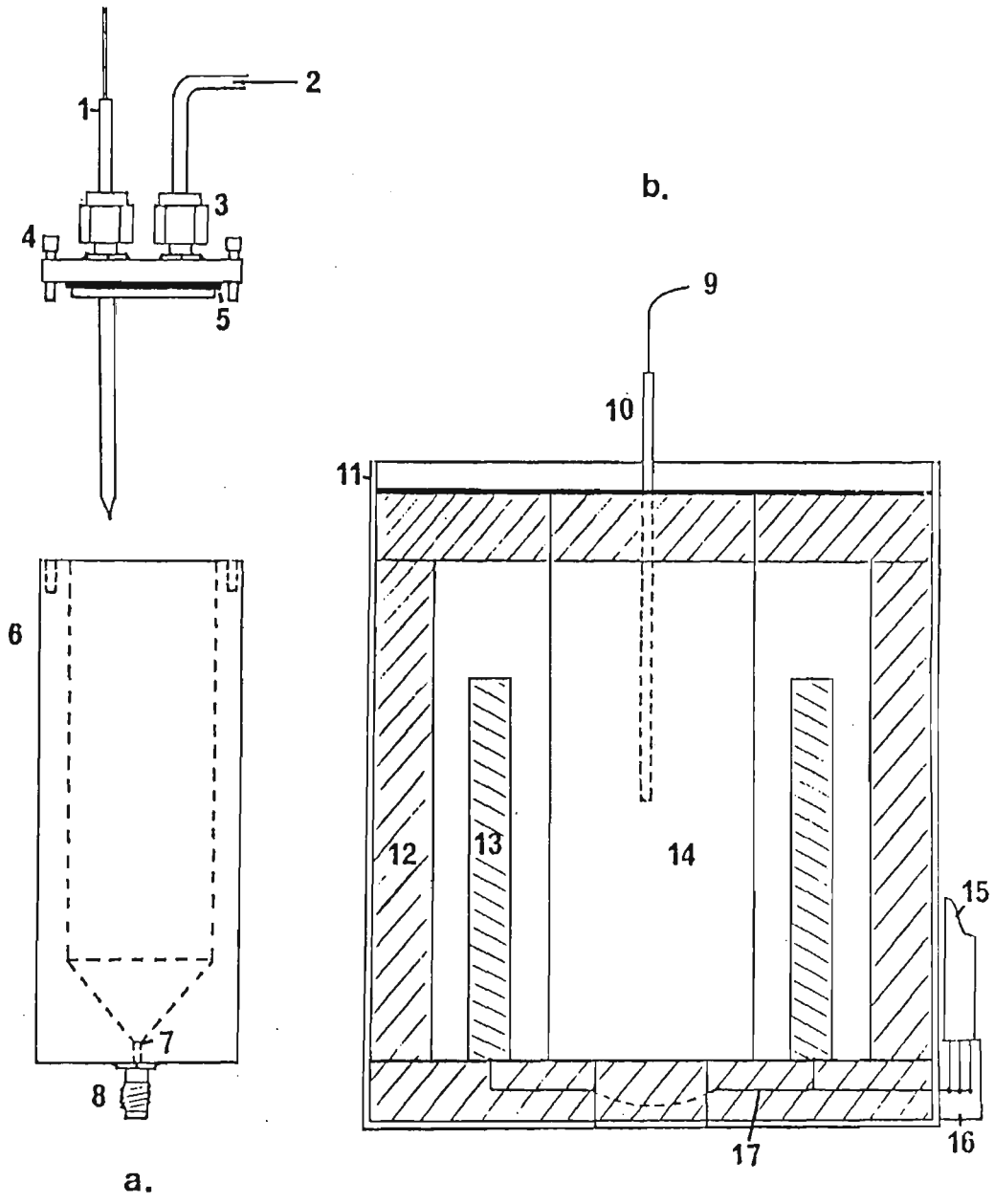

Figure 3-2.

Schematic diagram (0.5 x actual size) of stainless steel retort (a) and cut -away section of copper-tube furnace (b). 1, thermocouple probe; 2, sweep-gas inlet; 3, drilled through 1/8" Swagelok fitting; 4, fastening bolt; 5, silver-wire gasket; 6, retort; 7, stainless steel gauze; 8, 1/8" Swagelok fitting; 9, lead to temperature programmer; 10, furnace-control sensor; 11, aluminium can; 12, quartz-wool insulation; 13, Firerod cartridge heater @ 115 V, 300 W, connected in series; 14, copper furnace block; 15, electrical supply from temperature programmer; 16, ceramic terminal block; 17, lead connecting cartridge heaters.

The stainless steel retort exit tube was resistively-heated directly by a low-voltage high-current transformer. This ensured that all products left the tranfser tube and avoided the need for rinsing to achieve total product recovery. A purge-gas velocity of 50 mL min^{-1} was chosen to sweep pyrolysis products into the collection tubes. With an interstitial volume of ~30 mL for a normal retort charge of 60 g, this flow rate equates to a maximum product-residence time of ca.30 s. The whole assembly was located in a fume cupboard to minimise problems associated with fumes and unpleasent odours (Figure 3-3).

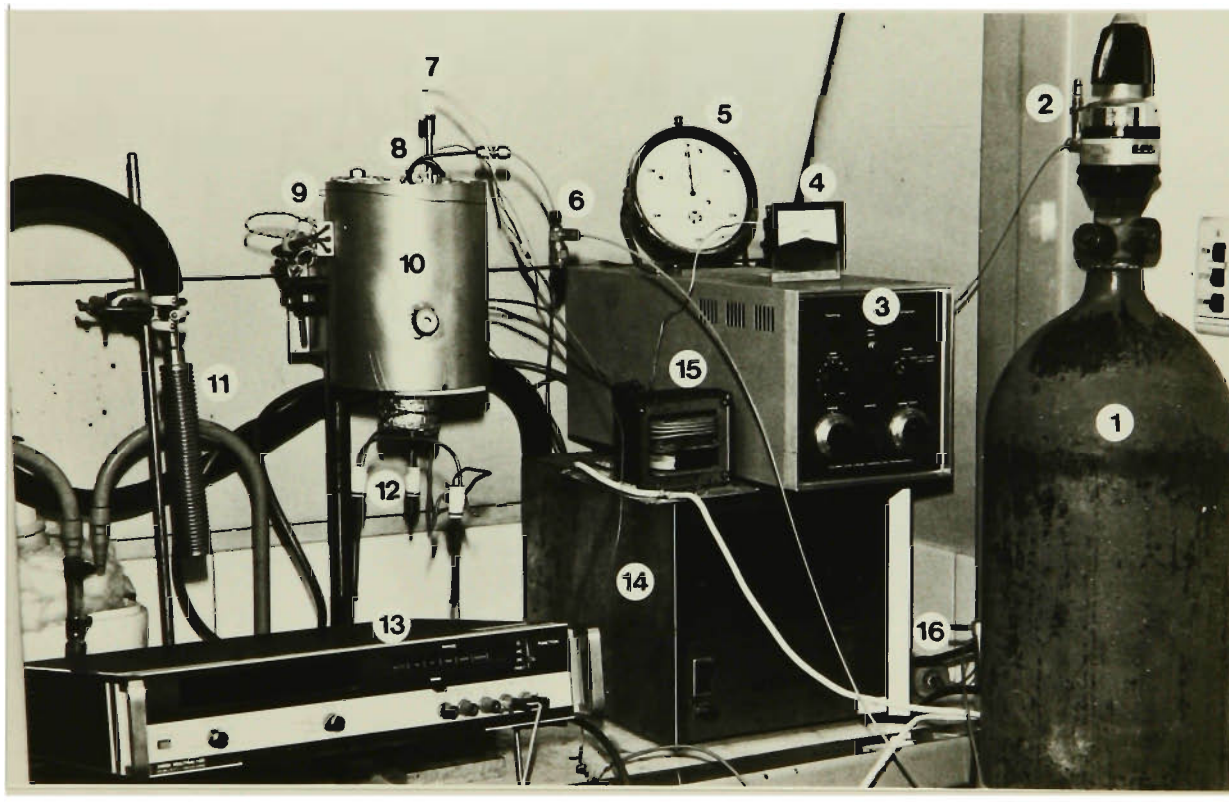

Figure 3-3.
Retort facility for producing shale oil. 1, sweep-gas cylinder; 2, needle valve; 3, linear temperature programmer; 4, pyrometer; 5, timer; 6, on/off toggle valve; 7, furnace-control sensor; 8, gas inlet; 9, ceramic terminal block; 10, aluminium can; 11, chiller "cold-finger"; 12, teflon stopper; 13, five figure digital volt meter; 14, Cryocool (Neslab) chiller; 15, low-voltage, high-current transformer.

Actual shale temperatures attained during retorting (Figure 3-4) were monitored by a chromel-alumel thermocouple probe fitted through the retort lid and connected via a 0°C reference junction to a five figure digital voltmeter or recorder. At maximum heating rate shale temperature was almost linear over the entire heating range and for the pyrolysis region (~300-500°C) had a gradient of 9.6°C min^{-1} (cf.10°C min^{-1} required for FA retort

studies). During step-wise retorting, samples corresponding to particular temperature regions were collected in 10 mL screw-cap vials. These were immediately sealed and stored in a freezer for subsequent analysis.

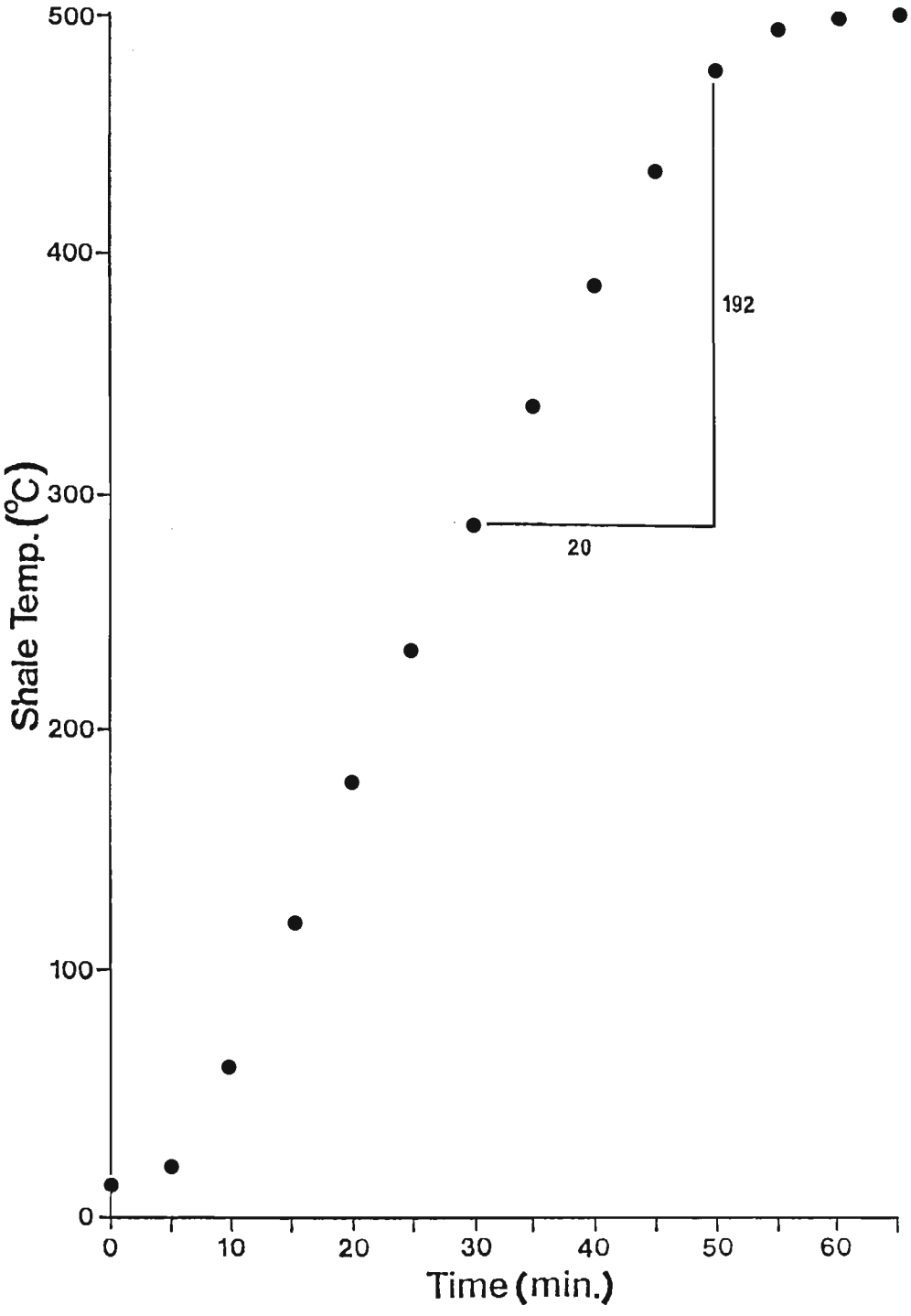

Figure 3-4.

Plot of actual shale temperatures during retorting. Values (●) were obtained by converting digital voltmeter readings from a chromel-alumel thermocouple located in the shale.

3.4 INSTRUMENTATION.

3.4.1 Gas chromatography.

GC analyses were carried out on a Varian Model 3700 gas chromatograph fitted with a FID and equipped with a thin film (0.25 micron) 25 m x 0.22 mm i.d.vitreous-silica BP5 column (S.G.E. code: 25QC2/BP5 0.25). The GC oven was temperature -programmed from 50°C to 280°C (isothermal) at a rate of 4°C min^{-1}. The inlet splitter was set to a split ratio of 15:1 and the pressure drop across the column was maintained at 100 kPa throughout the analysis. At 50°C this corresponded to a hydrogen carrier gas linear flow-rate of 19.4 cm s^{-1}, as determined from the retention time of methane. Hydrogen carrier gas was used for all of the GC analyses except for the initial phase of pyrolysis-GC (cf. section 3.5.2). GC profiles and quantitative data were obtained using a Shimadzu C-R3A integrator. The integrator was time-programmed to exclude any solvent contribution (< hexane) from the total peak area value (except for pyrolysis-GC, where all data were quantified). Peak detection parameters were chosen so that components present at levels greater than twice the background noise level contributed to the total area.

3.4.2 Mass spectrometry.

Direct insertion (DI) and GC-MS data were obtained from either a Vacuum Generators V.G. MM 12-12 or MAT-44 quadrupole mass spectrometer system. Both instruments have a 1200 amu mass range and each is able to operate in either EI or CI ionisation modes. The V.G. system also operates in a pulsed positive-negative ionisation mode and is equipped with a FAB source. For GC-MS analysis helium was used as carrier gas and a BP5 capillary column was connected directly to the ion-source (250°C) of the respective mass spectrometer via heated (250°C) deactivated vitreous silica transfer tubing. EI spectra were obtained at 70 eV. CI data were obtained using isobutane as reagent gas. Scan times for both modes were normally 1s, although faster rates were occasionally used to resolve closely eluting components. Mass-spectral data from the V.G. system were acquired and processed using a Data General Nova 3 computer interfaced to a top-load Pertec hard disk drive (2 x 5 megabyte). The MAT-44 mass spectrometer system operates under the control of its own microprocessor and stores spectra on single-sided 8" floppy-disks. Compounds were identified by matching their mass spectra with commercial libraries (M.S.D.C., 1974; Stenhagen et al., 1974) or by comparison with literature spectra (Anderson et al., 1969; Anders and Robinson, 1971; Gallegos, 1971, 1973; Simoneit et al. 1971; Simoneit, 1977; Seifert, 1978; Seifert and Moldowan, 1978, 1979; Mackenzie et al., 1981; Philp, 1985), or by comparison with spectra of reference compounds analysed using the above facilities.

FT-NMR analyses (^{1}H and ^{13}C) were carried out on either a 90 MHz (Jeol FX 90Q) or 400 MHz (Jeol JNM GX 400) spectrometer. Other instruments are described in those sections dealing with their specific application to oil shale and shale oil analysis.

3.5 PYROLYSIS PROCEDURES.

3.5.1 Pyroprobe calibration.

Pyrolysis-GC was performed using the platinum-coil probe of a CDS 150 Pyroprobe. To obtain accurate shale temperatures during flash pyrolysis, the pyroprobe was first calibrated in situ. This was done to establish accurate and reproducible instrument conditions and to obtain an indication of actual shale temperatures during pyrolysis. Prior to calibration the rubber septum-seal, normally used for the probe, was replaced by teflon tape. This was wound tightly around the probe shaft to a thickness slightly less than the internal diameter of the septum nut and was retained in it by a shallow stainless steel capture sleeve (Figure 3-5). A teflon seal was then formed by screwing the septum-nut onto an unused drilled-out (1/4") injection port of a Varian 2700 GC. The injection port was held at 300°C and the probe left in its position overnight to outgas the teflon, which deformed and compressed at this temperature to form an inert seal inside the nut. This seal has now been used on over 100 occasions without any problems or contributions to the chromatogram.

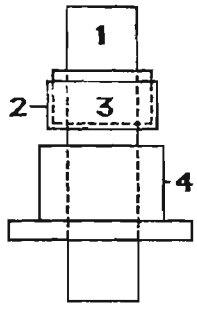

Figure 3-5.
Schematic diagram of CDS 150 Pyroprobe shaft-section showing teflon-tape seal and capture-sleeve arrangement. 1, pyroprobe shaft; 2, stainless steel capture sleeve; 3, tightly-wound teflon tape; 4, septum-nut.

The platinum coil was calibrated inside the injection port held at 300°C by placing a fine chromel-alumel thermocouple into the middle of a quartz pyrolysis tube located in the coil. The coil was positioned in the centre of the injection port and the thermocouple output referenced to a 0°C cold-junction. Pyroprobe instrument parameters were: RAMP: OFF; INTERVAL: 20 s; FINAL TEMPERATURE (DIAL): 300, 400,.....,999. Voltages generated during the pyrolysis period were recorded on a calibrated chart recorder against controller dial settings (Figure 3-6) and the maximum voltages reached during each run converted to temperatures using standard conversion tables. Individual profiles clearly show the poor heating rates (e.g. a rate of ca. 1200°C min^{-1} was achieved with the dial set to 700 -- curve 5 of Figure 3-6) and the restricted time interval during which the sample is actually in the region of the maximum temperature attained.

The maximum recorded temperature values of Figure 3-6 were plotted against respective controller dial settings to establish a calibration curve covering the entire range of available temperatures. Figure 3-7 shows the actual temperatures achieved are substantially lower than the settings on the instrument dial; a dial setting of 750 was satisfactory for flash pyrolysis. This gave a probe temperature of ~570°C, although any temperature gradient into the sample necessarily reduces the temperature which the entire sample actually experiences.

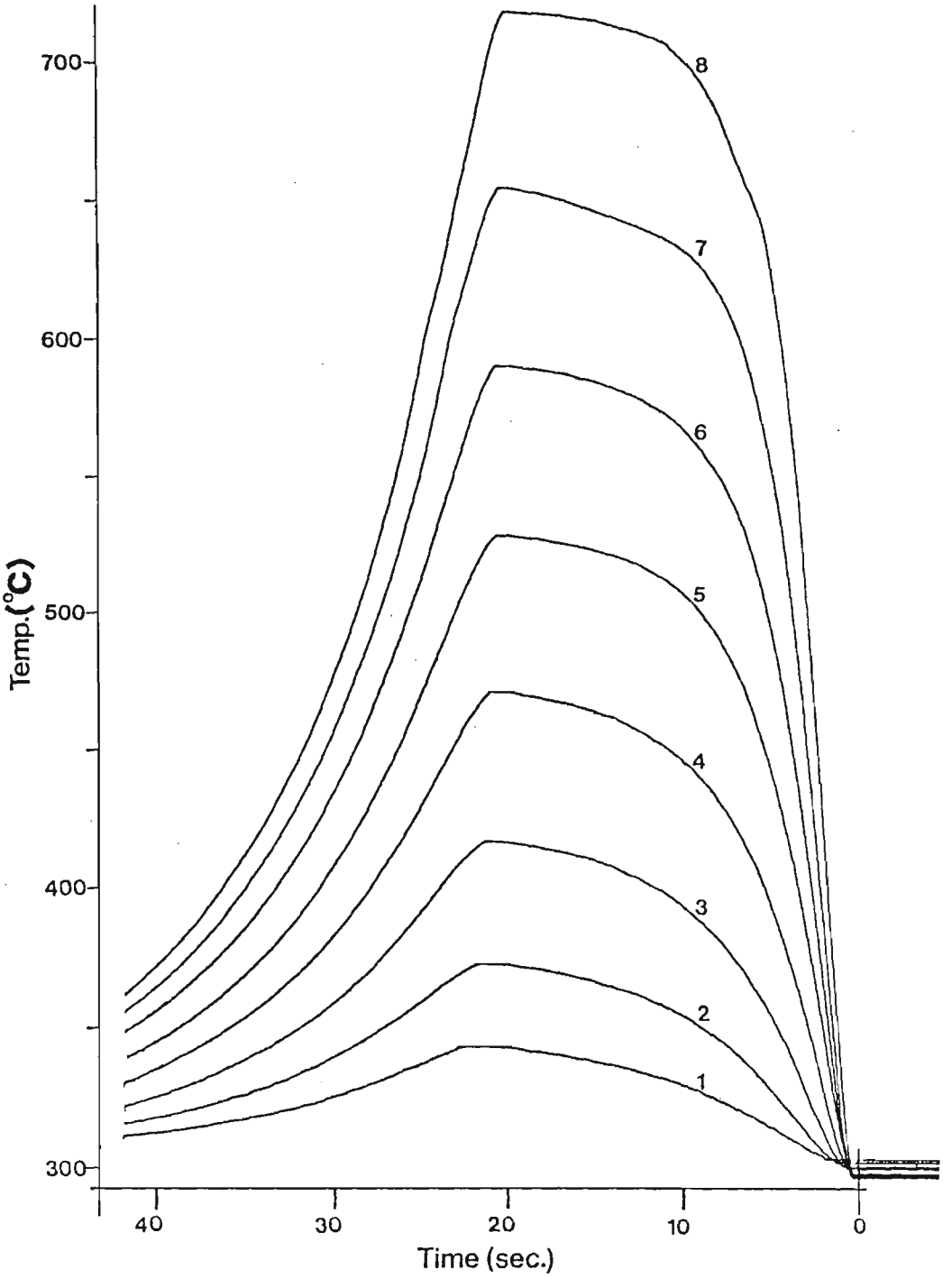

Figure 3-6.

Profiles of quartz-tube temperatures for platinum pyroprobe heater coil operated in the flash-pyrolysis mode. Curves 1-8 correspond to CDS controller dial settings of 300, 400, 500, ..., 999 respectively.

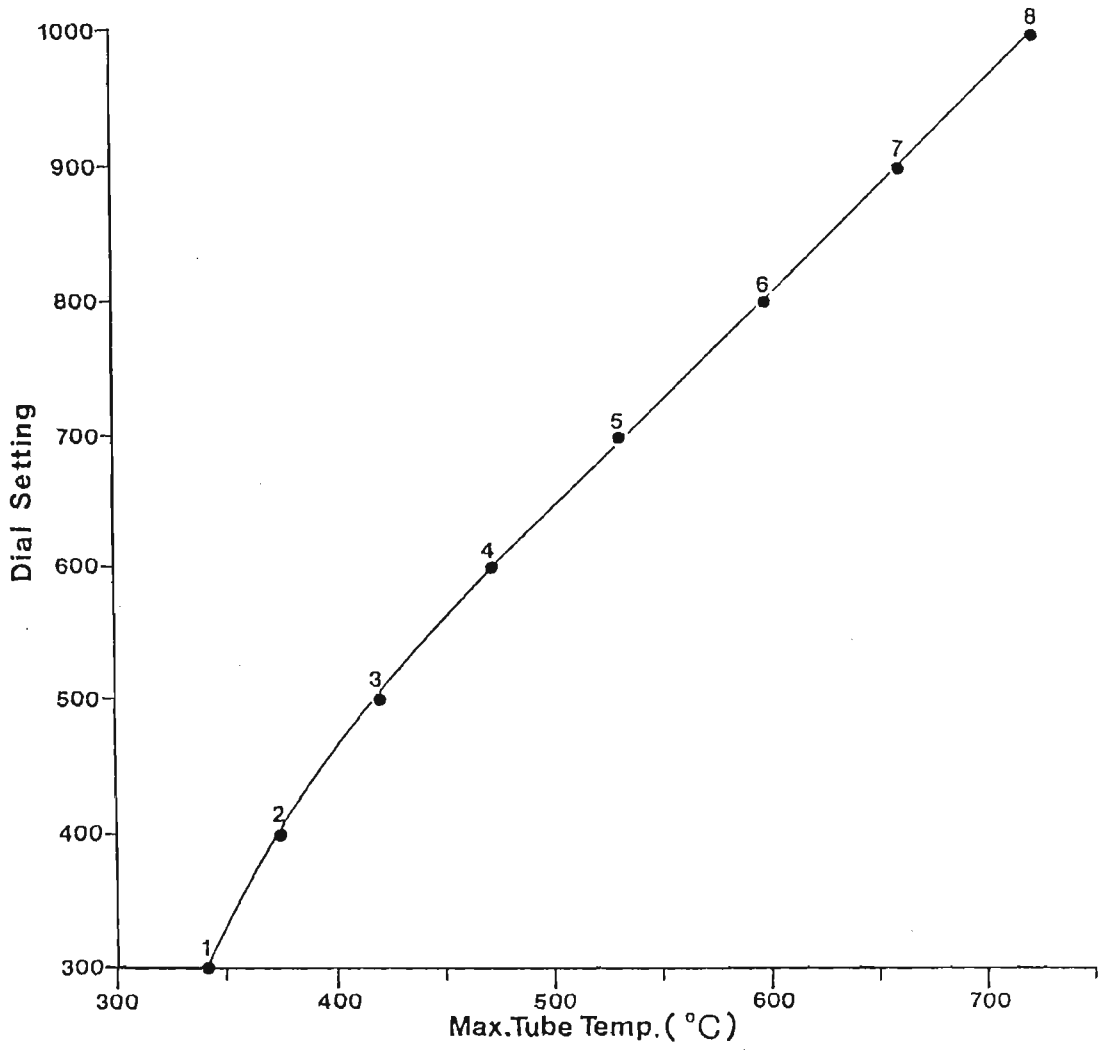

Figure 3-7 .

Plot of CDS pyroprobe dial-setting against maximum quartz-tube temperature attained during flash-pyrolysis. Maximum temperatures reached were obtained from appropriate curves 1-8 of Figure 3- 6 .

3.5.2 Pyrolysis gas chromatography

Finely crushed raw oil shale samples were flash-pyrolysed using a CDS 150 Pyroprobe and those instrument settings previously chosen to calibrate the platinum pyrolysis coil (final-temperature dial setting: 750). Quantities of shale, dependent on the richness of respective samples but usually within the range of 0.5 - 3 mg, were placed in a quartz pyrolysis tube (25mm x 2mm i.d.), which was then plugged at both ends with quartz wool. Prior to use this wool had been solvent extracted (CH_2Cl_2), DMCS deactivated and subsequently baked out (1h) in a muffle furnace at 800°C. The pyroprobe was introduced directly into the 1/4" injection port of a Varian 3700 gas

chromatograph, fitted with a splitter insert, cut down to accommodate the pyroprobe. Following lock-down of the probe shaft the sample was allowed to equilibrate for 10 s, after which the pyrolysis process was initiated. At the end of this period (20 s) the GC carrier gas was changed from helium to hydrogen, using a three-way switching valve, and the GC temperature program started. The carrier gas was changed back to helium once the analysis had been completed. This provided time adequate for reequilibration from hydrogen to helium during the GC cool-down phase (~10 min). All other GC operations and conditions were as described in section 3.4.1.

3.5.3 Pyrolysis-FID.

Although the CDS Pyroprobe platinum coil functioned satisfactorily for small samples (up to ~5 mg), its low thermal mass, axial thermal gradient and relatively slow heating rates were obvious limitations. To overcome at least some of these problems the platinum wire was replaced with a heater made from nichrome ribbon. 12 cm of nichrome ribbon (20 ohm m^{-1}) were wound tightly onto a 2.1 mm drill shaft (16 turns) and the preformed coil spotwelded to the pyroprobe. The finished heater is a closely spaced coil of comparatively high thermal mass which exhibits uniform heating along its entire axis; consequently it can accomodate samples up to 20 mg. The heater was calibrated as previously described, with appropriate CDS control-circuit potentiometers adjusted to compensate for the change in resistance between the two different coils. Figure 3-8 (a) shows the quartz-tube temperature profiles obtained for dial settings of 400, 500, 600 and 700 respectively, after the control circuits had been adjusted to produce an optimum heater response for the 500°C dial setting. As can be seen from the plots, the heater produces minimal temperature overshoot for that setting and exhibits a heating rate of ca. 4000°C min^{-1}, almost 4 times faster than that obtained for the platinum coil.

The CDS control circuits were further modified, and a temperature-ramp rate selection switch (two positions: x 1 and x 0.01) installed on the front panel of the instrument. By selecting one of the two switch positions, the probe functioned as either a flash-pyrolysis unit, or generated slow temperature ramps at rates roughly equivalent to 0.01 times the selected ramp dial setting. In practice linear heating rates of 9°C min^{-1} and 25°C min^{-1} were used to simulate the retorting of oil shales and to evaluate their oil and gas generating capacity by pyrolysis-FID (Figure 3-8 (b)).

To evaluate the oil and gas potential of oil shales, a known weight (1-2 mg) of air-dried raw shale was loaded into a quartz pyrolysis tube as described previously. The probe was then pushed into the injection-port of the gas-chromatograph (300°C) and locked-down. For pyrolysis-FID work the splitter was removed from the injection-port and the total products swept directly to the FID via a length of 1/16" o.d. deactivated glass-lined steel tubing (40 cm x 0.4 mm i.d.). To avoid product condensation in this transfer tubing the GC oven was held at 300°C throughout the procedure. The selectivity of the detector and the use of an integrator ensured that very accurate area values were

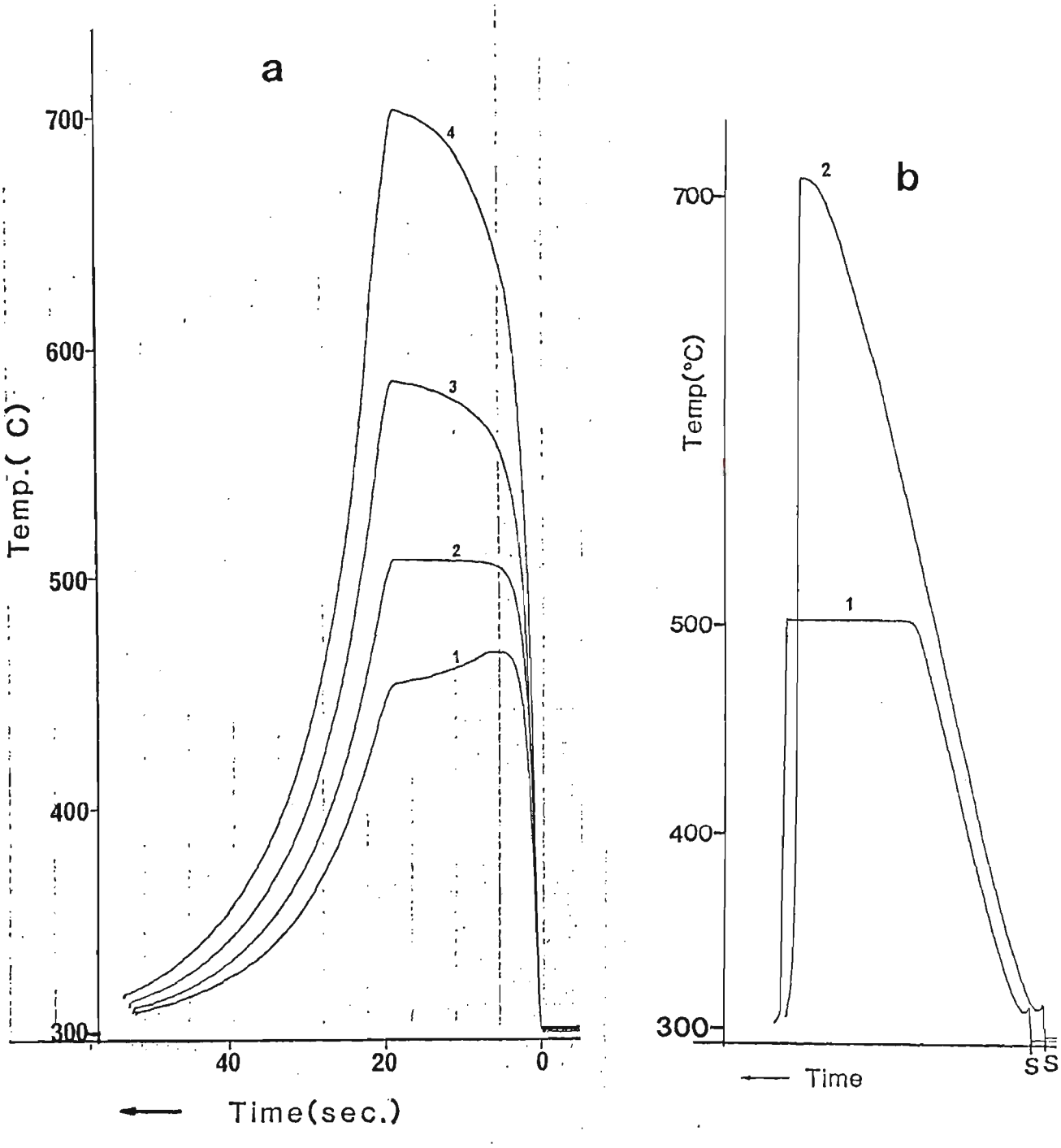

Figure 3-8 (a).

Pyroprobe quartz-tube temperature profiles for nichrome-ribbon heater coil operated under flash-pyrolysis conditions. Curves 1-4 correspond to dial settings of 400, 500, 600 and 700 respectively.

Figure 3-8 (b).

Pyroprobe quartz-tube temperature profiles obtained using the nichrome-ribbon coil under programmed temperature conditions (20 min total duration). Curves 1 and 2 correspond to final-temperature dial settings of 500 and 700°C. Heating rates obtained were 9.6°C min^{-1} and 25°C min^{-1} respectively. S denotes the start of each temperature programme; profiles were deliberately offset.

obtained for the oil and gas produced. These area values were converted to areas per unit mass of raw shale and were used to compare oil and gas generating potential for shales analysed under identical conditions. To enable comparisons to be made between samples analysed on different days, the Duaringa 5391-C sample was analysed 5 times to establish reproducibility and then used each day as a reference sample.

3.5.4 Thermogravimetric analysis.

Thermogravimetric and differential thermal analyses of finely-crushed raw oil shale (10-20 mg) and kerogen samples (ca. 10 mg) were carried out on a Rigaku thermal analyser. Samples were loaded into open aluminium pans and heated in either air or nitrogen gas to a final temperature of 600°C at a rate of 10°C min^{-1} (cf. rates used for oil shale retorting). The instrument was operated in the thermogravimetric-differential mode and TGA-DTA profiles were recorded simultaneously against Al_2O_3 reference material. Weight loss data from the pyrograms were normalised and plotted to predict kerogen type and to assess the oil and gas potential for the raw shale. Two raw oil shale samples were analysed in aluminium pans fitted with pin-holed crimped lids to assess the influence of a confined pyrolysis environment (increased product residence time) on their TGA-DTA curves.

3.6 CHEMICAL CHARACTERISATION OF SHALE OIL.

3.6.1 Asphaltenes.

Freshly retorted shale oil (2 g) was added to distilled pentane (20 mL) in a pyrex screw-neck culture tube (# 9826), vortex-mixed (2 min) and then allowed to stand for 1 h. The mixture was vortex-mixed for a further 2 min and again allowed to stand for 1h, then centrifuged and the supernatant decanted. The pentane insoluble material (asphaltenes) was transferred to a 5 mL Reactivial. The asphaltenes were vortex-mixed with fresh pentane (5 x 3 mL) and centrifuged. The isolated asphaltenes (ca. 20 mg) were dried to remove traces of solvent (50°C, 30 min) and retained for further studies.

3.6.2 Acid-base extraction.

Freshly retorted shale oil (1.5 g) was added to dichloromethane (20 mL) in a pyrex screw-neck culture tube (#9826) and vortex-extracted (2 min) with saturated sodium bicarbonate (3 x 2 mL), followed by distilled water (1 x 4 mL). The oil solution was retained and the aqueous extracts combined (culture tube #9826), saturated with sodium chloride and extracted with hexane (3 x 2 mL). The hexane extracts (containing water soluble neutrals and bases) were combined and dried ($MgSO_4$). The aqueous phase was acidified to pH <1 with 10N HCl and extracted with dichloromethane (3 x 10 mL). The

extracts, containing **carboxylic acids,** were pooled and dried ($MgSO_4$) and the aqueous phase discarded. The hexane was removed using a gentle stream of dry nitrogen (20°C). The acids were quantified gravimetrically and then converted to their methyl esters using 14% BF_3-MeOH (30 min at 100°C). The mixture was cooled, diluted with 1 mL of distilled water and the methyl esters vortex-extracted into hexane (2 mL). The hexane extract was dried ($MgSO_4$), centrifuged and the solution transferred to a clean vial. The solvent was evaporated under dry nitrogen until a concentration suitable for GC analysis was obtained.

The retained oil solution was vortex-extracted with 3M sodium hydroxide (3 x 2 mL), and distilled water (1 x 4 mL). The aqueous extracts were pooled (culture tube #9826), acidified to pH <1 with 10N HCl and extracted with hexane (3 x 10 mL). The aqueous phase was then discarded. The combined hexane extracts (containing **phenols**) were dried as above and the solution concentrated (dry nitrogen gas) to a component level suitable for GC analysis. Phenols extracted from the oil were quantified gravimetrically, or using GC quantitation with an internal standard (cf. section 3.6.4).

The remaining oil solution was vortex-extracted with 5N HCl (3 x 5 mL), distilled water (1 x 5 mL) and retained. The aqueous extracts were combined (culture tube #9826) saturated with sodium chloride and extracted with hexane to remove any water soluble neutrals (3 x 2 mL); the hexane extracts were pooled and dried as above. The remaining aqueous extract was basified to pH >10 and extracted with hexane (3 x 5 mL) to recover the basic components. The aqueous phase was discarded. The extract was dried ($MgSO_4$) and the solvent evaporated under a stream of dry nitrogen until concentrations of **bases** suitable for GC analysis were obtained, or completely for gravimetric quantitation.

3.6.3 Column chromatography.

The neutral shale oil solution was dried ($MgSO_4$), filtered and reduced in volume to ca. 3 mL under a stream of nitrogen at room temperature. The viscous oil solution was warmed gently with a hair dryer and applied to a combined alumina-silica column packed with pre-extracted (dichloromethane) activated adsorbents. To check for possible adsorbent contaminants, which could show up in the column eluates, the activated adsorbents were vortex-extracted with each of the previously analysed solvents (mixtures) of the eluant series. Each extract was filtered, concentrated and analysed by GC. The chromatography column (120 x 1.5 cm i.d.) was slurry-packed in hexane according to Regtop et al., (1982) with alumina (23 g, neutral activity 1, activated 12 h at 300°C) overlying silica gel (58 g Kieselgel 60, 70-230 US mesh, activated 12 h at 130°C). To obtain uniform packing densities for the respective adsorbents, the glass column was vibrated during slurry-packing until reproducible packing heights (silica: 86 cm, alumina: 105 cm) were obtained. These levels were indicated on the column and were used as calibration marks

for all subsequent column chromatography (Figure 3-9).

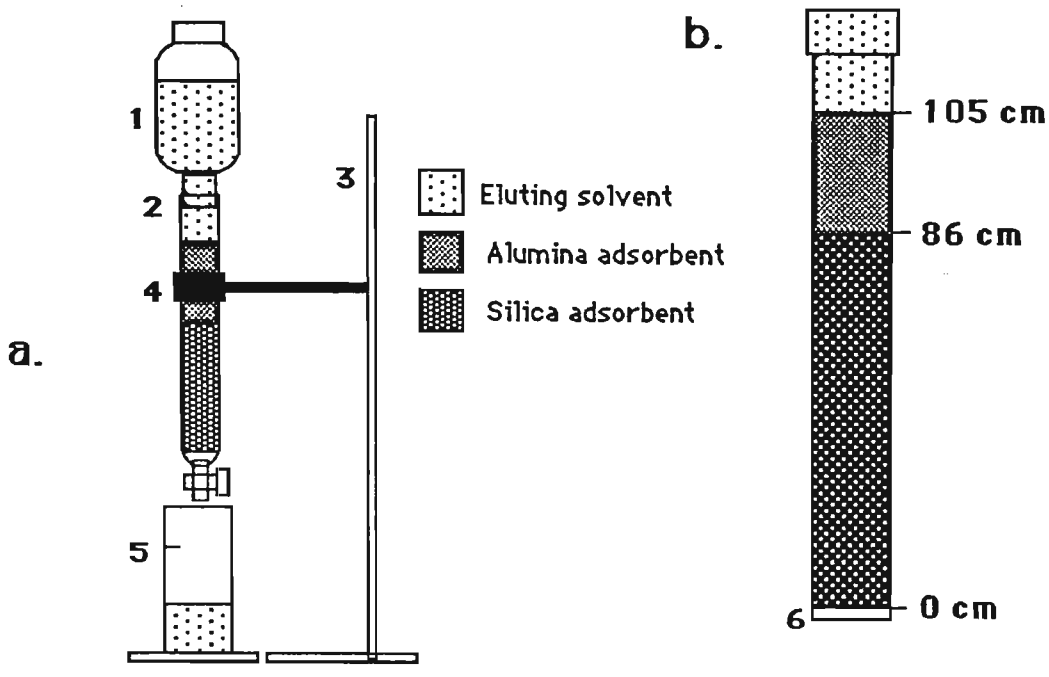

Figure 3-9.
Schematic diagram of the chromatographic separation of shale oil. The gravity-fed column assembly (**a**) comprises: 1, solvent reservoir; 2, adaptor; 3, retort stand; 4, glass column; 5, collection vessel (appropriate measuring cylinder). The adsorbent packing-heights indicated in (**b**) are relative to the column frit (6).

Shale oil components were eluted from the column using an eluotropic series of solvents and mixtures. Appropriate eluate volumes were collected in suitable measuring cylinders and the fractions concentrated to ca. 4 mL. using either a rotary evaporator (30°C, 4.7 kP), or dry nitrogen, or both. The reduced fractions were transferred to amber screw-cap vials (4 mL) and, where necessary, concentrated at room temperature under a gentle stream of dry nitrogen to a level suitable for GC and GC-MS analysis. For quantitation, fractions were further evaporated under dry nitrogen and the pre-tared vial monitored gravimetrically until an abrupt change was observed in a weight-time plot..

The chromatographic solvent program used was that adopted by Rovere et al. (1983) and comprised the column fractions, elution volumes and eluants listed in Table 3-1.

TABLE 3-1. Fraction, elution volume and eluant correspondence for the column chromatographic separation of neutral shale oil components.

FRACTION	VOLUME (mL)	ELUANT
0	0-95	hexane
1	95-125	hexane
1	125-130	hexane
2	130-135	hexane
2	135-140	hexane
3	140-145	hexane
3	145-175	hexane
4	175-215	hexane
5	215-315	hexane
6	315-400	hexane
7	400-450	hexane
8	450-500	hexane
9	500-600	hexane
10	600-750	hexane-dichloromethane (9:1, v/v).
11	750-850	hexane-dichloromethane (9:1, v/v).
12	850-1000	hexane-dichloromethane (4:1, v/v).
13	1000-1100	hexane-dichloromethane (4:1, v/v).
14	1100-1350	dichloromethane
15	1350-1600	dichloromethane-chloroform (9:1, v/v).
16*	1600-1750	chloroform-ether (9:1,v/v).
17	1750-1850	chloroform-ether (9:1,v/v).
18	1850-2100	ether
19	2100-2250	methanol

* Two distinct brown bands were resolved in this fraction and were collected separately.

Solvents (mixtures) were changed whenever the preceding eluant had reached a level 1 cm above the column packing. Fraction 0 represents the column void volume and was discarded. Aliquots of fractions 1 and 2, containing alkanes and alkenes respectively, were evaporated at room temperature under a stream of dry nitrogen and dissolved separately in cyclohexane (5 mL). Molecular sieve (2 g, 0.5 nm; preheated at 300°C for 5 h) was added and the solutions refluxed for 6 h. The molecular sieve, containing occluded linear components, was removed by filtration. The filtrates, containing branched and cyclic compounds, were evaporated under dry nitrogen to concentrations suitable for GC and GC-MS analysis.

3.6.4 Gas chromatographic determination of phenol in shale oil.

A standard solution of phenol (30 mg in 3.5 mL CH_2Cl_2) was prepared and stored in a 4.5 mL amber screw-cap vial fitted with an open-top cap and two teflon-lined silicon -rubber septum seals. An aliquot (50 µL) of a benzyl alcohol stock solution (300 mg in 3. mL CH_2Cl_2) was added to the phenol solution through the septum seals and the mixture

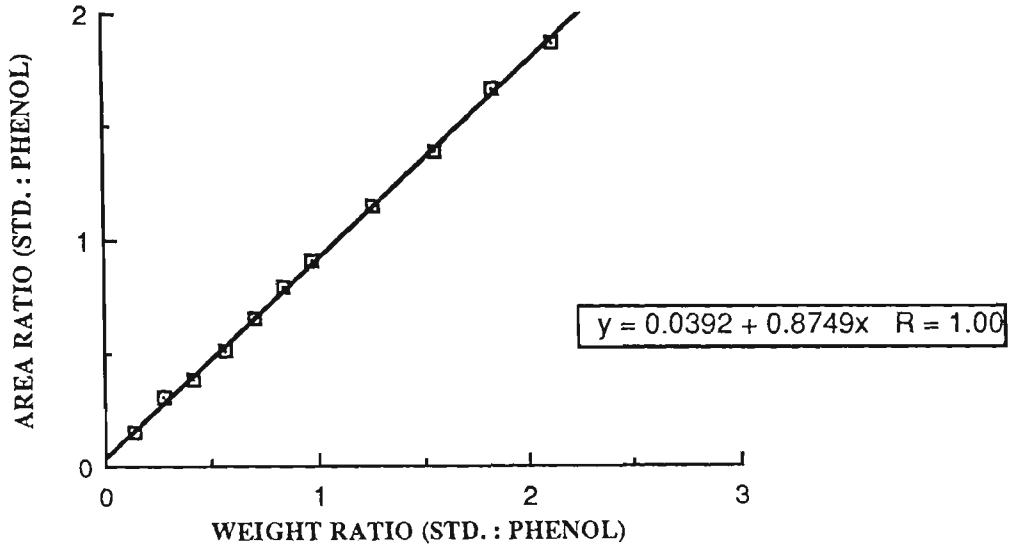

Figure 3-10.
Mass ratio versus area ratio plot for benzyl-alcohol (std.) and phenol. Area values were obtained from gas chromatographic data using a BP-5 fused-silica capillary column. Calibration curve equation was obtained by linear regression analysis of the data.

analysed by GC (split ratio: 10:1, oven temperature 150°C isothermal). Both compounds were found to be chromatographically pure since each produced only one component peak in the GC profile. Benzyl alcohol was chosen as a standard for GC quantitation because it has a structure similar to that of phenol and has suitable retention characteristics (on a BP-5 capillary column the alcohol is well resolved and elutes between phenol and

2-methylphenol). Further aliquots of standard were added to the previous mixture and the solution analysed as above after each addition (aliquots 8-11 comprised 100 µl each). The eleven mixtures analysed cover the wide range of phenol concentrations likely to be found in shale oil extracts. Alcohol : phenol mass and area ratios were plotted against each other and the calibration curve determined by linear regression analysis (Figure 3-10). Using the slope and intercept values given in the figure, the mass of phenol present in the the appropriate fraction from an oil shale extract is given by:

mass of phenol = 0.875 x (mass of std. added) / (area ratio - 0.0392).

A schematic diagram of the analytical sequence used for the chemical characterisation of oil shale and shale oil is given in Figure 3-11.

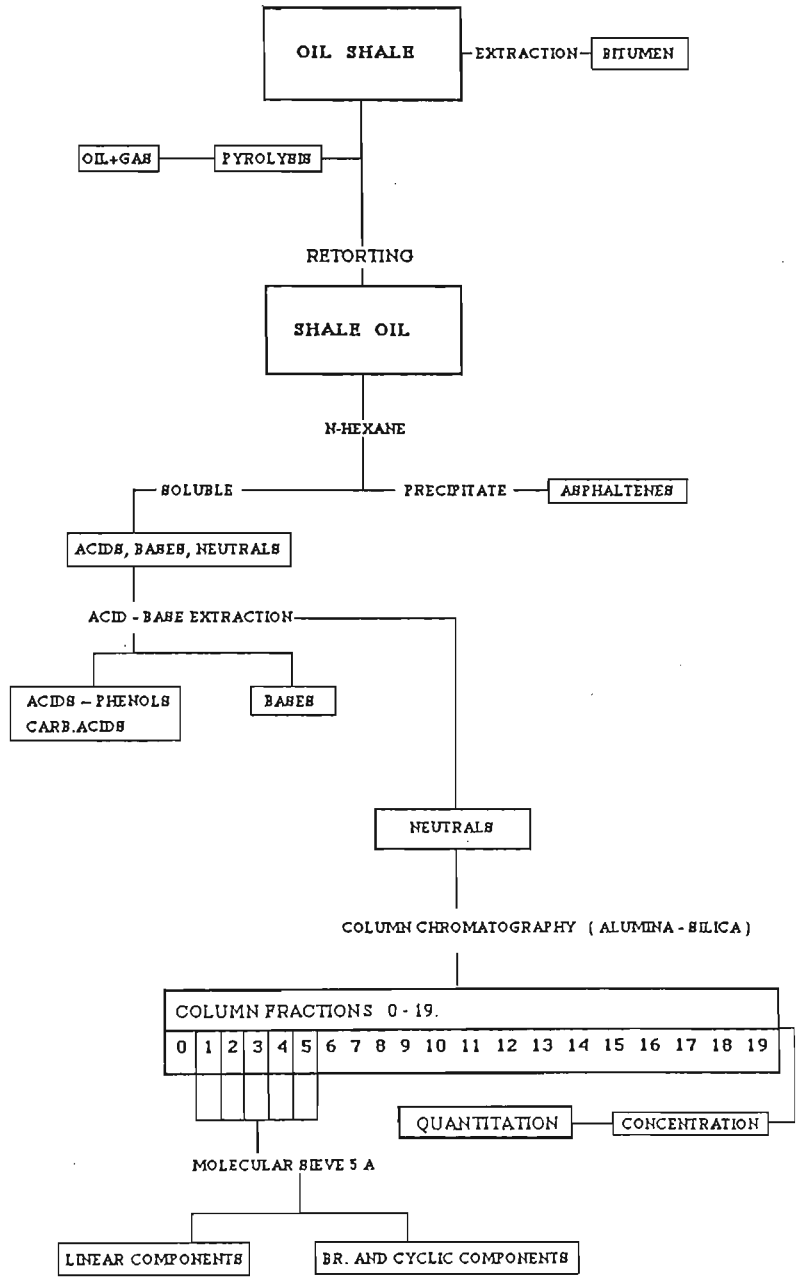

Figure 3-11.
Schematic diagram of the analysis sequence used for the chemical characterisation of oil shale and shale oil from the Duaringa deposit.

3.7 Oxidation of Prist-1-ene.

Prist-1-ene ((6R,10R) - 2,6,10,14 - tetramethylpentadec-1-ene) - (0.2g) was refluxed with acidified $KMnO_4$ (1g, 5h) in acetone (20mL). The $KMnO_4$ was added stepwise (ca. 0.1g) after each previous portion had been reduced. Distilled water (20mL), pre-extracted with hexane, was added and the acetone and volatile oxidation products recovered by distillation. The distillate was collected in a pear-shaped flask kept at 0°C. The residual aqueous phase was extracted with hexane (2x 20mL) filtered and dried ($MgSO_4$). The pooled hexane extracts were concentrated (ca. 1.5mL) and analysed using GC and GC-MS. Prist-1-ene remaining in the hexane extract was separated from more polar products (isoprenoid ketones) by column-chromatography on alumina (6g, neutral). Fraction 1 was eluted with 3 bed volumes of hexane (ca. 20mL). Fraction 2 was eluted with chloroform-hexane (3:1 v/v, 30mL). Both fractions were concentrated as above and analysed using GC and GC-MS where necessary.

Acidic compounds present in the aqueous phase (pH 9) were recovered by extraction (hexane, 2x 10mL) after acidifying the solution (HCl, pH 1) and saturating with NaCl. Recovered carboxylic acids were converted to their butyl esters (Rovere, 1980) and methyl esters (BF_3-MeOH). Derivatised acids were analysed using GC and GC-MS.

CHAPTER FOUR : CHEMICAL CHARACTERISATION OF OIL SHALE AND SHALE OIL FROM THE DUARINGA DEPOSIT QUEENSLAND, AUSTRALIA.

The bipartite Duaringa oil shale deposit comprises two resource seams (within an upper unit) and a lower unit consisting of several thin oil shale seams interbedded with carbonaceous oil shale, brown coal and claystone. The locality, history, geology, organic petrology, environment of deposition and development status of the resource were detailed in section 1-5.

Oil shales studied for the Duaringa deposit are listed in Table 4-1. Specimens were supplied by the venture partners SPP/CPM through Dr. A. Hutton (Geology Dept., University of Wollongong), who also provided data on their organic petrology (Table 4-2, 4-3).

All samples were analysed as received using (mainly) fast characterisation techniques such as solvent extraction, GC, pyrolysis-GC(-MS), pyrolysis-FID, TGA, etc. Data obtained from a large number of complementary (screening) procedures should allow samples to be categorised on the basis of observed similarities or differences. Two oil shale samples, 5391-C and 686, were fully characterised including GC-MS analysis of their open-column shale oil fractions. This is essential for the former oil shale since it represents a resource-seam sample with economic potential. The latter was studied in detail to determine the effects, if any, of deeper burial on oil shale and shale oil characteristics. It was chosen for comparison because its mineralogy and maceral analysis was very similar to that of 5391-C, with burial depth and time possibly the only major differences between the two samples.

4.1 Oil shale petrology.

Samples 5391-C to 812 (Table 4-1) are grey to olive-green oil shales comprising dominantly clay-sized quartz and clay minerals (95 % montmorillonite and 5 % illite), with

accessory apatite and pyrite (< 1 %). Sample 674 is a dark brown oil shale composed of four lithologies (lamosite, coal, carbonaceous lamosite and claystone) comprising dominantly clay-sized quartz and clay minerals (55 % montmorillonite, 30 % kaolinite and 15 % illite) with accessory apatite and anhedral pyrite (< 1 %).

TABLE 4-1. Sample designation, location and burial depth of oil shales studied for the Duaringa deposit, Queensland, Australia.

SAMPLE	LOCATION*	DEPTH (m)
5391-C	DD-51	86 - 88
686	GSQ-Duaringa 1-2R	1023 - 1026
789	GSQ-Duaringa 1-2R	86 - 90
822	GSQ-Duaringa 3-5RD	97 - 99
812	GSQ-Duaringa 3-5RD	95 - 97
674	GSQ-Duaringa 1-2R	920 - 922

* See location map Figure 1-11 (b). In the diagram drill-sites DD-51, 1-2R and 3-5RD are denoted by ■ and ● respectively.

TABLE 4-2. Maceral composition for the Duaringa oil shale samples.

	MACERAL ANALYSIS* (VOLUME % OF WHOLE ROCK)						
SAMPLE	LAM.	TEL.	VIT.	SPO.	S.FR.	PYR.	M. MATTER
5391-C	25.0	1.6	0.6	tr.			72.8
686	24.6	1.2	0.2	tr.	1.2	1.2	71.2
789	10.8	4.2	1.2	tr.	tr.	0.2	83.6
822	24.2	3.0	0.8	tr.		0.2	71.8
812**	14.0	2.0					84.0
674**	27.0		14.0				58.0

* Apart from the macerals tabulated above, sample 686 contained 0.4 % (v/v) of bitumen blebs and 674 contained 1 % resinite (v/v). ** Data from Crisp et al. (1987).

Abbreviations : LAM.- lamalginite, **TEL.** - telalginite, **VIT.** - vitrinite, **SPO.** - sporinite, **S.FR.** - shell fragments, **PYR.** - pyrite, **M.MATTER** - mineral matter, tr. - trace level.

Samples 5391-C to 822 (Table 4-2) have similar organic assemblages dominated by yellow to yellowish-green fluorescing lamalginite (rarely orange fluorescence - lamellae 0.02 - 0.1 mm long) derived in part from at least three species of the colonial alga *Pediastrum* , with small contributions from larger lamalginite of unknown affinity (yellow fluorescence 0.06 - 0.2 mm diameter) and telalginite with yellow fluorescence (< 0.4 mm diameter) derived from *Botryococcus*. Other macerals are found at very low to trace levels (Table 4-2). Sample 674, from the lower oil shale unit of GSQ-Duaringa 1-2R, is differentiated from the others by a very high percentage of vitrinite and a much higher vitrinite reflectance value (Table 4-3).

TABLE 4-3. Vitrinite reflectance data for Duaringa oil shale samples.

SAMPLE	MEAN MAX. REFL. (%).	RANGE	NO. OF READINGS	S.D. (n>10)
5391-C	0.19	0.12 - 0.31	16	0.06
686	0.26	0.22 - 0.30	12	0.02
789	0.25	0.20 - 0.26	21	0.04
822	0.23	0.21 - 0.26	17	0.05
812*	0.18	0.16 - 0.20		
674*	0.40	0.29 - 0.51		

* Data from Crisp et al. (1987).

4.2 Elemental composition of kerogen and shale oil.

The elemental composition for some of the retort oils and kerogens from the Duaringa resource are listed in Table 4-4. The retort oils were obtained using the stainless steel retort and tube-furnace, while the kerogens were produced by HCl-HF demineralisation of the raw shale. Analyses were carried out by Analytische Laboratorien (FGR), unless stated otherwise. All kerogen compositions were calculated on an ash-free basis. Those data obtained from Crisp et al. (1987) (footnote Table 4-4) are from duplicate

or triplicate analyses of the kerogens and have been adjusted for residual FeS_2, TiO_2, $ZrSiO_4$ and fluorides. Compositional data for other Duaringa resource samples are given by Lindner (1983).

TABLE 4-4. Elemental composition of Duaringa shale oils and kerogens.

SAMPLE	% C	% H	% N	% O	% S	H/C	O/C
5391-C (O)	85.64	11.92	0.99	1.12	0.37	**1.67**	**0.01**
686 (O)	82.42	11.96	0.92	3.38	0.97	**1.74**	**0.03**
789 (O)	85.40	11.79	1.04	1.37	0.28	**1.66**	**0.01**
822 (O)	84.34	12.10	1.13	1.82	0.38	**1.72**	**0.02**
674 (O)**	82.8	11.40	1.11	4.08	0.53	**1.65**	**0.04**
5391-C (K)*	71.64	9.67	1.90	16.78		**1.62**	**0.18**
686 (K)*	74.88	10.03	1.92	13.16		**1.61**	**0.13**
812 (K)**	74.1	9.58	1.60	13.8	0.89	**1.55**	**0.14**
674 (K)**	71.5	7.26	2.42	17.3	1.53	**1.22**	**0.18**

O = shale oil. K= kerogen.

* The percent elemental values were calculated on an ash- and sulphur-free basis to compensate for mineral residues and to exclude the contribution of sulphur from pyrite (the original elemental analysis figures did not differentiate between sulphur from pyrite or the kerogen).

** Elemental analysis values were taken from Crisp et al. (1987). Percentage values for oxygen were obtained by difference. Sulphur values were adjusted for residual pyrite.

Because sample preparation and subsequent analyses are both time consuming and costly, elemental analysis cannot be regarded as a rapid screening procedure which is routinely available; consequently only those samples considered most informative were analysed. Even when available, compositional data is (usually) not very precise and lacks the ability to resolve globally similar material disparate at the molecular level. For typing

and identifying kerogen source material not too much should be expected from it alone and it needs to be used in conjunction with other relevant analytical techniques; however, H/C ratios do give an indication of the aromatic nature of the sample.

Atomic ratios H/C and O/C for the kerogens were plotted on a van Krevelen diagram (Figure 4-1) to assess both the type and relative evolution (maturation) of the respective samples. The van Krevelen diagram is a practical means for the interpretation of the origin and evolution of sedimentary organic matter (cf. section 1.1.7) but again only in conjunction with data obtained from other techniques for the characterisation of kerogen. In the absence of other relevant information, the position of a singe sample or those for an unrelated series of samples is limited because elemental analysis provides only average compositional data and is inherently unable to distinquish between mixtures of different types in the one sample.

An interpretation of the position of samples 5391-C, 812 and 686 on the diagram suggests that all are highly-aliphatic type I kerogens, with the latter two more evolved than the former as indicated by their relative positions (displaced along the oxygen axis), consistent with defunctionalisation of oxygen moieties due to diagenetic changes. In the absence of geological data one cannot attribute the relative position for 686 solely to increased maturation due to burial (Table 4-1), since kerogen from sample 812 occupies a similar position on the diagram but originates from a shallow resource seam. Given that elemental oxygen values for 812 (and 674) were obtained by difference, errors inherent in this calculation may have had an effect on its position on the graph, particularly since oxygen values are in general less reliable than C and H data. Further uncertainties in elemental composition may arise as a consequence of the heterogeneity of the samples. In light of these comments and vitrinite reflectance data, which indicates an evolutionary stage of diagenesis for both, it seems reasonable to associate the relative positions of 812 and 686 predominantly with variations in organic matter for the former and a combination of this, and deeper burial, for the latter. Sample 674, on the contrary, is relatively poorer in hydrogen content. In conjunction with its petrology (particularly the maceral analysis) its position on the diagram is consistent with the incorporation of a

greater percentage of higher plant material in the organic matter and is relatable to a mixed type I (ca. 66 % - liptinite) and type III (ca. 33 % - vitrinite) kerogen, with overall properties expected to reflect this composite nature.

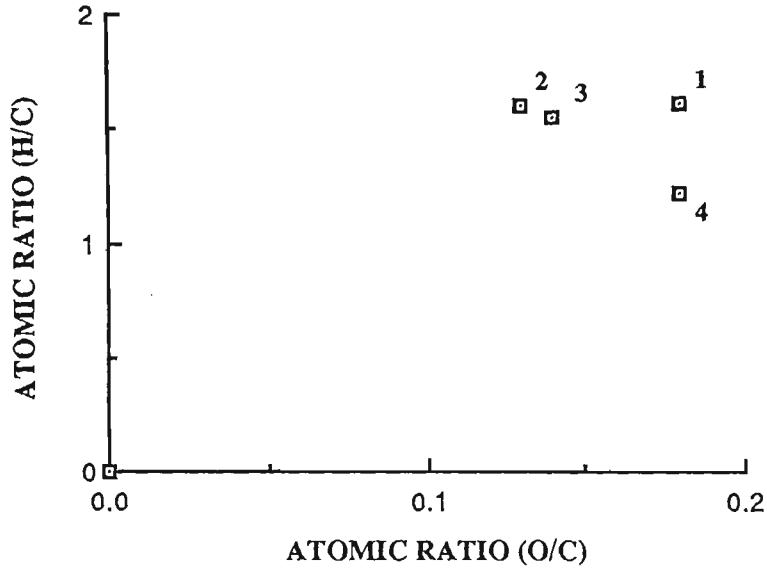

Figure 4-1.

Van Krevelen diagram for kerogens 5391-C (1), 686 (2), 812 (3) and 674 (4).

4.3 Solvent extracts (bitumen analysis).

Lipids deposited in lacustrine environments are derived from biological systems which may be autochthonous (planktonic and benthic vegetation), allochthonous (mainly higher plant vegetation from surrounding land areas) or detrital (material eroded from geological deposits). These diverse organic inputs may survive unaltered or be modified either by biota in the water column, or through biological or chemical alteration during diagenesis. Changes in the trophic status of the aquatic environment produce variations in composition of source materials and sedimentation rates affecting the preservation of lipid

components (Didyk et al. 1978). Certain lipids become inextractable from the sediment as a result of physical and/or chemical entrapment in the evolving kerogen or in the mineral matrix (Nishimura, 1977). Both bound and free lipids can provide valuable information about the biological inputs to sediments and their depositional environments, with the latter ideally suited to fast characterisation procedures. Lipidic fractions recovered from mixed biological sources usually contain compounds with similar chemical properties such as long-chain hydrocarbons, free fatty acids, alcohols and ketones. The common characteristic for fatty esters, acids and alcohols is that they contain an even number of carbon atoms, which is the result of their biosynthesis by means of acetyl-S-coenzyme A, which operates by successive additions of two carbon atoms (Vandenbroucke, 1980).

All Duaringa oil shale samples were extracted with dichloromethane as described earlier. Four of the samples (5391-C, 686, 789 and 822) were also soxhlet-extracted with dichloromethane (72 h) and compared with those above. Extracts of suitable concentration were analysed by GC, and various relevant parameters calculated from integrator data for each chromatogram (Table 4-5). Several of the extracts were analysed by GC-MS and the identity of components in other extracts subsequently inferred from relative retention data and the general appearance of the chromatogram.

In programmed-temperature gas chromatography, the simple expression of elution behaviour as retention relative to an arbitrary standard is not applicable, and the logarithmic relationship which exists under isothermal operation between *n*-alkane carbon number and retention in the Kovats Index is replaced by the approximately linear relationship:

$$RI = 100 \frac{T_u - T_C}{T_{C+1} - T_C} + 100\,C \qquad \ldots\ldots \quad (1)$$

where T_u is the retention time of the substance for which the retention index is to be calculated, T_C and T_{C+1} are the retention times for the linear alkane standards which bracket the substance of interest, and C is the number of carbons in the alkane that elutes just prior to the substance of interest (Lee et al., 1979).

The GC-profile for the ultrasonic extract from sample 5391-C (Figure 4-2a) shows a trimodal distribution of alkanes in the region C_{10} to C_{31} of the chromatogram, with local maxima at C_{11} and in the ranges C_{15} - C_{21} and C_{27} - C_{31}.

Regular isoprenoid alkanes are present at very low concentrations, although two isoprenoid ketones, identified by GC-MS as 6,10-dimethylundecan-2-one and 6,10,14-trimethylpentadecan-2-one in order of their elution, are very prominent. Cardoso and Chicarelli (1981) have suggested that the latter is an oxidation product of the labile alcohol phytol and that high relative abundances of acyclic isoprenoid ketones in conjunction with low concentrations of pristane and phytane are in keeping with oligotrophic conditions of deposition.

The extract is further characterised by a homologous series of linear alkanals ranging from nonanal to at least the C_{29}-aldehyde (Figure 4-4b, 4-5b, 4-6b). Modified Kovats retention indices (RI) were calculated for these components (equation 1) and a retention-index equation was obtained from the least-squares regression analysis of these data (Table 4-6, Figure 4-9a). Structural assignments for the alkanals were based on comparison with literature mass spectra and were verified from retention and GC-MS data for a mixture of standard linear aldehydes (Theta-Kit No.0151, Alltech Associates). The alkanals were found at comparatively high concentrations in the solvent extracts from all of the shallow oil shales studied and were present in 686, albeit at relatively lower concentrations. Quantitation of aldehydes relative to other components found in the extract was based on relevant discrete-peak areas in the total-extract profile. In general this is the most accurate approach for resolved constituents since it obviates the need for further separation-quantitation steps thereby reducing losses (volatile and labile components) attributed to sample handling.

Aldehydes have been rarely reported in sediments (Costa Neto et al., 1980; Dastillung et al., 1980; Cardoso and Chicarelli, 1981) and their origin is uncertain. The possibility of their formation during extraction or sample manipulation is excluded by their absence in other samples processed the same way. Chicarelli et al. (1984) cite the similarities between alkane, aldehyde and alkan-2-one distributions in their extracts from

Paraiba Valley oil shale, as first indications of the importance of microbial diagenesis in reworking the original biolipid profiles of this thermally unaltered sediment. They further report identification of alkan-2-ols in these samples, with a carbon number distribution qualitatively similar to the ketone profiles, to substantiate their conclusions. The authors used the correspondence of the alkanal distribution with those of alkanes extracted from Paraiba Valley oil shale to suggest a possible product-precursor relationship. Wils et al. (1982) have found long chain alkanals up to C_{28} in aerosol particulates and have postulated their formation by oxidation of epicuticular wax alcohols from terrestrial plants. Formation by oxidation of unsaturated acids has also been proposed (Gschwend et al., 1982).

Albaiges et al. (1984) have found small quantities of aldehydes and ketones in lagoon sediments, where these compounds occured as homologous series of alkanals and alkan-2-ones, ranging respectively from C_{14} to C_{30} and C_{21} to C_{31}. They point out that these compounds in coastal lagoons do not arise from primary plant input but as oxidation products of in-situ microbial activity. The authors found ketones in both free and bound fractions, whereas supposedly less stable aldehydes were only found in the bound fraction, from which they were released after saponification of the soxhlet-extracted sediment. Both bound and free lipids can provide valuable information about the biological inputs to sediments and their depositional environments, with the latter ideally suited to fast characterisation procedures. Their diagnostic use may be limited however since it has been suggested that bound lipids are characteristic of autochthonous sources, including bacteria, whereas those of free lipids are typical of terrestrial organic matter (Cranwell, 1978). Prahl and Pinto (1987) have studied long-chain aldehydes in Washington coastal sediments and consider these components to be common to depositional environments that receive substantial input of detrital organic matter from higher plants.

Regtop (1983) has studied the soxhlet extractable compounds (benzene-methanol 4:1 (v/v), 72 h) of oil shales from the Kerosene Creek seam of the Rundle formation. The bulk of the organics extracted comprised asphaltenes (66.2%) and polymeric material (8.7%). The balance (hexane-soluble fraction) was separated into various constituent classes using an open column procedure (silica-alumina) similar to that described earlier for

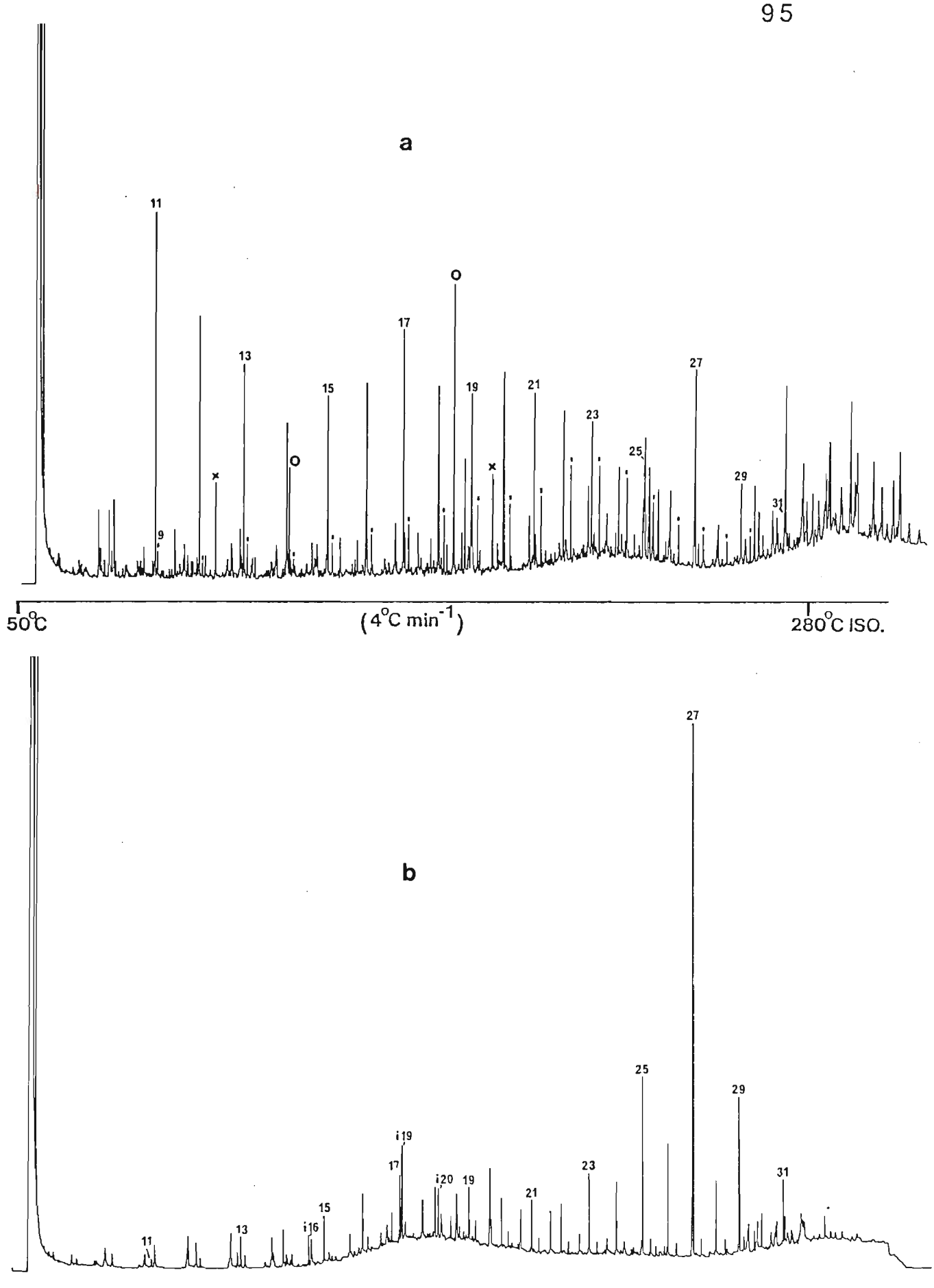

Figure 4-2.
Gas chromatographic profiles for the solvent extracts from Duaringa 5391-C (**a**) and 686 (**b**). Major components are linear alkanes with carbon numbers for odd alkanes indicated; alkanals from nonanal (**9**) are denoted by **ı** ; **x** denotes presumed artifacts; peaks denoted **o** are isoprenoid ketones, 6,10-dimethylundecan-2-one and 6,10,14 -trimethylpentadecan -2-one, in order of their elution; other components (alkanoic acids) are marked in Figure 4-3 to avoid obscuring peaks in the above profiles.

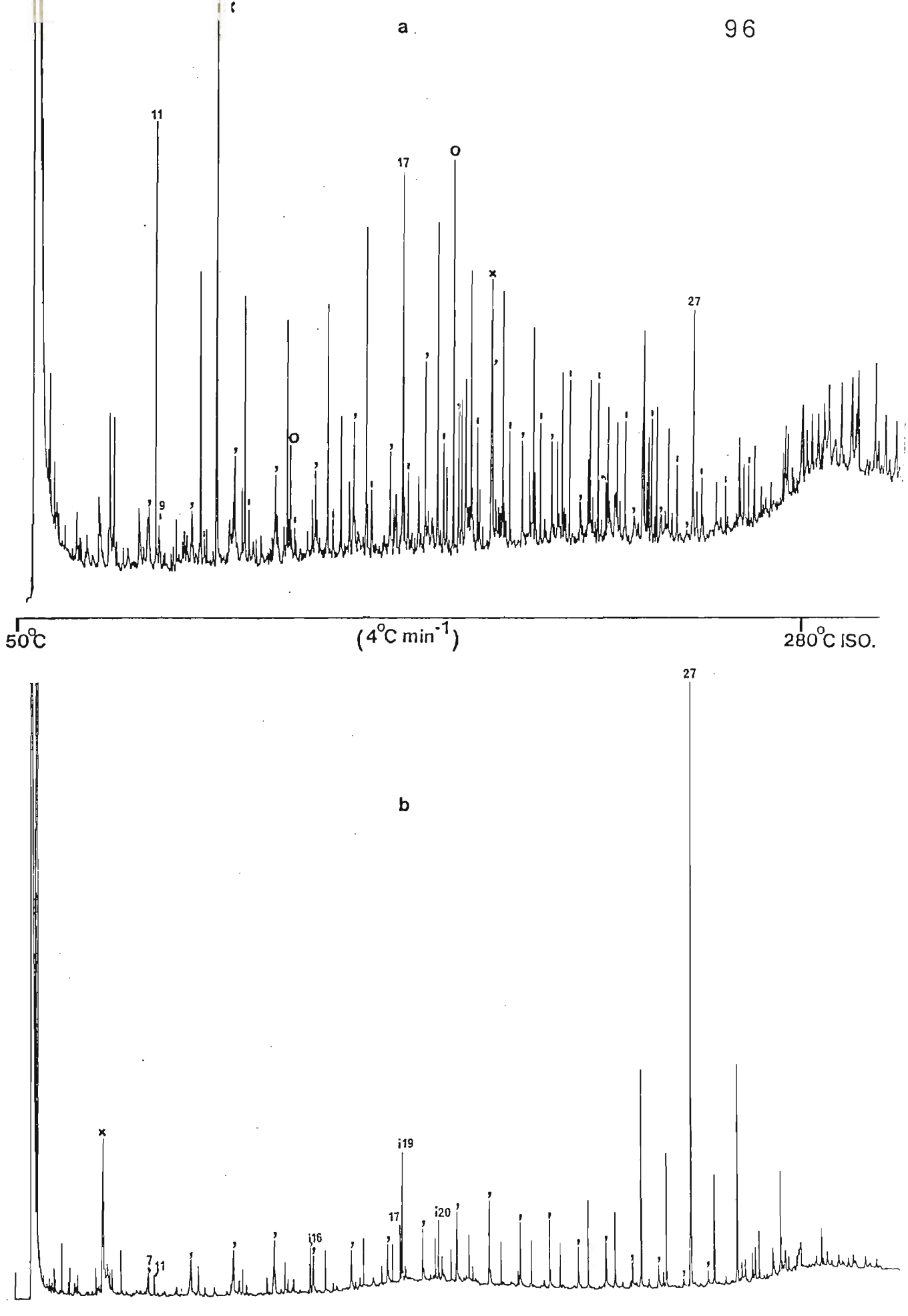

Figure 4-3.
Gas chromatographic profiles for the soxhlet extracts from Duaringa 5391-C (**a**) and 686 (**b**). Major components as in Figure 4-2 (key alkane components as marked); i19 and i20 in **b** are pristane and phytane respectively. Homologous series of linear alkanals (ı) from nonanal (**9**) and alkanoic acids (') from heptanoic acid (7) as indicated.

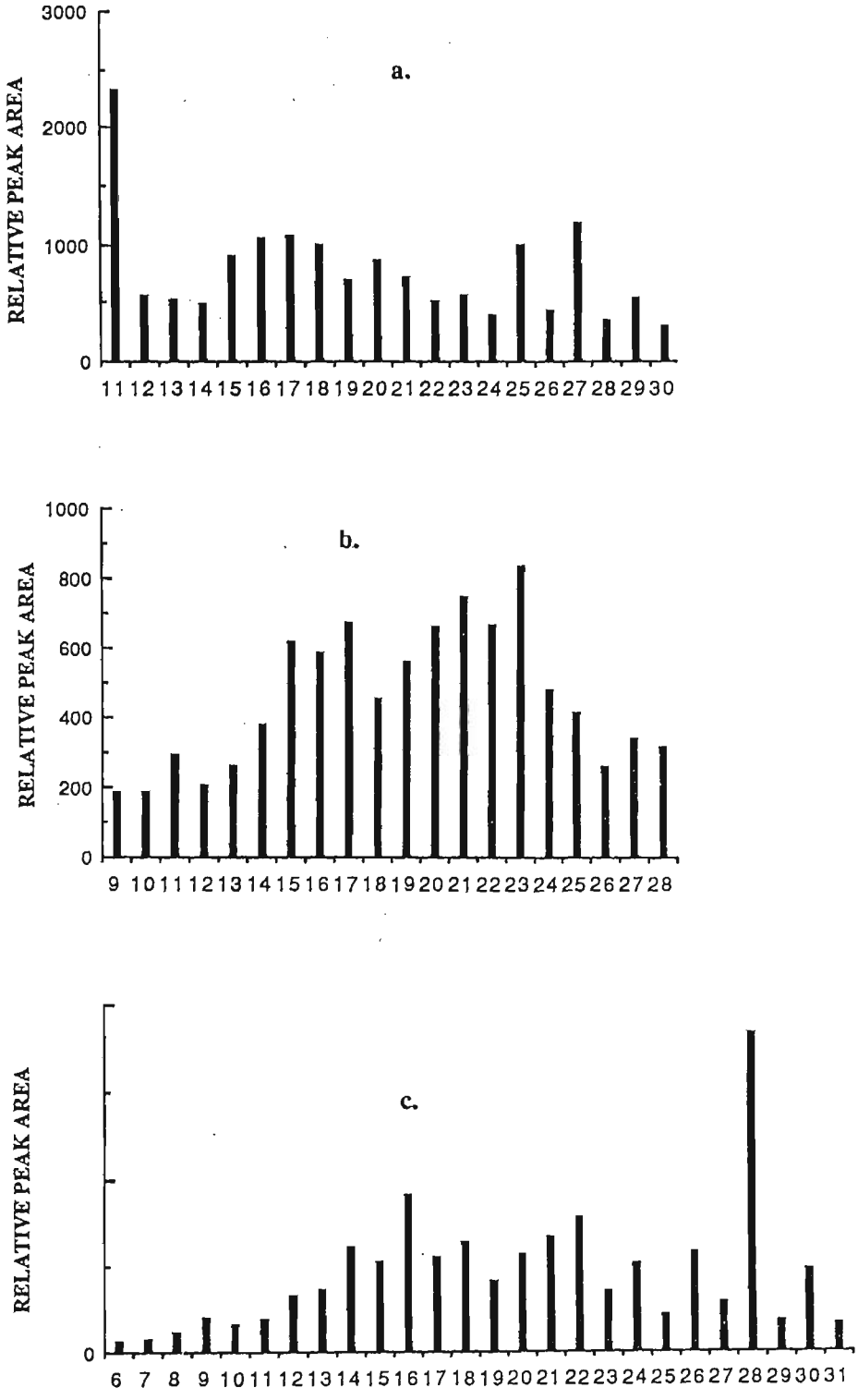

Figure 4-4.

Relative peak area distribution profiles, over the carbon number ranges indicated, for compound classes found in the solvent extract of oil shale from Duaringa 5391-C. Respective profiles comprise linear alkanes (**a.**), alkanals (**b.**) and alkanoic acid methyl esters (**c.**). Distributions **a.** and **b.** are directly comparable since peak areas were obtained from the same chromatogram. Profile **c.** is suitable only for a comparative analysis of the distribution of individual components.

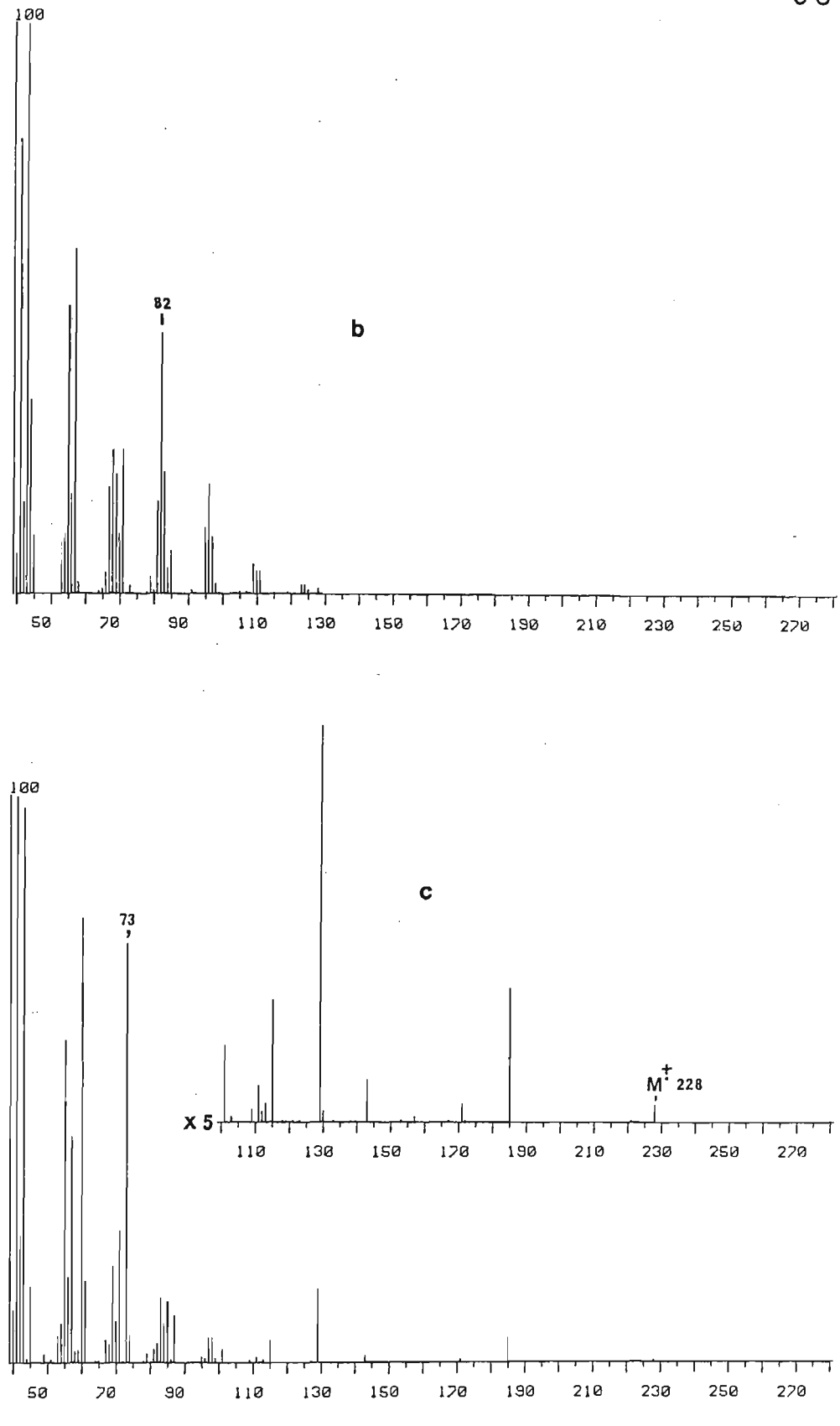

Figure 4-5.
Representative mass spectra for linear alkanals (C_{20}-homologue) and alkanoic acids (C_{14}-homologue) found in the solvent extracts of oil shales from the Duaringa resource are given in **b** and **c** above. Diagnostic fragment-ions m/z 82 and 73 were used to verify the continued presence of higher members of respective homologous series in unresolved regions of the gas chromatogram (see Figure 4-6).

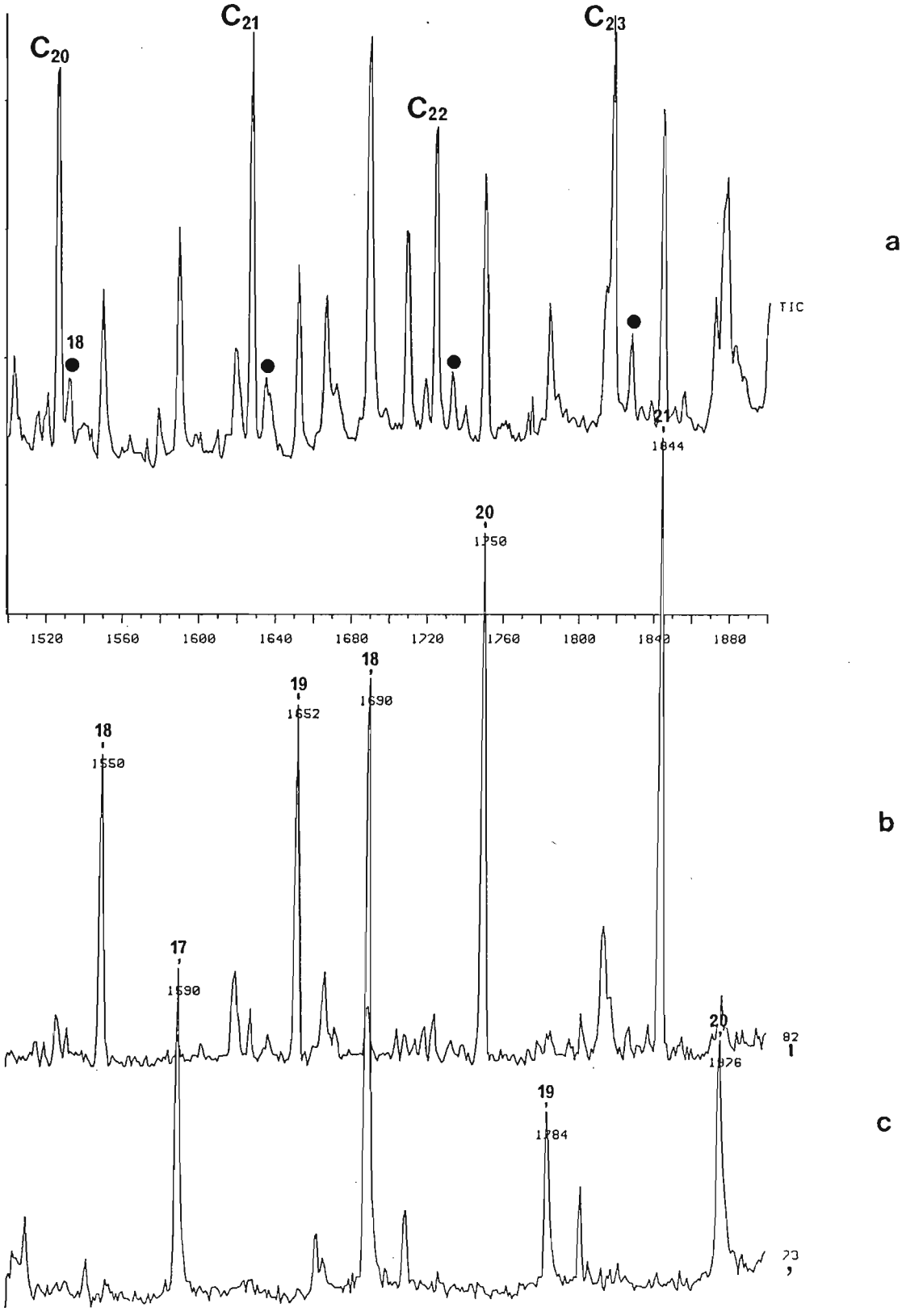

Figure 4-6.
Representative mass spectral data for the C_{20} - C_{23} region of the chromatogram for the soxhlet extract from Duaringa 5391-C. Trace **a** represents the total-ion current profile with alkanes as indicated; components marked ● are alkan-2-ones (see text for details). Trace **b** is the fragmentogram (m/z 82) corresponding to alkanals; trace **c** is the fragmentogram (m/z 73) corresponding to free alkanoic acids. Carbon numbers for each homologous series as indicated.

shale oil fractionation. Among other classes of compounds Regtop reported low concentrations (collectively < 1 % of total extractable organic matter) of homologous series of linear alkan-1-ols and alkan-2-ols, of even- and odd-carbon number preference respectively. Similar even- and odd-carbon number predominance for these primary and secondary alcohols have been reported in plant waxes by Eglinton and Hamilton (1967). Aliphatic alcohols could well be precursors for linear alkanals and alkanones previously reported, with oxidation of alkan-1-ols and alkan-2-ols producing alkanals and alkan-2-ones respectively. Regtop did not report any aldehydes or ketones in his soxhlet extract, probably due to their very low abundances and/or sample losses associated with his fractionation procedure (it has been reported that alumina adsorbs aldehydes irreversibly).

The relatively high concentrations of linear aldehydes in the extract from 5391-C and the prospect of their origin from alkanols prompted a closer examination of the profile in an attempt to identify alkan-2-ones possibly derived from similar sources. The latter were found by positive GC-MS identification of the C_{10} - C_{13} homologues (the members C_{13} - C_{16} coelute with the C_{15} - C_{18} alkanes) as well as fragment-ion profiles (m/z 58 and 59) and retention data for higher members up to C_{27} (Table 4-6). Alkan-2-ones in the 5391-C extract were present at relatively high concentrations (ca. 35 % of the aldehyde content), consistent with a high abundance of the isoprenoid ketones previously mentioned (Figure 4-6). Linear alkan-2-ones were also present in the extracts from the other shallow oil shale samples, though at reduced relative concentrations (< 10 % of the corresponding aldehyde content) and were not observed in the chromatogram for sample 686 (again consistent with the presence of the isoprenoid ketones in the former samples and their absence in the latter).

The bar graph below shows the relative distribution of alkanes (column 1), alkanals (column 2) and alkan-2-ones (column 3) for the 5391-C extract. Over the component range depicted it does not indicate any obvious genetic, or common-source relationship for these compounds. Quantitative data for the alkan-2-ones (from peak areas) was available only for a restricted range of carbon numbers because of resolution problems mentioned above.

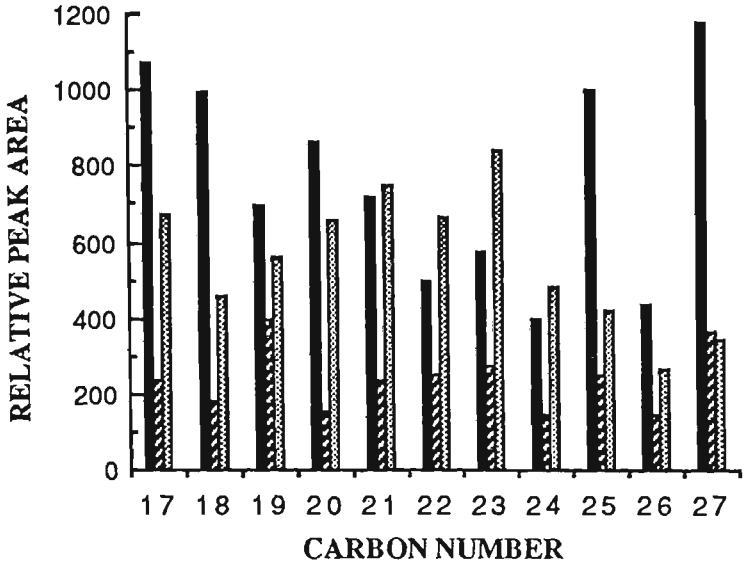

BAR GRAPH of relative abundances of alkanes (column1), alkan-2-ones (column 2) and alkanals (column 3) for the solvent extract of oil shale from Duaringa 5391-C.

The GC-profile for the ultrasonic extract from 686 (Figure 4-2b) shows a bimodal distribution of alkanes in the region C_{11} - C_{31} of the chromatogram, associated with a weak predominance in the C_{15} - C_{19} and a strong predominance in the C_{23} to C_{31} range. The linear alkane distribution is heavily biased towards the high molecular weight region, with C_{27} by far the most abundant component in the entire chromatogram (Figure 4-7a.), and shows a very pronounced CPI for odd alkanes in the latter part of the profile (Table 4-5). This rather common odd-carbon-number predominance of alkanes of high molecular weight is derived from epicuticular waxes of higher plants and is frequently reported for Recent detrital sediments, with an important contribution from contintental runoff and comprising both clay minerals or silts and organic material from plants. The heavy, predominently-odd alkanes are inherited as such from the continental higher plants, which synthesise them directly, or they may be obtained from an early diagenesis (defunctionalisation) from the even-numbered acids, alcohols or esters associated with higher plant accumulations (Tissot and Welte, 1984).

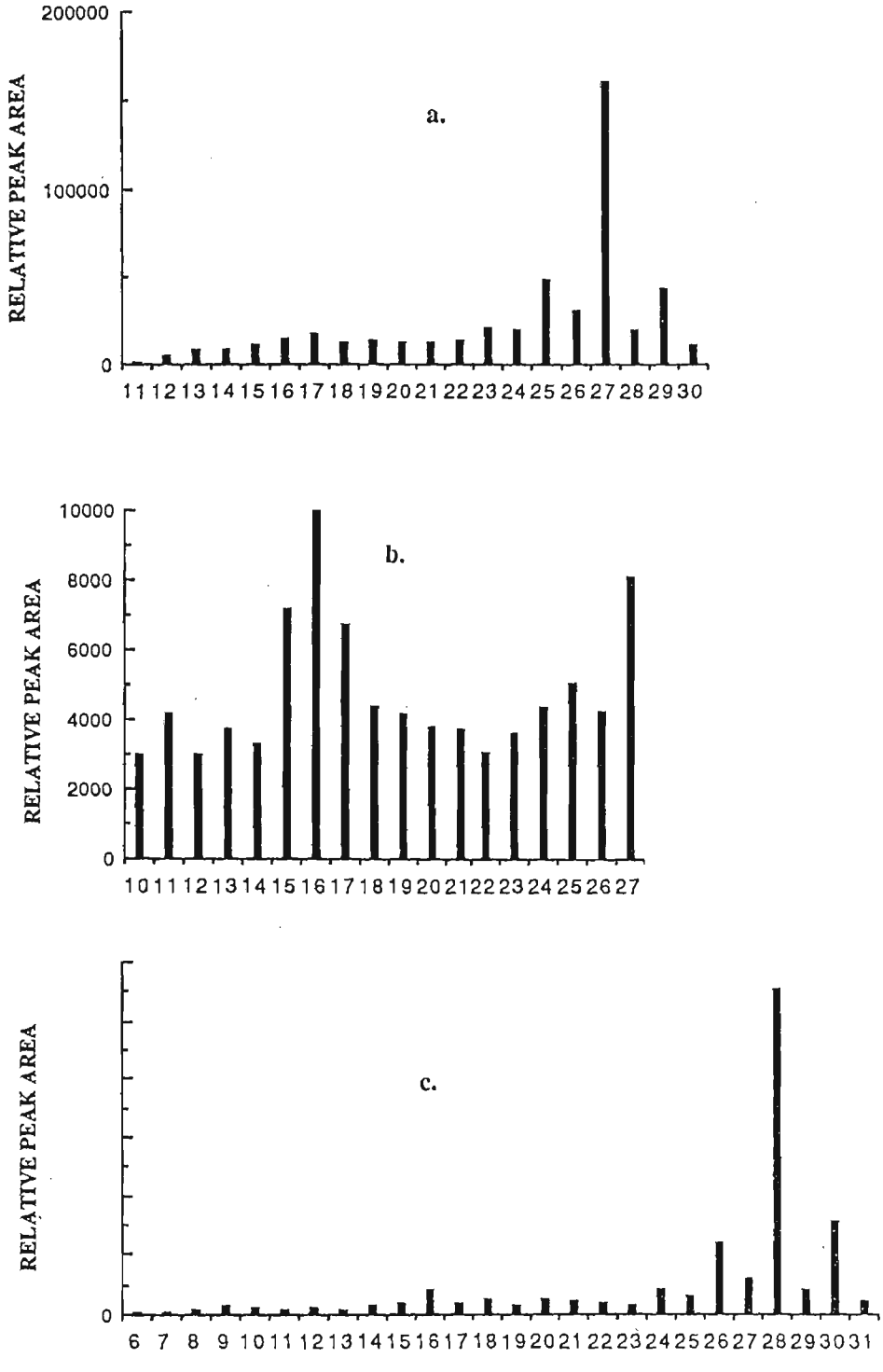

Figure 4-7.
Relative peak area distribution profiles, over the carbon number ranges indicated, for compound classes found in the solvent extract of oil shale from Duaringa 686. Respective profiles comprise linear alkanes (**a.**), alkanals (**b.**) and alkanoic acid methyl esters (**c.**). Distributions **a.** and **b.** are directly comparable since peak areas were obtained from the same chromatogram. Profile **c.** is suitable only for a comparative analysis of the distribution of individual components.

Table 4-5. Bitumen parameters obtained from GC data for the solvent-extracts of oil shale samples from the Duaringa deposit (bold numbers highlight major differences between 5391-C and 686).

PARAMETER	SAMPLE			
	5391-C	686	789	822
extract (mass % of raw shale)	1.57	1.16	0.6	0.6
pristane/phytane	2.17	2.04	4.0	2.2
pristane/ C_{17}	0.26	**1.69**	0.46	0.36
phytane/ C_{18}	0.13	**1.12**	0.18	0.22
alkane C No. range	10 - 31	10 - 31	10 - 31	10 - 31
alkane C No. maximum	11	**27**	14	27
C_{27} / C_{17}	1.1	**9.1**	0.8	1.5
CPI (alkanes)**	2.00	**3.25**	3.20	2.91*
% total GC peak area (for alkanes > C_6)	20	**51**	27	17

* C_{28} contribution to the CPI value was estimated to adjust for coeluting component.
** The CPI ratio was calculated using the equation:

$$CPI = \frac{2(C_{29} + C_{27} + C_{25} + C_{23})}{C_{30} + 2 (C_{28} + C_{26} + C_{24}) + C_{22}} \quad \ldots\ldots (2)$$

where C_{22}, C_{23}, ..., C_{30} are GC-peak areas for the respective linear alkanes (or appropriate areas for other components under consideration). Equation 2 ensures that a smooth distribution of compounds in this range is assigned a CPI ratio close to 1.

In ancient detrital sediments the important predominance of the original odd alkanes is preserved in relatively shallow shales and silts, where degradation of kerogen has not yet started. Odd alkanes derived from higher plants have been found in shallow European shales (Tissot and Welte, 1984) and have been reported in the Green River shales (Robinson et al., 1965). Alkanes in the region C_{10} - C_{20} are probably derived from a mixture of algal and bacterial sources. The latter is not linked to any pronounced carbon

number preference while the former is usually associated with odd-carbon-number alkanes of medium molecular weight, mostly C_{15} and C_{17}, which may represent a direct heritage from the hydrocarbons present in algae and from related acids. In upper beds of the Green River shales (Mahogany beds), C_{17} is the main alkane constituent in the medium molecular weight range. In the above context the predominance of undecane in the 5391-C extract is rather unusual.

Compared to linear C_{17} and C_{18}, the regular acyclic isoprenoids pristane (i19), phytane (i20) and i16 are substantially more abundant than in the solvent extract from 5391-C. Regtop (1983) has suggested that the ratios pristane/ C_{17} and phytane/ C_{18} can be used as maturation indicators in sediments, with both ratios decreasing as maturation progresses. This proposition is at variance with the results for the 686 oil shale sample, since it is arguably more evolved as a consequence of substantially deeper burial (note however that vitrinite reflectance values for this sample are close to those for 5391-C, with both values consistent with a diagenetic stage of evolution). A reduction of pristane and phytane concentrations through cracking of these components, and a further dilution by thermally produced alkanes, could be expected at a maturation stage which corresponds to (early) catagenesis and is associated with a higher vitrinite reflectance value. The relatively higher pristane and phytane concentrations may be due to selective depletion of linear alkanes through microbial degradation or may reflect diagenetic contributions from high concentrations of the phytol moiety of chlorophyll, consistent with input from allochthonous plant material evident in the high molecular weight alkane distribution. Work by Carreta et al. (1985) suggests that the selective depletion of algal-derived linear alkanes may be due to, at least in part, the action of syn-sedimentary bacteria and is consistent with the higher abundance of (framboidal) pyrite in 686, possibly derived from sulphate reducing bacteria (Table 4-2). Aldehydes present in the extract appear less abundant than in 5391-C; however, their relative abundance in the C_{23}- C_{31} region of the chromatogram is obviously influenced by the high concentration of alkanes covering that molecular weight range. From nonanal to the C_{21}-homologue, individual members

show a reduced but similar abundance to the alkane eluting before them as do the alkanals in 5391-C. Their reduced abundance may be due to their incorporation into the bound fraction of the sediment, which generally affords protection to the more labile compounds (Cranwell, 1981 ; Farrington and Quinn, 1973).

GC-MS analysis of the broad peaks (denoted by › in Figure 4-3b) identified them as members of a homologous series of alkanoic acids extending from hexanoic acid to at least the C_{23}-alkanoic acid. The fact that these free fatty acids were detected highlights the inert nature of the chromatographic column. The same homologous alkanoic acid series was also detected in each of the extracts from the shallow oil shale shale samples, albeit at lower concentration.

Soxhlet extracts of the above samples were identical to the ultrasonic extracts as regards the presence of the components described above and only minor quantitative differences were observed. The profiles differed markedly only in respect of the concentration of presumed artefacts (Figure 4-3, **X**) which were consistently higher in the soxhlet extracts.

Carboxylic acids in the solvent extracts were isolated from them by extraction of aliquots of the solution with NaOH (1N, 3 x 2 mL) and recovered with dichloromethane from the acidified aqueous phase (pH 1). The combined extracts were dried ($MgSO_4$), evaporated to dryness and the fatty acids converted to their methyl esters using BF_3/MeOH. The methyl ester profiles (Figure 4-8) were compared to the alkane distribution of the respective total extract chromatogram, to evaluate possible product -precursor relationships (Figure 4-4, 4-7). For 5391-C there is no genetic relationship between the fatty acid and alkane profiles, with the distribution probably reflecting differences in organic source material and possibly selective maturation and/or reworking by microorganisms. A possible genetic relationship between alkanes and fatty acids is clearly evident for the 686 sample, with some of the high molecular weight odd alkanes probably derived by decarboxylation of the corresponding even carboxylic acids. Welte and Waples (1973) suggest that in very reducing environments, reduction of linear fatty acids, alcohols from waxes, and phytanic acid or phytol is prevalent over decarboxylation, resulting in predominance of

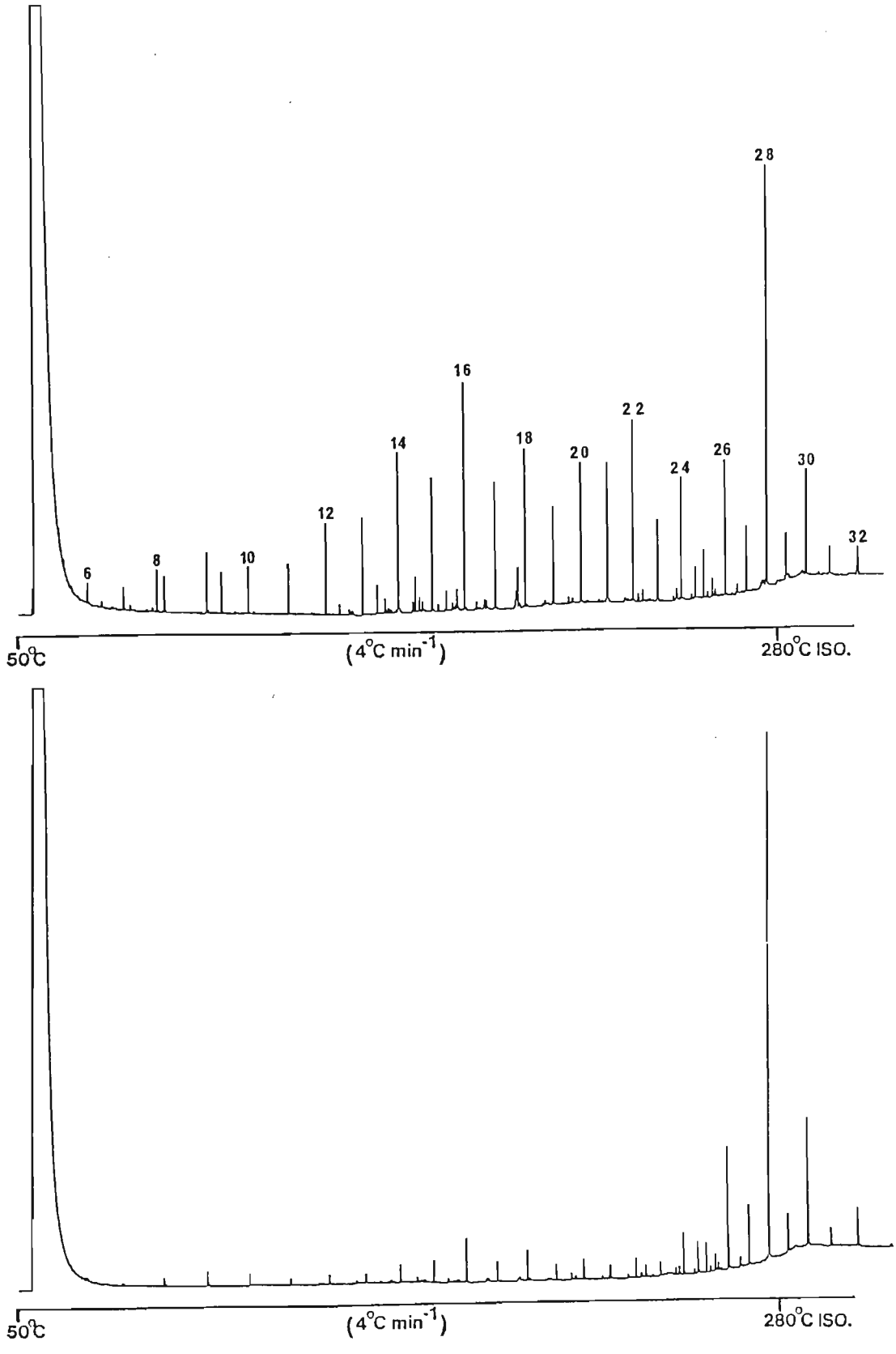

Figure 4-8.

Gas chromatographic profiles of alkanoic acid methyl-esters isolated from the solvent extracts from Duaringa 5391-C (a) and 686 (b). Acid carbon numbers as indicated.

even-carbon-numbered alkane molecules over odd molecules (CPI<1) and a predominance of phytane over pristane. In less reducing environments, decarboxylation results in a majority of odd alkanes (CPI>1) and a predominance of pristane over phytane. Shimoyama and Johns (1972) proposed an alternative interpretation of the even alkane predominance. They carried out experimental degradation of linear fatty acids in the presence of montmorillonite or calcium carbonate. The two minerals seem to have different catalytic effect: decarboxylation with loss of one carbon atom is favored by montmorillonite, while beta cleavage with loss of two carbon atoms is favored by calcium carbonate. Therefore, an original even-numbered fatty acid would generate mostly an odd alkane in shales and an even alkane in carbonates. Nishimura and Baker (1986) and Grimalt and Albaiges (1987)

Table 4-6. Modified Kovats retention indices for alkanals and alkanoic acids identified in the solvent extracts from the Duaringa oil shale samples.

C No.	RETENTION INDEX (RI)*		
	alkanals	**alkanoic acids**	**methyl esters****
7		1082.80	1024.57
8		1183.90	1125.63
9	1105.53	1279.70	1225.73
10	1207.04	1375.46	1326.12
11	1308.78	1471.10	1426.03
12	1410.30	1568.67	1526.24
13	1512.01	1666.67	1626.38
14	1613.88	1765.72	1726.91
15	1715.59	1865.10	1827.26
16	1817.84	1964.66	1927.82
17	1919.70	2063.95	2027.95
18	2022.28	2164.55	2128.74
19	2124.28	2265.00	2228.97
20	2226.25	2365.85	2330.06
21	2328.67	2466.75	2430.78
22	2430.48	2568.39	2531.48
23	2532.97		2632.71
24	2635.09		2733.49
25	2736.20		2834.66
26	2838.29		2935.28
27	2940.52		3035.61
28			3137.48

* Modified Kovats retention indices were calculated using equation (1).
** Retention indices for the methyl esters of the alkanoic acids are listed against the carbon number corresponding to the free fatty acid (e.g. octanoic acid methyl ester is listed against carbon number 8).

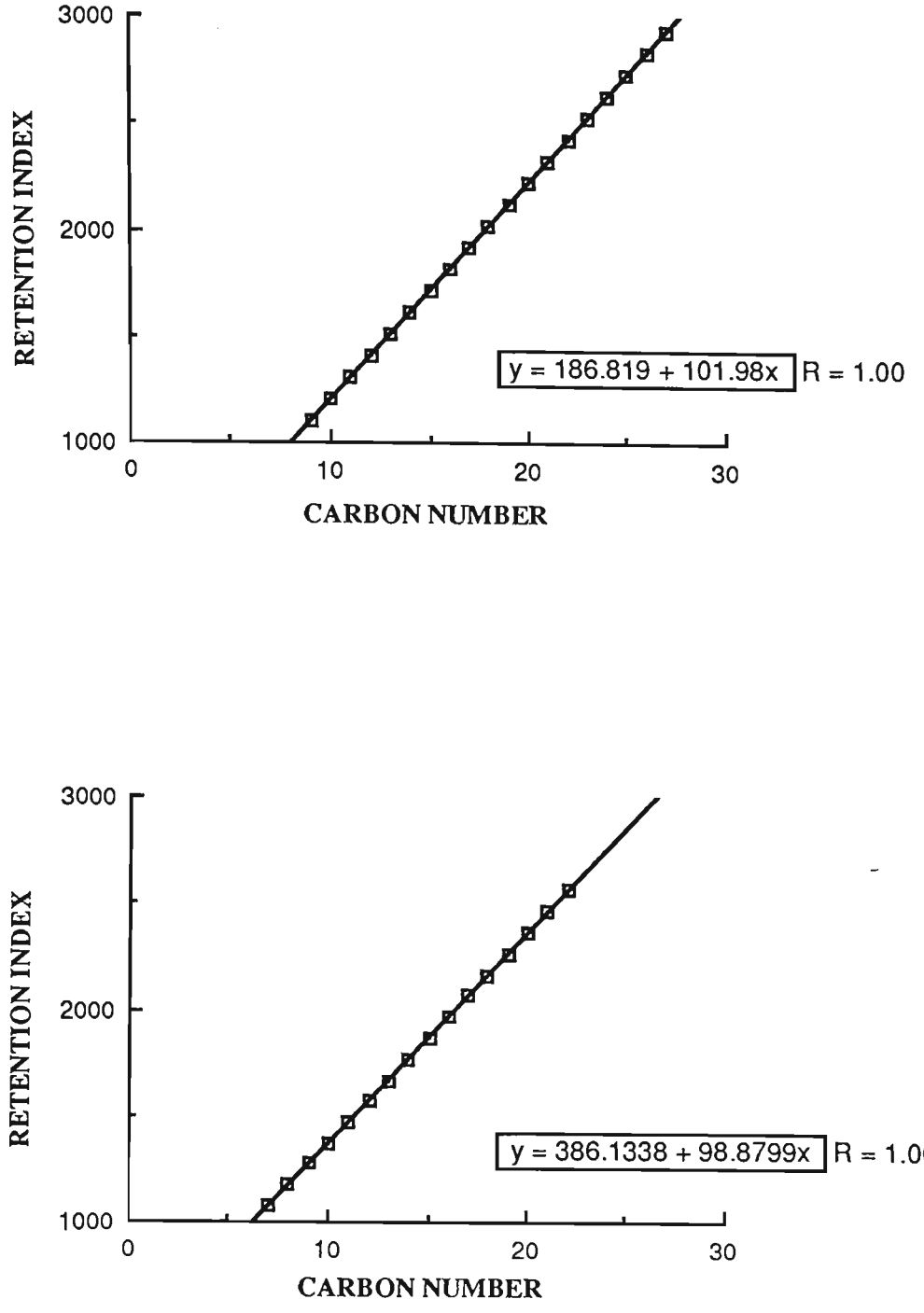

Figure 4-9 a.
Plot of modified Kovats retention indices (RI) against carbon numbers for alkanals (upper plot) and alkanoic acids (lower plot). Retention index equations (RI=mx +b), where x denotes the appropriate carbon number, and correlation coefficients (R) were obtained by least-squares regression analysis.

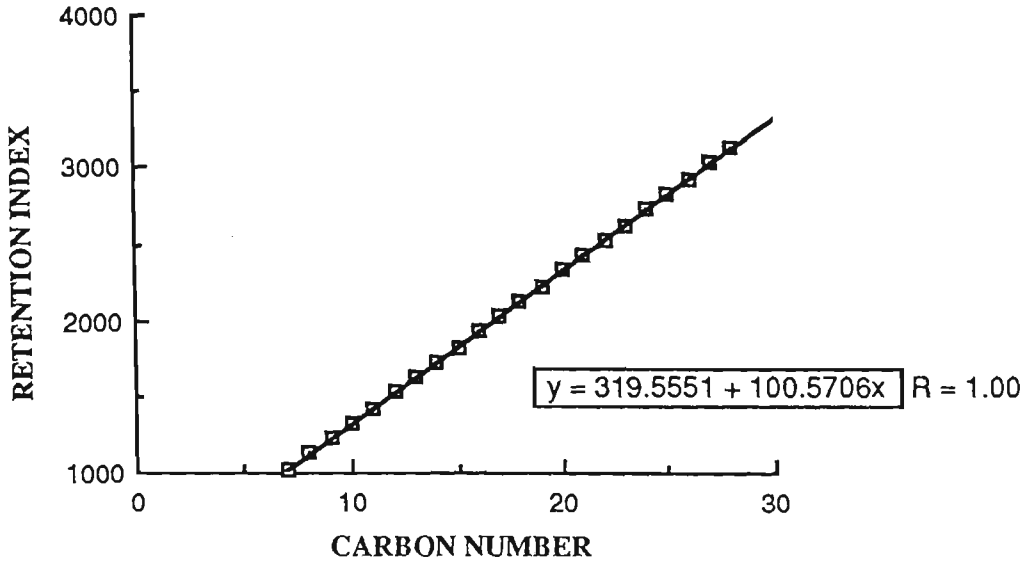

Figure 4-9 b. Plot of modified Kovats retention indices (RI) against carbon numbers for alkanoic acid methyl esters. Retention indices for the esters are plotted against the carbon number corresponding to the free fatty acid (e.g. octanoic acid methyl ester is plotted against carbon number 8). Retention index equation (RI=mx +b), where x denotes the above carbon number, and correlation coefficients (R) were obtained by least-squares regression analysis.

have shown that alkanes with a strong even CPI occur in a wider type of sedimentary environment than previously described. A variety of direct biological sources including both marine and freshwater bacteria as well as fungi and yeast species were suggested to account for their distributions.

The residual base extracted organic phase from each solvent extract was also analysed by GC, to determine whether the comparatively high concentrations of free fatty acids affected the original alkane distribution in the initial total-extract profile, through possible decarboxylation in the injection port of the gas chromatograph. In each case no relative differences between individual components were observed.

In conjunction with petrological data, the above results suggest that alkanes in the shallow oil shale samples were predominantly derived from algal lipids with probably (minor) contributions to the higher molecular weight regions from bacterial reworking of the algal biomass and comparatively little input from allochthonous or detrital higher plant material. The low pristane, phytane levels and the high relative abundance of the isoprenoid ketones suggest an oligotrophic environment of deposition, which is consistent with the shallow depth proposed for the ancestral Lake Duaringa in section 1.5.5. For the lower oil shale, petrology also indicates kerogen originating predominantly from an algal source.

The alkane profile suggests comparatively higher levels of detrital plant contributions responsible for probably the bulk of the high molecular weight components. Further alkane contributions in this region may have been derived through montmorillonite catalysed decarboxylation of the free fatty acids evident at similar distributions (CPI) and over the genetically required carbon number range. A depletion, relative to pristane and phytane concentrations, of alkanes normally associated with algal sources, may be due to the selective depletion of linear alkanes through more pronounced microbial reworking of the original biomass. The lower concentration of aldehydes and isoprenoid ketones as well as the absence of linear alkanones support this proposal, with oxygenated moieties in general possibly oxidised further to the respective free acids. This suggestion is not at variance with earlier remarks about the possible activity of sulphate reducing bacteria in the sediment, but merely reflects the changes from oxic to anoxic conditions which accompany deeper burial. Defunctionalisation, particularly of oxygenated components, is a well-documented process associated with these diagenetic changes due to progressive burial. It should be stressed at this stage that solvent extract information should not be overinterpreted in the absence of other relevant data.

4.4 Pyrolysis-GC-MS.

All of the Duaringa samples listed in Table 4-1 were analysed using flash-pyrolysis GC of the bitumen-free oil shales obtained from the solvent extraction procedure. The finely powdered and pre-extracted raw shales were dried under nitrogen (105°C, 1 h) and flash -pyrolysed using the modified CDS-150 pyroprobe and those experimental conditions detailed earlier.

Figure 4-10 shows the pyrolysis-GC profiles obtained for raw shale samples from 5391-C and 686. Both are dominated by 1-alkene/ alkane peaks extending over the entire region of the pyrolysate chromatograms. Except for sample 674, the pyrograms of the other oil shale samples show no major qualitative differences compared to those above and are again dominated by the alkene/alkane doublets, typical of algal shales. 1-alkenes and alkanes in the pyrolysates for the shallow oil shale samples are present at about the

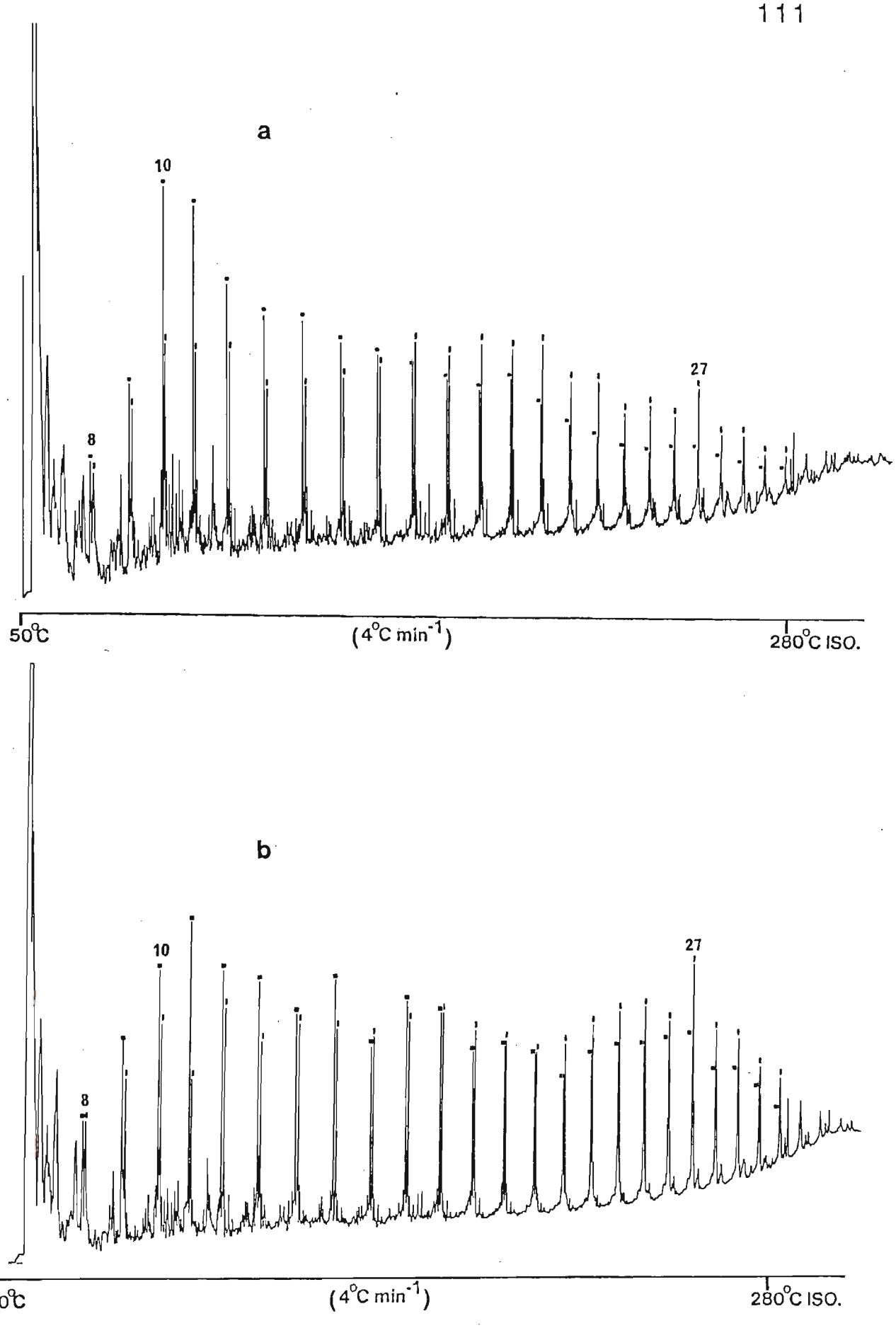

Figure 4-10.
Flash-pyrolysis-GC profiles (560°C, 20 s) obtained for ca.2 mg of raw oil shale samples from 5391-C (**a**) and 686 (**b**). Major components are alkanes (▮) and 1-alkenes (■) from octane (**8**) as indicated. Samples were pyrolysed using quartz pyrolysis tubes and the modified CDS-150 pyroprobe.

same relative concentrations. The latter exhibit broad modalities in the ranges C_{10} - C_{12} and C_{15} - C_{21} and at C_{27}; in each case they show a slight odd carbon-number preference in the region C_{23} - C_{27}. The alkane distribution for both of the deeper samples (686 and 674) show a comparative bias towards higher carbon number, particularly for sample 674 (Figure 4-11b) with again only slight odd carbon-number preference in the C_{25} - C_{27} region for both samples.

For each of the shallow samples the 1-alkene distribution is smooth and monotonically decreasing. It is biased towards the low molecular weight region with 1-decene the most prominent peak in each of the pyrograms. This distribution is consistent with an origin from cracking reactions, which generally result in the formation of low molecular weight hydrocarbons. The relatively greater abundance of alkenes in this region arises partly from the very short residence times for the pyrolysis products generated. This short residence time, associated with flash-pyrolysis conditions, prevents hydrogen capping reactions from saturating the alkyl radicals formed by the pyrolysis process and results in the relatively high concentrations of the alkenes. The 1-alkene distributions for the deeper oil shale samples are similar to those described, although the bias towards the low molecular weight region of the chromatogram is less pronounced for both.

The great similarity between most of the pyrograms indicates a common source for the oil shales; an inference consistent with their respective petrology. In addition to the major components, a number of other minor constituents were detected in the baseline of the chromatograms using pyrolysis-GC-MS. Several homologous series were inferred to be present after a number of representative individual components had been positively identified; the presence of each series was confirmed from appropriate fragment-ion profiles. For the above samples, homologous series of alkylbenzenes, alkylnaphthalenes and other substituted aromatics were detected.

The pyrogram for 674 differentiates it from the other samples on the basis of a pyrolysate which is relatively richer in the commonly observed isoprenoids prist-1-ene and prist-2-ene, and in higher carbon-number alkenes/alkanes. It is is generally agreed that

these pristenes, like other isoprenoid compounds, are derived from a biological source, although their biological precursors in sediments are unknown. It has been proposed that both are derived from a common source - the phytol side chain of chlorophyll (Didyk et al., 1978), although precursors such as the diphytanyl ethers of archaebacteria (Chappe et al., 1982) and tocopherols (Goossens et al., 1984) have also been proposed.

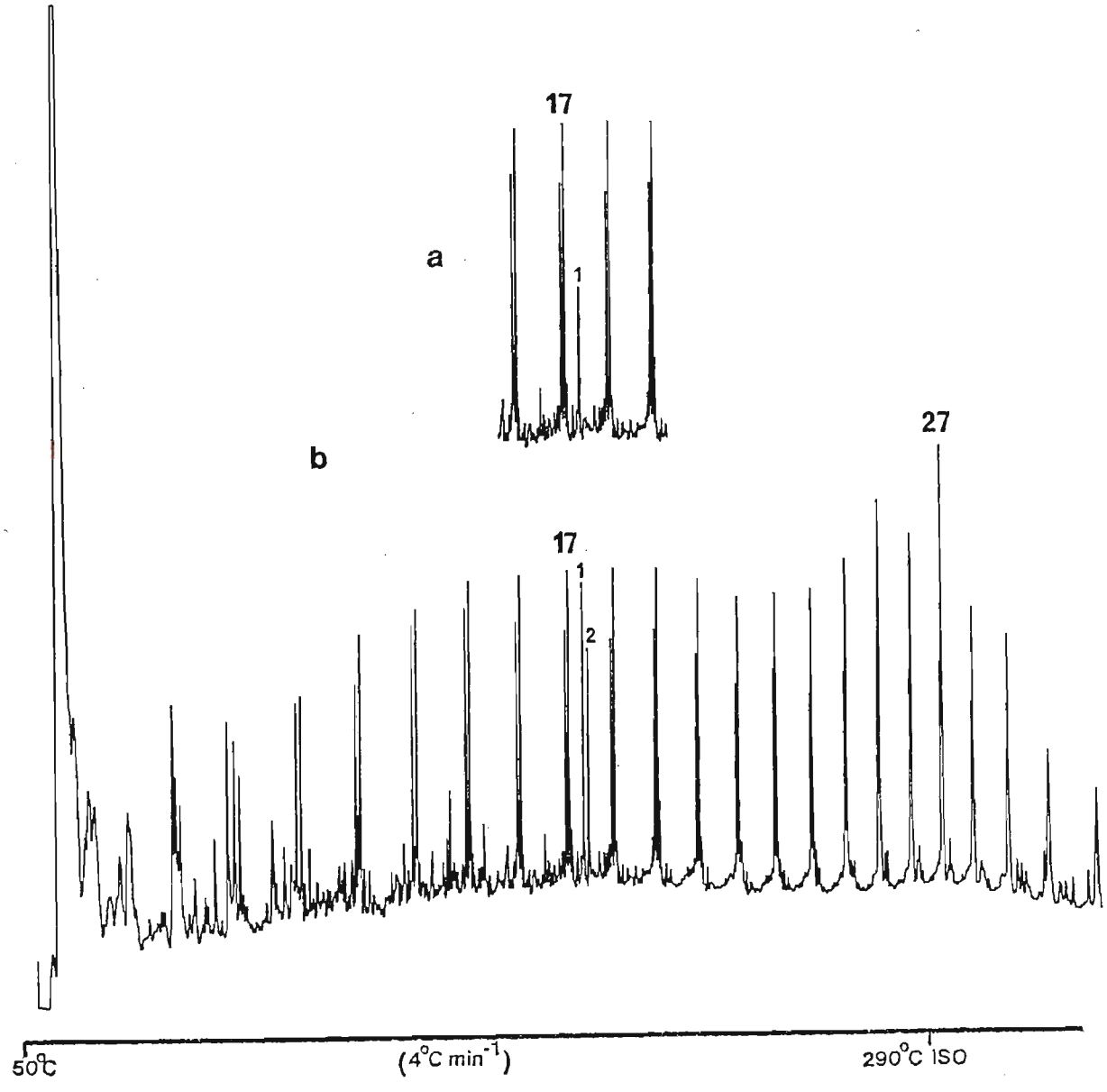

Figure 4-11.
Flash-pyrolysis-GC profile for raw oil shale from Duaringa 674 (b); notation as for Figure 4-10. Prist-1-ene and prist-2-ene are indicated by (1) and (2) respectively. Insert (a) shows a portion of the pyrogram obtained for kerogen from the same sample and highlights the catalytic effect of the mineral matrix on absolute and relative concentrations of the pristene isomers.

Regtop et al. (1986) have shown that the principal source of prist-2-ene in pyrolysates of the Tertiary Condor oil shale is prist-1-ene, which isomerises to prist-2-ene in the presence of mineral catalysts such as kaolinite and in proportions determined by the residence time of the pyrolysis vapours in contact with the catalyst. The production and subsequent isomerisation of shale-derived alkenes is generally considered to proceed via a thermolytic radical-induced mechanism, followed by clay-catalysed carbocationic processes involving double bond rearrangement (Alexander et al., 1984; Wilson et al., 1986; Williams, 1987). Based on these results, the relative abundance of the pristene isomers in the flash-pyrolysate of sample 674 reflects the thermocatalytic activity of the mineral matrix. In view of the maceral composition, the relatively higher concentrations of the pristenes and high molecular weight alkenes/alkanes for 674, are probably due to the genetic contribution to the pyrolysate of compounds (mainly) derived from the greater percentage of terrestrial content in its kerogen.

Although the Duaringa samples showed virtually no variation in their pyrolysate profiles, except where the oil shale was of mixed algal and terrestrial origin (674), a significant variation in the distribution of pyrolysis products has been observed for other oil shale samples representative of Australian deposits (Crisp et al., 1987). Where these variations do occur, they result from source and maturity differences. Generally speaking, pure algal shales are dominated by alkene/alkane components in the chromatogram whereas mixed algal and higher-plant shales contain mixtures of both aliphatic and aromatic products, with the latter often relegated to subordinate concentrations resulting from the lower generating potential (oil and gas) of type III kerogen.

In each case where shallow raw shale and the corresponding kerogen were pyrolysed, the respective profiles were qualitatively almost identical. This is not surprising since the mineral matrix plays an important role only for that portion of the kerogen or pyrolysis products which have actual contact with the mineral surface. Under those circumstances the former is likely to produce relatively more, but probably still subordinate concentrations of those mineral-catalysed products normally found in flash-pyrolysates. In Figure 4-11a the relatively reduced concentration of prist-1-ene and the virtual absence of prist-2-ene, in the pyrolysate of kerogen from sample 674, illustrate the catalytic effect of

the mineral matrix on pyrolysate composition in line with Regtop's findings above. The mineral matrix, through promoting cracking reactions, alters the C_{17}/ pristene ratio (the pristenes in Figure 4-11b are collectively much larger than C_{17}). Alternatively that portion of the total kerogen actually coating the mineral phase may have a lower generating potential (oil and gas) since it is likely to be involved to a greater extent in coking reactions than the rest of the kerogen (Espitalie et al., 1984).

For rapid screening of numerous samples the use of pre-extracted or raw shale is most suitable, since it obviates the need for costly and time-consuming kerogen isolation. The use of raw shale is particularly relevant in the commercial context since its pyrolysate relates more directly to the composition of pyrolysis products likely to be obtained using commercial retorts.

The relevance of flash-pyrolysis data can be enhanced further by quantitative information which allows a calculation of the yield of chromatographable pyrolysate produced as a percentage of raw shale used. To obtain these data the shale to be pyrolysed needs to be weighed and the profile peaks summed over the entire chromatogram; however, this procedure is limited to relatively low molecular weight, volatile compounds (up to C_{31} for the samples analysed) and ignores higher molecular weight compounds which may also be formed. Quantitation is further complicated by the fact that even for small samples of raw shale, in the 1-2 mg range, not all of the sample necessarily reaches the desired pyrolysis temperature and only a portion of the potential pyrolysate is observed in the pyrogram.

This situation of incomplete pyrolysis is demonstrated by sequential flash -pyrolysis of the one sample of raw shale from 5391-C (Figure 4-12). The shale was flash -pyrolysed repeatedly under conditions identical to those used for the above procedure but at a calibrated temperature of 500°C (20 s) and with a delay of 5 s between each cycle to allow the heater coil to cool down. The pyrolysate was passed directly into the FID via heated glass-lined stainless steel tubing under experimental conditions described earlier for thermal distillation pyrolysis-FID (cf. section 3.5.3). Sequential pyrolysis was continued until the pyrolysate-FID signal diminished to background levels (usually 25 cycles). The

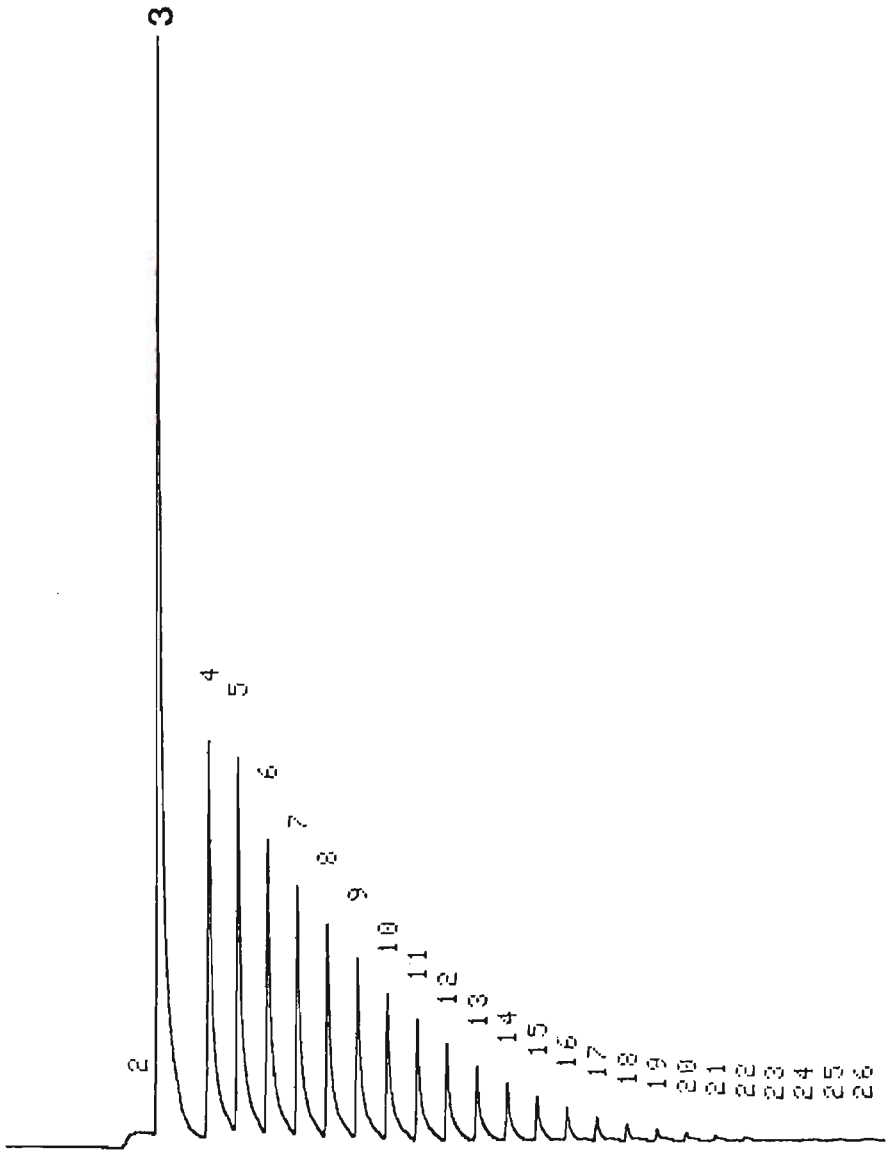

Figure 4-12.
FID-integrator trace for sequential flash-pyrolysis (500°C, 20 s) of raw oil shale 5391-C. Peak 3 corresponds to the first cycle of the sequence.

above procedure was repeated several times with fresh samples of the same raw shale, to determine the reproducibility of pyrolysate produced from the first cycle as a percentage of the total pyrolysate obtained. Results showed that the first pulse always produces the bulk of the total pyrolysate releasable from flash-pyrolysis, but varies sufficiently for repeated analysis of the same sample (between 30 - 35 % of total pyrolysate) to introduce errors into any absolute quantitation based on the above proposal. Larter and Senftle (1985) have overcome some of these limitations by adopting a quantitative approach for characterising

(typing) pre-extracted kerogen. The authors used an internal standard (polymethylstyrene) to directly determine the absolute concentrations of specific kerogen pyrolysis products. Using this approach for raw shale may resolve some of the problems outlined, but those of sample heterogeneity and incomplete pyrolysis would remain. Flash-pyrolysis of oil shales carried out at lower temperatures (e.g. 358°C - flash thermal desorption) has been shown to yield thermal desorbates virtually indistinguishable from the respective solvent extracts (Crisp et al., 1986). When used in conjunction, flash thermal-desorption and flash -pyrolysis are rapid procedures which provide information on the thermal history, hydrocarbon generating potential and shale oil composition.

4.5 Oil shale hydrocarbon potential - (Pyrolysis-FID).

All of the Duaringa oil shale samples were pyrolysed using the CDS-150 pyroprobe and those modifications of the device designed to achieve complete pyrolysis of the sample under conditions simulating retort environments (cf. section 3.5.3). Data obtained from this procedure provides immediate information on comparative hydrocarbon generating capacities of the shales, as well as related information, which may be used to assess the extent of their (thermal) evolution (cf. section 2.4.5).

During the assay, those hydrocarbons already present in the oil shale in a free or adsorbed state are first volatilised at the temperature of the injection port (300°C). This volatile (bitumen) fraction of the shale is flushed directly into the FID where it is detected as a (usually) small peak P_1. Crisp et al. (1986) have shown that when raw shale from Condor, Australia was pyrolysed using a Curie point pyrolysis device at 358°C, its thermal desorbate was virtually identical to the solvent extract obtained from the same sample. Subsequent heating of the shale results in pyrolysis of the kerogen and the generation of hydrocarbons and other compounds, whose yields and structures clearly dependend on both abundance and type of the organic matter. Other volatiles such as carbon dioxide and water are also produced, but are not detected by the FID, which is selective for combustible compounds and detects these components as a second peak P_2. Collectively P_1 and P_2 provide an evaluation of the genetic potential of the oil shale to produce hydrocarbons,

since their sum takes into account that portion of the kerogen which has already been transformed into hydrocarbons, as well as the residual hydrocarbon potential locked up in the kerogen and released during pyrolysis.

The genetic potential may be expressed in absolute units (kg hydrocarbons tonne^{-1} raw shale), or be related to a well characterised oil shale sample which then serves as a reference for subsequent analyses. The latter approach was adopted for the current studies since it obviates the need for time consuming calibration procedures. Used in that context, the procedure provides a rapid and inexpensive screening method for evaluating the relative genetic potentials of oil shale samples taken from different locations and stratigraphic sequences within a given resource. The method requires no sample pretreatment, and in conjunction with pyrolysis-GC, obtained using the same device in the flash-pyrolysis mode, yields data for both the quality and quantity of shale oil obtained from commercially-viable resource seams, first recognised as such by using hydrocarbon -generation criteria applied to the pyrolysis-FID data.

Another parameter available from the pyrolysis-FID technique is the temperature T_{MAX} corresponding to the maximum of hydrocarbon production during pyrolysis. For comparative work only relative T_{MAX} values are meaningful, since the temperature is obviously affected by experimental factors such as heating rates. For stratigraphic sequences of sedimentary rock containing kerogen of uniform type, T_{MAX} shows a systematic shift to relatively higher values in concert with deeper burial and is thus suitable for establishing relative maturation (rank of thermal evolution) under these conditions. Where these constraints are not met within a given deposit, T_{MAX} variations may reflect differences in kerogen type, rather than thermal evolution due to burial. In general the temperature T_{MAX} is lower for terrestrial kerogen of type III and higher in the marine or lacustrine types I and II (Tissot and Welte, 1984). Interpretations of a comparatively anomalous T_{MAX} value for a particular sequence of oil shale samples need to be made in conjunction with either petrographic data, elemental analysis or a cross-plot of hydrogen

indices (P_2/C_{org}) and oxygen indices (CO_2/C_{org}) obtained from the Rock-Eval procedure. The production of CO_2 was not monitored in the pyrolysis-FID procedure above, but CO_2 values could be obtained by installing a high-temperature switching valve in the GC oven and splitting the pyrolysate into two streams passing respectively through the FID and a thermal conductivity detector. A pyrolysis temperature range suitable for quantifying only kerogen-derived CO_2 would need to be chosen to obtain meaningful oxygen indices. In practice this temperature needs to lie below ca. 400°C, a value above which contributions are derived from the decomposition of labile carbonates, especially siderite (Espitalie et al., 1977).

Oil shale from Duaringa 5391-C was used to establish experimental conditions suitable to obtain all of the data required to calculate genetic potentials, transformation ratios and T_{MAX} values and to determine the reproducibility of the procedure. Initially parameters were chosen to simulate FA retort conditions (300°C to 500°C - isothermal, at 9°C min^{-1}). Hydrocarbon production continued at the final temperature at levels which made these conditions unsuitable for accurate peak area determinations. After various other protocols were evaluated, it was found that pyrolysis from 300 - 700°C at 25°C min^{-1} met all of the imposed requirements, including an acceptable cycle time of ca. 20 minutes for each analysis. Peak shapes obtained under these conditions are symmetric and easily processed by the integrator using appropriate parameters (Figure 4-13). Five different samples from 5391-C were sequentially analysed under identical conditions. Integrator data obtained from each run are given in Table 4-7, along with T_{MAX} values, calculated from the heating rate and the time difference between the P_1 and P_2 maxima. The reproducibility of the data in Table 4-7 show that the powdered shale represents a homogeneous sample in which kerogen is uniformly disseminated throughout the mineral matrix. This uniform composition made 5391-C an ideal choice as a standard against which other oil shale samples were subsequently compared. The use of a homogeneous, well characterised standard is absolutely essential to obtain meaningful comparative data between samples analysed at different times and under experimental conditions which may have varied

1. DUARINGA 5391-C 1.59 mg (Pyr-FID).

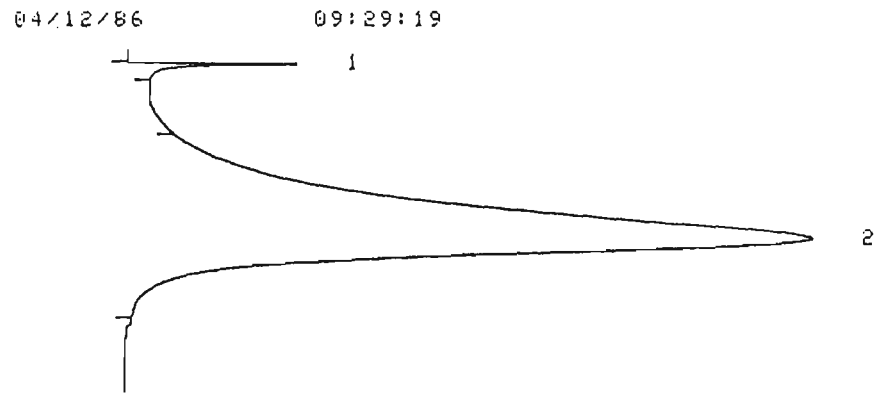

CHROMATOGRAM 1 MEMORIZED

CHROMATOPAC C-R3A
SAMPLE NO 0
REPORT NO 236

FILE 0
METHOD 221

PKNO	TIME	AREA	MK	IDNO	CONC	NAME
1	1	45139			1.6105	
2	13.42	2757663			98.3895	
	TOTAL	2802802			100	

Figure 4-13. Typical pyrolysis-FID profile and integrator data obtained for the pyrolysis of raw oil shale sample 5391-C from the Duaringa deposit.

TABLE 4-7. Statistical data for the determination of the hydrocarbon generating potential (oil and gas) of raw shale sample 5391-C from the Duaringa deposit.

		% PEAK AREAS		
SAMPLE No.	TOTAL AREA[1]	P_1	P_2	T_{MAX}
1	1760	1.5	98.5	618
2	1726	1.2	98.8	618
3	1708	1.5	98.5	620
4	1716	1.6	98.4	620
5	1698	1.3	98.7	619
MEAN:	**1722**	**1.4**	**98.6**	**619**
S. DEVIATION:	**24**			
REL STD. DEV:	**1.4%**			

1 Arbitrary peak area units (integrator peak area x 10^{-3}) per unit weight of raw shale.

during that period.

Pyrolysis-FID data obtained for the other oil shale samples from the Duaringa deposit are listed in Table 4-8. An evaluation of these data shows that the shallow samples are evidently too immature to show any large variations in the transformation ratios. The small relative differences probably reflect a combination of minor variations in the composition of these algal-derived kerogens and the combined influence of experimental errors, sample heterogeneity and sample history (handling and storage), which may result in a small but variable loss of some of the bitumen fraction.

Both of the deeper samples (686 and 674) are characterised by slightly lower transformation ratios. These relatively low ratios are at variance with those values expected from the effects of deeper burial based on the assumption of uniform kerogen type. For 686 a low ratio is in agreement with the petrology for the sample (vitrinite reflectance) which associates the kerogen with low thermal evolution, corresponding to the diagenesis stage of maturation; this is further substantiated by the corresponding T_{MAX} temperature. Both transformation ratio and T_{MAX} value for 674 appear anomalously low when

Table 4-8. Data relating to the hydrocarbon generating potential (oil and gas) of oil shales from the Duaringa deposit.

		PEAK AREAS[2]				
SAMPLE	% K[1]	P_1	P_2	TR.RATIO[3]	T_{MAX}	P_2 RATIO[4]
5391-C	10.5	31	1703	1.8	619	1.0
686	10.9	25	1800	1.4	615	1.06
789	nd	21	1371	1.5	619	0.81
822	nd	49	2880	1.7	615	1.69
812	12.5	64	2660	2.4	615	1.56
674	26.8	29	2895	1.0	605	1.70

1 % kerogen (dry, ash-free basis). **2** peak area (arbitrary units) per unit mass of raw shale. **3** transformation ratio (cf. section 2.4.5). **4** with respect to sample 5391-C. nd - not determined.

interpreted in isolation. The low transformation ratio could be due to migration losses (in -situ) of part of the pre-formed bitumen fraction, while the relatively lower T_{MAX} temperature is consistent with the maceral composition for the shale (ca. 66% liptinite and 33 % vitrinite content for the kerogen) and in agreement with comments above about the influence of type III kerogen on this parameter. The higher vitrinite reflectance values for 674 indicate a more advanced stage of thermal evolution for this sample and in conjunction with the pyrolysis-FID data suggest that at least some of the generating potential of the kerogen may have been realised in the formation of bitumen which subsequently migrated out of the seam. This would explain, in part, both the lower transformation ratio and the low relative hydrocarbon generating capacity (P_2 ratio - Table 4-8) when adjusted for kerogen abundance. On the other hand this interpretation is generally inconsistent with data for the deeper oil shale 686, particularly since maceral data for 674 shows that its kerogen is relatively more abundant and comprises a higher (absolute) percentage of lamalginite than that of the other shales. In addition the shale contains substantial vitrinite, which constitutes another hydrocarbon source, albeit at relatively reduced conversion levels.

The difficulty in finding a consistent interptetation for the various parameters obtained for sample 674 emphasise the fact that , especially for oil shales of mixed type, both optical and chemical data need to be used in a complementary fashion to explain some of the otherwise anomalous properties of the sample. Even then an interpretation of some of the behaviour is necessarily speculative. It would be easy to dismiss the above differences for 674 simply as due to variations in sample composition (heterogeneity) between those specimens examined by petrography and those subsequently pyrolysed. Sample heterogeneity will necessarily have some influence, possibly large for pyrolysis-FID, on the results obtained from these varied approaches but statistical data and representative sampling should minimise this influence. It is also possible that the low relative hydrocarbon production is due to interactions between kerogen moieties and the mineral matrix, which has a different composition for 674, and may result in the formation of greater quantities of coke and in the formation of pyrolysis products which are not detected by the FID (e.g. carbon dioxide and water). To determine the latter possibility it is necessary to analyse the total volatiles formed during pyrolysis. To achieve this

requires sophisticated equipment and complex calibration procedures to obtain a good mass balance by accounting for all of the products formed during pyrolysis. An analysis of this type, for some of the Duaringa samples, will be described in the following section.

Looked at in the absence of other data, the relative P_2 ratios for the shallow oil shales from Duaringa indicate that 822 and 812 are shales containing a greater percentage of kerogen than 5391-C, if it is assumed that all of these samples comprise organic matter of the same type. However, when the ratios are interpreted in conjunction with the kerogen abundance values obtained from demineralisation of the raw shale (these values would not normally be available) they also show a higher relative hydrocarbon generating capacity for sample 812. For the latter this greater production per unit weight of kerogen content may result from the heterogeneous nature of the shale, which is implied by the large discrepancy between kerogen abundances as determined by optical techniques (Table 4-2) and from demineralisation procedures (Table 4-8). The respective lower (higher) ratios for 789 and 822 are obtained primarily as a direct result of relatively lower (higher) maceral content (Table 4-2).

When using the above procedure to evaluate the resource potential of a given deposit the relative genetic hydrocarbon production of the raw shale is the most important criterion, since it determines the commercial viability of the deposit. Relative P_2 ratios provide this information, since all of the samples may be categorised as either potentially better or worse shale oil producers than a given standard. For the Duaringa samples absolute shale oil yields may be obtained by relating P_2 ratios to FA shale oil data for 5391-C.

Although the Duaringa resource seam samples (and 686) were not sufficiently different in type and evolution to display large differences in the pyrolysis-FID data, those for oil shales representative of other Australian deposits showed enough systematic variations in the data to allow their differentiation into consistent categories on the basis of correlations between pyrolysis-FID values and their various chemical and petrological properties (c.f. section 5.1.2).

4.6 Total pyrolysate composition.

A crucial test in the recognition of productive oil shale seams is their ability to produce relatively large quantities of hydrocarbons. This capacity is adequately determined by the previous pyrolysis-FID procedure since it gives yields, relative to a convenient standard, which may easily be converted to absolute values or related to FA shale oil yields (LTOM). Since hydrocarbons actually produced from the raw shale are dependent on both abundance and type of kerogen, the relative production of these compounds reflects the combined influence of these factors, without providing specific information about either of them. For quantitative appraisal of a resource this may not be required, however knowledge about both allows substantially better interpretations to be made about pyrolysis mechanisms, coke formation, potential oil yields etc. Kerogen abundance data are particularly important when all of the pyrolysis products are monitored and a good mass balance is obtained. Information obtained from the latter kind of approach provides comprehensive data on pyrolysate constitution and allows the kerogen to be typed using organic carbon (C_{org}) conversion calculations. Unless the oil shale comprises a single uniform type, this approach gives an average characterisation based on results obtained from the pyrolysis behaviour of the composite organic matter.

The kerogen content of an oil shale is most readily determined by combustion of the organic carbon to CO_2 in an oxygen atmosphere, after inorganic carbon has been removed by acid treatment of the finely ground (pre-extracted) raw shale. This procedure determines only C_{org} and needs to be adjusted to obtain the total organic matter. To compensate for the abundance of other elements (H, O, N, S) present in the kerogen, the C_{org} value has to be multiplied by a conversion factor, because the elemental composition of the kerogen depends on both type and level of evolution. For immature type I, II and III kerogen at the stage of diagenesis these factors are 1.25, 1.34 and 1.48 respectively (Tissot and Welte, 1984). Although the kerogen composition may vary within localised accumulations of oil shale, the predominent type and the general stage of evolution are generally known from the analysis of samples, representative for the deposit, using

appropriate optical and/or physicochemical techniques. For the Duaringa samples petrological data allow all shale kerogens, except sample 674, to be classified as immature type I, with the latter comprising a more evolved mixture of ca. 66 % type I and ca. 33 % type III kerogen.

To obtain comprehensive information about absolute abundances of all of the pyrolysis products, some of the Duaringa oil shales and kerogens were analysed using the procedure outlined in section 2.4.4 (kerogen, ca. 50 mg was pelletised prior to analysis to reduce possible fouling of the heater coil). The approach is that first described by Wall and Dung (1984), who used it primarily to obtain kinetic data for the pyrolysis of oil shales. However, the method may also be used as an ideal assaying procedure which provides excellent material balance (usually > 99 %) and requires less than 1 g of raw shale. Raw data for the samples submitted were kindly provided by the first author, who used an improved version of the procedure as described by Wall and Smith (1986). Organic carbon values were determined as outlined above, with C_{org} for the oil shales obtained from the difference between total C and inorganic C as determined by acid treatment of the raw shale. For the Duaringa samples output typically obtained from the (essentially) isothermal pyrolysis procedure is tabulated in Table 4-9. Oil shale samples are designated by their respective sample codes, with the first decimal place figure indicating the first or second analysis. Kerogen samples are denoted by the respective deposit number and the suffix-K. At the time the instrumentation was available only those kerogens listed in Table 4-9 had been prepared.

Major differences in pyrolysate composition for the various samples are easily recognised from the tabulated yield values; however the physico-chemical processes underlying major variations in the abundance of these constituents requires a more detailed examination of the available data. One parameter, which is dependent on kerogen type, is the extent of C_{org} conversion occuring in the oil shale kerogen during the formation of volatile products. This carbon conversion can be measured by comparing the C_{org} in both raw and spent shale and making appropriate adjustments for inorganic carbon. These data

Table 4-9. Yields of products obtained from the (isothermal) pyrolysis (500 °C, 500 s) of oil shale and kerogen from the Duaringa deposit. The raw data were provided by G. Wall, CSIRO Division of Energy Chemistry, Lucas Heights Research Laboratories.

YIELDS: Grams per 100 grams dry feed.

Pyrolysis Products.								
	SHALE NO.	812.1	812.2	674.1	5391-C.1	686.1	812-K	674-K
	RUN NO.	647	648	649	650	651	652	653
	TEMP.C	500	500	500	500	500	500	500
	TIMEsec	500	500	500	500	500	500	500
1 -	OIL C5+	7.09	6.82	10.78	5.04	5.95	64.71	35.62
2 -	ALKANES	0.168	0.150	0.313	0.149	0.116	0.978	0.794
3 -	ALKENES	0.145	0.136	0.167	0.119	0.072	0.844	0.552
4 -	METHANE	0.114	0.100	0.296	0.090	0.064	0.621	0.731
5 -	HYDROGEN	0.032	0.031	0.021	0.049	0.006	0.069	0.041
6 -	CO	0.226	0.218	0.470	0.392	0.042	1.529	1.336
7 -	CO2	0.953	0.930	3.123	1.974	0.750	3.388	4.520
8 -	WATER	3.50	3.42	5.60	3.52	5.07	3.09	7.87
	H2S	0.000	0.000	0.000	0.000	0.010	0.345	0.322
	SPENT	87.74	87.95	79.31	88.79	87.77	18.37	45.55
	TOTAL	99.97	99.75	100.07	100.13	99.85	93.94	97.34
2 -	ETHANE	0.083	0.073	0.173	0.068	0.052	0.465	0.432
2 -	PROPANE	0.053	0.049	0.095	0.047	0.037	0.298	0.214
2 -	N-BUTANE	0.028	0.028	0.040	0.029	0.023	0.215	0.148
2 -	I-BUTANE	0.004	0.000	0.006	0.004	0.005	0.000	0.000
3 -	ETHENE	0.054	0.049	0.063	0.036	0.023	0.243	0.182
3 -	PROPENE	0.072	0.064	0.076	0.061	0.035	0.363	0.222
3 -	BUTENES	0.019	0.023	0.028	0.021	0.014	0.238	0.148
	ANALYSIS OF RAW MATERIAL : GRAMS PER 100 GRAMS OF DRY MATERIAL							
	TOTAL CARBON	10.320		23.550	8.710	9.200	68.650	64.240
	HYDROGEN	1.970		2.830	1.710	2.010	9.020	6.740
	NITROGEN	0.490		0.960	0.410	0.390	1.800	2.550
	ANALYSIS OF SPENT SHALE : GRAMS PER 100 GRAMS OF SPENT SHALE							
	TOTAL CARBON	4.390		17.720	3.450	3.850		
	HYDROGEN	0.700		1.250	0.620	0.670		
	NITROGEN	0.350		0.940	0.300	0.240		
	YIELDS PER 100 GRAMS OF OIL							
	OIL C5+	100.000	100.000	100.000	100.000	100.000	100.000	100.000
	ALKANES	2.376	2.192	2.908	2.963	1.953	1.512	2.230
	ALKENES	2.048	1.987	1.547	2.359	1.212	1.304	1.550
	METHANE	1.602	1.462	2.745	1.789	1.077	0.960	2.054
	HYDROGEN	0.458	0.461	0.198	0.967	0.093	0.107	0.116
	CO	3.194	3.201	4.361	7.782	0.702	2.364	3.752
	CO2	13.447	13.631	28.974	39.155	12.606	5.235	12.692
	WATER	49.402	50.057	51.942	69.822	85.235	4.772	22.107
	H2S	0.000	0.000	0.000	0.000	0.173	0.534	0.904
	ETHANE	1.176	1.069	1.608	1.355	0.879	0.719	1.213
	PROPANE	0.750	0.711	0.877	0.938	0.617	0.461	0.601
	N-BUTANE	0.399	0.412	0.372	0.584	0.379	0.332	0.416
	I-BUTANE	0.051	0.000	0.052	0.085	0.077	0.000	0.000
	ETHENE	0.755	0.714	0.584	0.723	0.385	0.375	0.511
	PROPENE	1.018	0.934	0.705	1.213	0.589	0.562	0.623
	BUTENES	0.275	0.339	0.258	0.422	0.238	0.367	0.415

are given in Table 4-10 and show a substantial difference between C_{org} conversion levels for the shallow type I kerogens and that for the mixed type from sample 674. If it is assumed that the liptinite fraction in 674 behaves as it does in the shallow shales and that C_{org} conversion within the shale proceeds as two discrete processes for the (separate) liptinite and vitrinite fractions of the kerogen, then calculations using data from Table 4-10 result in a negative value for the carbon conversion of the vitrinite alone. This is clearly impossible, and illustrates that the vitrinite fraction in the shale has a marked influence on the overall C_{org} conversion capacity of the total kerogen contained within the shale. The significant overall reduction appears dependent on the abundance of vitrinite, which obviously interacts with organic matter from the liptinite macerals during pyrolysis to form relatively greater quantities of carbonaceous residues (char). Inorganic components alone are not responsible since mineral-free kerogens 812-K and 674-K, under the same experimental conditions, produced significantly different quantities of spent material (Table 4-9). For 812-K the kerogen conversion to volatile products was ca. 82 %, while that for 674-K was substantially lower at only ca. 54 %.

Table 4-10. Data for the conversion of organic carbon in the Duaringa oil shales to volatile products during pyrolysis at 500° C (500 s). Values are given as grams per 100 g of dry feed.

SAMPLE	C_{org} (raw shale)	C_{org} (spent shale)[1]	% C_{org} conversion
5391-C	8.10	2.84	65.0 %
686	8.97	3.62	59.5 %
812	10.16	4.23	58.4 %
674	23.19	17.36	25.1 %

1 total inorganic carbon is assumed to be retained in the spent shale. The inorganic carbon abundances for the raw shales, as listed, were: 0.61, 0.23, 0.16, 0.36.

These figures are not as accurate as those obtained for the raw shale because only 50 m g of kerogen were analysed each time (this reduced accuracy is reflected by the lower mass balance figures of 94 and 97 % respectively). If the percentage value of kerogen conversion for sample 812-K is applied to the liptinite fraction of 674-K, this results in a value of about 3 % for the conversion of the remaining vitrinite macerals in the kerogen of the latter. This low positive figure contrasts with the negative value obtained earlier from calculations for raw shale, but again indicates that significant interactions are taking place during pyrolysis of the two different types of macerals, despite the absence of mineral influences. The efficiency of conversion of organic matter to volatile products is much higher in both samples for the demineralised than for the raw shale (812-K raw minus 812-K spent - ca.80 %, C_{org} in the raw shale - ca.58 %; 674-K raw minus 674-K spent - ca.54 %, C_{org} in the raw shale - ca.25 %). This suggests that the mineral matrix (generally) plays a role in promoting the formation of organic residues (char and coke) during the pyrolysis of raw shale. Since there was insufficient spent kerogen available to determine the carbon content in the residue, no C_{org} conversion values could be calculated for either of the isolated kerogens. However, the preceding argument about kerogen conversion applies equally well to C_{org} conversion for these samples, albeit at lower values. This follows since pyrolysis results in relative carbon enrichment of the spent organic matter, as a consequence of hydrogen depletion through aromatisation -polycondensation reactions underlying residue formation.

Where C_{org} values have been determined for the raw shale, these data may be used with the relevant conversion factors given earlier for type I, II and III kerogen to predict the kerogen content of the oil shale. For Duaringa the values predicted were compared with those actually obtained from the demineralisation of the shale (Table 4-11). The values compare directly with those for the shallow kerogens of uniform type and also with that of the mixed type I/III kerogen from 674, provided the latter is partitioned into its constituent maceral fractions prior to performing the calculations. The predicted (found) kerogen values may be used to calculate relative hydrocarbon production (oil and gas) to be

Table 4-11. Oil shale kerogen content calculations from C_{org} data for the raw shale and conversion factors for type I and III kerogen. Values are given as grams per 100 g of dry oil shale.

SAMPLE	C_{org}	CF [1]	K^2 (predicted)	K^3 (found)
5391-C	8.10	1.25	10.1	10.5
686	8.97	1.25	11.2	10.9
812	10.16	1.25	12.7	12.5
674 [4]	15.3	1.25	26.6	26.8
	7.6	1.48		

1 conversion factors for the calculation of type I (1.25) and type III (1.48) kerogen content from C_{org} data for the raw shale. **2** kerogen content for the raw shale as predicted from C_{org} values (C_{org} x CF). **3** kerogen content values obtained from demineralised shale (dry, ash-free basis). **4** data for 674 are calculated from Table 4-10 according to its kerogen maceral composition i.e., 15.3 g C_{org} as liptinite (i.e. 66 % type I) and 7.6 g C_{org} as vitrinite (i.e. 33 % type III).

Table 4-12. Comparative data for relative hydrocarbon production from raw shale (oil and gas) as predicted from type-dependent production factors and kerogen content. Predicted values are compared with those obtained by isothermal pyrolysis of the raw shale

SAMPLE	K [1]	PF	Prod.(P)	Prod.(F)	Ratio (P)	Ratio (F)
5391-C	10.1	0.75	7.6	5.4	1	1
686	11.2	0.75	8.4	6.2	1.1	1.15
812	12.7	0.75	9.5	7.2	1.25	1.33
674 [2]	17.7	0.75	15.9	11.6	2.09	2.15
	8.8	0.30				

1 predicted kerogen content values (from table 4-11). **2** see **4** in footnote for Table 4-11.
KEY: PF - relative hydrocarbon production factor for type I (0.75) and type III (0.30) kerogen. **Prod.(P)** - hydrocarbon production (oil and gas) predicted from oil shale kerogen content (K x PF). **Prod.(F)** - hydrocarbon production data (oil and gas) as given in Table 4-9 (sum of pyrolysis products 1 - 4). **Ratio (P)** - ratio of Prod.(P) values relative to 5391-C. **Ratio (F)** - ratio of Prod.(F) values relative to 5391-C.

expected from pyrolysis of the raw shale, using approximate type-dependent production factors. These factors are respectively 0.75, 0.50 and 0.30 for kerogen of type I, II and III and correlate with the average H/C atomic ratios for the respective kerogen types. For the Duaringa samples both predicted and found values are listed in Table 4-12. The found values were taken from Table 4-9 and comprise total quantities of methane, alkanes ($< C_4$), alkenes ($< C_4$) and oil C_{5+} produced during pyrolysis. Again there is good agreement between predicted and found values for hydrocarbon oil and gas production relative to 5391-C for all of the seams. For the mixed-type oil shale 674 this demonstrates that total hydrocarbon production may be predicted by summing the separate yields expected from the type I and III fractions of the composite kerogen and treating the underlying production mechanisms as discrete additive processes. The consistently lower hydrocarbon production actually obtained (71, 74, 76 and 73% of the predicted yields for the samples as listed) shows the relatively uniform influence of the mineral matrix in reducing hydrocarbon yield by promoting coking reactions. This reduction is to be expected since the production factors (PF) used to predict the yields are based on statistical data obtained from kerogen pyrolysis. For demineralised kerogen an increase in porosity created by the loss of minerals will assist the rapid expulsion of volatile retort products and thereby reduce coking.

Ratios similar to the hydrogen and oxygen indices referred to in section 4-5 may be helpful in assessing the kerogen type of oil shales where this information is not available from other sources. The ratios mg HC / g C_{org} (where HC is the total hydrocarbon yield obtained from "isothermal" pyrolysis (products 1-4 in Table 4-9) or corresponds to absolute P_2 values obtained from pyrolysis-FID) and mg CO_2 / g C_{org} give values analogous to the indices obtained from the Rock-Eval procedure. The CO_2 data in Table 4-9 corresponds to total gas generated during pyrolysis by both the kerogen and mineral matrix (decomposition of carbonates) and is consequently higher than that normally derived from the kerogen alone. Values calculated for respective indices are given in Table 4-13. An examination of the "hydrogen index" shows a consistent average value of ca. 690 mg

HC / g C_{org} for each of the immature resource seam samples, while that for 674 is, as expected, substantially lower. The "oxygen indices" are all much higher than expected for reasons referred to above; for type I, II and III kerogens oxygen indices obtained by the Rock-Eval method are usually < 50, < 100 and < 150 respectively. For 674, the low "hydrogen index" results primarily from its high vitrinite abundance. Assuming an average "hydrogen index" of 690 for the liptinite fraction of the shale from 674 results in the assignment of a very low index value of ca. 110 for its remaining vitrinite content. This is a value normally associated with type III kerogens, which usually have indices that lie below 100. The hydrogen index obtained from the Rock-Eval method has been shown to correlate well with H/C ratios obtained from elemental composition. For a H/C value of 1.22 (sample 674) this correlation corresponds to a hydrogen index of just over 450 (Tissot and Welte, 1984), and is in good agreement with the above data (500) even though pyrolysis conditions are obviously different for the two procedures.

Table 4-13. "Hydrogen" and "oxygen indices" calculated for Duaringa oil shale samples from pyrolysis yield data in Table 4-9.

SAMPLE	C_{org}	HC [1]	CO_2	" H INDEX "	" O INDEX "
5391-C	8.10	5.4	1.974	666	243
686	8.97	6.2	0.750	691	83.6
812	10.16	7.2	0.930	708	91.5
674	23.19	11.6	3.123	500	134

1 Total hydrocarbons (yields 1-4 from Table 4-9).
" **H INDEX** " - mg HC / g C_{org} . " **O INDEX** " - mg CO_2 / g C_{org}.

Calculations based on CO_2 production from 812-K and 674-K yield "oxygen indices" of 50 and 70 respectively for these kerogens. These values, in conjunction with respective "hydrogen indices" obtained from the raw shale pyrolysis, characterise 812 kerogen as type I and 674 kerogen as lying between type II and III kerogen. Evolution of CO_2 from kerogen alone shows that for the two samples analysed respectively ca. 40 % and 50 % of the carbon dioxide evolved during pyrolysis of the raw shale was contributed

by the decomposition of carbonates. This percentage is still a low value in absolute terms and is consistent with both shale mineralogy and inorganic carbon values given above (footnote 1, Table 4-10). In line with similar mineralogies and inorganic carbon abundances, contributions of CO_2 derived from the mineral matrix of the other shales during pyrolysis are probably of the same order. The sources of CO_2 during isothermal pyrolysis will be discussed in greater detail later in this section.

Figure 4-14 summarises some of the data which may be obtained for raw shale from the basic information provided by the complementary methods of petrography and pyrolysis discussed above.

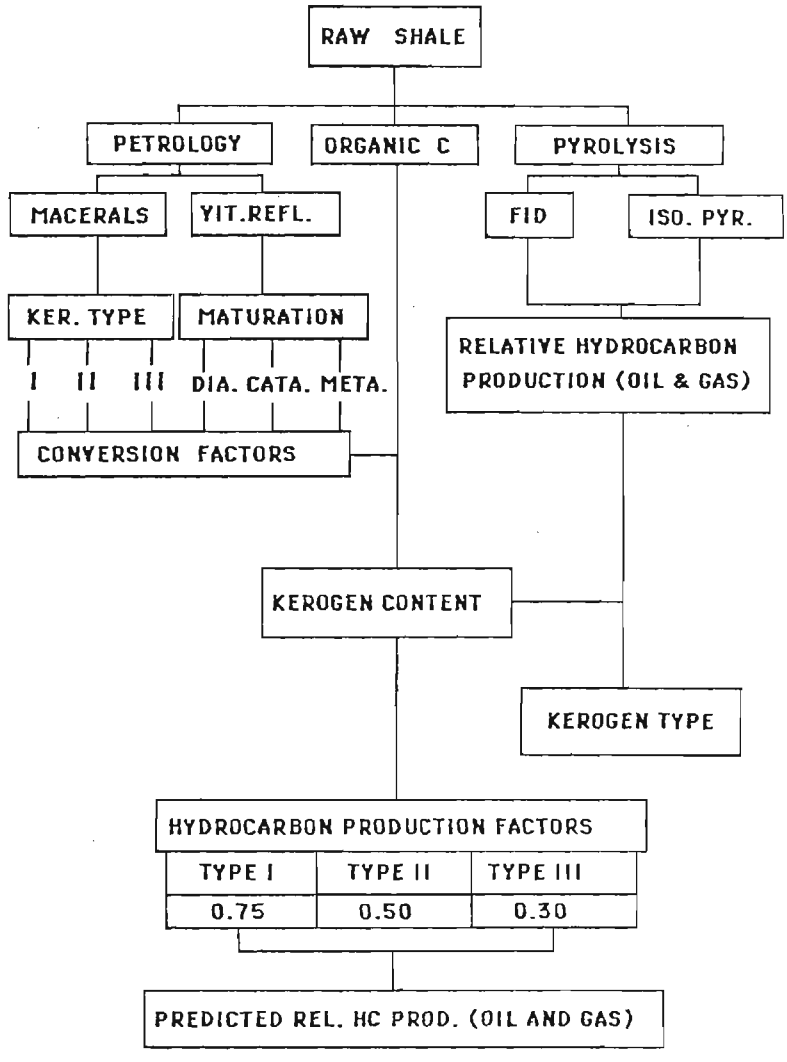

Figure 4-14. Schematic of some of the basic, interrelated data obtainable for oil shales using the complementary techniques of petrography and pyrolysis.

It should be emphasised that the predictions based on petrological data alone need to be checked against pyrolysis data for numbers of samples sufficient to support the validity of these predictions. Once petrological data for an appropriate number of samples representative of the deposit have been obtained, pyrolysis-FID should provide an adequate and rapid assessment procedure for determining the relative hydrocarbon production capacity of the reserve. The latter technique can also provide data for relative kerogen content in the raw shale, provided the deposit comprises organic matter of predominently uniform type. For kerogen of mixed type it gives kerogen content expressed as a percentage of the predominent organic matter type which would produce the yields (peak areas P_2) actually obtained during pyrolysis.

Wall and Smith (1986) used isothermal pyrolysis to study the production of oil and gaseous products from seven Australian oil shales as part of a broad investigation into their processing characteristics. They pyrolysed the raw shales isothermally at various temperatures and used the data to derive equations which give the yields of the various products as functions of time and temperature of pyrolysis. Although this was the main aim of the study, the authors pointed out that the method is also an attractive assaying procedure since it provides yields with a material balance closure at least equal to the Fischer assay. Used in that context, the data in Table 4-9 provide very accurate comparative information on both oil and volatile hydrocarbons produced by the organic matter contained in some of the raw shales from the Duaringa deposit. Comparative yield data for raw shale pyrolysis are particularly informative when they are calculated on the basis of production per unit weight of kerogen content. Under those circumstances the normalised comparative data provide information on the relative influence of the mineral matrix on respective hydrocarbon yields, provided the kerogen is of the same type for each sample. Even more information is obtained when both raw and demineralised shale from the same sample are analysed sequentially and under identical conditions. Since the same (relatively) unaltered kerogen is involved in both cases, combined data from these investigations differentiates between products derived from the mineral matrix and the kerogen and broadly quantifies mineral matrix influences and product contributions during pyrolysis.

For the two samples where these data are available, the contributions from and influence of, the mineral matrix are clearly evident from Table 4-14 and Figure 4-15.

Table 4-14. Yields of volatile products (grams per 100 g ash-free kerogen) obtained from the isothermal pyrolysis (500°C, 500 s) of raw and demineralised shale.

Sample	Oil C_{5+}	Alkanes	Alkenes	CH_4	H_2	CO	CO_2	H_2O
812[1]	55.00	1.25	1.11	0.84	0.25	1.74	7.41	27.24
	100.00	2.27	2.01	1.53	0.46	3.16		
812-K	67.37	1.02	0.88	0.65	0.07	1.59	3.53	3.22
	100.00	1.51	1.30	0.96	0.11	2.36		
674	40.53	1.18	0.63	1.11	0.08	1.77	11.74	21.01
	100.00	2.90	1.55	2.75	0.20	4.36		
674-K	37.40	0.83	0.58	0.77	0.04	1.40	4.75	8.26
	100.00	2.23	1.55	2.05	0.12	3.75		

1 The respective second row data for each sample are yields normalised against oil C5+ abundance and comprise those products derived (almost) exclusively from kerogen pyrolysis (see text for details).

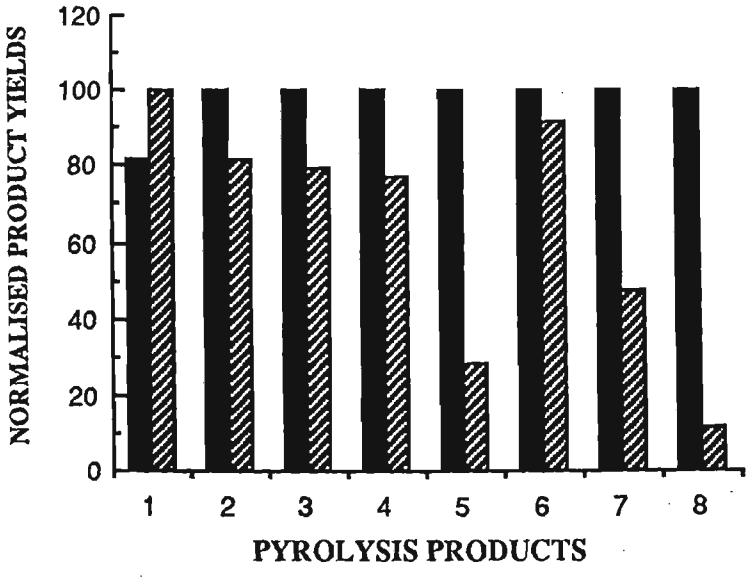

Figure 4-15. Plot of normalised relative yields (grams per 100 g kerogen) for individual products and component groupings obtained from the (isothermal) pyrolysis (500°C, 500 s) of oil shale ■ and kerogen samples ▨ from Duaringa 812. Products listed are: **1** - oil C_{5+}. **2** - alkanes (ethane, propane, butane, i-butane). **3** - alkenes (ethene, propene, butenes). **4** - methane. **5** - hydrogen. **6** - CO . **7** - CO_2 . **8** - water.

In both cases data for yields of CO_2 and H_2O show immediately that major contributions for these products are derived through the influence of, or directly from, the mineral matrix during raw shale pyrolysis (the contribution of CO_2 from the decomposition of carbonates was mentioned earlier). The bulk of the water is clearly contributed by the mineral matrix as interstitial H_2O derived from microreservoirs and pores and as water of hydration liberated from the minerals.

Although two samples do not constitute a sufficient number to allow generalisations to be made, the most obvious differences between raw shale and kerogen pyrolysis for the type I oil shales may be inferred from data for 812 and 812-K. Differences in the relative yields of individual products , or product groupings (e.g. alkanes $< C_4$ and alkenes $< C_4$) derived from the pyrolysis of these samples are most readily visualised in the form of a bar graph (Figure 4-15). When interpreting these data it is clear that differences in oil yield (per 100 g kerogen) from raw shale versus kerogen must be balanced by variations in other volatile products and/or char formation. Where variations do occur, they may be summarised as follows:

a) - kerogen produces relatively more oil C_{5+} (presumably because more char formation occurs during raw shale pyrolysis).

b) - abundances of low carbon number alkanes and alkenes are roughly the same; collectively they are slightly higher for the raw shale than for the kerogen, especially as a percentage of oil C_{5+} production (Figure 4-16). The latter is consistent with cracking reactions promoted by the thermo-catalytic activity of the mineral matrix. The similarity of the alkane/alkene ratios for both raw shale and kerogen pyrolysis (1.16 and 1.13 respectively) is in keeping with low residence times of the pyrolysate in the respective samples. The design of the pyrolysis-cell and experimental conditions used by Wall and Smith (1986) collectively ensure that coking and cracking are reduced as far as possible by chilling and condensing the evolved oil within a fraction of a second after its production.

c) - higher yields of methane from the raw shale (again consistent with more pronounced cracking).

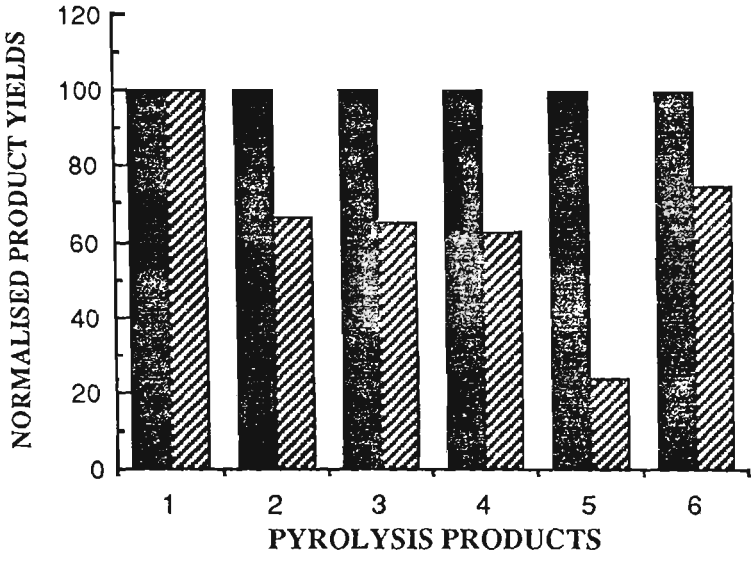

Figure 4-16.
Plot of normalised relative yields (grams per 100 g oil C_{5+}) for individual products and component groupings obtained from the (isothermal) pyrolysis (500°C, 500 s) of oil shale ■ and kerogen samples ▨ from Duaringa 812. Only yields for those products derived primarily from the pyrolysis of organic matter are plotted from data in Table 4-14. Products listed are : **1** - oil C_{5+} . **2** - alkanes (ethane, propane, butane, i-butane). **3** - alkenes (ethene, propene, butenes). **4** - methane. **5** - hydrogen. **6** - CO .

d) - substantially more hydrogen is obtained from the raw shale (ca.3x) and implicates the mineral matrix in H_2 production through cracking reactions.

e) - CO abundances (Figure 4-15) are about the same for both shale and kerogen (i.e. no major contribution through mineral matrix activity).

f) - CO_2 yields (Figure 4-15) show that about 50 % of the total production of the gas is derived from sources other than the direct pyrolysis of the kerogen. The additional yield from raw shale pyrolysis may be provided directly by the inorganic phase through the decomposition of thermally-labile carbonates, or indirectly through greater thermo-catalytic conversion of oxygen-containing moieties within the kerogen.

g) - H_2O yields (Figure 4-15) show that the bulk of the water is produced independently by the mineral matrix.

The data from Table 4-9 for the other oil shales analysed were also calculated as raw shale pyrolysis yields per 100 g of kerogen and are plotted in Figure 4-17 for samples 812, 5391-C and 686. The latter was included in the plot since earlier data (petrology, C_{org} conversion and "hydrogen index") suggest that this deeply-buried sample should produce similar yields of volatile pyrolysis products to those obtained from the shallow resource -seam oil shales.

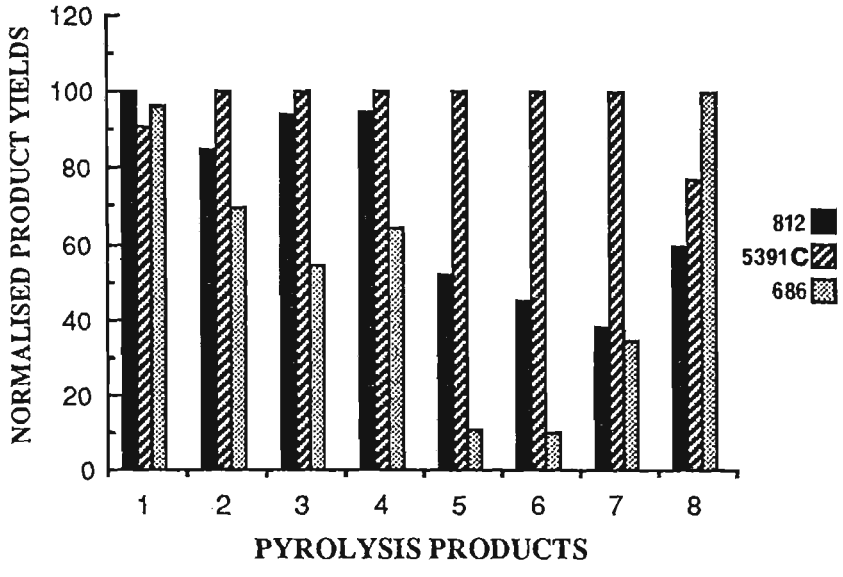

Figure 4-17.
Plot of normalised relative yields (grams per 100 g kerogen) for individual products and component groupings obtained from the (isothermal) pyrolysis (500°C, 500 s) of oil shale samples 812, 5391-C and 686 from Duaringa. Products listed are : **1** - oil C_{5+} . **2** - alkanes (ethane, propane, butane, i-butane). **3** - alkenes (ethene, propene, butenes). **4** - methane. **5** - hydrogen. **6** - CO . **7** - CO_2 . **8** - water.

Extending the inferences drawn from observations (a - g), to the isothermal pyrolysis data for all of the type I samples analysed supports the general propositions outlined below:

Variations in oil production between raw shale samples are primarily due to differences in kerogen composition and to subordinate mineral matrix effects (cracking, coking). These variations will be greatest when differences in the composition of organic matter are substantial (e.g. different uniform or mixed kerogen types). Where the oil shales comprise a uniform kerogen type, the mineral matrix effects may control pyrolysate composition. Where oil production is relatively higher (see data for 812 and 5391-C in

Figure 4-17) it is accompanied by less cracking to produce lower abundances of hydrocarbons < C_5. However total hydrocarbon production (per unit weight of kerogen) remains fairly constant as evidenced by the close "hydrogen indices" for all of the shales containing type I organic matter. Relatively higher oil yields may also be associated with relatively lower hydrogen and CO abundances, although data for 686 (Figure 4-17) contradicts this proposition, probably due to small cumulative differences in kerogen composition, mineralogy and maturation (note that for the three samples, CO yields correlate with O/C atomic ratios for respective kerogens in Figure 4-1).

CO appears to be derived almost entirely from the kerogen at this temperature of pyrolysis (500°C), but a small variable portion may result from the gasification of carbonaceous residues according to the equation: $C_{org} + CO_2 \longrightarrow 2\ CO$; and possibly from other reactions. The CO_2 required is derived both from kerogen and mineral matrix degradation and may participate in the above reaction of C_{org} gasification in quantities which depend on the reactivity of the char and the available surface area. The latter is a function of shale porosity and pore diameter. It should be noted that under the conditions of pyrolysis, the liberated CO_2 has ample opportunity to react with the hot carbonaceous residues, produced by both raw shale and kerogen pyrolysis, as a consequence of the confined environment within the sealed sample vessel.

If it is assumed that for the raw shales all of the inorganic carbon is in carbonate form, then the complete thermal degradation of the carbonate will produce a maximum yield of 3.66 g of CO_2 for each gram of inorganic carbon. For sample 812 the maximum yield of CO_2 obtainable from the pyrolysis of 787 g of raw shale (equivalent to 100 g kerogen content) through the total thermal-decomposition of inorganic C (0.16 % of raw shale - see footnote Table 4-10) in carbonate form is therefore 4.6 g. This figure is close to the absolute difference between the values of CO_2 for 812 and 812-K in Table 4-14. For 674, similar calculations for CO_2 yields from carbonates in the raw shale work out at a potential

maximum contribution of 4.95 g CO_2 from that source, again close to, but less than, the difference between 674 and 674-K in Table 4-14. This suggests that the major differences in CO_2 abundances between yields from raw shale and kerogen pyrolysis are due to contributions obtained directly from the thermal decomposition of labile carbonates.

Thompson and Thompson (1983) have shown that the thermal decomposition of calcite: $CaCO_3 \longrightarrow CaO + CO_2$ is a reversible process, in which recarbonisation of the oxide occurs in the presence of CO_2 via a two stage chemisorption-reaction process. This suggests that the carbonate source for the CO_2 from the Duaringa raw shales is probably a more labile carbonate such as siderite. This proposition is supported by data from Lindner (1983) who reported the absence of calcite and the presence of siderite (at accessory levels: 5 - 20 %) in the mineral constituents of oil shales from the resource seams of the Duaringa deposit. Although siderite may also undergo CO_2-induced recarbonisation reactions such as those proposed for calcite, these mineral data suggest that the bulk of the additional CO_2 obtained from the pyrolysis of the raw shale is probably obtained directly from its decomposition. Further subordinate quantities of CO_2 may possibly be liberated from oxygen-containing moieties of the kerogen through increased C_{org} conversion mediated by the thermo-catalytic activity of the mineral matrix.

The bulk of the water is obviously derived from the mineral matrix in the above cases (812 and 674) and in general is clearly dependent on the abundance of interstitial water present in mineral pores and microreservoirs, and on that derived from water of hydration liberated from the minerals.

Specific differences between 5391-C and 686 oil shale yields are clearly evident from Figure 4-17, with relative variations in hydrogen, CO and CO_2 abundance particularly noticeable. Hydrogen variations may be the result of differences in matrix-induced cracking reactions, while the relatively low yield of CO (kerogen derived) for 686, may reflect changes in maturity due to deeper burial. Little inference can be drawn from the CO_2 data

since, for both samples, quantities of the evolved gas correspond closely to relative values expected from the degradation of total inorganic C in carbonate form (22 g - 5391-C, 7.5 g - 686).

The total product yields are obviously relevant to the commercial exploitation of the deposit and provide data which have implications for resource potential (yield of gaseous and liquid hydrocarbons per gram of raw shale), waste disposal (spent material), energy balance (e.g. hydrogen yields, combustibility of carbonaceous residues) etc. Comparisons of pyrolysis yields for kerogens of the oil shales (e.g.from horizontal strata) should be restricted to oil and volatile hydrocarbons unless a uniform mineralogy for a given stratum has been established. This restriction is necessary since the possibility of secondary reactions and the derivation of variable quantities of carbon in the form of CO and CO_2 from sources other than the organic matter make a comparison of kerogen products speculative for these pyrolysate components.

When the results for the mixed-type samples (674 and 674-K) are compared, similar deductions about mineral matrix effects, product generation and cracking mechanisms can be made (Figure 4-18). Their relative total hydrocarbon composition is similar to that for the shallow resource-seam oil shales of type I, albeit at relatively reduced yields (per gram of kerogen). Moreover, the pyrolysis-GC profiles (which are dominated by the oil C_{5+} components) are also very similar. The pyrolysis products of the mixed type I - type III kerogen are dominated by the products corresponding to type I kerogen and for the samples studied the yields appear to be additive. Before these findings can be generalised this aspect requires further investigation, ideally using known artificial and natural mixtures of the two kerogen types.

a.

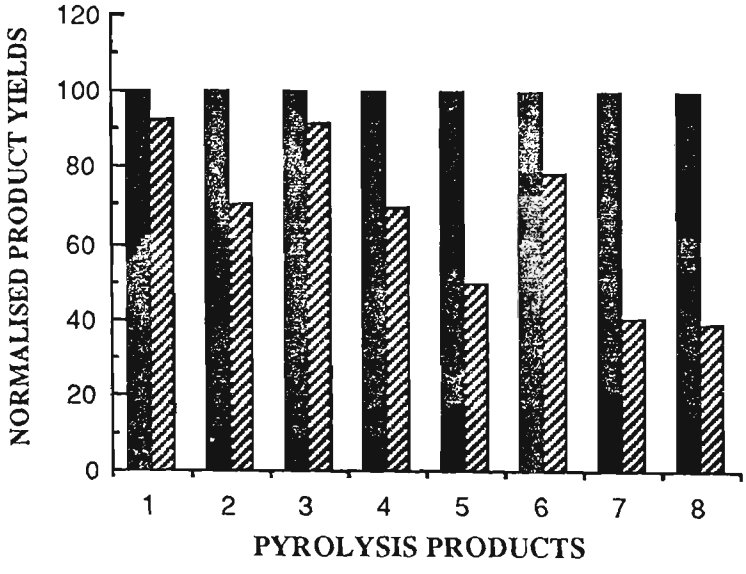

b.

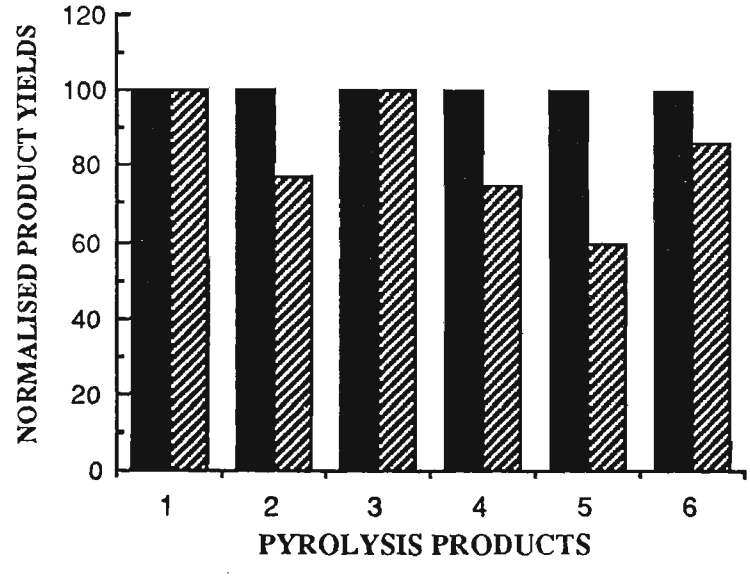

Figure 4-18.

a. Plot of normalised relative yields (grams per 100 g kerogen) for individual products and component groupings obtained from the (isothermal) pyrolysis (500°C, 500 s) of oil shale ■ and kerogen samples ▨ from Duaringa 674. Products listed are: **1** - oil C_{5+}. **2** - alkanes (ethane, propane, butane, i-butane). **3** - alkenes (ethene, propene, butenes). **4** - methane. **5** - hydrogen. **6** - CO . **7** - CO_2 . **8** - water.

b. Normalised relative shale ■ and kerogen ▨ yield data for Duaringa 674 (per 100 g oil C_{5+} - from Table 4-14)

4.7 Thermogravimetric analysis of raw shale and kerogen.

The application of, and results from, the TGA-DTA analysis of kerogens of different type were described in section 2.4.3. The general requirement for oil shale demineralisation limits the application of this procedure for the purposes of rapid stratigraphic screening of oil shale deposits. On the other hand, information obtained from the direct TGA-DTA analysis of raw shale is limited since it provides only global mass -loss data for the combined organic and inorganic phases, without differentiating between the mass losses attributable to each. This may be remedied, at least in part, by interfacing the thermobalance to other analytical instruments (any proposed coupling depends largely on the compatibility of respective instrument designs and in practice is very limited). The collection and independent analysis of pyrolysis gases, condensables (oil and water) and residues is also limited for the first two categories since only small quantities of raw material are (usually) accommodated in the instrument's sample holder. In isolation the technique is rather blunt, but may be used for the rapid assessment of horizontal strata of oil shale occurences within the one deposit, particularly for immature (shallow) samples. This follows since the kerogen contained in the mineral matrix undergoes a substantially higher percentage mass loss than the inorganic phase (up to ca. 97 % for type I kerogen - see later results for Duaringa 812), with the latter suffering relatively smaller mass losses associated primarily with the evolution of gas (CO_2) and H_2O (interstitial pore and microreservoir water and water of hydration). Consequently the procedure allows oil shale samples within common horizontal strata from geographically close regions of the same deposit to be compared directly, provided they comprise a uniform mineralogy and kerogen type. Where these requirements are generally met, direct comparisons of mass losses (per unit mass of raw shale) should provide a good indication of the relative organic content of any particular samples and allow predictions about their relative generating potentials (oil and gas) to be made. These predictions may then be verified independently, for a restricted number of representative samples, by more detailed complementary techniques (such as those described in previous sections of this chapter and in chapter 2), and the specific results applied more generally to previously obtained TGA-DTA data for the deposit.

Inferences with respect to relative kerogen content cannot be made, a priori, for raw shales obtained from different depths of a stratigraphic sequence, since mass losses from TGA analysis diminish in concert with increased evolution due to burial. Under special circumstances (same mineralogy, and known kerogen content), the data differentiate between kerogens of different types on the basis of large variations in mass losses (per unit mass of kerogen) associated with their pyrolytic conversion (cf. section 2.4.3).

Saxby (1981) overcame some of the inherent limitations of TGA analysis of oil shales by heating the samples in a series of steps and varying the pyrolysis atmosphere within a single run. The isothermal steps incorporated in the temperature profile were designed to briefly decrease the rate of evolution of volatiles so that losses from different samples during particular temperature intervals could be compared. The data provide information on the relative moisture content (25-150°C), volatile matter (150-500°C - oil-rich fraction, 500-900°C - gas fraction), char and ash produced by the raw shale sample.

When used with the same temperature profile employed for pyrolysis-FID, TGA provides very accurate complementary information which can be used in conjunction with results from the former approach to differentiate between pyrolysis products as residue (char and ash), combustible (oil and hydrocarbon gases) and volatile FID-negative fractions (CO, CO_2, H_2S, H_2O etc.). In this context the absence of losses, normally reported for FA procedures, ensures that the yield for each fraction is accurately determined. Although values for the combustible fractions (from pyrolysis-FID data) are normally only values relative to an adopted standard (e.g. 5391-C), these relative fractions may be converted to absolute values, which in turn provide absolute yield values for the volatile non-combustible fraction.

TGA-DTA data for the raw shale samples from the Duaringa deposit were obtained under atmospheres of air and nitrogen using the procedure described in section 3.5.4. Initially TGA results were compared for a single raw shale sample heated first in a sample pan fitted with a pin-holed crimped lid and then in an uncovered container. Data obtained for the uncovered sample showed that there was a ca. 50 % increase in mass loss when

using this open configuration; subsequently only open pans were used for all further analyses. The reduced mass loss associated with pyrolysis in a restricted environment shows the effects of secondary processes on the ultimate yields. A reduction in diffusion rates, with concomittant increases in the residence-time of pyrolysis products evidently allows more secondary processes, including hydrous pyrolysis and coking reactions to take place. The net result appears to be an overall reduction in carbon conversion to volatile products and is manifested in a subsequently lower mass loss.

When the TGA-DTA profiles for oil shale samples pyrolysed in air and nitrogen were compared, only minor differences were observed. These were confined almost entirely to the DTA curves which were virtually flat (i.e. no major exo- or endothermic reactions) for pyrolysis under nitrogen, but showed a very small endothermic as well as two variable and minor exothermic DTA peaks during pyrolysis in air. The very small endothermic peak (common to pyrolysis in both air and nitrogen) extends roughly over the temperature range 50 - 105°C and is probably related to the latent heat required to expel surface moisture. The other relatively larger exothermic peaks are poorly resolved and cover the temperature region 240 - 450°C. They comprise a first (usually) larger peak over the 240 - 370°C region of the pyrogram and a second overlapping peak extending from 330 - 450°C. Data obtained from investigations on coals suggest that the first peak is possibly associated with the oxidation of aliphatic chains, while the second may correspond to the oxidation of aromatic rings (Durand-Souron, 1980).

The mass-loss profiles for the Duaringa raw shales heated in air were plotted from respective TGA data and are given in Figures 4-19 and 4-20. The mass-loss curve for 5391-C is again depicted in Figure 4-21, with points labeling those temperature regions delineated by points of inflection. Pyrolysis processes underlying these temperature domains for the TGA analysis of kerogens were discussed in section 2. ; below they are interpreted along similar lines for the raw shale, with specific reference to data available for the sample from other procedures. The pyrograms for sample 812, 812-K, 674 and 674-K were plotted from TGA data obtained in an inert atmosphere (nitrogen) and results for these samples will be contrasted with information previously obtained in section 4.6 from their isothermal pyrolysis.

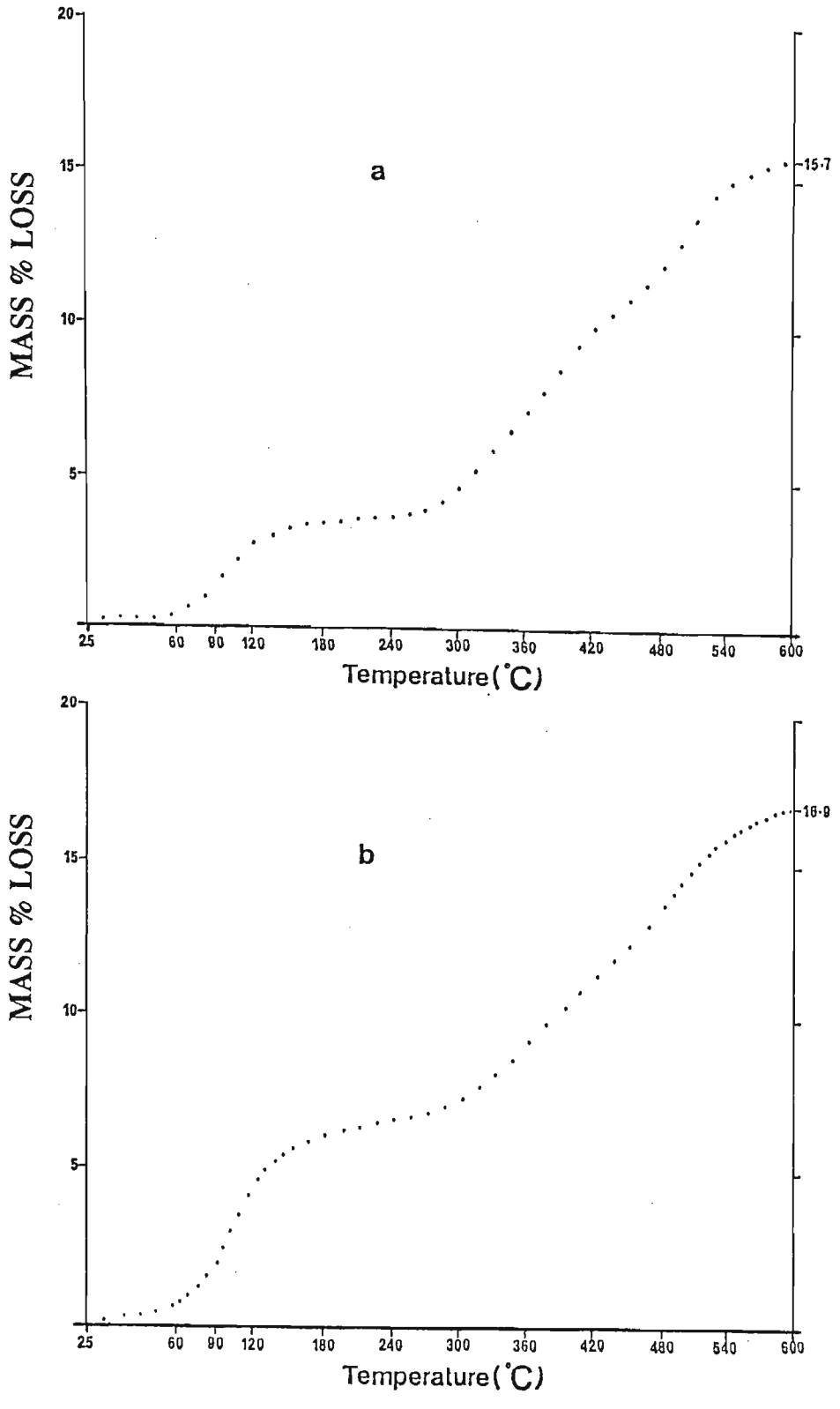

Figure 4-19.

Percent mass-loss profiles for Duaringa raw shale samples 5391-C (a) and 686 (b). The profiles were obtained from respective TGA pyrograms of the raw shales heated in air (without pre-drying) over the temperature range indicated, at a rate of 10°C min^{-1}.

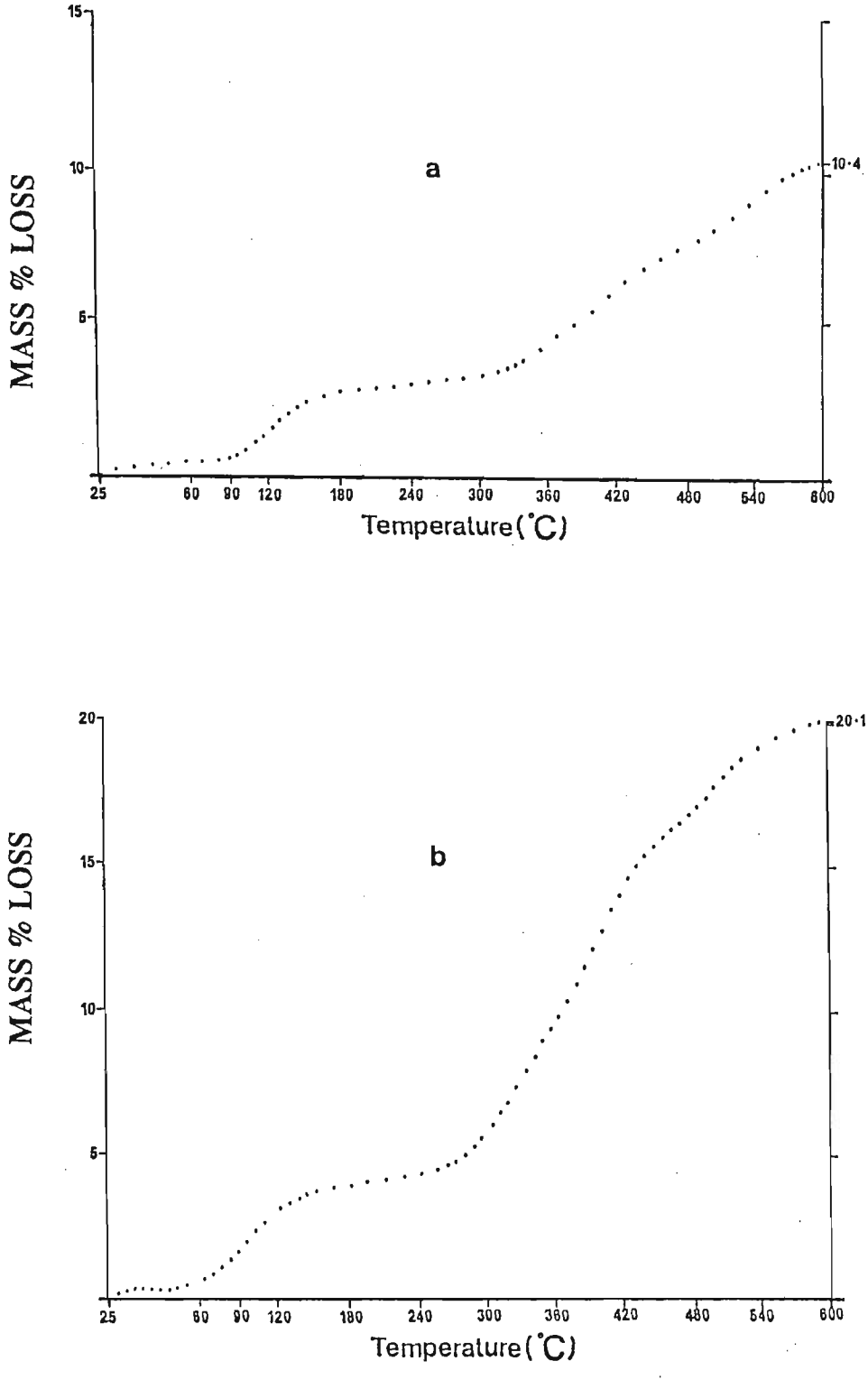

Figure 4-20.

Percent mass-loss profiles for Duaringa raw shale samples 789 (a) and 822 (b). The profiles were obtained from respective TGA pyrograms of the raw shales heated in air (without pre-drying) over the temperature range indicated, at a rate of 10°C min^{-1}.

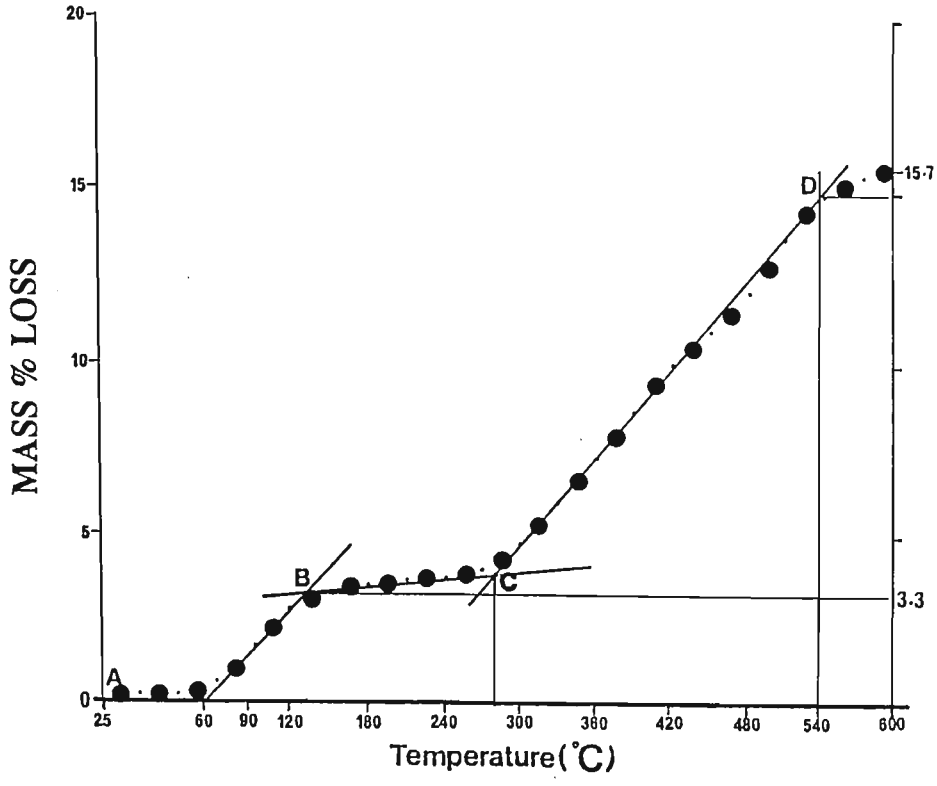

Figure 4-21.
Percent mass-loss profile for Duaringa raw shale 5391-C heated in air (conditions as for Figure 4-19).

For all of the TGA analyses the raw shale was used as received and for 5391-C the three regions above, corresponding to (major) mass losses, may be associated with the following physicochemical processes:

REGION AB (25 - 130°C) : Major loss of adsorbed water (ca. 3 %) as well as the loss of small amounts of volatile adsorbed organic matter (bitumen).

REGION BC (130 - 280°C) : Further (minor) loss of adsorbed water and continued loss of volatile organics(< 1 %). Onset of major oil formation after point C (ca. 280°C).

REGION CD (280 - 540°C) : Major oil formation zone due to pyrolysis of kerogen; also mass losses due to formation of water and gas from the inorganic phase (combined losses ca. 11 %). Only minor further mass loss after 540°C.

Residue remaining after pyrolysis to 600°C (char and ash) is 84.3 g (per 100 g of raw shale).

The TGA data for the other raw shales may be interpreted in the same way as for 5391-C and provide comparative TG results for moisture, volatile matter, char and mineral residues (ash). The volatile matter produced in the 280 - 600°C region of the pyrogram should provide qualitative data on relative kerogen abundance, since all of the shallow raw shales and 686 have similar petrologies (Table 4-15).

Table 4-15. Comparative TG results for oil shales from Duaringa (grams per 100 g of raw shale). Samples were heated in air from 280 - 600°C at 10°C min^{-1}.

SAMPLE	MOISTURE (25 - 130°C)	VOLATILE MATTER (130 - 600°C)	RESIDUE (char and ash)	RATIO[1] (volatile matter)
5391-C	3.3	12.4	84.3	1.00
686	5.0	11.9	83.1	0.96
789	2.5	7.9	89.6	0.64
822	3.8	16.3	79.9	1.31

1 Ratio of volatile matter relative to sample 5391-C.

The residue values in Table 4-15 are close to, but lower than, those found for the samples analysed by isothermal pyrolysis. This is not surprising, since the TGA temperatures and duration of heating are higher in both cases. An ab initio attempt to reconcile the volatile losses in Table 4-15 with the data for maceral and mineral content (Table 4-2) proved unsucessful. Expressing the total loss incurred as comprising the additive losses due to maceral (kerogen) and mineral changes in the raw shale during heating produces a series of linear equations which may be solved simultaneously under certain assumptions. For the petrologically most similar shales 5391-C and 822, these are respectively:

$$(1) \qquad 27.2\,x + 72.8\,y = 12.4$$

$$(2) \qquad 28.1\,x + 71.9\,y = 16.3$$

where x represents the mass loss in grams per volume percent of liptinite maceral content

in the raw shale, y denotes the mass loss in grams per volume percent of mineral matter contained in the raw shale and the RHS of the equations are respective TG values corresponding to losses of volatile matter (Table 4-15). (N.B. equation (2) has been adjusted for mineral pyrite.).

The very close values of the coefficients for the respective organic and inorganic phases of the two samples suggest that mass losses actually obtained should be similar (contrary to what was found) if the underlying percentage mass losses are in fact constant for both samples (as assumed). Solving the equations simultaneously confirms the underlying problems of reconciling TGA data for the raw shales by giving a negative mass loss (i.e. a mass gain) for the mineral phase and an impossible value of ca. 450 % mass loss for the kerogen. This underscores the difficult task of interpreting all of the complex processes arising from interactions between pyrolysis mechanisms, possible sample heterogeneity, mineral matrix influences etc. from one isolated approach. (The initial interpretation of the process as comprising two first order processes is of course far too simplistic, but serves to highlight the complexities of the combined mechanisms operating during the analysis).

As expected, more direct comparative inferences may be drawn when isolated kerogens are analysed. The Duaringa samples 812 and 674 were analysed by TG in an inert nitrogen atmosphere under identical experimental conditions (Figure 4-22). Although data from the raw shale analyses are again only global losses and reveal very little about the contained organic matter (other than to suggest (erroneously) that both shales are very similar), the pyrograms for the kerogens clearly differentiate between the type I kerogen from 812 and that of the different type from 674. Without samples representative of other types of kerogens, it remains speculative to assign a definitive type to that of 674, although other data has indicated a mixed type I/III composition. This again emphasises the need for complementary data required to characterise correctly both raw shales and kerogens.

In isolation, TGA-DTA is clearly best suited for the comparative study of the same sample (raw shale or kerogen) under variations in heating rates, final retorting temperatures and inert or reactive pyrolysis atmospheres. In that context the procedure provides valuable

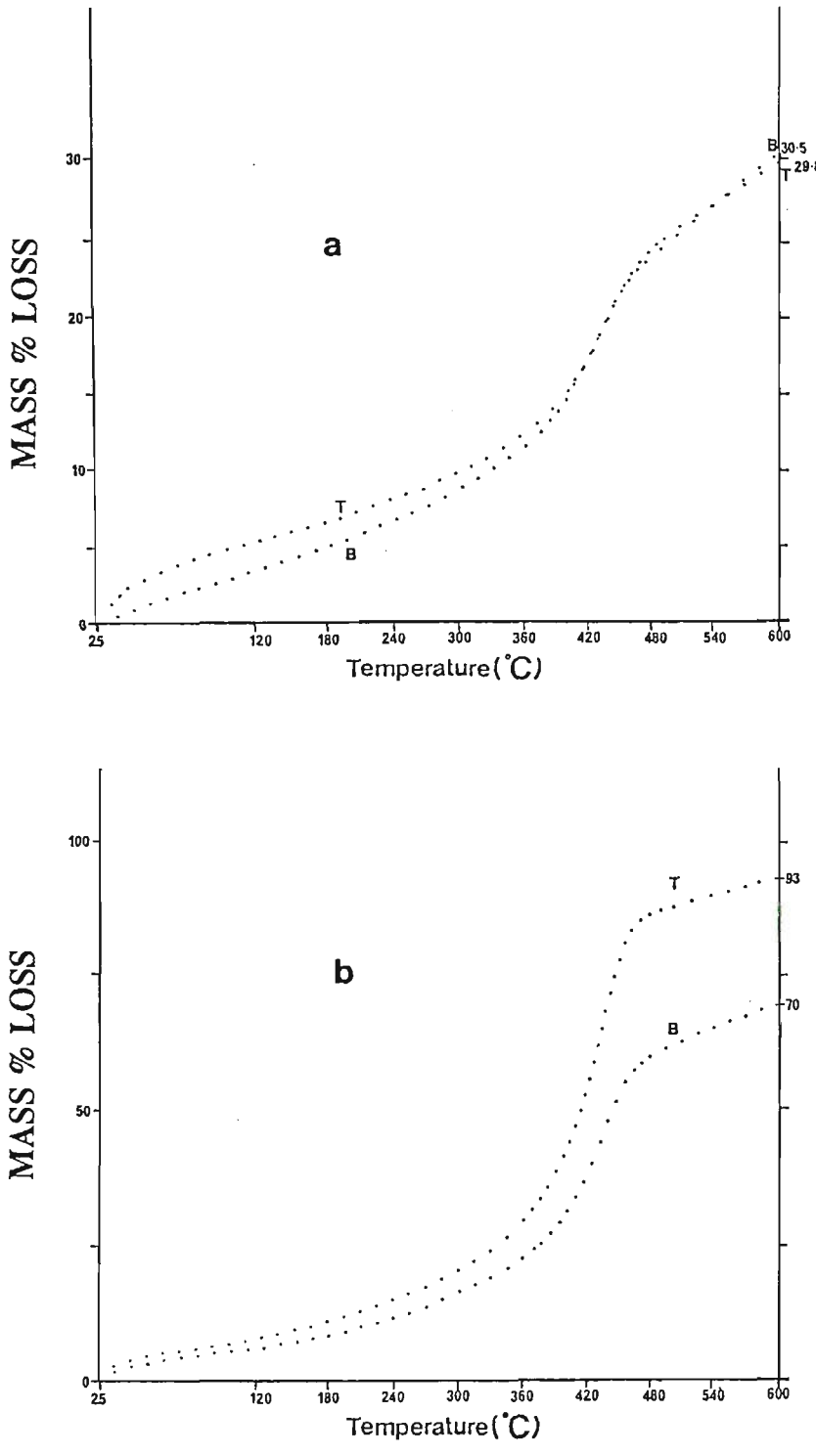

Figure 4-22.

Percent mass-loss profiles for Duaringa raw shale samples 812 (T) and 674 (B) - (a), and for the corresponding demineralised shales (b). The profiles were obtained from respective TGA data of pre-dried samples (105°C, 2 h) heated in nitrogen over the temperature range indicated at a rate of 10°C min^{-1}.

data on the retorting characteristics of the sample and should assist in choosing retorting parameters which will maximise hydrocarbon yields (oil and gas) from commercial operations. It may also be used as a preliminary step in the more detailed analysis of potentially promising samples.

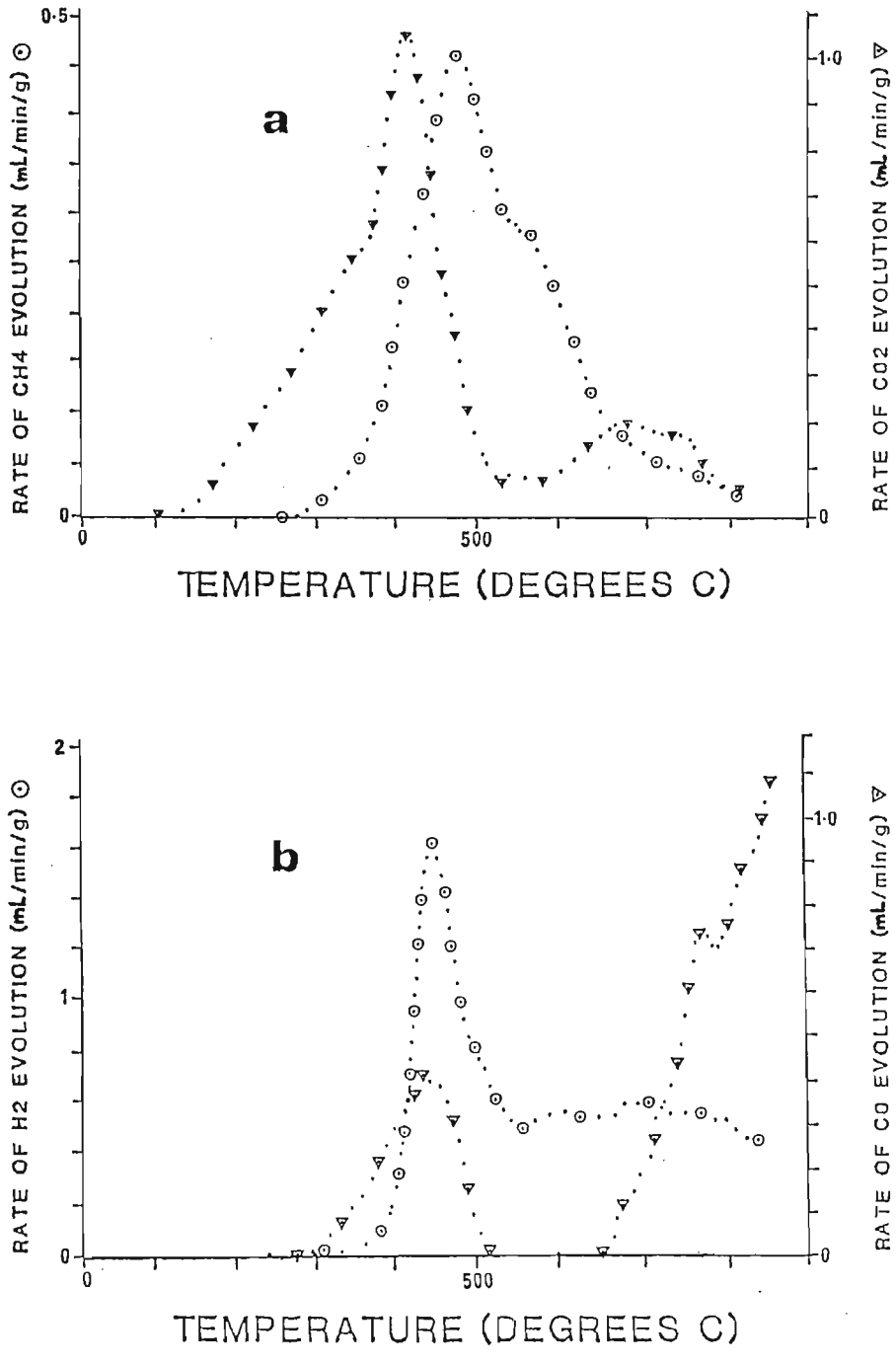

Figure 4-23. Gas evolution profiles (for a "representative" Duaringa resource-seam shale heated at 3°C min^{-1} in argon) expressed per gram of organic carbon. The profiles correspond to CH_4 and CO_2 (a) and H_2 and CO (b), with respective symbols as indicated. (Data were taken from Ekstrom et al. 1983).

Ekstrom et al. (1983) have reported on the chemical and retorting properties of selected Australian oil shales and obtained gas evolution profiles for samples from five deposits (the samples were retorted at a linear rate of 3°C min^{-1} in an inert atmosphere of argon). The various profiles of gas evolution for a "representative" Duaringa oil shale sample are given in Figures 4-23. Most of the gas evolution traces show sharp peaks at or near the temperature at which oil formation is at a maximum. For the Duaringa resource -seam samples analysed by isothermal pyrolysis this indicates that their formation at 500°C is (primarily) associated with the thermal degradation of organic matter, in agreement with speculative conclusions reached in section 4.6 from their respective yield data.

4.8 SHALE OIL CHARACTERISATION.

The previous sections in this chapter were primarily concerned with rapid assessment procedures for the oil shales and furnished data on kerogen type, maturity, hydrocarbon production potential (oil and gas) and commercial viability of the deposit. It is clear however that a detailed knowledge of the constituents of crude shale oil is essential for the (general) development of refining procedures capable of handling the diverse range of compounds normally found in these syncrudes. In that context it is particularly important to evaluate the effects of certain fractions of the shale oil on overall performance in distillation and catalytic cracking units, where the presence of certain classes of compounds in the feedstock (e.g. nitrogen-containing components) is known to poison catalysts. Detailed knowledge of constituents is also needed to determine the effect on raw oil composition of varying retorting conditions or high-grading the syncrude (e.g. removal of heteroatoms (N,S) by catalytic hydrogenation) and to assess the potential of contained classes of compound as feedstocks for the chemical industry.

4.8.1 Raw shale oil.

Shale oil for all of the Duaringa oil shale samples was obtained using the stainless-steel retort (cf. section 3.3). In addition to these (**tube-furnace**) oils, further oil was produced for Duaringa 5391-C using the FA retort and procedure. The latter (**FA**

oil) was used as a reference sample for subsequent shale oil characterisations. Tube furnace oil yields (Table 4-20) were generally higher than available FA retort data (Queensland Government Analyst), probably due to the combined effects of better retort design, the use of sweep-gas and a shorter, independently heated, collection tube and the collection of the pyrolysate at -20°C.

Aliquots of each of the raw shale oils (50 mg) were separately dissolved in dichloromethane (1 mL), dried ($MgSO_4$) and centrifuged. The supernatant oil solutions were analysed by GC and GC-MS and the various profiles compared. All of the chromatograms were qualitatively similar, with each GC-trace dominated by the alkene-alkane components previously observed in the pyrolysis-GC profiles of the respective samples (Figure4-24).

TABLE 4-20. Tube-furnace retort yields (grams per 100 g of dry feed) obtained for some of the raw shales from the Duaringa deposit.

SAMPLE	OIL	WATER	SPENT SHALE	GAS AND LOSSES
5391-C	4.9	7.5	83.6	4.0
686	5.8	8.9	85.5	3.5
812	5.9	10.7	78.1	5.3
674	12.7	8.6	75.4	3.3

NB! Insufficient raw shale was retorted for 789 and 822 to enable accurate yield determinations to be obtained for these samples.

A notable feature of each of the raw oil gas-chromatographic profiles is the relatively lower abundance of alkenes (relative to the corresponding alkanes) when compared with the appropriate pyrolysis-GC profiles. This comparative reduction in absolute alkene concentrations in the raw oils is due to differences in pyrolysate residence times during the two retorting procedures. Regtop et. al (1985) have shown that a decrease in the concentration of alkenes derived from the pyrolysis of oil shales correlates positively with

an increase in pyrolysate residence-times. Differences in the relative abundance of dimethyl -benzenes were also observed for 5391-C and 686, but variations in the concentration of these components are not restricted to these samples and were also found in the raw oil profiles from the other shallow oil shale samples. Consequently these variations reflect differences in the organic content rather than changes caused by maturation due to burial.

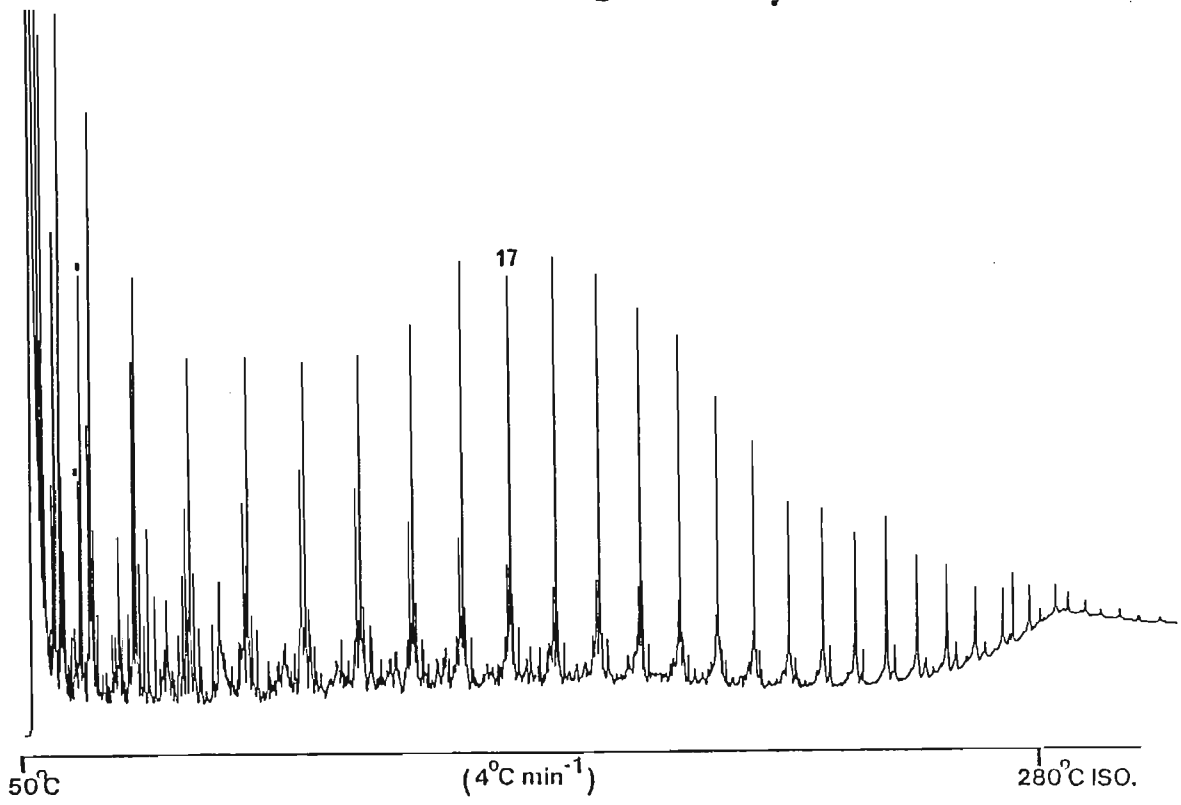

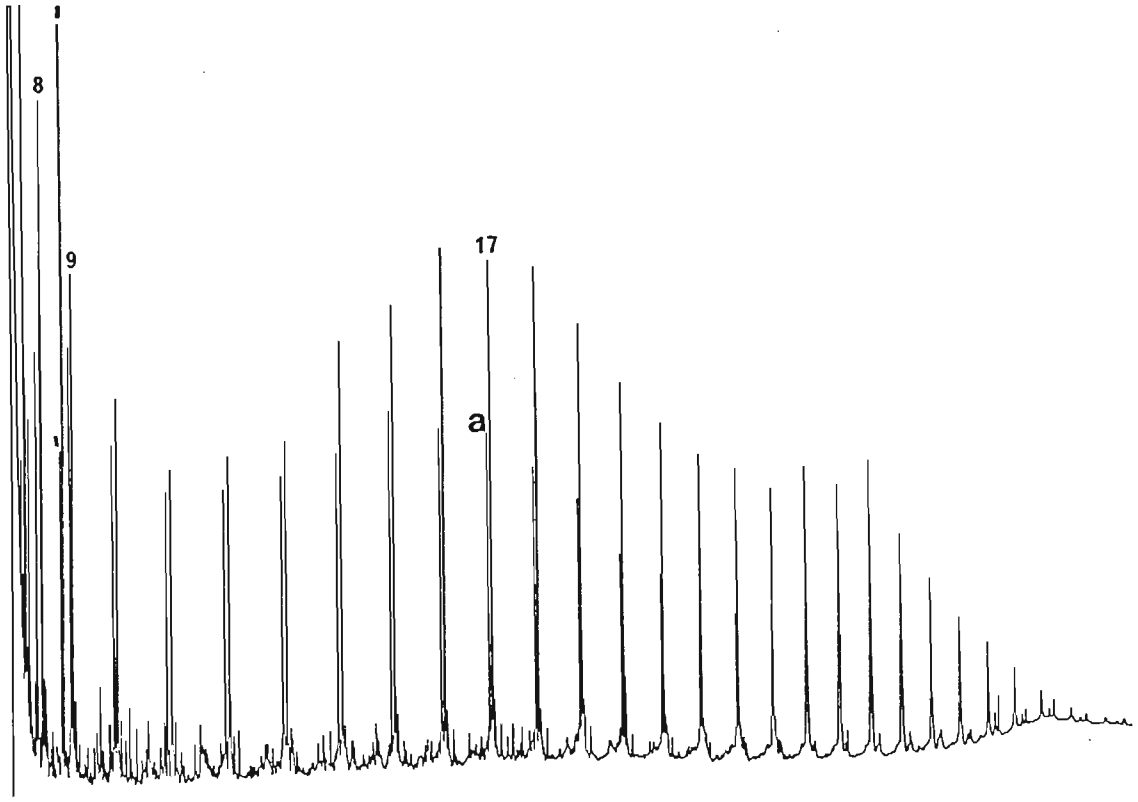

Figure 4-24.
GC profiles for tube-furnace oils obtained from Duaringa 5391-C (upper trace) and 686. Each profile is dominated by 1-alkenes (a) and alkanes (17),which show differences in their relative abundances. Further variations are evident in the concentration of dimethylbenzenes, denoted by ' in the chromatograms.

4.8.2 Shale oil asphaltenes.

A common property of fossil fuels derived from heavy oils, bituminous sands, oil shales and coals is their high content of N, S, O compounds (resins and asphaltenes). Asphaltenes is the general name given to the fraction of these oils and bitumens which is precipitated by the addition of a large excess of low-boiling hydrocarbons such as pentane or hexane (different compounds may be precipitated with the same procedure from different crudes and also from shale oils and coal liquids). Tissot and Welte (1984) have suggested that (natural) asphaltenes are formed during the diagenetic stage of sediment maturation and that they are similar to kerogen (based on data from EA, IR etc.) but of lower molecular weight; this makes them soluble in the usual organic solvents such as benzene, dichloromethane etc.

The N, S, O compounds appear as possible intermediates in some of the reaction pathways from kerogen to petroleum, with generation of high molecular weight heterocompounds preceding the formation of hydrocarbons. The latter would mostly result from successive reactions in which heavy heterocompounds act as intermediate products (Ishiwatari et al. 1976).

Asphaltenes precipitated from crude oils have been studied by numerous physical and chemical techniques such as EA, IR, X-ray diffraction and fluorescence, NMR etc. (Yen, 1972). Using these data Yen has proposed a generally accepted, structural model for asphaltenes :

The basic unit is a pericondensed polyaromatic sheet consisting of aromatic cycles substituted by methyl groups and a small number of long chains. Heteroatoms represent a defect in the aromatic structure and are found in benzothiophene groups (S), quinoline groups (N) and ether bonds (O). Individual aromatic sheets are usually stacked (ca. 5 layers) to form particles or crystallites by intermolecular or intramolecular association. The stacked aromatic sheets show some disorder, probably induced by chains of aliphatic- and/or napthenic-ring systems, which link the edges of the aromatic sheets and tend to hold the sheets apart. Several crystallites may form aggregates or micelles of different size. In crude oils (shale oils) asphaltenes are probalbly dispersed by the action of resins which keep these aggregates in suspension.

The molecular weights of asphaltenes depend on the source from which they are derived and on the method by which they are isolated. Wen et al. (1978) list the molecular weights of various asphaltenes isolated using methods such as freezing point, vapour pressure osmometry, gel-permeation chromatography etc. but stress that the values given represent average values only. The molecular weights of petroleum asphaltenes range from 1,000 - 10,000 or more. By contrast, the asphaltenes isolated from Green River shale oil by Yen and coworkers have a molecular weight range of 600 - 750 daltons (Wen et al., 1978). Structurally petroleum and shale oil asphaltenes are similar, with shale oil asphaltene sheets generally more closely spaced and the average number of carbon atoms per saturated substituent (2 - 3) about half that for those obtained from petroleum.

Pyrolysis methods have provided new insights into asphaltene structure, especially for side chains on polyaromatic nuclei (Philp and Gilbert, 1985; Behar and Pelet, 1985). The former have used pyrolysis-GC-MS and multiple-ion detection to characterise source rock and asphaltene biomarkers. The biomarkers (steranes, triterpanes, hopanes) derived from asphaltenes were compared with those produced from the corresponding bitumen and extracted rock to investigate the theory that "asphaltenes are liquid kerogen". Behar et al. (1984) have used pyrolysis-GC at 450 and 500°C to investigate asphaltenes derived from both oil and the corresponding source rock kerogen and bitumens. Their profiles for pyrolysates from bitumen asphaltenes show a distribution of alkanes and alkenes extending up to C_{30}, and very similar to the pyrograms of the kerogen isolated from the same sample. The authors interpreted these observations in terms of a geochemical relationship between the kerogens and asphaltenes; both appear to be able to generate, by thermal evolution, the same types of compounds. The authors concluded that asphaltene structure is very close to the structure of the kerogen isolated from the same sample and allows asphaltenes to be regarded as kerogen moieties, resulting from its early evolution. This interpretation supports the characterisations of Tissot and Welte given above.

Pentasphaltenes isolated from Duaringa shale oil were washed, dried (cf. section 3.6.1) and analysed by GC, pyrolysis-GC, pyrolysis-GC-MS, NMR and elemental anlaysis. Results obtained from these procedures are discussed below.

A portion (5mg) was taken up in dichloromethane (200 μL) and 1μL of the solution analysed by GC. At this concentration (ca. 25 mg mL^{-1}) the chromatographic profile was identical to a dichloromethane blank analysed under identical conditions. This demonstrates the absence of any free (occluded or adsorbed) chromatographable material (e.g. alkanes) which may have remained in the asphaltene fraction despite the thorough washing procedure to which the sample had been subjected. The asphaltenes were analysed further by flash-pyrolysis-GC (4 mg, 570°C) using the CDS 150 pyroprobe. The pyrolysate profile was dominated by alkene/alkane peaks in the range C_8 - C_{30}, superimposed on a monotonously rising unresolved hump, extending from ca. $C_{12} > C_{30}$. The peak heights of the alkene/alkane doublets diminished progressively over the same region, with component levels barely above the unresolved baseline material at the upper temperature. The overall chromatogram was virtually identical to the total-ion-current profile obtained from the pyrolysis-GC-MS analysis of the sample analysed under identical conditions (Figure 4-25). This in turn is similar to, but not identical with, the pyrolysis-GC obtained from the raw shale under the same conditions (Figure 4-10). Compared to the GC analysis of the asphaltene solution, the mass of asphaltenes pyrolysed equates to potentially 100 times the level of any free chromatographable material introduced into the GC. This increase in sample size could possibly contribute at least some of the major components (alkanes and alkenes) observed in the subsequent pyrolysis profiles. However, the fact that 1-alkenes are found at approximately the same levels as the alkanes seen in the profiles mitigates against that proposition, since it is known that alkenes are produced pyrolytically (they are not found in the solvent extracts of raw shales or kerogens).

An examination of the components listed in Table 4-21 shows a relatively high abundance of nitrogen-containing compounds (pyridines, pyrroles, aniline, toluidine, indoles, quinolines, cinnolines, pyrazoles, carbazoles). Substituted pyrroles are well represented amongst the latter and these constituents, as well as other nitrogen heterocycles, have been implicated in gum formation during the storage of synfuels derived from shale oil (Brinkman et al., 1980). Other components and homologous series present (but not listed in the table) were difficult to identify positively since they were found at

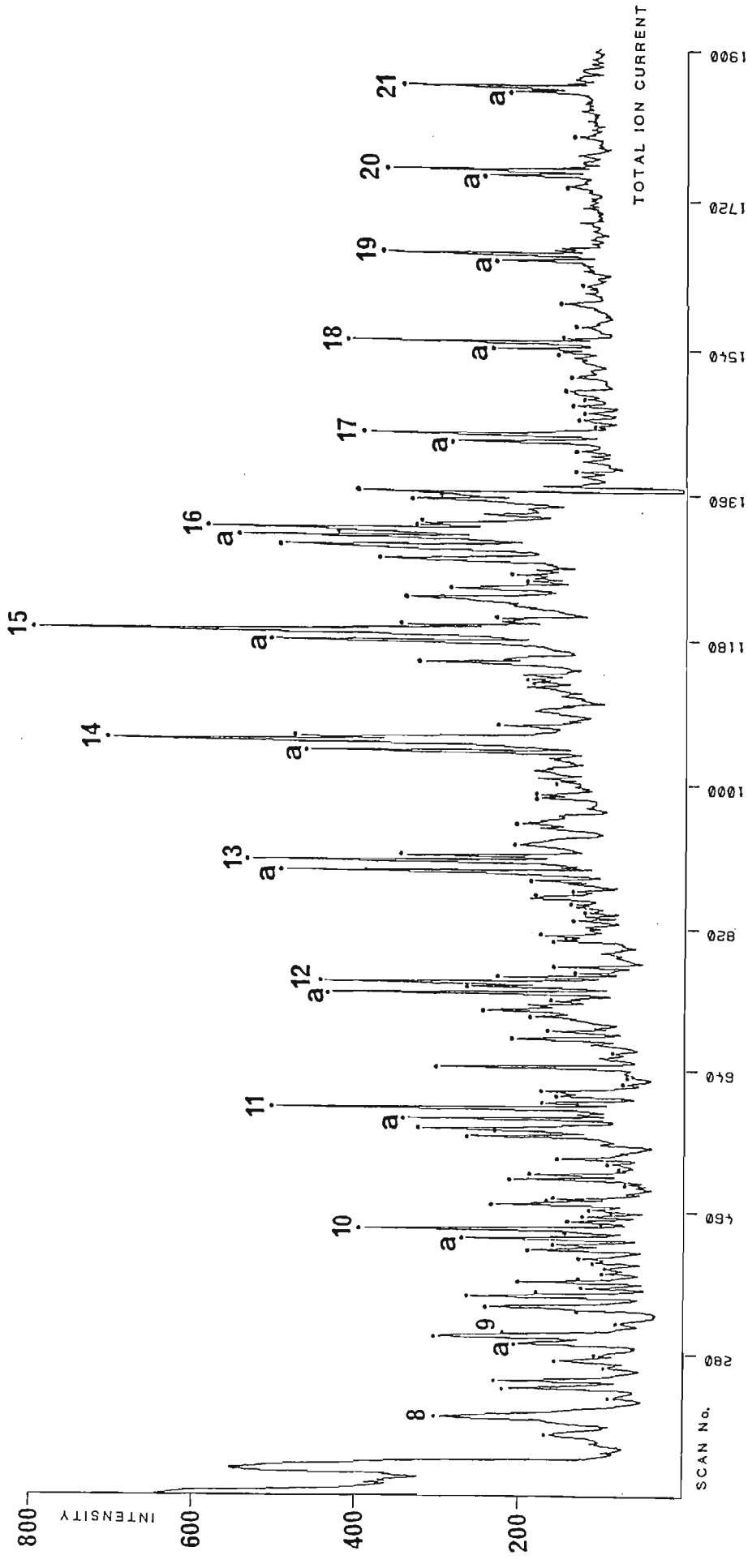

Figure 4-25. Part of the total-ion current (TIC) obtained for the pyrolysis-GC-MS analysis of pentasphaltenes isolated from Duaringa 5391-C shale oil. For clarity, only the alkanes (C_8 - C_{21}) and alkene peaks (a) are labeled. Dotted peaks indicate identified compounds which elute discretely or coelute with minor unidentified components. The former are listed against a component position number in Table 4-21. The baseline dip at scan # 1360 corresponds to a deliberate change in mass spectrometer sensitivity.

TABLE 4-21. List of compounds identified in the pyrolysate obtained from the pyrolysis GC-MS analysis (Figure 4-21) of asphaltenes (5391-C) from the Duaringa deposit.

Pk.No.[a]	Compound Name	Pk.No.	Compound Name
7.1	toluene	11.15	C4-pyrrole + acetyldimethyl -pyrrole *
8.1	methylpyridine		
8.2	methylpyrrole	12.1	2-dodecene
8.3	methylpyrrole	12.2	C3-pyridine
8.4	C2-benzene	12.3	branched alkane
8.5	dimethylpyrrole	12.4	?
8.6	C2-benzene	12.5	trimethylphenol + methylindole
8.8	C2-benzene	12.6	trimethylphenol + methoxy -benzylamine *
9.1	ethylpyridine		
9.2	ethyl + dimethylpyridine	12.7	methylindole + N-ethyl-O-toluidine *
9.3	dimethylpyrrole		
9.4	dimethylpyrrole	12.8	C4-pyridine *
9.5	dimethylpyrrole	12.9	C4-pyridine
9.6	ethylpyrrole	12.10	C4-pyridine + dimethylindan
9.7	dimethylpyrrole	12.11	C4-pyridine + dimethylindan
9.8	dimethylpyrrole	12.12	C9 H17 N *
9.9	C3-pyrrole	13.1	indole + 2-tridecene
9.10	C3-benzene	13.2	dimethylindan +acetyldimethyl -pyrrole *
9.11	C3-pyridine *		
9.12	C3-pyrrole *	13.3	acetyldimethylpyrrole+C8 H15 N*
9.13	aniline	13.4	dimethylindole + methylquinoline
9.14	phenol	13.5	tetrahydroquinoline
9.16	C3-benzene	13.6	phenylheptane + C7 H10 N4 *
10.1	2-decene	14.0	C14 + methylindole
10.2	C3-pyrrole *	14.1	methylindole
10.3	C3-pyrrole *	14.2	2-tetradecene
10.4	C3-pyrrole	14.3	ethylindole
10.5	trimethylpyridine + C3-pyrrole	14.4	C10 H10 N2 *
10.6	C3-pyrrole *	14.5	dimethylindole
10.7	C3-pyrrole *	15.0	C15 + dimethylindole
10.8	C3-benzene	15.1	C2-indole
10.10	C3-pyrrole	15.2	2-pentadecene
10.11	C3-pyrrole	15.3	dimethylindole
10.12	indene	15.4	trimethylindole
10.13	C4-pyrrole + C4-benzene	15.5	C10 H8 N2 *
10.14	cresol	15.6	trimethylindole
10.15	toluidine	15.7	trimethylindole
10.16	cresol	15.8	dimethylcinnoline
10.17	C4-pyrrole + methylaniline	15.10	C8 H8 N2 *
11.1	trimethylpyridine	16.1	2-hexadecene +
11.2	2-undecene + C4-pyrrole	16.2	trimethylindole
11.3	C4-pyrrole	16.3	trimethylindole
11.4	C4-pyrrole	16.4	dimethylcinnoline
11.5	C4-benzene	16.5	dimethylcinnoline
11.6	C4-benzene	16.6	methylphenylpyrazole *
11.7	C4-pyrrole * + amino cresol *	16.7	acetylmethylindole *
11.8	methylindan + ethylphenol	16.8	1-heptadecene + C3-cinnoline *
11.9	ethylphenol	17.1	C3-cinnoline *
11.10	C3-pyridine + acetyldimethyl -pyrrole *	17.2	carbazole * + ?
		17.3	C3-dihydroquinoline
11.11	C3-pyridine	17.4	C3-cinnoline
11.12	C3-pyridine	17.5	C3-hydroquinoline * + ?
11.13	ethylphenol	17.7	C3-cinnoline

TABLE 4-21 (cont.).

Pk.No.[a]	Compound Name	Pk.No.	Compound Name
17.1	dimethylhydrindacine *	18.4	carbazole
18.1	2-octadecene	19.1	methylcarbazole *
18.2	trimethylnaphthol	20.1	methylcarbazole *
18.3	trimethylnaphthol		

a Peak number refers to position of component in the pyrolysis-GC-MS total-ion-current chromatogram (Figure 4-25). Integral parts of the number denote the alkane component preceding the compound in question and are intended to locate the component quickly in the profile (e.g. **10**.8 denotes the 8th marked component eluting after decane (C-**10**). This position index should not be confused with the retention index (**RI**). * Tentative identification.

only low concentrations and/or coeluted with other more abundant constituents. However the presence of two homologous series of alkyl-substituted benzenes was detected from appropriate plots of fragment ions (m/z=92 and m/z=105) diagnostic for the respective series (Figure 4-26).

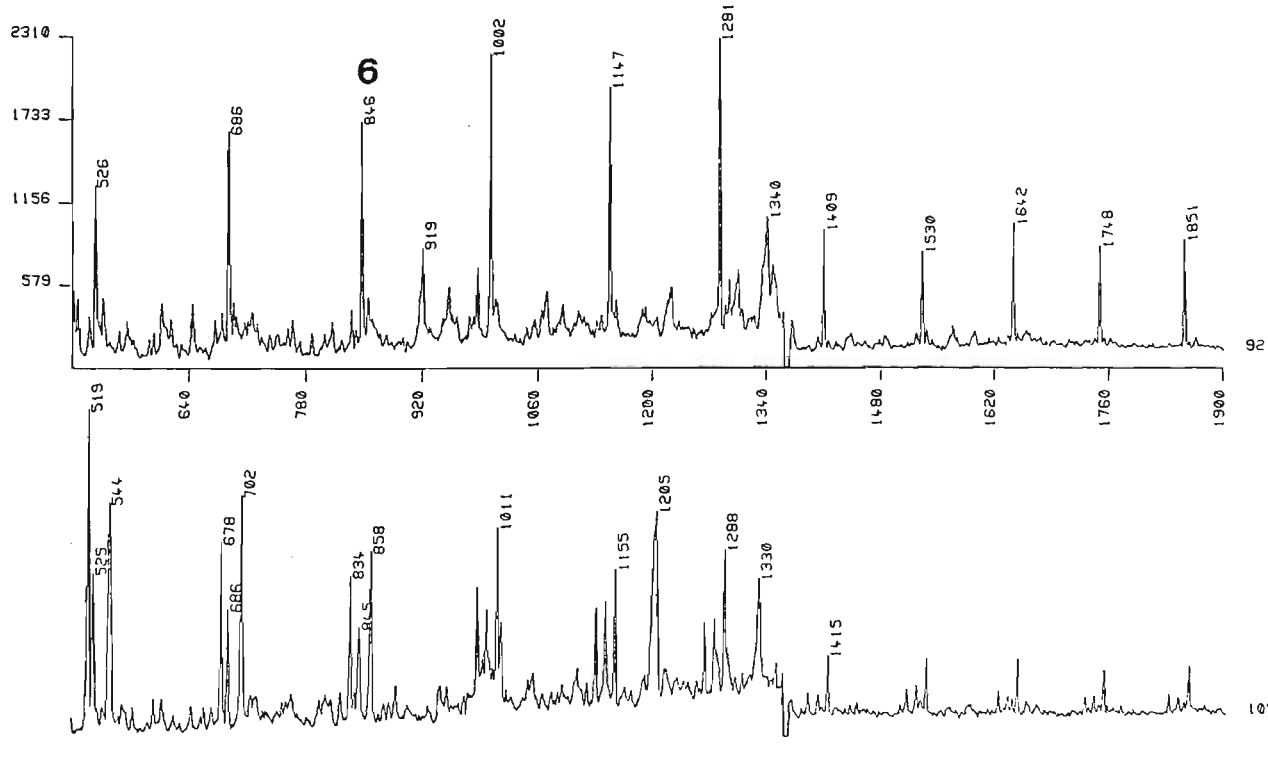

Figure 4-26. Fragment-ion plots of alkyl substituted benzenes (m/z=92) and m/z=105 (probably corresponding to alkyl-substituted toluenes; cf. section 4.9 - fraction 5), obtained from the pyrolysis-GC-MS analysis of asphaltenes from Duaringa 5391-C. Hexylbenzene denoted by **6**.

A plot of the parent-ion (m/z=156) for C_2- naphthalenes revealed the presence of these diaromatic constituents (mainly dimethylnaphthalenes) in the pyrolysate, albeit at very low concentrations and in a poorly resolved region of the chromatogram (Figure 4-27).

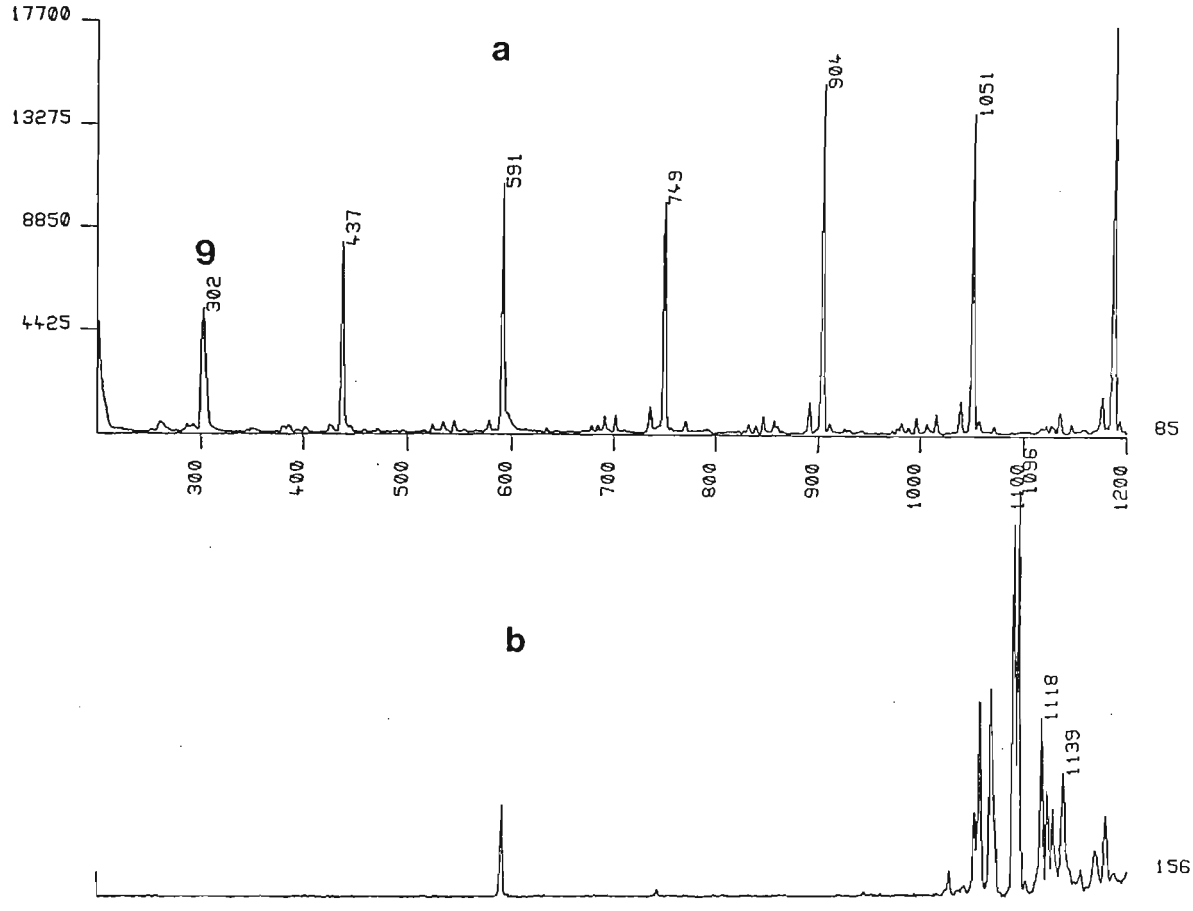

Figure 4-27. Parent-ion plot (m/z=156) corresponding to C_2-naphthalenes (mainly dimethylnaphthalenes) found in the flash-pyrolysate of asphaltenes isolated from Duaringa shale oil (**b**). Trace **a** corresponds to alkanes (diagnostic fragment ion m/z=85) and locates the substituted napthalenes in the TIC profile relative to these marker compounds i.e. between C_{14} and C_{15} (nonane denoted by **9**).

The asphaltenes were also analysed using a pyrolysis-FPD procedure, with the flame-photometric detector (FPD) selected for the sulphur detection mode. The flash -pyrolysis chromatogram showed only one large "solvent peak", consistent with the release of hydrocarbon gases detected earlier during the normal pyrolysis-GC analysis (the FPD is not entirely selective for sulphur-containing molecules). The lack of volatile sulphur -containing compounds in the pyrolysate was confirmed by plotting fragmentograms of masses 97, 111 and 125, obtained during the pyrolysis-GC-MS analysis. These fragment

ions are characteristic of alkyl-substituted thiophenes (usually the most abundant volatile sulphur constituents in raw shale oil) but were not observed for these compounds; peaks obtained for masses 97 and 111 in the respective fragmentograms were found to correspond to alkene fragment ions. Benzothiophenes (parent ion at mass 156) were not detected. The only oxygen-containing components found in the pyrolysate (at detectable concentrations) were phenol and its C_1 - C_3 analogues. Direct insertion-MS of the asphaltenes provided no meaningful data since the mass spectra at various probe temperatures (up to 500°C) consisted primarily of a large envelope of sequential masses of similar intensities.

NMR has found wide application in the study of asphaltenes and provides (average) information on the degree of aromatic-ring substitution, aliphatic chain lengths and aromaticity etc. The NMR spectrum and NMR and IR data of asphaltenes isolated by Yen and coworkers from Green River shale oil (produced by the Paraho Retort process) have been published (Wen et al., 1978). The 400 MHz ^1H NMR spectrum for the Duaringa asphaltenes (Figure 4-28) was virtually identical to that published by these authors but provided little structural information. All sharp signals could be assigned to solvent impurities and, although the solution was treated with D_2O, small water peaks remained at 1.6 and 4.8 ppm. The signals from the sample itself are very broad and indicate that the asphaltenes are either very large or have paramagnetic metal ions associated with them. Their aromaticity is relatively high (H_a= 17%) with a high degree of substitution (H_a= 32%). Signals which may be assigned to long-chain alkyl fragments (residues) are also prominent near 0.9 and 1.2 ppm and yield an average aliphatic chain length of ca. 9. Since the alkanes found in the pyrolysis-GC trace extend at least to C_{30}, the low average chain length indicated by NMR data means that the long alkyl chains are not relatively abundant (Behar et al., 1984).

Only ca. 20 mg of asphaltenes were isolated initially and elemental analysis was necessarily confined to C, H and N data (C: 67.9%, H: 5.6%, N: 4.2%). Since a mass balance was not attained, it would be speculative to attribute the large remainder (22.3%)

solely to oxygen and sulphur. However, a comparison with elemental data of the raw shale oil for the latter (Table 4-4) suggests that oxygen should be relatively more abundant. In that context it appears that only the increased nitrogen abundance in the asphaltene appears in its pyrolysis products.

Asphaltenes formed in shale oil during storage are clearly derived from components produced during the retorting of raw shale. This restricts their formation in the oil to polymerisations involving relatively volatile and reactive constituents. These may include heteroatoms derived from kerogen structures involved in cross-linking or in functional groups and removed by thermal treatment; heteroatoms (particularly N and S) engaged in

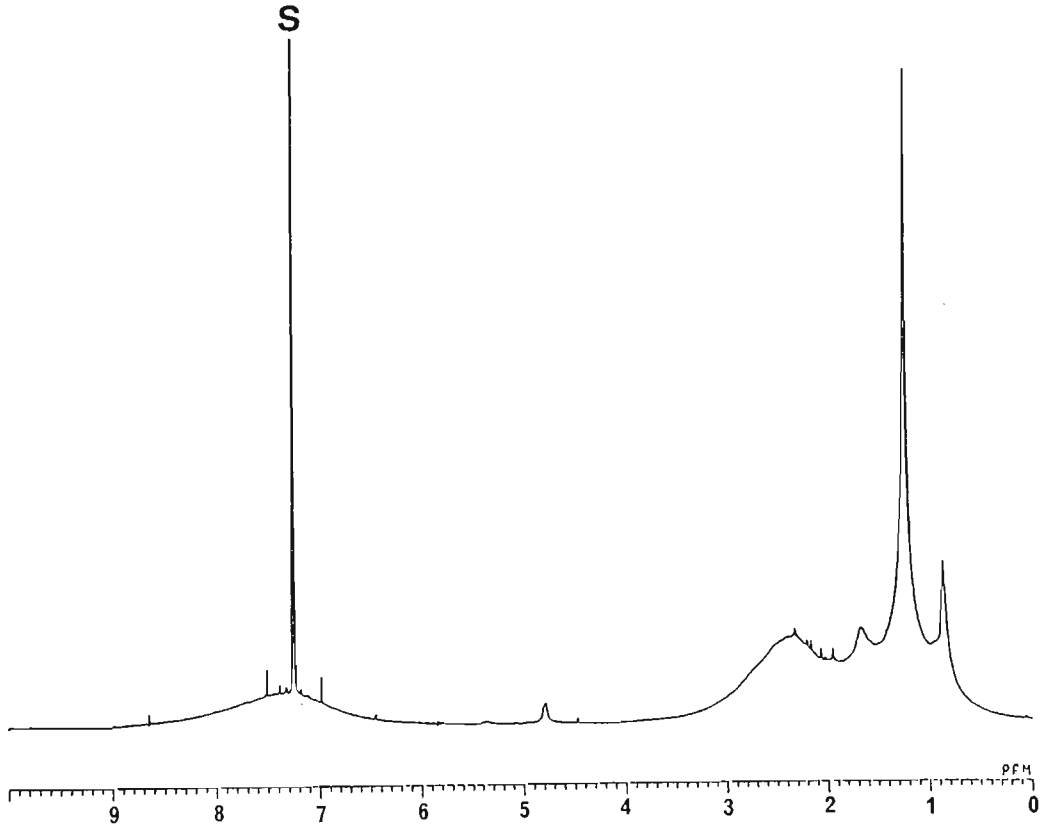

Figure 4-28. 400 MHz ^{1}H NMR spectrum for pentasphaltenes ($CDCl_3$ + D_2O) isolated from Duaringa 5391-C. S denotes solvent impurity.

heterocycles of the polyaromatic nucleus of oil shale kerogen are usually found in the residual coke (Speight et al., 1979). Larger molecules which may be associated with their formation (e.g. porphyrins, which have been isolated from shale oil by Ekstrom et al., 1983) are presumably carried into the shale oil as an aerosol.

When subjected to flash-pyrolysis, the gas chromatographic constituents of the shale oil asphaltenes reveal information about smaller structural units contained within the asphaltenes. GC-MS data obtained from this procedure indicate that at least part of the polymeric structure of Duaringa pentasphaltenes is made up of nitrogen-containing heterocycles (e.g., pyrroles, indoles, quinolines) and aliphatic hydrocarbon chains ranging in length up to 30 carbon atoms. It is not clear from this approach whether these heterocycles are directly associated with the alkyl residues or not. However, it seems likely that part of the polymer has been formed through polymerisations involving alkenes and a range of reactive nitrogen-containing heterocyclic oil shale components. Other less volatile hetero-containing constituents (e.g. large polycyclic fragments) of the asphaltenes are presumably retained in the pyrolytic residue (char and coke). In this context the pyrolysis of the asphaltenes would be expected to conform to the same mechanisms as those applying to the pyrolysis of kerogen. This partly explains the low concentration of oxygen and sulphur components found in their flash-pyrolysate, since the latter comprises only the "oil" obtained from that procedure.

4.8.3 Acid-base extractable compounds.

Acid-base extractions from hexane solutions of raw shale oils invariably produce significant quantities of acid-base catalysed polymers (tars, artefacts) as well as stable emulsions. Neutral oil recovered from the extraction = raw shale oil - (acid- and base-extractable compounds + extractable neutrals + tars and other polymers), where the quantities in parenthesis are difficult to recover and quantify gravimetrically. The latter is due to:

a) - evaporative losses (e.g. phenols and bases, volatile carboxylic acids);

b) - poor recovery of material (e.g. sludges);

c) - possible formation of artefacts.

Collectively the above factors make it extremely difficult to obtain an accurate value for the amount of neutral oil ultimately recovered from the procedure and loaded onto the open column for separation into constituent fractions. However an accurate figure for the recovered neutral oil is important to establish absolute masses for fractions obtained from the chromatographic column and to establish where (major) losses occur in the entire shale oil characterisation procedure. The above problems apply particularly to old oil, where polymerisation caused by autoxidation due to storage may prevent relatively large amounts of the oil from going into solution. These hexane-insoluble asphaltenes may contain occluded compounds, some of which could be released through dissolution in dichloromethane to be subsequently recovered from the open column procedure by one of the polar solvents (mixtures) of the eluotropic series.

Isolation of acidic and basic compounds from a dichloromethane solution of freshly-obtained shale oil goes part of the way to overcoming the latter problems and keeps most of the normally precipitated tars and polymers in solution during the extraction sequence. This cleaner procedure (cf. section 3.6.2) also circumvents the need for separating funnels and further provides a simple method for determining the quantity of neutral oil recovered after the extraction; this aspect will be discussed later in this section.

The **carboxylic acids** isolated from the sat. $NaHCO_3$-extract were quantified gravimetrically, but were present at such low concentrations that these data were not considered sufficiently accurate. The acids were consequently converted to the methyl-ester derivatives and their total relative abundances (for each raw shale oil) determined from respective GC-profiles. These tabulated data (Table 4-22) show that the shallow-seam raw oils contain relatively similar quantities of volatile carboxylic acids while shale oil from 686 contains ca. 17 times the quantity of those isolated from 5391-C. The chromatograms (Figure 4-29) are similar to those previously reported for Kerosene Creek shale oil (Regtop, 1983), with components restricted to the C_6 - C_{11} carboxylic acids. However, these traces are not a complete representation of the entire range of alkanoic acids contained in the raw shale oils. The higher members of the homologous series obviously require higher concentrations of OH-ions to convert them to their salts, from which they are

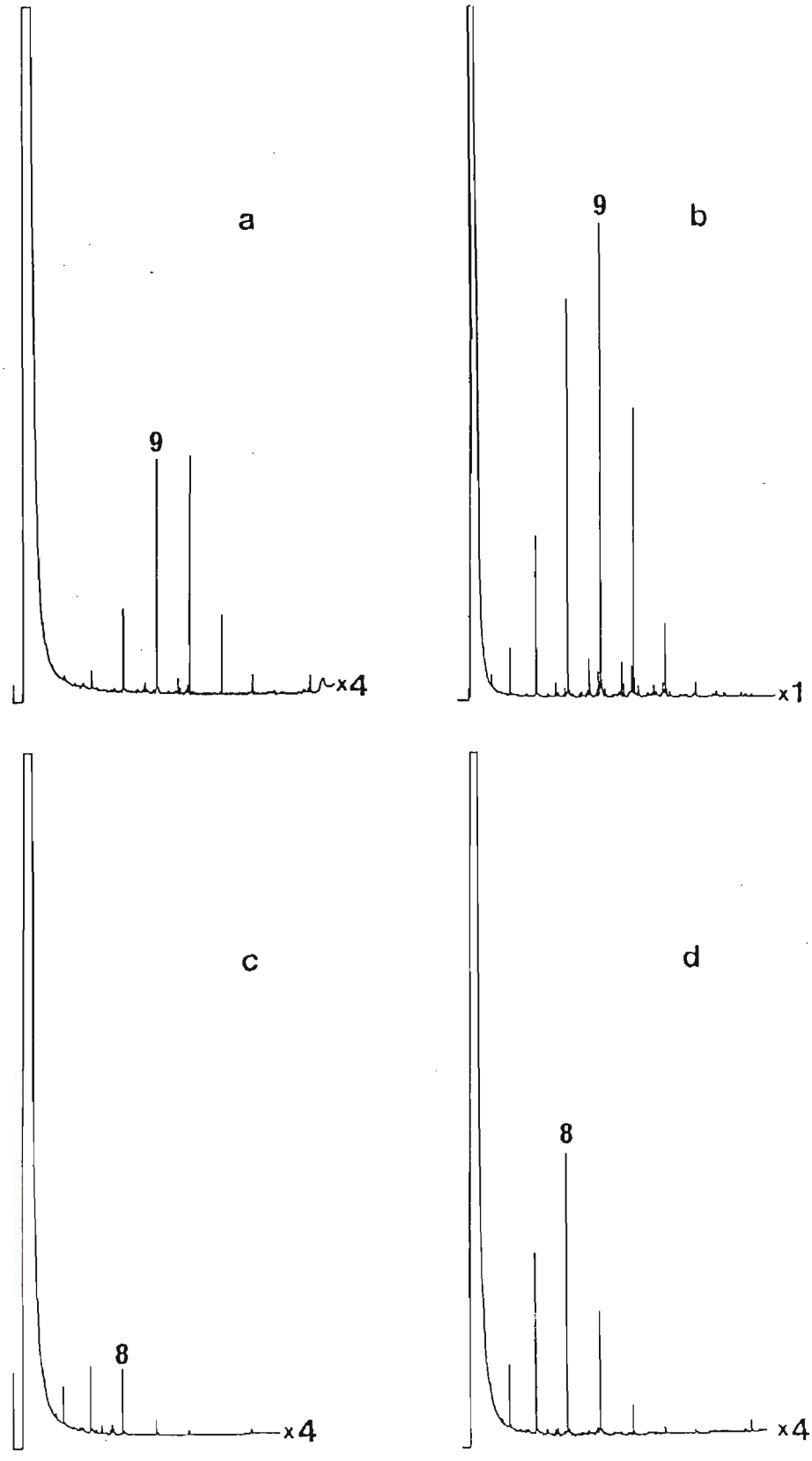

Figure 4-29. Profiles of alkanoic acids (methyl-esters) isolated from the sat. $NaHCO_3$ -extracts of raw shale oil from Duaringa 5391-C (a), 686 (b), 789 (c) and 822 (d). Carbon numbers as indicated.

Table 4-22. Determination of relative quantities (per gram of raw shale oil) of alkanoic acids (C_6 - C_{11}) isolated from the sat. $NaHCO_3$-extracts of shale oil from the Duaringa deposit.

SAMPLE	REL. PEAK AREA[1]	GRAV. DET.	mass % OF RAW OIL[2]
5391-C	6		~ 0.01
686	100	0.18	0.18
789	1.5		~ 0.003
822	3		~ 0.006

1 Relative total peak areas for the methyl-esters of alkanoic acids (C_6 - C_{11}). **2** From GC relative peak areas (relative to gravimetric data for 686)

subsequently released as the free acid. The latter is clearly evident from Figure 4-30, which depicts the carboxylic acids (methyl-esters) isolated from the NaOH-extract of the raw shale oil from Duaringa 686, following the preliminary sat. bicarbonate extraction. Similar profiles and range of acid components were obtained for the other raw shale oils. Collectively the alkanoic acids range from C_6 to C_{26} and exhibit a smooth monotonically decreasing distribution with a maximum in the C_9 - C_{10} region of the profiles. This is indicative of cracking processes which (generally) favour the production of volatile components without carbon-number preference. The need to isolate higher molecular weight acids from the NaOH-extract, which also contains phenols and other base-extractable compounds, makes it difficult to quantify this fraction gravimetrically. Given earlier comments about the very low abundances of the acids in the bicarbonate extract, it appears that quantitation of total carboxylic acid content is best achieved using GC-analysis of the two extract fractions after the addition of appropriate internal standards to the raw oil (e.g. a C_9 and C_{19} branched carboxylic acid not indigenous to the raw oil).

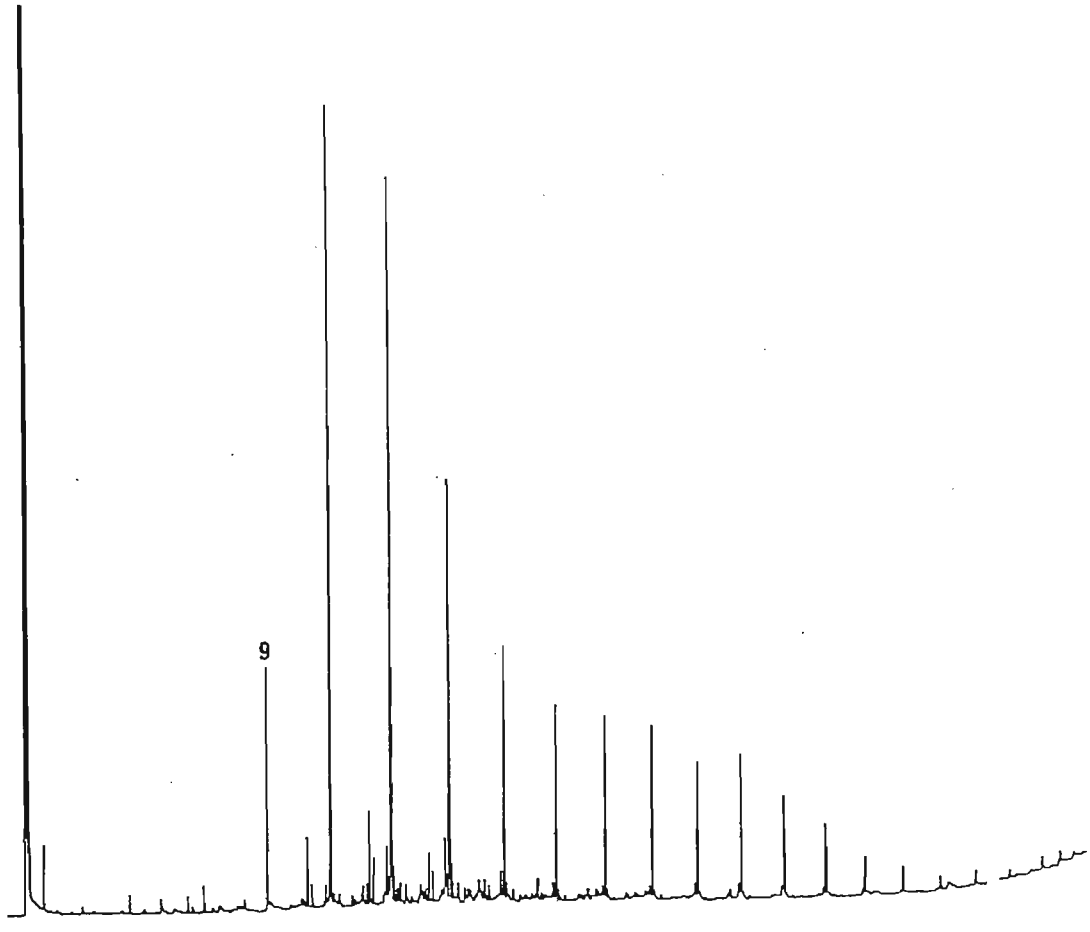

Figure 4-30. Profile of alkanoic acids (methyl-esters) isolated from the NaOH-extract of raw shale oil from Duaringa 686 (compare with Figure 4-29 (**b**)). Carbon numbers as indicated.

Phenol and alkyl-substituted phenols were isolated from the NaOH-extract of the raw shale oils. In addition to these acidic compounds, the extracts also contained alkanoic acids (C_9 - C_{26} , cf. above section), pigments (reddish-brown) and water-soluble neutral compounds. The latter were recovered by back-extraction with dichloromethane from the NaOH-solution and were pooled and quantified together with those base-extractable neutrals previously recovered fromt the sat. bicarbonate extract. For the Duaringa oils the volatile (chromatographable) constituents in these pooled fractions comprise trace amounts of those components found in large concentrations in the respective phenol fraction. The

gas chromatographic profile of the phenol fraction from Duaringa shale oil 5391-C (Figure 4-31) contains mainly phenol and its alkyl-substituent forms, up to trimethylphenol (Table 4-23). Those for the other shale oils were qualitatively identical, with only minor variations in the relative abundances of the constituents observed. The composition of the phenol fractions from Duaringa is similar to those reported for shale oils from the Rundle deposit (Regtop, 1983) and virtually identical to that for Condor shale oil (Rovere, 1986). **NB!** any further comparisons of Duaringa data with that for Rundle and Condor shale oil will imply the above references unless stated otherwise. Quantitation of the fractions was carried out using gravimetric and chromatographic procedures, the latter utilising both

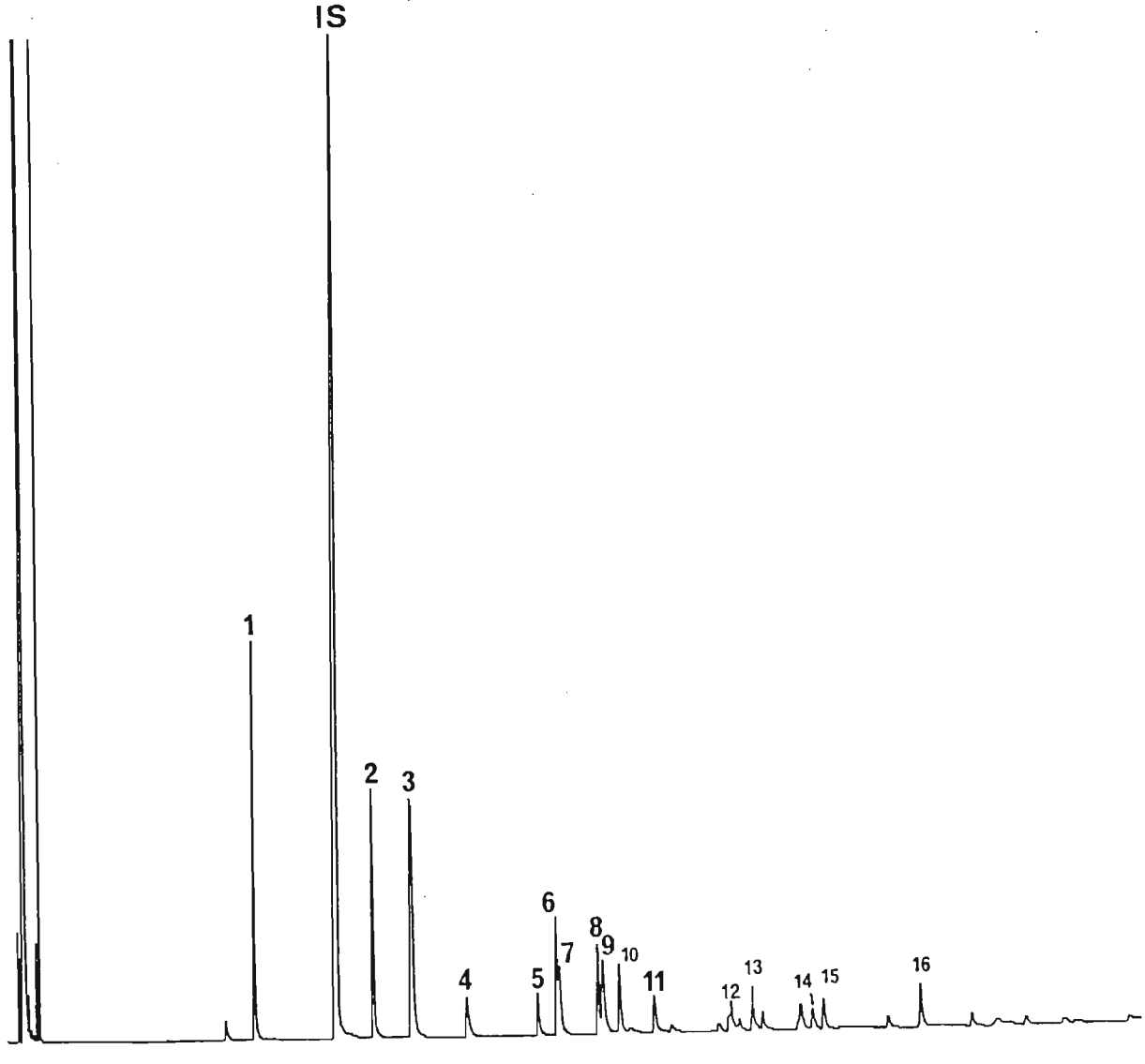

Figure 4-31.
Gas chromatogram of the phenolic fraction isolated from the NaOH-extract of raw shale oil from Duaringa 5391-C. Numbers refer to compounds listed in Table 4-23 ; IS denotes the internal standard (benzyl alcohol). GC-oven heating rate 2°C min^{-1}.

TABLE 4-23. List of some of the compounds identified in the phenol fraction (NaOH-extract) of raw shale oil from Duaringa 5391-C (Figure 4-31).

Pk. No.	Compound Name[1]	Retention Index (RI)[2]
1	phenol	979.77
2	2-methylphenol	1052.80
3	4- and 3-methylphenol	1075.37
4	2,6-dimethylphenol	1104.75
5	2-ethylphenol	1138.24
6	2,4-dimethylphenol	1147.16
7	2,5-dimethylphenol	1148.55
8	4-ethylphenol	1166.52
9	3,5-dimethylphenol	1169.30
10	2,3-dimethylphenol*	1176.71
11	3,4-dimethylphenol	1192.82
12	trimethylphenol	1228.65
13	isopropylphenol	1237.83
14	trimethylphenol	1265.37
15	2,3,5-trimethylphenol*	1270.13
16	3,4,5-trimethylphenol	1314.28

1 Where definite isomeric assignments are given, identification is based on mass-spectral data and the close agreement between RI values in the table and those given for analytical standards by Rostad and Pereira (1986). 2 Heating rate 2°C min^{-1}. * Tentative isomeric assignment.

relative total peak areas as well as absolute quantitation using an internal standard (cf. section 3.6.4). The "total phenols" were quantified using the internal standard (benzyl -alcohol) by assuming constant relative FID-response factors for the alkyl-substituted phenol components. This results in a slightly higher figure for the chromatographic determination for components other than phenol, since the FID mass-response (relative to the IS) is higher for the substituted compounds. Absolute data obtained for the shale oils from this approach shows that 45 - 65 % of the NaOH-extractable material comprises non-volatile compounds not directly accessible via GC (Table 4-24). Some of these compounds were listed above and may be quantified separately (carboxylic acids), whereas the isolation and determination of pigments and high molecular weight components is more difficult. The bulk of the phenols found in the NaOH-extracts of the raw shale oils are probably derived from lignins and tannins, which are both abundant in higher-plant tissues and characterised by phenolic structures. Lignins is a collective term for high molecular

weight polyphenols which form structural elements of the supporting tissues of higher plants while tannins which are quantitatively less important are complex derivatives of gallic or ellapic acids which have phenolic groups on their aromatic structures (Tissot and Welte, 1984).

Table 4-24. Quantitative data for acid- and NaOH-extracts of raw shale oil from Duaringa. Except for the chromatographic determination of volatile bases (see footnote 3) all values are given in milligrams per gram of raw oil . **NB**. gravimetric data for NaOH- and acid-extracts do not include back-extracted "neutrals"- see text for details.

SAMPLE	ARTEFACTS[1]		NaOH-EXTRACT		ACID-EXTRACT	
	Base-extractions	Acid-extraction	Gravimetric	Phenols[2]	Gravimetric	Bases[3]
5391-C	10.1	1.2	12.1	6.9	28.8	100
686	15.6	2.4	7.3	2.5	13.1	36
789	9.6	1.5	10.4	6.5	7.8	32
822	8.7	1.2	8.3	4.5	8.1	43

1 Sludges etc. formed during acid- and base-extraction (pooled sat.$NaHCO_3$ and NaOH ppt.) and recovered by filtration. 2 Absolute values as determined from GC data using IS. 3 Ratio of GC peak areas (relative to 5391-C) for total chromatographable bases.

The acid-extracts of the raw shale oils contain volatile **organic bases** with GC-profiles that are substantially more complex than the corresponding phenol fractions and which vary more widely between the different oils. A representative chromatogram (Figure 4-32) shows that most components are poorly resolved, which makes positive identification of individual compounds very difficult. Only some of the components identified by GC-MS are listed in Table 4-25 and comprise those constituents commonly found in shale oil extracts (e.g. Rundle and Condor). For the Duaringa shale oils these include predominantly pyridine and alkyl-substituted pyridines, with lesser quantities of tetrahydroquinolines as well as quinoline, isoquinoline and alkyl-substituted quinolines. For the base fractions the presence of most homologous series is obscured by co-eluting

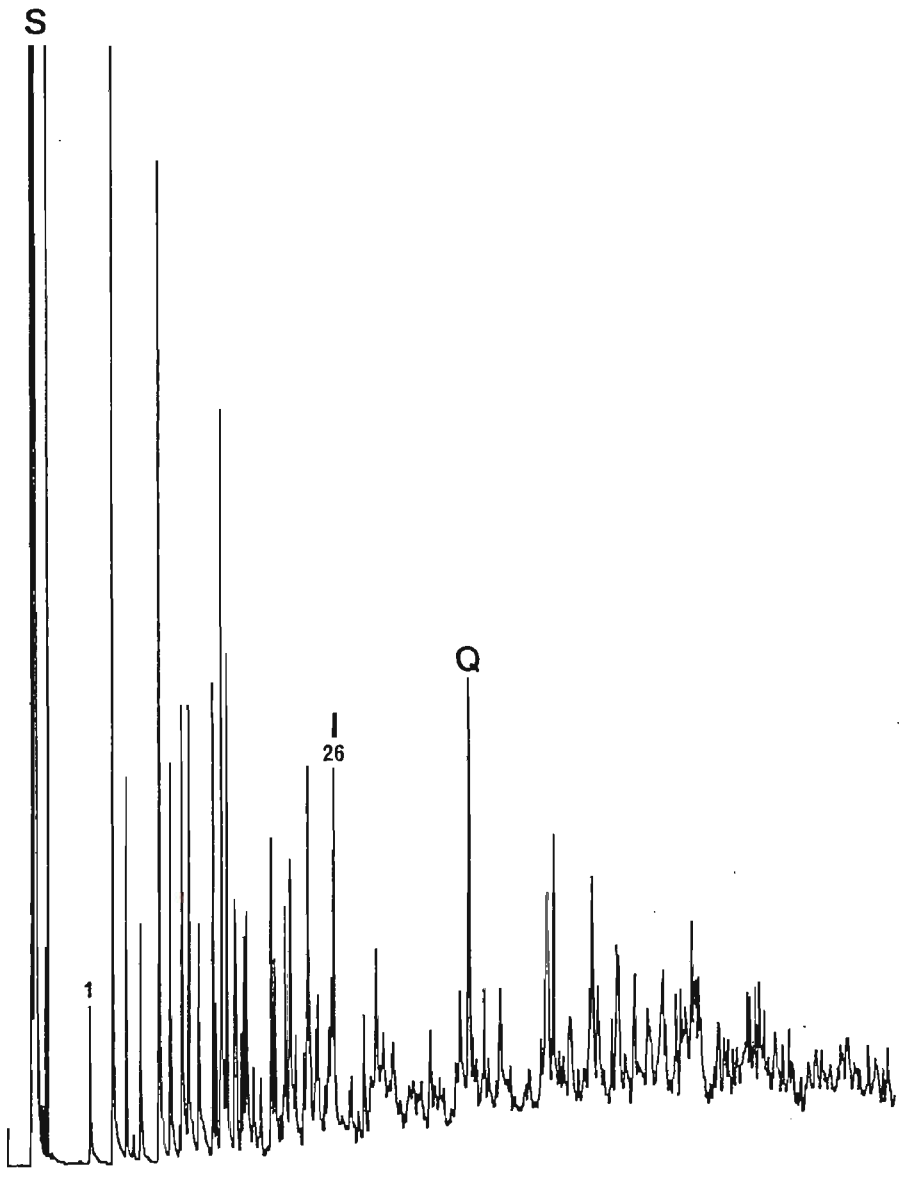

Figure 4-32.
Gas chromatogram of the acid-extract (bases) of raw shale oil from Duaringa 5391-C. For clarity, the profile region between peaks #1 - #26 has been expanded in Figure 4-33. Peaks marked denote solvent (S), indoline (I) and quinoline (Q).

peaks and their presence can only be seen clearly from profiles of representative fragment-ions (Figure 4-34). Similarly, the distribution of the large number of isomers (e.g. methylquinolines) can only be visualised effectively from either fragment- or parent -ion plots (Figure 4-35). The Duaringa acid-extracts are not stable over long periods of storage (amber glass vials) and comparative GC-profiles corresponding to fresh and stored solutions (1 year) generally showed a depletion in chromatographable components other

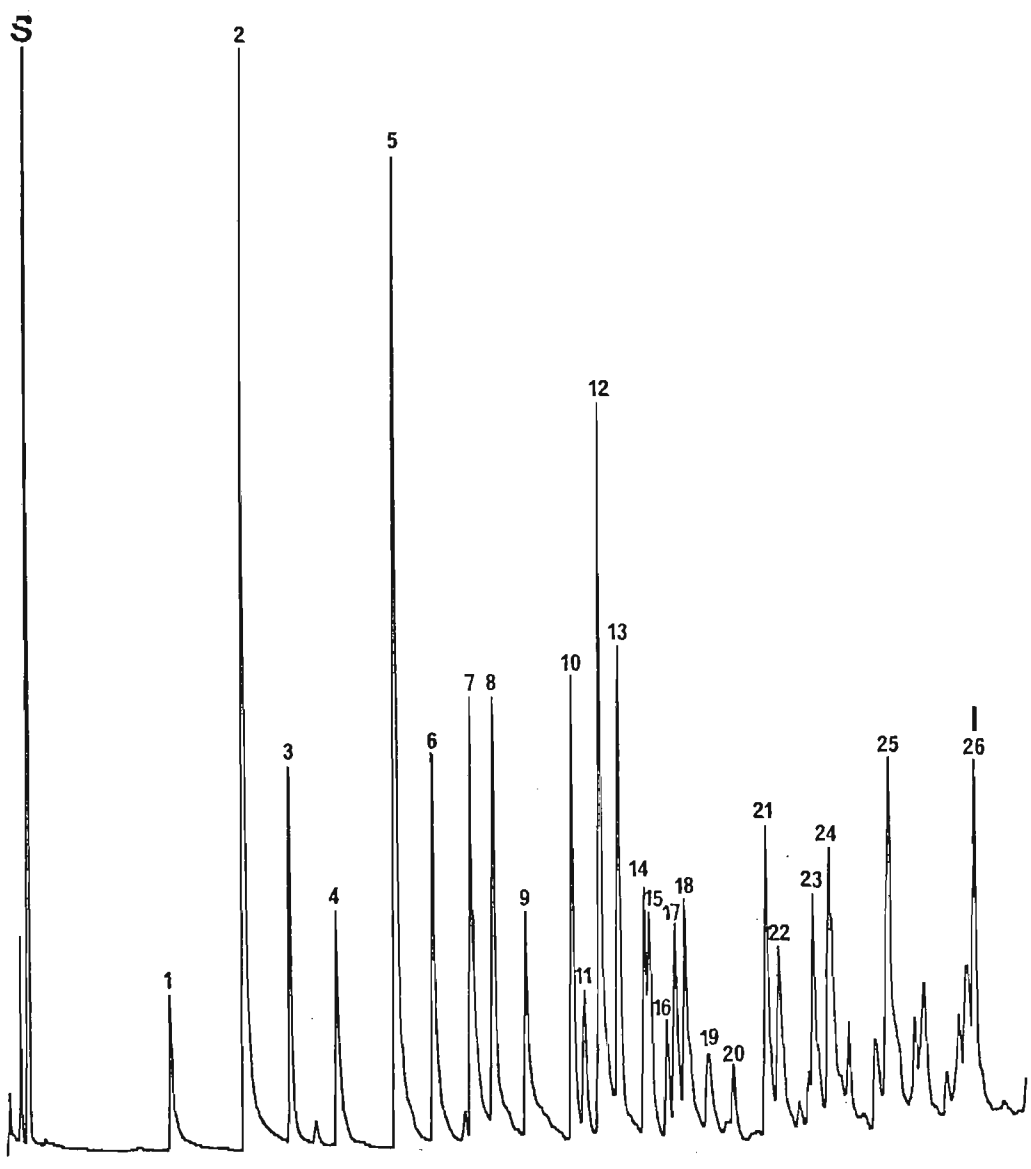

Figure 4-33. Expanded chromatographic region (peaks #1 to #26 - Figure 4-32) of the acid extract (bases) of raw shale oil from Duaringa 5391-C. Numbered peaks were positively identified from their mass-spectra and are listed in Table 4-25.

Table 4-25. List of compounds positively identified in the acid-extract fraction (bases) of raw shale oil from Duaringa 5391-C (Figure 4-33).

Pk. No.	Compound Name	Pk. No.	Compound Name
1	methylpyridine	14	methyl-ethylpyridine
2	methylpyridine	15	methyl-ethylpyridine
3	dimethylpyridine	16	methyl-ethylpyridine
4	ethylpyridine	17	N-ethylaniline
5	dimethylpyridine	18	trimethylpyridine
6	dimethylpyridine	19	methyl-ethylpyridine
7	3-ethylpyridine	20	dimethyl-ethylpyridine
8	methyl- ethylpyridine	21	Mixture (M.Wt. 121, base peak m/z = 92).
9	dimethyl-ethylpyridine	22	trimethylpyridine
10	dimethyl-ethylpyridine	23	dimethyl-ethylpyridine & trimethylpyridine
11	2-propylpyridine	24	methyl-ethylpyridine
12	dimethylpyridine	25	dimethyl-ethylpyridine & trimethylpyridine
13	trimethylpyridine	26	indoline

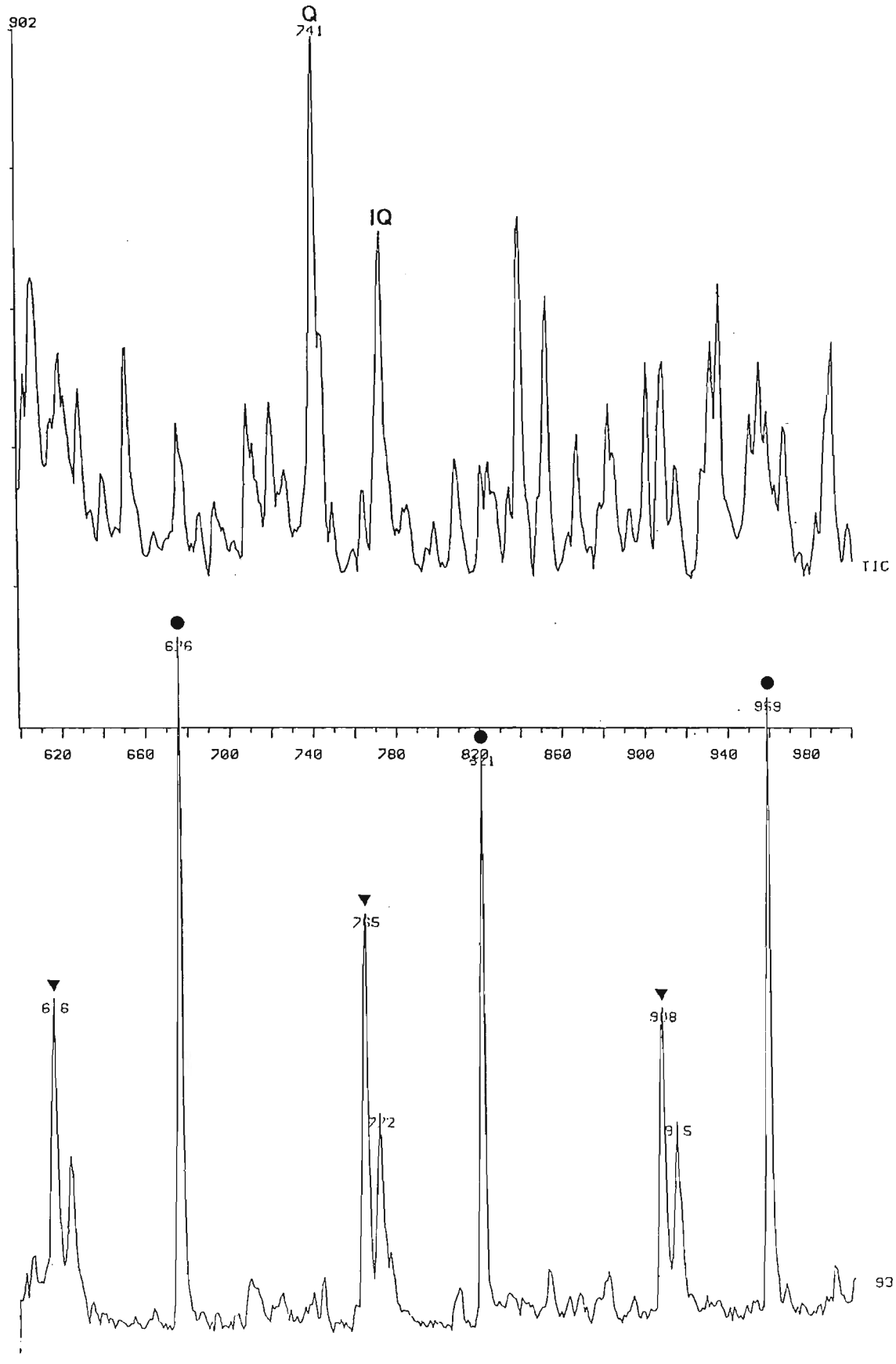

Figure 4-34.
Part of the total ion-current (TIC) and corresponding fragment-ion trace (m/z = 93) obtained from the mass-spectral analysis of the acid extract (bases) of raw shale oil from Duaringa 5391-C (Figure 4-32). The fragment-ion peaks characterise alkyl-substituted pyridines, with peaks marked ● and ▼ denoting 2- and 3-alkylpyridines respectively. Peaks marked in the TIC profile denote quinoline (Q) and isoquinoline (IQ).

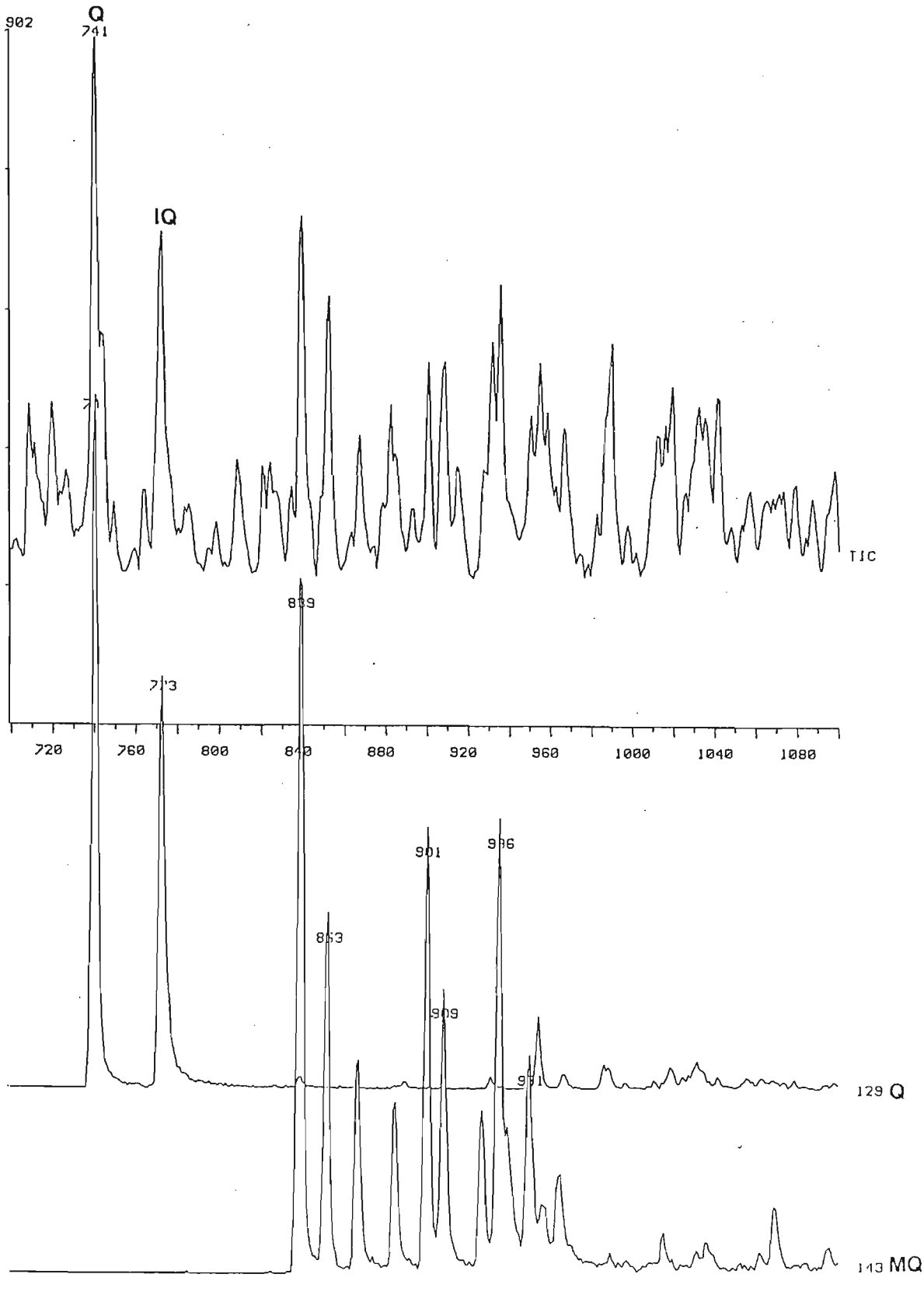

Figure 4-35.
Part of the total ion-current (TIC) and corresponding parent-ion trace for quinoline and isoquinoline (m/z=129) and methylquinolines (m/z=143;) obtained from the mass-spectral analysis of the acid extract (bases) of raw shale oil from Duaringa 5391-C (Figure 4-32). Peaks marked in the TIC profile denote quinoline (Q) and isoquinoline (IQ).

than pyridine and alkyl-substituted pyridines. This suggests that the bases are participating in the formation of less volatile high molecular weight products. Nitrogen heterocycles are known to reduce fuel stability (Brown and Karn, 1980); their presence has also been found to reduce catalyst lifetimes during refining processes.

All of the acid-extracts were coloured (yellowish-brown) partly due to pigments derived from both plant and animal sources. The complexity of the profiles and the poor resolution and diversity of components makes the choice of internal standard(s) for GC-quantitation of the volatile bases very difficult. It is clear however that chromatographable components do not comprise the entire mass of the fraction, since DI-MS of the solvent-free concentrates yielded mass-spectral information at odd molecular weights (nitrogen containing) higher than those which can be assigned to GC-components.

Although proteins and nucleic acids are presumed to be the original source of most nitrogen heterocycles in shale oil (Mapstone, 1951), Whitehead (cited in Tissot and Welte, 1984) has suggested that nitrogen compounds (pyridines, quinolines, carbazoles) are probably derived from skeletal fragments of plant alkaloids. Once incorporated into the kerogen structure, it seems reasonable to believe that at least some of the heterocycles are released during pyrolysis and with alkyl-substituents which reflect their attachment within the complex polymeric network.

The water-soluble "neutrals", isolated by back-extraction from the sat. $NaHCO_3$- and NaOH- extracts were pooled for each oil and quantified gravimetrically. Those isolated from the acid extracts were also determined gravimetrically and the combined masses were used with other gravimetric data to calculate the quantity of neutral oil recovered for further analysis. Quantities (per gram of raw oil) for the pooled base-extractable "neutrals" varied widely between the different oils and for those samples listed in Table 4-24 were ca.: 0.3, 0.1, 8.7 and 7.3 mg respectively. Quantities for "neutrals" recovered from the acid-extracts of respective oils were generally higher at ca.: 0.1, 0.9, 20.5 and 23.7 mg.

Where a very accurate material balance is required, the quantity of neutral oil recovered after acid-base extraction may be determined directly and without incurring the loss of volatile components. This serves as a check against the collective total of those masses, obtained for extractable fractions and artefacts, which are normally summed and

subtracted from the original mass of raw shale oil to arrive at an (assumed) mass of recovered neutral oil. The procedure is also suitable for the determination of the density of raw oil, particularly on cold days when the manipulation of the viscous raw oil makes an accurate value difficult to obtain. The method is as follows:

Weigh out accurately approximately 1.5 g of dry raw shale oil into a pre-tared and pre-calibrated volumetric flask (25 mL). Record the mass of flask plus oil and add dichloromethane to the graduation mark. The volume of dichloromethane added may be calculated from the mass of solvent added and the density ($\mathbf{D_2}$) of dichloromethane previously determined using the same calibrated volumetric flask. Assuming additivity of volumes for the oil and solvent, the density $\mathbf{D_1}$ of raw oil is then given by:

$$\mathbf{D_1} = \frac{(\text{mass of 25 mL raw oil solution}) - (\text{mass of dichloromethane})}{(25 - \text{volume of dichloromethane added}).}$$

Otherwise the value for $\mathbf{D_1}$ represents the density of raw oil in solution at the above concentration. In either case the value of $\mathbf{D_1}$ as calculated is the value required in the equations below to determine the mass of neutral oil recovered after acid-base extraction. The latter may be achieved as follows:

After acid-base extraction recover the neutral oil solution quantitatively. Filter the dichloromethane solution into a suitable stoppered flask and determine the mass of solution recovered ($\mathbf{W_S}$). Using the pre-calibrated volumetric flask take an exact aliquot (25 mL) of solution if the volume available is greater than 25 mL; otherwise fill to the calibration mark by addition of solvent (CH_2Cl_2). For simplicity of notation it will be assumed that the pre-determined flask volume is exactly 25 mL, although in practice this will not necessarily be the case.

The mass ($\mathbf{W_{S(25)}}$) of 25 mL of the recovered neutral oil solution is given by:

$$\mathbf{W_{S(25)}} = \mathbf{V_1 D_1} + (25 - \mathbf{V_1})\mathbf{D_2} \quad \ldots\ldots\ldots\ldots (\mathbf{I}),$$ where

$\mathbf{V_1}$ = volume of neutral oil in 25mL of solution,

D_1 = density of the raw oil in solution (as determined earlier),

D_2 = density of CH_2Cl_2 at the appropriate temperature,

In equation (I) it is assumed that the densities of raw oil and neutral oil are equal. This assumption is necessary since efforts to reduce dissolved neutral oil back to solvent-free neutral oil results in unknown losses of volatile components.

Simplifying equation (I) yields:

$$V_1 = \frac{W_{S(25)} - 25\ D_2}{D_1 - D_2} \qquad \text{.....(II),}$$

Since all values on the right of equation (II) are known (i.e. given or determined), the mass of neutral oil recovered and contained in 25 mL is given by:

$$W_{OIL(25)} = V_1\ D_1 \qquad \text{.....(III).}$$

Equation (III) gives the mass of total oil recovered if the initial volume of recovered-oil solution is equal to or less than 25 mL. Where the initial volume exceeds 25 mL, the total mass of recovered oil is given by:

$$W_{OIL} = W_{OIL(25)}\ \frac{W_S}{W_{S(25)}} \qquad \text{.....(IV).}$$

Equation (II) shows that an accurate value for V_1 depends on a relatively large difference between the densities of the raw oil and the solvent used. This makes dichloromethane an obvious choice for the determination since it is substantially more dense (1.336 g mL^{-1} at 20°C) than shale oil (ca. 0.9 g mL^{-1}). Since the entire acid-base extraction procedure takes no more than a few hours, temperature corrections are (normally) not necessary.

The above procedure was tested on an aliquot of raw oil from Duaringa 5391-C. The dry raw oil was used for both density and recovery determinations, with a recorded but unknown mass of the raw oil determined in solution from equation **(III)** above. The accuracy of the method was demonstrated by the very close agreement between the actual mass of raw oil added (1.49375 g) and that determined from solution (1.48992 g); a difference of less than 4 mg, or less than 0.3%. The procedure is particularly useful in those circumstances where only neutral oil is required for further accurate analysis since it obviates the need for the quantitative recovery of artefacts and acid- and base-extractable compounds.

4.9 OPEN COLUMN CHROMATOGRAPHY OF NEUTRAL FRACTIONS FROM DUARINGA SHALE OILS.

The detailed chemical composition of the neutral fraction of shale oils obtained from Duaringa 5391-C and 686 is discussed below. The two oil fractions were obtained under identical conditions, which allows a comparison to be made between their respective chromatographic fractions in terms of similarities and specific differences. The gravimetric results for each raw oil are given in Table 4-26 and show the excellent material balance obtained in each case. The relative masses of neutral oil fractions, normalised against the total neutral oil recovered from the open column, were also calculated. These data are (generally) more informative than absolute values and inferences based on their relative values will be included in the detailed discussions of individual fractions.

Fraction 1 (90-130 mL: alkanes).

GC-MS analysis of fraction 1 (90-130 mL, hexane) shows that it contains linear, branched and cyclic alkanes. GC analysis of sequential subfractions of this eluent volume shows that solute affinities for the open-column adsorbents cause high molecular weight components to elute slightly earlier than the more volatile ones. The gas chromatogram of the total fraction is dominated by alkanes (C_7 - C_{32}), which comprise 86 % of total peak area over that component range and represent the major portion of volatile constituents in the eluate. The linear alkanes exhibit a tetramodal distribution, with relative maxima at C_{10} and in the regions C_{15}- C_{17}, C_{19} - C_{21} and C_{25} - C_{27} (Figure 4-36a). However, an overlap of further alkanes (primarily in the lower molecular weight region) coeluting with alkenes from the open-column up to ca.140 mL, influences their relative and total abundance in fraction 1 above. To obtain a composite "total alkane" profile, normalised alkane peak areas from column volumes (130-140 mL) were added to those obtained directly from the gas-chromatographic data for fraction 1. The resultant profile shows a broad bimodal distribution with slight maxima in the regions C_{19} - C_{21} and C_{25} - C_{27} and very little odd over even carbon preference (Figure 4-36b). Direct insertion mass spectrometry (DI-MS)

of an aliquot (10 µL) of fraction 1 has shown that alkanes are present at low levels up to at least C_{50}. This makes chromatographic quantitation of these constituents (using an internal standard) rather difficult, since it requires assumptions about their distribution beyond the highest-eluted member of the homologous series. Gravimetric quantitations, on the other hand, result in low values due to the partial loss of volatile constituents

TABLE 4-26. Gravimetric results for the acid, base and neutral fractions of shale oil from Duaringa 5391-C and 686. Both oils were produced by retorting the raw shales in a stainless steel retort using nitrogen sweep-gas.

FRACTION	RAW OIL[1]		NEUTRAL OIL[2]	
	5391-C	686	5391-C	686
Asphaltenes	9.6	7.9		
Phenols[3]	12.1	7.3		
Carb. Acids[4]	< 0.1	1.8		
Bases	28.8	13.1		
Artefacts[5]	11.6	19.0		
1	210.0	278.3	22.6	29.6
2	92.5	84.5	9.9	9.0
3	66.5	63.0	7.1	6.7
4	26.0	24.4	2.8	2.6
5	44.7	42.2	4.8	4.5
6	33.3	31.9	3.6	3.4
7	14.6	13.1	1.6	1.4
8	10.2	9.3	1.1	1.0
9	19.4	17.8	2.1	1.9
10	53.2	57.3	5.7	6.1
11	29.8	18.7	3.2	2.0
12	29.0	20.6	3.1	2.2
13	10.3	11.2	1.1	1.2
14	103.0	84.5	11.1	9.0
15	12.8	30.0	1.4	3.2
16	50.8	77.0	5.5	8.2
17	50.3	17.8	5.4	1.9
18	65.3	45.0	7.0	4.8
19	8.8	14.9	1.0	1.6
TOTAL	992.7	990.4	100.0	100.0

1 mg per gram of raw oil. **2** percent mass of total column-recovered material. **3** see Table 4-24 for mass of phenol and alkyl-substituted phenols. **4** gravimetric estimate only (cf. 4.8.3 for details). **5** this value represents the polymers, tars etc. formed during acid-base extraction of the raw shale oil, as well as those water-soluble "neutrals" recovered by back-extraction from the $NaHCO_3$ -, NaOH- and acid-extracts (cf. 4.8.3 for details).

(up to C_{15}) during solvent removal; however, when used under controlled conditions, both may be used for comparative studies.

Alkane distributions and relative abundance (CPI ratio) in shale oil provide little information about the oil shale kerogen. This is because precursor products are affected by random pyrolytic processes, such as thermal and catalytic cracking, during retorting. Some

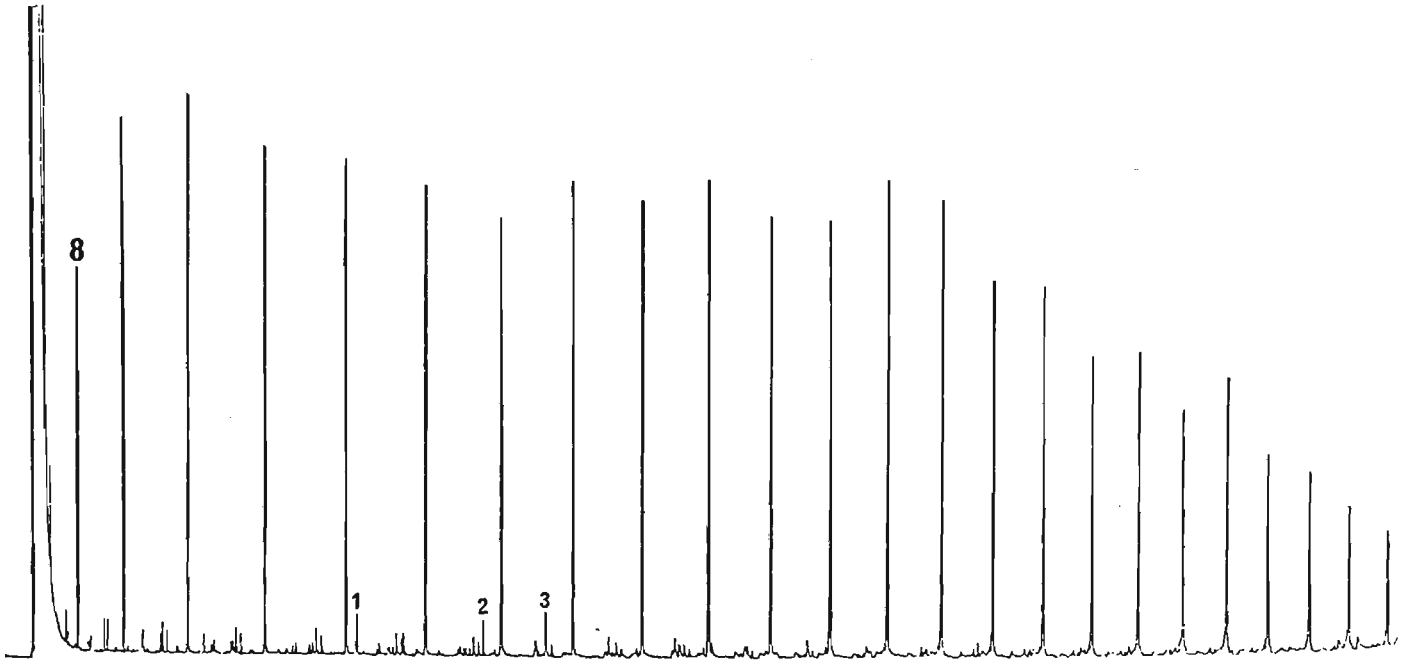

Figure 4-36a.
Gas chromatogram of fraction 1 from the open-column separation of Duaringa 5391-C neutral shale oil. Major components are alkanes, with octane (8) indicated. Components 1, 2 and 3 are acyclic regular isoprenoids: 2,6-dimethylundecane, 2,6,10-trimethyldodecane and 2,6,10 -trimethyltridecane.

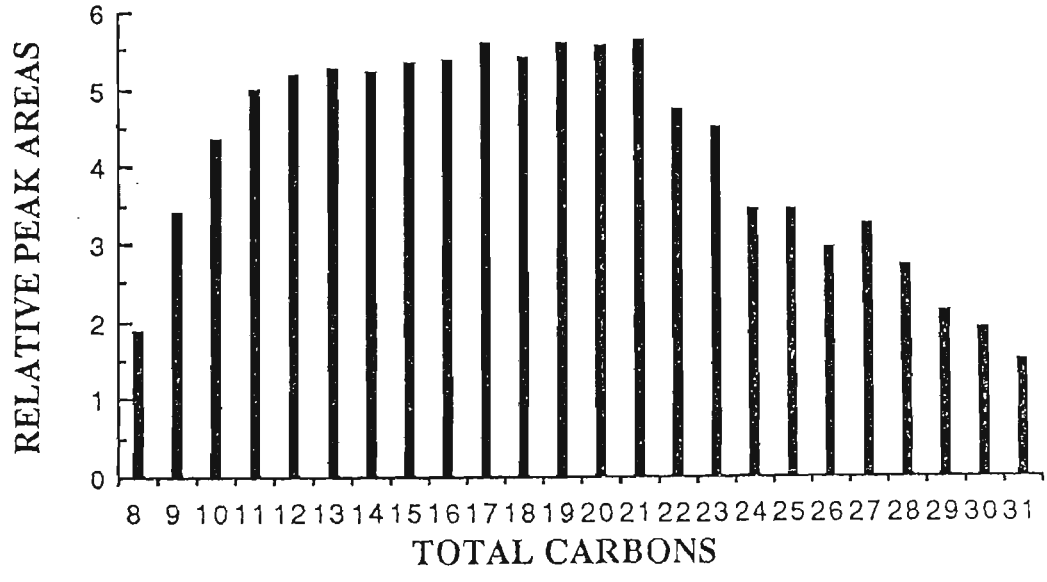

Figure 4-36b.
Composite "total alkane" profile for open-column fraction 1 from Duaringa 5391-C neutral shale oil.

of the high molecular weight alkanes ($>C_{24}$) however, are probably produced by pyrolytic fission of kerogen moieties derived from higher plant waxes, since the latter are known to contain linear alkyl chains of suitable length (Eglinton and Hamilton, 1963). Some of the very high molecular weight alkanes, found by DI-MS, may have been produced by radical intermediates derived from fatty acid pyrolysis according to the reaction scheme proposed by Eisma and Jurg (1969). The authors heated behenic acid ($C_{21}H_{43}COOH$) and from an analysis of the products formed described several radical mechanisms (initiation, propagation, scission and termination), by which odd- and even-numbered alkanes and fatty acids can be formed from an even-numbered fatty acid initially present in a living organism. Fraction 1 alkanes in the range C_8 - C_{23} are partly derived as secondary products from the thermal cracking (cleavage of C-C bonds) of higher molecular weight alkanes (possibly formed initially as suggested above), with the major portion probably formed directly by the pyrolytic scission of terrestrial lipid material or from kerogen moieties derived from algal or bacterial lipids (Regtop et al., 1983).

The fraction 1 chromatogram for the neutral Fischer retort oil (Duaringa 5391-C) is virtually identical to that of Figure 4-36a. That of fraction 1 for neutral shale oil from Duaringa 686 is again very similar, with only slight differences in the overall alkane distribution.

GC analysis of the branched and cyclic components, isolated from fraction 1 by occlusion of the linear alkanes with molecular sieves (0.5 nm), produced over 400 (resolved) peaks (Figure 4-37). GC-MS analysis identified more than 200 of these constituents as members of major homologous series of alkylcyclopentanes, alkylcyclohexanes, 2-, 3-, 4-, and 5-methylalkanes (listed in the order of decreasing relative abundance), with four minor series, possibly corresponding to methylalkylcyclopentanes, methylalkylcyclohexanes and dimethylalkanes, also detected. To guard against artefact formation and possible rearrangements, cyclisation, isomerisation etc., which could occur during removal of the linear alkanes, each series detected in the branched and cyclic fraction was verified as indigenous to the shale oil by demonstrating its

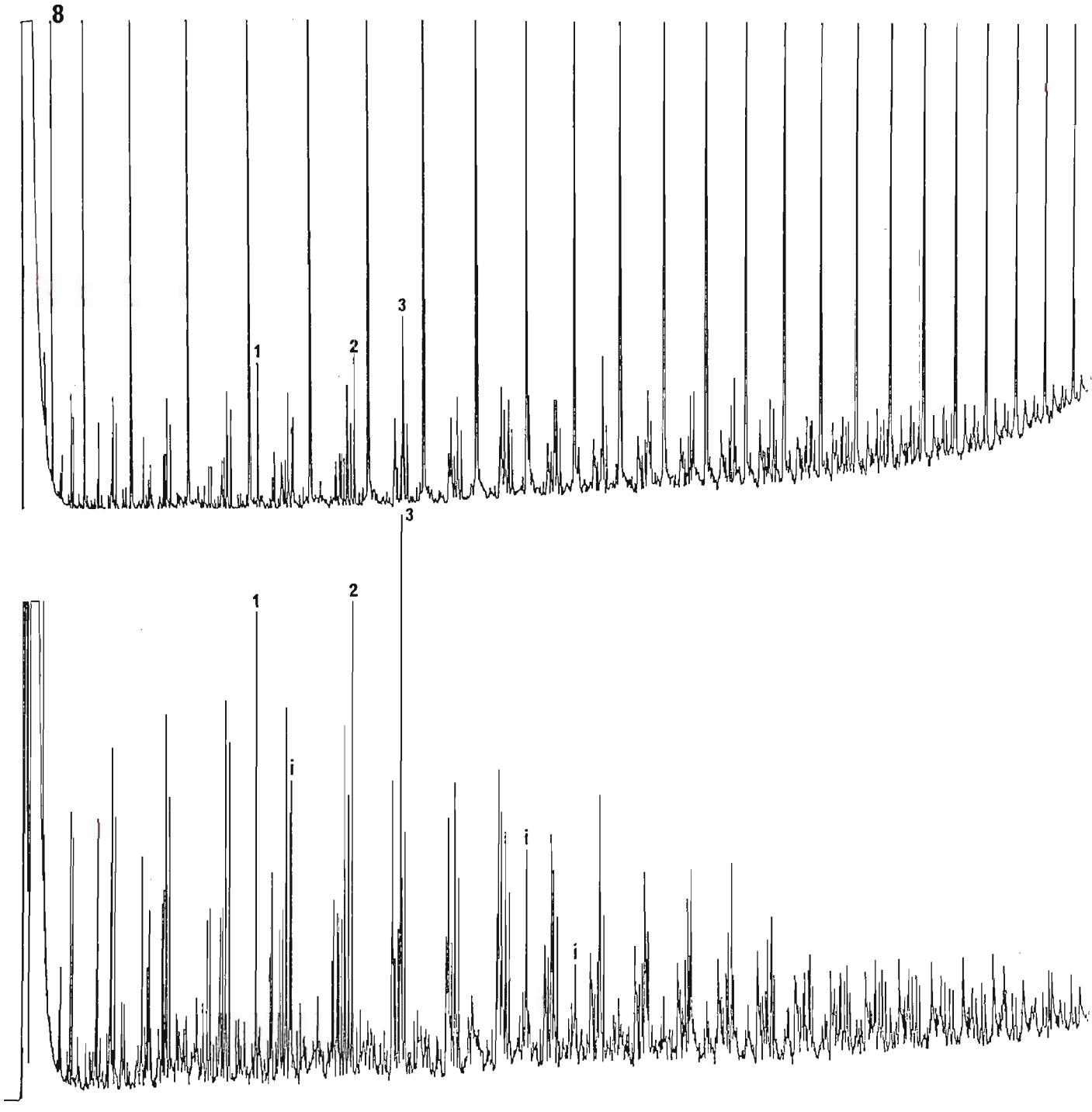

Figure 4-37.
Gas chromatogram of branched and cyclic components isolated from Duaringa 5391-C neutral shale oil fraction 1 (lower trace); components 1, 2 and 3 as in Figure 4-36; other acyclic regular isoprenoids (i) are, in order of elution: 2,6-dimethyldodecane, pristane and phytane. The upper trace is the fraction 1 profile (Fig. 4-36) replotted at high sensitivity, to enhance the visibility of non-linear components.

presence in the column eluent from which it was isolated (i.e. fraction 1).

For resolved GC peaks, modified Kovats retention indices (RI) were calculated from equation (**1**) in section 4.3, using component retention times obtained under standard GC analysis conditions (cf.section 3.4.1). For the above fraction this was particularly straightforward, since all of the components were bracketed by appropriate alkanes prior to clathration of the sample (Figure 4-37). Retention index equations were calculated using least-squares analysis of the retention indices obtained for positively identified components (GC-MS) of the appropriate homologous series (Table 4-27 - 4-30; Figure 4-38 and 4-39).

Gas chromatographic resolution degraded with an increase in the molecular weight of constituents and many components coeluted at elevated temperatures. Under these circumstances diagnostic mass-spectra cannot always be obtained during GC-MS analysis, and plots of characteristic fragment-ions (fragmentograms) are needed to establish the presence of higher members of previously identified homologous series. To identify as many series as possible, suitable well-resolved regions of the total ion-current profile were chosen and the presence of all discrete components recognised by manual deconvolution of mass-spectra across each peak (Figure 4-40). Where possible these discrete components were identified and the presence of prospective homologous series inferred from appropriate fragmentograms of masses specific for each particular class of compounds. Once recognised from these single-ion current profiles, the identity of particular components was verified by looking at their complete mass spectra. This approach was limited in the high molecular weight region through interference from coeluting components. However, the agreement between retention indices calculated for peaks in the single-ion current profile and those values obtained from retention index equations derived from previously identified lower members of the homologous series, is sufficient to establish the presence of the higher molecular weight constituents. Figure 4-41 shows part of the single-ion current profile for alkylcyclopentanes and alkylcyclohexanes found in the branched and cyclic fraction of the retort shale oil. For respective series individual members were positively identified up to C_{15} cyclopentane and C_{14} cyclohexane (Table 4-27) from both their mass spectra and diagnostic single-ion fragmentograms. For each series,

Table 4-27. Modified Kovats retention indices calculated for cyclic components positively identified in the branched and cyclic alkane fraction isolated from Duaringa 5391-C neutral shale oil.

C No.	RETENTION INDEX (RI)*	
	alkylcyclopentanes	alkylcyclohexanes
9	930.83	
10	1034.14	1029.94
11	1137.62	1133.28
12	1240.99	1237.27
13	1344.46	1341.44
14	1447.65	1445.87
15	1554.47	1550.95
16	1657.15	1654.19
17	1762.25	1756.82
18	1861.88	1861.88
19	1961.98	1967.05
20	2066.17	2070.00

* Modified Kovats retention indices were calculated using equation (1).

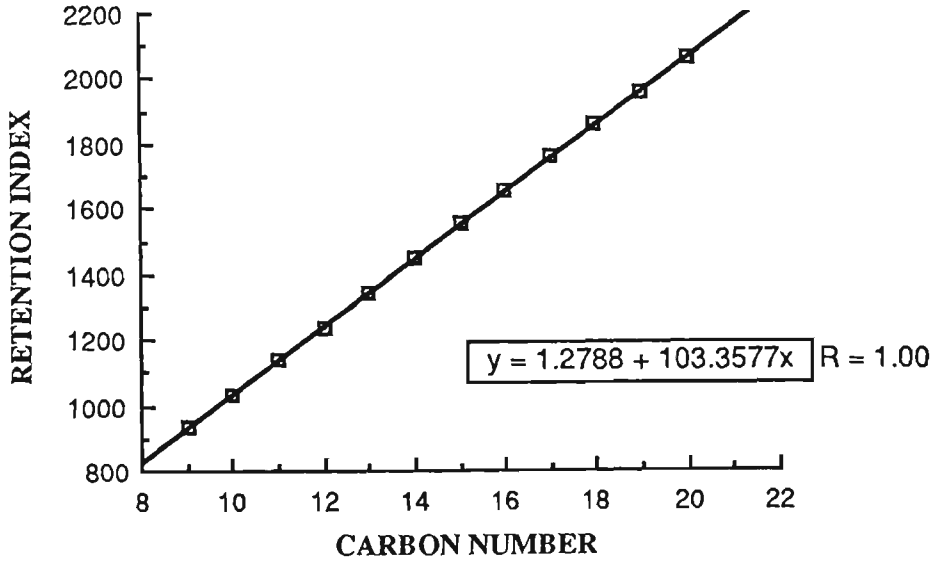

Figure 4-38.
Plot of retention indices (RI) for positively identified alkylcyclopentanes contained in the branched and cyclic alkane fraction isolated from Duaringa 5391-C neutral shale oil.

TABLE 4-28. Retention index equations (RI = m (C No.) + b), obtained by least -squares analysis of the tabulated retention indices for cyclic components in the Duaringa branched and cyclic alkane fraction (Table 4-27).

COMPOUND	EQUATION	RESIDUALS
alkylcyclopentanes	**RI** = 103.358 **C** + 1.279	4.41
alkylcyclohexanes	**RI** = 104.075 **C** - 11.250	4.05

TABLE 4-29. Modified Kovats retention indices calculated for positively identified methyl alkanes in the branched and cyclic alkane fraction isolated from Duaringa 5391-C neutral shale oil (compounds listed in order of elution).

C No.	RETENTION INDEX (RI)*			
	5-methyl	**4-methyl**	**2-methyl**	**3-methyl**
10		958.52	961.43	968.33
11	1054.14	1059.02	1062.56	1069.17
12	1155.16	1159.10	1163.43	1169.85
13	1254.04	1258.79	1263.35	1269.97
14	1353.21	1358.11	1363.24	1369.87
15	1452.35	1457.72	1461.75	1470.03
16	1550.95	1557.50	1562.68	1569.96
17	1651.46	1657.15	1662.54	1669.93
18			1762.25	1770.00
19			1861.88	1869.99
20			1961.98	1970.13
21			2061.18	2070.00

* Modified Kovats retention indices were calculated using equation (1).

TABLE 4-30. Retention index equations (RI = m (C No.) + b), obtained by least -squares analysis of the tabulated retention indices for methyl alkane components in the Duaringa branched and cyclic alkane fraction (Table 4-29).

COMPOUND	EQUATION	RESIDUALS
5-methylalkanes	**RI** = 99.352 **C** - 37.88	2.31
4-methylalkanes	**RI** = 99.738 **C** - 38.224	11.87
2-methylalkanes	**RI** = 99.911 **C** - 36.262	4.95
3-methylalkanes	**RI** = 100.099 **C** - 31.762	1.5

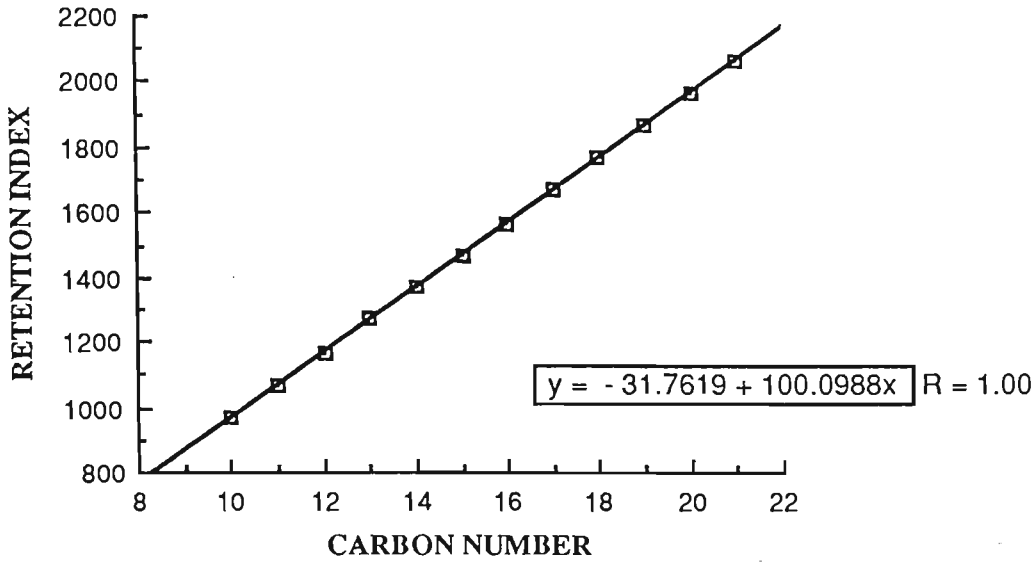

Figure 4-39.
Plot of retention indices (RI) for positively identified 3-methylalkanes contained in the branched and cycloalkane fraction isolated from Duaringa 5391-C neutral shale oil.

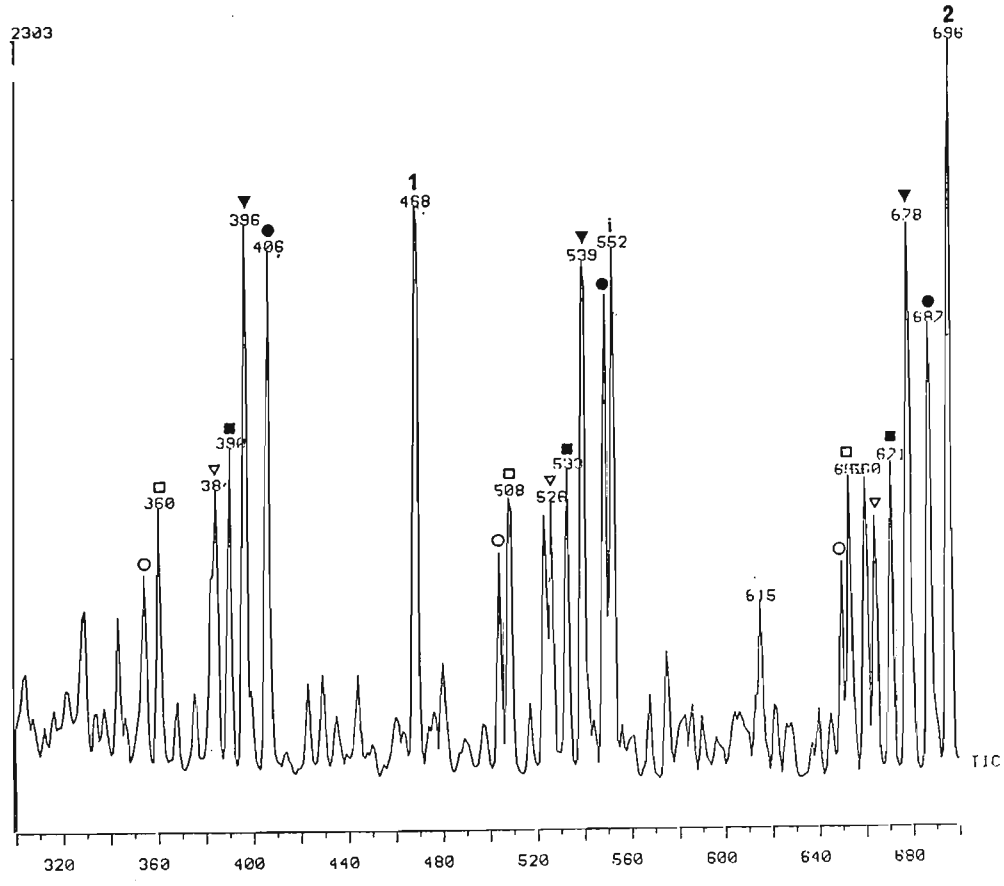

Figure 4-40.
Part of the total ion-current profile (TIC) for the branched and cyclic alkane fraction isolated from Duaringa 5391-C neutral shale oil (scan range #300 - #700 - see Figure 4-41). Components 1 (#468), 2 (#696) and (i) (#552) as in Figure 4-37. Other marked components denote, in order of elution, sequential components of homologous series of alkylcyclohexanes, alkylcyclopentanes, 5-, 4-, 2- and 3-methylalkanes.

fragmentograms and retention data were used to establish the presence of substituent alkyl chains ranging up to at least C_{27} and C_{26} respectively.

Regular acyclic isoprenoid hydrocarbons and several series of methyl alkane homologues were also identified on the basis of their mass spectra, with high molecular weight components of the latter characterised by specific-fragment-ion plots and retention data (Figure 4-37). As can be seen from Table 4-29, the methyl alkanes elute sequentially as 5-, 4-, 2-, and 3-methylalkanes. For the corresponding methylnonanes, the boiling points (°C) are : 165.1, 165.7, 166.8 and 167.8; the BP-5 stationary phase thus separates these methylalkanes according to their boiling points.

Naturally occuring isoprenoids which have been proposed as possible precursors to the regular isoprenoid alkanes detected in sediments include squalene, the polyprenoids, carotenoids, the phytol side chain of chlorophyll, the isoprenoid acids, alcohols and other biolipids (Gallegos, 1976). The presence of regular isoprenoids in the shale oil and their suggested biogenic origin indicates that at least some of them were formed by pyrolysis of one or more of the proposed precursors listed above.

Mass spectra of methylalkanes usually differentiate between isomers of the various identified homologous series by exhibiting fragment ions specific for position of the methyl substituent on the alkyl chain; this allows different individual components to be resolved even in chromatographically congested regions of the profile (Figure 4-42). Although only 2-, 3-, 4- and 5-methylalkanes were positively identified in the fraction, the presence of low concentrations of other positional isomers, associated with longer alkyl chains (e.g. 6- and 7-methylalkanes etc.), was inferred from appropriate ion-current traces. This suggests that all possible positional isomers of the methyl alkanes may be present in shale oil and indicates a pyrolytic origin for at least some of the less commonly observed isomers. The observation of these series is predicted by a study of the pyrolysis of $C_{24}H_{50}$ by Kissin (1987). Almon, cited by Tissot and Welte (1984), has investigated the mechanism of fatty acid decarboxylation and shown that anhydrous smectite favours the formation of branched alkanes, with a distribution of isomers approaching thermodynamic equilibrium. He further showed that the presence of water favours some sort of free radical reaction and results in a strong predominance of alkanes. Iso- and anteiso- alkanes have been isolated

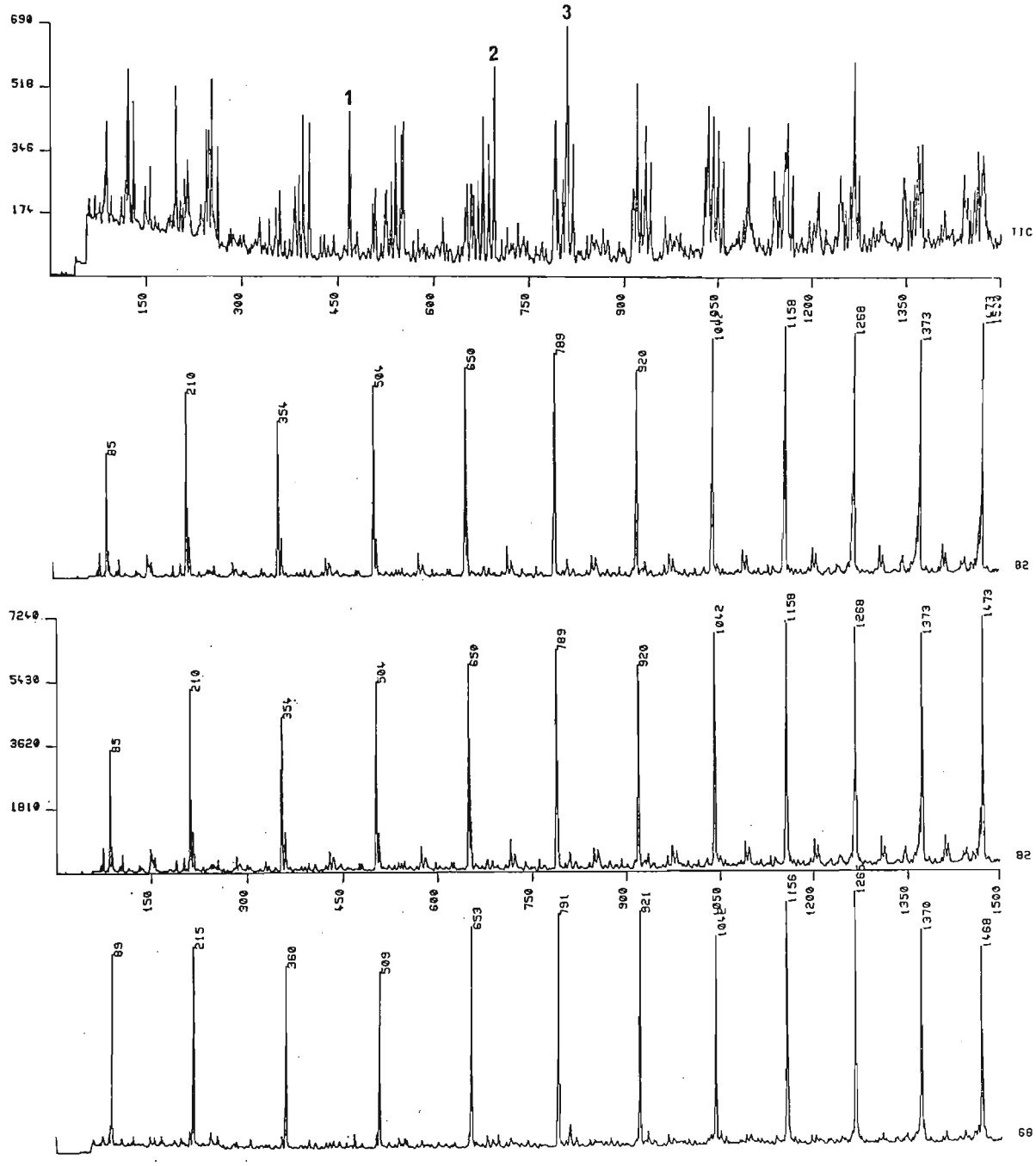

Figure 4-41.
Part of the total ion-current profile for the branched and cyclic alkane fraction isolated from Duaringa 5391-C neutral shale oil (trace 1), with numbered components as in Figure 4-37. Trace 2 is the fragment-ion profile of mass 82, corresponding to a homologous series of alkylcyclohexanes contained in the fraction, and shows the position of this series in relation to the total ion-current profile. Traces 3 and 4 are respectively fragment-ion profiles of masses corresponding to homologous series of alkylcyclohexanes (m/z=82) and alkyl -cyclopentanes (m/z=68) and show the relative elution pattern of these components. Peak numbers in traces 2-4 denote mass-spectral scan numbers, with # 85 and # 89 respectively denoting ethylcyclohexane and propylcyclopentane. Note the change in elution order after scan # 1042.

from a number of sources including bacteria, higher plants, Recent and ancient sediments and have been reported as constituents of shale oil (Regtop et al. 1982; Rovere et al. 1983), although 4- and 5-methyl alkanes were not reported by these authors.

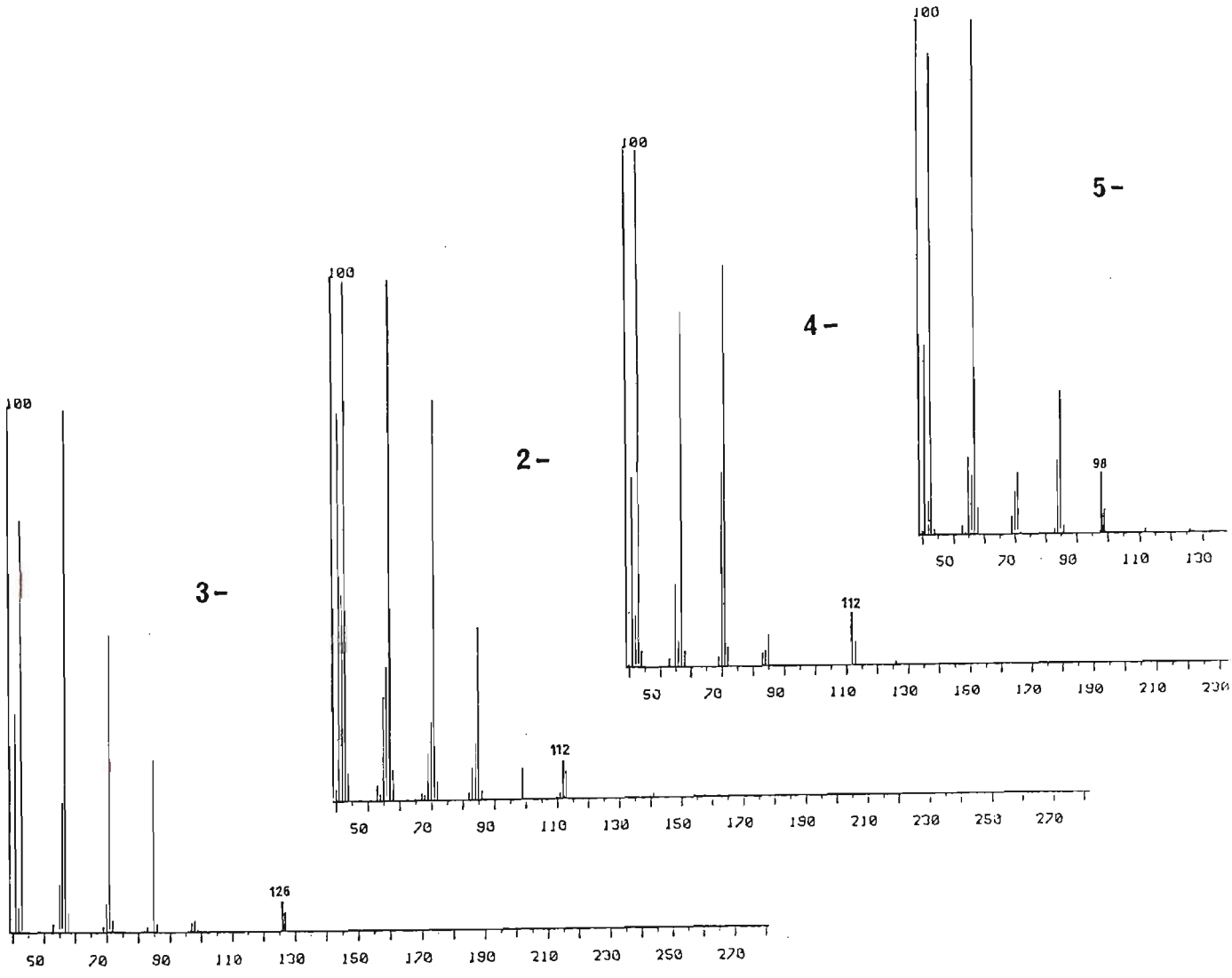

Figure 4-42.
Mass spectra for 5-, 4-, 2- and 3-methyldecane (M.Wt. 156), identified in the branched and cyclic alkane fraction of open column fraction 1 from Duaringa 5391-C neutral shale oil. Diagnostic fragment ions, relating to methyl-branch position on the alkyl chain, are highlighted. The 4- and 2-methyldecane isomers were identified on the basis of diagnostic fragment-ion differences at the low-mass end (e.g. ratio of ions at m/z = 57 and 71) and complementary retention data.

Levy et al. (1963) have shown the presence of iso- and anteiso- alkanes, as well as both 4- and 5-methylalkanes in paraffin wax. A homologous series of iso- and anteiso alkanes, with an odd carbon number preference, generally indicates a contribution from plant wax sources. For the branched/cyclic fraction the problem of insufficient component resolution at high molecular weight makes the calculation of relevant CPI ratios very difficult, while the thermal cracking of long alkyl chains during the retorting of the oil shale produces lower molecular weight fragments and consequently destroys its diagnostic value. The source of the methylalkanes remains speculative given the possibility of contributions from both of the above sources.

Fraction 2 (130-140 mL: alkanes-alkenes).

Fraction 2 was collected as two separate eluate volumes (130-135 and 135-140 mL) to facilitate quantitation of the low carbon number alkanes, which continue to elute from the column in this fraction. Eluate components comprise predominantly alkanes and high carbon number alkenes, which elute prior to the lower alkene homologues. The former alkenes were quantified from gas-chromatographic data based on the proportion of their collective peak areas relative to the total peak area of all chromatographable constituents contained in the fraction. The percentage of their total peak area was converted to an approximate alkene mass from absolute (gravimetric) values obtained for the solvent-free concentrate. This value was added to the gravimetric data for fraction 3 to obtain a total alkene concentration for the raw oil. Alternatively the total fraction 2 eluate may be concentrated and the olefins quantified gravimetrically after isolating these components from saturated constituents using silver nitrate impregnated silica gel and either TLC (Gupta and Dev, 1963) or column chromatography (Iida et al., 1966).

Fraction 3 (140-175 mL: alkenes).

Fraction 3 comprises both linear and branched alkenes ranging from C_8 to greater than C_{32}. Major (resolved) linear alkenes in the C_{10}-region of the chromatogram were identified by comparative gas chromatography and GC-MS analysis of authentic decene

standards, as 1-, (4- and 5-), 3-, 2- (trans) and 2- (cis) decene, listed in the order of their elution, with co-eluting isomers bracketed together (Figure 4-43).

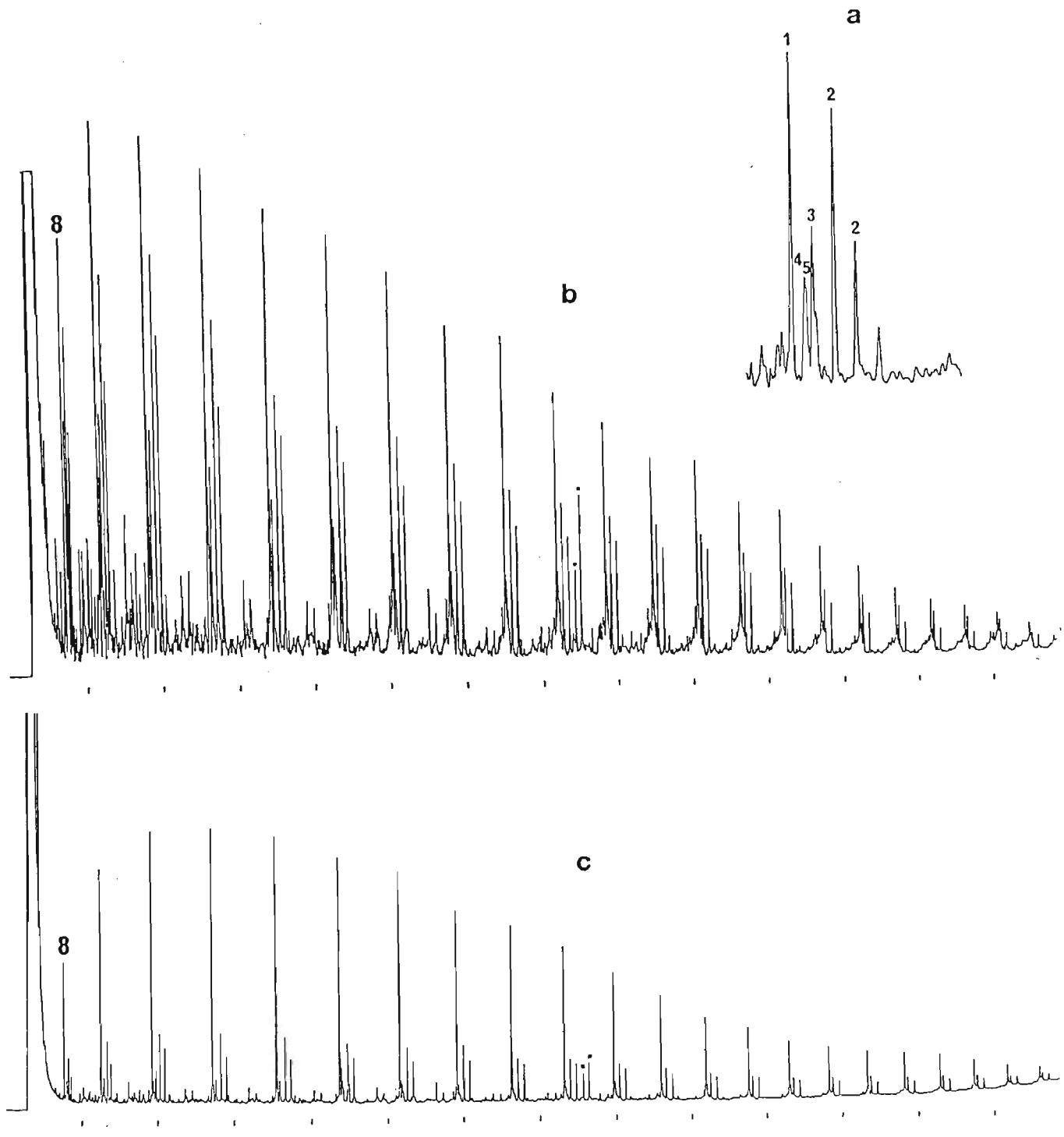

Figure 4-43. Gas chromatograms of alkenes contained in the fraction 3 eluent of neutral shale oil from Duaringa 5391-C (b) and 686 (c); carbon numbers for 1-alkenes as indicated. Major components are 1-, (4- and 5-), 3-, 2- (trans) and 2- (cis) alkenes, listed in the order of their elution (see insert a, given for decene-isomers). Other components marked ▪ are prist-1-ene and prist-2-ene listed in the order of their elution.

Inspection of the chromatograms and GC-MS analysis of higher molecular weight components, in conjunction with fragment-ion plots diagnostic for monoolefins (m/z=83), confirmed the continued presence of these series of isomeric homologues up to at least C_{32}. The 1-alkenes are the most prominent single components in the GC-profiles of fraction 3 for both oils, although variations exist between the two oils in their relative abundances. They are relatively more concentrated in the eluate from 686, whereas their abundance in 5391-C is subordinate to that of the combined peak areas of the respective 2-alkenes (trans and cis). The presence of internal alkenes in retort oils suggests mineral matrix induced isomerisation of the 1-alkenes during retorting, since only the latter are prominent in the flash-pyrolysis GC-profiles of raw oil shales. This line of reasoning is supported by the discussions below, which confirm that the relative abundances of the various isomers are largely determined by the thermo-catalytic activity of the mineral matrix. For the Duaringa oils this indicates greater catalytic activity for 5391-C as a consequence of the higher concentrations of internal olefins. Branched and cyclic alkenes were not separated from this fraction but their presence was established from chromatographic retention data and corresponding GC-MS analysis. The latter was used in particular to produce fragment-ion plots characteristic for cyclopentenes (m/z=67) and cyclohexenes (m/z=81).

Alkenes derived from the retorting of oil shales are present in quantities and isomeric distributions which are largely dependent on the combined effects of heating rates (Burnham et al., 1982), pyrolysis temperature, pyrolysate residence time, the conditions of pyrolysis (e.g. hydrous) and the activity of the mineral matrix. Hutton et al. (1986) have shown that Condor oil shale needs to be heated above 350°C to produce appreciable quantities of 1-alkenes, which are virtually absent below that temperature. Saxby et al. (1986) have demonstrated that very slow heating of torbanite (100 - 400°C at 1°C / week) in a sealed tube produced alkanes only. Other authors have produced pyrolysates free of olefins and similar to natural crude oils by heating dried organic-rich shales in sealed tubes at 330°C and in the presence (hydrous) and absence (anhydrous) of free water (Hoering, 1984; Comet et al., 1986). Although these conditions suppressed the formation of alkenes,

the above work by Hutton and co-workers showed for Condor shale that neither sealed environments, nor slow heating rates, nor the addition of water are necessary prerequisites to prevent their formation below sample-dependant threshold temperatures.

An examination of a likely mechanism for the release of hydrocarbons from pyrolysing kerogen may explain the formation of alkenes. It is known that the concentrations of alkenes and alkanes with the same carbon number are generally similar in high temperature (> 450°C) pyrolysates of oil shales, suggesting common precursors for the two classes of compounds. The most likely precursors for both are alkyl-radicals since these may form alkanes by unimolecular dissociation or through collision-induced coupling with another free alkyl-radical or hydrogen-radicals; alternatively they may lose a hydrogen-radical to form alkenes. The extent to which these competing processes take place during retorting ultimately determines the relative alkane-alkene content of the pyrolysate. A likely source of the hydrogen-radicals needed to convert free alkyl-radicals into alkanes is water derived from the kerogen or the mineral matrix (free interstitial pore- and microreservoir-water as well as water of hydration released from minerals) and the thermally degrading (aromatising) kerogen. Given that all oil shale retorting processes are essentially hydrous procedures, at least up to those temperatures corresponding to the depletion of free or bound water, the overall suppression of alkenes is influenced by the availability and rate at which hydrogen-radicals are released from both sources. The extent to which one source predominates is dependent on the oil shale composition, but hydrogen-radicals derived from mineral matrix water are likely to predominate in the lower temperature range, possibly up to 400°C, since very little kerogen degradation (aromatisation) occurs below this temperature.

In the temperature range of maximum oil formation (400 - 500°C) the shortened residence time of components in the pyrolysate, in conjunction with a possible depletion of hydrogen-radicals, is sufficient to guarantee the survival of relatively abundant quantities of alkenes. Initially these alkenes are predominantly 1-alkenes partly derived from simple cleavage of pre-formed alkanes according to a mechanism postulated by the Rice theory for thermal unimolecular radical decomposition (Fanter et al., 1968; Brown, 1971). Once

formed, these terminal alkenes may be transformed to internal alkenes by the thermo -catalytic influence of the mineral matrix, which promotes the migration of double bonds along the carbon chain. The latter was demonstrated by Regtop et al. (1986) who showed that prist-2-ene in the pyrolysate of Condor oil shale was derived from prist-1-ene by mineral-catalysed isomerisation in relative abundances dependent upon the residence time of the vapour in the catalyst bed. Fookes and Johnson (1984) have used high field ^{13}C NMR analysis of the alkenes isolated from a Condor shale oil to show the presence and quantify the abundance of all of the possible 1- to 6- cis and trans double bond isomers of linear alkenes in the fraction. They interpreted their quantitative data as indicating that 1-enes are the initially-formed olefins and that the double bond subsequently migrates along the carbon chain. They concluded that the terminal carbon is the likely site of the original linkage to the kerogen, consistent with the widespread occurence in the biosphere of long chain fatty acids and, to a lesser extent, primary alcohols and their isolation from the hydrolysis of kerogens.

The presence of high concentrations of relatively reactive alkenes in retort oil is known to have an effect on its composition and storage properties. Lambert and Saxby (1987) have simulated long-term storage conditions by subjecting a fresh sample of Rundle shale oil to a variety of storage conditions over a 26 week period. Ageing of the oil in sunlight caused the biggest decrease (79 %) in the amount of straight-chain mono-alkenes present, with internal alkenes (both cis and trans) more susceptible to further reactions than the corresponding 1-alkenes. The authors postulated that the monoolefins may have polymerised into materials which remained bound to the GC-column support. These findings support the need to fractionate shale oil as soon as possible after production. If long-term storage of samples is required, they should be kept frozen and under nitrogen.

Fraction 4 (175-215 mL: dienes).

Fraction 4 is characterised by very complex GC-profiles for both oils and comprises at least 10 homologous series, with terminal dienes the most abundant compounds in the eluate of each (Figure 4-44). Because of the chromatographic complexity the column eluate for fraction 4 of the reference oil from 5391-C (FA retort oil)

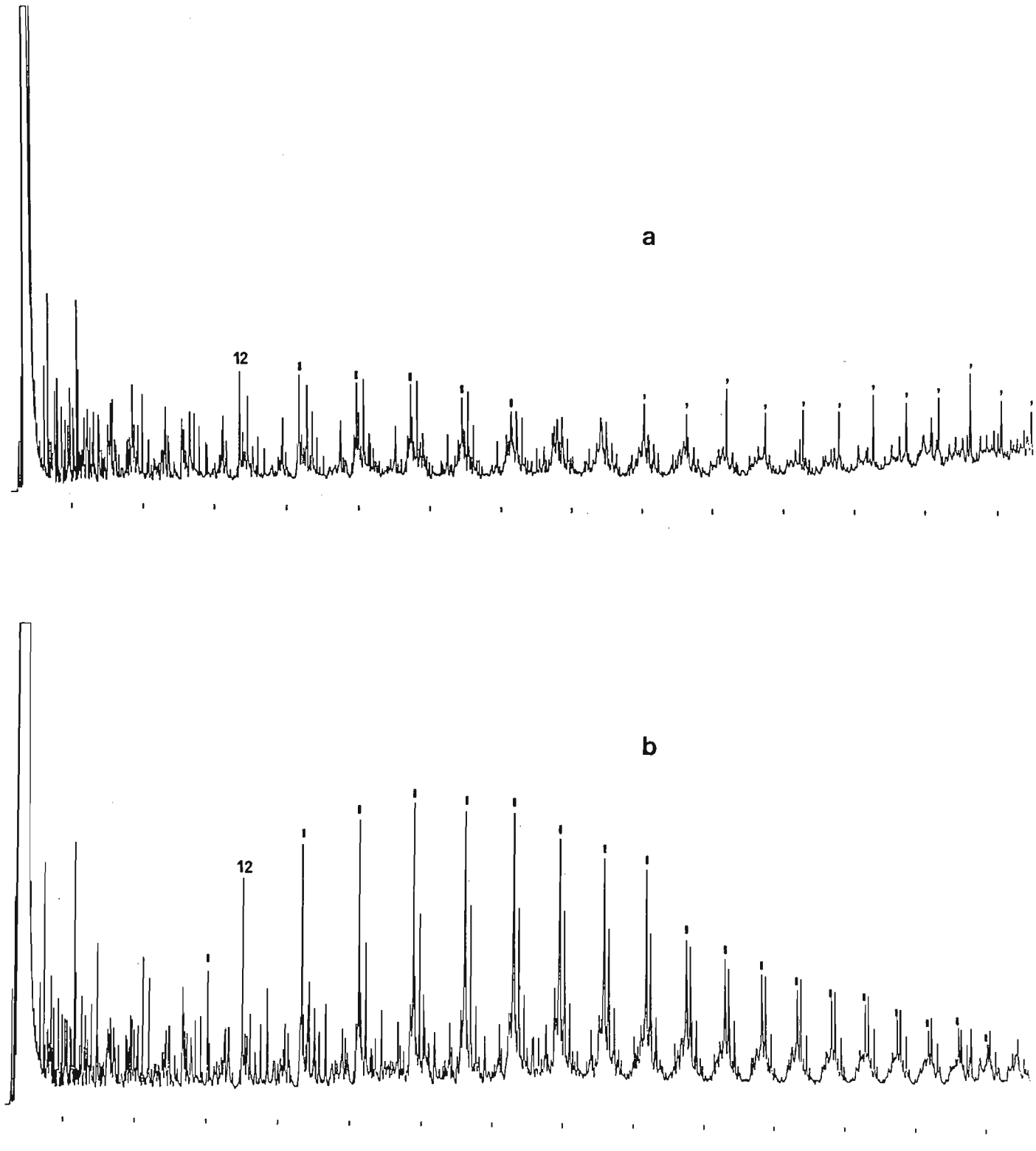

Figure 4-44.
Gas chromatogram of fraction 4 for neutral shale oil from Duaringa 5391-C (a) and 686 (b). Components marked ı in each profile are terminal dienes with carbon numbers as indicated. Other components (,) in profile a denote high molecular weight alkylbenzenes which have partly overlapped with this fraction.

was collected as sequential volumes of 5mL each, which were then analysed separately by GC and GC-MS. The first column volume (175-180 mL) consisted mainly of traces of low carbon number alkenes (predominantly cyclic and branched) which were still eluting from the column at this stage. These alkenes were also found in low concentrations in the total fraction 4 eluate for each of the two oils analysed (Figure 4-45).

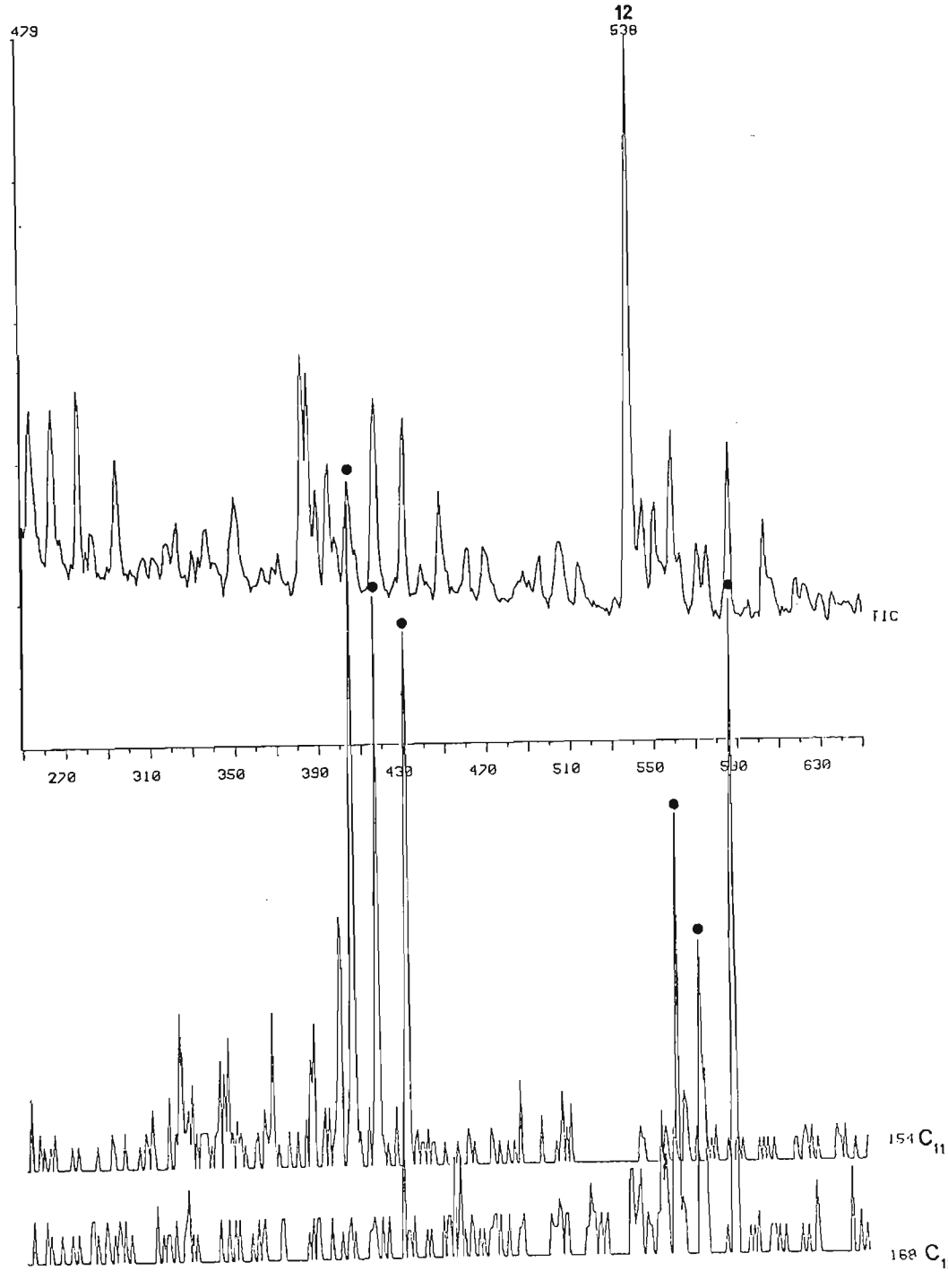

Figure 4-45.
Part of the total-ion-current (TIC) profile for fraction 4 from 5391-C and corresponding fragment-ion plots for alkenes with molecular weights of 154 (C_{11}) and 168 (C_{12}) daltons respectively. Similar concentrations of residual alkenes were also detected in the gas chromatogram of fraction 4 from 686.

Later sequential sub-fractions showed a progressive increase in the relative abundance of dienes, particularly terminal dienes, which were identified by comparison with literature mass spectra for 1,11-dodecadiene and 1,12-tridecadiene. There was also mass spectral evidence for the presence of two homologous series of linear alkynes, characterised by the appropriate molecular weights and fragment-ions at m/z: 95, 68, **67**, 55 and 41 (base peak listed in bold print). Three minor (isomeric) homologous series were also identified ranging from C_9 (M.WT: 124) to at least C_{17} (M.WT: 236); beyond this carbon number these series were poorly resolved and co-eluted with other more abundant components. The molecular weights for these compounds are characterised by the general formula C_nH_{2n-2} and mass spectra for individual components contain prominent fragment-ions at m/z: 95, 81, **68**, 67, 53 and 41. The other 5 homologous series found comprised dienes ranging from C_{10} - C_{20} for 5391-C and C_8 - C_{32} for 686, with terminal dienes clearly predominant in the gas chromatogram of the latter (Figure 4-46). Mass spectra for compounds representative of each of the homologous series are given in Figure 4-47.

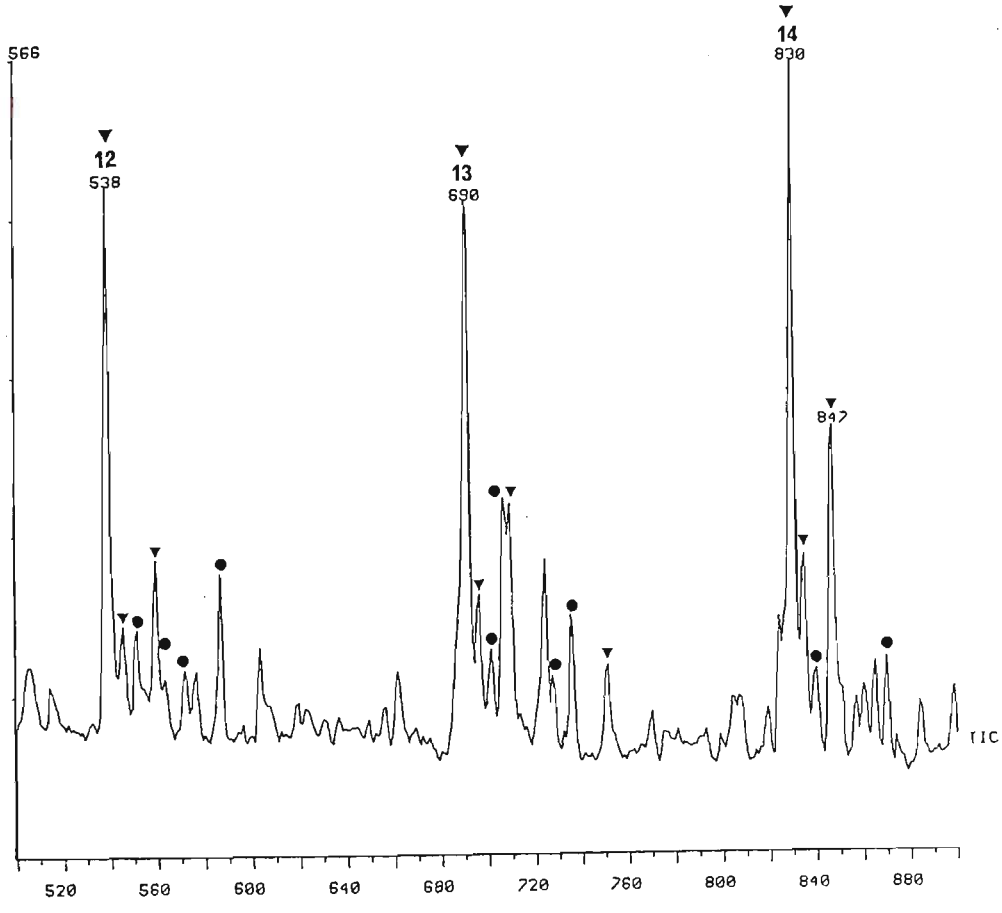

Figure 4-46. Part of the total-ion-current (TIC) profile for fraction 4 from 5391-C. Dienes are denoted by ▼, with major components corresponding to terminal dienes having carbon numbers as indicated. Other compounds (●) are low molecular weight residual alkenes from fraction 3.

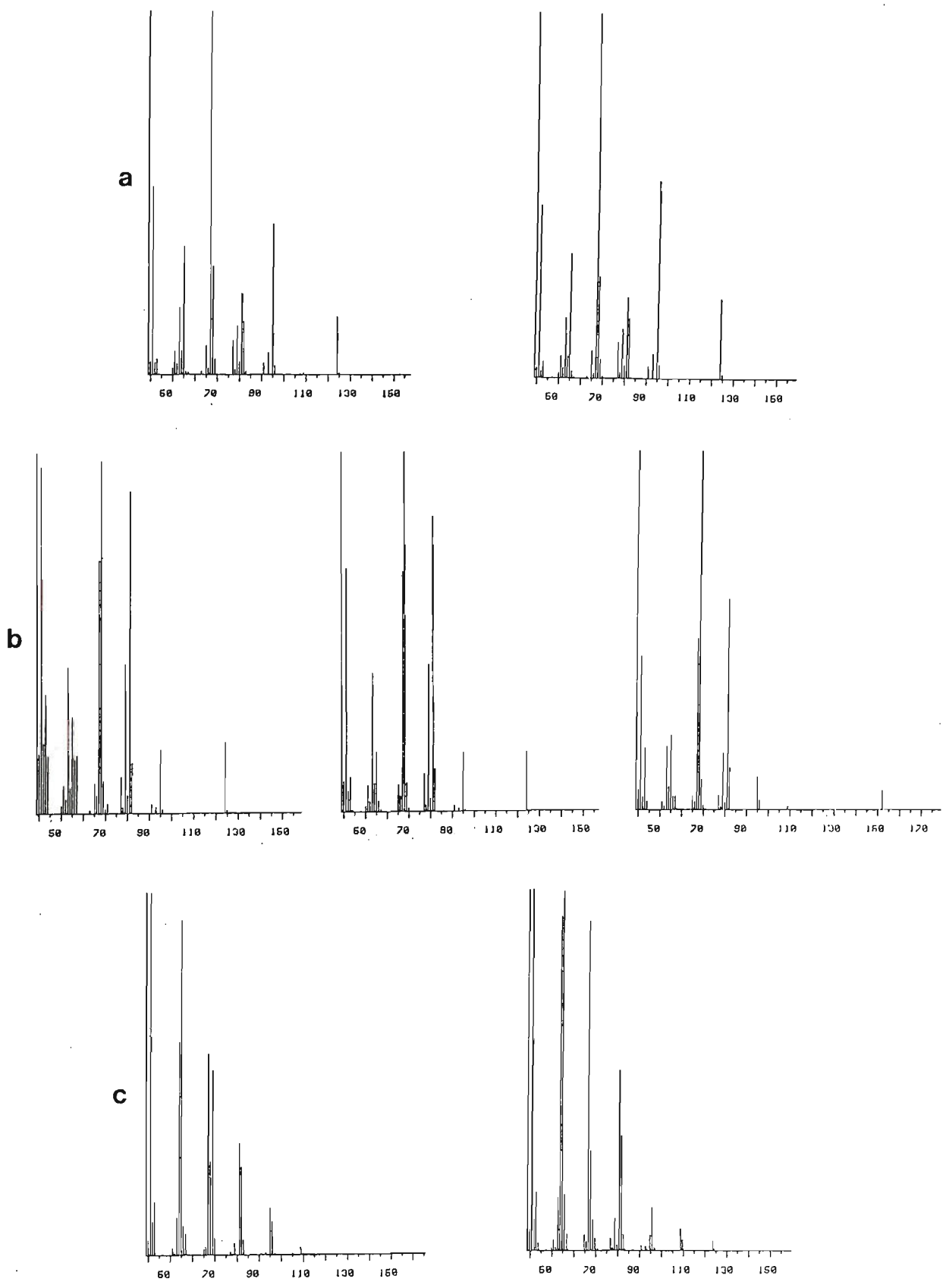

Figure 4-47.
Representative mass spectra of some of the homolgous series of compounds identified in fraction 4 from Duaringa 5391-C. Series **a** are possibly alkynes; series **b** are unidentified dienes (possibly branched) previously detected in neutral oil from Condor; spectra depicted in **c** are representative of the five series of homologous linear dienes found in the fraction.

The abundance of terminal dienes in the gas chromatogram for 5391-C was relatively diminished in relation to internal isomers. This is consistent with greater catalytic activity of the mineral matrix in raw shale from 5391-C, as proposed earlier to account for the comparatively lower 1-alkene/internal alkene ratio for fraction 3 from this oil. Dienes have previously been reported in FA retort oil from Condor by Rovere et al. (1983), who reported the presence of three major and six minor series of alkadienes with the same diagnostic fragment-ions as those found for both oils from the Duaringa deposit. The author found a UV absorption maximum for the fraction at 216 nm with $E^{0.01\%}$ equal to 0.61 and concluded that the majority of the dienes were unconjugated.

Fraction 5 (215-315 mL: monoaromatics).

For both oils this fraction comprises substituted monoaromatics (predominantly alkyl-substituted benzenes) with subordinate concentrations of alkyl-substituted toluenes and xylenes.

The more complex fraction obtained for neutral oil from 5391-C was analysed first using both GC and GC-MS analysis. The latter was carried out in detail over the chromatographically well-resolved molecular weight range of 134-162 daltons and revealed the presence of trace quantities of residual dienes apart from abundant monoaromatic compounds. Both oil fractions are dominated by alkylbenzenes, with the alkyl substituents ranging in carbon number from 2 to at least 26 in each case. The profile for 5391-C is substantially more complex than that for 686, with the latter characterised by relatively more abundant 1-phenylalkanes (Figure 4-48).

Aromatic hydrocarbons are characterised by well-defined mass spectra with relatively intense molecular ion peaks and few, but prominent, fragment ions. The most characteristic fragments of alkyl-substituted aromatic hydrocarbons correspond to cleavages ß to the aromatic ring. For mono-substituted alkylbenzenes this results in the formation of an ion at mass m/z=91, which is the most abundant peak of the mass spectrum. Further substitution on the ring is accompanied by a shift of this peak by the appropriate mass increment. Thus peaks at m/z values of 105, 119 and 133 are (generally) diagnostic for alkyltoluenes, alkylxylenes and alkyltrimethylbenzenes respectively. Another characteristic

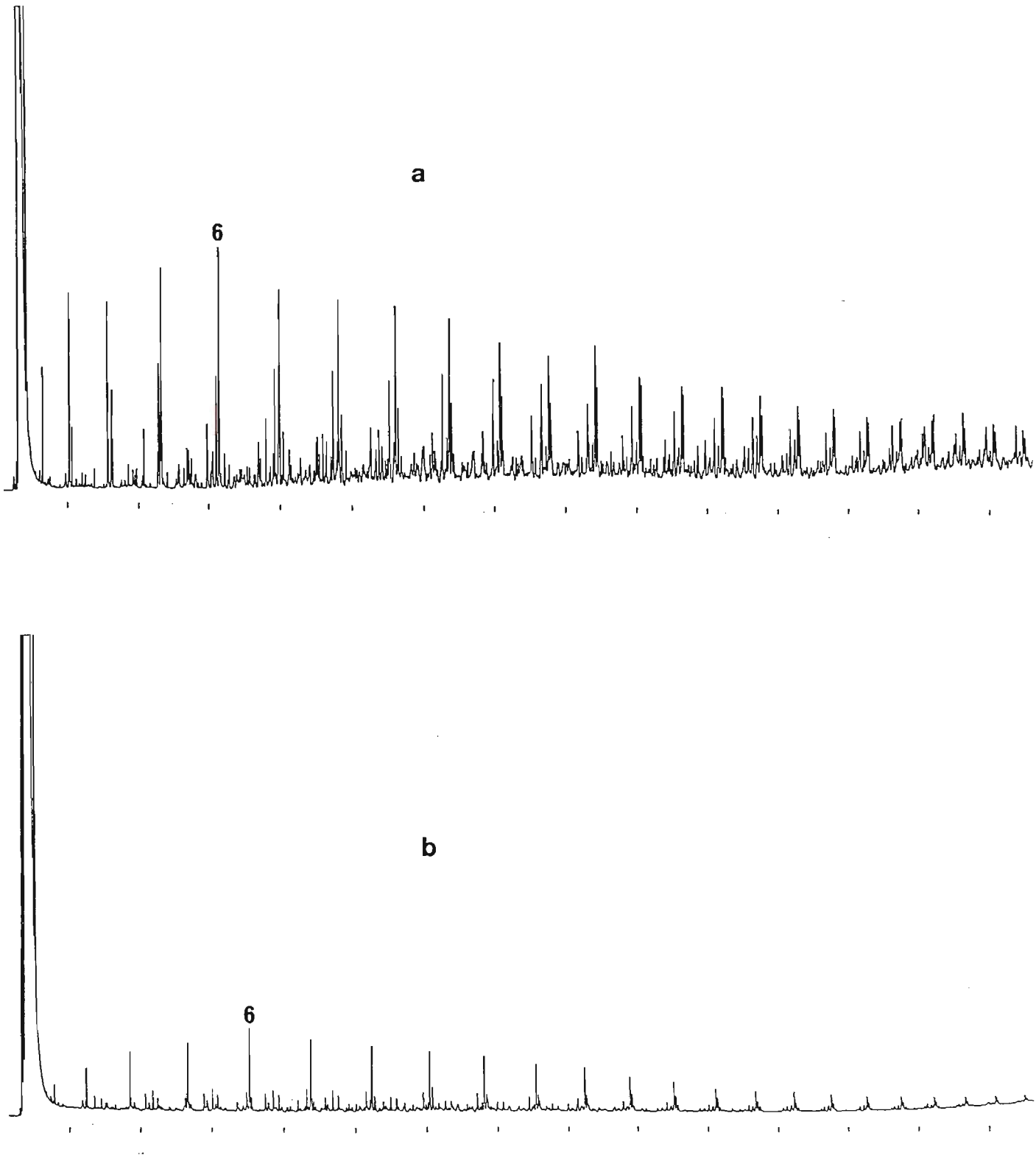

Figure 4-48.
Gas chromatogram of fraction 5 from the open column chromatography of neutral oil from Duaringa 5391-C (**a**) and 686 (**b**). Major components are alkylbenzenes which have an alkyl chain length as indicated (e.g. 1-phenylhexane is denoted by **6**).

feature of aromatics with alkyl chains of more than three carbon atoms are intense rearrangement ions at even masses again due to cleavage ß to the ring (Burlingame and Schnoes, 1969). For the above series these occur at m/z values 106, 120 and 134 respectively, with intensities generally similar to, but less than, those corresponding to respective ions at 105, 119 and 133 (cf. Figure 4-50 spectra 1 and 2). Mass spectra of monoaromatics in Green River shale have been discussed by Gallegos (1973) and a comprehensive review on the mass spectra of alkylbenzenes has been compiled by Grubb and Meyerson (1963).

Detailed GC-MS analysis of 5391-C enabled at least six series of homologous alkyl-substituted monoaromatics to be identified (Figure 4-49) on the basis of molecular weight information (all of the monoaromatics had molecular ions at masses defined by C_nH_{2n-6}) and diagnostic fragment-ions as described above (Figure 4-50).

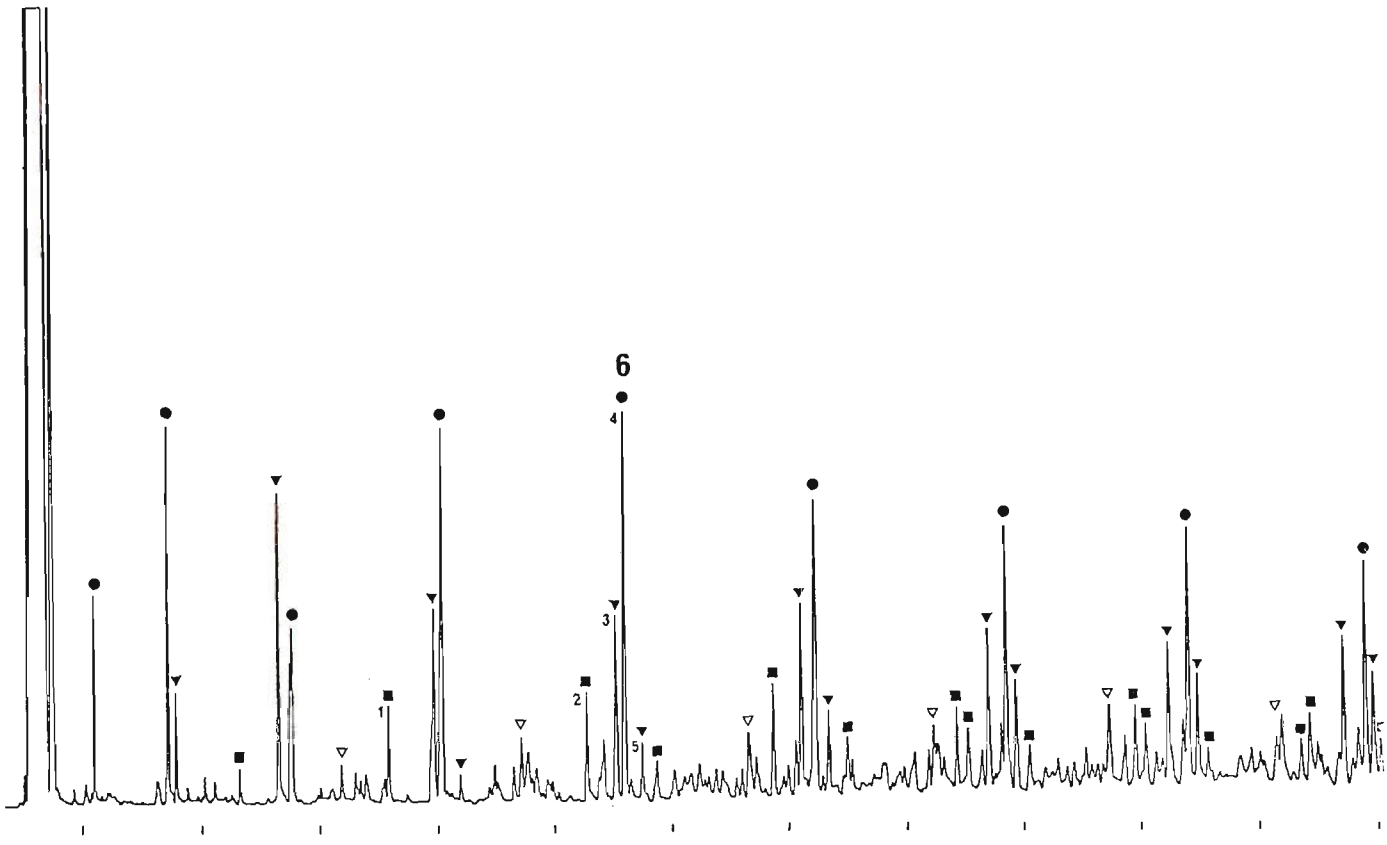

Figure 4-49. Expanded section of the gas-chromatogram (Figure 4-48) for fraction 5 of neutral oil from Duaringa 5391-C, showing the position of components of the various homologous series identified from GC-MS data. Respective symbols denote individual components of 1-phenylalkanes (●), toluylalkanes (▼) - 2 isomers, xylylalkanes (■) - up to 3 isomers and alkyltrimethylbenzenes (▽). Alkyl chain length for 1-phenylalkanes as indicated. Mass spectra for peaks 1-5 are given in Figure 4-50.

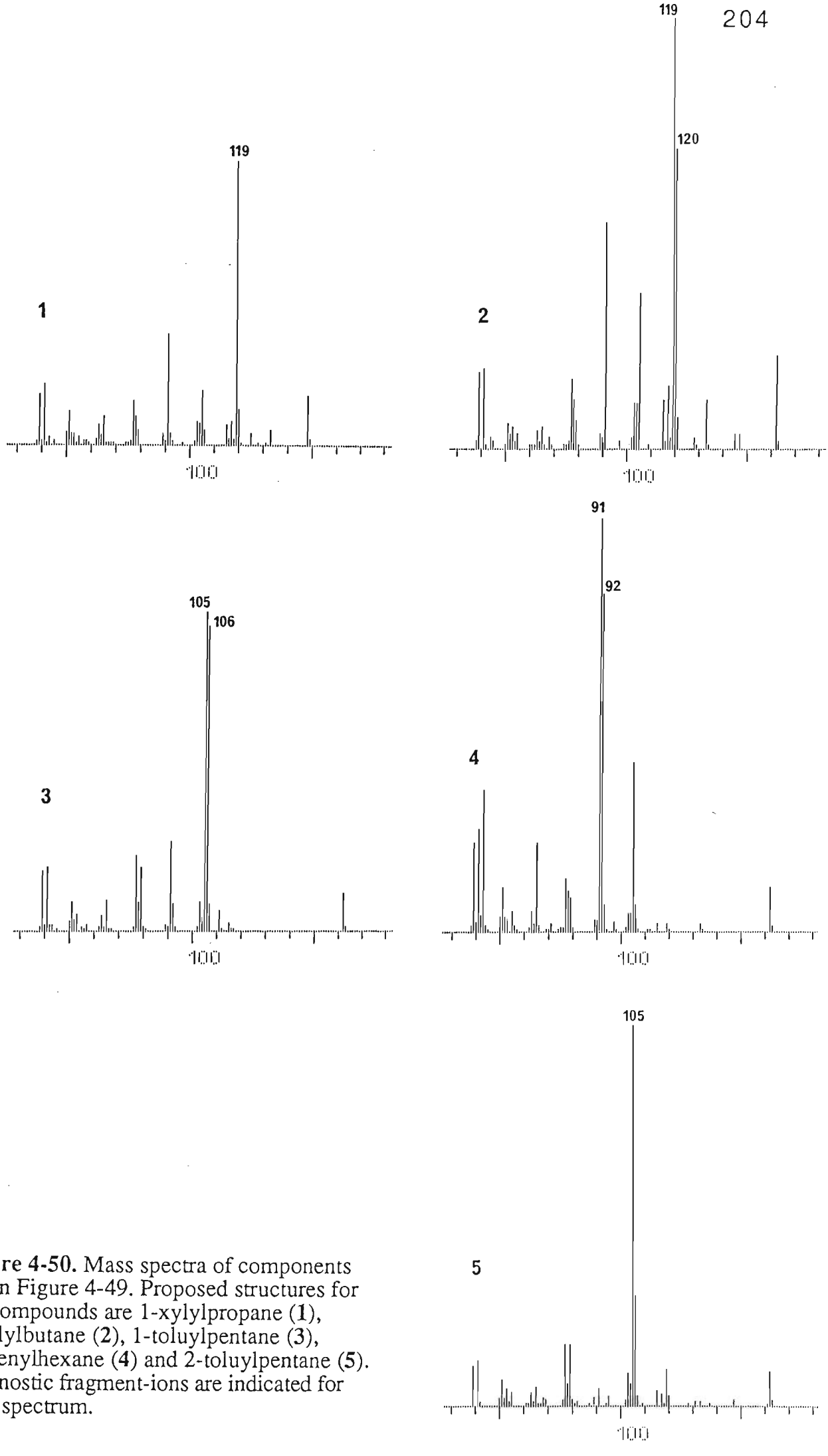

Figure 4-50. Mass spectra of components 1-5 in Figure 4-49. Proposed structures for the compounds are 1-xylylpropane (**1**), 1-xylylbutane (**2**), 1-toluylpentane (**3**), 1-phenylhexane (**4**) and 2-toluylpentane (**5**). Diagnostic fragment-ions are indicated for each spectrum.

The presence (or absence) and range of both lower and higher molecular weight homologues for fraction 5 of each oil was verified by fragment-ion plots diagnostic for each series. Some of the monoaromatic compounds found in fraction 5 of neutral oil from both samples are the same as those previously reported in neutral oil from Condor and Rundle, although Regtop et al. (1982) did not resolve these components in the Rundle oil from alkenes or bicyclic aromatics. A summary of mass spectral and abundance data for components with a molecular weight of 162 daltons detected in fraction 5 of each oil from Duaringa is given in Table 4-31.

Table 4-31. Summary of mass spectral and abundance data obtained from detailed GC-MS analysis of monoaromatic compounds contained in column fraction 5 of neutral oil from Duaringa 5391-C and 686.

Diagnostic Fragment Ion(s)	Molecular Weight	Peak[1] Number	Spectrum[2] Number	Symbol[3]	Compound[4] Class	Abundance relative to 1-Phenylalkane[5] 5391-C	686
91/92	**162**	**4**	**4**	●	1-phenylalkanes(6)	**100**	**100**
105/106	**162**	**3**	**3**	▼	1-toluylalkanes(5)	**51**	**24**
119/120	**162**	**2**	**2**	■	1-xylylalkanes(4)	**31**	**11**
133/134	**162**			▼	1-trimethylbenzene-alkanes(3)	**18**	**10**
91	**162**				3- or 4-phenylalkanes(6)	**nd**	**nd**
105	**162**	**5**	**5**	▼	2-phenylalkanes(6) or 3- or 4-toluylalkanes(5)	**15**	**nd**
119	**148**	**1**	**1**	■	2-toluylalkanes(4) or 3-xylylalkanes(3)	**15**	**nd**
133	**162**				2-xylylalkanes(4) or 3-trimethylbenzene-alkanes(3)	**10**	**nd**

1 Peak number of component in Figure 4-49. **2** Spectrum number of component in Figure 4-50. **3** Symbol denoting the homologous series as depicted in Figure 4-49 and characterised in the profile by respective fragment-ion(s). **4** Compound class proposed on the basis of detailed GC-MS data and respective fragment-ion plots; numbers given in brackets denote the number of carbon atoms in the substituent alkyl chain corresponding to the molecular weight for which the data was obtained. **5** Isomeric abundance relative to 1-phenylalkane concentration (GC peak area). **nd** not detected at the given molecular weight.

The abundances of isomeric alkyl-(polymethyl)-benzenes, given in Table 4-31 relative to 1-phenylalkanes for each oil, are sufficiently different to suggest variations in both the composition of respective source kerogens and the influence of clay minerals, which comprise the inorganic matrix for each shale. The potential for major variations in the organic phase of oil shales to influence the composition of respective shale oils is obvious, while the influence on pyrolysate composition of the inorganic phase has been demonstrated by Regtop et al. (1985). The authors showed that alkanes and alkenes, both of which are by far the most prominent components of typical shale oil (cf. Figure 4-24), are readily converted into aromatic and branched aliphatic compounds through the catalytic action (cracking, isomerisation and aromatisation) of clay minerals.

For the Duaringa oil shales, a role (possibly predominant) for the mineral matrix (montmorillonite) in producing higher concentrations of monoaromatic positional isomers relative to alkylbenzenes (i.e., 1-phenylalkanes) in shale oil from 5391-C may involve production of the former by matrix-catalysed addition reactions between (polymethyl) -substituted benzenes and internal olefin precursors. This proposed mechanism to form (predominantly 2-) monoaromatic alkanes is speculative, but the higher concentrations and relative distributions of the isomeric monoaromatic compounds found in the neutral oil from 5391-C are consistent with the relative variations in the abundances and distributions of internal alkenes observed earlier in fraction 3 of each oil.

It is only possible to observe meaningful consistent and systematic variations in the shale oil produced from different sources if the oils are produced and fractionated under identical experimental conditions. Where these are met, differences observed in the composition of the various well-resolved column fractions may then be attributed to differences in the composition of the oil shale kerogens and / or variations in the influence of the inorganic matrix on the formation of secondary products. Mechanisms, proposed to explain differences which involve the latter, may be tested under conditions which either suppress the formation of one or more of the postulated precursor compounds, or by using oil shale samples which are known to produce only specific precursor isomers. For Duaringa the former could be achieved by retorting the shale from 5391-C in an enclosed environment under hydrous conditions (this should suppress the formation of alkenes),

while the latter could be investigated by detailed examination of fraction 5 of neutral shale oil from the Green River Formation. Ingram et al. (1983) have shown that the FA retort oil from Green River contains no internal olefins and neither of the homologous 1- and 2-phenylalkane series, although several other substituted benzene series ranging from $C_{11}H_{16}$ to $C_{31}H_{56}$ were reported by the authors. These findings suggest that the relatively inert carbonate matrix in Green River shale is unable to catalyse the formation of either internal olefins or the long chain alkyl-substituted monoaromatics referred to above. The pyrolysis of Green River shale pellets, formed by compressing a mixture of finely-crushed shale and catalytically-active clay, should produce a retort-oil composition which reflects the influence of increased catalytic activity of the admixed inorganic phase and establish whether 1-alkenes are involved in the formation of either of the two phenylalkane series.

Where it can (generally) be demonstrated that particular differences in the composition of raw shale oil may be attributed to specific differences in precursor type and abundance, the systematic study of column fractions of neutral oil produced by retorting diverse types of raw shales will increase our understanding of the complexities of retorting processes. In particular it may help in understanding the molecular processes, which occur during pyrolysis of oil shales to produce those (isomeric) compounds not normally found in crude oil (a comprehensive discussion on the principal types of hydrocarbons found in crude oil is given by Tissot and Welte, 1984).

The purity and gas-chromatographic resolution of fraction 5 from each oil allowed accurate retention indices to be obtained over a wide range of carbon numbers. These values are tabulated for 1-phenylalkanes (Table 4-32) along with the corresponding index equation derived from least-squares analysis of the retention data. Retention indices for other monoaromatic components are listed only for identified compounds with a molecular weight of 162 daltons (peaks 2, 3 and 5 in Figure 4-49). Although the relative retention differences between these values and those for the 1-phenylalkane series vary for other molecular weight groupings, they may be used to provide a guide to the relative elution order and position for both lower and higher molecular-weight homologues.

Table 4-32. Modified Kovats retention indices (RI) calculated for 1-phenylalkanes and components corresponding to peaks 2, 3 and 5 (Figure 4-49) identified in column fraction 5 isolated from Duaringa 5391-C and 686 neutral shale oil.

CARBON NO.[1]	RI[2]		CARBON NO.[1]	RI[2]
4	951.49		8	1362.78
5	1055.10		9	1466.22
6	1136.48	(2)	10	1570.32
6	1151.89	(3)	11	1674.35
6	1156.60	(4)	12	1778.60
6	1159.75	(5)	13	1882.93
7	1258.93			

RI Equation (1-phenylalkanes): **RI = 103.478 (carbon no.[1]) + 536.172**

Correlation coefficient = 1.00.

The index equation was obtained by least-squares analysis and extrapolation of the retention data tabulated above. It covers the carbon-number range 4-26 in the chain length of the alkyl substituents.

1 Number of carbon atoms in the alkyl substituent chain. 2 Modified Kovats retention indices were calculated using equation (1).

Fractions 6-13 (315-1100 mL: di- and polyaromatics).

The sequential column-eluates 6-9 may be classified collectively as the "diaromatic" fraction of the neutral shale oil since individual fractions from both oils contain abundant quantities of naphthalene and its alkyl-substituted forms (mainly methylnaphthalenes), although polymethyl-substituted benzenes are also prominent in fractions 6-8 in each case. Except for fraction 6, the respective gas-chromatographic profiles for each oil are qualitatively the same, with only relatively minor differences evident in the concentrations of some of the prominent components. Column fraction 6 from 686 (Figure 4-51) is differentiated from that of 5391-C (Figure 4-52) by the presence of a homologous series of alkyl-substituted benzenes. Mass spectra for individual components of the latter contain prominent parent peaks at masses defined by C_nH_{2n-6} and diagnostic fragment-ions at mass values m/z=105. The homologous series has retention characteristics which are consistent with a structural assignment of branched 2-phenylalkanes for each of the individual

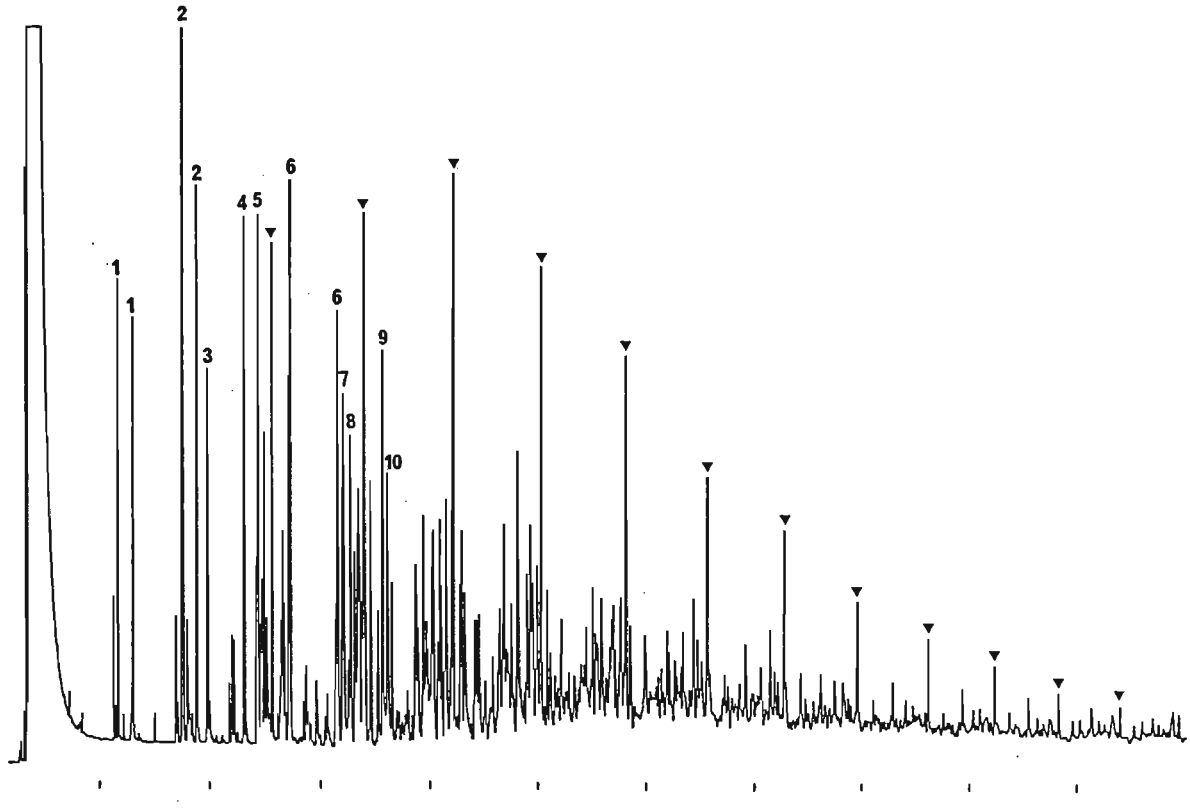

Figure 4-51.
Gas chromatogram for column-fraction 6 of neutral shale oil from Duaringa 686. The identities of numbered components are listed in Table 4-33. Peaks denoted ▼ are members of a homologous series of alkyl-substituted benzenes, probably branched 2-phenylalkanes.

members. Detailed GC-MS analysis of fractions 6-9 identified xylenes, tri- and tetramethylbenzenes, indan, mono- di- and trimethylindans, methylnaphthalenes and C4-tetrahydronaphthalene as the most abundant components in the respective fractions (Table 4-33). Alkylnaphthalenes in the shale oil may be derived from the dehydrogenation of cyclic sesquiterpenes (Streibl and Herout, 1969). Less abundant compounds comprised primarily isomeric alkyl-substituted components of the parent compounds listed above, in particular C5- and C6-benzenes, C1 to C3-tetrahydro- naphthalenes, traces of C3- and C4-thiophenes and a homologous series of 2- and 1-alkylnaphthalenes. The fractions also contained homologous series of alkyl-substituted thiophenes (fractions 6 and 7) and alkenylbenzenes (fraction 7), both present at trace concentrations. The former series is characterised by a prominent fragment-ion at mass m/z=111, while the latter series elutes prior to the more prominent series of 2- and 1-alkylnaphthalenes and has a diagnostic

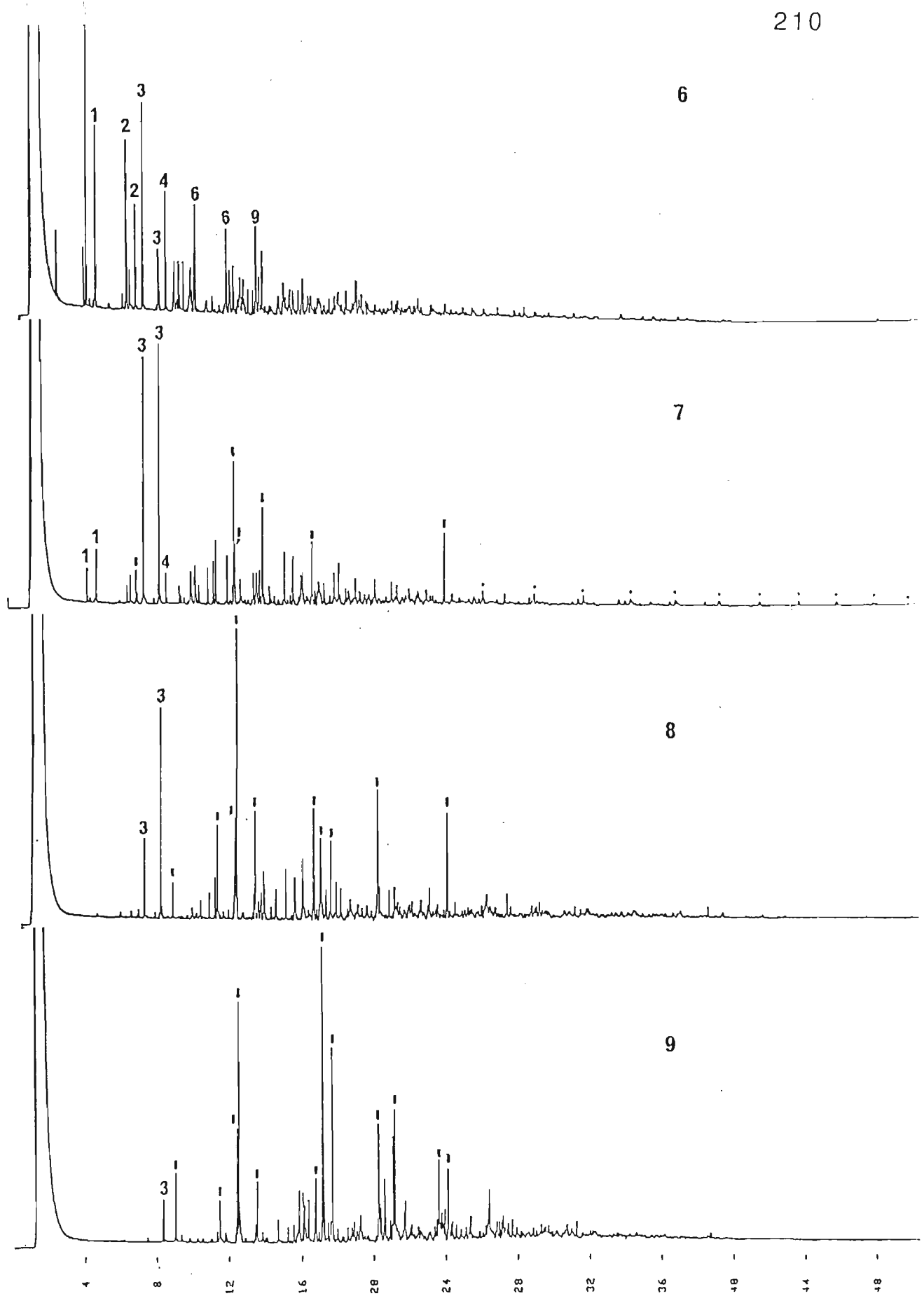

Figure 4-52. Gas-chromatograms of column fractions 6-9 for neutral shale oil from Duaringa 5391-C. Numbered peaks as in Figure 4-51 for 686 and Table 4-33 (bold peak numbers). Peaks marked • in **7** denote members of a homologous series of 2- and 1-alkylnaphthalenes (see also Figure 4-54). The identities of other peaks, denoted ı in each profile are listed in the order of their elution against compounds given in Table 4-33.

Table 4-33. Numbered and marked components identified by GC-MS in column-fraction 6 of neutral shale oil from Duaringa 686 (Figure 4-51) and fractions 6-9 from 5391-C (Figure 4-52). Peaks denoted ı in each profile are listed against their compound name under respective fraction headings in the order of their elution.

		FRACTION			
Pk. No.	**COMPOUND NAME**	**6**	**7**	**8**	**9**
1	xylene	1			
2	methyl-ethylbenzene	2			
3	trimethylbenzene	3			
4	indan	4			
5	C4-benzene	5			
6	methylindan	6			
7	C5-benzene	7			
8	C4-toluene	8			
9	dimethylindan	9			
10	ethylindan	10			
11	methylethylbenzene		1		
12	trimethylthiophene		1		
13	indene			1	1
14	tetramethylbenzene			2	2
15	methylindan		2		
16	1-methyl-1H-indene			3	3
17	tetramethylbenzene		3	4	4
18	naphthalene			5	5
19	C5-benzene & dimethylindan		4		
20	dimethylindan		5	6	6
21	2-methylnaphthalene			7	7
22	1-methylnaphthalene			8	8
23	ethylnaphthalene & trimethylindan			9	9
24	tetrahydronaphthalene				10
25	C3-naphthalene				11
26	C4-tetrahydronaphthalene		6	10	12
27	C3-naphthalenes				

fragment-ion at mass m/z=104 as its base peak (Figure 4-54, 390-410 mL). A comparison between the gravimetric data for the two oils showed that individual fractions 6-9 constitute an almost equal percentage of the total mass of neutral oil recovered from the open column in each case.

The gas-chromatographic profiles of the polycyclic aromatic hydrocarbons (PAH), corresponding to fractions 10-12 of the neutral oils are given for 5391-C in Figure 4-53. The sequence of chromatograms shows a progression of complexity in the profiles

due to the large number of (alkyl-substituted) structural isomers that are possible as the number of aromatic rings increases. The compounds in fraction 13 were not volatile enough to elute from the capillary column.

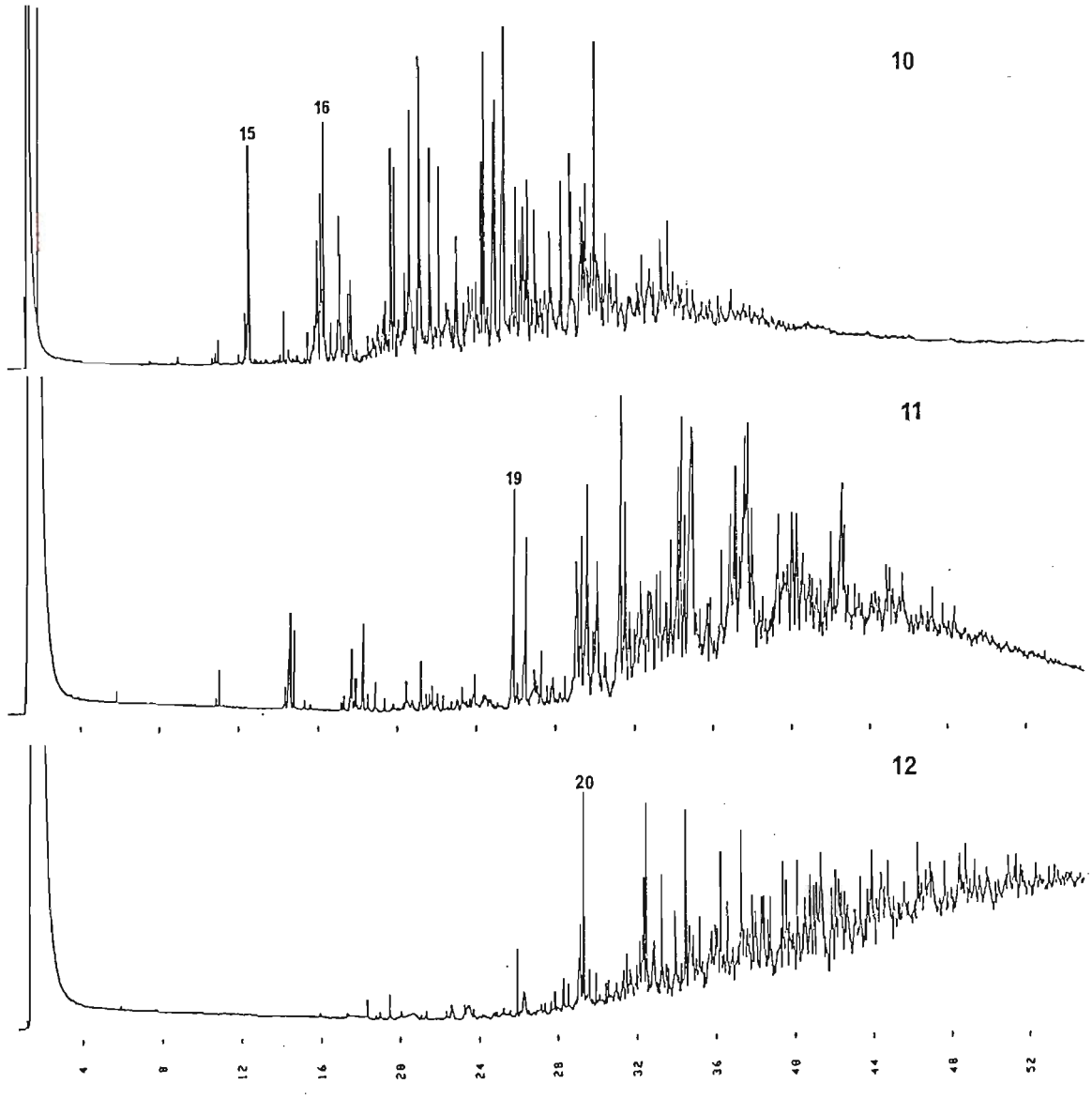

Figure 4-53. Gas-chromatograms of column fractions 10-12 for neutral shale oil from Duaringa 5391-C. Numbered peaks as in Figure 4-55 (15,16) and Table 4-34 (19,20). For more detailed chromatographic information see profiles corresponding to column sub -fractions i.e., volumes 700-840 mL (Figures 4-55, 4-56).

GC-MS analysis of the polyaromatic fractions detected indenes, fulvenes, biphenyls, acenapthene, fluorenes, phenanthrenes, indanones, pyrenes or fluoranthenes and several unidentified components (Table 4-34). Most of the PAH exhibit diagnostic mass spectra which show very little fragmentation and have the molecular ion as base peak . This is due to the high ionisation potentials of these molecules, which results from the stability conferred on them by the fused aromatic-ring systems. This feature allows PAH and their alkyl-substituted derivatives to be characterised according to ring number from appropriate molecular weight profiles derived from mass-spectral information. For the two oils these procedures showed that parent compounds with multiple alkyl substituents were (usually) more abundant than those with only single alkyl chains of increasing length. This distribution becomes obscured for PAH with increasing ring number since structural isomerism of the ring system influences the underlying alkyl-substitution patterns. However, where the pattern was observed, the greater concentration of polyalkyl PAH substituted by short alkyl chains may reflect the relatively greater abundance of these small, thermally more stable alkyl radicals formed during the retorting process. Most of the aromatic compounds described above have been detected in Condor shale oil. Regtop (1983) used a different open-column method which did not resolve the PAH as well as the current procedure but also reported 3-5 ring PAH and their partially hydrogenated derivatives in the polyaromatic fraction of shale oil from Rundle.

It is generally accepted that the hydrogen produced during retorting is derived from (mineral-catalysed) dehydrogenation reactions. This progressive aromatisation of the organic phase produces a kerogen which becomes enriched in fused aromatic-ring structures as the temperature increases. The hydrogen generated during this phase of retorting may participate in secondary reactions (e.g., hydrogen-capping of alkyl radicals) or escape from the retort as gas. Gravimetric data for fractions 10-13 show a difference of ca. 30% between the relative masses of fractions 11 and 12 for the respective neutral oils. The relatively higher concentration of polyaromatics in these fractions of neutral oil from 5391-C are consistent with the greater abundance of hydrogen previously found in the total pyrolysate of raw shale from that sample (cf. 4.6). The comparatively lower abundance of PAH in the oil from 686 may be due to differences in the parent kerogen (possibly

lower lignitic contributions derived from allochthonous terrestrial input), or to the reduced activity of the mineral matrix functioning as a catalyst in promoting aromatisation reactions. The latter is consistent with, and adds further support to, arguments previously advanced to explain differences in the composition of those earlier fractions known to be largely dependent on mineral matrix effects.

Although most components in the diaromatic fractions 6-9 are well resolved it is difficult to characterise these column eluates using gas-chromatography alone. This is because there are no homologous series of components to serve as reference peaks in the chromatographic profiles. Fractions 10-12 are substantially more complex, primarily due to the presence of a large number of poorly resolved PAH structural isomers, formed during the retorting process. An appreciation of the potential problems encountered in the identification of components in these fractions can be gained by considering the number of possible isomers ranging from three to five cata-condensed rings. Although there are only two possible stuctures for the three-ring PAH this number increases to 12 possible structures for the five-ring compounds; adding only a single methyl group to the respective PAH results in an increase to 8 and 117 isomers respectively (the isomeric possibilities for polysubstituted PAH are enormous).

As a consequence of this complexity the retention indices of marker compounds (prominent) in each profile are very important, since they serve to relate those of other components in the chromatogram to either Kovats or Lee retention indices, many of which are available from the literature (Futoma et al., 1981; Rostad and Pereira, 1986) or from commercial sources in both hard-copy or data-base form (Sadtler Research Laboratories, Division of Bio-Rad Laboratories, Inc.). They are particularly important to detect and confirm (GC-MS) the presence of certain isomers e.g., benz(a)anthracene, benzo(c)-phenanthrene and chrysene, all of which are known carcinogens among the five possible structural isomers for the four-ring PAH with molecular weight 228 (Lee and Wright 1980). Lee indices of compounds are derived (in a way analogous to that used for the determination of Kovats retention indices) from retention times relative to those of selected marker PAH, with ring number n and n+1, which bracket the components of interest. The marker compounds chosen are naphthalene (n=2), phenanthrene (n=3), chrysene (n=4)

and picene (n=5), which have respective Lee retention indices of 200, 300, 400 and 500 assigned to them (Lee et al., 1979).

In order to resolve as many of the di- and polyaromatic constituents as possible the open-column neutral oil fractions for the reference FA retort oil from 5391-C were collected as sequential aliquots of ca. 20mL each. Each of these sub-fractions was analysed using both GC (Figure 4-54 - 4-56) and GC-MS. The latter was carried out on a restricted number of pooled or individual column eluents comprising resolved (major) components previously observed in the GC-profiles. The detailed mass-spectrometric analysis of this reduced number of samples provided definitive (clean) mass spectra and accurate relative retention data for a very large number of components. It is not within the scope of the present study to publish all of this data, however the work has established a comprehensive data-base, which should make comparative studies on these classes of compounds, derived from a variety of sources, substantially easier in the future. Rovere (1986) has developed an inexpensive low-pressure LC procedure for the isolation of PAH from shale oil which broadly separates these components according to aromatic ring number. He used sieved alumina (neutral, activity 1) of narrow-range particle size and mixtures of Freon 113 and benzene as sequential eluents to attain improved resolution of these compounds.

Polycyclic aromatic hydrocarbons have been isolated from many diverse sources and are invariably present in crude oils, coal tars and synthetic fuels derived from coal and oil shales (Romanowski et al., 1983; Novotny et al., 1984). Efficient procedures are needed to determine their concentrations and identities in synfuels since their presence influences the utilisation of these refinery feed-stocks and is of major environmental concern, particularly if these components are isolated for disposal. It is in this context that the collection of a great number of open-column fractions, such as those obtained for the FA reference oil may be advisable since it provides clean and well-resolved sub-fractions, which may subsequently be analysed (pooled or separately) using one of the many techniques developed for the isolation and analysis of PAH from complex mixtures (Novotny et al., 1974; Lee et al., 1976 **a**; Lee et al., 1976 **b**; Schultz et al., 1979; Lee and Wright, 1980; Romanowski et al., 1983; Novotny et al., 1984; Wood et al., 1984).

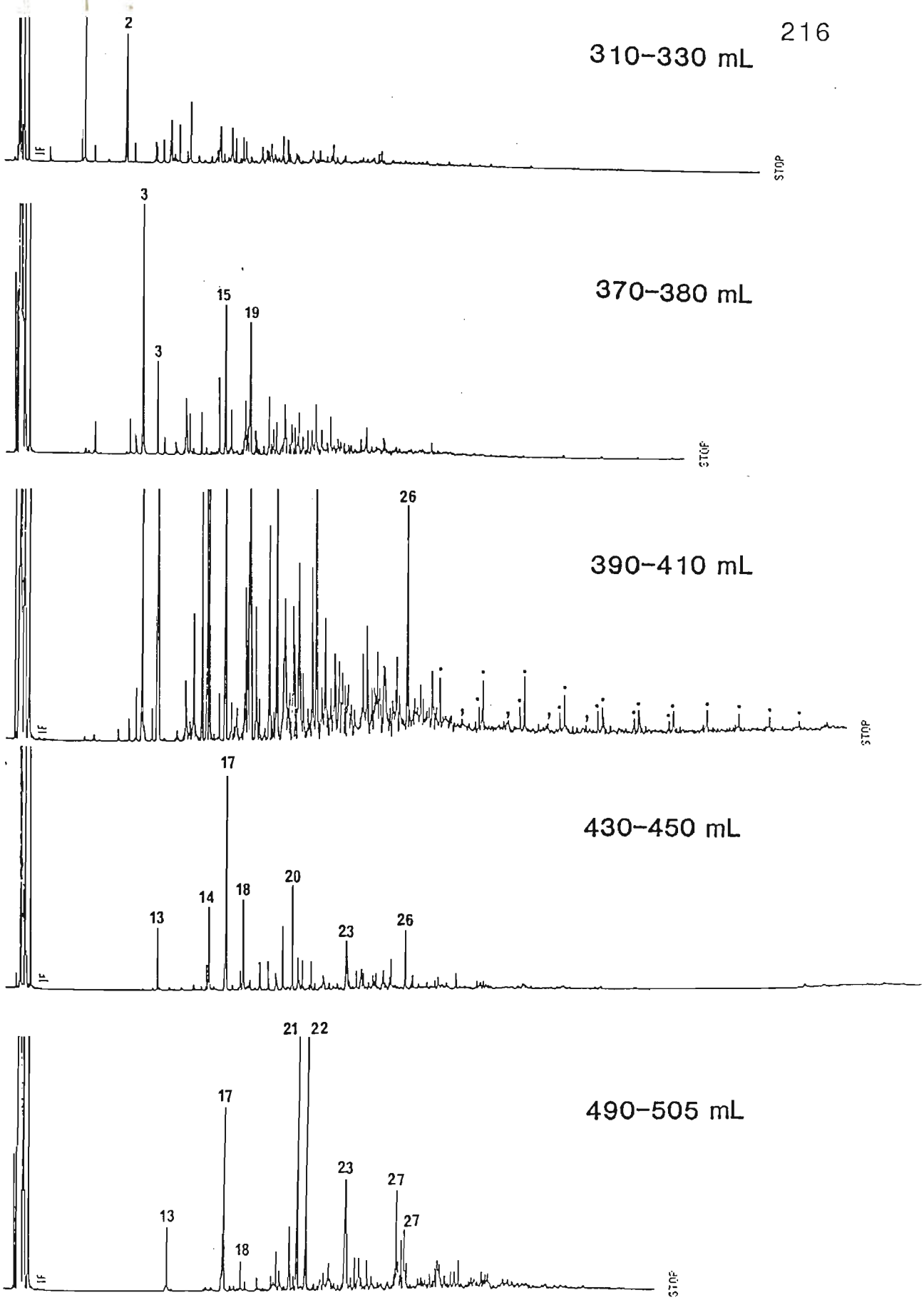

Figure 4-54.
Selected gas-chromatographic profiles of sequential open-column fractions for neutral oil from Duaringa 5391-C. Numbered peaks refer to peak numbers in Table 4-33. The trace for column eluent 390-410 mL was re-plotted at high sensitivity to enhance peaks corresponding to the homologous series of 2- and 1-alkylnaphthalenes (■) and alkenylbenzenes (❜). Continued .....

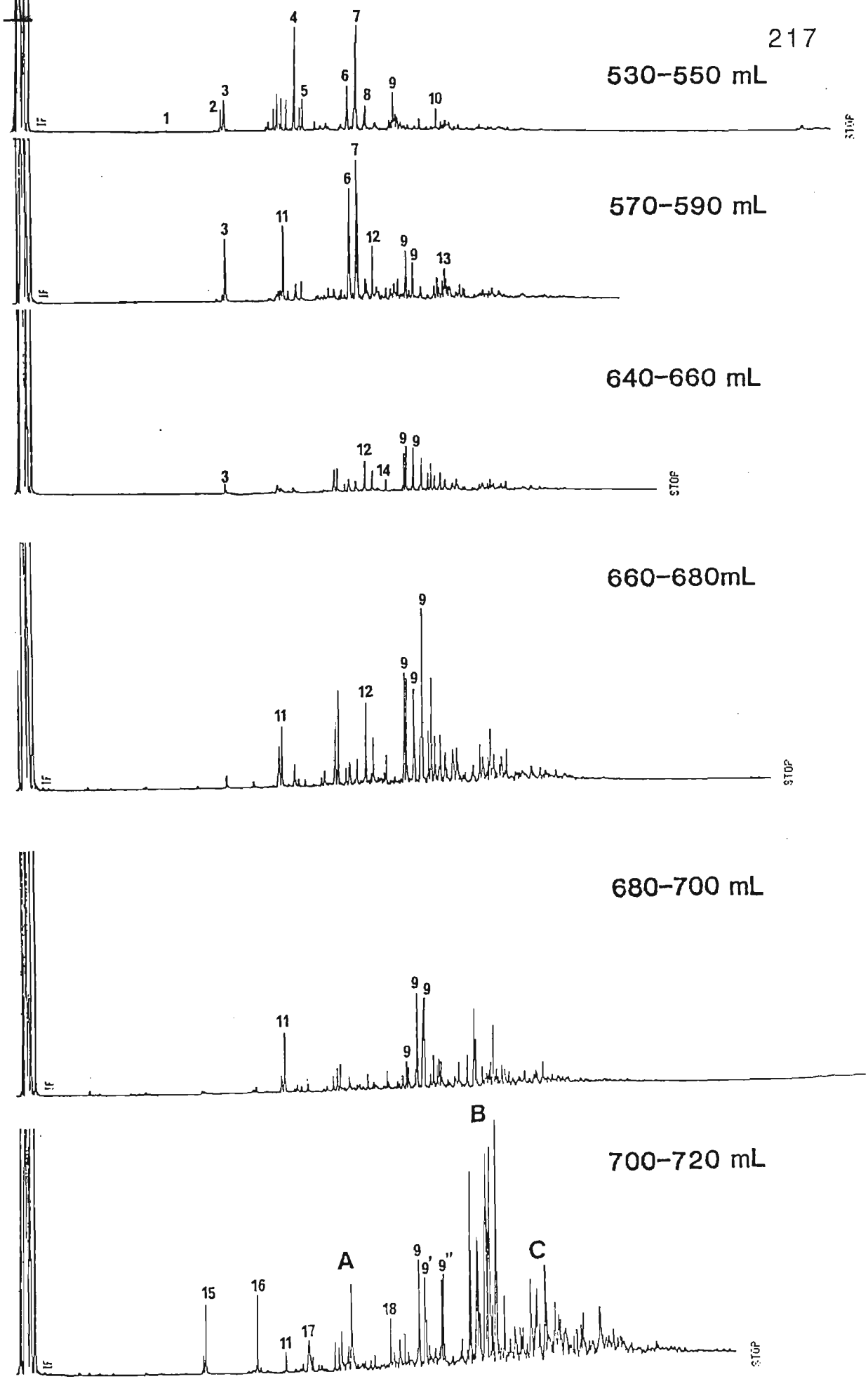

Figure 4-55.
Selected gas-chromatograms of sequential open-column fractions for neutral oil from Duaringa 5391-C. Numbered peaks and regions denoted by letters refer to Table 4-34. Continued ...

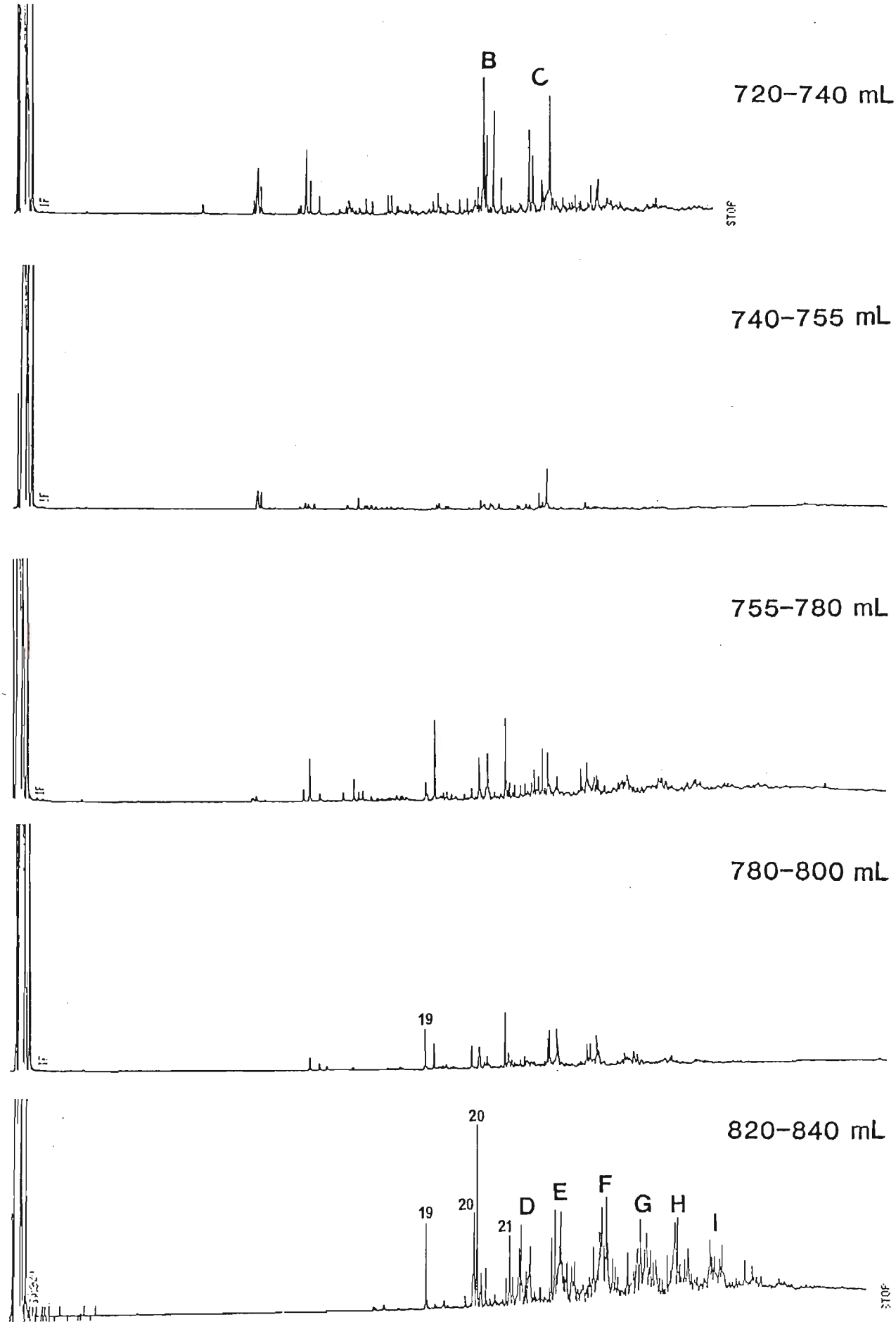

Figure 4-56.
Selected gas-chromatograms of sequential open-column fractions for neutral oil from Duaringa 5391-C. Numbered peaks and regions denoted by letters refer to peak numbers in Table 4-34. For gas chromatograms of higher column volumes refer to profiles in later figures.

Table 4-34. List of components identified by GC-MS in open-column volumes 530-840 mL of neutral shale oil from Duaringa 5391-C.

Pk. No.	COMPOUND NAME	Pk. No.	COMPOUND NAME
1	indene	16	dimethylbenzofuran
2	1-methyl-1H-indene	17	trimethylindan
3	methylindene	18	methylbiphenyl
4	2-methylnaphthalene	19	fluorene
5	1-methylnaphthalene	20	methylfluorene
6	dimethylnaphthalene	21	phenanthrene
7	dimethylnaphthalenes	22	pyrene or fluoranthene
8	dimethylnaphthalenes		
9	trimethylnaphthalenes	A	includes tri- and tetramethylindanones
9	trimethylnaphthalene & fluorene	B	M. Wt. 184 region
9	trimethylnaphthalene & methylphenylfulvene	C	M. Wt. 198 region
		D	dimethylfluorenes
10	methylbiphenyl	E	methylphenanthrenes*
11	methyldihydronaphthalene	F	trimethylphenanthrenes*
12	ethylnaphthalene	G	C4-phenanthrenes*
13	ethylnaphthalenes	H	C5-phenanthrenes*
14	acenapthene	I	C6-phenanthrenes*
15	phenylpropanal		

* proposed major components in the regions indicated in the gas chromatograms (may also be anthracenes).

Fraction 14 (1100-1350 mL: nitriles).

The gas chromatograms of fraction 14 from each oil are dominated by linear aliphatic nitriles which range in carbon number from C_6 to at least C_{32} (Figure 4-57). The profile for 5391-C shows a trimodal distribution with relative maxima in the regions C_6 - C_{10}, C_{18} - C_{22} and at C_{28}, which collectively indicate precursors derived from both algal and higher-plant sources. The pronounced even/odd carbon number preference (CPI = 0.44) covering the C_{24} - C_{30} region of the profile is similar to values reported for shale oil from Rundle B, Nagoorin and Stuart North by Evans et al. (1985) and indicates a pyrolysis mechanism which maintains the biological bias for compounds with even carbon numbers (e.g., fatty-acid biosynthesis). The smooth distribution covering the region C_6 - C_{15} is probably due to nitrile formation involving precursors previously cracked during pyrolysis.

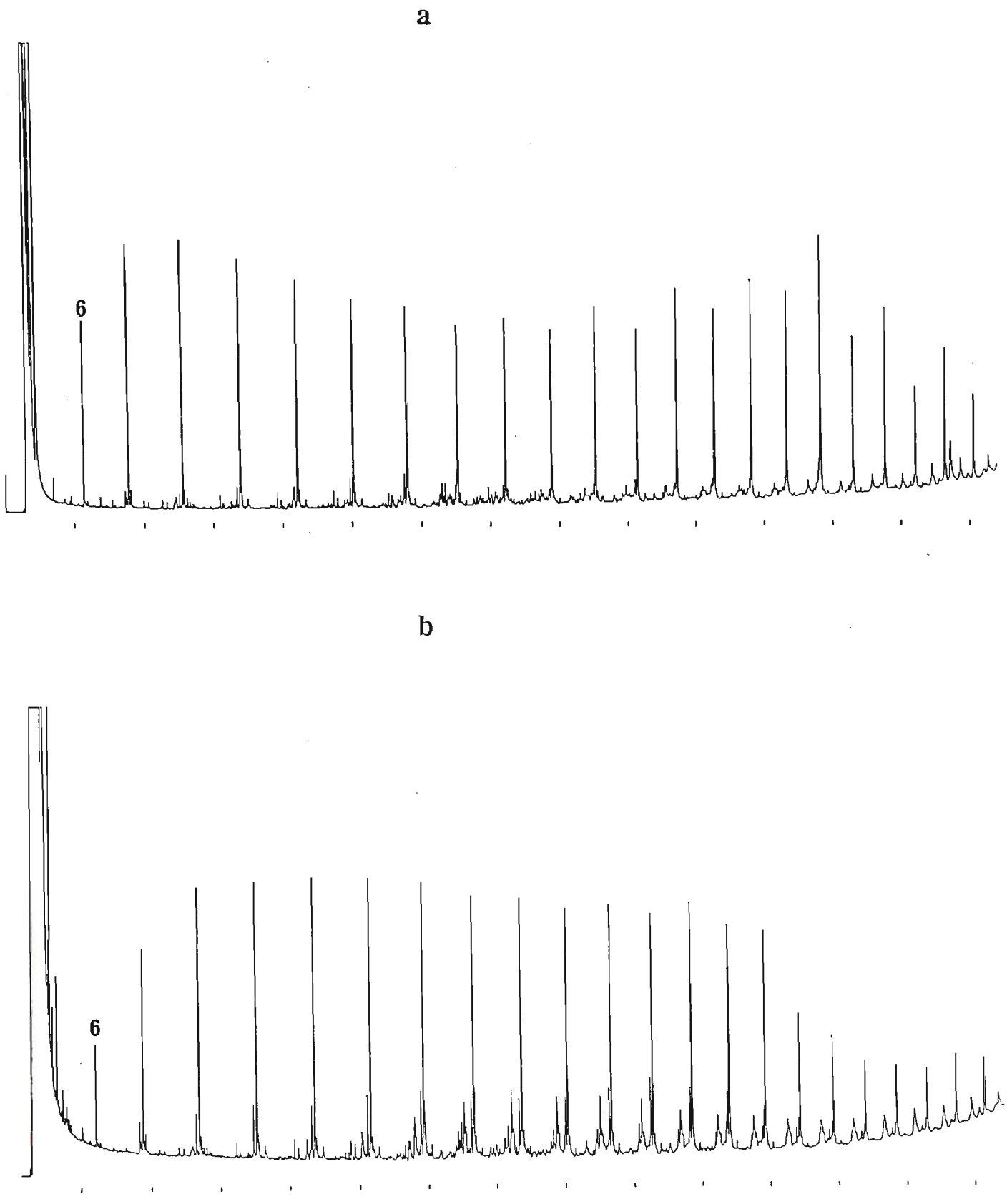

Figure 4-57.
Part of the gas chromatograms (C_6 - C_{30}) for open-column fraction 14 of neutral shale oil from Duaringa 5391-C (a) and 686 (b). Major components comprise a homologous series of alkanonitriles with carbon numbers as indicated. For quantification both series were analysed up to the C_{32} -nitrile.

The distribution of alkanonitriles in fraction 14 from Duaringa 686 is bimodal and exhibits a smooth envelope of these components over a wide range of carbon numbers (C_6 - C_{20}) and a localised maximum at C_{28}. A higher CPI value of 0.59 for this fraction is less pronounced in favour of even carbon numbers, but still strongly indicative of a bias for specific biological precursors.

The gravimetric data for 5391-C and 686 show that the two fractions constitute respectively 10.3 and 8.45 % by mass of the raw oils. The total peak area obtained by gas chromatography for fraction 14 from each oil was compared with that obtained for fraction 1 (comprising only linear and branched alkanes), after the total areas for the different fractions had been adjusted for variations in solute concentrations.The relatively large differences found in the areas between the nitrile and hydrocarbon peaks for each oil were heavily in favour of the alkane components (based on equal solute masses) and indicated clearly that the linear nitriles comprise only a small percentage (w/w) of the total mass for each fraction. The actual mass of nitriles in the respective fractions was determined using gas chromatography over the component range C_6 - C_{32} and decane as an internal standard (the choice of a suitable alkane standard is restricted by the retention characteristics of the nitrile series - Table 4-36). Since nitriles have a lower FID response than the same concentration of hydrocarbons (w/w), a weight-response factor of 0.9 was used to compensate for this difference in the relative sensitivity of the FID. This response factor was used for all of the alkanonitriles (total area divided by 0.9) and slightly overestimates the nitrile content. This follows because their distribution for both oils is biased towards the medium to high molecular weight region of the chromatogram and their relative weight-response (FID) gets progressively closer to that of a saturated hydrocarbon (unity) as the length of the nitrile carbon chain increases (the relative response for butyronitrile was found to be 0.88 - average of 5 determinations).

For 5391-C the linear nitriles comprise ca. 83 % of the total gas-chromatographic peak area, with nitrogen constituting 4.7% by mass of this value. The latter was obtained from integrator peak areas of individual alkanonitriles, which enables a value for the nitrogen mass to be calculated for each of these molecules. Summing these values yields a

total nitrogen content for all of the alkanonitriles over the range C_6 - C_{32}, which may then be compared with the nitrogen content of the original raw oil. Mass-spectral data suggest that the remaining 17% of the total peak area for each oil also comprises nitriles, both branched and unsaturated, and justifies its inclusion for the purpose of chromatographic quantification. It is clear from the respective profiles that the range of alkanonitriles extends beyond C_{32} (for the alkanes in fraction 1 it extended up to C_{54}), so an upward adjustment for the total nitrile peak area needs to be made to account for this extended range of molecular weights. An estimate of a 10 % increase in total area due to additional nitriles (relative to that for C_6 - C_{32}) was made for components larger than C_{32}. This estimate is again deliberately high (based on the relative distribution of components over the entire profile) and is designed to keep the actual nitrile abundance close to, but below, the value calculated from integrator peak areas.

Quantitative data for each oil (Table 4-35) show that the nitriles comprise respectively ca. 15 and 10% by mass of each fraction. The balance of the total mass is made up of reddish-brown material which coelutes with the nitriles from the open-column but does not contribute to the gas-chromatographic area (as indicated by a flat baseline for the entire chromatogram). The nitriles constitute ca. 1.5 and 1.0% by mass of the two oils while their nitrogen content represents only ca. 0.1 and 0.07% respectively. The former two values agree well with data reported by Evans et al. (1985) for the concentration of aliphatic nitriles in a range of Australian shale oils, particularly with those for Rundle B (1.27%; w/w). The low values for the nitrogen content indicate that most of it is tied up in non-volatile (polymeric) material in this or later fractions and in structures such as nitrogen heterocycles, pigments (e.g., porphyrins) and artefacts; further (small) quantities of nitrogen are accounted for in asphaltenes and in the basic fraction (e.g., pyridines).

Retention data were obtained for the well-resolved fraction 14 from 5391-C and used to determine modified Kovat's retention indices and a retention-index equation for the alkanonitrile components (Table 4-36, Figure 4-58); the former agree well with those data published for a restricted number of analytical standards by Rostad and Pereira (1986).

Table 4-35. Quantitative data (gravimetric and chromatographic) for nitriles isolated in open-column fraction 14 of neutral shale oil from Duaringa 5391-C and 686.

QUANTITATIVE DATA	SAMPLE 5391-C	686
Mass (mg) - fraction 14.	103	84.5
Mass (mg) of volatile nitriles (C_6 - C_{32+}) in fraction 14.[1]	15	10
% volatile nitriles (C_6 - C_{32+}) in fraction 14 (w/w).	ca. 15	ca. 12
% volatile nitriles (C_6 - C_{32+}) in raw oil (w/w).	ca. 1.5	ca. 1.0
% nitrogen (raw oil) derived from volatile nitriles (C_6 - C_{32+}) in fraction 14 (w/w).[2]	ca. 0.1	ca. 0.07
CPI[3]	0.44	0.59

1 based on peak area data relative to IS - decane. **2** based on the nitrogen content of individual alkanonitrile (calculated from the mass equivalent for each homologue in the gas chromatogram).

3 **CPI** = $$\frac{2(C_{29} + C_{27} + C_{25})}{C_{30} + 2(C_{28} + C_{26}) + C_{24}}$$

Nitrogen-containing compounds produced in shale oils during retorting represent a potential problem in the utilisation of these synfuels as refinery feedstocks. The work on Duaringa has shown that only a small fraction of these compounds, which need to be removed from feedstock crudes to avoid poisining refinery catalysts, are present as nitriles. Despite the potential for these compounds to cause problems in upgrading and refining processes, surprisingly little quantitative data is available in the literature. Batts et al., (1983) have carried out a general study of the principal nitrogen functional groups present in a range of shale oils, while aliphatic nitriles have previously been reported in relatively high concentrations in Rundle (Regtop et al., 1982), Green River (Ingram et

Table 4-36. List of modified Kovat's retention indices (RI) for alkanonitriles isolated in open-column fraction 14 of neutral shale oil from Duaringa 5391-C.

CARBON No.	RI[1]	CARBON No.	RI
6	877.66	18	2108.63
7	980.62	19	2211.54
8	1083.63	20	2315.55
9	1185.61	21	2418.56
10	1287.70	22	2522.34
11	1389.79	23	2624.74
12	1492.20	24	2727.48
13	1594.64	25	2830.30
14	1697.07	26	2933.45
15	1800.27	27	3036.25
16	1900.00	28	3123.78
17	2006.16		

1 Calculated using equation 1.

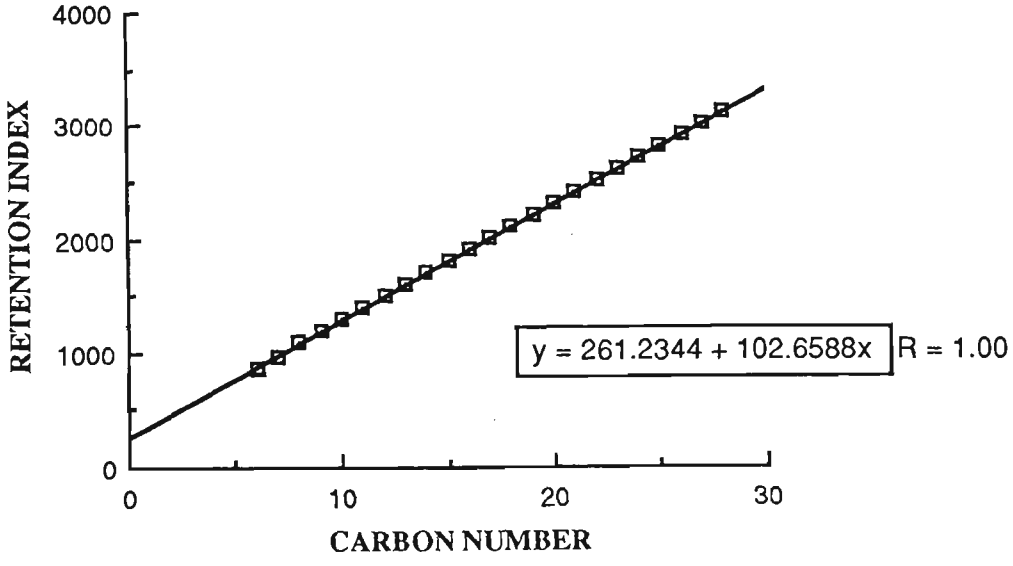

Figure 4-58.
Plot of modified Kovat's retention indices for alkanonitriles isolated in fraction 14 of neutral oil from Duaringa. The retention index equation and correlation coefficient (R) are also given.

al., 1983) and Condor shale oil (Rovere et al., 1983). The results for Duaringa shale oil suggest that the concentrations of nitriles reported for these oils were overestimates.

Regtop and co-workers (1982) have proposed a derivation of alkanonitriles from the dehydration of amides during pyrolysis, but conceded that there may be a number of other potential precursors. Evans et al. (1985) have shown that alkanonitriles are most probably derived from the conversion of fatty acids during retorting. Their proposed mechanism proceeds via the following reaction sequence:

$$\text{R-COOH} + \text{NH}_3 \xrightarrow{-\text{H}_2\text{O}} \text{R-CONH}_2 \xrightarrow{-\text{H}_2\text{O}} \text{R-C}\equiv\text{N}.$$

The ammonia required for the conversion is probably liberated from ammonium ions (e.g. ammonium feldspars such as buddingtonite) in the mineral matrix during pyrolysis, rather than from an organic source. Following the systematic study of a variety of samples retorted in the presence and absence of ammonia they concluded that the production of nitriles during retorting requires the presence of both fatty acids or esters and ammonia.

Fractions 15-16 (1350-1750 mL: ketones).

Open-column fraction 15 isolated from both oils comprises oxygenated compounds (ketones) as the only gas-chromatographable components. The compounds elute late in the eluotropic solvent sequence because of their relatively high affinity (polarity) for the chromatographic adsorbents. The column eluate from both oils is "clear" (as collected) and comprises linear 2-, 3-, 4- and 5-alkanones listed in the order of decreasing abundance (Figure 4-59). The distribution of the 2-alkanones varies substantially between the two oils, with that for 5391-C heavily biased towards the high molecular weight region of the chromatogram and ranging in carbon number from C_{17} to at least C_{31}. The distribution of individual components shows three relative maxima at C_{19}, C_{23} and C_{29} respectively with a pronounced odd number CPI. The distribution for the 3-alkanones is smooth and restricted to a narrower range; the chromatographically resolved

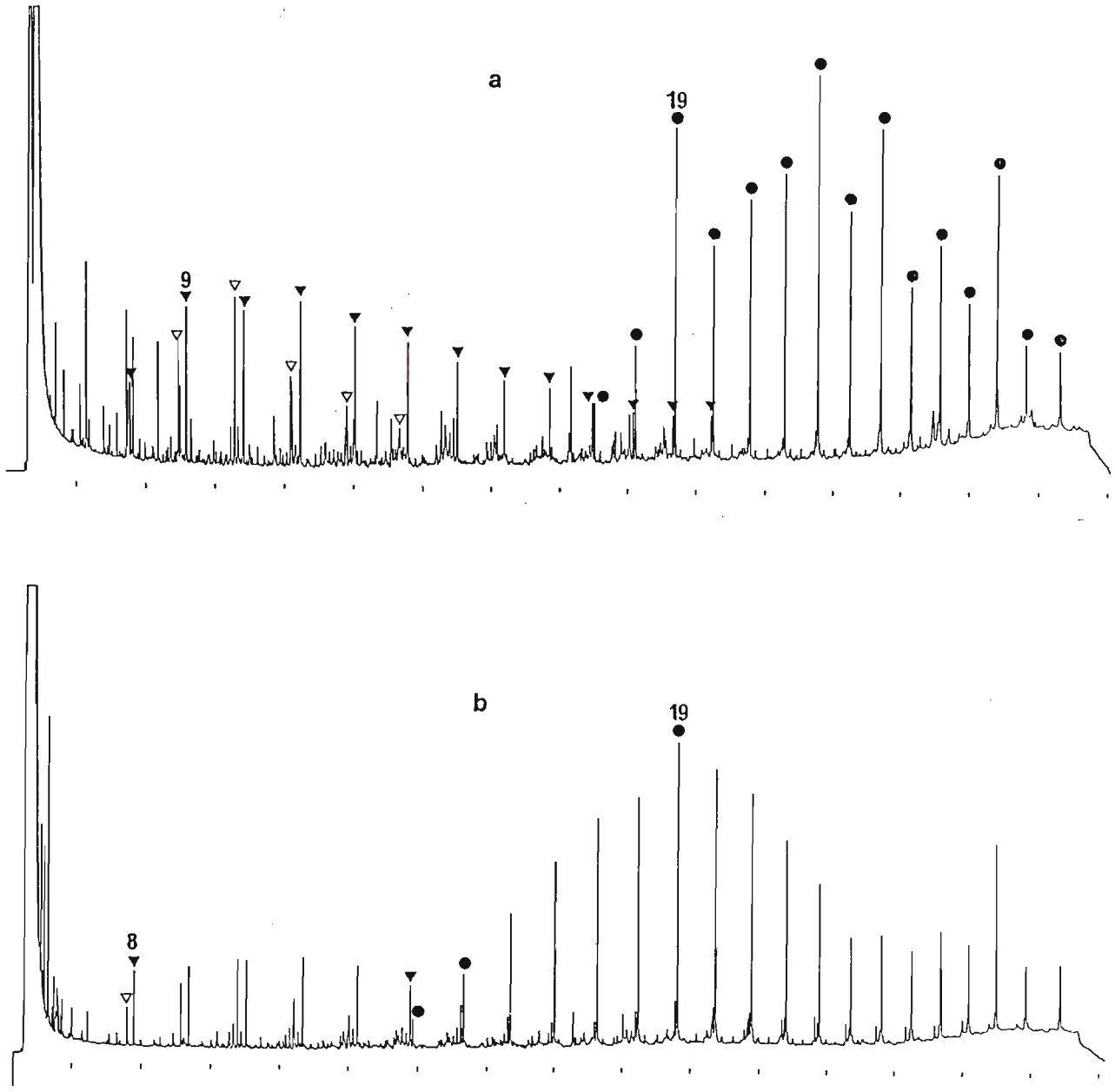

Figure 4-59.
Gas chromatograms for open-column fraction 15 of neutral shale oil from Duaringa 5391-C (**a**) and 686 (**b**). Major components (●) comprise a homologous series of 2-alkanones with carbon numbers as indicated. Other symbols denote a series of 3-alkanones (▼) and 4- and 5-alkanones (▽), which coelute in the region C_{10}- C_{14}. Peaks for profile **b** correspond with those for **a** and only key components are indicated.

constituents range from C_7 to at least C_{20} in the profile although higher homologues, up to C_{27}, were inferred to be present from a plot of mass-spectral fragment ions diagnostic for this series (m/z = M^+ - 29 and 72).

The gas chromatogram for 686 exhibits a bimodal distribution for the 2-alkanones, characterised by a smooth and extensive envelope of components over the range C_{14} - C_{24} and a more localised maximum at C_{29}. The CPI for this series is less pronounced than that for 5391-C, but still shows a clear bias towards odd carbon number compounds over the same region of the chromatogram. The relative distribution of 3-alkanones covers a range of molecular weights similar to that for 5391-C, with a predominance of low molecular weight constituents again evident. For both oils 4- and 5-alkanones are present at relatively lower concentrations and are only discernable in the chromatogram over a restricted range of carbon numbers (Figure 4-59). Mass-spectral data obtained for these two series of closely-eluting homologues indicate that the 5-alkanone series appears only at even carbon numbers. However, the interpretation of relevant spectra is complicated by the fact that the two series co-elute over the region where their concentrations are sufficient to produce meaningful data. The various isomeric series of alkanones are readily differentiated by mass spectra of well-resolved individual homologues, which exhibit the following characteristic fragment ions (fragment ions in bold print denote the base peak; numbers in parentheses denote the carbon number of the ketone from which the data were obtained):

HOMOLOGOUS SERIES	DIAGNOSTIC FRAGMENT IONS.
2-alkanones	85, 71, 59, 58, **43** (10).
3-alkanones	M^+ - 29, 85, 72, 57, **43** (10).
4-alkanones	M^+ - 43, 86, 71, 58, 57, **43** (10).
5-alkanones	M^+ - 57, 85, 71, 58, 57, **43** (10).

It should be noted that any interpretation of the relative distribution of components, both within and between the series of ketones in each oil is inappropriate for this fraction alone since the 2-alkanones continue to elute from the open-column beyond 1600 mL.

Fraction 16 (1600-1750 mL) for each oil was collected as two sub-fractions, comprising a pooled "clear" column eluent (ca. 1600-1644 mL and 1668-1750 mL - Figure 4-60) and a

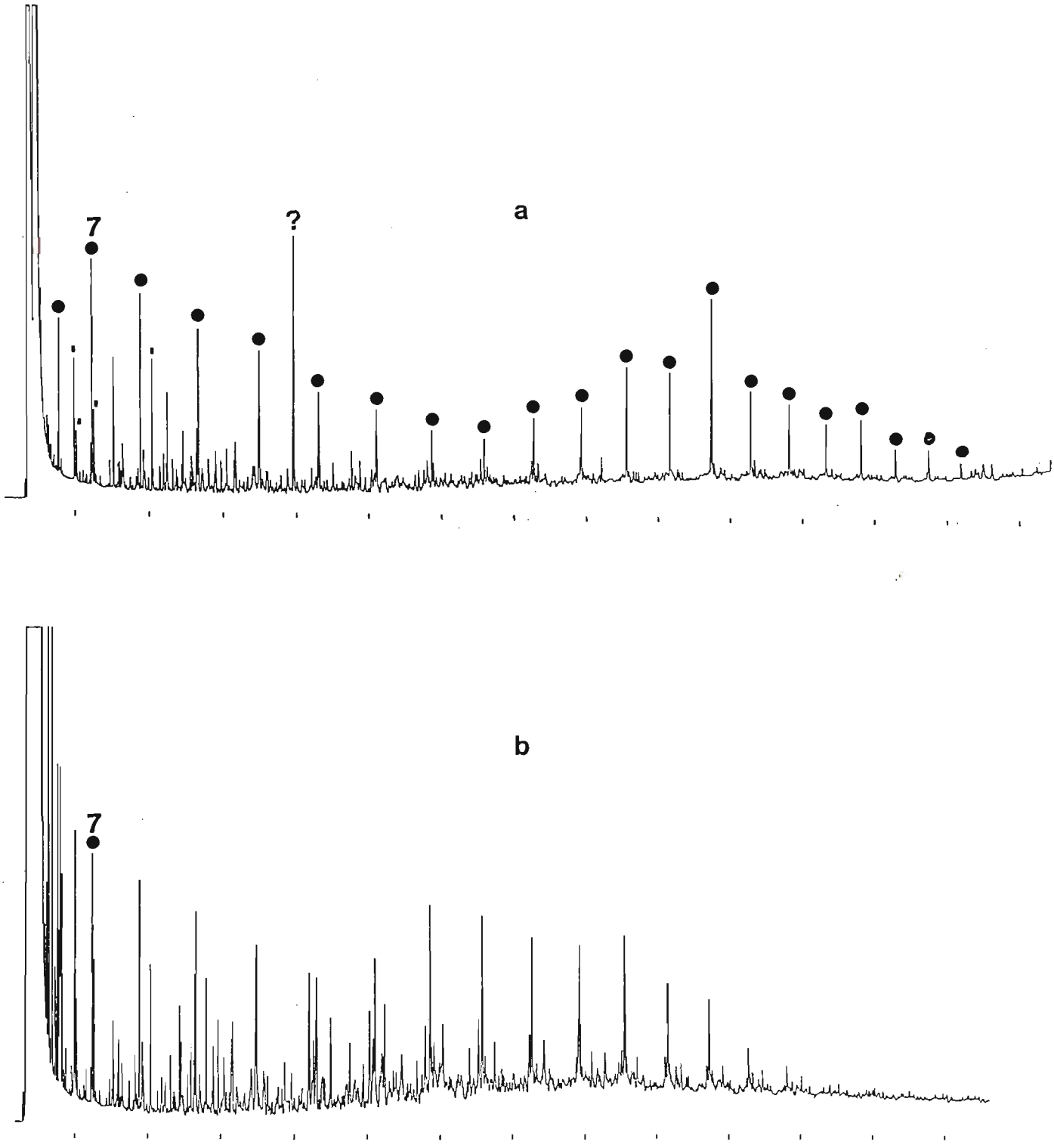

Figure 4-60. Gas chromatogram of the pooled "clear" column eluent (ca. 1600-1644 mL and 1668-1750 mL) of open-column fraction 16 from Duaringa 5391-C (a) and 686 (b). Major components are 2-alkanones with carbon numbers as indicated. Other components denoted (ı) are methyl-substituted cyclopentanones and cyclohexanones.

brown band (ca. 1644 -1668 mL - Figure 4-61). Both sub-fractions were analysed separately using GC , GC-MS and gravimetric quantification.

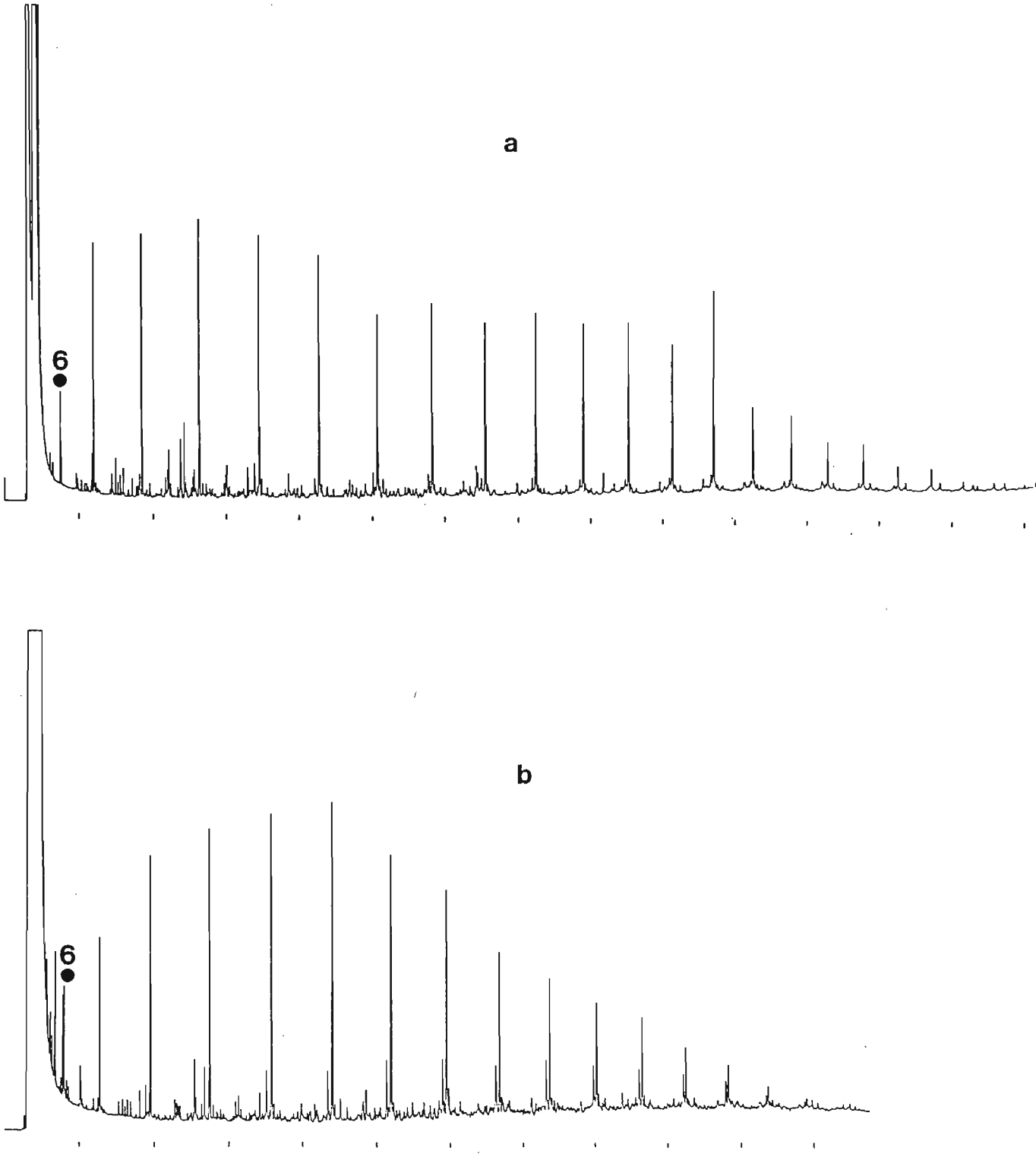

Figure 4-61. Gas chromatogram of the brown band (ca. 1644 -1668 mL) of open-column fraction 16 from Duaringa 5391-C (a) and 686 (b). Major components are 2-alkanones with carbon numbers as indicated.

The gravimetric data for both oils showed that the total mass for fraction 16 was partitioned between the pooled "clear", and the dark-brown eluent at ca. 40 and 60% respectively.

Following the gravimetric work, fractions 15 and 16 were reconstituted in dichloromethane and combined to obtain a composite and representative profile for the distribution and relative abundances of the 3- and 2-alkanone series in each of the oils (Figure 4-62). The bimodal distributions and odd/even carbon number preferences (CPI = 1.66 and 1.47 respectively - Table 4-37) over the C_{24} - C_{30} region of the chromatograms indicate a pyrolysis mechanism which involves both algal and higher-plant precursors. The conspicuously high concentration of the C_{19} -ketone for 5391-C suggests a relatively more abundant precursor for this component and/or an additional source (possibly unique). Work by Regtop et al. (1985) on the pyrolysis of model compounds on spent shales, minerals and charcoal has shown that many components of oil shale pyrolysates may be derived from secondary reactions of primary pyrolysis products, mediated by catalysts such as minerals or carbonaceous char. They identified specific, though not necessarily unique, precursors for the above ketones and other compounds; implications arising from their work will be discussed later in this section. The distribution of the 2-alkanones over the low molecular weight region of the gas chromatogram is smooth in both cases and suggests the influence of cracking processes which generally obscure any carbon number preferences. The more restricted distribution of the 3-alkanones is similar to that for the 2-alkanones (where both series are abundant) but does not show any obvious genetic relationship for the C_{19} -homologue in the oil from 5391-C.

The pooled ketones were quantified using decane as the internal standard. Assumptions similar to those used earlier to determine an upper limit for the concentration of nitriles in each oil were again made to calculate the maximum possible ketone concentration in the combined fractions. Total GC peak area was assumed to be of ketone origin (there is mass-spectral evidence to support the presence of traces of branched, cyclic and unsaturated ketones) and the total peak area was multiplied by 1.1 to account for homologues greater than C_{32}. The resultant area was then divided by 0.9 to adjust for the difference between the relative FID mass response factors of the ketones and the

internal standard. As for the nitriles this factor was used at a value deliberately lower than the response factor determined from several replicate analyses (5) of a known mass of

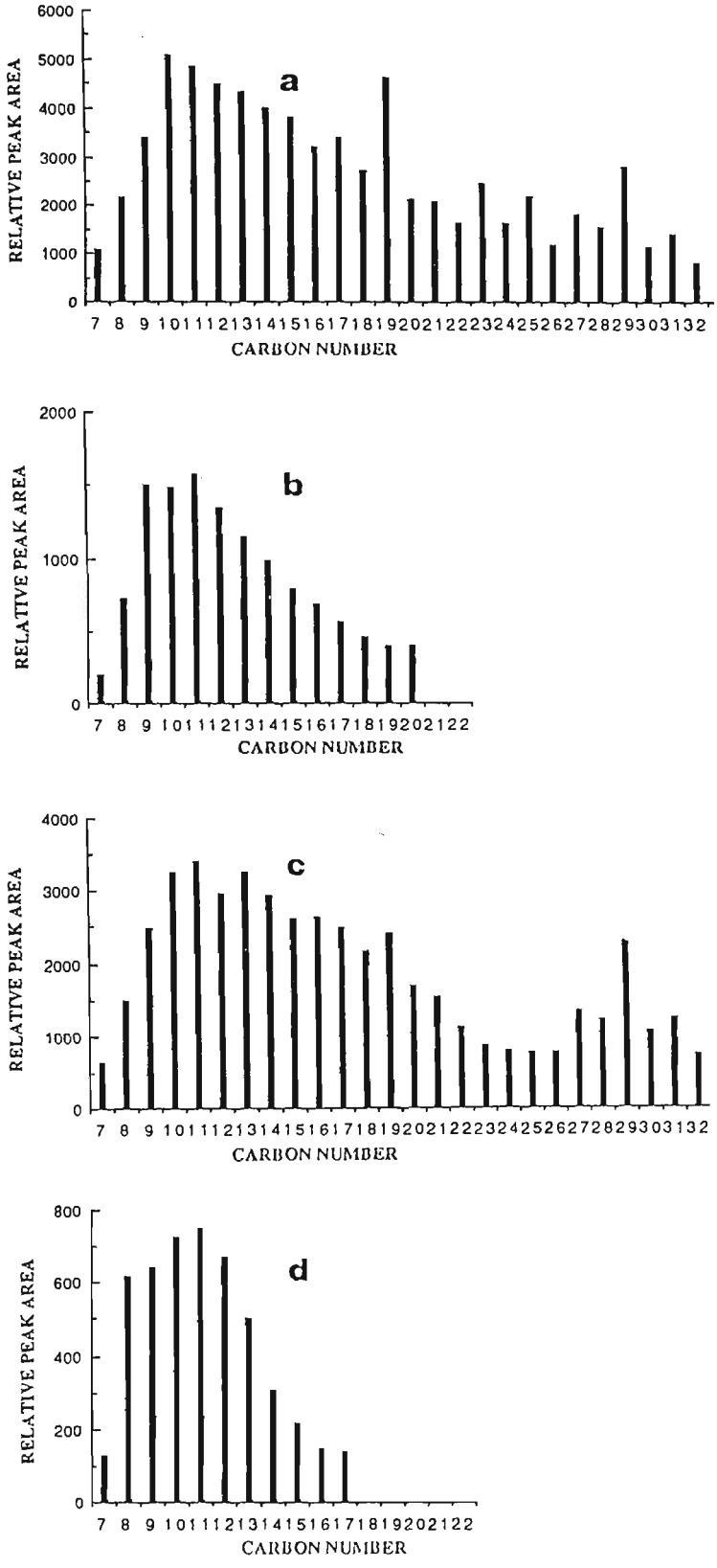

Figure 4-62. Total 2-alkanone and 3-alkanone profiles of combined open-column fractions 15 and 16 from Duaringa 5391-C (a and b) and 686 (c and d).

tridecane and 2-tridecanone. The latter showed relative response values in the range 0.95 - 0.98, which is greater than the value used above to account for the reduced FID sensitivity of the ketones relative to alkanes.

Quantitative data for the combined fractions for each oil (Table 4-37) show that the ketones comprise respectively ca.9 and 6% by mass of each fraction. As for the nitriles, the balance of the total mass of the fractions comprises reddish-brown (polymeric) material which does not contribute to the total gas-chromatographic peak area. The ketones constitute ca. 0.6% of the raw oil in each case and account for only a very small portion of its total oxygen content. A comparison of the gravimetric data for each fraction of the raw oils (Table 4-37), interpreted in conjunction with the relatively large difference between their oxygen content (Table 4-4), makes it reasonable to speculate that the bulk of the oxygen is associated with the polymeric portion of combined fractions 15 and 16

Table 4-37. Quantitative and chromatographic data for ketones (pooled open-column fractions 15 and 16) isolated from neutral oil - Duaringa 5391-C and 686.

	SAMPLE	
QUANTITATIVE DATA	**5391-C**	**686**
Mass (mg) - combined fractions 15, 16.	63.6	106.8
Mass (mg) of volatile ketones (C_7 - C_{32+}) in combined fractions 15, 16.[1]	5.7	6.1
% volatile ketones (C_7 - C_{32}) in combined fractions 15, 16 (w/w).	ca. 9	ca. 6
% volatile ketones (C_7 - C_{32+}) in raw oil (w/w).	ca. 0.6	ca. 0.6
% oxygen (raw oil) derived from volatile ketones (C_7 - C_{32+}) in combined fractions 15,16 (w/w).[2]	ca. 0.04	ca. 0.04
CPI[3]	1.66	1.47

1 based on peak area data relative to IS - decane. **2** average for the total oxygen content in the volatile ketones (C_7 - C_{32}) based on the oxygen content in 2-hexadecanone.

3 **CPI** = $$\frac{2(C_{29} + C_{27} + C_{25})}{C_{30} + 2(C_{28} + C_{26}) + C_{24}}$$

(possibly in pigmented material derived from higher plants). The latter may be verified by elemental analysis of the ketone-free solute. Other (small) quantities of oxygen are accounted for in the acid fraction (phenols and carboxylic acids) as well as in artefacts and asphaltenes.

Retention data for the 2-alkanones present in the combined fractions were used to determine modified Kovat's retention indices for these components (Table 4-38) and to derive a retention index equation (Figure 4-63). The former agree well with those data published for a restricted number of analytical standards by Rostad and Pereira (1986).

Table 4-38. List of modified Kovat's retention indices (RI) for 2-alkanones isolated in combined open-column fractions 15 and 16 of neutral shale oil from Duaringa 5391-C.

CARBON No.	RI[1]	CARBON No.	RI
7	890.96	16	1800
8	991.98	17	1903.58
9	1093.68	18	2005.50
10	1194.59	19	2107.25
11	1295.53	20	2208.90
12	1396.65	21	2310.47
13	1500.00	22	2412.37
14	1600.00	23	2514.14
15	1700.00		

1 Calculated using equation 1.

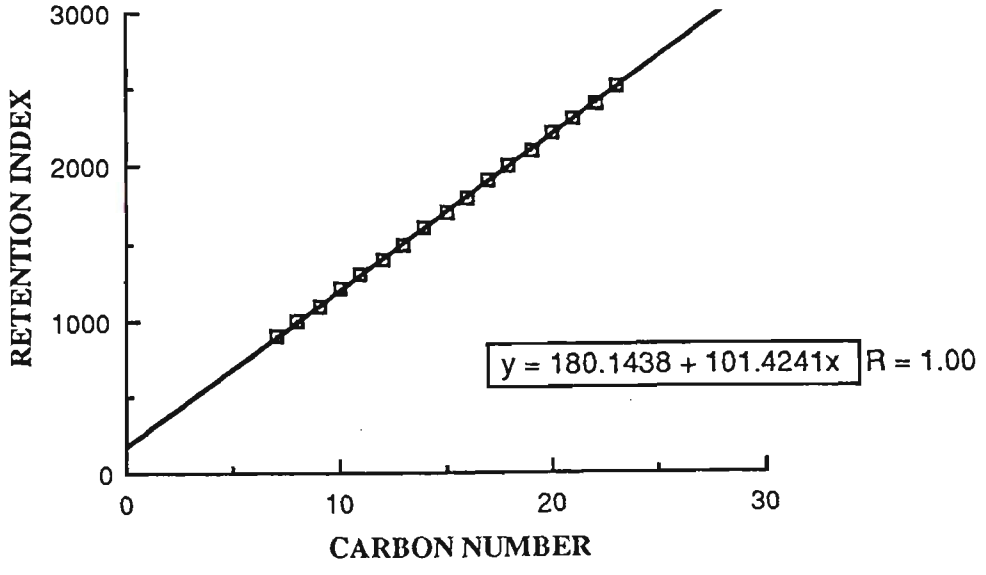

Figure 4-63.
Plot of modified Kovat's retention indices for 2-alkanones isolated in combined open -column fractions 15 and 16 of neutral oil from Duaringa 5391-C.

Although homologous series of linear ketones have been reported by a number of authors this is the first report of the presence of a clearly identified series of 4- and 5-alkanone components in shale oil. Regtop (1983) has reported 2-alkanones in the shale oils from the various units of the Rundle deposit. The chromatograms he obtained for the Kerosene Creek, Munduran Creek and Brick Kiln units are very similar to the composite 2-alkanone profile for both Duaringa oils, with all traces characterised by relatively abundant C_{19} and C_{29} homologues. He also reported evidence for trace quantities of 3-, 4- and 6-alkanones in the nitrile fraction of light, middle and heavy shale oil produced from the Kerosene Creek unit by the Lurgi-Ruhrgas process. Both 2- and 3-alkanones were found in shale oil from Condor (Rovere et al., 1983) and from the Mahogany Zone of the Green River Formation (Ingram et al., 1983). Rovere (1986) also suggested the presence of a homologous series of 4-alkanones in a fraction of neutral shale oil isolated from the latter using low-pressure liquid chromatography and a range of thermally modified alumina adsorbents.

The absence of 2-alkanones in the solvent extracts from Rundle oil shale has been cited as evidence for their pyrolytic origin (Rovere et al., 1983); however they have now been found in the solvent extracts of raw shale from Duaringa 5391-C and 686, albeit at low concentrations (cf. section 4.2). The distribution of 2-alkanones in the solvent extract from 5391-C (Figure 4-6) is similar to that in pooled fractions 15 and 16 from that sample and indicates that early diagenesis (possibly oxidation of alkan-2-ols, which are known to be biosynthesised in higher plants) may be sufficient to produce small quantities of these molecules; the retorting process would be expected to accelerate their formation from this source. The listed authors have cited β-oxidation of fatty acids followed by decarboxylation of the resultant β-keto acid (Davis, 1967), direct oxidation of hydrocarbons (Morrison, 1969) and thermolysis of β-keto esters (March, 1968) as possible mechanisms for the production of 2-alkanones during retorting.

The restricted unimodal distribution and reduced abundance of the 3-, 4-,and 5-alkanones may indicate lower thermodynamic stability for these compounds or suggest a unique source. Some of these components may be derived by cracking of mid-chain ketones known to occur in cuticular wax components (Cranwell, 1984).

Regtop et al. (1985) have studied the pyrolysis of model compounds on spent shales, minerals and charcoal, to assess the implication of product formation on the composition of shale oil. The authors found that the catalytic properties of the spent shale cannot be attributed to any single parameter such as residual carbon, but is probably a function of both surface area and composition of the residual char and the surface properties of pyrolysed mineral constituents. Pyrolysis of decanoic acid over Julia Creek spent shale (500°C, 5 min) yielded a range of alkanones showing systematic variation in the keto position with carbon number, i.e. $RCO(CH_2)_8CH_3$, R = CH_3 to C_9H_{19}, with 2 -undecanone being the most abundant component. At higher space velocities (ca. 15s residence time) much less cracking occured and 10-nonadecanone (probably formed by coupling reactions involving an acyl radical) was the most abundant ketone formed; it was followed by trace amounts of all other members of the series. Other specific ketones were also produced by the pyrolysis of 2-octanol (2-octanone), 1-octen-3-ol (3-octanone), 6-undecanone (2-heptanone) and 1-octen-3-one (3-octanone).

These results show that a mixture of relatively few carboxylic acids may be sufficient to produce the range and relative distributions of ketones observed in the Duaringa shale oils. A (small) quantity of the required medium to high molecular weight precursors occur as free fatty acids in the oil shales (cf.section 4.3), while others may be formed by β-elimination reactions from esters bound to the kerogen. Low molecular weight carboxylic and dicarboxylic acids are (usually) abundant in oil shale retort waters. The small amounts of cycloalkanones found in fractions 15-16 may be derived from the cyclisation of the latter (Regtop et al. 1985).

Fractions 17-19 (1750-2250 mL: polymeric material).

These column fractions require relatively polar solvents for elution and contain non -volatile (polymeric) material not accessible by GC-analysis. Some of the material may have been carried out of the retort in aerosol form, or formed shortly after production of the oil by oxidation through contact with air and light. The formation of further polymeric substances may have been catalysed during acid-base extraction of the raw oil. It has also

been reported that partitioning of polar compounds can cause the formation of tars (Regtop, 1983). The latter is a potential source of polymeric material as the constituent classes comprising the neutral oil are partitioned, on the basis of solubility, by the increasingly polar solvents (mixtures) of the eluotropic series. Other non-volatile material may subsequently form on the open-column through reactions facilitated by the catalytic activity of the chromatographic adsorbents. Rovere et al. (1983) have suggested that the latter source generates the majority of this material and cite the insoluble nature of these column fractions (pentane) as evidence to support their supposition. However, it should be noted that other constituents present in the raw oil may act as co-solvents during initial dissolution in the solvent.

The isolated fractions may be characterised further using NMR, IR, pyrolysis-GC and elemental analysis; research in these areas is continuing. Rovere et al. (1983) have reported several percent of nitrogen in these fractions of shale oil from the Condor deposit. These findings may implicate pyrroles and other nitrogen-containing heterocycles in the formation of their constituents, since alkyl-subsituted forms of the latter are known to form polymeric material (gums) during the storage of synfuels (Brinkman et al., 1980).

The fractions collectively constitute 13.4 and 8.3% of the raw oil mass for Duaringa 5391-C and 686 respectively. However, the total polymeric fraction for the oils is greater in each case since the non-volatile constituents of the nitrile and ketone fractions need to be included in the total mass. The combined gravimetric values are listed for each oil in Table 4-39, along with gravimetric data for other combined fractions of associated compound classes comprising the raw oil. As these data show, only ca. 67-70 % of the syncrudes from the two Duaringa deposits comprise compounds readily utilised by a potential synfuel industry. These figures need to be revised downwards if any of the alkene, diene and polyaromatic fractions are not suitable for refining purposes. For the worst-case scenario, where each of them is unsuitable, this leaves respectively only ca. 28 to 33% (alkanes and mono-aromaticcs) for each oil; hydrotreating of the synfuels should increase this value and will improve the long-term storage properties of these liquids.

Table 4-39. Combined gravimetric and chromatographic data (mg per gram of raw shale oil) for the masses of grouped fractions obtained from the acid-base extraction and open-column fractionation of raw shale oil from Duaringa 5391-C and 686.

	Compound Class	Grouped Fractions (open-column)	mass % of Raw Oil 5391-C	686
1	Asphaltenes		1	0.8
2	Phenols		1.2	0.7
3	Carboxylic Acids		0.01	0.2
4	Bases		2.9	1.3
5	Artefacts		1.2	1.9
6	Alkanes	1 - 2	23.8	28.6
7	Alkenes	2 - 3	13.1	13.9
8	Dienes	4	2.6	2.4
9	Monoaromatics	5	4.5	4.5
10	Di- and polyaromatics	6 -13	20	18
11	Nitriles	14	1.5	1
12	Ketones	15	0.6	0.6
13	Polymeric Material	14-19	27	25.3
	TOTAL		**99.4**	**99.2**

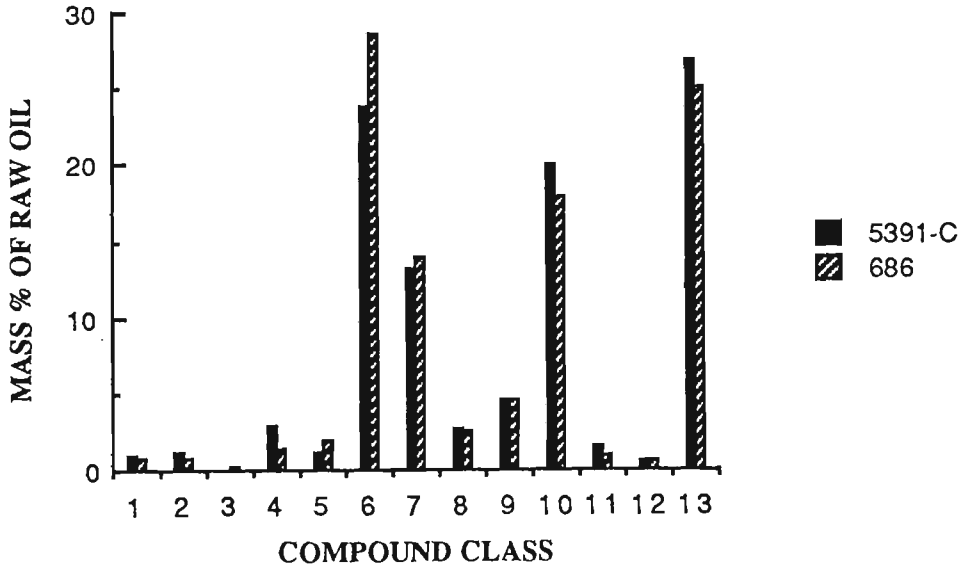

Figure 4-64. Bar graph of Table 4-39 values for the masses of grouped fractions obtained from the acid-base extraction and open-column fractionation of raw shale oil from Duaringa 5391-C and 686. Compound class numbers refer to those listed in Table 4-39.

CHAPTER FIVE: COMPARATIVE ANALYTICAL STUDIES ON AUSTRALIAN OIL SHALES.

5.1 THERMAL CHARACTERISATIONS.

5.1.1 Effects of temperature and time on the composition of oil shale retort products.

The design of the tube furnace and stainless-steel retort provides good control over retorting parameters (sweep-gas, heating rates) and allows accurate monitoring of the actual shale temperature during pyrolysis. This makes the device ideally suited to fundamental studies on the composition of retort products obtained at various temperatures. It was used in that context to study the low temperature pyrolysis (350°C) of selected Tertiary oil shales from the Rundle, Stuart and Condor oil shale deposits in Queensland (Hutton et al., 1986).

The three oil shales are termed lamosites since they contain abundant lamellar alginite (lamalginite) which is derived from planktonic precursors. Minor constituents of the oil shales include vitrodetrinite and sporinite (both derived from terrestrial plants), telalginite (derived from the colonial green alga *Botryococcus*) and rare bituminite (Hutton, 1982). During pyrolysis of the oil shales, most of the shale oil is derived from the alginite and shale yields are proportional to alginite content (Hutton, 1985), with a maximum of 75 % of the organic carbon of the oil shale converted to oil under Fischer assay conditions (Gannon and Henstridge et al., 1984). Estimates of shale oil yields from commercial retorts vary from 70 - 110 % of the Fischer assay yield.

Comparative aspects of the chemical and petrographic properties of these deposits were discussed based on data from the low temperature retorting. Interpretation of these data provides a better understanding of pyrolysis mechanisms and may serve as a guide to increasing the efficiency of converting oil shale organic matter to useable fossil fuels. The gas chromatograms of oil from the Stuart deposit have been published. Comparable chromatograms from Rundle were similar to those obtained for Stuart, while those for Condor were different in several respects. Gas chromatograms for the solvent extract and the 350°C pyrolysates (0.5h and 48h) of the latter are given in Figure 5-1. Apart from

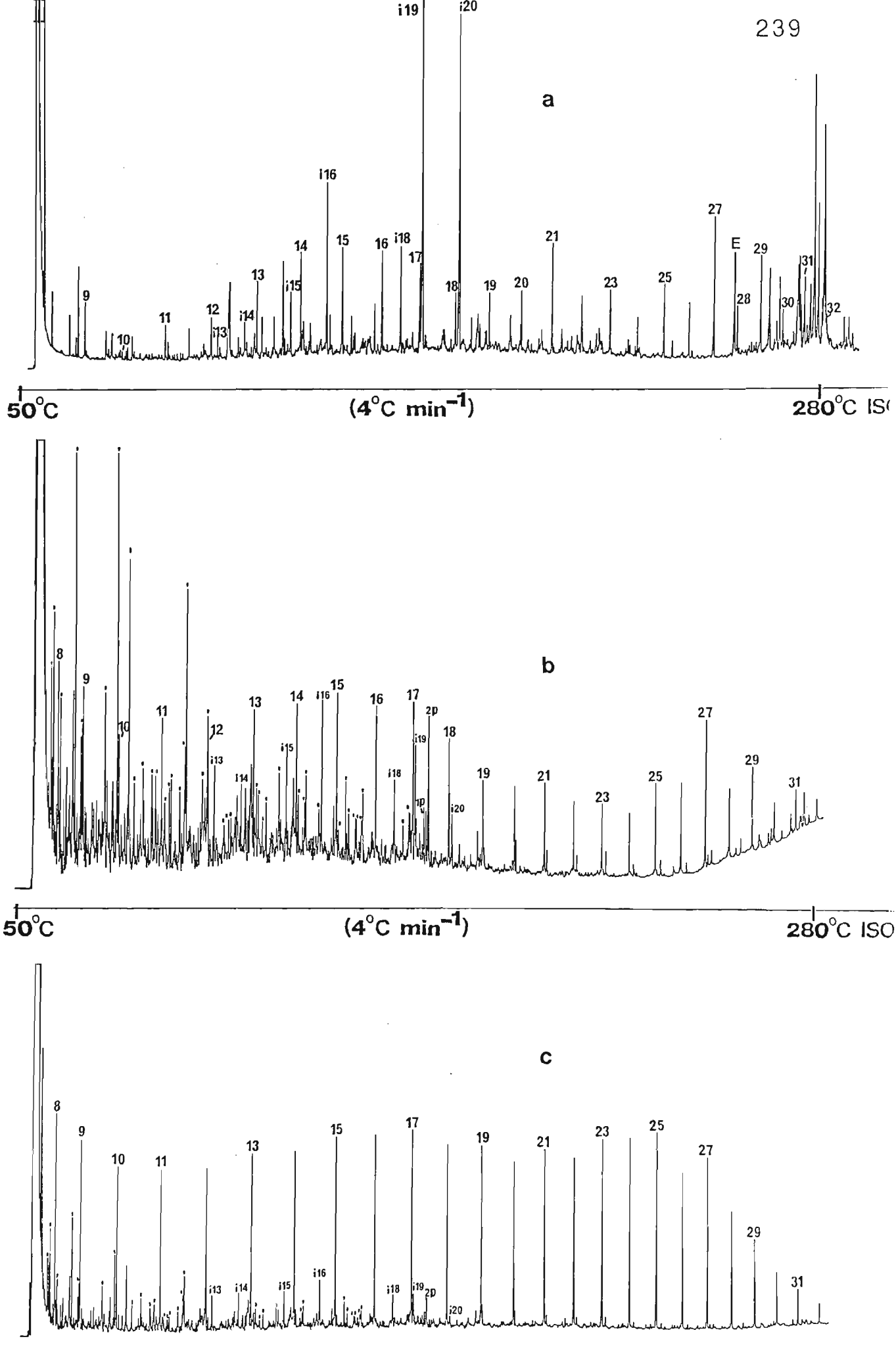

Figure 5-1. Gas chromatograms of solvent extract **a** and thermal desorbates (350°C; 0.5h - **b**, 48h - **c**) for raw shale from Condor (Brown unit). Major components are alkanes and isoprenoid hydrocarbons (i13 - i20) with carbon numbers as indicated, erucamide (E) and steranes and pentacyclic triterpanes over the alkane region C_{29} - C_{32}. Components denoted i are listed in Table 5-1. 1p = prist-1-ene, 2p = prist-2-ene.

the major compounds labeled in the respective profiles, GC-MS analysis of each sample also identified those listed in Table 5-1.

Table 5-1. Identity of (minor) components found in the thermal desorbate (350°C, 0.5h and 48h) of raw oil shale from Condor, Australia (Brown unit).

Pk.No.[1]	Compound Name	Pk.No.	Compound Name
7.1	methylhexadiene	12.2	C6-benzene
7.2	methylbenzene	12.3	dimethylindan
8.1	dimethylhexadiene	13.1	C6-benzene + tetramethylindan
8.2	dimethylbenzene	13.2	methylnaphthalene
8.3	dimethylbenzene	13.3	C6-benzene
9.1	C3-benzene + methylnonane	13.4	C6-benzene
9.2	trimethylbenzene	13.5	tetramethylindan
10.1	trimethylbenzene	14.1	dimethylnaphthalene
10.2	indan	14.2	ethyl- or dimethylnaphthalene
10.3	C4-benzene	14.3	dimethylnaphthalene
10.4	C4-benzene	14.4	C6-benzene + br.alkane (226)
10.5	C4-benzene + methylindan	15.1	isopropylnaphthalene
11.1	C4-benzene	15.2	butyl-tetrahydronaphthalene
11.2	C4-benzene	15.3	trimethylnaphthalene
11.3	C4-benzene	15.4	trimethylnaphthalene
11.4	methylindan	15.5	trimethylnaphthalene
11.5	methylindan	15.6	C3-naphthalene
11.6	C4-benzene	15.7	C3-naphthalene
11.7	dimethylindan	16.1	C4-naphthalene
11.8	dimethylindan	16.2	C4-naphthalene
12.1	C5-benzene		

1 Peak code as for Figure 4-25; numbers refer to Figure 5-1 (**b**) and equivalent peaks marked in profile (**c**). The listed compounds were identified from complete mass spectra.

The gas chromatograms of the solvent extract and thermally desorbed components (350°C, 0.5 h) show large differences which illustrate the effects of retort residence time and secondary reactions.

A notable feature of the Condor chromatograms is the relatively high concentration of steranes and pentacyclic triterpanes in the solvent extract (over the alkane region C_{29} - C_{32}) and the virtual absence of alkenes in the thermal desorbates, even after 48 h at 350°C. The former components were characterised by GC-MS (complete spectra) and plots of diagnostic fragment ions; relevant profiles, mass-spectral data and retention indices are given in Figure 5-2 and Table 5-2. Crisp et al. (1986) have found that the flash thermal desorbate obtained from powdered Condor shale using a Curie-point pyrolyser (358°C,

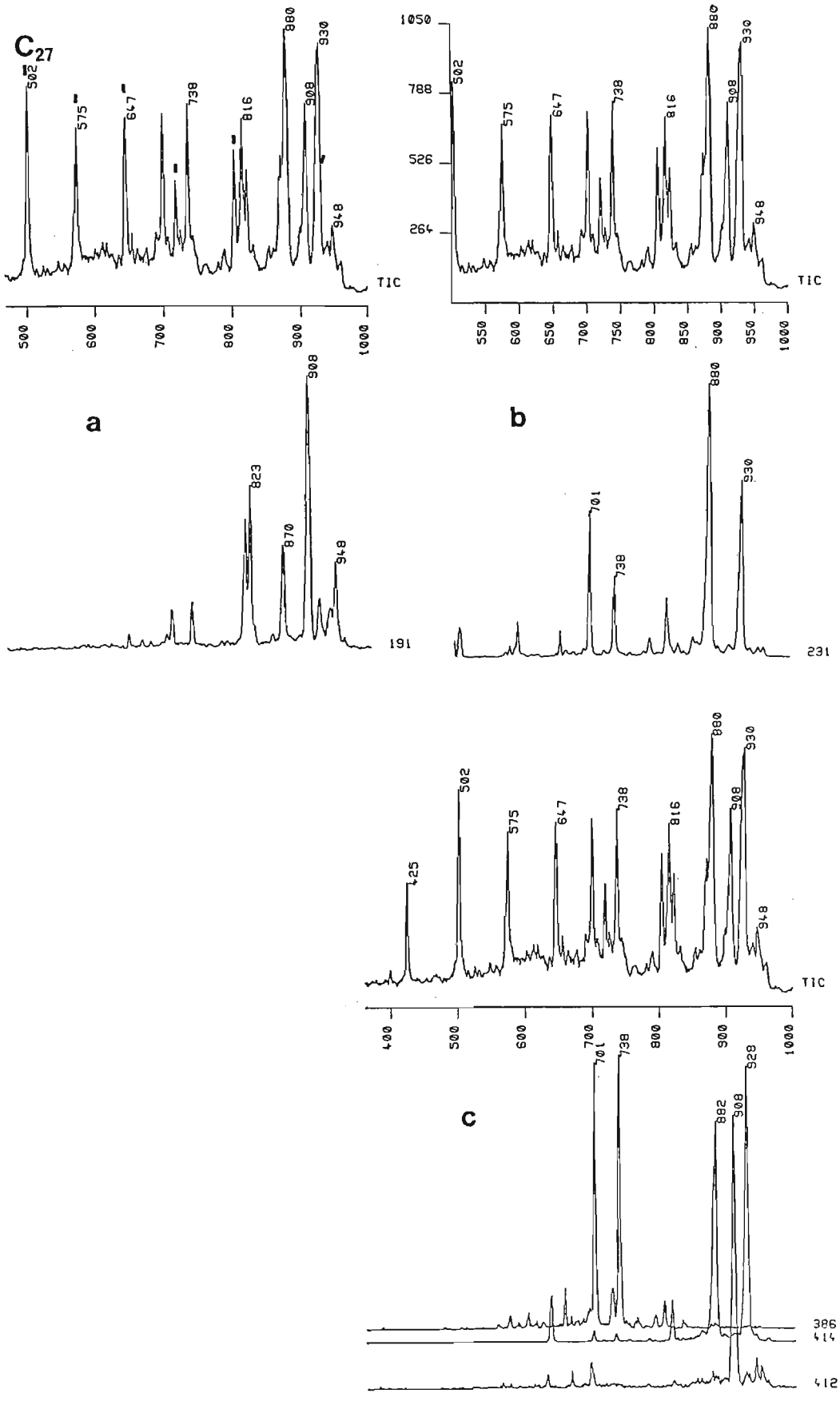

Figure 5-2. GC-MS data for the sterane-pentacyclic triterpane region of the solvent extract from Condor (Brown unit). Figures **a**, **b** and **c** depict the total ion current (TIC) over the high molecular weight region of the chromatogram (alkanes C_{27}-C_{32} in **a** denoted by ı) and the corresponding fragment-ion plots characteristic for pentacyclic triterpanes (m/z=191 - **a**), steranes (m/z=231 - **b**) and molecular weights (386, 412, 414) for the major components of the two series (**c**).

Table 5-2. Mass-spectral and retention data for steranes and pentacyclic triterpanes identified in the solvent extract of oil shale from Condor, Australia (Brown unit).

Pk.No.[1]	M.Wt.	Formula[2]	FI[3]	RI[4]	Compound Name	Ref.
701	386	$C_{28}H_{50}$	231	2940.74	methylcholestane	Philp, 1985.
738	386	$C_{28}H_{50}$	231	2985.99	methylcholestane	Philp, 1985.
816	414	$C_{30}H_{54}$	231	3077.22	4-methylsterane (C_{30})[5]	
823	398	$C_{29}H_{50}$	191	3113.52	triterpane (C_{29})[5]	
870	414	$C_{29}H_{50}$	191	3127.04	triterpane (C_{29})[5]	
880	414	$C_{30}H_{54}$	231	3145.95	4-methylsterane (C_{30})[5]	
908	412	$C_{30}H_{52}$	191	3163.49	gammacerane	Philp, 1985.
930	414	$C_{30}H_{54}$	231	3189.74	4-methylsterane (C_{30})[5]	

1 Peak number in TIC profile of Figure 5-2. **2** Empirical formula based on MS molecular weight data. **3** Characteristic fragment-ion. **4** Modified Kovats retention index. **5** Tentative identification (in the absence of reference spectra).

10s) is practically identical to the solvent extract for the deposit. In contrast with their findings the current study shows that the steranes and pentacyclic triterpanes, prominent in the solvent extract, are virtually absent from the thermal desorbate at 350°C (0.5h) and suggests that these components degrade (readily) to more volatile (cyclic) products. This postulate was examined by isolating these compounds from the solvent extract and pyrolysing the solvent-free concentrate on a platinum ribbon over a range of temperatures (300-500°C) at 50°C increments.

The concentrate was isolated from the extract using clathration (5nm molecular sieve) to remove the linear components, followed by vacuum sublimation (ca. 1 kPa, 75°C, 1h) to remove the volatile components. A small portion of the fraction was examined after each step of the procedure using GC (Figure 5-3). The isolated sterane-triterpane fraction was dissolved in dichloromethane (ca. 1mg mL^{-1}) and 1μL of the solution was used to coat the platinum ribbon of the CDS-150 pyroprobe. Separate samples of air-dried films of the material were pyrolysed at progressively higher temperatures over the

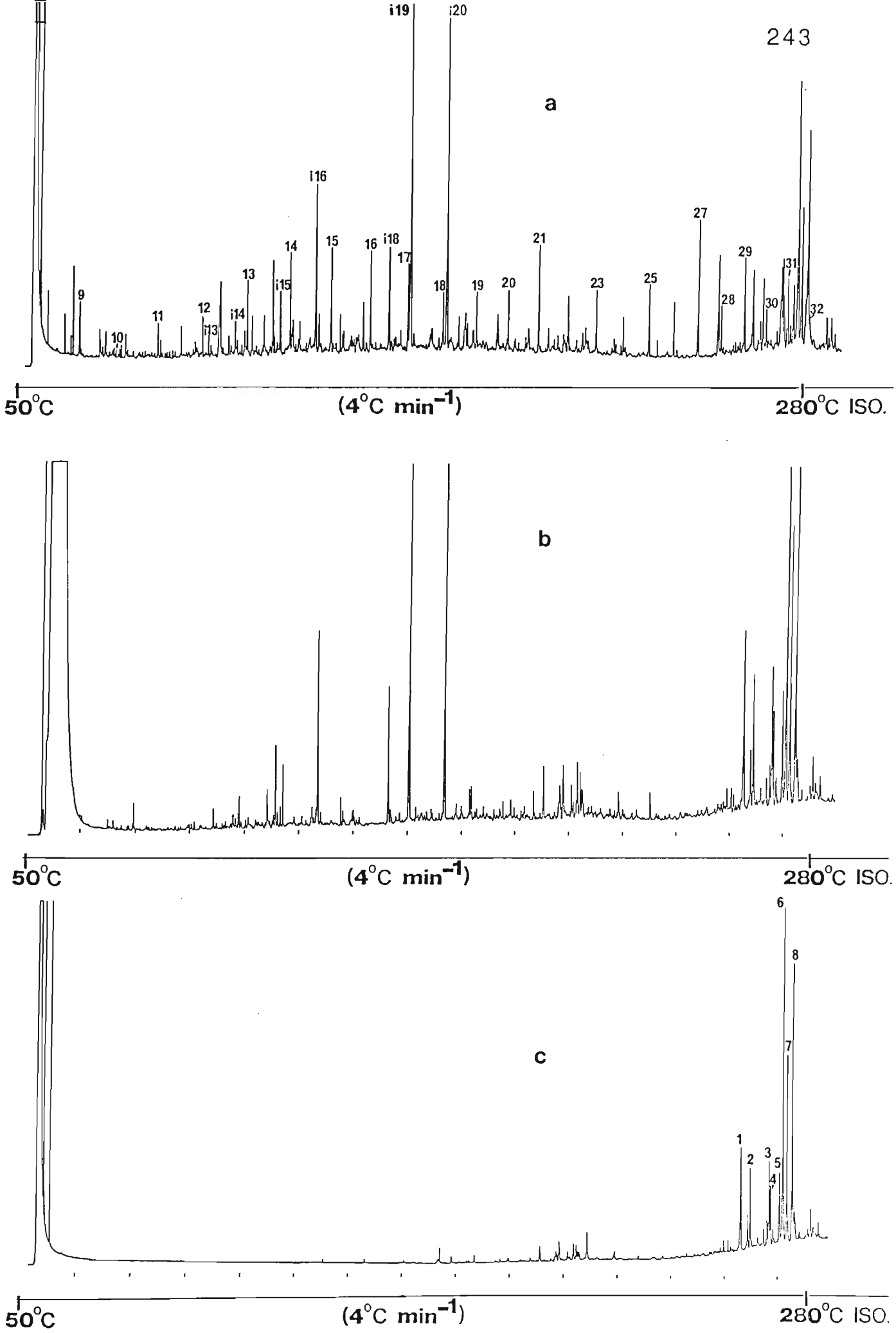

Figure 5-3. Gas chromatograms for the total solvent extract from Condor raw oil shale (Brown unit) **a** and the branched-cyclic fraction **b** and sterane-pentacyclic triterpane fraction **c** isolated from the extract. Components 1-8 (c) correspond in sequence to the steranes and triterpanes (TIC numbers 701-930) listed in Table 5-2.

above range of temperatures and using the same experimental conditions as those described for the pyrolysis of raw shale. The pyrolysis-GC profiles in each case were virtually indistinguishable from the gas chromatogram of the isolated fraction (Figure 5-3 c) and illustrate the high thermal stability of these compounds. In interpreting these results it must be considered that flash-pyrolysis from a relatively inert platinum surface differs markedly from the conditions prevailing in the retort. Rapid heating of the high-surface-area ribbon may facilitate cracking (for the above sample there is no evidence for this), but offers little opportunity for secondary pyrolysis reactions to occur. Consequently the pyrolysis profile may simply represent the result of rapid volatilisation of the compounds from the ribbon without any evident change in pyrolysate composition. Possible formation of non-volatile material must also be considered but is not significant under these conditions since chromatograms obtained from 1μL injections of the same material gave quantitatively similar results. To obtain a more realistic pyrolysis profile the isolated concentrate needs to be added to spent shale from Condor, or to a mixture of minerals comprising its mineral matrix. These approaches will be the subject of further research.

The profiles for solvent extracts and flash Curie-point desorbates (358°C, 10s) published by Crisp and co-workers for the Condor deposit were almost identical and, in particular, contained relatively constant abundances of both sterane and pentacyclic triterpane components. They introduced solvent extracts onto the GC-column by evaporating a film of the solvent-free extract from a Curie-point nickel wire at 358°C. Their profile differs from Figure 5-1**a** by the absence of erucamide, which is a prominent peak in the latter (component **E**). This amide of erucic acid (13-docosenoic acid) which constitutes 40 to 80% of the total fatty acids of rapeseed, mustard-, wallflower- and nasturtium-seeds (Merck Index) does not appear to be an artefact, since it was not isolated in extracts from other deposits obtained under identical conditions. The absence of this compound in the chromatogram of Crisp et al. may be related to their flash-desorption injection procedure, since the amide would be expected to dehydrate readily to the nitrile. The continued presence of the sterane and triterpane components in their flash thermal -desorption profile of Condor powdered shale supports the above findings of high thermal stability for these components using platinum-ribbon pyrolysis. Evidently, longer residence times than those

encountered using the Curie-point device (10 s) and secondary interactions with the hot shale in a (confined) retort environment are required to induce changes in the structure of these compounds.

The absence of alkenes in the total Condor pyrolysate, even after exposure to 350°C for 48h, prompted a further investigation of this oil shale to determine the changes occuring in pyrolysate composition during step-wise retorting up to 500°C. Results obtained from the pyrolysate collected during each of the sequentialy-increasing temperature intervals should provide a clearer understanding of retort processes generally and may help to understand the underlying mechanisms with a view to optimising the process.

Air-dried and sieved raw shale (< 1mm, 15g) from the Condor deposit (Brown unit) were heated as received in the stainless-steel retort. Eight fractions were collected during the retorting experiment. The temperature profile over which individual samples were collected is shown in Figure 5-11 **a**. Oil fractions collected are shown as numbered intervals in the latter and correspond to details given in Table 5-5. For example, sample 3 was collected over the temperature range 350-375°C by heating the shale from 350 to 375°C (2.5°C min^{-1}) and maintaining it at that value for a period of 15 min. Collected fractions were treated as detailed for step-wise retorting in section 3.3 of the experimental procedures. Gas chromatograms for volatile hexane-soluble compounds collected over the various temperature regions are depicted in Figures 5-4 and 5-5. When necessary, post-run replotting was performed to bring all peaks on scale.

Detailed GC-MS analysis of sample 2 (Figure 5-6) identified alkanes (C_{10} - C_{31}), prist-1-ene and prist-2-ene as the major components. Other (minor) components identified are listed in Table 5-3 along with respective retention indices. The relatively high concentrations of di-, tri- and tetramethylbenzenes in sample 1 (see also Figure 5-1**b**) and alkyl-substituted indans and naphthalenes in sample 2 are particularly noteworthy. The substituted benzenes are practically absent from the solvent extract (Figure 5-1**a**) and Curie-point raw shale desorbate at 358°C (Crisp et al., 1986). This indicates that secondary reactions associated with relatively long residence times are important factors facilitating

their formation from thermally-labile precursors under relatively mild conditions (<350°C). The relatively high abundance of these compounds in the Fischer retort oil from Condor carbonaceous shales and their absence in the oil from the Condor Brown unit (Crisp et al., 1987) suggests that they may be derived from (aromatic) higher-plant precursors. Crisp and coworkers have commented on the higher yield of compounds (< C_{15}) they obtained from the thermal degradation of Condor raw shale (relative to solvent extraction) but did not attribute these differences to low temperature pyrolysis reactions. Their "injection" technique precluded them from detecting components < C_{11} in their desorbates and they were not in a position to observe the low molecular weight substituted benzenes described above.

The high concentration of prist-1-ene and prist-2-ene in sample 2 indicates that shale-dependant temperature thresholds may have to be overcome for the formation of these components from different deposits. Crisp et al. have found approximately equal quantities of both isomers in the 358°C Curie-point flash-desorbate from Stuart oil shale, but failed to detect either of these in desorbates from Condor or Julia Creek under identical experimental conditions. However, they found both isomers in the Curie-point flash pyrolysate of Condor at 510°C. The current work on Condor (Figure 5-4 - **2** and **3**) shows relatively high concentrations of both components with prist-1-ene predominant in each case. The respectively low (high) abundances of both in the condensate of sample **1** (**2**) again supports the earlier proposition that relatively long residence times and sustained exposure to a (moderate) temperature of 350°C are required for the formation of certain components from thermally-labile precursors. Sequential Curie-point pyrolysis of the same Condor sample at 510°C produced the usual (similar) profiles, but only the prist-1-ene isomer in the second pyrolysate (Crisp, unpublished data). Evidently residual char deposited on the shale after the first pyrolysis prevents formation of the prist-2-ene, which is known to be derived by mineral-catalysed isomerisation of the latter (Regtop et al., 1986). During the above step-wise retorting the formation of the pristenes ended at a temperature of ca. 400°C (Figure 5-4 - **4**).

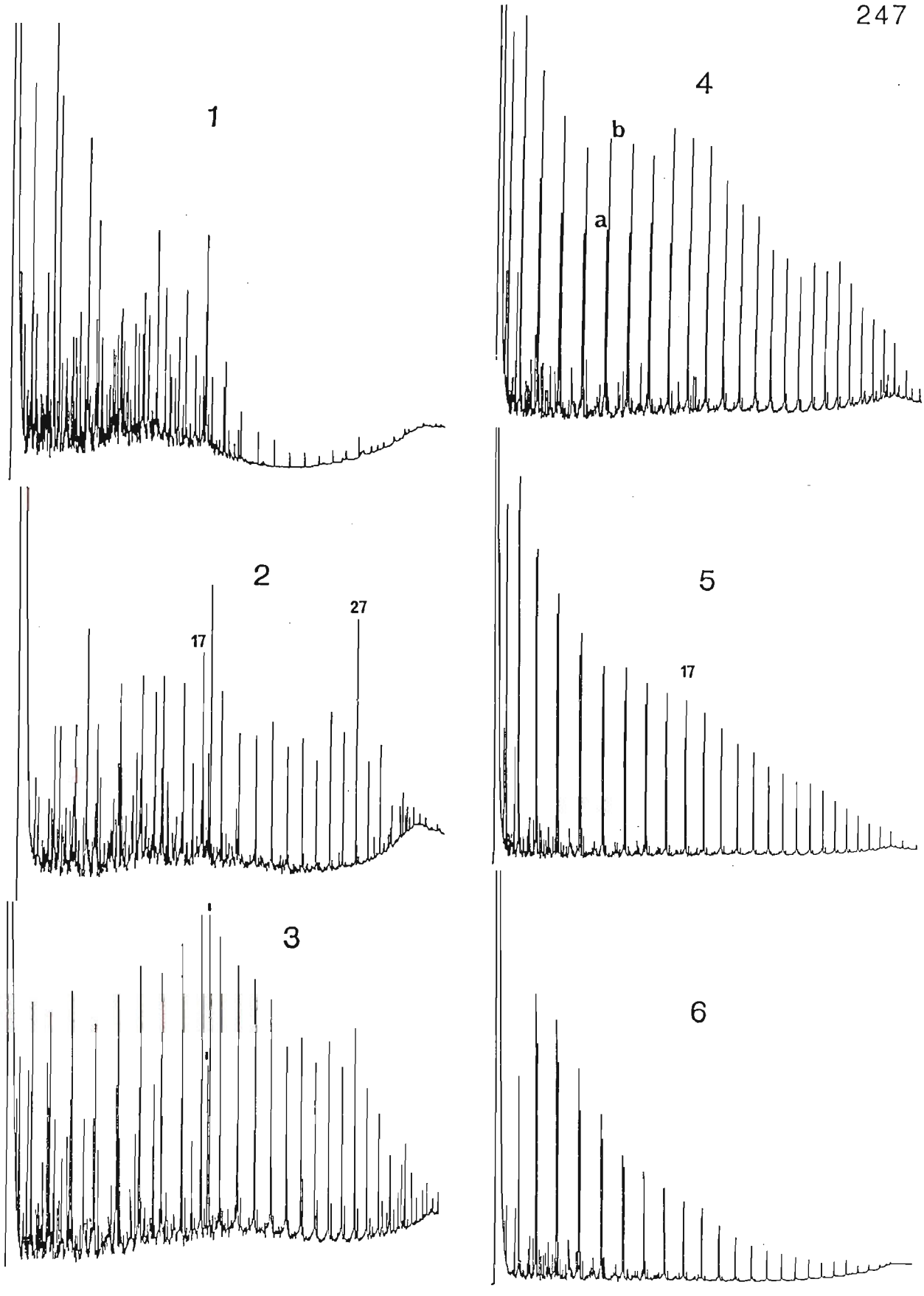

Figure 5-4. Comparative gas chromatograms of condensable retort products obtained from the step-wise retorting of raw shale from Condor (Brown unit). Sequential profiles **1** - **6** correspond to samples collected over the temperature regions 1-6 listed in Table 5-5. Major components (profiles **1** - **3**) comprise alkanes (carbon number as indicated) and those compounds identified earlier in the low temperature pyrolysates (Figure 5-1, Table 5-1). Other marked components(') denote prist-1-ene and prist-2-ene in the order of their elution. Detailed GC-MS analysis of sample **2** is described in the text. Profiles **4** - **6** are dominated by linear 1-alkenes **a** and alkanes **b**.

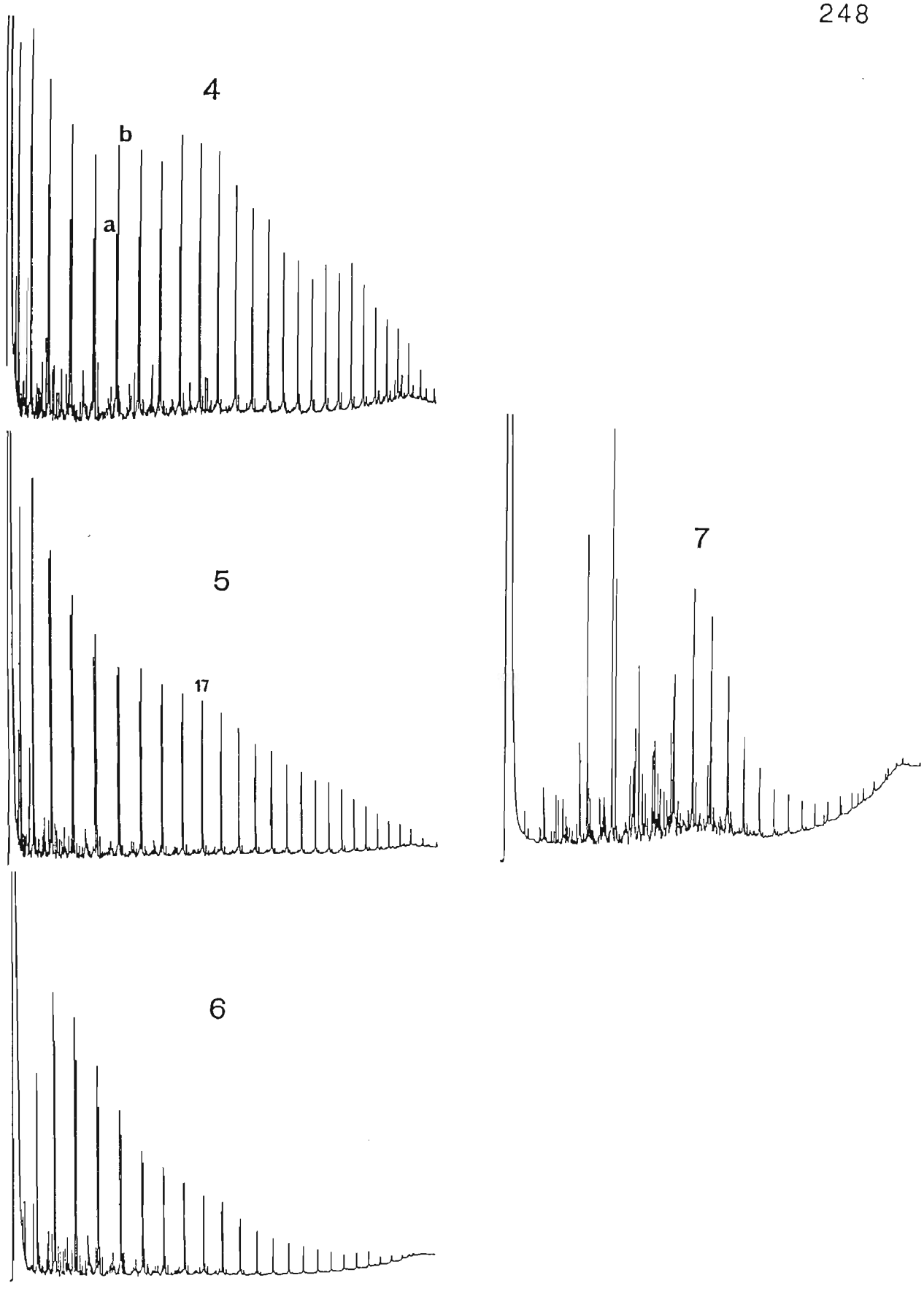

Figure 5-5. Comparative gas chromatograms of condensable retort products obtained from the step-wise retorting of raw shale from Condor (Brown unit). Sequential profiles **4 - 7** correspond to samples collected over the temperature regions 4-7 listed in Table 5-5. Major components (profiles **4 - 6**) comprise linear 1-alkenes **a** and alkanes **b** with carbon numbers as indicated. Sample 7 contains predominant aromatic components - see detailed GC-MS analysis in text. Sample 8 (not shown) contained lower concentrations of components found in sample 7.

A close examination of pyrolysis-GC data published for Australian oil shales by Crisp et al. (1987) suggests that there may be a correlation between input from land-based plants and high prist-1-ene concentrations in the flash-pyrolysates (570°C) for the listed shales. However, apparent exceptions (based on maceral data) make inferences about higher-plant precursors for this compound rather speculative.

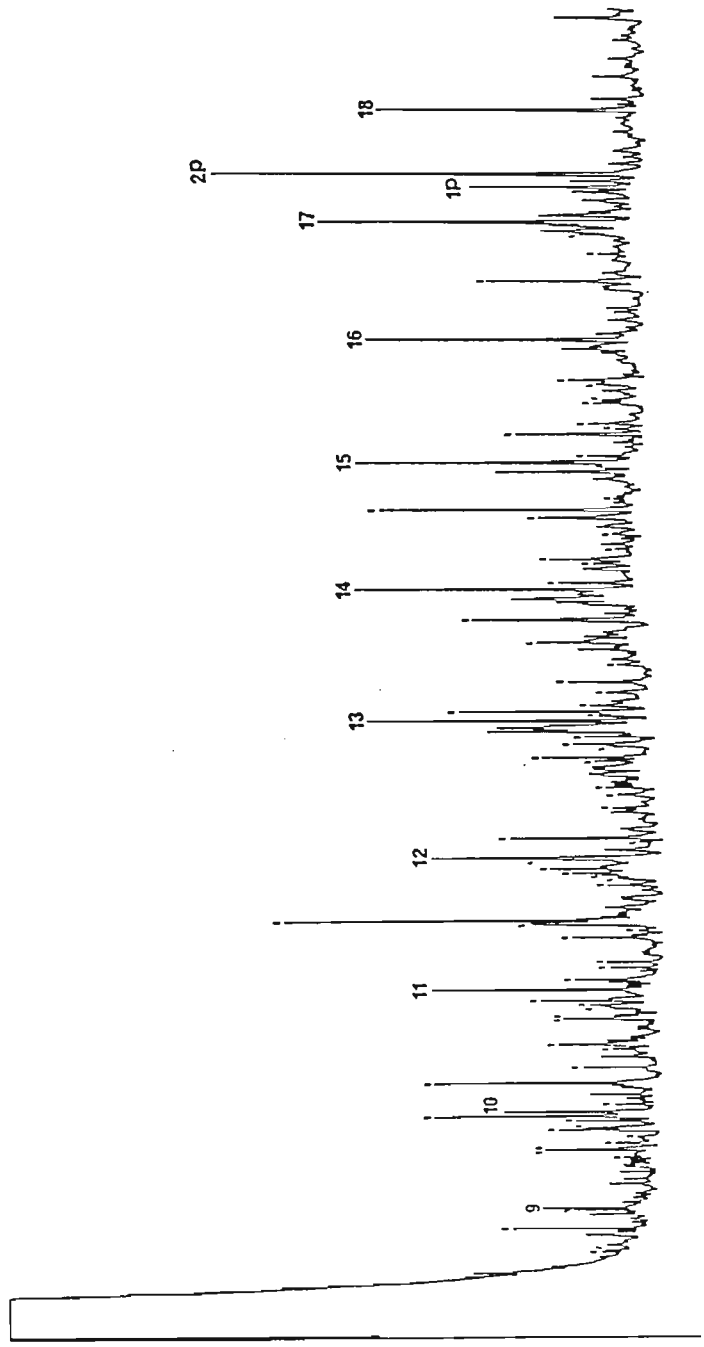

Figure 5-6. Part of the total-ion-current profile (TIC: C_9 - C_{19}) of retort sample 2 (350°C, 0.25h) from Condor (Brown unit) - (cf. Figure 5-4 -2). Major components are alkanes with carbon numbers as indicated; prist-1-ene (1p) and prist-2-ene (2p). Other components denoted ı are listed in Table 5-3.

TABLE 5-3. Retention index and component identification for retort-product profile Figure 5-6 (350°C, 0.25h).

Pk.No.[a]	R.I.	Compound Name	Pk.No.[a]	R.I.	Compound Name
8.1		dimethylheptane	12.2	1213.66	2,6 dimethylundecane
8.2		trimethylcyclohexane	12.3	1235.37	trimethylethylbenzene
8.3	817.17	dimethylbenzene	12.4	1245.53	C6-benzene
8.4	896.14	dimethylbenzene	12.5	1250.09	dimethylindan
9.1	953.51	?	12.6	1270.19	dimethylindan
9.2	960.52	2-methylnonane	12.7	1272.86	2,6,10-trimethylundecane
9.3	960.52	C3-benzene	12.8	1282.17	3C,C2-benzene
9.4	967.26	3-methylnonane	12.9	1282.17	dimethylindan
9.5	974.28	?	12.10	1287.76	C6-benzene
9.6	979.73	C3-benzene	13.1	1303.39	2-methylnaphthalene
9.7	982.62	1-decene*	13.2	1307.4	C6-benzene
9.8	990.66	4-decene*			+ tetramethylindan
9.9	994.31	trimethylbenzene	13.3	1311.29	1-methylnaphthalene
10.1	1005.84	2-decene	13.4	1320.89	C6-benzene
10.2	1022.53	trimethylbenzene	13.5	1328.79	C6-benzene
10.3	1035.52	indane	13.6	1341.60	tetramethylindan
10.4	1050.88	C4-benzene	13.7	1359.05	tetramethylindan
10.5	1055.84	C4-benzene	13.8	1376.78	2,6,10-trimethyldodecane
10.6	1077.27	C4-benzene	14.1	1404.68	dimethylnaphthalene
10.7	1077.27	C4-benzene	14.2	1419.84	C2-naphthalene
10.8	1085.71	C4-benzene	14.3	1423.18	dimethylnaphthalene
10.9	1085.71	?	14.4	1430.69	tetramethylindan
10.10	1092.01	C4-benzene	14.5	1442.48	ethylnaphthalene
11.1	1106.76	C4-benzene	14.6	1454.78	?
11.2	1116.20	C4-benzene	14.7	1462.59	2,6,10-trimethyltridecane
11.3	1120.50	C4-benzene	14.8	1470.92	dimethylnaphthalene
11.4	1138.72	?	15.1	1505.25	isopropylnaphthalene
11.5	1144.07	C5-benzene	15.2	1522.75	butyltetrahydronaphthalene
11.6	1150.00	?	15.3	1526.76	trimethylnaphthalene
11.7	1152.24	C4-benzene	15.4	1531.69	trimethylnaphthalene
11.8	1178.80	?	15.5	1548.10	trimethylnaphthalene
11.9	1183.19	dimethylindan	15.6	1550.92	trimethylnaphthalene+alkane
11.10	1187.71	dimethylindan	15.7	1563.38	C3-naphthalene
11.11	1189.95	dimethylindan	15.8	1567.11	C3-naphthalene
11.12	1193.24	dimethylindan	16.1	1650.00	2,6,10-trimethylpentadecane
11.13	1198.34	dimethylindan	16.2	1672.91	C4-naphthalene + alkane
12.1	1210.34	?	16.3	1689.17	C4-naphthalene

a Peak code as for Figure 4-25. * Tentative identification.

As previously found for low-temperature pyrolysis studies on Condor (Hutton et al., 1986) the formation of alkenes during step-wise retorting did not proceed until a temperature greater than 350°C had been attained. The authors attributed the absence

of alkenes to efficient hydrogen-capping of alkyl radicals, with the hydrogen required to prevent their formation donated by the decomposing (aromatising) kerogen. Saxby (personal communication) has suggested that the relatively late formation of alkenes may also be facilitated by the decomposition of siderite, abundantly present in Condor shale. This labile carbonate decomposes at relatively low temperatures and the generation of CO_2 may promote the rapid expulsion of alkanes without major cracking (disproportionation) processes occuring. During any phase of abundant gas (vapour) release the residence time of primary pyrolysis products should be reduced by their expulsion through microscopic vents. The formation of these vents serves to minimise secondary reactions generally by reducing the tortuosity of the pathway the products follow out of the shale.

With reference to GC-MS data and profiles **1** - **7** (Figure 5-5, 5-6) it is possible to describe accurately the production of individual volatile components and the qualitative and quantitative changes which occur in Condor retort oil composition (chromatographable fraction) with progressively increasing temperature.

As the temperature rises volatile free and adsorbed components (bitumen distillates) are released up to about 350°C (**1**). These are the compounds normally found in solvent extracts from the raw shale (alkanes, isoprenoids) although alkyl-substituted benzenes, possibly derived from mild thermal degradation of aromatic higher-plant material were also found. As the temperature increases further, thermally-labile precursors produce those compounds found in high concentrations in the transition from bitumen constituents to products formed at moderately-high retort temperatures (350-375°C) - (profiles **2** and **3**). In particular these include prist-1-ene and prist-2-ene in proportions dependent on the catalytic effect of the mineral matrix (Regtop et al., 1986). At higher temperatures cracking reactions predominate and both alkanes and alkenes are formed (**4** - **6**). Sequential profiles resemble those of raw oil chromatograms and show progressively higher abundances of low carbon number 1-alkene/ alkane doublets. Coburn and Campbell (1977) have shown that ratios of the latter correlate with retort oil yield. The relative increase in 1-alkene concentration for the profiles supports a formation from high-temperature cracking reactions dependent on residence times. Literature data suggests that 1-alkenes isomerise,

reduce, or coke to a degree that is a function of the time they spend in the condensed or adsorbed phase before leaving the retort (Coburn and Campbell, 1977; Lambert et al., 1984; Regtop et al., 1985).

As the temperature rises above 450°C oil production diminishes and the influence of mineral-catalysis subsides. Retort products formed become more dependent on the thermocatalytic influence of the hydrogen-depleted and aromatising carbonaceous residue (char), which coats the inorganic matrix. The overall effect is one which favours the formation of aromatic compounds (e.g. alkyl-substituted benzenes and naphthalenes), although 1-alkene and alkane components are still prominent (7). Detailed GC-MS and retention data for components in profile 7 are given in Figure 5-7 and Table 5-4.

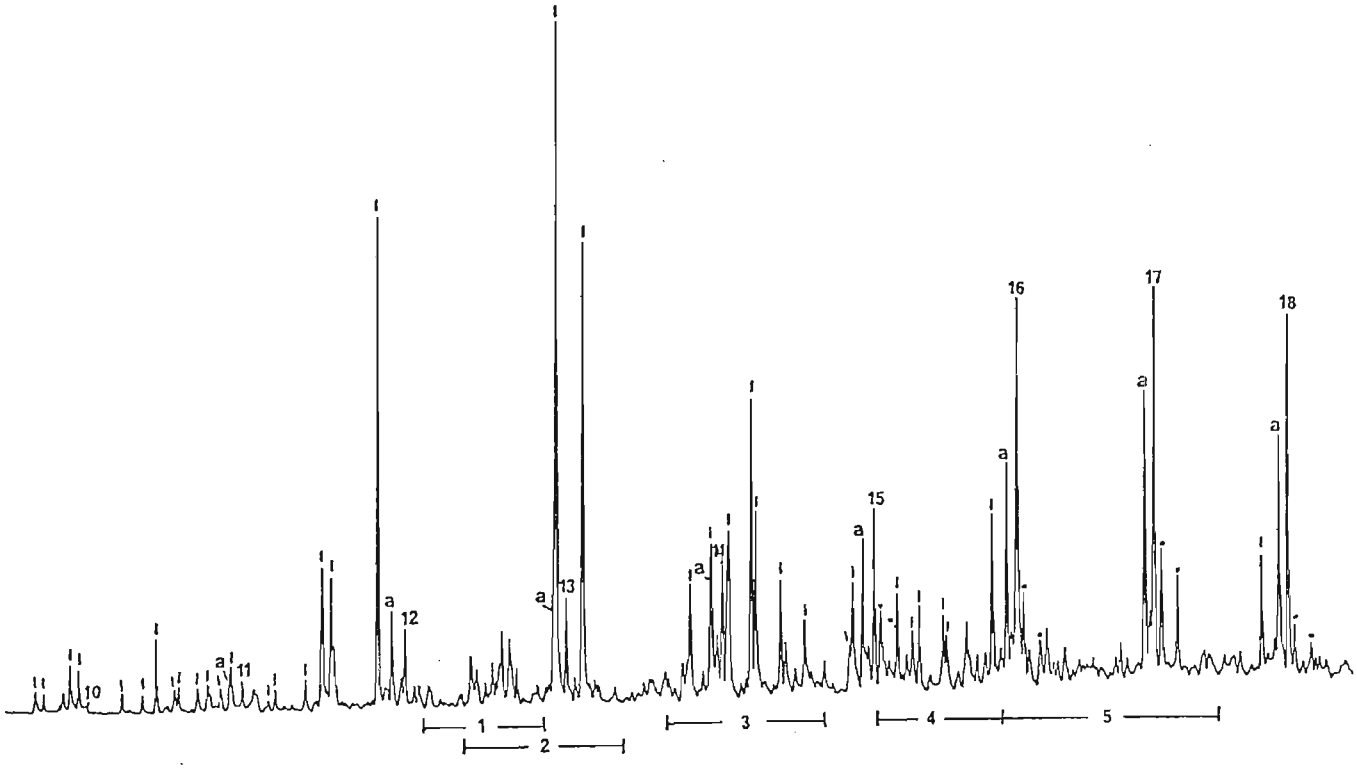

Figure 5-7. Expanded section of gas chromatogram (FID-trace 7). Carbon numbers for alkanes as indicated; other notation as in Figure 5-4. Retention index and compound identification for peaks denoted ı given in Table 5-4. Components denoted · are 2-alkenes; regions numbered 1-5 represent elution areas of C2-indans (1), C2-indenes (2), C2-naphthalenes and C2-benzothiophenes (3), C3-naphthalenes (4) and C4-napthalenes (5). Details for 1 to 5 are given in Figures 5-8 - 5-10.

TABLE 5-4. Retention index and identification of (minor) components denoted by in Figure 5-7. Components listed were identified from complete mass spectra.

Pk.No.[a]	R.I.	Compound Name	Pk.No.[a]	R.I.	Compound Name
9.1	960.41	C3-benzene	12.1	1293.59	2-methylnaphthalene
9.2	967.18	C3-benzene	13.1	1310.50	1-methylnaphthalene
9.3	987.12	benzonitrile	13.2	1379.52	biphenyl
9.4	994.21	C3-benzene	13.3	1392.75	dimethylbenzothiophene
10.1	1022.31	C3-benzene	14.1	1404.30	dimethylnaphthalene
10.2	1035.22	indane	14.2	1419.19	ethylnaphthalene
10.3	1043.91	indene	14.3	1422.34	dimethylnaphthalene
10.4	1055.42	C4-benzene	14.4	1438.83	ethylnaphthalene
10.5	1058.09	C4-benzene	14.5	1454.40	ethylnaphthalene
10.6	1070.13	C4-benzene	14.6	1483.51	phenylfulvene
10.7	1077.16	C4-benzene + methylindane	14.7	1485.78	methylbiphenyl
			15.1	1515.46	dibenzofuran
10.8	1085.62	C4-benzene + toluonitrile	15.2	1515.89	C3-naphthalene + C2-biphenyl
10.9	1092.24	toluonitrile	15.3	1524.64	C3-naphthalene
11.1	1116.18	C4-benzene	15.4	1547.14	C3-naphthalene
11.2	1120.34	C4-benzene	15.5	1549.75	C3-naphthalene
11.3	1138.65	methylindane	15.6	1582.14	fluorene
11.4	1148.67	methylindene	17.1	1779.82	phenanthrene
11.5	1154.52	methylindene			
11.6	1183.16	naphthalene			

a Peak code as for Figure 4-25.

It is unlikely that the aromatic compounds are formed from a unique source, rather than from abundant precursors which require these high temperatures for their formation. It seems plausible that they are derived from a combination of dehydrogenation aromatisation reactions involving residual aliphatic moieties which are exposed to the combined thermo -catalytic effects of high temperature and char. The relatively high concentrations of methylindenes, naphthalene and methyl- and dimethylnaphthalenes are consistent with their prominence in the diaromatic fractions of neutral oil from Condor (Rovere, 1986). They were also the most abundant components in the respective fractions isolated from Duaringa neutral shale oil. Other less volatile aromatics (fluorene, phenanthrene) are also abundant in profile **7**, while less abundant compounds containing greater numbers of fused aromatic rings would be obscured in the chromatogram or remain in the shale residue.

Lambert et al. (1984) have used NMR techniques to study the conversion of aliphatic to aromatic carbon during the pyrolysis of Rundle oil shale. They found that the yield of

aromatic carbon in the retort oil increased with temperature up to 475°C, whereas that of the residues appeared to be independent of temperature above 400°C. They demonstrated that processes such as aromatisation (oil and residue) are dependent on retort design, reaction temperature and residence times, with all three parameters evidently able to influence the degree of secondary reactions. Surprisingly they found that as much as 25 % of the original aliphatic carbon is aromatised (oil and residue) when shale is pyrolysed at a standard retorting temperature of 500°C.

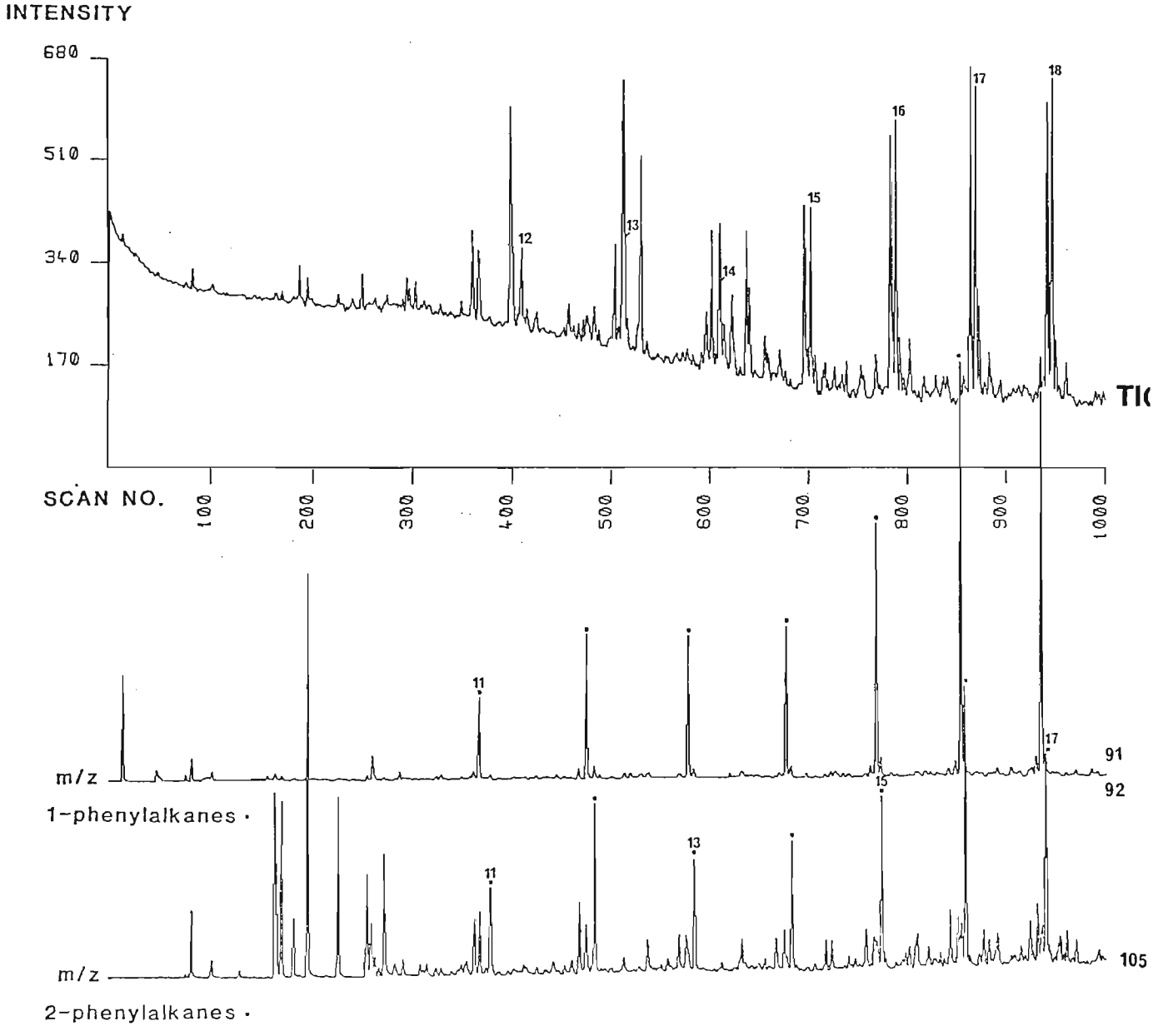

Figure 5-8. Section of the total-ion-current profile (TIC) of sample 7 from the sequential retorting of raw shale from Condor (Brown unit) and corresponding fagment-ion plots characteristic for 1-phenylalkanes (m/z =91 and 92) and 2-phenylalkanes (m/z = 105). Carbon numbers for alkanes (TIC) and phenylalkanes as indicated (e.g. phenylheptane is denoted by **13**).

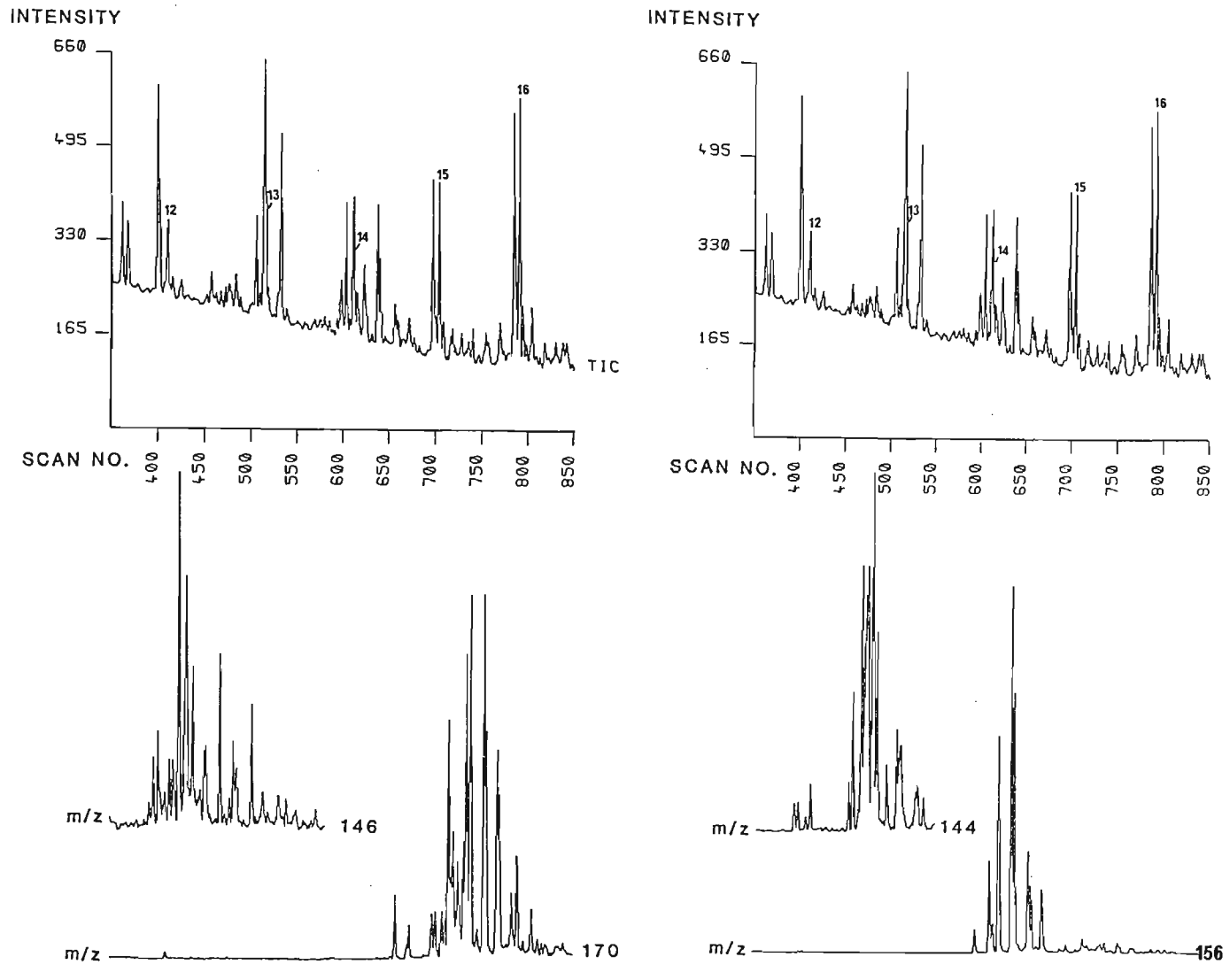

Figure 5-9. Section of the total-ion-current profile (TIC) of sample 7 from the sequential retorting of raw shale from Condor (Brown unit) and corresponding fagment-ion plots characteristic for C2-indans (m/z = 146 -region (1) Fig. 5-7), C2-indenes (m/z = 144 -region (2) Fig. 5-7), C2-naphthalenes (m/z = 156 - region (3) Fig. 5-7) and C3-naphthalenes (m/z = 170 - region (4) Fig. 5-7). Other notation as for Fig. 5-8.

Relative quantities of all of the chromatographable components contained in the various fractions corresponding to particular retort temperatures were calculated using normalised total peak areas (Table 5-5, Figure 5-11). The above GC-MS analyses and earlier work on the Duaringa deposit show that these volatile components comprise those compounds isolated from the open-column procedure which were subsequently amenable to analysis by GC and GC-MS. For Duaringa they comprised ca. 70% of the raw retort oil. For Condor this figure is ca. 80 %, based on quantitative data for volatile components

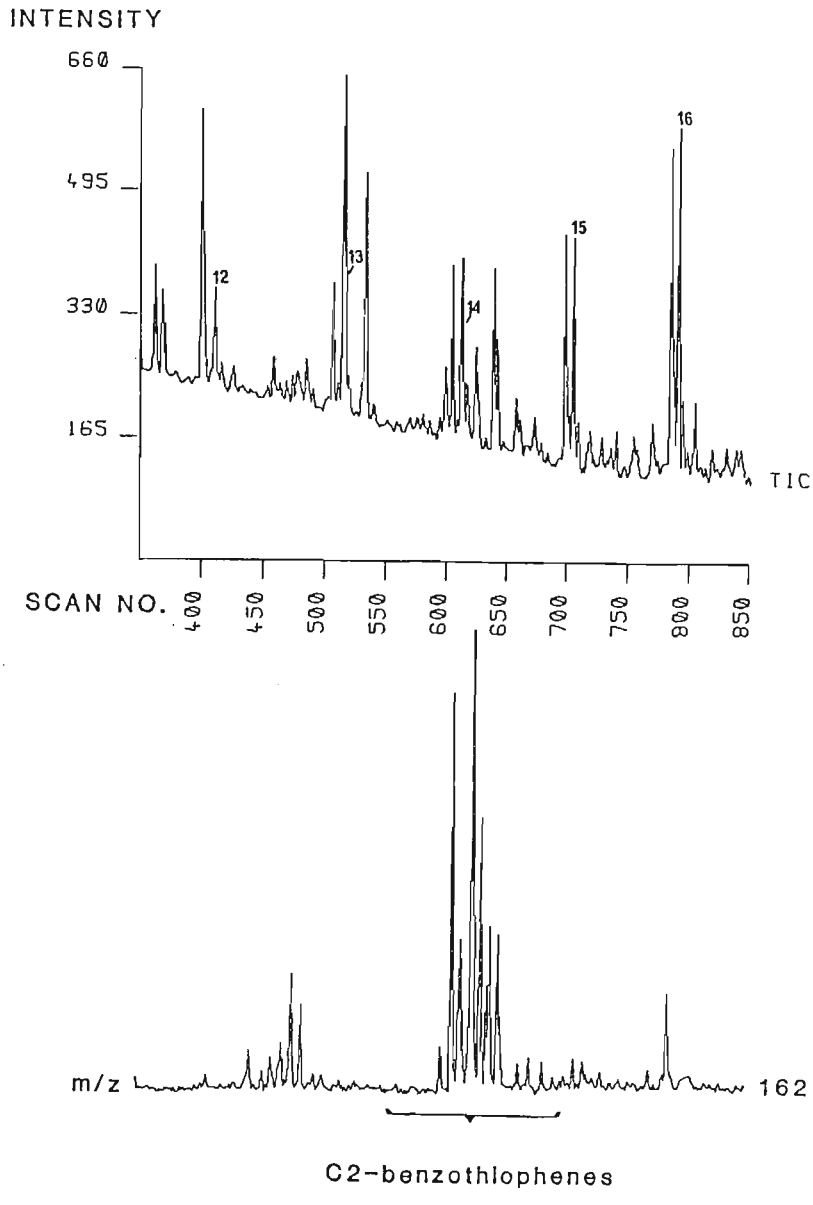

Figure 5-10. Section of the total-ion-current profile (TIC) of sample 7 from the sequential retorting of raw shale from Condor (Brown unit) and corresponding fagment-ion plots characteristic for benzothiophenes (m/z = 162 - region (3) Fig. 5-7). Other notation as for Fig. 5-9.

(open-column fractions 1- 19) published by Rovere et al. (1983). Relating the data from Table 5-5 to the latter shows that ca. 9% of the Condor FA retort oil is formed at temperatures < 350°C (samples 1 and 2) and comprises primarily bitumen distillates and low temperature pyrolysis products. The bulk of the oil (ca. 70%) is formed over the temperature range 350-450°C (samples 3 to 6) and this fraction is dominated by alkanes and alkenes in relative proportions dependent on retort temperature. The balance of the volatile material in the FA oil (< 1%) is produced at temperatures greater than 450°C and comprises a mixture of (alkyl-substituted) aromatic compounds and residual aliphatics (mainly > C_{16}).

TABLE 5-5. Quantitative data for gas-chromatographable retort products (> hexane) obtained at various temperatures during the retorting of raw oil shale from the Condor brown unit. (* See text for details. ** Estimate).

SAMPLE	TEMP. RANGE (°C)	TIME (min)	% OF TOTAL CHROMATOGRAPHABLE MASS*
1	30 - 350	30	8.4
2	350 - 350	15	2.8
3	350 - 375	25	17.9
4	375 - 400	25	24.5
5	400 - 425	25	41.3
6	425 - 450	25	4.7
7	450 - 475	25	0.4
8	475 - 500	25	0.1**

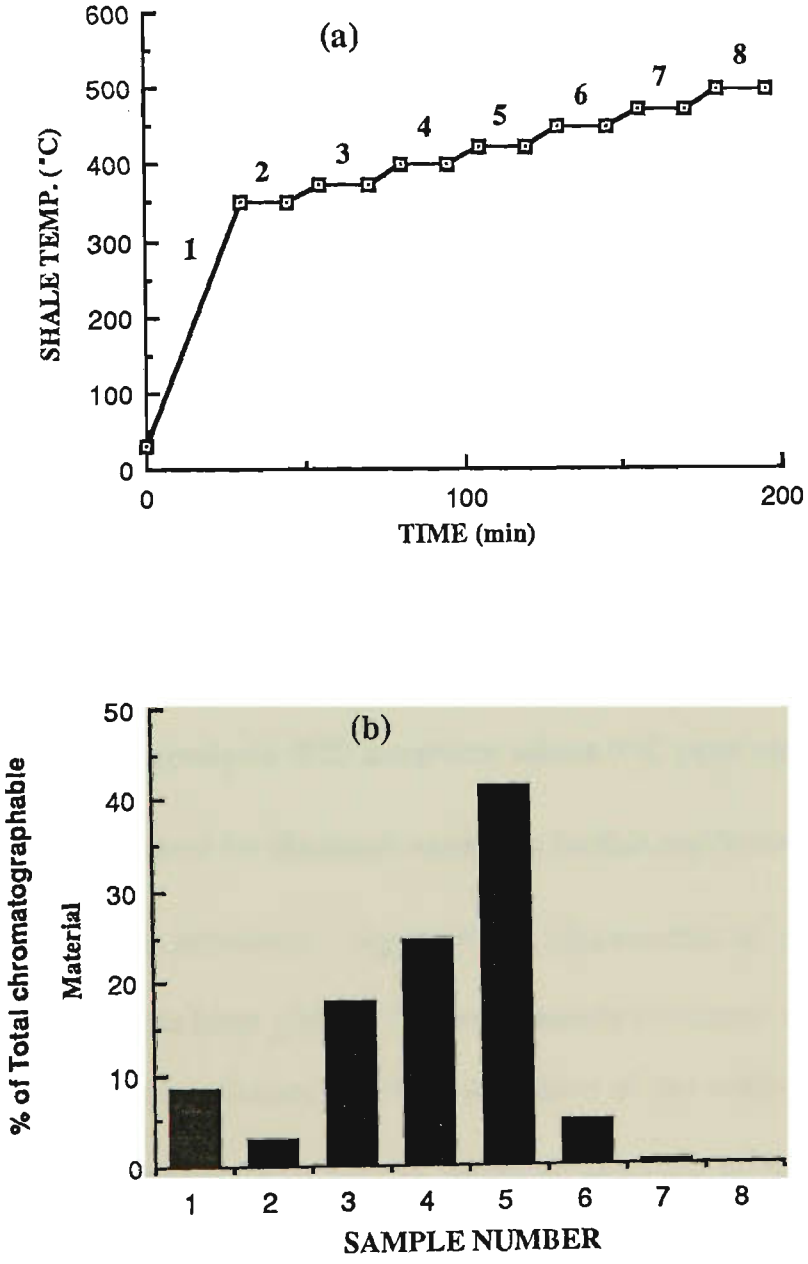

Figure 5-11.
Shale temperature-profile and corresponding sample number (a) and percent mass distribution of total gas-chromatographable material obtained from retorting Condor raw oil shale (b). Data for (b) is based on gas-chromatography data for volatile condensable retort products (> hexane) obtained using the retort profile depicted in (a) - see text for details.

5.1.2 Rapid assessment of hydrocarbon generating potential and kerogen type of selected Australian oil shales using a modified CDS-150 pyroprobe.

The ability of the pyrolysis-FID procedure to differentiate between oil shales containing kerogen of different types and mixtures on the basis of hydrocarbon-generating capacity (oil and gas) was demonstrated in section 4.5 for samples from the Duaringa deposit. It was also suggested that pyrolysis-FID data, both in isolation and in conjunction with other relevant information should predict FA oil yields, kerogen content and correlate positively with other chemical and petrographic data. The same pyrolysis-FID procedure was extended to a suite of Australian and overseas oil shales (Crisp et al., 1987). Those from the Green River Formation and the Paris Basin (Toarcian) are particularly important in this context since they are shales comprising definitive type I and II kerogens (Durand and Monin, 1980). An Australian brown coal sample (Morwell) was also included to characterise hydrocarbon production from a sample containing kerogen of type III. In what follows the term oil shale will continue to be used (loosely) as a matter of convenience to describe all of the samples examined.

Raw shale from Duaringa 5391-C, which had previously been shown to give very reproducible pyrolysis-FID data (cf. 4.5) was used as a reference sample and analysed immediately prior to and after each set of other shales investigated. For the range of samples studied pyrolysis -FID integrator values (GC peak areas $\mathbf{P_1}$, $\mathbf{P_2}$ and temperature $\mathbf{T_{MAX}}$) were adjusted for the small variations (within and between days) which occured in the data for the reference. Appropriate adjustments to sample areas P_1 and P_2 to compensate for the latter yielded a set of relatively consistent area values for each sample which were further adjusted for the initial mass of the various raw shales used (ca. 2-4 mg). These normalised data for the randomly analysed oil shales (i.e. P_2 areas per unit mass of raw shale - arbitrary units) were related to the kerogen content (determined gravimetrically - Crisp et al., 1987) and each sample was subsequently categorised as containing organic matter with a capacity to generate high, medium or low quantities of

hydrocarbons (oil and gas) under identical experimental conditions. Typical pyrolysis -FID data for a representative of each of the three categories and Mt. Coolon are given in Figure 5-12.

Grade 1: Glen Davis

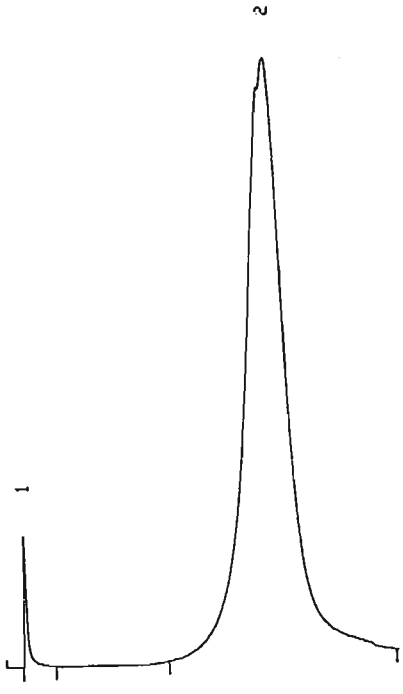

Grade 2: Camooweal

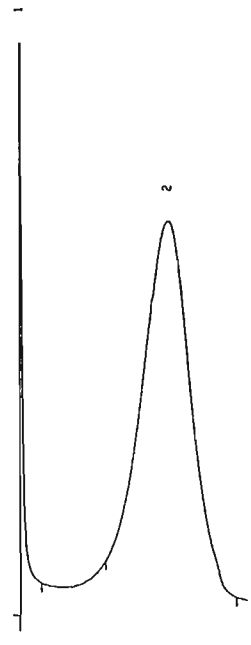

Grade 3: Morwell (brown coal)

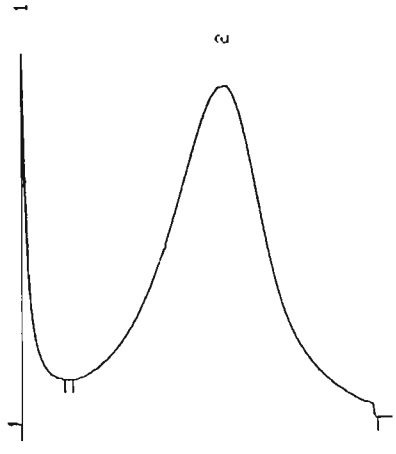

Grade 2: Mt. Coolon

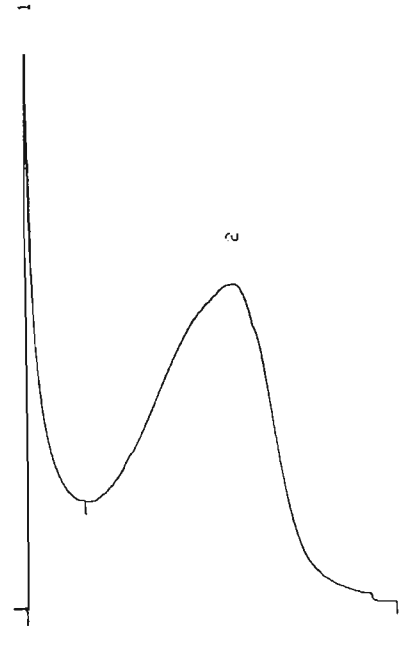

Figure 5-12. Typical pyrolysis-FID profiles for raw shales having relatively high (grade 1), medium (grade 2) and low (grade 3) hydrocarbon-generating potentials. The Mt. Coolon sample is a high-wax shale and the hydrocarbon production profile suggests a relatively early evolution of hydrocarbons from this source. All samples were heated as received from 300 - 700°C at 25°C min^{-1}.

The Mt. Coolon sample has a high transformation ratio (18.8), which is consistent with the relatively large quantities of solvent-extractable bitumen found in this sample (ca.10 mass % of raw shale - Chaffee et al., 1984). The extensive first peak (P_1) in its pyrolysis-FID profile is derived initially from this source, with continued early hydrocarbon release possibly derived from abundant wax esters known to occur in the shale (Chaffee et al., 1984). This illustrates the ability of the modified pyroprobe to display relative variations in the temperature-hydrocarbon production relationship during pyrolysis. This feature makes the device extremely useful for fundamental retorting studies involving the effects of changes in heating rates, maximum retort temperatures and variations in the composition of sweep gases. The procedure also offers the possibility of examining any profile region of interest by introducing the corresponding pyrolysate directly onto a capillary column through a high-temperature switching valve. Volatile constituents may then be analysed using a variety of GC or GC-MS procedures.

The range of values for the generating potential, defined here as (P_2 / mass % kerogen in the raw shale) varied from 32 to 226, with the reference samples characterised by 185 (Green River), 112 (Toarcian) and 32 (Morwell) respectively. Each of the oil shales was categorised relative to these samples as containing kerogen with a hydrocarbon generating potential of grade 1 (high), 2 (medium) or 3 (low). These grades are analogous to characterisations based on hydrocarbon production criteria for kerogens of type I, II and III since the latter types are known to produce relative hydrocarbon yields (oil and gas per unit mass of kerogen) of ca. 75, 50 and 30% respectively (Durand and Monin, 1980). A major difference between these classifications based on relative hydrocarbon production criteria (shale grade and kerogen type) is the fact that the shale grade is determined directly from the raw sample and reflects mineral matrix influences (if any) which occur during pyrolysis. Consequently it is more relevant to retorting studies. Pyrolysis-FID and various other relevant chemical and petrographic data for each shale analysed are listed in Table 5-6.

The range of values for shale generating potentials listed in Table 5-6 exhibits a relatively smooth transition between the various production categories. This lack of clear

Table 5-6. Pyrolysis-FID and other chemical and petrographic data (columns 1-13) obtained for the raw oil shale samples listed. For column entries see key at the foot of the table. Other details are given in the text.

SAMPLE	1	2	3	4	5	6	7	8	9	10	11	12	13
1. Glen Davis	75	257	15823	1.6	650	211	1	1.46	109.5	56.2	70	10	0.32
2. Yaamba	20	41	4090	1.0	625	204	1	1.61	32.2	17.4	36	7	0.27
3. Stuart K. Cr.	36	79	7051	0.9	625	196	1	1.64	59.0	27.0	69	3	0.32
4. Green River	18	157	3338	4.5	622	185	1	1.55	28.0	16.5	15	5	0.19
5. Condor Br.	11	43	2033	2.1	622	185	1	1.44	15.8	8.0	31	1	0.30
6. Alpha	80	233	14343	1.6	627	179	1	1.45	116.0	65.1	75	19	0.27
7. Rundle R.C.	23	76	3719	2.0	622	162	2	1.64	37.7	14.4	43	2	0.27
8. Nagoorin S.	16	32	2593	1.2	620	162	2	1.46	23.4	9.5	20	2	0.31
9. Byfield	13	61	2033	2.9	610	156	2	1.36	17.7	7.5	28	4	0.40
10. Rundle M.C.	31	88	4819	1.8	620	155	2	1.57	48.7	17.9	51	5	0.26
11. Lowmead	14	75	1965	3.7	622	140	2	1.38	19.3	9.0	24	2	0.31
12. Joadja	79	124	11160	1.1	640	141	2	1.39	109.8	48.0	67	10	0.40
13. Duaringa	10.5	26	1421	1.8	619	135	2	1.62	17.0	4.9	27	1	0.19
14. Irati	18	249	2196	10.2	590	122	2	1.31	23.6	7.7	55	7	0.46
15. Julia Creek	12	69	1527	4.3	587	127	2	1.21	14.5	5.4	42	4	0.50
16. Camooweal	4	53	447	10.5	600	112	2	1.25	5.0	2.1	12	6	0.41
17. Tasmanite	15	91	1689	5.1	620	112	2	1.53	23.0	14.2	31	0	0.52
18. Toarcian	14	27	1566	1.7	597	112	2	1.23	17.2	4.6	18	1	0.46
19. Mt. Coolon	50	1060	4580	18.8	595	92	2	1.12	56.0	17.4	38	29	0.44
20. Kentucky S.	19	102	1788	5.4	583	94	3	1.03	19.6	5.9	70	2	0.35
21. Nagoorin Carb.	38	133	3200	4.0	597	84	3	1.01	38.4	9.8	18	57	0.41
22. Nagoorin Br.	16	29	1224	2.3	607	77	3	1.17	18.7	6.2	13	5	0.37
23. Stuart H.C.	33	17	2486	0.7	615	75	3	1.04	34.3	8.2	26	32	0.32
24. Kentucky C.	16	65	1146	5.4	597	72	3	1.06	17.0	4.6	17	3	0.34
25. Condor Carb.	47	69	2931	2.3	607	62	3	0.86	40.2	6.2	5	56	0.59
26. Morwell	82	222	2621	7.8	580	32	3	0.81	66.4	7.8	7	93	0.26

Abbreviated samples: Stuart K. Cr. = Stuart Kerosene Creek member; Condor Br. = Condor Brown Unit; Rundle R.C. = Rundle Ramsay Crossing member; Nagoorin S. = Nagoorin South; Rundle M.C. = Rundle Munduran Creek member; Duaringa = Duaringa 5391-C; Kentucky S. = Kentucky Sunbury shale; Nagoorin Carb. = Nagoorin Carbonaceous; Nagoorin Br. = Nagoorin Brown; Stuart H.C. = Stuart Humpy Creek member; Kentucky C. = Kentucky Cleveland member; Condor Carb. = Condor Carbonaceous.

COLUMN

1 **% kerogen** (w/w) - (Crisp et al., 1987).
2 normalised pyrolysis-FID area P_1 (arbitrary units per unit mass raw shale).
3 normalised pyrolysis-FID area P_2 (arbitrary units per unit mass raw shale).
4 transformation ratio ($P_1/ P_1 + P_2$)
5 T_{MAX}
6 hydrocarbon generating potential (P_2/ **mass % kerogen**).
7 oil shale **grade** (capacity to produce hydrocarbons (oil and gas).
8 atomic ratio **H/C** - (Crisp et al., 1987).
9 **%K x H/C**
10 **FA oil yield** (mass %) - (Crisp et al., 1987).
11 Liptinite macerals (volume % of whole shale) - (Crisp et al., 1987).
12 other macerals (volume % of whole shale) - (Crisp et al., 1987).
13 vitrinite reflectance (R_o**max**).

delineation between the grades is not surprising however, since similar overlap problems occur for other type-based characterisations of oil shale kerogens, with many exhibiting features common to types I and II. However, with respect to hydrocarbon generating potential of the shales the question of kerogen type is largely academic, since the main criterion for the purpose of resource evaluation is the relative hydrocarbon (oil) yield. The latter is clearly expressed in the values listed in Table 5-6 (column 6) but any positive resource assessment (based on relatively high values) needs to be followed by pyrolysis-GC or an analysis of whole retort oil to obtain a comprehensive chemical characterisation of the crude. Collectively these procedures are required to establish the potential of the raw oil as a suitable feedstock for refining purposes.

The normalised P_2 value for the reference sample Duaringa 5391-C listed in Table 5-6 is 1421. This is lower than that given earlier in Table 4-8 because the GC-electrometer gain was reduced slightly to accommodate the wide range of sample values encountered during the analyses. This variation does not introduce any problems since only relative areas, with respect to this reference sample, are important for comparative purposes. The Mt. Coolon sample (19) was grouped with the grade 2 shales because decomposition of its high-wax kerogen produced a rather broad profile with poorly defined peaks (Figure 5-12). Its total generating potential appropriately based on the sum of the areas for P_1 and P_2 is 113. This value places it into the grade 2 production category and will be used for all subsequent calculations.

For raw shale, the ability to produce hydrocarbons (oil and gas) is governed by kerogen quantity and quality (type). The latter is determined by the compositon of macerals comprising the organic matter and is reflected in its elemental composition, most notably in atomic ratios H/C. For kerogen of type I, II and III these ratios are ca. 1.6, 1.3 and 0.9 respectively (Durand and Monin, 1980). Consequently there should be a high positive correlation between data which measure or are dependent on the above parameters. In particular, the normalised P_2 areas (Table 5-6 - column 3) should correlate with:

1) - FA oil yields

2) - petrographic data (i.e. maceral content and composition)

3) - elemental analysis data - particularly atomic H/C ratios.

These and other possible correlations arising from the data in Table 5-6 were initially examined using the MINITAB statistical computer program by generating a correlation matrix for columns 1-13. Any underlying relationships were analysed in more detail and, where required, data were converted into a more relevant format. Each of the various correlations will be discussed in detail below.

Clearly the most important values required for the assessment of a potential oil shale deposit are the FA oil yields since these data determine the commercial viability of the resource. The ability of the pyrolysis-FID procedure to assess these yields depends on the extent to which the approach successfuly simulates retort conditions and is reflected in the agreement between predicted oil yields and those actually found using the standard Fischer assay. As expected the relative oil shale hydrocarbon potential (column 3) correlated positively with the FA oil yields for the corresponding shales (column 10) for the entire range of samples analysed. For all grades of shale the relationship between FA oil yields (mass % of raw shale) and the normalised P_2 values (area per unit mass of raw shale - arbitrary units) was calculated using a least-squares regression analysis of the relevant data. Figure 5-13 shows a plot of the correspondence between the latter and gives the derived first-order linear equation.

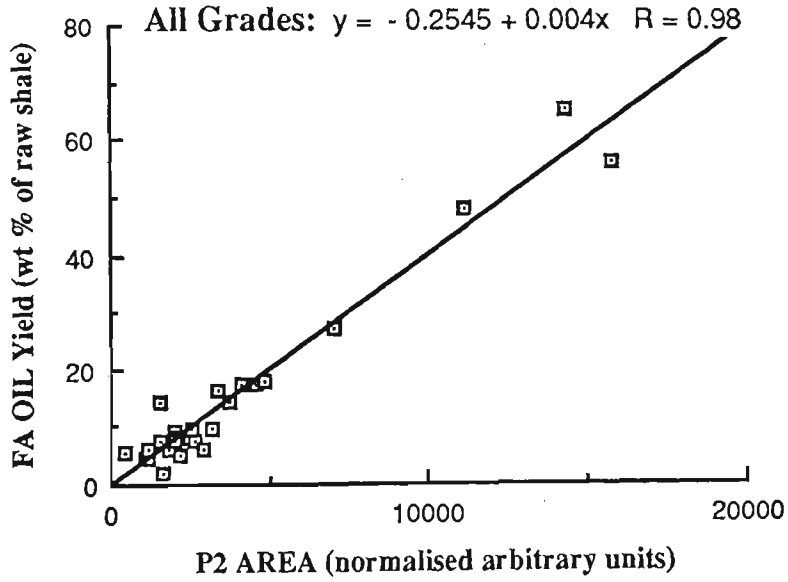

Figure 5-13. Plot of the correspondence between FA oil yields and P_2 areas for the range of oil shales listed in Table 5-6. The equation relating the two variables was derived by least-squares regression analysis of the relevant data (Table 5-6: column 10 v column 3).

The relationship is characterised by a high correlation coefficient (R = 0.98) and, as required, the plot does not go through the origin since the FA assay gives only recovered oil yields, whereas non-condensable hydrocarbon gases such as CH_4 and C_2H_6 are also detected and recorded by the pyrolysis-FID procedure.

As expected, the equation which correlates FA oil yield with normalised P_2 areas varies considerably if calculated for those samples belonging to one of the restricted production categories. Although grades 1 and 2 are separately governed by virtually the same equation as that derived for the entire range of shales, the data for grade 3 samples are widely scattered and the correlation coefficient has values of 0.98, 0.98 and 0.78 for grades 1, 2 and 3 respectively. For the grade 3 shales these variations illustrate the combined effects on hydrocarbon yields (oil and gas) of differences in hydrocarbon production mechanisms and kerogen type (mixtures). The wide scatter for these data makes the equation in Figure 5-13 at best only a crude approximation for this category. This is not surprising however when it is considered that the maceral composition for these samples ranges from bituminite (70 mass % for Kentucky S) to virtually pure vitrinite (93 mass %) for the brown coal from Morwell. Evidently hydrocarbon production from these widely-differing organic materials cannot be expressed by a simple linear relationship. It should be noted however that the pyrolysis-FID procedure should still give relative hydrocarbon productions for different samples from the same grade 3 shale deposit (based on relative kerogen abundances in the raw shale) provided the maceral composition remains reasonably uniform.

The relationship between FA oil yield and P_2 areas relative to a given standard is most useful when the various normalised P_2 area values are expressed relative to that of the standard. Under these circumstances the equation for FA oil yield as a function of the P_2 areas ratios is independent of instrument parameters such as detector sensitivity or electrometer gain. Plots and equations derived from this approach are given in Figure 5-14 for the combined shales from grade 1 and 2, since these were found to be the groups which determine the underlying relationship for the entire range investigated. The first plot of the

figure includes the tasmanite sample (T) which was identified by the MINITAB program as having a marked influence on the slope (and intercept) of the equation. The given equation has a positive y-intercept, which corresponds to a situation of a 0.2 wt % FA oil yield without any pyrolysis-FID signal. This is clearly impossible and the data were re-analysed without this shale. Later correlations involving different parameters indicate

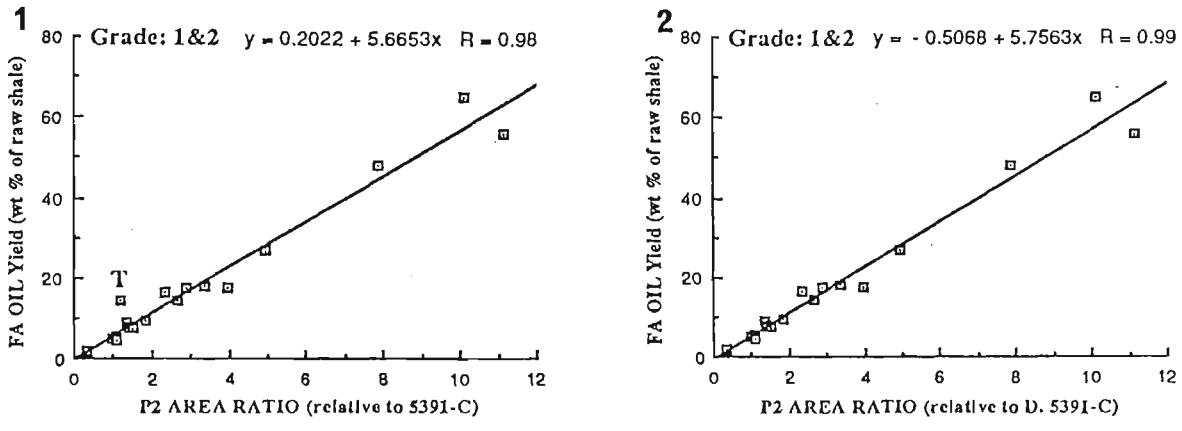

Figure 5-14. Plot of FA oil yield versus P_2 area ratios (relative to Duaringa 5391-C) for oil shales of grade 1 and 2 as listed in Table 5-6. Data were correlated with (**1**) and without (**2**) the tasmanite sample (**T**) - see text for details.

that the tasmanite sample analysed using the micro-scale approach was low in kerogen relative to the charge used for FA oil yield determinations. This sample heterogeneity justifies its exclusion at this stage for the purpose of deriving a consistent equation relating FA oil yield and total hydrocarbons (oil and gas) produced relative to the well-characterised standard from Duaringa 5391-C. The second plot (Figure 5-14) shows that the intercept is now negative (as required) and that the slope has only changed marginally along with an overall improvement in the correlation. The given equation may now be used to calculate predicted FA oil yields for any oil shale analysed under those experimental conditions used above. For grade 1 and 2 type shales these predicted yields (relative to Duaringa 5391-C or any other standard chosen from the grade 1 and 2 samples listed) should correspond closely to those actually found, provided the analysed sample is sufficiently homogeneous. The equation was used to calculate a FA oil yield for Duaringa 5391-C and for other

samples from the deposit, previously examined using pyrolysis-FID (Table 4-8). It should be noted here that even though Duaringa 5391-C was used as a standard it was not one of the samples analysed and reported in the compendium published by Crisp et al. (1987). It was chosen for that function because statistical analysis of its pyrolysis-FID data showed it to be a homogeneous sample giving extremely reproducible pyrolysis data. The latter is a fundamental requirement for any potential reference standard. Substituting a value of 1 for x in the equation for grade 2 shales: $y = - 0.5068 + 5.7563x$ (Figure 5-14: 2) gives a predicted FA assay oil yield of 5.2 mass % for raw shale from Duaringa 5391-C. This value is very close to that found using the standard Fischer assay procedure (4.9 mass %) and isothermal pyrolysis (5.04 mass % - section 4-6). Specific oil yield data predicted from the equation for the other Duaringa samples, previously analysed using a variety of procedures, will be examined in detail later in this section.

Hydrocarbon generating potentials should also correlate positively with maceral data since the latter directly determine kerogen content and type. Hutton (1985) has shown that shale oil yield, as determined by modified Fischer assay, is directly related to the volume per cent of alginite for selected Australian Rundle-type oil shales (i.e. characterised by abundant lamalginite). However any petrographic method is unlikely to give either accurate or reproducible results where poor contrast between the organic and mineral matter makes any quantitative maceral determination uncertain or where a large proportion of the oil is derived from two or more components with significantly different specific oil yields.

In Australian Tertiary oil shales or lamosites the dominant liptinite maceral is lamalginite, much of which is derived from the colonial green alga *Pediastrum*. Minor components include other liptinite macerals (such as telalginite, liptodetrinite and sporinite) and vitrodetrinite. In carbonaceous lamosites (> 5 vol% vitrinite) ulminite, corpohuminite, resinite and cutinite occur. Earlier work on the Duaringa samples has confirmed that liptinite macerals have higher specific shale oil yields than vitrinite macerals so that the bulk of hydrocarbons generated during any pyrolysis procedure will be predominantly derived from the former source where these are the major constituents. Where non-liptinite macerals are also relatively abundant the total hydrocarbon production will be predicted more accurately by additivity of the combined maceral production capacities, generated at

different rates of conversion from both sources (cf. section 4.6).

Although Hutton derived useful first-order equations for the Tertiary lamosite deposits he investigated, it is inappropriate to plot mass % FA oil yield data against volume % maceral data, unless the specific gravities for the mineral and organic phases in the shale are equal. Only in the latter case will petrographic volume % data approximate mass % data and FA oil yield (expressed as volume or mass per tonne of raw shale) plot linearly against volume % liptinite content. However, since the mineral phase is always denser than the kerogen, usually by an unknown amount, the relationship between oil yield (based on mass of raw shale) and volume % of liptinite (alginite) content is actually a quadratic equation. This is most easily visualised by examining the relationship between alginite content and FA oil yield for a hypothetical (ideal) deposit containing varying amounts of uniform kerogen (alginite) with an assumed density of 1g mL^{-1} within a uniform mineral matrix with a density of 2g mL^{-1} (say). If the shale oil production per gram of organic matter remains constant at 75% per unit mass of kerogen - (this is an appropriate conversion rate for type I kerogen) then for a 100g charge of dry shale containing varying amounts of alginite (volume % of raw shale) the retort oil produced from the hypothetical raw shale of the described type will yield oil (mass % of raw shale) in those quantities listed in Table 5-7.

Table 5-7. Relationship between liptinite content (vol % of raw shale), liptinite mass (mass % of raw shale) and FA oil yield (mass % of raw shale) for a hypothetical (ideal) oil shale sample containing varying amounts of kerogen of uniform composition and oil yield per unit mass of raw shale.

Liptinite Content[1]	Liptinite Mass[2]	FA OIL Yield[3]
0	0	0
10	5.26	3.95
20	11.11	8.33
30	17.64	13.23
40	25.00	18.75
50	33.33	25.00
60	42.86	32.14
70	53.85	40.38
80	66.66	50.00

1 (vol % of raw shale); **2** (mass % of raw shale); **3** (mass % of raw shale)

The variable differences in the liptinite content (vol % as seen under the microscope) and liptinite mass (mass %) listed in the Table arise from the difference between the densities of the organic and inorganic phases. Consequently the relationship between liptinite content (vol %) and FA oil yield is governed by a quadratic equation and for a given deposit is generally determined by the difference in density between the kerogen and mineral phase as well as the rate of conversion of organic matter to oil.

It is thus not surprising that Hutton (1985) found a poor correlation for interdeposit comparisons of oil yields and respective liptinite content (vol %). In particular he found substantial differences in the gradients of the linear equations expressing specific shale oil yields for the five deposits in terms of the latter. He suggested that these variations may be related either to the maturity of the sequences or to the abundance of telalginite. Where these differences are substantial they will undoubtedly have some influence on oil yield. However, the poor correlation and slope changes are not merely an expression of the differences between the composition of the organic matter from the various deposits (i.e. different rates of production of hydrocarbons per unit mass of kerogen) but also reflect interdeposit variations in the relative differences of densities between the organic and inorganic phases for each deposit. Oil yield data from Table 5-6 presented and discussed below supports a conclusion that for grade 1 and 2 shales the latter may well account adequately for the interdeposit differences found by Hutton. It should be noted that where the organic composition within a given deposit does not vary significantly, and where the mineral matrix remains relatively uniform, the FA oil yield may be approximated within these constraints by a first-order equation. This is illustrated in the ideal case for the data in Table 5-7 below. Figure 5-15**a**, which is a plot of FA oil yield versus liptinite content data (vol %) shows clearly that the equation is a quadratic (it should be noted that the equation would be linear if the FA oil yield data were given as shale oil yield per unit volume of shale rather than unit mass as is customary). However, by analysing the data using a least-squares linear regression procedure (although inappropriate for this case) the relationship is approximated by a linear expression (Figure 5-15**b**). This equation has a high correlation coefficient and is sufficiently accurate for maceral contents up to 40 vol % of liptinite for intraseam calculations of this hypothetical deposit. It should be evident from

this illustration that both the quadratic and linear equations will be influenced by changes in composition (density) of the mineral matrix even where the kerogen composition remains constant. In practice the deviation of the linear equation from actual values is obviously greater and Hutton (1985) obtained correlation coefficients of 0.91 - 0.96 for the oil yield and liptinite content (vol %) correspondences within the specific Tertiary lamosite deposits which he investigated. For the combined deposits the overall correlation was only 0.94.

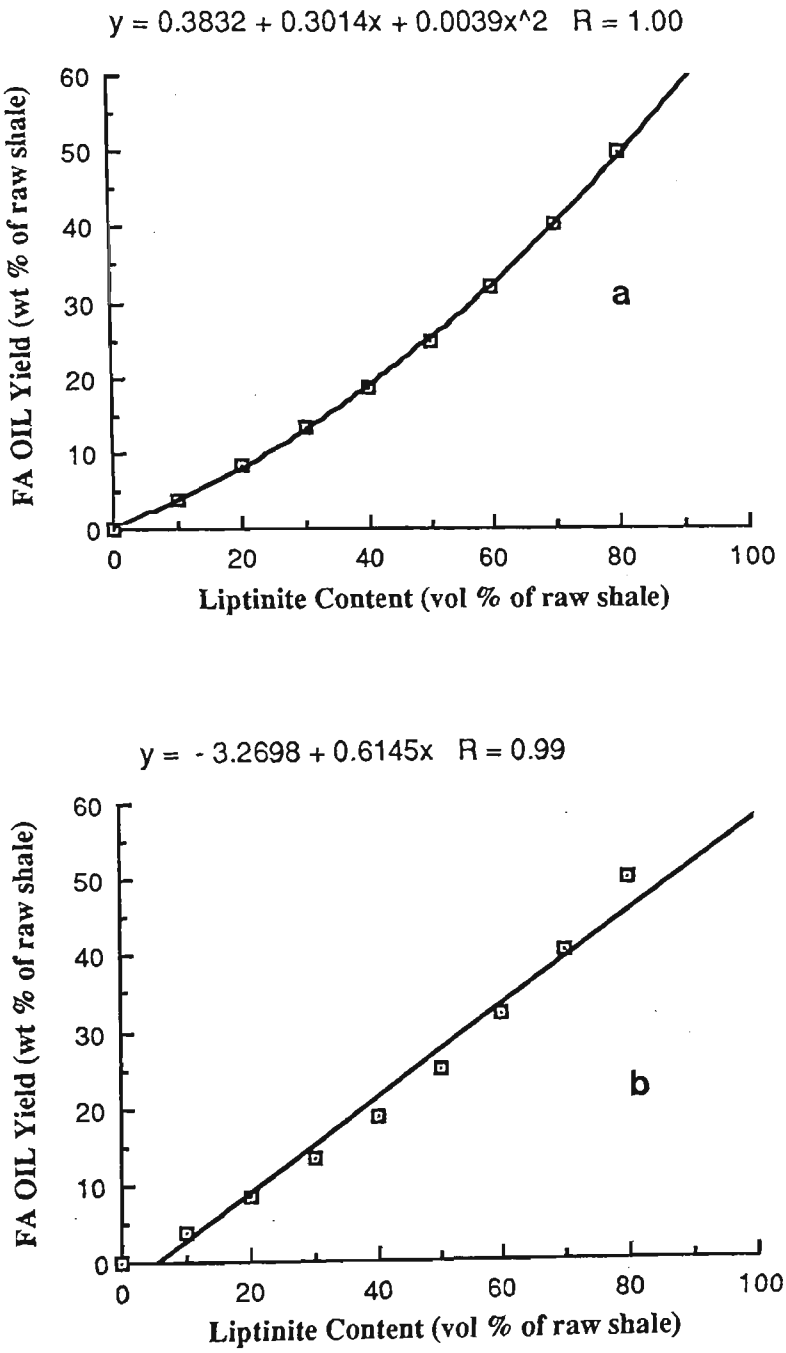

Figure 5-15. Relationship between FA oil yield (mass % of raw shale) and liptinite content (vol % of raw shale) for a hypothetical (ideal) deposit (see text for details on composition). Respective plots show the actual (quadratic) relationship which exists between the two variables (**a**) and the approximate linear equation derived by least-squares regression analysis of the data (**b**).

For the entire range of samples listed in Table 5-6, the correlation between FA oil yield and liptinite content (vol %) is very poor (Figure 5-16: **1**) due to the combined effects of the various influences discussed above. The correlation improves only slightly to 0.80 for samples within the combined grade 1 and 2 shales. However, it improves dramatically if the FA oil yield is related to the constituent maceral groups on the basis of their relative capacities to produce hydrocarbons per unit mass of kerogen. For specific maceral groups this hydrocarbon production capacity was calculated as the product:

(vol % maceral group / total maceral volume) x kerogen content (mass % of raw shale) x hydrocarbon production factor (oil and gas).

For liptinite macerals (type I kerogen) the production factor is ca. 75 % hydrocarbons (oil and gas) per unit mass of kerogen (Durand and Monin, 1980) and the capacity values are a general expression of hydrocarbon production from the shale in terms of the mass % maceral composition of its constituent kerogen.

Where liptinite macerals predominate (grade 1 and 2 shales) this capacity may be directly proportional to FA oil yields, although the latter is usually predicted more accurately by the total maceral production capacity of the raw shale. For the Duaringa deposit (cf. section 4.6) this was shown to be additive and expressed by the sum of the production capacities of the liptinite and non-liptinite maceral groups. For the oil shales studied the latter (mainly vitrinite - type III kerogen) were assigned a hydrocarbon production factor of 30% per unit mass of kerogen in the total capacity calculations. The correspondence between FA oil yield and liptinite or total maceral production capacities are given for grade 1 and 2 shales in Figure 5-16: **2 - 5**. It should be noted that the tasmanite sample (**T**) continues to show a relatively high oil production compared to other grade 2 shales. The high correlations between oil yields and both liptinite and total maceral production capacity for these interdeposit correlations of grade 1 and 2 shales show that the specific oil yields for the constituent maceral groups remain remarkably constant within each grade and appear practically unaffected by the wide variations in mineral matrix content (e.g. 20 and 96% respectively for Alpha and Camooweal) and compositon.

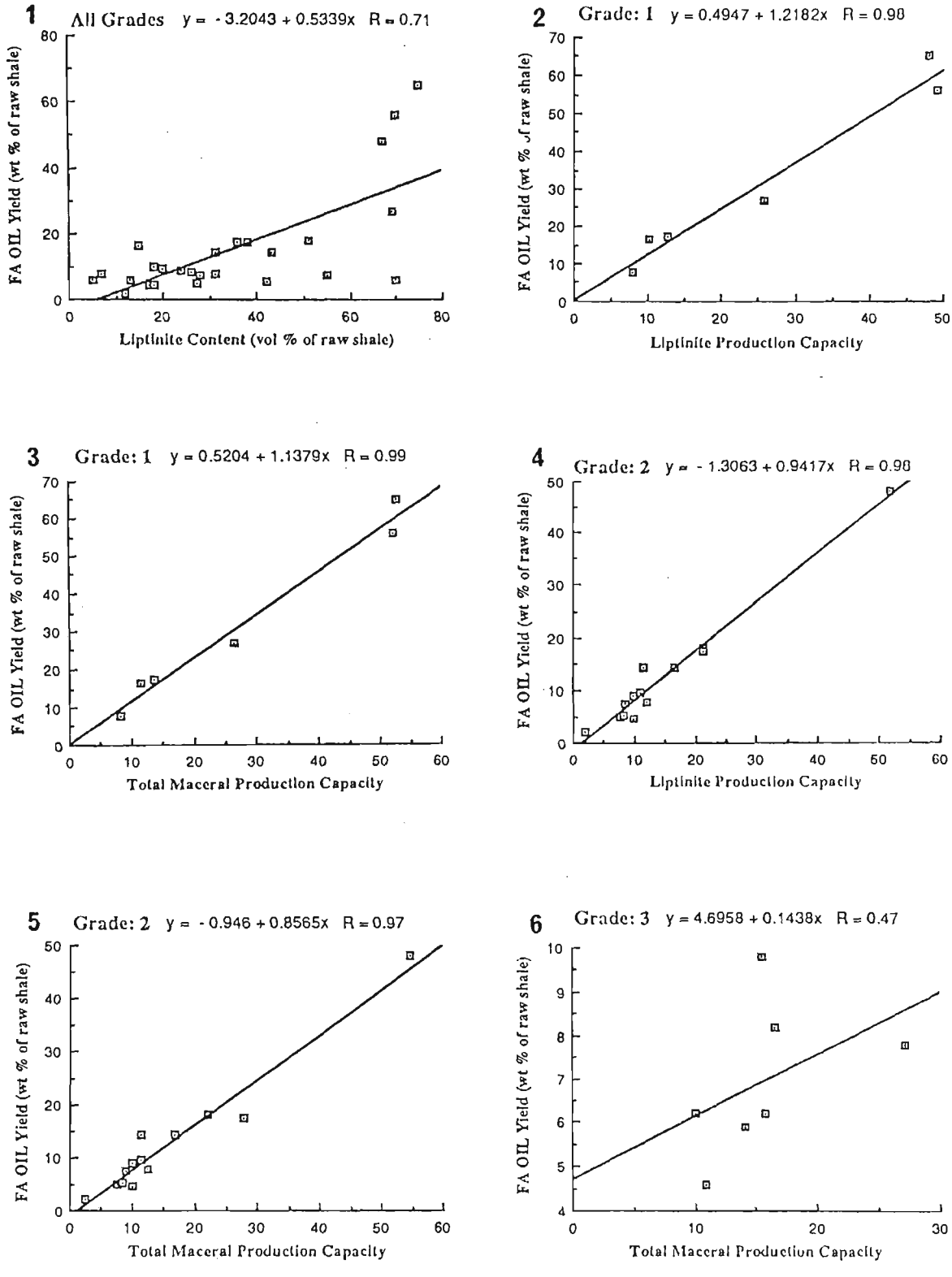

Figure 5-16.

Linear-regression analyses of the relationship between retort oil obtained by modified Fischer assay and the hydrocarbon production capacity of the liptinite and total maceral groups comprising the kerogen of the various shale grades. The definition of maceral hydrocarbon production capacities is given in the text.

The decrease in the gradient between grade 1 and 2 shales shows that the macerals comprising the former have a higher specific capacity to produce oil and is consistent with the generally higher H/C atomic ratios for kerogens within this group. A comparison between the two groups shows that hydrocarbon production from liptinite macerals belonging to grade 2 shales is ca. 77 % of that for the group 1 samples. This represents a relative hydrocarbon production factor of ca. 58 % per unit mass of kerogen for this maceral group and is close to the value of approximately 50 % given by Durand and Monin (1980) for kerogen of type II. For an analysis of the combined grade 1 and 2 raw shales the data are slightly more scattered (R = 0.96) particularly for shales with high kerogen contents. Note that the torbanite deposit at Joadja is categorised as a grade 2 shale. This classification is consistent with its low oil yield relative to the other torbanites (Alpha and Glen Davis) and its different kerogen composition, which is characterised by a relatively low atomic H/C ratio of 1.39.

The uniform oil production of the constituent maceral groups (per unit mass of kerogen) comprising grade 1 and 2 shales is evidently independent of variations in the composition and content of the mineral matrix and suggests that it should be possible to predict oil yields from petrographic data (vol % maceral composition of raw shale) in conjunction with relevant data for the density of the raw shale and the constituent maceral groups. For this purpose the above data suggest that grade 1 or 2 lamosites or torbanites may be characterised as comprising primarily two discrete kerogens having appropriate densities, which need to be determined accurately for each of the major maceral groups (lamalginite, telalginite and vitrinite). Petrographic data (maceral composition and content - vol %) may then be converted to kerogen type and mass values once the density of the whole rock has been established. The above work has shown that maceral mass data correlates well with FA oil yields since the production capacities for type I and II kerogens remain virtually invariant when oil yield is expressed as production per unit mass of maceral group comprising the various shales within the respective grades. For grade 3 shales the correlation is substantially worse (Figure 5-16: 6). The low correlation between the two variables is not surprising since this group comprises kerogen composed of organic matter ranging from 70% bituminite (Kentucky S.) to 93% vitrinite (Morwell

brown coal), with other samples also containing varying quantities of these and liptinite macerals. The scattered data in the graph show clearly that the former maceral groups produce hydrocarbons (oil) at different rates per unit mass of kerogen.

An even clearer and more direct indication of the production capacities (oil and gas) of constituent shale macerals is given by the correspondence between the latter and the respective normalised P_2 areas obtained from the pyrolysis-FID procedure. These relationships are depicted in Figure 5-17: **1-5** for the various shale grades. It is noteworthy that the correlations are substantially better for each grade than those obtained above for respective FA oil yield correspondences, both for liptinite and total maceral production capacity. In particular the differences in the gradients for grade 1 and 2 samples equate to a relative hydrocarbon production factor of ca. 52% for the total macerals comprising the kerogen of grade 2 shales. This figure is very close to the value of 50% associated with the relative hydrocarbon production capacity of type II kerogens by Durand and Monin (1980).

The increased linearity between maceral oil and hydrocarbon gas production and P_2 areas is not surprising, since the latter includes the total contribution from both sources. The absence of any losses in the pyrolysis-FID procedure suggests that the (small) remaining scatter in the data may well occur as a result of inaccuracies in the determination of kerogen content. This follows since maceral production capacities are based on the latter and will consequently reflect these errors. The poor correlation between the two variables for the grade 3 shales arises from the fact that the constituent maceral groups were simply treated as comprising liptinite or non-liptinite material and assigned hydrocarbon production factors of 75% and 30% respectively. The latter may be appropriate for the conversion of vitrinite macerals to volatile hydrocarbons, whereas the former value is evidently inappropriate, for example, to characterise the conversion of organic matter to hydrocarbons for the bituminite comprising almost the entire kerogen content of the Kentucky S. shale. An indication of its hydrocarbon production (relative to the liptinite group of macerals in grade 1 shales) can be obtained by comparing its P_2 area with that for Condor Brown Unit shale since both shales comprise predominantly only one maceral group. The latter produces a P_2 area of 185 arbitrary units per unit mass of kerogen (Table

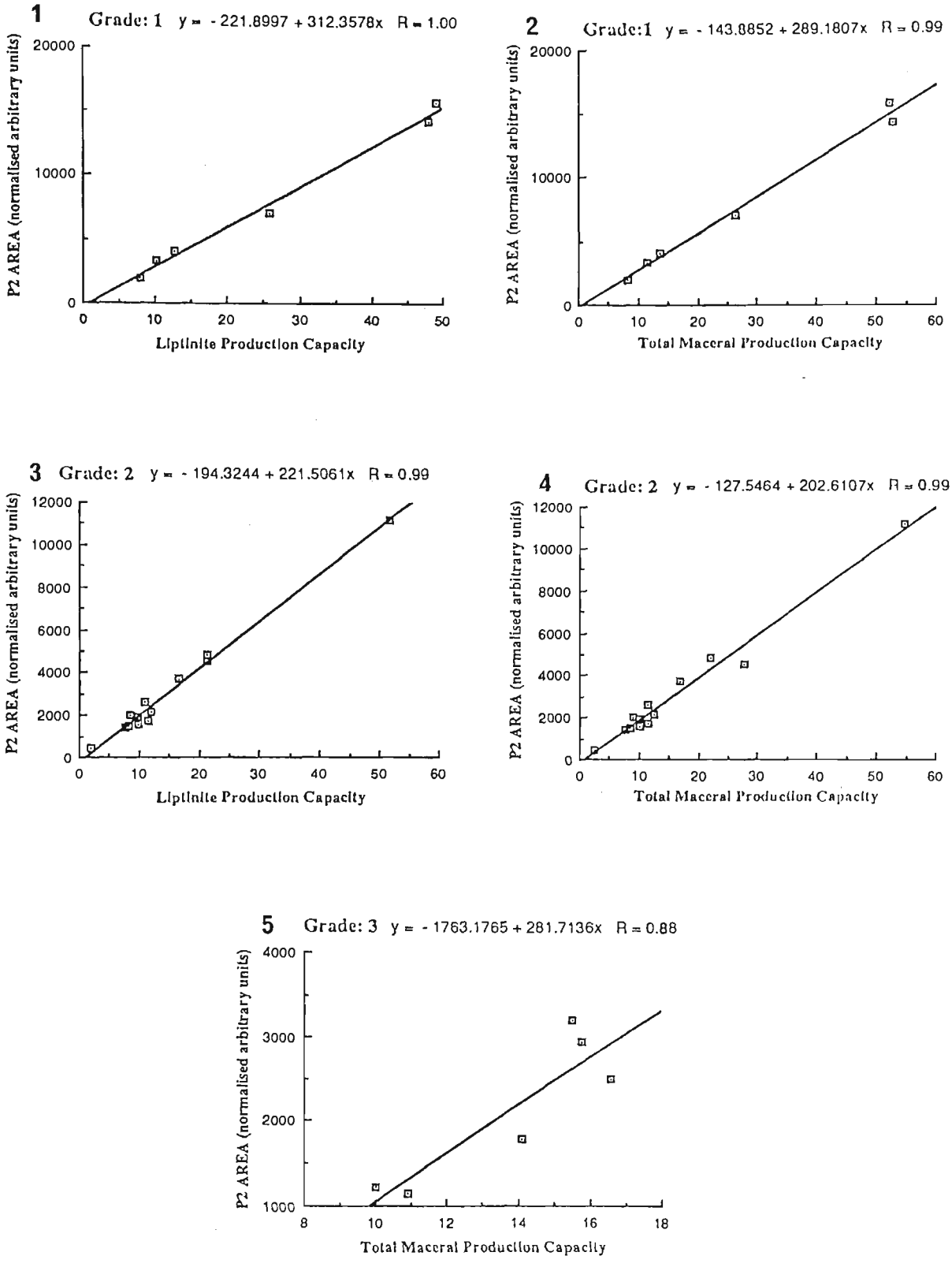

Figure 5-17.

Linear-regression analyses of the relationship between the normalised P_2 area values obtained from the pyrolysis-FID procedure and the production capacity of the liptinite and total maceral groups for the kerogen of the various shale grades. The definition of maceral hydrocarbon production capacities is given in the text.

5-6: column **6**) whereas shale from Kentucky S. produces at a corresponding rate of only 94 area units. Since a production factor of 75% was used for Condor, this equates the production capacity of the bituminite to a relative value of ca. 38%. This rate of bitumen maceral conversion to hydrocarbons (oil and gas) is slightly higher than the accepted figure of ca. 30% for type III kerogen (vitrinite).

An examination of the plot for grade 2 shales shows that the telalginite macerals in tasmanite produce hydrocarbons at the same rate of conversion as the liptinite group of macerals for the other samples within this group. This suggests that the earlier relatively high FA oil yields associated with this sample arose from variations in the bulk composition of the shale used for retorting and micro-scale pyrolysis-FID. Evidently the small sample used for the latter had a relatively lower abundance of kerogen. This interpretation is further substantiated by results presented later in this section.

The quantity of hydrocarbons that can be generated during rapid pyrolysis is a crucial factor in oil shale conversion studies and provides a rapid assessment of potential reserves. The normalised P_2 areas give an immediate indication of oil shale richness, whereas the hydrocarbon generating potential grades the shales on the basis of relative yields, which are dependent on the type of the constituent kerogen. Another common approach to assessing oil-shale richness involves the relationship between oil yield and elemental analysis data, particularly organic carbon content. Earlier work on Duaringa has shown that C_{org} values may be used to derive kerogen content for the raw shales by multiplying these values by type-dependent conversion factors (cf. section 4.6). Where the shale comprises a mixture of different kerogen types petrographic data is needed to identify and delineate these and kerogen abundance (mass % of raw shale) may then be obtained by additivity. Many researchers have derived equations for specific deposits by relating FA oil yield to C_{org} shale content. Smith (1966) and Cook (1974) have calculated these respectively for the Mahogany Zone and Parachute Creek member of the Green River Formation under the assumptions that the organic matrix is of uniform structure and composition and that pyrolysis is consistent and reproducible. Cook has further suggested that hydrogen content is a critical parameter for predicting oil yields from any pyrolytic process and

noted that the atomic H/C ratio remained reasonably constant for the large number of core samples which he analysed. He interpreted this as indicating that the kerogen had a relatively uniform hydrocarbon framework stratigraphically down the core and that the overall high efficiency of hydrocarbon production from the shale was basically invariant throughout the deposit. He further showed that pyrolysis of the kerogen in shale preferentially cleaves and volatilises aliphatic and alicyclic moieties, leaving predominantly aromatic and nitrogen-containing heteroaromatic structures in the residue. Saxby (1980) has shown the dependence of oil yield from demineralised kerogen on both atomic H/C and O/C ratios, although atomic H/C ratios are usually used as a direct measure of their oil-forming potential under pyrolysis or diagenesis conditions.

The dependence of P_2 areas from pyrolysis-FID and FA retort oil yields on H/C ratios for respective shales listed in Table 5-6 is clearly evident in Figures 5-18 and 5-19.

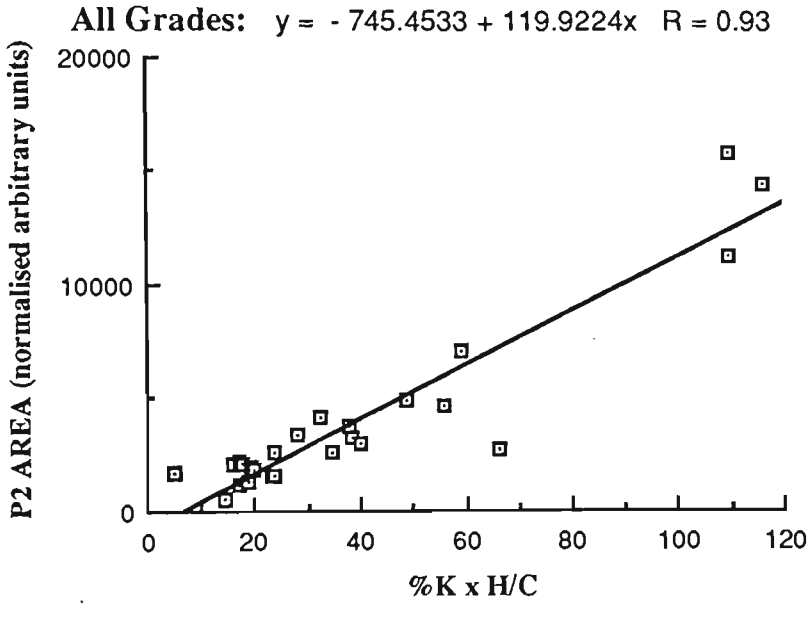

Figure 5-18. Plot of the relationship between hydrocarbons produced by pyrolysis-FID of the raw shale (oil and gas) and shale richness as expressed by the product of its kerogen content (**%K**) and aliphatic nature (**H/C**).

However, the above plot shows that the P_2 areas are not as dependent on H/C ratios as might be expected. The scatter in the data obviously reflects a combination of variations

in kerogen composition and differences in degradation processes between the various types of organic matter undergoing thermal decomposition. Relative differences in intragrade dependence of hydrocarbon production on H/C ratios are particularly pronounced for the grade 3 shales mainly due to large variations in the composition of their constituent kerogens. However, scatter in the data for all shale grades are also due, in part, to the cumulative effect of errors in the determination of the X-axis variables. Multiplying the errors in the kerogen percentage (% K) and H/C ratio values may fortuitously cancel these in certain cases, while compounding them in others. The correlation between H/C atomic ratios and FA oil yields for all grades of shale is slightly lower than that obtained from the pyrolysis-FID procedure (Figure 5-19: **1**) This slight difference may be associated with possible variations in the relative partitioning of the kerogen into hydrocarbon gas and oil fractions during the two pyrolysis processes. An appropriate restriction of the correlation to combined grade 1 and 2 shales shows a dramatic improvement in the value of the coefficient in both cases (Figure 5-19: **2** and **3**).

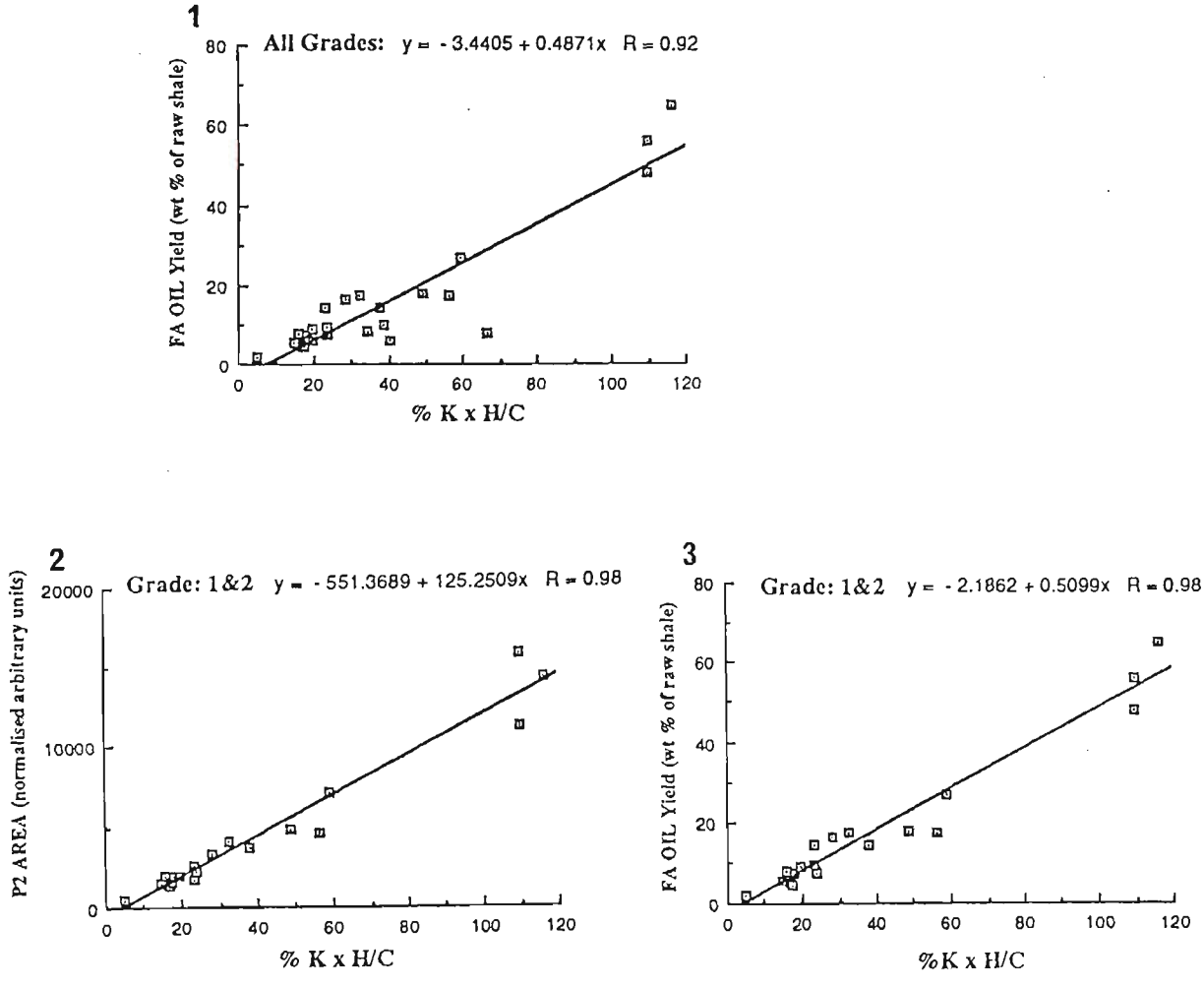

Figure 5-19. Linear-regression analysis of the relationship between hydrocarbon production (pyrolysis-FID and FA oil yields) and shale richness as expressed by the product of its kerogen content (%K) and aliphatic nature (H/C).

In line with generally higher H/C ratios for these richer shales this improvement is consistent with the formation of oil and hydrocarbon gases from predominantly aliphatic and alicyclic moieties as suggested above. The tasmanite sample again conforms closely to the governing equation relating hydrocarbon oil and gas production to H/C atomic ratios within these grades and supports earlier remarks about the effects on micro-scale data of heterogeneity for this sample.

Collectively the various correlations established above have shown that for raw shale valuable information about potential shale oil yield is immediately available from pyrolysis-FID data. Other strong correlations also link important shale parameters such as kerogen content, maceral composition and elemental data to the production of hydrocarbon gases and oil. Estimates for some of the latter may be obtained indirectly by combining information from various analytical procedures. In particular it is evident that a C_{org} value for the raw shale is extremely useful for estimating kerogen content. Initially this will yield three values which are respectively obtained by multiplying the C_{org} value by conversion factors corresponding to kerogen of type I, II or III (cf. section 4.6). A refinement of the assignment of kerogen type can be achieved by comparing the assumed shale production capacities (normalised P_2 area actually obtained from pyrolysis-FID / calculated mass % kerogen corresponding to each of the assigned types) with the range of values listed in Table 5-6: column **6**. Although a type III assignment can be readily confirmed or eliminated on the basis of the pyrolysis data, any differentiation between type I and II kerogen will in practice remain uncertain since there is no clear-cut delineation based on production capacities between the two grades of shale. It is clear however that any raw shale with a relatively high assumed production capacity (e.g. >180), calculated as above, must contain type I kerogen. It is only those shales which exhibit values corresponding to regions of potential overlap which are hard to categorise. It should be noted that, at best, a combination of the above information can only give a value for the average kerogen type as characterised by relative pyrolysis-FID data; only petrographic studies can differentiate between the constituent maceral groups. Once the correspondence between the assigned kerogen type has been verified by an appropriate value for the hydrocarbon production

potential the correlation in Figure 5-18 or 5-19: **2** may be used to estimate the H/C ratio for the constituent kerogen. Since the C_{org} value is known this also allows an estimate for the elemental H value of the kerogen to be calculated. A diagram summarising the various interrelationships between pyrolysis, elemental analysis and petrographic data is given in Figure 4-14.

Apart from the researchers specifically mentioned above many others have established various correlations between some of the chemical and petrographic data obtainable from oil shale analysis (Giraud, 1970; Barker, 1974; Tissot et al., 1974; Claypool and Reed, 1976; Harwood, 1977. Espitalie et al., (1977) have shown that P_2 peak areas obtained using the Rock-Eval procedure correlated well with Fischer assay oil yields for the samples they investigated. These researchers also found that the yields of organic CO_2 and the P_2 peak areas respectively correlated well with the O/C and H/C ratios of contained kerogen. They defined oxygen and hydrogen indices based on the former quantities and plotted these in place of the conventional H/C and O/C ratios in the van Krevelen diagram (cf. section 4.6). For the shales analysed above a plot of the latter is given in Figure 5- 20.

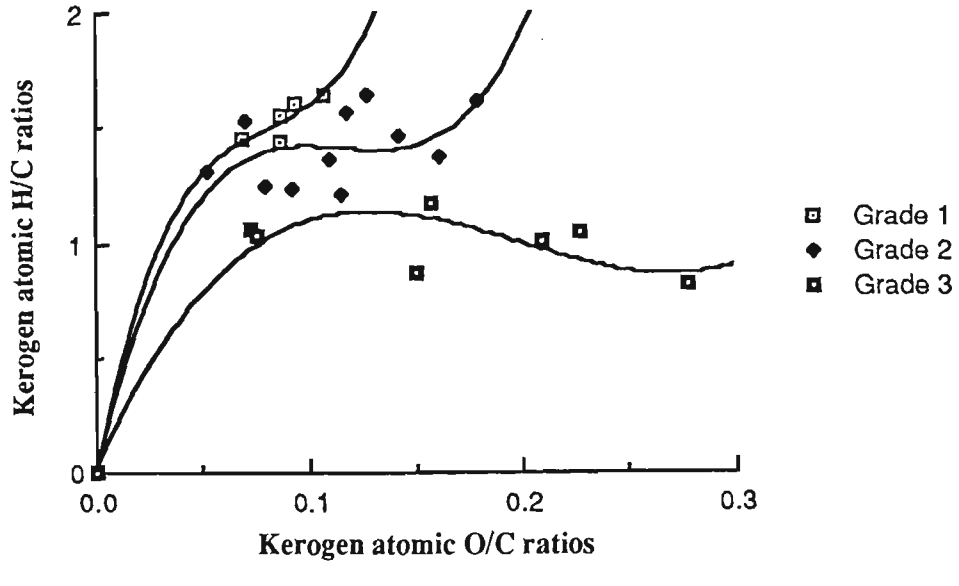

Figure 5-20. van Krevelen diagram of the elemental analysis of the shales listed in Table 5-6. Respective plots for shales of grade 1, 2 and 3 were approximated by a polynomial function of degree 3. The trace for each shale grade approximates the evolutionary changes in composition which occur in the respective kerogen types with increases in maturation (i.e. progression towards the carbon pole).

In each case the relationships between H/C and O/C atomic ratios for the kerogens of the shales within specific grades may be approximated by a polynomial function of degree 3. Although the latter is not necessarily the underlying relationship which defines the equations of the evolutionary paths, it nevertheless serves to visualise these over the restricted domain of values depicted in the graph. Initially this approximation was carried out for all of the shales contained within the various grades. However, data for the samples from Glen Davis, Joadja and Mt. Coolon were omitted from the above graph (Figure 5-20) since their inclusion caused severe distortion in the plot of the equations approximating the mean evolutionary paths for the respective kerogen types (I and II). The remaining samples, including all of the grade 3 shale kerogens follow a maturation path broadly similar to those given for type I, II and III kerogens by Durand and Monin (1980). The diagram should only be used for approximating relative kerogen maturity within each particularly shale grade. Any samples lying close to the carbon pole along the respective evolutionary path for each grade may be considered relatively more mature than comparatively remote samples. However, these interpretations may not hold for samples closely positioned in the diagram and any inference about relative maturity of the organic matter needs to be substantiated by other supporting data.

Plotting the correspondence between hydrogen and oxygen indices obviates the need for elemental analysis of the kerogen, although the latter remains an important procedure for spot-checking data obtained from other techniques. As a routine method for continuous logging of cuttings with depth, it is expensive and time consuming. Kerogen concentrates from solvent-extracted rocks are also susceptible to oxidation and this may cause artificially high oxygen values to be obtained.

Apart from its relative position in a van Krevelen diagram the level of organic maturity of the kerogen in oil shales may also be estimated from a hydrogen-oxygen index diagram, the transformation ratio, the relative temperature maxima (T_{MAX}) and vitrinite reflectance data. However, it should be appreciated that any natural variability in the hydrogen content of kerogen will obscure the interpretation of the hydrogen index if the other two associated maturation indicators are not present to support it. It should also be

noted that although the transformation ratio will always increase in the mature zone, if the kerogen is capable of generating oil or gas, this increase will not be completely reflected in the data where there has been substantial migration of bitumen out of the seam.

Espitalie and coworkers postulated that families of samples which have undergone a systematic change in maturity would show a decline in the oxygen index during early catagenesis, followed by a decrease in the hydrogen index in the principal zone of oil and gas formation. They analysed Tertiary core samples from West Africa (800 - 2,770m) and showed that the transformation ratio increased systematically with depth and in line with observed relative shifts to higher T_{MAX} values of ca. 7 %. This small systematic variation in the relative T_{MAX} values over ca. 2,000m shows that the T_{MAX} parameter is not sensitive enough as a maturity indicator for differentiating between immature shallow samples. However it is suitable for categorising the kerogen as relatively immature, mature, or metamorphosed providing the samples have been buried over sufficient depth and comprise organic matter of uniform compositiion. Interdeposit comparisons need to be carried out under identical experimental conditions and relative to a common suitable reference sample. Hunt (1979) has pointed out that different kerogen types require different activation energies to yield hydrocarbons and that as the kerogen in a rock matures, higher temperatures are required to form hydrocarbons.

Vitrinite reflectance has the advantage over other maturation techniques of covering the entire temperature range from early diagenesis through catagenesis into metamorphism. It is the most useful subsurface prospecting tool for determining the present and past stages of maturation where the maceral group is relatively abundant. It does not , however, define the oil- or gas-generating capability of any sediment.

Some of the above parameters have been shown to vary systematically for cuttings from oil shale deposits comprising stratigraphic sequences of uniform kerogen type. However, an examination of transformation ratios, relative T_{MAX} values and vitrinite reflectance data for those samples listed in Table 5-6 (columns **4, 5** and **13**) show that these parameters are not necessarily consistent indicators of relative maturity for intra- and

interdeposit comparisons. This is illustrated, for example, by the conflicting data for oil shales from Glen Davis and Green River. Relative transformation ratio and vitrinite values suggest that the examined Green River shale is more mature than that from Glen Davis, whereas the relative T_{MAX} temperature contradicts this ranking. Other inconsistencies in these parameters for individual samples as well as between samples from different deposits show clearly that their use as maturity indicators is dependent on sample composition and thermal history. Consequently they need to be restricted to measuring relative changes in maturity of uniform organic matter contained in shale sequences obtained from the same core.

Although some of the above procedures provide valuable information in isolation it is their combined application that provides consistent characterisations for oil shales in general. This comprehensive approach will be demonstrated for the samples from Duaringa and illustrates that all available information (both chemical and petrographic) is (usually) required for the characterisation of otherwise anomalous shales (with respect to apparently inconsistent data obtained from different procedures). This is particularly the case where the latter contain organic matter comprising a mixture of different kerogen types.

The Fischer assay oil yields for two Duaringa samples (812 - upper lamosite and 674 - lower carbonaceous lamosite) were obtained as part of the compendium series (Crisp et al., 1987). The oil yields listed in Table 5-8 and 5-9 for Duaringa shales 5391-C and 686 were obtained using the standard retort procedure referred to in the experimental section. Pyrolysis-FID data for these and other Duaringa samples (Table 4-8) gave normalised P_2 area ratios of 1.06 (Duaringa 686), 1.56 (Duaringa 812) and 1.70 (Duaringa 674) relative to the standard oil shale from Duaringa 5391-C. These and other chemical and petrographic data for raw shales from the Duaringa deposit are listed in Table 5-8. It should be noted that although the kerogens for samples 1, 2 and 3 below comprise lamalginite (almost exclusively), these shales are categorised as belonging to different grades (column 7). Given the consistency of hydrocarbon production data for the liptinite maceral groups comprising shales from the various deposits listed in Table 5-6, this difference is probably due to the combined effects of sample heterogeneity and inaccuracies in the

Table 5-8. Pyrolysis-FID and other chemical and petrographic data (columns **1-13**) obtained for raw oil shale samples from the **Duaringa** deposit. Pyrolysis-FID data were obtained by adjusting those values in Table 4-8 for the different integrator gain settings used for characterising those shales listed in Table 5-6. For column entries see key at the foot of Table 5-6. Other details as given in the text.

SAMPLE	1	2	3	4	5	6	7	8	9	10	11	12	13
1. 5391-C	10.5	26	1421	1.8	619	135	2	1.62	17.0	4.9	27	1	0.19
2. 686	10.9	21	1502	1.4	615	138	2	1.61	17.5	5.8	26	0	0.26
3. 812	12.5	53	2220	2.4	615	177	1	1.55	19.4	5.9	16	0	0.18
4. 674	26.8	24	2416	1.0	605	86	3	1.22	34.7	12.7	27	15	0.40

determination of the kerogen content. Errors in the latter and differences (heterogeneity) between the bulk retort shale and micro-scale quantities will have a major effect on shale grade calculations.

For 812 there appears to be a further anomaly, between the relatively low volume % liptinite content and an inconsistently high kerogen content, which can only be explained on the basis of sample heterogeneity or a high content of poorly defined amorphous organic material which was petrographically assigned as mineral matter. The anomaly is further accentuated by the low FA oil yield derived from the relatively more abundant type I kerogen. Oil yields predicted (pyrolysis-FID) and found (total pyrolysate compositon from isothermal flash pyrolysis - cf. section 4-6) are both higher than that listed in the compendium (Crisp et al., 1987) and indicate that the micro-scale sample contained more kerogen (mass % of raw shale) than the reported 12.5% listed in Table 5-8. Pyrolysis-FID analysis of a shale sample from 812, actually richer than presumed, would reduce the hydrocarbon generating potential of the constituent kerogen from 177 to a value closer to that of the other shallow seam shales. It would also account for the relatively higher FA oil yield predicted from the equation in Figure 5-14: 2 and that found using flash isothermal pyrolysis (Table 5-9). Although the predicted and found oil yields agree closely for samples from 5391-C and 686, their H/C ratios derived from equation 2 in Figure 5-19 are low in both cases. The atomic H/C ratio for 812 on the other hand is relatively high. Again the predicted values are critically dependent on accurate kerogen content values (mass % of raw shale) relevant to the micro-scale sample.

Table 5-9. Fischer assay oil yield and compositional data (H/C) for oil shale samples from the Duaringa deposit, as predicted from pyrolysis-FID and petrographic data and found using conventional techniques.

	FA OIL YIELD			H/C RATIO	
SAMPLE	PREDICTED[1]	FOUND (a)[2]	(b)[3]	PREDICTED[4]	FOUND[5]
1. 5391-C	5.2	5.04	4.9	1.50	1.62
2. 686	5.6	5.95	5.8	1.51	1.61
3. 812	8.4	7.09	5.9	1.76	1.55
4. 674	9.3	10.78	12.7	0.98	1.22

1 as calculated from Pyrolysis-FID data using the equation given in Figure 5-14: **2** ; **2** as determined from total pyrolysate data listed in Table 4-9; **3** modified Fischer assay retort yield. Samples 812 and 674 from compendium data published by Crisp et al. (1987); **4** as calculated from maceral and pyrolysis-FID data using the equation given in Figure 5-19: **2** (samples 1-3) and Figure 5-18 (sample 4); **5** from elemental analysis data for demineralised kerogen (Table 4-4).

If it is assumed that the H/C ratio for the sample from 812 used for pyrolysis-FID data is similar to those for samples 1 and 2, which is consistent with similar maceral content (i.e. lamalginite) then solving the equation gives a kerogen content of 14.7 mass % of raw shale. This translates into a hydrocarbon production potential of 151, which still places it above both 5391-C and 686 in terms of shale grade, but brings it into the grade 2 category. Based on a kerogen content of 14.7 mass % the FA oil yield (based on uniform bulk composition for the retort sample at this kerogen value) would be expected to be 5.9 x 14.7/12.5 , or 6.93 mass % of of the raw shale. The latter % is close to that obtained from the isothermal flash-pyrolysis procedure. The above calculations illustrate that, with sufficient data available from different procedures, it may be possible to reconcile some of the otherwise inconsistent data obtained from these approaches, which in some cases involve vastly different quantities of sample. It is this large difference in the quantity of the samples used which makes data obtained from micro-scale techniques so dependent on sample homogeneity. On the other hand data from relatively large-scale procedures such as Fischer assay retorting may be regarded as average values for samples obtained from that location within the deposit.

The predicted data for 674 are also difficult to reconcile with some of the average

found values because for this sample both shale richness (relative changes in kerogen content for the bulk and micro-scale sample) and composition (variations in the relative proportions of its constituent kerogen types I and III) are reflected in the results obtained from micro-scale procedures. The FA oil yield predicted from relative P_2 area ratios is lower than both of the isothermal flash-pyrolysis determination and the standard Fischer assay. Given that 674 contains ca. 33 % vitrinite, it was considered that this fraction of the total organic matter may behave differently during the relatively high temperatures encountered during the pyrolysis-FID analysis (i.e. possibly more coking) and consequently produce a lower yield than that obtained from the other two methods, which only go to ca. 500°C. This possibility was investigated by simulating the isothermal pyrolysis conditions. The shale sample was analysed using a sequential pulsed pyrolysis-FID approach (fifty 20s pulses) and the total normalised hydrocarbon area was compared with that obtained from the standard shale from 5391-C analysed under identical experimental conditions (Figure 5-21).

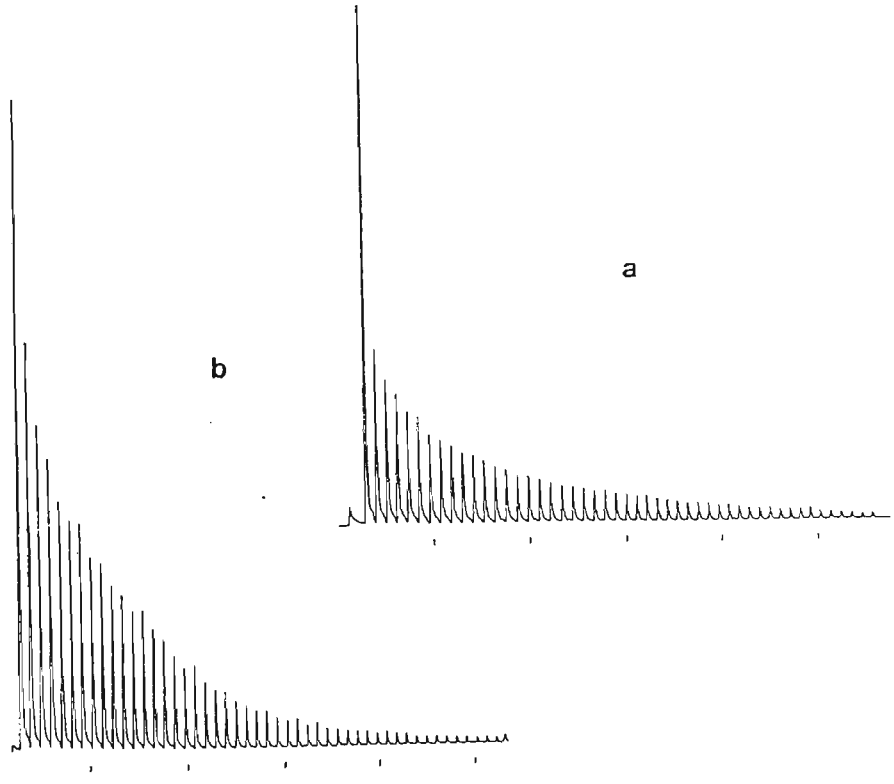

Figure 5-21. Integrator profiles for pulsed-pyrolysis-FID analysis of raw shales from Duaringa 5391-C (a) and 674 (b). Each sample was sequentially pulsed fifty times (20s, 500°C) - i.e. until the integrator signal had been reduced to near noise level. Total hydrocarbons generated were obtained by summing peak areas corresponding to sequential pulses.

The ratio of the two normalised areas remained the same (1.7) as that obtained previously using the pyrolysis-FID procedure and eliminated temperature as a major influence in the determination of the predicted FA oil yield in this case. Given the composite nature of the oil shale from Duaringa 674, the consistently low oil yield data obtained from the isothermal pyrolysis and both pyrolysis-FID procedures are attributed to variations in kerogen composition.

The H/C atomic ratio for 674 (Table 5-9) was calculated using the equation given in Figure 5-18. The latter was used since the correlation restricted to Grade 3 shales was unacceptably low. A H/C value of 0.98 is again below that found by elemental analysis of the demineralised kerogen. However, the relative differences between the predicted H/C atomic ratios for samples 1 - 3 and 674 correctly indicate that the latter comprises a relatively more aromatic kerogen and is consistent with its maceral composition.

In general the pyrolysis-FID procedure should be more accurate than FA for assessing oil shales with very low kerogen content, in particular where the latter comprise organic matter of type III. Under these circumstances, quantitative recovery of the small amount of oil produced during conventional retorting is difficult to achieve since some of it remains in the retort assembly (transfer tube) and collection apparatus. Further problems are encountered in separating small yields from the retort water, since part of the oil is emulsified. None of these problems arise with the pyrolysis-FID method which is capable of detecting hydrocarbons, initially present (bitumen) or subsequently produced, at trace concentrations. Where large variations in relative data are encountered for proximal samples, the potential problem of sample heterogeneity can be partly overcome by analysing several specimen from the one shale and averaging the results.

5.2 Solvent Extracts.

An important application of organic geochemistry to oil shale characterisation involves the analysis of the extractable bitumen fraction. High-resolution gas chromatography and mass spectrometry, both separately and used in conjunction (GC-MS), yield substantial information about the distribution of various classes of biomarkers (e.g. alkanes, branched and cyclic hydrocarbons, aromatics, aldehydes, ketones, steranes, triterpanes) and the latter approach has enabled hundreds of individual components to be identified.

With the development of high-speed instrumentation, mass-spectrometric techniques commonly referred to as single ion monitoring (SIM) or multiple ion detection (MID) have been used extensively to determine the distribution of components present at low concentrations in the extract. This technique can be used for virtually the entire range of biomarkers by choosing appropriate fragment ions characteristic for a particular class of compounds. The approach is substantially more sensitive than the normal mode of operation, which acquires a full spectrum during each scanning cycle. This increase in sensitivity is due to the long dwell-times associated with preselected masses corresponding to a single or range of ions. However, ambiguities may arise for unknown extracts since other components present in the mixture may also produce the specific fragment ions monitored during the analysis. These ambiguities are largely resolved by analysing the extract in the normal full-scan mode and generating fragment-ion plots of masses diagnostic for particular classes of compounds. Ambiguities in the resulting mass-fragmentogram may then be resolved by examining the full spectra corresponding to the components in question. The application of some of these procedures, particularly the latter, to the study of solvent extracts from the Duaringa deposit was described earlier (cf. section 4.3).

More detailed information about compounds present at only low concentrations may be obtained using any of the above approaches after first separating the solvent extract into various constituent classes using appropriate fractionating techniques (e.g. column and thin-layer chromatography). Very comprehensive information may be obtained by treating

the solvent extract as a crude oil and analysing it as detailed for Duaringa shale oil in chapter 4. Unfortunately these separation procedures are time consuming, require large quantities of extract and are not suitable for the routine analysis of bitumen constituents. Analysing extracts without prior fractionation, however, restricts the analysis to relatively abundant components and may not detect important biomarkers due to their relatively low concentrations. This is unfortunate since detailed mass-spectrometric analysis of the latter (steranes and triterpanes) have been shown to provide source (Seifert and Moldowan, 1978), maturity (Mackenzie et al., 1980) and biodegradation parameters in petroleum studies (Alexander et al., 1983).

Constraints of speed and simplicity for the rapid screening of solvent extracts obtained from raw shale samples necessarily restrict these to gas chromatography (primarily) and an examination of the distribution and presence of only the most abundant volatile components. Nevertheless, these data may still provide comparative information about the source, depositional environment and bacterial reworking of the organic matter. Interpretations based on parameters calculated in this context need to be made in conjunction with data obtained from other independent procedures.

Raw oil shales, other than Duaringa 5391-C (Table 5-6), were added to screw-neck vials, bundled together and extracted with solvent (dichloromethane) as detailed in the experimental section (cf. 3.2). The suspension was filtered and the recovered components analysed using GC and GC-MS procedures. The latter were performed only on samples which contained prominent peaks other than alkanes in their gas chromatograms.

Gas chromatograms for the extracts were grouped according to shale grades (Table 5-6) to assess similarities in the compositon of the bitumen fraction within each category. The wide variations, both in the composition of the extracts as well as in the relative abundances and distributions of constituent components, show clearly that these were not pronounced for the above samples (Figures 5-22 to 5-25). The identities of most of the prominent components in each extract are self-evident from the respective gas chromatograms. Quantitative data and a summary of the most conspicuous features of each profile are given in Table 5-10.

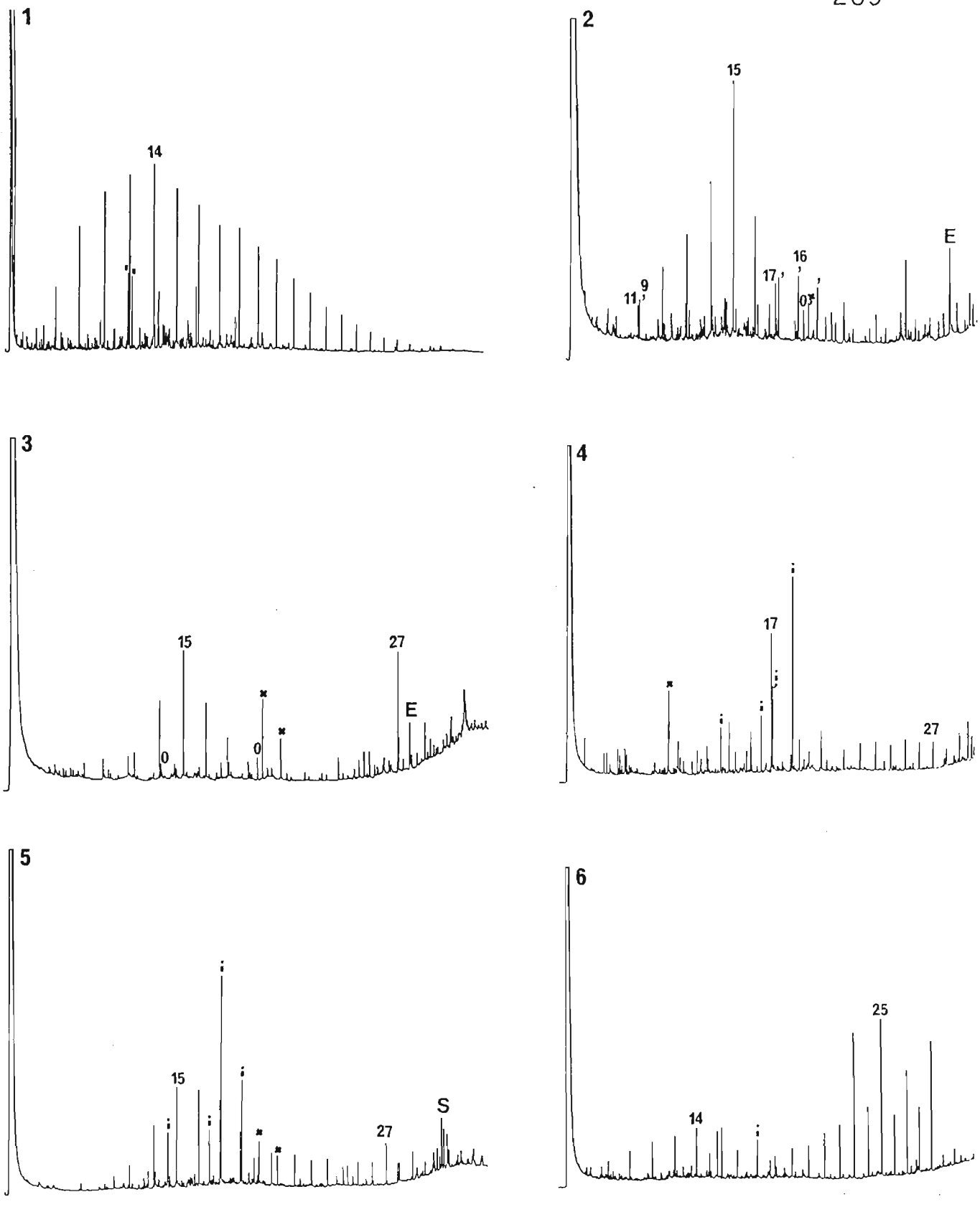

Figure 5-22. Gas chromatograms for the solvent extracts of raw shale samples **1-6** listed in Table 5-10. To avoid obscuring the profiles only key alkane peaks are numbered. Since all of the chromatograms were obtained under identical conditions, the alkane positions relative to the solvent front in profile **1** (major peaks) defines their positions in the remaining chromatograms. Other common components in their order of elution: **i** - isoprenoids (i16, i18, i19 and i20); **O**- ketones (6,10-dimethylundecan-2-one, 6,10,14-trimethylpentadecan-2-one); **x** - artefacts (< C_{13} - imide, > C_{13} phthalates); **E** - 13-docosenamide. Specific compounds: 2- and 1-methylnapthalene (') - sample **1**; aldehydes (') - sample **2**, only major members numbered; sterane-triterpane region (S) - sample **5**. Other relevant details in Table 5-10 and text.

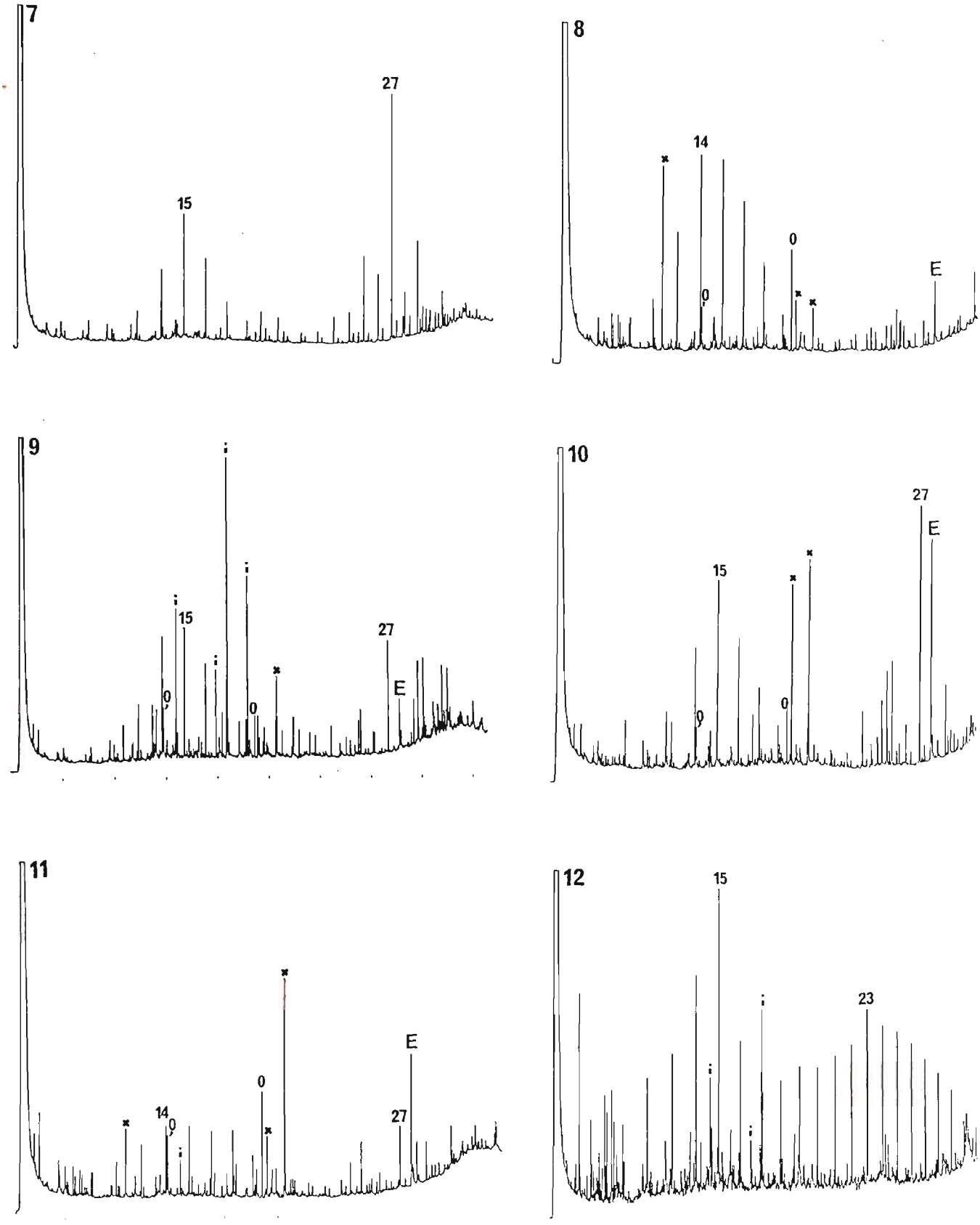

Figure 5-23. Gas chromatograms for the solvent extracts of raw shale samples 7 - 12 listed in Table 5-10. To avoid obscuring the profiles only key alkane peaks are numbered. Since all of the chromatograms were obtained under identical conditions, the alkane positions relative to the solvent front in profile 1 (major peaks) defines their positions in the remaining chromatograms. Other common components in their order of elution: **i** - isoprenoids (i16, i18, i19 and i20); **O**- ketones (6,10-dimethylundecan-2-one, 6,10,14-trimethylpentadecan-2-one); **x** - artefacts (< C_{13} - imide, > C_{13} phthalates); **E** - 13-docosenamide. Other relevant details in Table 5-10 and text.

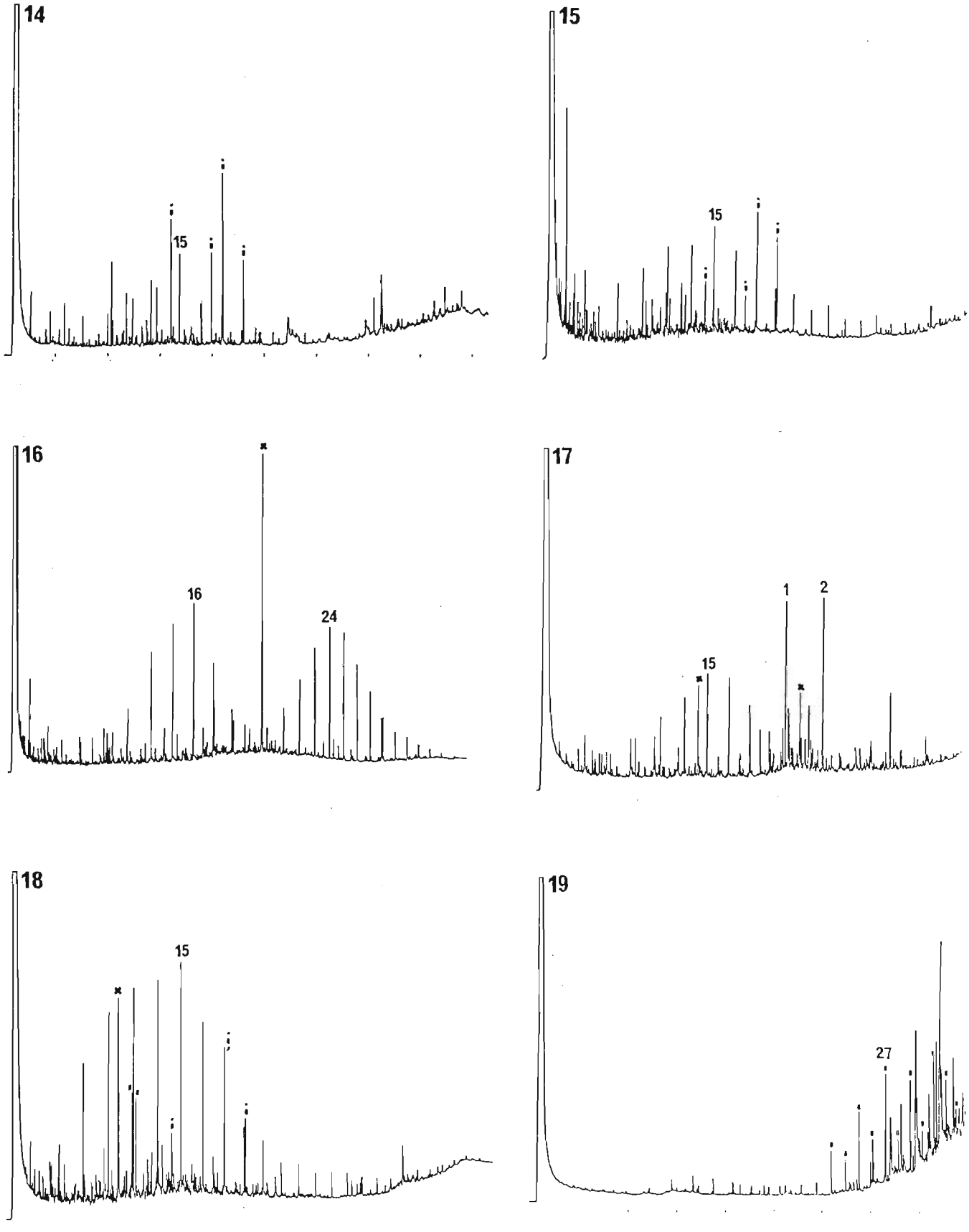

Figure 5-24. Gas chromatograms for the solvent extracts of raw shale samples **14-19** listed in Table 5-10. To avoid obscuring the profiles only key alkane peaks are numbered. Since all of the chromatograms were obtained under identical conditions, the alkane positions relative to the solvent front in profile **1** (major peaks) defines their positions in the remaining chromatograms. Other common components in their order of elution: **i** - isoprenoids (i16, i18, i19 and i20); **x** - artefacts (< C_{13} -imide, > C_{13} - phthalates). Specific compounds: 2- and 1-methylnapthalene (') - sample **18**; alkanes (') C_{23} - C_{33} - sample **19**. Other relevant details in Table 5-10 and text.

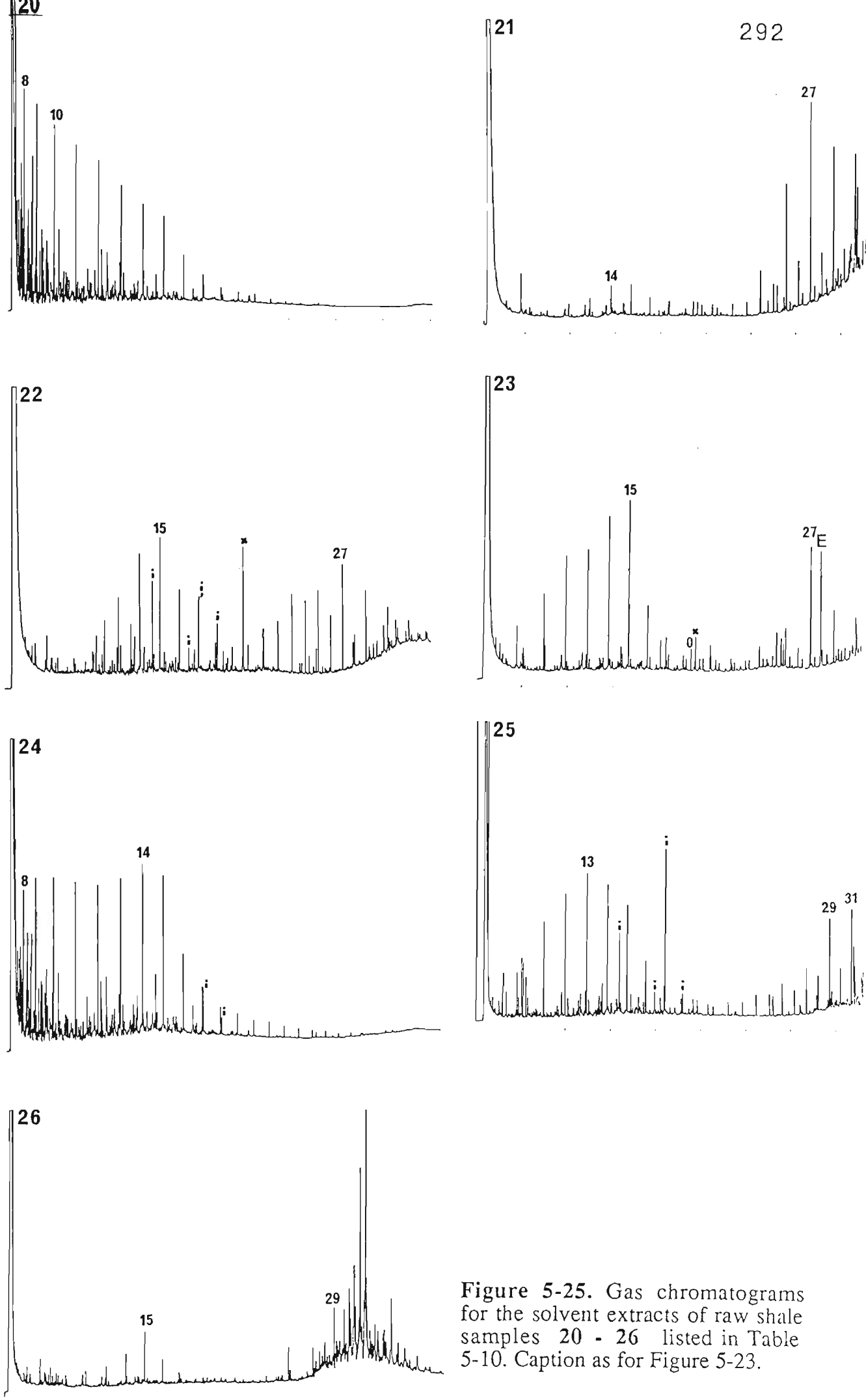

Figure 5-25. Gas chromatograms for the solvent extracts of raw shale samples **20 - 26** listed in Table 5-10. Caption as for Figure 5-23.

Table 5-10. Gas-chromatographic data for the solvent extracts of raw oil shale samples listed (abbreviations as for Table 5-6. Duaringa 5391-C (sample **13** - Table **5-6**) was analysed in section 4.3. Individual chromatograms are depicted in Figures 5-22 to 5-25.

Sample	Alkanes a.	b.	c.	CPI	PR/PH	C_{14}	Remarks
1. Glen Davis	mono	8-30	14	1.0	>1	36000	2- and 1-methylnaphthalene (')
2. Yaamba	mono	10-28	15	-	ca. 3	1190	aldehydes (+++), ketones (O), erucamide (E), artefact (X).
3. Stuart K C.	bi	11-30	**15,27**	5.3	ca. 2	1340	aldehydes (+), ketones (O), erucamide (E), artefacts (X).
4. Green River	mono	12-32	17	1.2	0.5	790	isoprenoids (i) - (+++), artefact (X).
5. Condor B.	mono	12-32	15	1.5	1.9	1080	isoprenoids (i) - (+++), steranes & triterpanes (S), artefacts (X).
6. Alpha	bi	10-32	**14,25**	2.5	3.4	1700	very pronounced CPI (C_{23} - C_{29}).
7. Rundle R C.	bi	10-32	15,27	2.9	ca. 2.5	1080	aldehydes (+).
8. Nagoorin S.	mono	10-30	14	2.9	1.5	1520	aldehydes (++), ketones (O), erucamide (E), artefacts (X).
9. Byfield	bi	10-32	**15,27**	3.1	1.6	2320	isoprenoids (i) - (+++), ketones (O), erucamide (E), artefact (X), similar profile to Condor Brown.
10. Rundle M C.	bi	10-32	15,27	4.5	ca. 2	1440	ketones (O), erucamide (E), artefacts (X).
11. Lowmead	bi	10-30	**14,27**	3.5	1.6	500	aldehydes (+), ketones (O), erucamide (E), artefacts (X).
12. Joadja	bi	10-32	**15**,23	1.1	5.9	2340	isoprenoids (i) - (++).
14. Irati	mono	10-20	15	-	1.8	5230	isoprenoids (i) - (+++).
15. Julia Creek	mono	10-27	15	-	1.2	950	isoprenoids (i) - (+++).
16. Camooweal	bi	10-33	**16**,24	0.97	1.6	4760	alkane maxima at even carbon numbers, artefact (X)
17. Tasmanite	mono	10-27	15	-	ca. 2	590	two prominent unidentified peaks: M Wt: 262(**1**), 256(**2**); artefacts (X).
18. Toarcian	mono	10-27	15	-	1.9	1300	isoprenoids (i) - (++), artefact (X), 2- and 1-methylnaphthalene (')
19. Mt. Coolon	mono	12-33	27	2.7	-	180	unidentified (broad) high molecular weight peaks.
20. Kentucky S.	mono	8-21	8	-	2.3	7600	this sample comprises mainly bituminite macerals.
21. Nagoorin C.	bi	11-32	14,27	3.9	ca. 5	470	pronounced CPI
22. Nagoorin B.	bi	10-32	**15**,27	1.7	1.5	1035	isoprenoids (i) - (++), artefact (X).
23. Stuart H C.	bi	10-32	**15**,27			3520	aldehydes (+), ketone (O), erucamide (E), artefact (X).
24. Kentucky C.	mono	8-27	14	-	2.5	6590	similar to Kentucky S.
25. Condor C.	bi	9-32	**13**,31	1.8	8.5	10700	isoprenoids (i) - (++).
26. Morwell	bi	10-32	**15,29**	-	-	400	brown coal extract; mainly terpenoid -derived high mol. wt compounds.

Key: Alkanes **a.** modality of distribution (i.e. **mono**- or **bi**modal)
b. minimum carbon number range
c. carbon number of most abundant alkane

CPI carbon preference index - see footnote Table 4-5.

PR/PH ratio of pristane (i19) to phytane (i20)

C_{14} normalised peak area of tetradecane (per unit mass of raw shale). This value allows relative attenuator scale settings to be calculated when comparing individual gas chromatograms.

General features listed for each chromatogram in Table 5-10 include the distribution (modality) of the entire range of volatile constituent alkanes, the most abundant homologue in that range and the CPI, where applicable. Collectively these data provide information about kerogen source and maturity. Distributions of alkanes (C_{25} - C_{35}) with a marked predominance of odd over even carbon numbers are, in the majority of cases, derived from higher plant waxes, whereas those in the medium molecular weight range are generally attributed to algal and/or bacterial input. The CPI may also provide some information on the relative maturities of extracts. Immature sediment extracts generally contain low concentrations of even-carbon-number alkanes, but as maturation progresses their abundance increases as they continue to be formed by a number of diagenetic reactions from aliphatic moieties (alkanes, alcohols, esters etc.) present in the kerogen. Ultimately (catagenesis) a smooth distribution of alkanes (CPI=1) may result. The alkane maxima within a given distribution may also provide information on source material since specific alkanes may be associated with photo- and non-photosynthetic bacteria, cyanobacteria, fungi, algae, zooplankton and higher plants (Philp, 1985). However, inferences about possible sources of organic matter must take into account the preferential removal of alkanes through bacterial degradation. Where the latter has been pronounced their use as a reliable indicator is virtually eliminated.

The relative abundances of acyclic isoprenoids, particularly the ratio of pristane (i19) to phytane (i20), have been widely used to obtain information on depositional environments (Didyk et al., 1978; Larter et al., 1979). A ratio >1 is considered to reflect oxidising conditions of deposition, while a ratio of <1 is associated with reducing environments. These inferences are based on the premise that both isoprenoids are formed from a common precursor (phytol - from the side chain of chlorophyll) by various oxidation and decarboxylation reactions (pristane) or hydrogenation and dehydration (phytane) - Brooks et al. (1969).

The application of the above parameters to extracts from the Duaringa deposit were discussed in section 4.3. Other criteria relating to source, maturation, migration and biodegradation are only obtainable using GC-MS, primarily in the SIM or MID mode, and have been summarized by Philp (1985).

By way of example, an examination of each chromatogram for the grade 1 shales (Figure 5-22) shows that the extract data generally agree with the maceral composition and environments of depositon (Crisp et al., 1987). The alkane distributions for samples 1-5 appropriately suggest that these shales comprise kerogen derived predominantly from algal sources. The relatively high concentrations of high molecular weight alkanes in sample 6 (Alpha - torbanite) illustrate that terrestrial biomarkers may dominate the extract profile at concentrations disproportionate to the abundance of the respective maceral content (vitrinite) in the shale kerogen. The pristane/phytane ratios of all of the extracts, except sample 4, indicate that the sediments were deposited and matured under oxidising conditions. This is consistent with the shallow fresh to brackish lake environments associated with the formation of most of the shales (Crisp et al., 1987). A pristane/phytane ratio of only 0.5 for the Green River shale suggests predominantly reducing conditions in the stratified lake, which is considered a likely model for the environment of its deposition. The relatively high concentrations of isoprenoids in the extracts of samples 4 and 6 are (generally) indicative of selective removal of alkanes by bacterial reworking of the algal ooze during deposition. An interpretation of the prominence of isoprenoid ketones in some of the extracts was given in section 4.3 and will be developed further later in this section.

Extract data for the grade 2 shales (Figure 5-23, 5-24) may be interpreted as outlined above and again indicate correctly that most of the kerogens in these shales were derived from algal sources under oxic conditions of deposition. This interpretation of respective alkane distributions is only clearly evident where bacterial reworking is not pronounced (i.e. low isoprenoid concentrations), although abundant artefact peaks (**X**) may distort the relative distributions if they are not recognised as such. Grade 3 shale extracts are more difficult to interpret since they comprise substantially more diverse organic material including high concentrations of bituminite and vitrinite (Crisp et al., 1987). Since most of these samples are not true oil shales any interpretation of their chromatograms should only be made in conjunction with other chemical and petrographic data.

Semi-quantitative data for the solvent extracts were obtained by relating the total gas-chromatographic peak area for each extract to the mass of raw shale. The mass -adjusted areas for each sample were further adjusted for the mass of solution from which

they were injected. The calculated normalised peak areas (total peak area of volatile constituents per unit mass of raw shale) allow a comparison to be made between the relative quantities of shale bitumen extracted from each sample (Table 5-11).

Table 5-11. Total peak area of volatile (chromatographable) compounds extracted from the listed raw shale samples. Data are given as total gas-chromatographic area per unit mass of raw shale.

GRADE[1]	SAMPLE	PEAK AREA[2]	GRADE[1]	SAMPLE	PEAK AREA[2]
1	1. Glen Davis	134,460	1	2. Yaamba	8,040
1	3. Stuart K. C.	8,210	1	4. Green River	23,940
1	5. Condor B.	13,650	1	6. Alpha	17,060
2	7. Rundle R. C.	11,770	2	8. Nagoorin S.	7,380
2	9. Byfield	27,070	2	10. Rundle M. C.	10,600
2	11. Lowmead	7,030	2	12. Joadja	20,180
2	14. Irati	53,570	2	15. Julia Creek	9,770
2	16. Camooweal	35,470	2	17. Tasmanite	8,070
2	18. Toarcian	6,420	2	19. Mt. Coolon	16,630
3	20. Kentucky S.	90,390	3	21. Nagoorin C.	16,710
3	22. Nagoorin B.	9,110	3	23. Stuart H. C.	10,840
3	24. Kentucky C.	50,900	3	25. Condor C.	74,500
3	26. Morwell	19,060			

1 raw shale grade as given in Table 5-6. **2** total peak area of volatile (chromatographable) compounds extracted from the listed raw shale samples.

Data for the normalised areas were correlated with the thermal-desorbate values (P_1 area values listed in Table 5-6) to determine any underlying relationship between them. Relevant values were plotted and show clearly that there is no correlation between these data (Figure 5-26). The same approach was adopted for data restricted to each shale grade category and again showed no correlation between the respective values. This lack of correlation between these quantitative data is perhaps not surprising given the dependence of solute concentrations on the solvent (polarity, mixtures), the procedure used (e.g. soxhlet, sonication, shaking) and parameters of time and temperature. For example, although gas chromatograms of benzene-methanol extracts of some of the above oil shales were virtually indistinguishable from those obtained using dichloromethane, greater quantities of bitumen

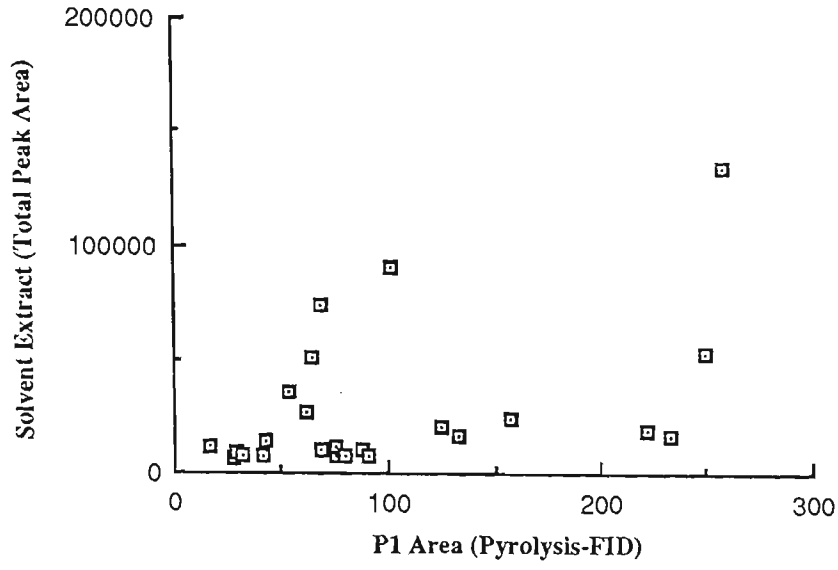

Figure 5-26. Plot of solvent extract (total peak areas of chromatographable components per unit mass of raw shale) versus P_1 area data obtained by pyrolysis-FID for shales listed in Table 5-11.

may have been extracted using the former and in each case the procedure may have failed to liberate occluded compounds expelled during thermal desorption. Gas chromatographic areas are further restricted to volatile components and do not account for any extracted non-volatile material. On the other hand the release of bitumen components by the action of heat is clearly governed by different mechanisms and is influenced by reactions occuring during thermal treatment of the raw shale. For example, prist-1-ene and prist-2-ene are present in the thermal desorbate (350°C) of raw shale from the Stuart deposit but are absent from the solvent extract. Heating of the shale may also cause secondary reactions to occur. These could involve thermally-labile components in the formation of non-volatile products thereby reducing the P_1 area. Further differences may arise from the retention of volatile free and adsorbed components due to shale pore closure caused by kerogen softening and swelling at elevated temperatures (300-400°C).

It has been shown that the transformation ratio increases with maturity as uniform shale from a given deposit is subjected to increasing depths of burial (Barker, 1974). It appears therefore that quantitative bitumen data need to be restricted to the respective approaches (thermal desorption or solvent extraction) for comparative purposes. For transformation ratios the severe restriction to stratigraphic sequences within the same

deposit may need to be imposed. However, the solvent extracts show clearly that under the same experimental conditions the sample from Glen Davis contains the relatively greatest quantity of volatile extractable bitumen (134,460 area counts (arbitrary units) per unit mass of raw shale) while the lowest quantity was extracted from the Toarcian shale (6,420 area counts).

Some of the solvent extracts from grade 1 and 2 shales are characterised by the presence of erucamide (E) and prominent isoprenoid compounds. The former (13-docosenamide) has been detected by Hutton et al. (1986) and was observed in the extract of raw shale from the Condor deposit (cf. section 5.1.1). The component was positively identified by coinjection (RI= 2787.43) and comparison with mass-spectral data of an authentic standard of the amide synthesised from erucoyl chloride (Sigma).

The similarity in structure of isoprenoids to phytol is considered as an indication that this labile alcohol is the natural precursor of all open-chain isoprenoid compounds found in sediments and oils; those < C_{20} are considered to have originated from the precursor by carbon bond cleavage of the main chain. This reasoning may explain the absence of the C_{17} and C_{12} -isoprenoid hydrocarbons, since their structure cannot be derived by this mechanism. The extract chromatograms show that the presence of isoprenoid ketones (O) in shale extracts is not uncommon. They have been reported in solvent extracts of Messel and Aleksinac oil shales (De Leeuw et al., 1973; Saban et al., 1979). Hutton et al. (1986) identified 6-methylheptan-2-one, 6,10-dimethylundecan-2-one and 6,10,14-trimethylpentadecan-2-one as major peaks in the gas chromatogram of a solvent extract from Stuart oil shale (Figure 5-27 **a**).

The C_{18}-isoprenoid ketone has been shown to form from phytol by biological (Brooks and Maxwell, 1973) and clay-catalysed mechanisms (de Leeuw et al., 1973). When phytol was heated at 60°C for four weeks with montmorillonite and water, it gave the C_{13} and C_{18} -isoprenoid ketones and saturated isoprenoid acids. In the absence of clay, the C_{18} -isoprenoid ketone was the only significant product. A multi-step mechanism was

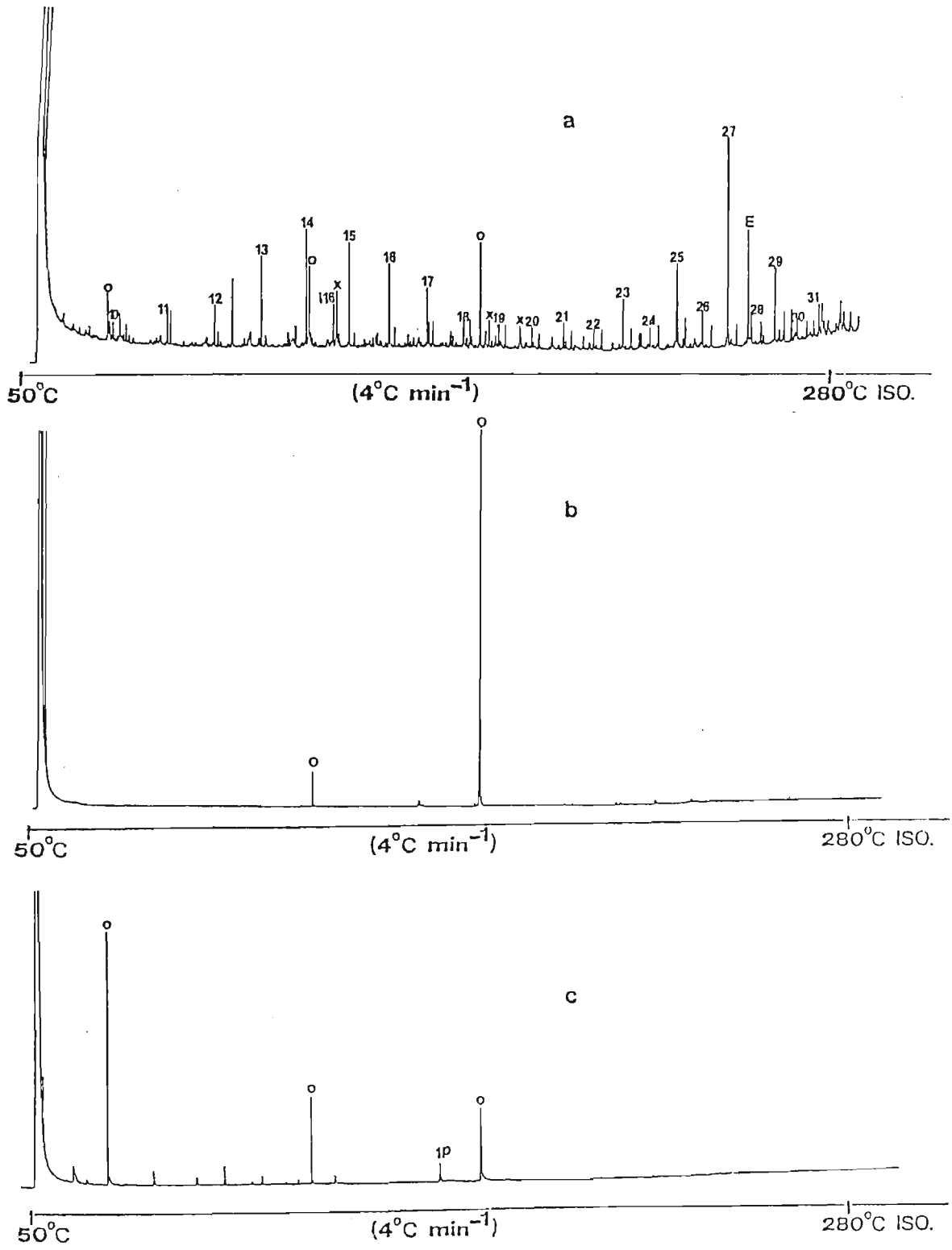

Figure 5-27. Gas chromatograms of the solvent extract from Stuart raw shale (a) and isoprenoid ketones isolated from the $KMnO_4$ oxidation of prist-1-ene (b) and (c). The Stuart extract was obtained from the raw shale described by Hutton et al. (1986). Alkanes in **a** are numbered sequentially; other notation as for Figure 5-22. Components denoted in chromatogram **b** are isoprenoid ketones (O - C_{13} and C_{18} - listed in order of their elution) isolated by column chromatography from the hexane extract of the aqueous phase of the crude oxidation mixture. Chromatogram **c** was obtained from the crude acetone distillate of the original oxidation mixture and comprises the C_8, C_{13} and C_{18} -isoprenoid ketones and residual prist-1-ene (**1P**). Chromatograms were recorded using various integrator settings and are not directly comparable for quantitative purposes.

proposed, with the first step being clay-catalysed dehydration to diphytyl ether (Figure 5-28. 1).

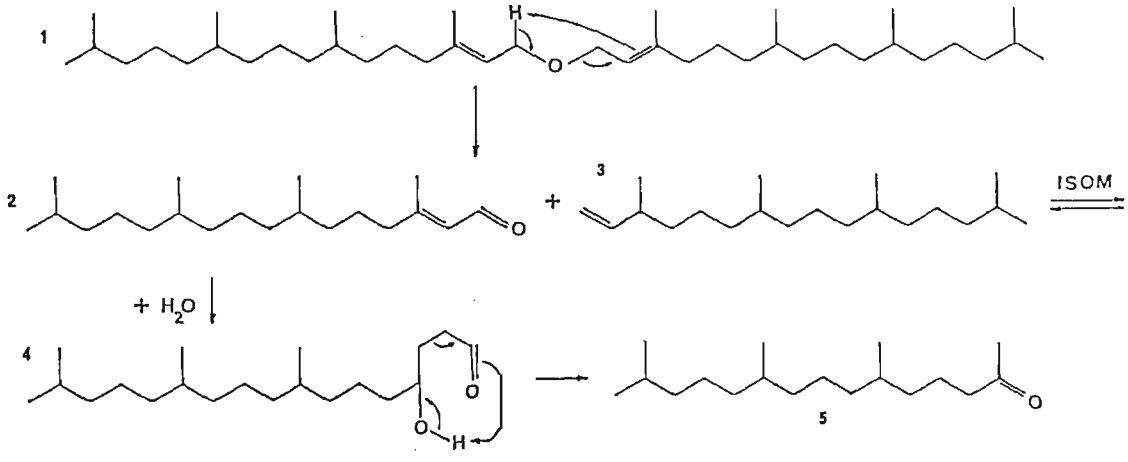

Figure 5-28. Proposed mechanism for the formation of the C_{18} -isoprenoid ketone (6,10,14- trimethylpentadecan-2-one: compound 5) via thermocatalytic break-down of phytol (de Leeuw et al., 1973).

The reference compounds needed to confirm the extended series of isoprenoid ketones found in the present work were easily prepared by permanganate oxidation of pure prist-1-ene (cf. section 3.7). The same oxidation also yielded a series of isoprenoid acids which were analysed by GC-MS of their methyl and butyl esters. The latter were produced according to the procedure of Rovere (1980) to resolve volatile constituents from the solvent front. Mass spectra (Figure 5-30 and 5-31) and retention indices (Table 5-12) allowed components 5-8 to be identified in the acid fraction of the solvent extract of Stuart raw shale (Figure 5-29).

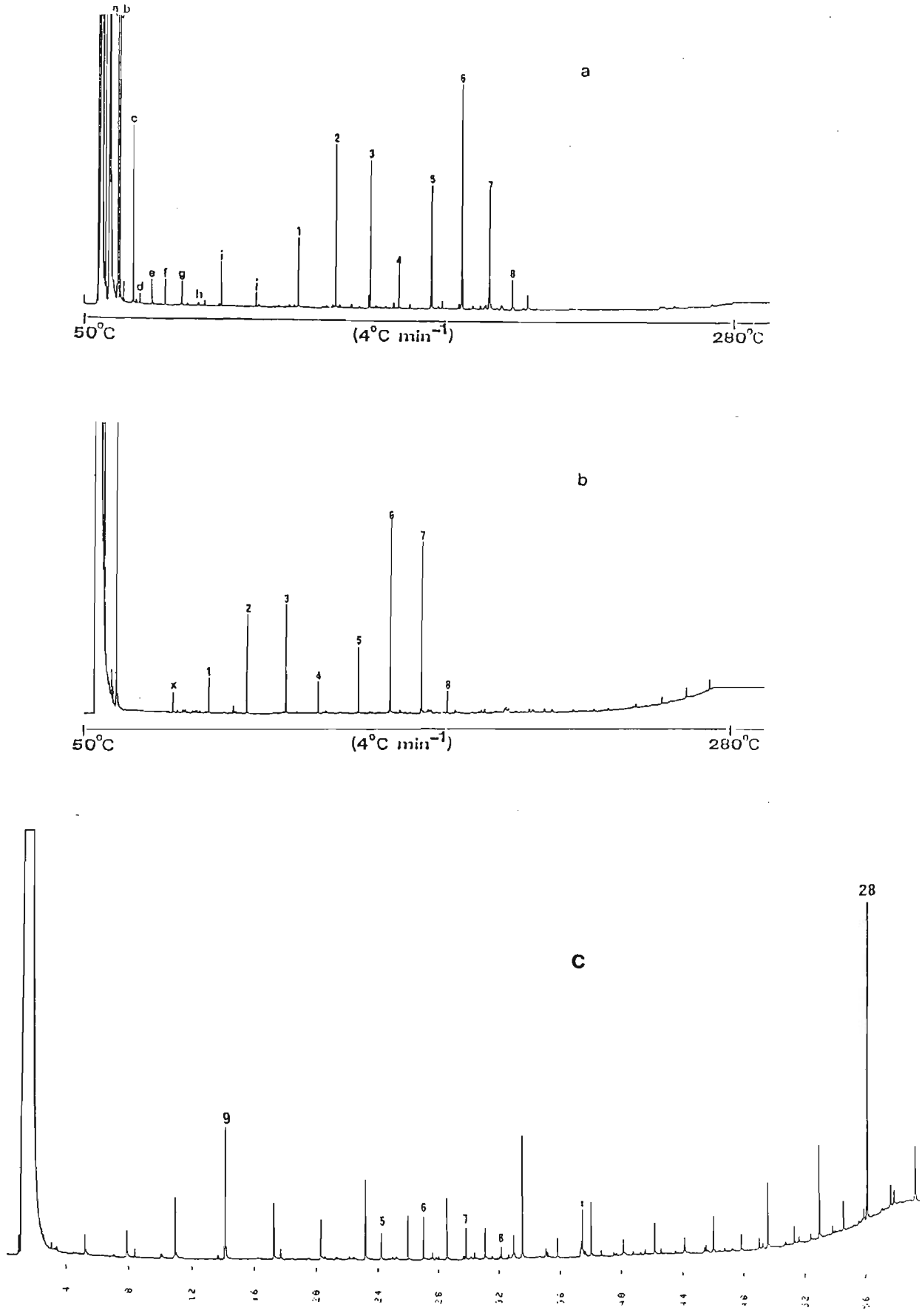

Figure 5-29. Gas chromatograms of carboxylic acids isolated from the $KMnO_4$ oxidation of prist-1-ene (**a** and **b**) and the solvent extract from Stuart raw shale (**c**). Respective chromatograms depict butyl-ester (**a**) and methyl-ester derivatives (**b** and **c**). Lettered and numbered peaks (**a-8**) refer to compounds listed in Table 5-12. Major peaks in profile **c** are alkanoic acids with carbon numbers as indicated. Isoprenoid acids **5-8** as in **b**. Peak marked (:) in **c** denotes monunsaturated C_{18} -alkanoic acid.

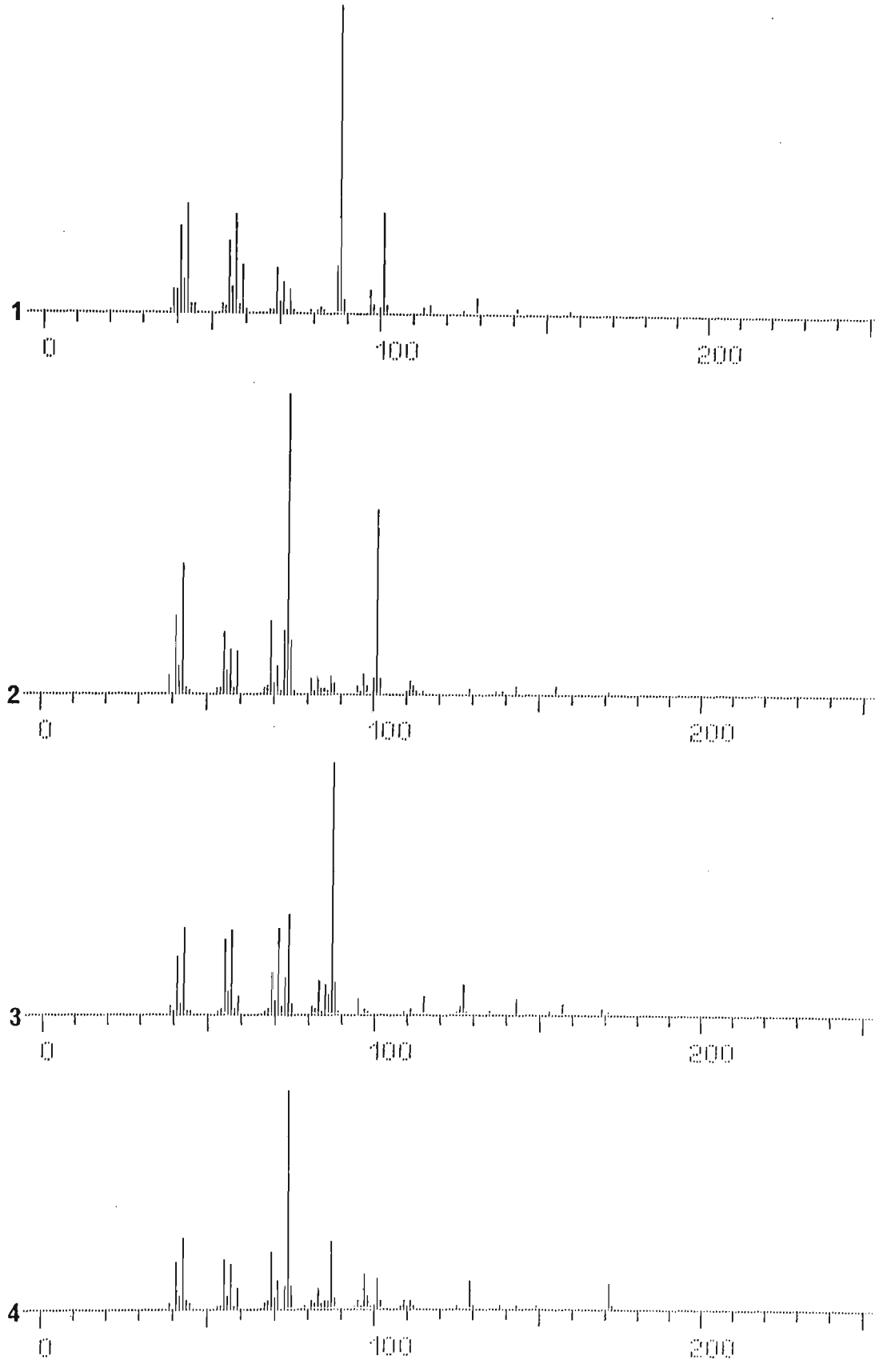

Figure 5-30. Mass spectra of the methyl ester derivatives (components **1-4** - Figure 5-29**b**) of isoprenoid acids isolated from the $KMnO_4$ oxidation of prist-1-ene. The identities of the acids are given in Table 5-12 and were obtained by comparison with library spectra. Where the latter were not available the proposed structures were inferred from a combination of the above data as well as molecular weight (GC-MS-CI: isobutane) and retention information.

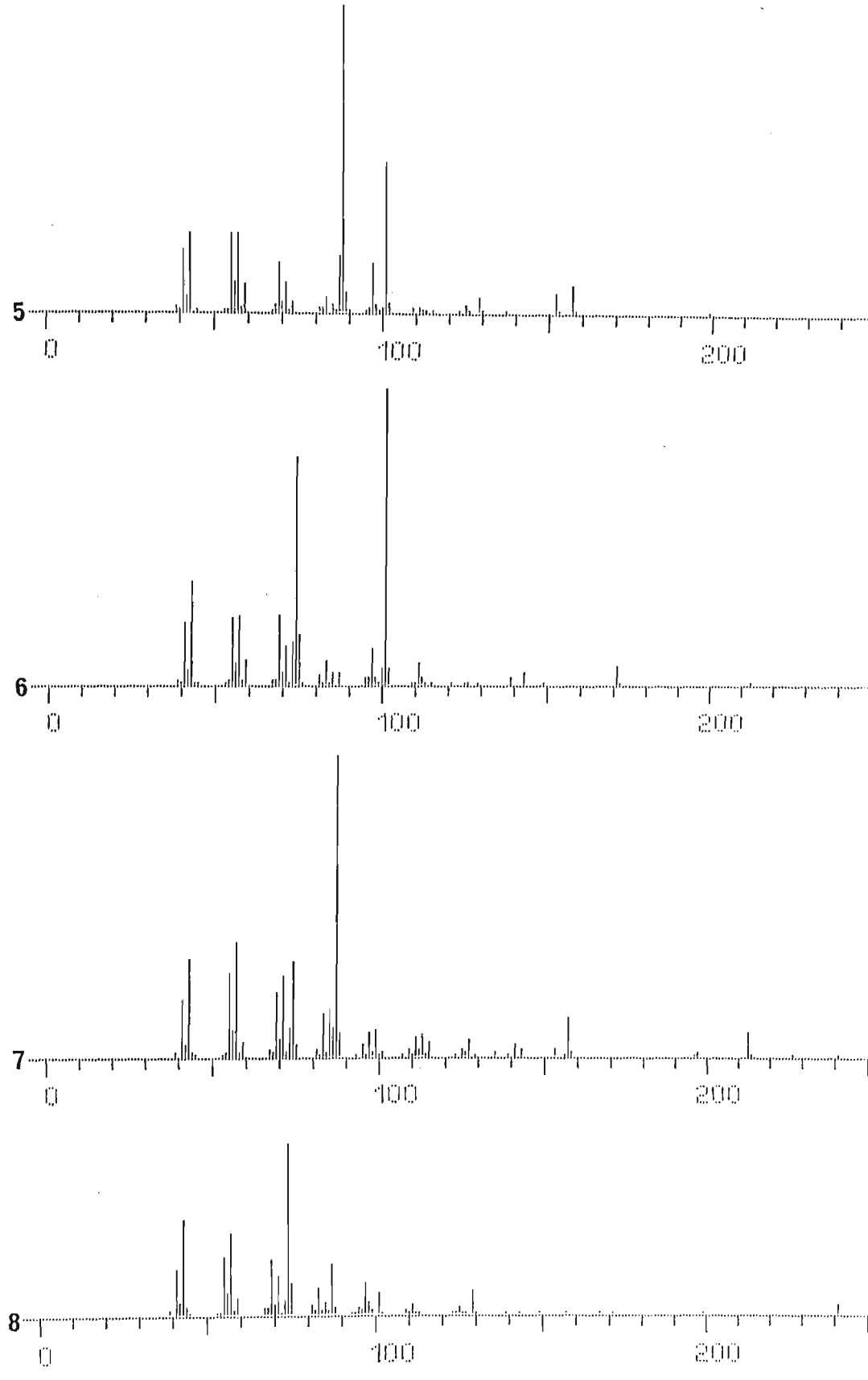

Figure 5-31. Mass spectra of the methyl ester derivatives (components **5-8** - Figure 5-29b) of isoprenoid acids isolated from the $KMnO_4$ oxidation of prist-1-ene. The identities of the acids are given in Table 5-12 and were obtained by comparison with library spectra. Where the latter were not available the proposed structures were inferred from a combination of the above data as well as molecular weight (GC-MS-CI: isobutane) and retention information.

Table 5-12. List of compounds identified in the acid fraction isolated from the $KMnO_4$ oxidation of prist-1-ene. Peak numbers refer to components depicted in respective chromatograms of Figure 5-29. Retention indices (RI) were obtained by coinjection with alkane standards.

PEAK	ACID	M WT		RI (ESTERS)	
		m	b	methyl	butyl
a	methyl-penten-2-one*				
b	acetic		116		811.9
c	glyoxylic*		130		881.1
d	propanoic		130		910.2
e	2-methylpropanoic		144		952.4
g	3-methylbutanoic		158		1047.3
h	pentanoic		158		**nd**
i	4-methylpentanoic*		172		1157.9
j	5-methylhexanoic*		186		1254.3
1	2, 6-dimethylheptanoic	172	214	1124.16	1373.97
2	3, 7-dimethyloctanoic	186	228	1229.44	1486.16
3	4, 8-dimethylnonanoic	200	242	1340.59	1595.71
4	5, 9-dimethyldecanoic*	214	256	1436.05	1692.50
5	2, 6, 10-trimethylundecanoic	242	284	1563.19	1803.87
6	3, 7, 11-trimethyldodecanoic	256	298	1666.52	1918.30
7	4, 8, 12-trimethyltridecanoic	270	312	1776.10	2027.17
8	5, 9, 13-trimethyltetradecanoic*	284	326	1870.41	2122.58

* tentative assignment; **m, b** molecular weights corresponding to the methyl (**m**) and butyl esters (**b**) of the respective acids - see text for details; **nd** - not determined.

The isoprenoid acids can be derived from prist-1-ene via migration of the double bond along the main carbon chain, followed by oxidation of the double bond (Table 5-13). Components 4 and 8 (Table 5-12) were tentatively identified as 5,9-dimethyldecanoic acid and 5,9,13-trimethyltetradecanoic acid (Figure 5-32). The structures of these two acids suggest that they may be formed by oxidation of an enol-form of the ketone components. To test this hypothesis the C_{18} -isoprenoid ketone was isolated and oxidised under the same experimental conditions as those used for prist-1-ene. Compounds isolated included acids 1-8 previously obtained, however the components of specific interest (4 and 8) were relatively less abundant than in the prist-1-ene oxidation mixture.

The similarity of the series of isoprenoid ketones and acids to the permanganate

Table 5-13. Proposed precursor-product relationship for the components isolated from the $KMnO_4$ oxidation of prist-1-ene. Due to structural symmetry of the molecule only prist-1-ene to prist-7-ene precursors need to be considered.

SOURCE	PRODUCTS		
	KETONE	ACIDS	PEAK[1]
Prist-1-ene	6,10,14-trimethylpentadecan-2-one		
Prist-2-ene	acetone	4,8,12-trimethyltridecanoic	(7)
Prist-3-ene		2-methylpropanoic	(e)
		3,7,11-trimethyldodecanoic	(6)
Prist-4-ene		3-methylbutanoic	(g)
		2,6,10-trimethylundecanoic	(5)
Prist-5-ene	6,10-dimethylundecan-2-one	4-methylpentanoic	(i)
Prist-6-ene	6-methylheptan-2-one	4,8-dimethylnonanoic	(3)
Prist-7-ene		2,6-dimethylheptanoic	(1)
		3,7-dimethyloctanoic	(2)

1 peaks listed refer to components depicted in Figure 5-29a.

(a)

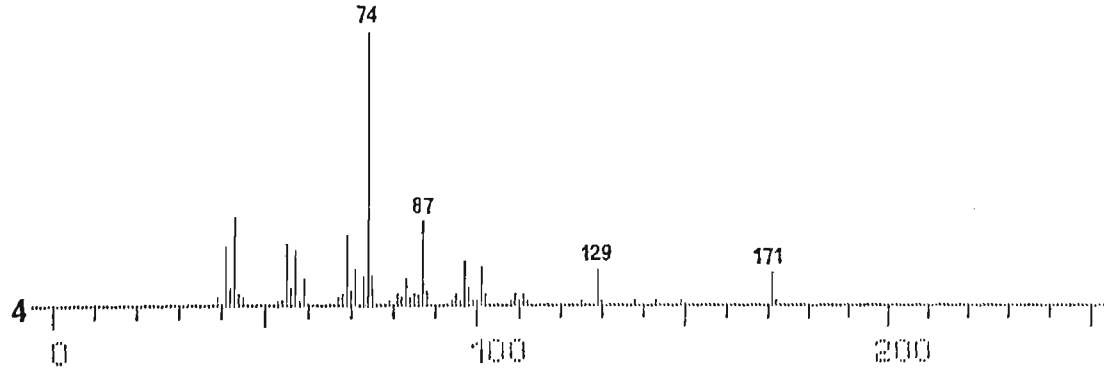

Base peak: m/z = 74 -Mc Lafferty rearrangement-ion:

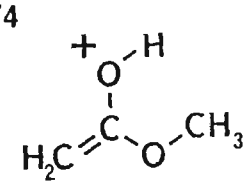

Other major fragment ions as detailed in the Proposed Structure:

(b)

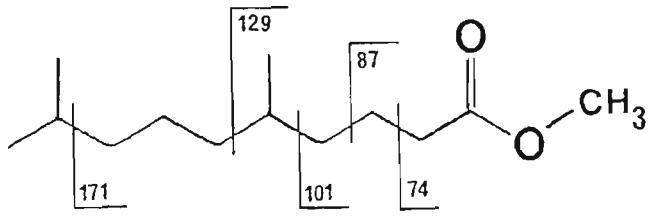

Other Data.

1. M Wt. (from CI: isobutane) = 214
2. Isoprenoid Acid (methyl ester) - from precursor information (prist-1-ene)
3. Molecular Formula: $C_{13}H_{26}O_2$ - from molecular weight and retention data

Figure 5-32. Structural elucidation of the methyl ester of component 4 (Figure 5-29b). Mass spectrum (a) and proposed structure (b). Similar reasoning applied to the determination of the structure for component 8.

degradation products of prist-1-ene suggests the possibility of biogenic and mineral -catalysed oxidation of prist-1-ene as a geological pathway. While prist-1-ene does not occur in solvent extracts of oil shale, it is readily formed by pyrolysis of an unidentified precursor (Hutton et al., 1986) and might therefore have a transient existence during maturation. However, attempted laboratory experiments on aerial oxidation of prist-1-ene supported on raw shale did not produce detectable quantities of isoprenoid ketones. If prist-1-ene is an intermediate in their formation, its conversion to ketones is most probably via biogenic pathways.

CONCLUSION.

In agreement with petrographic data, solvent-extract results for the bipartite Duaringa oil shale deposit suggest that the kerogens in the shallow oil shale samples were predominantly derived from algal lipids with further (minor) contributions from bacterial reworking of the algal biomass and comparatively little other input from allochthonous or detrital higher-plant material. Low pristane and phytane levels coupled with high relative abundances of isoprenoid ketones indicate an oligotrophic environment of deposition, which is consistent with the shallow depth proposed for the ancestral Lake Duaringa. Extract and petrographic information for the lower oil shales also indicates kerogen originating from predominantly algal sources.

The great similarity between flash-pyrolysis-GC profiles of raw shales from Duaringa indicates a common source for the oil shales and is consistent with their respective petrologies. For rapid screening of numerous samples the use of raw shale is most suitable, since it obviates the need for costly and time-consuming kerogen isolation. The use of raw shale is particularly relevant in the commercial context since its pyrolysate relates more directly to the composition of volatile products likely to be obtained using commercial retorts. Flash-pyrolysis-GC reveals structural information about the kerogen contained in the raw shale samples analysed. Pyrolysate chromatograms for an extensive range of Australian and several overseas reference oil shales studied suggest that algal-derived kerogens contain predominantly linear alkyl-chains up to at least C_{32} in chain length and possibly as long as C_{50}. Algal kerogens which have been microbially degraded or reworked are also dominated by aliphatic structures. When substantial higher-plant contributions are present in the kerogen they produce enhanced concentrations of phenols in the pyrolysate. Compositional differences in volatile constituents between retort oils and flash pyrolysates obtained for the raw shales can be largely attributed to an increased contribution of secondary pyrolysis reactions promoted by the greater opportunity for contact between organic vapour and minerals and char which is afforded in a retort. Oils from carbonaceous shales appear to be richer in pristenes than the dominantly algal

lamosites. Oil yield (relative to organic carbon content) is lower than for the algal-derived shales.

Micro-scale pyrolysis screening techniques, particularly pyrolysis-FID, are ideally suited to the preliminary assessment of oil shale properties such as hydrocarbon generating potential (oil and gas). Data obtained from this procedure provides immediate information on comparative hydrocarbon generating capacities of the shales, as well as related information, which may be used to assess the extent of their (thermal) evolution. When used in conjunction with a well-characterised standard oil shale sample it provides absolute oil-yield data for a given (uniform) deposit and is a fast and inexpensive first approach in assessing the economic viability of potential reserves. For oil shales containing type I or II kerogens the hydrocarbon generating potential is directly proportional to Fischer assay oil yield over a range of kerogen content varying from ca. 5-80 %. Total hydrocarbon quantities (oil + gas) released during pyrolysis of the raw shales appear virtually independent of the abundance and composition of the mineral matrix, which functions primarily to promote coking and to produce compositional changes in the pyrolysate due to isomerisation and cracking reactions. During pyrolysis-FID analysis of raw shale coking has a surprisingly uniform and relatively small influence in reducing the hydrocarbon generating potential of either lean or kerogen-rich shales, presumably due to the small sample sizes used for the procedure. Evidently the use of micro-scale quantities induces the rapid expulsion of volatile products and reduces their residence time in the raw shale sufficiently to reduce coking reactions.

Where C_{org} values have been determined for raw shale, these data may be used with relevant conversion factors for type I, II and III kerogen to predict the kerogen content of the oil shale. For Duaringa the kerogen contents predicted agreed closely with those actually obtained from the demineralisation of the shale. Kerogen contents calculated from C_{org} agreed closely with experimental kerogen concentrations for the shallow kerogens of uniform type I organic matter and also with that of the mixed type I/III kerogen from the lower unit. In the latter case, the relative proportions of type I and type III macerals (determined microscopically) were needed to make this calculation accurate.

TGA-DTA studies on oil shales appear best suited to the comparative study of the same sample (raw shale or demineralised kerogen) using variations in heating rates, final retorting temperatures and inert or reactive pyrolysis atmospheres. In that context the procedure provides valuable data on the retorting characteristics of the sample and should assist in choosing retorting parameters which will maximise hydrocarbon yields (oil and gas) from commercial operations. It may also be used as a preliminary step in the more detailed analysis of potentially promising samples.

Asphaltenes formed in shale oil during storage are clearly derived from polymerisations involving relatively volatile and reactive constituents. These compounds may include heteroatoms derived from kerogen structures involved in cross-linking or in functional groups and subsequently released by thermal treatment. Larger molecules which may be associated with their formation are presumably carried into the shale oil as an aerosol. The pentasphaltene isolated from a lamosite oil from the Duaringa deposit showed a relatively high abundance of nitrogen containing compounds (pyridines, pyrroles, aniline, toluidine, indoles, quinolines, cinnolines, pyrazoles, carbazoles) in the gas chromatogram of its pyrolysate. These constituents, as well as other nitrogen heterocycles, appear to be implicated in gum formation during the storage of synfuels derived from shale oil.

Although the asphaltenes contain higher proportions of N, O and S than the retort oil, when the asphaltenes are pyrolysed the volatile components of the pyrolysate are enriched in N only. Presumably the O and S remain in the char or are released in gases not detected by the FID.

Pyrolysis-FID may be used as an independent comparative approach to assess the economic potential of a given deposit. However, many of the other diverse chemical and petrological screening procedures such as solvent extraction, pyrolysis-GC, TGA and microscopy must be interpreted with caution when used in isolation. In particular, differences may occur where amorphous organic material of unknown origin is observed in the oil shale or where it is difficult to detect this using optical techniques. However, as part of an integrated approach involving both disciplines they can supply complementary data and may provide consistent information about oil shales which

includes the environment of their deposition as well as the extent of biodegradation and maturation of the deposit. Even when used in this context, disparate but complementary data is most relevant for single oil shale deposits of uniform kerogen type. For example, pyrolysis-FID screening data is capable of showing trends in maturation with increasing depth of burial where the latter requirements are met. Where these preconditions do not apply within the one deposit, or for interdeposit comparisons generally, there appears to be no consistent correlation between relative evolution of oil shales and some of the screening data (e.g. T_{MAX} and transformation ratio) considered to reflect maturational variations related to changes in depth.

For interdeposit comparisons this lack of correlation is primarily due to differences in kerogen composition, while for all deposits the effect of sample heterogeneity continues to be a severe restriction to the generalisation of any interpretations based on micro-scale procedures. Since the composition of oil shale normally changes and may be cyclic with depth, no truly representative sample exists for any given deposit although in much of the literature this is implied. To overcome this restriction the analysed sample must be fully described and bulk properties of the oil shale obtained by averaging the results obtained from several finely-divided samples obtained from different locations within the same seam of the one deposit.

The retort oils from the upper and lower seam lamosites are very similar both in composition and in terms of oil yield relative to kerogen content. This shows that there is no significant difference in the extent of maturation of their alginite macerals, despite a difference for this deposit in burial depth of about 1000m. This lack of differentiation, as expressed in retort-oil composition, is consistent with the similar elemental composition of their constituent kerogens. For each sample it is also in keeping with respective vitrinite reflectance data although accuracy of the latter is restricted by the small point count of this maceral in the deeper sample.

The retort oil from the lower lamosite has a higher proportion of alkanes in the neutral fraction of the oil and a smaller proportion of polymeric material. Although the oxygen content of the lower lamosite kerogen is less than that of the upper unit, the oxygen

content of the lower unit oil is greater than the upper unit oil. Presumably a greater part of the oxygen in the lower kerogen is chemically incorporated in relatively more stable molecules which survive retorting and end up in the oil. For the less evolved upper unit a greater proportion of the kerogen oxygen is associated with more labile moieties and expelled as carbon monoxide and carbon dioxide during retorting.

With detailed chemical data now available for retort oils from Duaringa plus two other Tertiary oil shale deposits of Queensland lamosites (Rundle/Stuart; Condor), some generalisations are possible:

All of the oils are highly aliphatic (H/C 1.6 - 1.7) and exhibit relatively small variations in the composition of their volatile fractions. These variations probably reflect differences in the relative proportions of algal and terrestrial macerals coupled with changes caused by secondary pyrolytic reactions catalysed by minerals and char. In particular, alkanones, nitriles and internal alkene isomers (including pristenes) appear to be derived mainly by secondary reactions.

The concentrations of linear nitriles and ketones in the Duaringa lamosite retort oils are substantially lower than those previously reported for other Tertiary Australian oil shale deposits. For the latter the reported abundances, based on gravimetric data, appear to be an overestimate of their actual concentrations in the oils. This follows since the polar fractions of the neutral oils in which the nitriles and ketones are isolated contain substantial proportions of compounds having too little volatility to be amenable to GC. While some of these compounds could have been transported as an aerosol during the initial retorting of the shale (e.g. porphyrins) it is likely that much of this material is formed on the silica/alumina adsorbents of the fractionating column and/or during storage of the oil (e.g. asphaltenes).

With the exception of zones adjacent to an igneous intrusion (e.g. Rundle - Gilbert and Philp,1983) differences in maturation within each of the deposits appear to have little expression in the solvent extracts or retort oils. In particular, the upper and lower lamosites from Duaringa are chemically very similar, despite differences of ca. 1000 m in depth of burial. The uniformity of the macerals and minerals in the oil shale seams of this deposit

make it ideal for microscopic pyrolysis screening of core sections to estimate its overall oil yield potential.

The present work has generated a large number of accurate GC-retention indices for many homologous series identified in the oil by mass spectrometry. The reproducibility of the combined open-column and gas-chromatographic procedures used for Duaringa indicate that it is possible to establish these retention indices with such precision that these homologues contained in the specified open-column fractions may be identified in other shale oils by retention index alone or with only minor recourse to mass spectrometry.

A knowledge of the detailed chemical characterisation of a given shale oil will greatly assist an assessment of its suitability for upgrading and an evaluation of the catalysts and conditions required for hydrotreating upgrading and refining processes. In that context the abundances and carbon-number distributions of the major homologous series of volatile components are of particular economic interest.

ACKNOWLEDGEMENTS.

This thesis is dedicated to my wife and daughter, mother and father. The former for the support and understanding they have shown throughout its preparation and the latter for guiding me in the right direction.

I would like to thank my supervisor Dr. J. Ellis for his willing guidance and assistance during the entire course of the research.

Thanks are also extended to Dr. A. Hutton for providing the oil shale samples used for these studies and for performing the petrography on them. I am grateful to Southern Pacific Petroleum NL, Central Pacific Minerals and the Queensland Geological Survey for making them available.

I acknowledge the assistance of G. Wall and his research staff (Lucas Heights Research Laboratories, CSIRO Division of Energy Chemistry) for providing the raw isothermal-pyrolysis data.

Special thanks must go to the late Professor B. Halpern for the warm personal interest and support he gave me during his tenure as foundation professor of the department.

AUTHORS PUBLICATIONS.

Hutton, A.C., Korth, J., Ellis, J. and Crisp, P. (1984). Petrography of oil shales and geochemistry of shale oil, Duaringa. In: *Geoscience in Development of Natural Resources, Proc. 7th Australian Geological Convention. Geol. Soc. Austr. Abstr. Series* No. 12, 271-273.

Hutton, A.C., Korth, J., Crisp, P.T. and Ellis, J. (1986). Low temperature pyrolysis of three Tertiary oil shales from Queensland, Australia. *J. Anal. Appl. Pyrol.,* 9, 323-333.

Crisp, P.T., Ellis, J., Hutton, A.C., Korth, J., Martin, F.A., Saxby, J.D. (1987). *Australian oil shales: A compendium of geological and chemical data.* The University of Wollongong.

Korth, J., Ellis, J., Crisp, P.T. and Hutton, A.C. (1987). Chemical studies on the Duaringa oil shale deposit. *Proc. 4th Aust. Workshop on Oil Shale,* 81-85.

BIBLIOGRAPHY.

Albaiges, J., Algaba, J. and Grimalt, J. **(1984).** Extractable and bound neutral lipids in some lacustrine sediments. *Org. Geochem.*, 6, 223-236.

Alexander, R., Kagi, R.I., Woodhouse, G.W. and Volkman, J.K. **(1983).** The geochemistry of some biodegraded Australian oils. *APEA J.*, 23(1), 53-63.

Alexander, R., Kagi, R.I. and Larcher, A.V. **(1984).** Clay catalysis of alkyl hydrogen exchange reactions-reaction mechanism. *Org. Geochem.*, 6, 755-760.

Anders, D.E. and Robinson, W.E. **(1971).** Cycloalkane constituents of bitumen from Green River shale. *Geochim. Cosmochim. Acta,* 35, 661-678.

Anders, D.E., Doolittle, F.G. and Robinson, W.E. **(1973).** Analysis of some aromatic hydrocarbons in a benzene-soluble bitumen from Green River shale. *Geochim. Cosmochim. Acta,* 37, 1213-1228.

Anderson, P.C., Gardner, P.M., Whitehead, G.V., Anders, D.G. and Robinson, W.E. **(1969).** The isolation of steranes from Green River oil shale. *Geochim. Cosmochim Acta,* 33, 1304-1307.

Arpino, P. and Ourisson, G. **(1971).** Interactions between rock and organic matter. Esterification and transesterification induced in sediments by methanol and ethanol. *Anal. Chem.*, 43, 1656-1657.

Barker, C. **(1974).** Pyrolysis techniques for source-rock evaluation. *AAPG Bull.*, 58, (11), 2349-2361.

Batts, B.D., Evans, E., Finseth, D. and Kaur, S. **(1983).** A study of the principal nitrogen functional groups present in a range of shale oils. *Proc. 1st Aust. Workshop on Oil Shale*, 157-160.

Behar, F., Pelet, R. and Roucache, J. **(1984).** Geochemistry of asphaltenes. *Org. Geochem.*, 6, 587-595.

Behar, F., Pelet, R. **(1985).** Pyrolysis-gas chromatography applied to organic geochemistry. Structural similarities between kerogens and asphaltenes from related rock extracts and oils. *J. Anal. Appl. Pyrol.*, 8, 173-187.

Berezkin, V.G. **(1981).** The development of pyrolysis gas chromatography. In *CRC Critical Reviews in Anal. Chem.*, pp. 1-48.

Blumer, M. **(1973).** Chemical fossils: trends in organic geochemistry. *Pure Appl. Chem.*, 34, 591-609.

Blumer, M., Mullin, M.M., Thomas, D.W. **(1963).** Pristane in zooplankton. *Science,* 140, 974.

Blumer, M., Guillard, R.R.L. and Chase, T. **(1971).** Hydrocarbons of marine phytoplankton. *Mar. Biol.*, 8, 183-189.

Brinkman, D.W., Bowden, J.N., Frankenfeld, J. and Taylor, B. **(1980).** Synfuel stability: Degradation mechanism and actual findings. *B. Am. Chem. Soc. Div. Fuel Chem. Prepr.*, 25(3), pp. 110-115.

Brooks, J.D., Gould, K. and Smith, J. **(1969).** Isoprenoid hydrocarbons in coal and petroleum. *Nature*, 222, 257-259.

Brooks, P.W. and Maxwell, J.R. **(1973).** Early fate of phytol in a recently-deposited lacustrine sediment. In *Advances in Organic Geochemistry 1973*. Tissot, B., Bienner, F. (eds.), pp. 977-991. Editions Technip, Paris. 1974.

Brown, F.R. and Karn, F.S. **(1980).** Stability studies of coal-derived liquids. *Fuel*, 59, 431-435.

Brown, R.A. **(1971).** Identification of alkanes by pyrolysis gas chromatography. *Anal. Chem.*, 43, 900-907.

Brown, S., Bailie, T.A. and Burlingame, A.L. **(1979).** Analytical approaches to the investigation of kerogen structure by mass spectrometric techniques. In *Advances in Organic Geochemistry 1979*. (Physics and Chemistry of the Earth Vol. 12). Douglas, A.G. and Maxwell, J.R. (eds.), pp. 475-484. Pergamon Press, Oxford.

Burlingame, A.L., Haug, P.A., Schnoes, H.K. and Simoneit, B.R. **(1968).** Fatty acids derived from Green River formation oil shale by extractions and oxidations. A Review. In *Advances in Organic Geochemistry, 1968*. Schenck, P.B. and Havenaar, I. (eds.), pp. 85-129. Pergamon Press, Oxford.

Burlingame, A.L. and Schnoes, H.K. **(1969).** Mass spectrometry in organic geochemistry. In *Organic Geochemistry*. Eglinton, G., Murphy, M.T.J. (eds.), pp. 81-160. Springer, Berlin-Heidelberg-New York.

Burnham, A.K., Clarkson, J.E., Singleton, M.F., Wong, C.M. and Crawford, R.W. **(1982).** Biological markers from Green River kerogen decomposition. *Geochim. Cosmochim. Acta*, 46, 1243-1251.

Cane, R.F. **(1976).** The origin and formation of oil shales. In *Oil Shale*, T.F. Yen and G.V. Chilingarian, (eds.). pp. 27-60. Elsevier, Amsterdam.

Cardoso, J.N. and Chicarelli, M.I. **(1981).** The organic geochemistry of the Paraiba Valley and Marau oil shales. In *Advances in Organic Geochemistry, 1981*. Bjoroy, M. et al. (eds.), pp. 828-833. John Wiley, Chichester.

Carreta, Z., Da Silva, C. and Cornford, C. **(1985).** The kerogen type, depositional environment and maturity, of the Irati Shale, Upper Permian of Parana Basin, Southern Brazil. *Org. Geochem.*, 8, 399-411.

Chaffee, A.L., Ekstrom, A., Fookes, C.J.R., Glickson, M. and Loeh. H. **(1984)**. An examination of the oil shale from the Mt. Coolon deposit. *Proc. 2nd Aust. Workshop on Oil Shale*, 56-61.

Chaffee, A.L. and McLaren, K.G. **(1986).** Structure of kerogen in Julia Creek oil shale revealed by a simple oxidation technique. *Proc. 3rd Aust. Workshop on Oil Shale*, 151-155.

Chappe, B., Albrecht, P. and Michaelis, W. **(1982).** Polar lipids of archaebacteria in sediments and petroleums. *Science*, 217, 65-66.

Chicarelli, M.I., Damasceno, L.P and Cardoso, J.N. **(1984).** Diagenetic chemistry of the Paraiba Valley oil shale. *Org. Geochem.*, 6, 153-155.

Claypool, G.E. and Reed, P.R. **(1976).** Thermal-analysis technique for source rock evaluation: Quantitative estimate of organic richness and effects of lithologic variation. *AAPG Bull.*, 60 (4), 608-626.

Coburn, T.T. and Campbell, J.H. **(1977)**. Oil shale retorting: Variation in product oil chemistry during retorting of an oil shale block. *Report to U.S. Energy Research & Development Administration*. Contract No. W-7405-Eng-48.

Comet, P.A., McEvoy, J., Giger, W. and Douglas, A.G. **(1986).** Hydrous and anhydrous pyrolysis of DSDP Leg 75 kerogens - A comparative study using a biological marker approach. *Org. Geochem.*, 9, 171-182.

Cook, E.W. **(1974)**. Green River shale-oil yields: correlation with elemental analysis. *Fuel*, 53, 16-20.

Costa Neto, C., Macaira, A.M.P., Pinto, R.C.P., Nakayama, H.T. and Cardoso, J.N. **(1980).** New analytical approaches to organic geochemistry: Solid phase functional group extraction for bitumens and functional group markers for kerogens. In *Advances in Organic Geochemistry 1979*. Douglas A.G. and Maxwell, J.R. (eds.), pp. 249-263. Pergamon Press, Oxford.

Costa Neto, C., Lachter, E.R. and Cardoso, J.N. **(1984).** The stepwise aqueous alkaline permanganate oxidation of Irati formation shale kerogen and of its reaction product with N-bromosuccinimide. *Org. Geochem.*, 8 (6), 391-397.

Cranwell, P.A. **(1978).** Extractable and bound lipid components in a freshwater sediment. *Geochim. Cosmochim. Acta,* 42, 1523-1532.

Cranwell, P.A. **(1981).** Diagenesis of free and bound lipids in terrestrial detritus deposited in a lacustrine sediment. *Org. Geochem.*, 3, 79-89.

Cranwell, P.A. **(1984).** Alkyl esters, mid chain ketones and fatty acids in late glacial and postglacial lacustrine sediments. *Org. Geochem.*, 6, 115-124.

Crisp, P.T., Ellis, J., de Leeuw, J.W. and Schenck, P.A. **(1986).** Flash thermal desorption as an alternative to solvent extraction for the determination of C_8-C_{35} hydrocarbons in oil shales. *Anal. Chem.*, 58, 258-261.

Crisp, P.T., Ellis, J., Hutton, A.C., Korth, J., Martin, F.A. Saxby, J.D. **(1987).** *Australian oil shales: A compendium of geological and chemical data.* The University of Wollongong.

Curnow, W.J. **(1986).** The prospects for shale oil in Australia. *Proc. 3rd Aust. Workshop on Oil Shale,* 3-8.

Dark, W.A., McFadden, W.H. and Bradford, D.L. **(1977).** Fractionation of coal liquids by HPLC with structural characterization by LC-MS. *J. Chromatog. Sci.*, 15 (10), 454-460.

Dastillung, M., Albrecht, P. and Ourisson, G. **(1980).** Aliphatic and polycyclic ketones in sediments, C_{27} - C_{35} ketones and aldehydes of the hopane series. *J. Chem. Res.* (S), 166-167.

Davis, J. **(1967).** *Petroleum Microbiology.* p.299, Elsevier, Amsterdam.

Dembicki, H., Horsfield, B. and Ho, T.T.Y. **(1983).** Source rock evaluation by pyrolysis-gas chromatography. *AAPG Bull.*, 67, 1094-1103.

Didyk, D.M., Simoneit, B.R.T., Brassel, S.C. and Eglinton, G. **(1978).** Organic geochemical indicators of paleoenvironmental conditions of sedimentation. *Nature,* 272, 216-222.

Douglas, A.G. **(1969).** Gas chromatography. In *Organic Geochemistry.* Eglinton, G., Murphy, M.T.J. (eds.), pp. 161-180. Springer, Berlin-Heidelberg-New York.

Duncan, D.C. **(1976).** Geologic setting of oil-shale deposits and world prospects. In *Oil Shale*. T.F. Yen and G.V. Chilingarin (eds.), pp. 1-26. Elsevier, Amsterdam.

Durand, B. **(1980).** Sedimentary organic matter and kerogen. Definition and quantitative importance of kerogen. In *Kerogen*. Durand, B. (ed.), pp. 13-34. Editions Technip, Paris.

Durand, B. and Nicaise, G. **(1980).** Procedures for kerogen isolation. In *Kerogen*. Durand, B. (ed.), pp. 35-53. Editions Technip, Paris

Durand, B. and Monin, J.C. **(1980).** Elemental analysis of kerogens. In *Kerogen*. Durand, B. (ed.), pp. 113-142. Editions Technip, Paris.

Durand-Souron, C. **(1980).** Thermogravimetric analysis and associated techniques applied to kerogens. In *Kerogen*. Durand, B. (ed.), pp. 143-162. Editions Technip, Paris.

Eglinton, G. and Hamilton, R.J. **(1963).** The distribution of alkanes. In *Chemical Plant Taxonomy*. T. Swain, (ed.), pp. 187-208. Academic Press.

Eglinton, G. and Calvin, M. **(1967).** Chemical fossils. *Sci. Am.*, 216, 32-43.

Eglinton, G. and Hamilton, R.J. **(1967).** Leaf epicuticular waxes. *Science,* 156, 1322-1335.

Eisma, E. and Jurg, J.W. **(1969).** Fundamental aspects of the generation of petroleum. In *Organic Geochemistry*. Eglinton, G., Murphy, M.T.J. (eds.), pp. 676-698. Springer, Berlin-Heidelberg-New York.

Ekstrom, A., Loeh, H. and Dale, L. **(1983).** An examination of the petroporphyrins found in oil shale from the Julia Creek deposit of the Toolebuc Formation. *Am. Chem. Soc. Div. Fuel Chem.,* 28 (3), 166-176.

Ellacott, M. **(1986).** A Geochemical Investigation of Marine Oil Shale. B.Sc. Honours Thesis. The University of Wollongong.

Espitalie, J., La Porte, J.L., Madec, M., Marquis, F., Leplat, P., Paulet, J. and Boutefeu, A. **(1977).** Methode rapide de caracterisation des roches meres de leur potentiel et de leur degre d'evolution. *Rev. de l'Inst. Francais Petrol.,* 32 (1), 23-42.

Espitalie, J., Senga Makadi, K. and Trichet, J. **(1984).** Role of mineral matrix during kerogen pyrolysis. *Org. Geochem.,* 6, 365-382.

Evans, E.J., Batts, B.D., Cant, N.W. and Smith, J.W. **(1985).** The origin of nitriles in shale oil. *Org. Geochem.,* 8 (5), 367-374.

Evans, E.J., Batts, B.D. and Cant, N.W. **(1986).** The yield of Australian oil shales as determined in nuclear magnetic resonance and infrared spectroscopy. *Proc. 3rd Aust. Workshop on Oil Shale,* 89-93.

Fanter, D.L., Walker, J.Q. and Wolf, J. **(1968).** Pyrolysis-gas chromatography of hydrocarbons. *Anal. Chem.,* 40, 2168-2175.

Farrington, J.W. and Quinn, J.G. **(1973).** Biogeochemistry of fatty acids in Recent sediments from Narraganset Bay Rhode Island. *Geochim. Cosmochim. Acta*, 37, 259-268.

Fookes, C.J.R. and Johnson, D.A. **(1984).** An investigation of the primary reactions in the pyrolysis of kerogen. *Proc. 2nd Aust. Workshop on Oil Shale,* 176-181.

Futoma, D.J., Smith, S.R., Tanaka, J., Smith, T.E. **(1981).** Chromatographic methods for the analysis of polycyclic aromatic hydrocarbons in water systems. *CRC Critical Reviews in Analytical Chemistry,* 12, 2, 69-153.

Gallegos, E.J. **(1971).** Identification of new steranes, terpanes and branched paraffins in Green River shale by combined capillary gas chromatography and mass spectrometry. *Anal. Chem.*, 43, 1151-1160.

Gallegos, E.J. **(1973).** Identification of phenylcycloparaffin alkanes and other mono -aromatics in Green River shale by gas chromatography-mass spectrometry. *Anal. Chem.*, 45, 1399-1402.

Gallegos, E.J. **(1975).** Terpane-sterane release from kerogen by pyrolysis-gas chromatography-mass spectrometry. *Anal. Chem.*, 47, 1524-1528.

Gallegos, E.J. **(1976).** Biological fossil hydrocarbons in shales. In *Oil Shale,* T.F. Yen and G.V. Chilingarian, (eds.), pp. 149-180. Elsevier, Amsterdam.

Gannon, A.J. and Henstridge, D.A. **(1984)**. Kerogen conversion relationships for selected Australian oil shales. *Proc. 2nd Aust. Workshop on Oil Shale*, 123-128.

Gelpi, E., Schneider, H., Mann, J. and Oro, T. **(1970).** Hydrocarbons of geochemical significance in microscopic algae. *Phytochemistry*, 9, 603-612.

Gilbert, T.D. and Philp, R.P. **(1983).** Triterpane stereochemistry; maturation effects due to an intrusion in Rundle oil shale. *Proc. 1st Aust. Workshop on Oil Shale*, 84-86.

Giraud, A. **(1970)**. Application of pyrolysis and gas chromatography to geochemical characterisation of kerogen in sedimentary rocks. *AAPG Bull.*, 54, 439-455.

Goossens, H., de Leeuw, J.W., Schenck, P.A. and Brassel, S.C. **(1984).** Tocopherols as likely precursors of pristane in ancient sediments and crude oils. *Nature,* 312, 440-442.

van Graas, G. de Leeuw, J.W., Schenck, P.A. and Haverkamp, J. **(1981).** Kerogen of Toarcian Shales of the Paris basin. A study of its maturation by flash pyrolysis techniques. *Geochim. Cosmochim. Acta,* 45, 2465-2474

van Graas, G., Viets, T.C., de Leeuw, J.W. and Schenck, P.A. **(1983).**A study of the soluble and insoluble organic matter from the Livello Bonarelli, a Cretaceous black shale deposit in the Central Apennines, Italy. *Geochim.Cosmochim Acta.,* 47, 1051-1059.

Grimalt, J. and Albaiges, J. **(1987).** Sources and occurence of C_{12} - C_{22} n-alkane distributions with even carbon-number preference in sedimentary environments. *Geochim. Cosmochim. Acta,* 51, 1379-1384.

Grubb, H.M. and Meyerson, S. **(1963).** Mass spectra of alkyl benzenes. In *Mass Spectrometry of Organic Ions*. F.W. McLafferty, (ed), pp. 453-527. Academic Press, New-York.

Gschwend, P.M., Zatiriou, O.C., Mantoura, R.F.C., Schwarzenbach, R.P. and Gagosian, R.B. **(1982).** Volatile organic compounds at a coastal site. 1. Seasonal variations. *Environ. Sci. Technol.,* 16, 31-38.

Gupta, A.S. and Dev,S.**(1963).** Thin-layer chromatography of olefins. *J. Chromatog.,* 12, 189-195.

Hagaman, E.W., Schell, F.M.and Cronauer, D.C. **(1984).** Oil shale analysis by CP/MAS-^{13}C n.m.r. spectroscopy. *Fuel,* 63, 915-919.

Harvey, T.G., Matheson, T.W., Pratt, K.C. **(1984).** Chemical class separation of organics in shale oil by thin-layer chromatography. *Anal. Chem.*, 56, 1277-1281.

Harwood, R.J. **(1977).** Oil and gas generation by laboratory pyrolysis of kerogen. *AAPG Bull.,* 61 (12), 2082-2102.

Haselhurst, D. **(1986).** The good oil on a bad oil scenario for Australia. *The Bulletin,* June 10, pp. 120-123.

Hertz, H.S., Brown, J.M., Chesler, S.N., Guenther, F.R., Hilpert, L.R., May, W.E., Parris, R.M. and Wise, S.A. **(1980).** Determination of individual organic compounds in shale oil. *Anal.Chem.*, 52, 1650-1657.

Hirata, Y., Novotny, M., Peaden, P.A., Lee, M.L. **(1981).** A comparison of capillary chromatographic techniques for the separation of very large polycyclic aromatic molecules. *Anal. Chim. Acta,* 127, 55-61.

Hirsch, D.E., Hopkins, R.L., Coleman, H.J., Cotton, F.O., Thompson, C.J. **(1972).** Separation of high-boiling petroleum distillates using gradient elution through dual-packed (silica gel-alumina gel) adsorption columns. *Anal. Chem.*, 44, 915-919.

Hoering, T.C. **(1984).** Thermal reactions of kerogen with added water, heavy water and pure organic substances. *Org. Geochem.,* 5, 267-278.

Horsfield, B. and Douglas, A.G. **(1980).** The influence of minerals on the pyrolysis of kerogens. *Geochim. Cosmochim. Acta,* 44, 1119-1131.

Huc, A.Y. and Roucache, J.G. **(1981).** Quantitative thin-layer separation of heavy petroleum fractions. *Anal. Chem.,* 53, 914-917.

Hunt, J. M. **(1972).** Distribution of carbon in the crust of the earth. *AAPG Bull.*, 56 (11), 2273-2277.

Hunt, J.M. **(1979).** In *Petroleum Geochemistry and Geology*. Freeman, San Francisco.

Hurtubise, R.J., Phillip, J.D. **(1979).** Characterization of polycyclic aromatic hydrocarbons in shale oil by chromatography and fluorescence densitometry. *Anal. Chim. Acta,* 110, 245-251.

Hutton, A.C. **(1981).** Organic petrology of samples of oil shale from G.S.Q. Duaringa 1/2 A. A report prepared for *Geological Survey of Queensland.*

Hutton, A.C. **(1982).** Organic petrology of oil shales. PhD thesis, University of Wollongong.

Hutton, A.C. **(1985).** Determination of oil shale yields by petrographic analysis. *Fuel,* 64, 1058-1061.

Hutton, A.C. **(1986).** Duaringa - A bipartite oil shale deposit. *Aust. Coal Geol.,* 6, 27-40.

Hutton, A.C., Kantsler, A.J., Cook, A.C. and McKirdy, D.M. **(1980).** Organic matter in oil shales. *APEA J.*, 20, 1-11.

Hutton, A.C., Korth, J. Crisp, P.T. and Ellis, J. **(1986).** Low temperature pyrolysis of three Tertiary oil shales from Queensland, Australia. *J. Anal. Appl. Pyrol.*, 9, 323-333.

Iida, T., Yoshii, E. and Kitatsuji, E. **(1966).** Identification of normal paraffins, olefins, ketones and nitriles from Colorado shale oil. *Anal. Chem.,* 38, 1224-1227.

Ingram, L.L., Ellis, J., Crisp, P.T. and Cook, A.C. **(1983).** Comparative study of oil shales and shale oils from the Mahogany Zone, Green River Formation (U.S.A.) and Kerosene Creek Seam, Rundle Formation (Australia). *Chem. Geol.,* 38, 185-212.

Ishiwatary, R., Ishiwatary, M., Kaplan, I.R., Rohrbach, B.G. **(1976).** Thermal alteration of young kerogen in relation to petroleum genesis. *Nature*, 264, 347-349.

Ivanac, J.F. **(1983).** Stuart, Nagoorin - Nagoorin South, Lowmead and Duaringa oil shale deposits: A review. *Proc 1st Aust. Workshop on Oil Shale*, 12-17.

Jennings, W. **(1980).** Gas Chromatography with Glass Capillary Columns. (2nd Edition). Academic Press.

Jewell, D.M., Ruberto, R.G.and Davis, B.E. **(1972).** Systematic approach to the study of aromatic hydrocarbons in heavy distillates and residues by elution adsorption chromatography. *Anal. Chem.,* 44, 2319-2321.

Jones, A.R., Guerin, M.R. and Clark, B.R. **(1977).** Preparative-scale liquid chromatographic fractionation of crude oils derived from coal and shale. *Anal. Chem.,* 49, 1766-1771.

Kalman, J.R. and Saxby, J.D. **(1983).** Solid state NMR spectroscopy of oil shales and its application to in-situ pyrolysis at Rundle. *Proc 1st Aust. Workshop on Oil Shale*, 80-83.

Kissin, Y.V. **(1987).** Catagenesis and composition of petroleum: Origin of n-alkanes and isoalkanes in petroleum crudes. *Geochim. Cosmochim. Acta,* 51, 2445-2457.

Krevelen, D. W. van **(1961).** In *Coal.* Elsevier, Amsterdam.

Krishnan, K. **(1981).** Some applications of fourier transform infrared photoacoustic spectroscopy. *Appl. Spectroscopy,* 35, 549-557.

Lambert, D.E., Wilson, M.A. and Collin, P.J. **(1984).** Conversion of aliphatic to aromatic carbon during pyrolysis of Rundle oil shale and the characterisation of oil product. *Proc. 2nd Aust. Workshop on Oil Shale*, 164-169.

Lambert, D.E. and Saxby, J.D. **(1987).** Effects of storage on the chemical composition of shale oil from Rundle, Australia. *Fuel*, 66, 396-399.

Larter, S.R. **(1984).** Application of analytical pyrolysis techniques to kerogen characterization and fossil fuel exploration/exploitation. In *Analytical Pyrolysis.* Voorkees, K.E. (ed.), Vol.II. pp. 212-272, . Butterworths, London.

Larter, S.R., Solli, H. and Douglas, A.G. **(1978).** Analysis of kerogens by pyrolysis-gas chromatography-mass spectrometry using selective ion detection. *J. Chromatogr.*, 167, 421-431.

Larter, S.R., Solli, H., Douglas, A.G., De Lange, F. and De Leeuw, J.W. **(1979).** Occurence and significance of prist-1-ene in kerogen pyrolysates. *Nature,* 279, 405-408.

Larter, L.R. and Senftle, J.T. **(1985).** Improved kerogen typing for petroleum source rock analysis. *Nature,* 318, 277-280.

Later, D.W., Lee, M.L., Bartle, K.D., Kong, R.C., Vassilaros, D.L. **(1981).** Chemical class separation and characterisation of organic compounds in synthetic fuels. *Anal. Chem.*, 53, 1612-1620.

Laude, D.A., Brissey, G.M., Ijames, C.F., Brown, R.S. and Wilkins, C.L. **(1984).** Linked gas chromatography/fourier transform infrared/fourier transform mass spectrometry with integrated electron impact and chemical ionization. *Anal . Chem.*, 56, 1163-1168.

Lee, M.L., Novotny, M., Bartle, K.D. **(1976a).** Gas chromatography/mass spectrometric and nuclear magnetic resonance spectrometric stidies of carcinogenic polynuclear aromatic hydrocarbons in tobacco and marijuana smoke condensates. *Anal. Chem.*, 48, 405-416

Lee, M.L., Novotny, M., Bartle, K.D. **(1976b).** Gas chromatography/mass spectrometric and nuclear magnetic resonance determination of polynuclear aromatic hydrocarbons in airborne particulates. *Anal. Chem,* 48, 1566-1572.

Lee, M.L., Vassilaros, D.L., White, C.M., Novotny, M. **(1979).** Retention Indices for programmed-temperature capillary-column gas chromatography of polycyclic aromatic hydrocarbons. *Anal. Chem.*, 51, 768-773.

Lee, M.L. and Wright, B.W. **(1980).** Capillary column gas chromatography of polycyclic aromatic compounds: A review. *J.Chromatog. Sci.*, 18, 345-358.

Lee, R.F., Nevenzei, J.C., Pfaffenhofer, G.A. **(1970).** Wax esters in marine copepods. *Science,* 167, 1510-1511.

Leeuw, J.W. de, Correira, V.A. and Schenck, P.A. **(1973).** On the decomposition of phytol under simulated geological conditions and in the top layer of natural sediments. In *Advances in Organic Geochemistry 1973.* Tissot, B., Bienner, F. (eds.), pp. 993-1004. Editions Technip, Paris. 1974.

Leventhal, J.S. **(1976).** Stepwise pyrolysis-gas chromatography of kerogen in sedimentary rocks. *Chem.Geol.*, 18, 5-20.

Levy, E.J., Galbraith, E.J. and Melpolder, F.W. **(1963).** Interpretive techniques for the determination of paraffin wax composition by mass spectrometry and gas chromatography. In: *Advances in mass spectrometry,* Vol. 2, p. 395. Elliot, R.M. (ed.). Macmillan, New York.

Levy, J.H. and Stuart, W.I. **(1983).** Thermal analysis of some Australian oil shales. *Proc. 1st Aust.Workshop on Oil Shale,* 135-138.

Levy, J.H. and Stuart, W.I. **(1984).** Characterisation of Australian oil shales by thermal methods. *Proc. 2nd Aust.Workshop on Oil Shale,* 91-96.

Lijmbach, G.W.M. **(1975).** On the origin of petroleum. Proc. 9th World Petroleum Congress, Tokyo, 2, 357-369.

Lindner, A.W. **(1983).** Geology and geochemistry of some Queensland Tertiary oil shales. In: *Geochemistry and Chemistry of Oil Shales*, ACS Symp. Ser. 230, Miknis, F.P. and McKay, J.F. (eds), pp. 97-118. Amer. Chem. Soc., Washington.

McFarlane, I. **(1984).** Why we need Queensland shale oil. Keynote address to *2nd Aust.Workshop on Oil Shale*, Brisbane, 1984.

McNair, H.M. and Bonelli., E.J. **(1969).** *Basic Gas Chromatography.* (5th Edition) Varian (Insrument Division), Palo Alto, U.S.A.

Mackenzie, A.S., Hoffman, C.F. and Maxwell, J.R. **(1981).** Molecular parameters of maturation in the Toarcian shales, Paris Basin, France, III- Changes in aromatic steroid hydrocarbons. *Geochim. Cosmochim. Acta,* 45, 1345-1355.

Mackenzie, A.S. Disko, V. and Rullkoter, J. **(1983).** Determination of hydrocarbon distributions in oils and sediment extracts by gas chromatography-high resolution mass spectrometry. *Org. Geochem.,* 5 (2), 57-63.

Mapstone, G.E. **(1951).** In *Oil Shale and Cannel Coal.* Sell, G. (ed.). Vol. 2, p.787.

March, J. **(1968).** *Advanced organic chemistry: Reactions, mechanisms and structure.* McGraw-Hill.

Marchand, A. and Conrad, J. **(1980).** Electron paramagnetic resonance in kerogen studies. In *Kerogen.* Durand, B. (ed.), pp. 243-270. Editions Technip, Paris.

Marcovich, B.J. **(1983).** In-situ retorting of Julia Creek oil shale. *Proc 1st Aust. Workshop on Oil Shale,* 47-50.

Maxwell, J.R., Pillinger, C.T., Eglinton, G. **(1971).** Organic Geochemistry. Quar. Rev., 25, 571-628.

Miknis, F.P., Netzel, D.A. Smith, J.W., Mast, M.A., Maciel, G.E. **(1982).** ^{13} C NMR measurements of the genetic potential of oil shales. *Geochim. Cosmochim. Acta,* 46, 977-984.

Miknis, F.P., Lindner, A.W., Gannon, A.J., Davis, M.F.and Maciel, G.E. **(1984).** Solis state ^{13}C NMR studies of selected oil shales from Queensland, Australia. *Org. Geochem.,* 7, 239-248.

Miller, R. **(1982).** Hydrocarbon class fractionation with bonded-phase liquid chromatography. *Anal. Chem.,* 54, 1742-1746.

Moore, A.J., Wright, B.C., Reddan, P.J. and Gannon, A.J. **(1986).** Implications from several oil shale project studies. *Proc. 3rd Aust. Workshop on Oil Shale,* 26-31.

Morrison, R.I. **(1969).** Soil lipids. In *Organic Geochemistry.* Eglinton, G., Murphy, M.T.J. (eds.), pp. 558-575. Springer, Berlin-Heidelberg-New York.

M.S.D.C. (Mass Spectrometry Data Centre). **(1974).** Eight Peak Index of Mass Spectra. *Mass Spectrometry Data Centre,* Reading, 2nd ed., 2933 pp.

Neale, R.C. and Thompson, B.J. **(1986).** Technical status of the Rundle oil shale project. *Proc. 3rd Aust. Workshop on Oil Shale,* 21-25.

Nishimura, M. **(1977).** The geochemical significance in early sedimentation of geolipids obtained by saponification of lacustrine sediments. *Geochim. Cosmochim. Acta,* 41, 1817-1823.

Nishimura, M. and Baker, E. **(1986).** Possible origin of n-alkanes with a remarkable even-to-odd predominance in recent marine sediments. *Geochim. Cosmochim. Acta,* 50, 299-305.

Noon, T.A. **(1986).** Oil shale exploration activity in Queensland during 1985-1986. *Proc. 3rd Aust. Workshop on Oil Shale,* 9-14.

Novotny, M., Lee, M. and Bartle, K. **(1974).** The methods for fractionation, analytical separation and identification of polynuclear aromatic hydrcarbons in complex mixtures. *J. Chromatog. Sci.,* 12, 606-612.

Novotny, M., Hirose, A. and Wiesler, D. **(1984).** Separation and characterization of very large neutral polycyclic molecules in fossil fuels by microcolumn liquid chromatography and mass spectrometry. *Anal. Chem.*, 56, 1243-1248.

Oberlin, A., Boulmier, J.L., Villey, M. **(1980).** Electron microscopic structure of kerogen microtexture. Selected criteria for determining the evolution path and evolution stage of kerogen. In *Kerogen.* Durand, B. (ed.), pp. 191-241. Editions Technip, Paris.

Oil Shale Data Book (1979). Published by TRW Energy Systems Group (Mc Lean, Va.).

Ourisson, G., Albrecht, P. and Rohmer, M. **(1984).** The microbial origin of fossil fuels. *Sci. American*, 251, 44-51.

Paine, G.G. **(1983).** Explosives fracturing of oil shale for an experimental in-situ retort at the Julia Creek project. *Proc 1st Aust Workshop on Oil Shale*, 51-54.

Philp, R.P. **(1985).** Fossil Fuel Biomarkers. Applications and spectra. Elsevier, Amsterdam-Oxford-New York-Tokyo.

Philp, R.P.and Gilbert, T.D. **(1984).** Characterisation of petroleum source rocks and shales by pyrolysis-gas chromatography-mass spectrometry-multiple ion detection. *Org. Geochem.*, 6, 489-501.

Philp, R.P.and Gilbert, T.D. **(1985).** Source rock and asphaltene biomarker characterisation by pyrolysis-gas chromatography-mass spectrometry-multiple ion detection. *Geochim. Cosmochim. Acta,* 49, 1421-1432.

Prahl, F.G. and Pinto, L.A. **(1987).** A geochemical study of long-chain n-aldehydes in Washington coastal sediments. *Geochim. Cosmochim. Acta,* 51, 1573-1582.

Prien, C.H. **(1976).** Survey of oil shale research in the last three decades. In *Oil Shale,* T.F. Yen and G.V. Chilingarian, (eds.), pp. 233-267. Elsevier, Amsterdam.

Reddan, P.J. and Poole, D.R. **(1984).** The status of the Condor oil shale project. *Proc. 2nd Aust. Workshop on Oil Shale*, 15-19.

Reedy, G.T., Bourne, S., Cunningham, P.T. **(1979).** Gas chromatography/infrared matrix isolation spectrometry. *Anal Chem.*, 51, 1535-1540.

Reedy, G.T., Ettinger, D.G. and Schneider, J.F. **(1985).** High-resolution gas chromatography/matrix isolation infrared spectrometry. *Anal. Chem.*, 57, 1602-1609.

Regtop, R.A. **(1983)**. Gas chromatographic-mass spectrometric studies of shale oil and oil shale from the Rundle deposit, Queensland. PhD thesis, University of Wollongong.

Regtop, R.A., Crisp, P.T. and Ellis, J. **(1982).** Chemical characterisation of shale oil from Rundle, Queensland. *Fuel,* 61, 185-192.

Regtop, R.A., Crisp, P.T. and Ellis, J. **(1983).** Molecular markers and other extractable components from Rundle oil shale. *Proc. 1st Aust. Workshop on Oil Shale,* 73-75.

Regtop, R.A., Ellis, E, Crisp, P.T., Ekstrom, A. and Fookes, C.J.R. **(1985).** Pyrolysis of model compounds on spent oil shales, minerals and charcoal. *Fuel,* 64, 1640-1646.

Regtop, R.A., Crisp, P.T., Ellis, J. and Fookes, C.J.R. **(1986).** 1-Pristene as a precursor for 2-pristene in pyrolysates of oil shale from Condor, Australia. *Org. Geochem.*, 9, 233-236.

Robinson, W.E. **(1969).** Isolation procedures for kerogens and associated soluble organic materials. In *Organic Geochemistry*. Eglinton, G., Murphy, M.T.J. (eds.), pp. 181-195. Springer, Berlin-Heidelberg-New York.

Robinson, W.E. and Lawlor, D.L. **(1961).** Constitution of hydrocarbonlike materials derived from kerogen oxidation products. *Fuel* , 40, 375-388.

Robinson, W.E., Cummins, J.J., Dinneen, G.U. **(1965).** Changes in Green River oil shale paraffins with depth. *Geochim. Cosmochim. Acta*, 29, 249-258.

Romanowski, T., Funcke, W., Grossmann, I.G., Konig, J. and Balfanz, E. **(1983).** Gas chromatographic/mass spectrometric determination of high-molecular -weight polycyclic aromatic hydrocarbons in coal tar. *Anal. Chem.*, 55, 1030-1033.

Rostad, C.E. and Pereira, W.E. **(1986).** Kovats and Lee retention indices determined by gas chromatography/mass spectrometry for organic compounds of environmental interest. *J. HRC & CC*. 9, 328-334.

Rouxhet, P.G., Robin, P.L., Nicaise, G. **(1980).** Characterization of kerogens and of their evolution by infrared spectroscopy. In *Kerogen*. Durand, B. (ed.), pp. 163-190. Editions Technip, Paris.

Rovere, C. **(1980).** The quantitation of short chain fatty acids in human physiological fluids. A study of inherited diseases. BSc (Honours) thesis. University of Wollongong.

Rovere, C. **(1986).** Analytical studies on Australian shale oils. PhD thesis, University of Wollongong.

Rovere, C., Crisp, P.T., Ellis, J. and Bolton, P.D. **(1983).** Chemical characterisation of shale oil from Condor, Australia. *Fuel,* 62, 1274-1282.

Saban, M., Porter, S., Costello, C., Vitorovic, D. **(1979).** Polar constituents isolated from Aleksinac oil shale. In *Advances in Organic Geochemistry 1979*. Douglas, A.G., Maxwell, J.R. (eds.), pp. 559-566. Pergamon Press, Oxford, 1980.

Saxby, J.D. **(1970).** Isolation of kerogen in sediments by chemical methods. *Chem. Geol.,* 6, 173-184.

Saxby, J.D. **(1976).** Chemical separation and characterization of kerogen from oil shale. In *Oil Shale*. T.F. Yen and G.V. Chilingarin (eds.), pp. 103-128. Elsevier, Amsterdam.

Saxby, J.D. **(1980).** Atomic H/C ratios and the generation of oil from coals and kerogens. *Fuel,* 59, 305-307.

Saxby, J.D. **(1981).** Thermogravimetric analysis of oil shales. *Thermochimica Acta.*, 47, 121-123.

Saxby, J.D., Bennett, A.J.R., Corcoran, J.F., Lambert, D.E. and Riley, K.W. **(1986).** Petroleum generation: Simulation over six years of hydrocarbon formation from torbanite and brown coal in a subsiding basin. *Org. Geochem.*, 9, 69-81.

Schultz, R.V., Jorgenson, J.W., Maskarinec, M.P., Novotny, M. and Todd, L.J. **(1979).** Characterisation of polynuclear aromatic and hydrocarbon fractions of solvent-refined coal by glass capillary gas chromatography/mass spectrometry. *Fuel,* 58, 783-789.

Schwatzky, H., George, A.E., Smiley, G.T., Montgomery, D.S. **(1976).** Hydrocarbon-type separation of heavy petroleum fractions. *Fuel,* 55, 16-20.

Seifert, W.K. **(1978).** Steranes and terpanes in kerogen pyrolysis for correlation of oils and source rocks. *Geochim. Cosmochim. Acta,* 42, 473-484.

Seifert, W.K. and Moldowan, J.M. **(1978).** Applications of steranes, terpanes and mono-aromatics to the maturation, migration and source of crude oils. *Geochim. Cosmochim. Acta,* 42, 77-95.

Seifert, W.K. and Moldowan, J.M. **(1979).** The effect of biodegradation on steranes and terpanes in crude oils. *Geochim. Cosmochim. Acta,* 43, 111-126.

Shanks, W.C., Seyfried, W.E., Meyer, W.C. and O'Neil, T.J. **(1976).** Mineralogy of oil shale. In *Oil Shale*. T.F. Yen and G.V. Chilingarin (eds.), pp. 81-100. Elsevier, Amsterdam.

Shimoyama , A., Johns, W.D. **(1972).** Formation of alkanes from fatty acids in the presence of $CaCO_3$. *Geochim. Cosmochim. Acta,* 36, 87-91.

Shue, F.F., Yen, T.F. **(1981).** Concentration and selective identification of nitrogen and oxygen containing compounds in shale oil. *Anal. Chem.,* 53, 2081-2084.

Simoneit, B.R. **(1977).** Diterpenoid compounds and other lipids in deep-sea sediments and their geochemical significance. *Geochim. Cosmochim. Acta,* 41, 463-476.

Simoneit, B.R., Schnoes, H.K., Haug, P. and Burlinghame, A.L. **(1971).** High resolution mass spectrometry of nitrogenous compounds of the Colorado Green River Formation oil shale. *Chem. Geol.,* 7, 123-141.

Smith, J.W. **(1966).** Conversion constants for Mahogany-zone oil shale. *AAPG Bull.,* 50, 167-170.

Smith, S.L. **(1986).** Two-dimensional capillary GC/FT-IR. *J. Applied Spectroscopy,* 40 (2), 278-281.

Solli, H., Larter, S.R. and Douglas, A.G. **(1981).** Analysis of kerogens by pyrolysis-gas chromatography-mass spectrometry using selective ion monotoring.III. Long chain alkylbenzenes. In *Advances in Organic Geochemistry* . Douglas, A.G. and Maxwell, J.R. (eds.), pp. 591-597. Pergamon Press, Oxford.

Speight, J.G., Moschopedis, S.E. **(1979).** Some observations on the molecular nature of petroleum asphaltenes. *Preprints. Div. Pet. Chem., Am. Chem. Soc.,* 24 (4), 910-923.

Stanfield, K.E. and Frost, I.C. **(1949).** Report of investigation 4477 US Bureau of Mines, Washington, DC.

Starsinic, M., Otake, Y., Walker, Jr. P.L.and Painter, P.C. **(1984).** Application of FT-i.r. spectroscopy to the determination of COOH groups in coal. *Fuel,* 63, 1002-1007.

Stenhagen, E., Abrahamsson, S. and McLafferty, F.W. **(1974).** *Registry of mass spectral data.* Wiley, New York.

Streibl, M. and Herout, V. **(1969).** Terpenoids- Especially oxygenated nono, sesqui-, di- abd triterpenes. In *Organic Geochemistry.* Eglinton, G., Murphy, M.T.J. (eds.), pp. 401-424. Springer, Berlin-Heidelberg-New York.

Thompson, L.G. and Thompson, W.J. **(1983).** Mineral reactions of two Colorado oil shale samples - A comparison. In: Miknis, F.P. and McKay, J.F. (editors), *Geochemistry and Chemistry of Oil Shales* ACS Symp. Ser. 230, pp. 513-528. Amer. Chem. Soc., Washington.

Tissot, B.P., Durand, J., Esspitalie, J. and Combaz, A. **(1974).** Influence of nature and diagenesis of organic matter in formation of petroleum. *AAPG Bull.,* 58 (3), 499-506.

Tissot, B.P. and Welte, D.H. **(1984).** In *Petroleum Formation and Occurence*. Springer, Berlin-Heidelberg-New York.

Tolmie, D.B. **(1986).** Status of the Julia Creek oil shale project. *Proc. 3rd Aust. Workshop on Oil Shale,* 15-20.

Treibs, A. **(1936).** Chlorophyll and hemin derivatives in organic materials. *Angew. Chem.,* 49, 628-686.

Uchida, T. and Yabushita, T. **(1986).** Oil shale development activities in Japan-Construction of oil shale pilot plant. *Proc. 3rd Aust. Workshop on Oil Shale,* 175-180.

Vandenbroucke, M. **(1980).** Structure of kerogens as seen by investigations on soluble extracts. In *Kerogen.* Durand, B. (ed.), pp. 415-443. Editions Technip, Paris.

Vitorovic, D.K. **(1980).** Structure elucidation of kerogen by chemical methods. In *Kerogen.* Durand, B. (ed.), pp. 301-338. Editions Technip, Paris.

Vitorovic, D.K. and Pfendt, P.A. **(1967).** Investigation of the kerogen of a Yugoslav (Aleksinac) oil shale. *Proc. 7th World Pet. Congr.*, 3, 691-694.

Vitorovic, D.K. Ambles, A. and Djordievic, M. **(1984).** Relationship between kerogens of various structural types and the products of their multistep oxidative degradation. *Org. Geochem.,* 6, 333-342.

Wakeham, S.G., Schaffner, C. and Giger, W. **(1980).** Diagenetic polycyclic aromatic hydrocarbons in Recent sediments: Structural information obtained by high performance liquid chromatography. In *Advances in Organic Geochemistry* 1979. (Physics and Chemistry of the Earth Vol. 12). Douglas, A.G. and Maxwell, J.R. (eds.), pp. 353-363. Pergamon Press, Oxford.

Wall, G.C. and Dung, N.V. **(1984).** The isothermal pyrolysis kinetics of Condor oil shale. *Proc. 2nd Aust. Workshop on Oil Shale*, 129-134.

Wall, G.C. and Smith, S.J.C. **(1986).** Kinetics of production of individual products from the isothermal pyrolysis of seven Australian oil shales. *Proc. 3rd Aust.Workshop on Oil Shale,* 109-114.

Welte, D.H. and Waples, D. **(1973).** Ueber die Bevorzugung geradezahliger *n*-alkane in Sedimentgesteinen. *Naturwissenschaften,* 60, 516-517.

Wen, C.S, Chilingarian, G.V. and Yen, T.F. **(1978).** Properties and structures of bitumen. In *Bitumens, Asphalts and Tar Sands.* Chilingarian,G.V. and Yen, T.F (eds.). pp. 154-190. Elsevier, Amsterdam.

Whelan, J.K., Hunt, J.M., Huc, A.Y. **(1980).** Applications of thermal distillation -pyrolysis to petroleum source rock studies and marine pollution. *J. Anal. Appl. Pyrol.,* 2, 79-96.

Williams, P.F.V. **(1987).** Organic geochemistry of the British Kimmeridge Clay. *Fuel,* 66, 86-91.

Wils, E.R.J., Hulst, A.G. and Den Hartog, J.C. **(1982).** The occurence of plant wax constituents in airborne particulate matter in an urbanised area. *Chemosphere*, 11, 1087-1096.

Wilson, M.A., McCarthy, S.A., Collin, P.J. and Lambert, D.E. **(1986).** Alkene transformations catalysed by mineral matter during oil shale pyrolysis. *Org. Geochem.* 9 (5), 245-253.

Wood, K.V., Schmidt, C.E., Cooks, R.G., Batts, B.D. **(1984).** Identification of partially hydrogenated nitrogen-containing polycyclic aromatic hydrocarbons in coal liquids by tandem mass spectrometry. *Anal. Chem.*, 56, 1335-1338.

Yen, T.F. **(1972).** Present status of the structure of petroleum heavy ends and its significance to various technical applications. *Am. Chem. Soc. Div. Petr. Chem.*, (Preprint), 102-114.

Yen, T.F. and Chilingarian, G.V. **(1976).** Introduction to oil shales. In *Developments in Petroleum Science, 5.Oil Shale*. Yen, T.F and Chilingarian, G.V. (eds.). pp. 1-12. Elsevier, Amsterdam.